INSTITUTE OF APPLIED ASTRONOMY
of the
RUSSIAN ACADEMY OF SCIENCES

OBSERVATOIRE DE PARIS
SYSTÈMES DE RÉFÉRENCE TEMPS-ESPACE

Astrometry, Geodynamics and Solar System Dynamics: from milliarcseconds to microarcseconds

Astrométrie, Géodynamique et Dynamique du Système solaire: de la milliseconde à la microseconde

Edited by

(Actes publiés par)

A. FINKELSTEIN and N. CAPITAINE

JOURNÉES 2003 ⋆

SYSTÈMES DE RÉFÉRENCE SPATIO-TEMPORELS

⋆ ST.PETERSBURG, 22-25 SEPTEMBER

INSTITUTE OF APPLIED ASTRONOMY
of the
RUSSIAN ACADEMY OF SCIENCES

10 Kutuzov Quay, 191187, St.Petersburg
Russian Federation

OBSERVATOIRE DE PARIS
SYSTÈMES DE RÉFÉRENCE TEMPS-ESPACE
UMR8630 / CNRS

61, avenue de l'Observatoire, Paris
F-75014, France

Astrometry, Geodynamics and Solar System Dynamics: from milliarcseconds to microarcseconds

Astrométrie, Géodynamique et Dynamique du Système solaire: de la milliseconde à la microseconde

Edited by

(Actes publiés par)

A. FINKELSTEIN and N. CAPITAINE

JOURNÉES 2003 ⋆

SYSTÈMES DE RÉFÉRENCE SPATIO-TEMPORELS

⋆*ST.PETERSBURG, 22-25 SEPTEMBER*

ISBN 5-93197-019-3

ISBN 2-901057-50-0

TABLE OF CONTENTS

PREFACE

The Journées 2003 "Systèmes de référence spatio-temporels", with the sub-title "Astrometry, geodynamics and solar system dynamics: from milliarcseconds to microarcseconds", have been held from 22 to 25 September 2003 in Saint Petersburg. They have been organized with the help of the Ministry of Science and Technology of Russian Federation, the Russian Foundation for basic Research, St Petersburg Scientific Center of RAS and Institute of Applied Astronomy. The Conference took place in the buildings of Saint Petersburg Scientific Center and of the Institute of Applied Astronomy (IAA) of Russian Academy of Sciences. A one-day visit of the Svetloe Radio Astronomical Observatory (SvRAO) was organized by the IAA on the third day, which allowed the participants to see real VLBI observations performed with this radiotelescope during a VLBI session in the framework of the International VLBI Service for geodesy and astrometry. The meeting ended with a typical Russian buffet organized at the IAA.

These Journées, which were the fifteenth conference in this series, have been organized jointly by the IAA and Paris Observatory, reflecting the long term tradition of cooperation between our two institutes. The previous Journées have been organized in Paris each year from 1988 to 1992 and alternately, since 1994, in Paris and the following European cities: Warsaw (1995), Paris (1996), Prague (1997), Paris (1998), Dresden (1999), Paris (2000), Brussels (2001) and Bucharest (2002).

The main goal of the Journées 2003 was to discuss the most recent results in astrometry, geodynamics, ephemeris astronomy and celestial mechanics in the context of improving the celestial and terrestrial reference systems and determining their mutual orientation at a sub-milliarcsecond level of accuracy. Special attention has been paid to develop the methods of processing high precision observations of VLBI, SLR and GPS techniques on the basis of the new standards of the IERS Conventions (2003). About 100 participants from 14 countries attended this meeting that included 14 invited papers, 38 oral communications and 41 posters. The general sessions were "Celestial and Terrestrial Reference Frames: Techniques, Definitions and Links", "Rotation of the Earth and other Planets: Observations and Models (Orlov's Session)", "Plate tectonics, Crustal deformations and Geophysical fluids", "Solar System Dynamics" and "Relativity and Time". Each session included invited papers and oral contributions and the poster sessions were summarized with short oral presentations. In addition, a special session on "Highlights of the 25th IAU General Assembly on Reference Systems and Fundamental Astronomy" provided information about the scientific meetings in these topics that took place at the latest General Assembly of the International Astronomical Union in July 2003 in Sydney; the session included summaries of the major IAU Division I meetings and a panel discussion.

These Proceedings are divided into six sections corresponding to the sessions of the meeting. The list of participants is given on pages vii and viii, the scientific programme on pages ix to xiii. A Table of Contents and a Postface are given on pages iii to v and 355, respectively. The Postface gives the announcement for "Journées" 2004 in Paris.

We thank the Scientific Organizing Committee for its valuable contribution to the elaboration of the scientific programme and all the authors of the papers who have sent their contribution in the required form and within the required deadline. We would like to thank the Local Organizing Committee and especially Victor Brumberg and Nadia Shuygina for their very efficient work before and during the meeting and the staff of the Institute of Applied Astronomy as well for their kind welcome at IAA. We are grateful to N. Shuygina, D. Ryzhkova and O. Becker for their efficient technical help for the publication.

The organizers of the "Journées 2003",

Andrey FINKELSTEIN, Nicole CAPITAINE

19 July 2004

LIST OF PARTICIPANTS

Bagrov A.	Moscow, Russia	abagrov@inasan.rssi.ru
Barkin Yu.	Alikante, Spain	yuri.barkin@ua.es
Benishek V.	Belgrade, Serbia	vlaben@yahoo.com
Bizouard Ch.	Paris, France	christian.bizouard@obspm.fr
Bobylev V.	St.Petersburg, Russia	vbobylev@gao.spb.ru
Boehm J.	Vienna, Austria	johannes.boehm@tuwien.ac.at
Bolotin S.	Kiev, Ukraine	bolotin@mao.kiev.ua
Bourda G.	Paris, France	Geraldine.Bourda@obspm.fr
Bronnikova N.	St.Petersburg, Russia	bronn@gao.spb.ru
Brumberg V.	St.Petersburg, Russia	brumberg@quasar.ipa.nw.ru
Brzeziński A.	Warszawa, Poland	alek@cbk.waw.pl
Capitaine N.	Paris, France	capitain@syrte.obspm.fr
Coll B.	Paris, France	bartolome.coll@obspm.fr
Débarbat S.	Paris, France	Suzanne.Debarbat@obspm.fr
Eroshkin G.	St.Petersburg, Russia	eroshkin@gao.spb.ru
Escapa A.	Alicante, Spain	alberto.escapa@ua.es
Fienga A.	Paris, France	fienga@imcce.fr
Finkelstein A.	St.Petersburg, Russia	amf@quasar.ipa.nw.ru
Folgueira M.	Madrid, Spain	martafl@mat.ucm.es
Fukushima T.	Tokyo, Japan	Toshio.Fukushima@nao.ac.jp
Gambis D.	Paris, France	gambis@obspm.fr
Gayazov I.	St.Petersburg, Russia	gayazov@quasar.ipa.nw.ru
Gontcharov G.	St.Petersburg, Russia	georgegontcharov@yahoo.com
Gorshkov V.	St.Petersburg, Russia	vigor@gao.spb.ru
Gozhy A.	Poltava, Ukraine	pgo@poltava.ukrtel.net
Groten E.	Darmstadt, Germany	groten@ipg.tu-darmstadt.de
Gubanov V.	St.Petersburg, Russia	gubanov@quasar.ipa.nw.ru
Ilyasov Yu.	Puschino, Russia	ilyasov@prao.psn.ru
Ivanova T.	St.Petersburg, Russia	itv@quasar.ipa.nw.ru
Ivantsov A.	Nikolaev, Ukraine	anatoly@mao.nikolaev.ua
Izmailov I.	St.Petersburg, Russia	melon@gao.spb.ru
Kalinitchenko O.	St.Petersburg, Russia	melon@gao.spb.ru
Kharin A.	Kiev, Ukraine	kharin@mao.kiev.ua
Kholshevnikov K.	St.Petersburg, Russia	kvk@astro.spbu.ru
Khovritchev M.	St.Petersburg, Russia	deimos@gao.spb.ru
Khrutskaya E.	St.Petersburg, Russia	deimos@gao.spb.ru
Kiseleva T.	St.Petersburg, Russia	melon@gao.spb.ru
Kočer M.	Czech Republic	kocer@klet.cz
Kolaczek B.	Warszawa, Poland	kolaczek@cbk.waw.pl
Kolesnik Yu.	Moscow, Russia	kolesnik@inasan.rssi.ru
Korsun' A.	Kiev, Ukraine	akorsun@mao.kiev.ua
Kosek W.	Warszawa, Poland	kosek@cbk.waw.pl
Krasinsky G.	St.Petersburg, Russia	kra@quasar.ipa.nw.ru
Kudryavtsev S.	Moscow, Russia	ksm@sai.msu.ru
Kumakshev S.	Moscow, Russia	kumak@ipmnet.ru
Kumkova I.	St.Petersburg, Russia	kumkova@quasar.ipa.nw.ru

Kurzynska K.	Poznan, Poland	kurzastr@main.amu.edu.pl
Kuznetsov E.	Ekaterinburg, Russia	Eduard.Kuznetsov@usu.ru
Lambert S.	Paris, France	Sebastien.Lambert@obspm.fr
Le Poncin-Lafitte Ch.	Paris, France	leponcin@danof.obspm.fr
Lopez J.	Castellon, Spain	lopez@mat.uji.es
Lubkov M.	Poltava, Ukraine	pgo@poltava.ukrtel.net
Malkin Z.	St.Petersburg, Russia	malkin@quasar.ipa.nw.ru
Marco F.	Castellon, Spain	marco@mat.uji.es
McCarthy D.	Washington, USA	dmc@maia.usno.navy.mil
Mozhaev M.	St.Petersburg, Russia	melon@gao.spb.ru
Ogrizovic V.	Belgrade, Serbia	vukan@grf.bg.ac.yu
Panafidina N.	St.Petersburg, Russia	nap@quasar.ipa.nw.ru
Pashkevich V.	St.Petersburg, Russia	apeks@gao.spb.ru
Pasynok S.	Moscow, Russia	pasynok@sai.msu.ru
Petit G.	Sevres, France	gpetit@bipm.org
Pireaux S.	Toulouse, France	sophie.pireaux@cnes.fr
Pitjeva E.	St.Petersburg, Russia	evp@quasar.ipa.nw.ru
Protitch-Benishek V.	Belgrade, Serbia	vprotic@aob.bg.ac.yu
Rodin A.	Puschino, Russia	rodin@prao.psn.ru
Ron C.	Prague, Czech Republic	ron@ig.cas.cz
Rusinov Yu.	St.Petersburg, Russia	rusinov@quasar.ipa.nw.ru
Schuh H.	Vienna, Austria	harald.schuh@tuwien.ac.at
Seidelmann K.	USA	pks6n@virginia.edu
Sekido M.	Kashima, Japan	sekido@crl.go.jp
Shabun C.	St.Petersburg, Russia	clara_sh@mail.ru
Shlyapnikova A.	St.Petersburg, Russia	ann@AS3597.spb.edu
Shuygina N.	St.Petersburg, Russia	nvf@quasar.ipa.nw.ru
Sidorenkov N.	Moscow, Russia	sidorenkov@rhmc.mecom.ru
Skurikhina E.	St.Petersburg, Russia	sea@quasar.ipa.nw.ru
Soffel M.	Dresden, Germany	soffel@rcs.urz.tu-dresden.de
Sokolova Ju.	St.Petersburg, Russia	S0lei@yandex.ru
Sôma M.	Tokyo, Japan	somamt@cc.nao.ac.jp
Souchay J.	Paris, France	Jean.Souchay@obspm.fr
Stavinschi M.	Bucharest, Romania	magda@aira.astro.ro
Tatevian S.	Moscow, Russia	statev@inasan.ru
Tesmer V.	Munchen, Germany	tesmer@dgfi.badw.de
Teyssandier P.	Paris, France	pierre.teyssandier@obspm.fr
Titov O.	Canberra, Australia	olegtitov@auslig.gov.au
Tsvetkov A.	St.Petersburg, Russia	tsvetkov@ast.usr.pu.ru
Vityazev V.	St.Petersburg, Russia	vityazev@venvi.usr.pu.ru
Wooden W.	Washington, USA	whw@usno.navy.mil
Yagudina E.	St.Petersburg, Russia	eiya@quasar.ipa.nw.ru
Yatskiv Ya.	Kiev, Ukraine	yatskiv@mao.kiev.ua
Zhang H.	Nanjing, China	jupiter@nju.edu.cn
Zharov V.	Moscow, Russia	zharov@sai.msu.ru
Zhu Z.	Nanjing, China	zhuzi@nju.edu.cn
Zotov L.	Moscow, Russia	tempus@sai.msu.ru

SCIENTIFIC PROGRAM

September 22, 2003: 9^h40^m – 14^h30^m

OPENING OF THE JOURNÉES 2003: V. Brumberg (Russia), N. Capitaine (France)

SESSION I:
CELESTIAL AND TERRESTRIAL REFERENCE FRAMES: TECHNIQUES, DEFINITIONS AND LINKS

Chair: V. Brumberg, N. Capitaine

V. Gubanov (Russia): *Project of global analysis of the 1979-2003 VLBI data*
D. D. McCarthy (USA), G. Petit (France): *IERS Conventions 2000*
N. Capitaine (France): *Microarsecond models for the celestial motions of the CIP and CEO*
Z. Malkin (Russia): *Comparison of IAU2000 precession–nutation model with observations*
A. Finkelstein, A. Ipatov, S. Smolentsev, V. Gratchev, I. Rahimov, Z. Malkin, E. Skurikhina (Russia): *The first results of VLBI observations at the Svetloe observatory in the framework of the IVS programs*
Ya. Yatskiv, A. Kur'yanova, S. Bolotin (Ukraine): *Consistency check of ICRF–Ext.1 by comparing it with catalogues of GAOUA type*
O. Titov (Australia): *Comparison of the individual ICRF solutions*
A. Rodin, Yu. Ilyasov (Russia): *Pulsar astrometry: status and prospects*
G. Gontcharov (Russia): *Statistics of double stars for ICRS optic realizations*
Yu. Kolesnik (Russia): *A new approach to representation of the catalogue systematic differences*
V. Vityazev (Russia): *Does Precession derived from FK5–HIPPARCOS agree with the VLBI?*
S. Bolotin (Ukraine): *Estimation of the Celestial Intermediate Pole motion in the Terrestrial and Celestial reference frames from VLBI observations on the interval 1979–2003*

September 22, 2003: 16^h00^m – 18^h00^m

SESSION VI:
HIGHLIGHTS OF THE 25TH IAU GENERAL ASSEMBLY ON REFERENCE SYSTEMS AND FUNDAMENTAL ASTRONOMY

Chair: M. Soffel

N. Capitaine (France): *Highlights of the scientific meetings of Division I*
D. D. McCarthy (USA): *Highlights of the Joint Discussion on the International Celestial Reference System*
K. Seidelmann (USA): *Thoughts about the implementation of the IAU 2000 Resolutions*
T. Fukushima (Japan): *Summary of Division I and IAU EC discussion on the Future organization of Division I*

Panel discussion

September 23, 2003: 9^h00^m – 14^h45^m

SESSION II:
ROTATION OF THE EARTH AND OTHER PLANETS: OBSERVATIONS AND MODELS (A. Ya. Orlov's session)

Chair: A. Finkelstein, Z. Malkin

A. Brzeziński, W. Kosek (Poland): *Free core nutation: stochastic modelling versus predictability*

G. Krasinsky (Russia): *Body tides in the Earth–Moon system and the Earth's rotation*

D. Gambis (France): *State of the art in the Earth Rotation monitoring*

T. Fukushima (Japan): *New formulation of precession and GST–UT1 relation*

A. Korsun' (Ukraine): *The history of the Orlov's sessions*

M. Sôma, K. Tanikawa, K. Kawabata (Japan): *Earth's rate of rotation between 700 BC and 1000 AD derived from ancient solar eclipses*

S. Débarbat, M. -P. Lerner (France): *The rotation of the Moon from Antiquity to Cassini*

G. Eroshkin, V. Pashkevich (Russia): *High–precision numerical analysis of the rigid Earth rotation problem using a high performance computer*

C. Ron, J. Vondrák (Czech Republic): *Earth Orientation Parameters in 1899–1992 based on the new Earth Orientation Catalogue*

B. Kolaczek, J. Nastula (Poland): *Impact of the addition of the ocean to the atmospheric excitation of polar motion on variability of spectra and correlation with polar motion*

A. Escapa, J. Getino, J. Ferrandiz (Spain): *Influence of the redistribution tidal potential on the rotation of the non–rigid Earth*

C. Bizouard (France): *Interactive Earth rotation parameters through the Web*

W. Wooden, T. Johnson, M. Carter, A. Myers (USA): *Near Real–time IERS Products*

W. Kosek (Poland), D. D. McCarthy (USA), T. Johnson (USA), M. Kalarus: *Comparison of polar motion prediction results supplied by the IERS Sub–bureau for Rapid Service and Predictions and results of other prediction methods*

Yu. Rusinov (Russia): *Averaging of individual EOP series by least-squares collocation*

S. Pasynok (Russia): *IAU2000: Comparison with the VLBI observations and other nutation theories*

N. Shuygina (Russia): *Determination of EOP from combination of SLR and VLBI data at the observational level*

S. Kuzin, N. Sorokin, S. Tatevian (Russia): *On the use of DORIS data for determination of the EOP and geocenter motion*

I. Gayazov (Russia): *Variation of C_{21}, S_{21} geopotential coefficients from SLR data of Lageos satellites*

September 23, 2003: 16^h00^m – 18^h00^m

SESSION III:
PLATE TECTONICS, CRUSTAL DEFORMATIONS AND GEOPHYSICAL FLUIDS

Chair: A. Brzeziński

H. Schuh, G. Estermann (Austria): *Atmospheric, non–tidal oceanic and hydrological loading investigated by VLBI*

N. Sidorenkov (Russia): *Influence of the atmospheric and oceanic circulation on the plate tectonics*

O. Titov (Australia): *Post-seismic motion of the Gilcreek VLBI site after the 03–Nov–2002 earthquake by VLBI*

V. Zharov (Russia): *New models for reduction of the VLBI data*

Review of posters for the Sessions I and III

September 24, 2003: 9^h00^m – 18^h00^m

VISIT TO THE OBSERVATORY SVETLOE

September 25, 2003: 9^h00^m – 10^h50^m

SESSION IV:
SOLAR SYSTEM DYNAMICS
Chair: Ya. Yatskiv

E. Pitjeva (Russia): *Numerical ephemerides of planets and the Moon — EPM and improvement of some astronomical constants*

S. Kudryavtsev (Russia): *Improved Harmonic Development of the Earth Tide Generating Potential*

V. Mioc, M. Stavinschi (Romania): *Stability of equatorial satellite orbits*

A. Fienga, J.-L. Simon (France): *Future of the IMCCE planetary ephemerides*

J. Souchay (France): *Characteristics of the rotation of asteroid EROS 433*

I. Izmailov, M. Khovritchev, E. Khrutskaya, T. Kiseleva (Russia): *CCD-observations of Galilean satellites of Jupiter during their munual occultations eclipses in 2003 at Pulkovo Observatory*

J.-E. Arlot (France), G. Gorel, L. Hudkova, A. Ivantsov, Eu. Kozyrev (Ukraine): *Photometric observations of the mutual events of the Galilean satellites of Jupiter made at Nikolaev Astronomical Observatory in 2002–2003*

September 25, 2003: 11^h30^m – 14^h45^m

SESSION V:
RELATIVITY AND TIME
Chair: D.D. McCarthy

M. Soffel, S. Klioner (Germany): *The BCRS and the large scale structure of the universe*

V. Brumberg (Russia), J.-L. Simon (France): *Relativistic indirect third–body perturbation in the SMART Earth's rotation theory and their effect on the ITRS/GCRS relationship*

G. Petit (France): *A new realization of Terrestrial Time*

M. Sekido, T. Fukushima (Japan): *Relativistic VLBI model for Finite distance Radio Source*

P. Teyssandier, C. Le Poncin-Lafitte (France): *Relativistic theory of light deflection and time transfer up to the order G^2/c^4 using the world function*

M. Soffel (Germany): *The BCRS, GCRS and the classical astronomical reference system*

Review of posters for the Sessions II, IV, and V

CLOSING OF THE JOURNÉES 2003: N. Capitaine (France), V. Brumberg (Russia)

LIST OF POSTERS

SESSION I:

A. Bagrov, Yu. Kolesnik (Russia): *Scientific objectives of a small size catalogue based on the space–born optical interferometric mission*

V. Bobylev (Russia): *Kinematical test of the ICRS inertiality*

A. Kharin (Ukraine): *All–wave astrometry. Basic problems*

M. Khovritchev, E. Khrutskaya, N. Bronnikova (Russia): *The positions and proper motions of 58483 stars in the Pulkovo fields with galaxies on the Tycho–2 system (Pul–3)*

M. Khovritchev, E. Khrutskaya (Russia): *Comparisons USNO–B1.0 catalogue with Pul–3 and UCAC1 in selected fields*

I. Kumkova, M. Stepashkin (Russia): *Transformation between ICRS and ITRS under IAU(2000) resolutions*

K. Kurzynska (Poland): *Optical realization of ICRF with Liquid Mirror Telescope*

J. Lopez, F. Marco, M. Martinez (Spain): *A numerical method for the analysis of the systematic errors in reference systems from non–regular samples*

F. Marco (Spain): *Compatibility among dynamical and kinematical correction models*

V. Ogrizovic (Serbia): *A motorized system for rapid defection of vertical determiation*

A. Shlyapnikova, V. Vityazev (Russia): *FK5–HIPPARCOS: systematic differences without assumption of rigid mutual rotation*

E. Skurikhina, N. Panafidina, J. Sokolova (Russia): *Comparison station position time series from VLBI and GPS*

J. Sokolova (Russia): *The distribution of post–fit residuals from the VLBI observational data*

A. Tsvetkov, A. Popov (Russia): *Tycho–2 and Hipparcos: intercomparison of the catalogues*

I. Verestchagina (Russia): *Processing of VLBI–data: application of different estimation methods*

E. Yagudina (Russia): *Problems of the dynamical reference frames construction at the modern stage*

Z. Zhu (China): *NPM2 and Hipparcos proper motions*

SESSION II:

J. Ferrandiz, Yu. Barkin (Spain): *New approach to development of Moon rotation theory*

Yu. Barkin, J. Ferrandiz (Spain): *Mercury resonant translatory–rotary motion as "core-mantle" system*

G. Bourda, N. Capitaine (France): *Modelisation of Earth rotation using temporal variations of the Earth's gravity field*

M. Folgueira (Spain), J. Souchay (France): *A new formulation of the damping effect in the Earth's and Mars' free polar motion*

V. Gubanov, C. Shabun (Russia): *Three–angle parametrisation of the Earth's orientation in VLBI data analysis*

T. Ivanova, N. Shuygina (Russia): *Geopotential coefficient J_2 from the analysis of the Etalon 1 & 2 SLR observations*

L. Akulenko, S. Kumakshev, Yu. Markov (Russia): *Motion of the Earth's pole*

S. Lambert (France): *Coupling effects between nutation and zonal variations in Earth's rotation*

M. Lubkov (Ukraine): *The definition of the forced nutations of rotating elastic Earth by finite element method*

L. Zotov (Russia): *High frequency variations in the Earth rotation*

SESSION III:

A. Gozhy (Ukraine): *On the expediency of creation of the network of the same type points of joint astronomical, geodetic and geophysical determinations of their position changes in Eurasia*

V. Gorshkov, N. Shcherbakova, N. Miller, E. Prudnikova (Russia): *Earth tidal variations from local astrometric EOP sets (1904–2002) recomputed in IERS Convention 2000*

SESSION IV:

N. Bronnikova, T. Vasil'eva: *Astrometric observations of Uranus in 2002 with normal astrograph*

H. Zhang (China): *Internal structure models of Mars*

A. Ivantsov (Ukraine): *Comparison analysis of measured coordinates at CCD*

L. Kazantseva, V. Kislyuk (Ukraine): *Comparative analysis of Kyiv database of lunar occultations*

K. Kholshevnikov, E. Kuznetsov (Russia): *Evolution of a two–planetary regular system on a cosmogonic time scale*

T. Kiseleva, O. Kalinitchenko, M. Mozhaev (Russia): *The determination of coordinates of Saturn by the observations of their satellites with 26–inch Refractor at Pulkovo Observatory*

M. Kočer, J. Tichá, M. Tichý (Czech Republic): *KLENOT — practical use of solar system dynamics in follow–up astrometry observations of small solar system bodies*

V. Protitch–Benishek, V. Benishek (Serbia): *Transits of Mercury: observations and analysis from Belgrade Astronomical Observatory*

V. Protitch-Benishek (Serbia): *Newcomb's data on ancient eclipses revisited: conclusions*

M. Sôma, T. Hayamizu, T. Setoguchi, T. Hirose (Japan): *Precise position of Saturn obtained from a stellar occultation by Tethys*

SESSION V:

B. Coll, A. Tarantola (France): *A Galactic Positionning System*

S. Pireaux, J. -P. Barriot, G. Balmino (France): *Basis for a native relativistic software integrating the motion of satellites*

Section I)

CELESTIAL AND TERRESTRIAL REFERENCE FRAMES: TECHNIQUES, DEFINITIONS AND LINKS

SYTÈMES DE RÉFÉRENCE CÉLESTES ET TERRESTRES: TECHNIQUES, DÉFINTIONS ET LIENS

PROJECT: GLOBAL ANALYSIS OF 1979-2004 VLBI DATA

V.S. GUBANOV
Institute of Applied Astronomy of R.A.S.
Kutuzov quay, 10, St.Petersburg, Russia, 191187
e-mail: gubanov@ipa.nw.ru

ABSTRACT. VLBI observations for the last 25 years will be used for new revision of the International Celestial Reference Frame (ICRF), the International Terrestrial Reference Frame (ITRF) and the IERS Earth's Orientation Parameters (EOP) with the help of a new software QUASAR (Quantitative Analysis and Series Adjustment in Radioastrometry). The package QUASAR allows to compute the residuals (O − C) according to IERS Conventions (2003) and to analyze their by single-/multi-series or global adjustment using parametric, stochastic and dynamical models of data.

1. GENERAL STATEMENT

There are approximately 2200 radio sources and 150 stations in about 5 million VLBI observations that were curried out during last 25 years. The goal objective is reanalysis of these data for revision and extension of ICRF-Ext.1 and ITRF(VLBI) reference frames and correction of IERS(EOP)C04 reference series. The main components of this project are following:

a) Data base: all observation at global VLBI-network during 1979-2004.

b) Theoretical foundation: IERS Conventions (2003) (McCarthy, Petit, 2003) and Genaralized Least-Squares Techniques (Gubanov, 1997, 2001).

c) Expected results: new versions of ICRF, ITRF and IERS(EOP) series; proper motion of source position due to changing structure effects; variation of base lines; parametrization of free core nutation as stochastic process; refined luni-solar precession and nutation terms; more precise Love/Shida numbers, tidal phase lag; tropospheric wet-delay, its horizontal gradients and mupping function; antenna offsets, and atmospheric loading coefficients for all sites, etc.

d) Period of realization: 2003-2005.

e) Research group: V.S.Gubanov, I.F.Surkis, Yu.L.Rusinov (IAA) and post-graduate students of SPbSU.

f) Financial support: grant No. 03-02-17591 of the Russian Foundation for Basic Research.

2. PACKAGE QUASAR: CONFIGURATION, TUNING AND CONTROL

Software QUASAR was developed during 1998-2002 by Prof. V.S.Gubanov and Ph.D. I.F.Surkis with collaboration of Dr. I.A.Vereschagina (Kozlova) and Dr. Yu.L.Rusinov. The description of astronomical reductions, data analysis techniques, application results and user guide have been published by these co-authors in IAA Communications, No. 141–145, 2002.

As is obvious from below flow diagram (Fig. 1) the programmed package QUASAR allows to carry out single-series, multi-series and global solutions. As well seven different methods for analysis of diurnal stochastic signals may be used. The iteraton process can be realized with respect to both unknown parameters and covariance of signals.

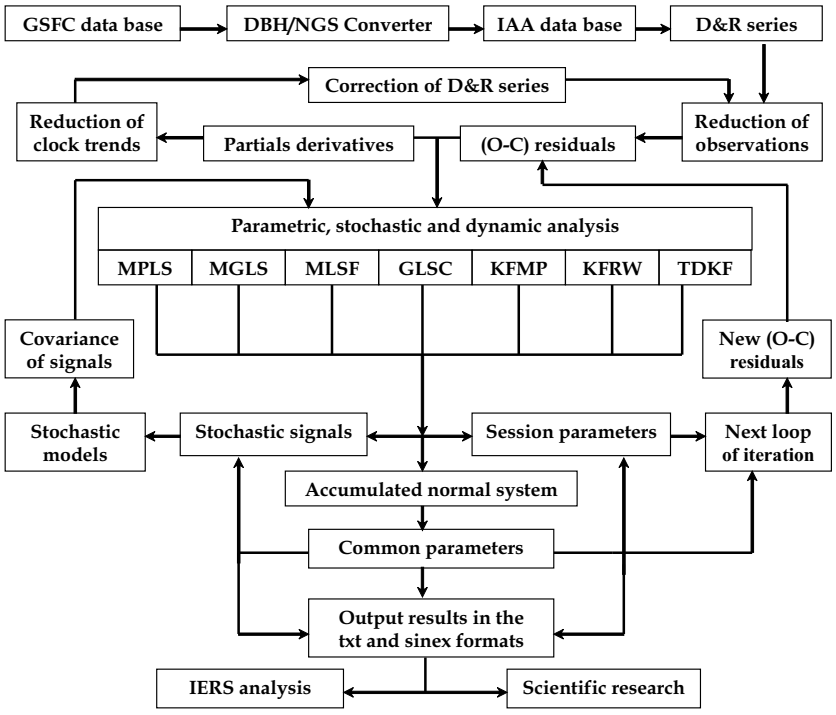

Figure 1: Configuration of the package QUASAR.

The main tuning and control functions are following: a) support and visualization of data base; b) reduction of delay/rate measurements and calculation of partials; c) correction of local clocks diurnal trend to quadratic model; d) parametrization of covariance function for all type stochastic signals; e) choice of stochastic analysis techniques; f) control of single-/multi-series or global solution processes; g) estimation of all signals and session or global parameters; h) regularization of random parameters; i) iteration process; j) preparation of ICRF, ITRF and EOP corrections in the IERS formats.

3. REDUCTION OF CLOCK TREND TO QUADRATIC MODEL

Sometimes the quadratic model for daily clock trend was not acceptable, because of local hydrogen masers have not been stable enough. For this reason the residuals (O – C) for all available VLBI observations were corrected using QUASAR graphic system. As a result, the RMS of clock stochastic component is decreased by 10 times. In all other respect these corrected data are not changed practicaly. For example, this process is demonstrated on Figs. 2-5 for the NEOS-A 011106xe session.

--- All ---	ALGOPARK FORTLEZA	KOKEE WETTZELL
ALGOPARK NYALES20	FORTLEZA WETTZELL	
ALGOPARK WETTZELL	FORTLEZA KOKEE	
NYALES20 WETTZELL	FORTLEZA NYALES20	
KOKEE NYALES20	ALGOPARK KOKEE	

Fig. 2 - The base line names for NEOS-A 011106xe session.

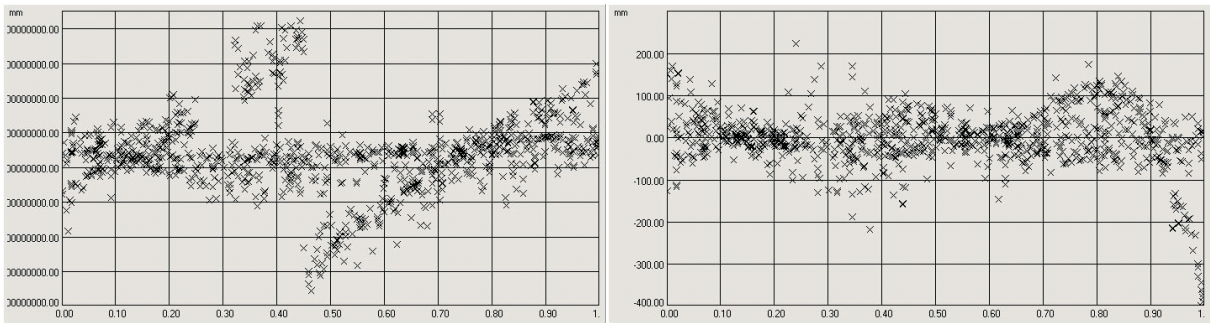

Figure 3: Original residuals (O − C) after elimination of clock quadratic trends for all VLBI stations (left) and then after elimination of the phase breaks (right).

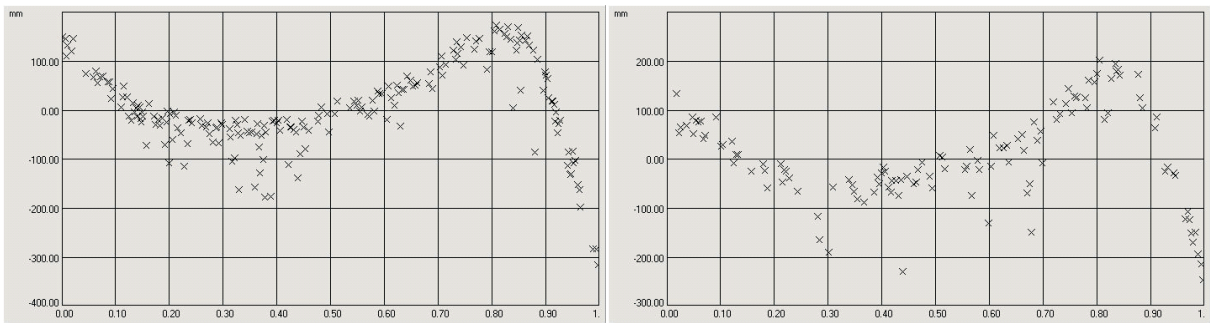

Figure 4: (O − C) residuals for Wettzell - Fortaleza (left) and Wettzell - Kokee baselines (right).

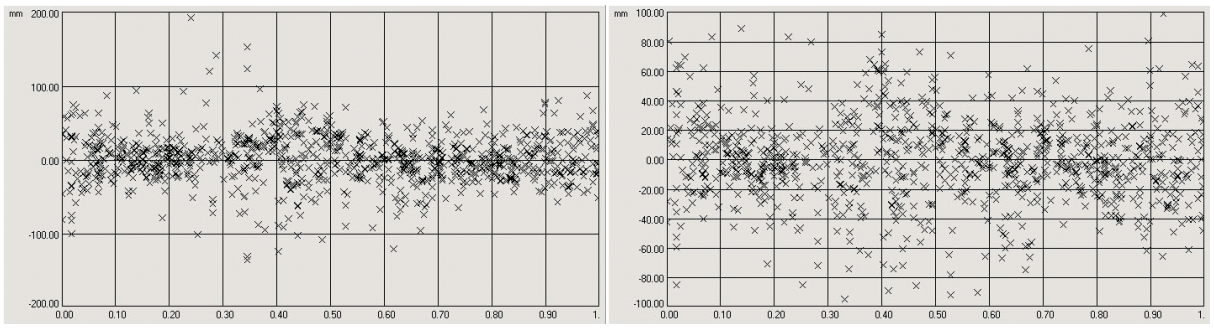

Figure 5: Reduction of Wettzell clock trend to quadratic model (left) and filtration of all residuals (O − C) under "4-sigma" criterion (right).

4. PARAMETRIC AND STOCHASTIC ANALYSIS TECHNIQUES

The diurnal variable parameters (DVP) may be analysed by seven different techniques: a) Multi-Parameter Least-Squares (MPLS), b) Multi-Group Least-Squares (MGLS), c) Moving Least-Squares Filter (MLSF), d) Global Least-Squares Collocation (GLSC), e) Kalman Filter of Markov's Process (KFMP), f) Kalman Filter of Random Walk (KFRW), g) Two-Dimension Kalman Filter (TDKF).

The first two of them (MPLS and MGLS) are well known. They use the Least-Squares (LS) techniques and DVP representation showed in Fig. 6. As opposed to MPLS, the MGLS technique have to do with a few fragmets (groups) of diurnal session duration of each about 1 hours. In general, the change of DVP inside every group may be presented as bound constrained polynomial trend (Gubanov, Kozlova and Surkis, 2002).

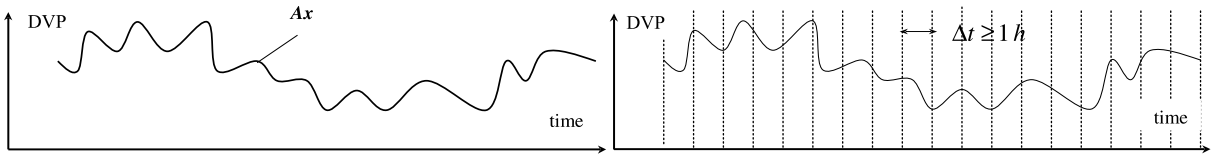

Figure 6: DVP representations being used by MPLS (left) and MGLS (right) techniques.

The MLSF technique is given as following recurrence relations (Gubanov, 2001):

$$\hat{\mathbf{x}}_{k,k+1} = \mathbf{D}_{k,k+1}\mathbf{D}^{-1}_{k-1,k}(\hat{\mathbf{x}}_{k-1,k} - \mathbf{K}_{k-1,k}\mathbf{l}_{k-1}) + \mathbf{K}_{k,k+1}\mathbf{l}_{k+1},$$
$$\mathbf{D}_{k,k+1} = (\mathbf{I} - \mathbf{K}_{k,k+1}\mathbf{A}_{k+1})(\mathbf{I} - \mathbf{K}_{k-1,k}\mathbf{A}_{k-1})^{-1}\mathbf{D}_{k-1,k},$$

where $(\mathbf{l}_k, \mathbf{A}_k, \mathbf{Q}_k)$ are data for group number $k = 0, 1, 2, \ldots$; $\mathbf{l}_k$ is the vector of $(\mathrm{O}-\mathrm{C})_k$ residuals, $\mathbf{A}_k, \mathbf{Q}_k$ are the matrices of their partials and covariances, respectively; $\hat{\mathbf{x}}_{k-1,k}$ and $\mathbf{D}_{k-1,k}$ are estimates of parameters vector and its a posteriori covariance matrix derived from combined LS-solution for two preceding groups with numbers $k-1$ and k; $\hat{\mathbf{x}}_{k,k+1}$ and $\mathbf{D}_{k,k+1}$ are similar solution for next two groups k and $k+1$ (see left side of Fig. 7). The amplification matrices are follows:

$$\mathbf{K}_{k-1,k} = \mathbf{D}_{k-1,k}\mathbf{A'}_{k-1}\mathbf{Q}^{-1}_{k-1},$$
$$\mathbf{K}_{k,k+1} = \mathbf{D}_{k-1,k}\mathbf{A'}_{k+1}(\mathbf{Q}_{k+1} + \mathbf{A}_{k+1}\mathbf{D}_{k-1,k}\mathbf{A'}_{k+1})^{-1}.$$

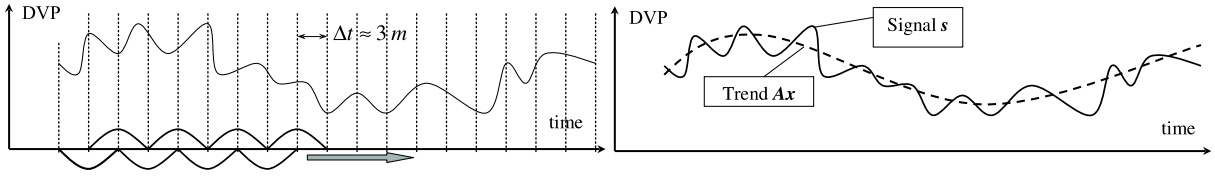

Figure 7: DVP representation being used by MLSF (left) and GLSC (right) techniques

The GLSC technique deals with DVP representation in the form DVP $= \mathbf{Ax} + \mathbf{s}$, where $\mathbf{Ax}$ is diurnal polinomial trend and $\mathbf{s}$ is correlated random component the auto-covariance of which must be a priori known (see right side of Fig. 7). Preliminary analysis of NEOS-A VLBI data (Gubanov, Surkis, Kozlova and Rusinov, 2002) shows that the normalized auto-covariance functions of wet and clock random components are very similar for all stations (see Fig. 8). Their pecularities and variances may be corrected by iteration (see Fig. 1).

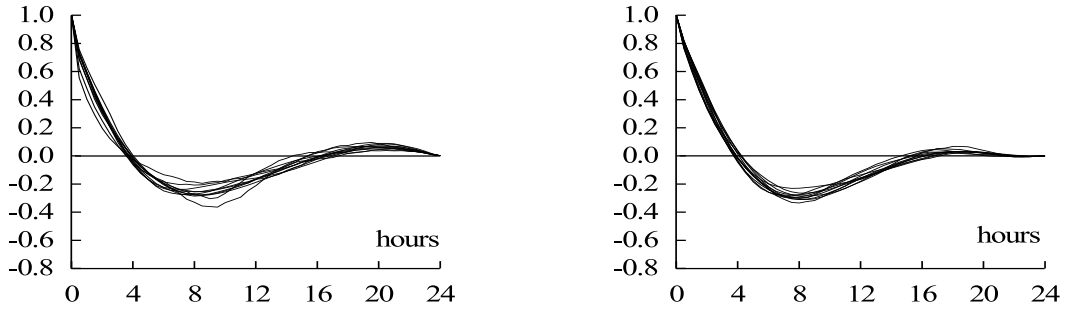

Figure 8: Normalized auto-covariance functions of wet (left) and clock (right) random componets for each NEOS-A stations after averaging by all session of observations

Being averaged for all stations these covariance functions may be modeled by expression

$$q(\tau) = \sigma^2 \sum_{n=0}^{n=2} \frac{b_n}{\cos\phi_n} e^{-\alpha_n|\tau|}\cos(\omega_n\tau + \phi_n), \quad (\omega_0 = 0, \phi_0 = 0), \tag{1}$$

where ω_n is cyclic frequency of n-th component of covariance function, $\alpha_n > 0$ – damping factor, b_n – dimensionless coefficients such as $\sum_{n=0}^{n=2} b_n = 1$, ϕ_n – phase under condition $|\phi_n| \leq |\arctan(\alpha_n/\omega_n)|$ that provide the positive definite function $q(\tau)$.

The GLSC-technique is developed in detail (Moritz, 1983; Gubanov, 1997). As far as a priori information about unknown parameters and random signals is used in this technique GLSC-estimates are the most precise and reliable then some kind of other linear estimates. Serious difficulties arising from inversion very large matrix in analysis of VLBA, Bb023 and other programs may be eliminated by sharing their sessions onto several sub-sessions.

If a priori exponential auto-covariance function or, at last, its leading segment are known then the KFMP technique may be used for analysis of Markov's process. However, GLSC-analysis of VLBI data shows that the mean values b_0 in expression (1) for wet and clock stochastic components are not exceed 0.1 so that one-dimension Markov's process is not representative for these signals. In an opposite way the KFRW tecnique have not to do with a priori covariance and, therefore, is very popular. In this technique the transition matrix is equal of unit-matrix and KFRW-solution provides non-stationary random walk identical of Brownian motion.

The TDKF technique is more acceptable from theoretical and practical points of view (Gubanov, Kozlova and Surkis, 2002). It is known that if some stationary random process $u(t)$ have continuously derivative $v(t) = du/dt$, two-dimension process $z(t) = (u(t), v(t))$ is Markov's one. In this case the discrete dynamic system perturbed by "white" noise $w(i)$ proves to be form

$$z(i+1) = \Phi(i+1, i)z(i) + w(i)$$

with the transition matrix

$$\Phi(i+1,i) = \begin{bmatrix} q_{uu}(\tau_i) & q_{uv}(\tau_i) \\ q_{vu}(\tau_i) & q_{vv}(\tau_i) \end{bmatrix} \begin{bmatrix} q_{uu}(0) & 0 \\ 0 & q_{vv}(0) \end{bmatrix}^{-1},$$

where auto-covariance function $q_{uu}(\tau)$ is defined by (1), $q_{uv}(\tau) = -q_{vu}(\tau) = dq_{uu}(\tau)/d\tau$, $q_{vv}(\tau) = -d^2 q_{uu}/d\tau^2$ and $q_{uu}(0) = \sigma^2$, $q_{vv}(0) = \sigma^2 \sum_{n=0}^{n=2} b_n(\alpha_n^2 + \omega_n^2)$.

5. STOCHASTIC REGULARIZATION

Stochastic regularization is taking into account of a priori auto-covariance of unknown random parameters in LS-solutions. Let we have the linear system $\mathbf{l} = \mathbf{A}\mathbf{x} + \mathbf{r}$ where $\mathbf{l}$ is (O – C) residuals, $\mathbf{A}$ – the matrix of partials, $\hat{\mathbf{x}}$ – the vector of corrections to reference systems such as ICRF, ITRF or EOP and $\mathbf{r}$ – the random vector of observation errors with known auto-covariance matrix $\mathbf{Q}_{rr}$. The LS-technique using principle $\mathbf{r}'\mathbf{Q}_{rr}^{-1}\mathbf{r} = min.$ leads to normal system $\mathbf{W}\hat{\mathbf{x}} = \mathbf{h}$ and its solution $\hat{\mathbf{x}} = \mathbf{W}^{-1}\mathbf{h}$. According to Fisher's theory of information (Gubanov, 1997) the matrix of normal system have to contain the total amount of information on vector $\mathbf{x}$ both *a posteriori* and *a priori* ones. In considered case the matrix $\mathbf{W} = \mathbf{D}_{xx}^{-1}$ presents only a posteriori information deribed from LS-solution. However, if the vector $\mathbf{x}$ is the centered random set or sequence and its a priori information $\mathbf{R} = \mathbf{Q}_{xx}^{-1}$ is known the more precise regularizated corrections $\hat{\mathbf{x}}_R$ may be obtained by relation

$$\hat{\mathbf{x}}_R = (\mathbf{W} + \mathbf{R})^{-1}\mathbf{h} \tag{2}$$

that should be also from Generalized Least-Squares (GLS) principle $\mathbf{r}'\mathbf{Q}_{rr}^{-1}\mathbf{r} + \mathbf{x}'\mathbf{Q}_{xx}^{-1}\mathbf{x} = min.$

The relation (2) is equivalent to the follows:

$$\hat{\mathbf{x}}_R = (\mathbf{W} + \mathbf{R})^{-1}\mathbf{W}\hat{\mathbf{x}}, \tag{3}$$

$$\hat{\mathbf{x}}_R = \mathbf{Q}_{xx}(\mathbf{Q}_{xx} + \mathbf{D}_{xx})^{-1}\hat{\mathbf{x}}. \tag{4}$$

It is easy to see that the eqs. (3) - (4) represent the generalized weighting and LSC-filtering of LS-solution $\hat{\mathbf{x}}$, respectively (Gubanov, 1997). In order to the estimates $\hat{\mathbf{x}}_R$ were found as unbiased the errors of revised referense systems $\mathbf{x}$ have to be centered random sets or sequences. To this objective the parameters of their systematic errors must be included to common ones in process of multi-series or global solution (see Fig. 1).

The regularization leads to decrease the corrections $\hat{\mathbf{x}}_R$ and their a posteriori variances. If we have precise reference systems and rough or not enough observations this effect may be very essential. On the contrary, it become negligible. In fact, the precise reference system can not be improved by using of poor observations.

6. PRELIMINARLY RESULTS OF NEOS-A DATA COLLOCATION

The results demonstrated at Figs. 9 - 10 may be considered as the proof of this that the GLSC-estimations of wet-component of troposperic path-delay are real.

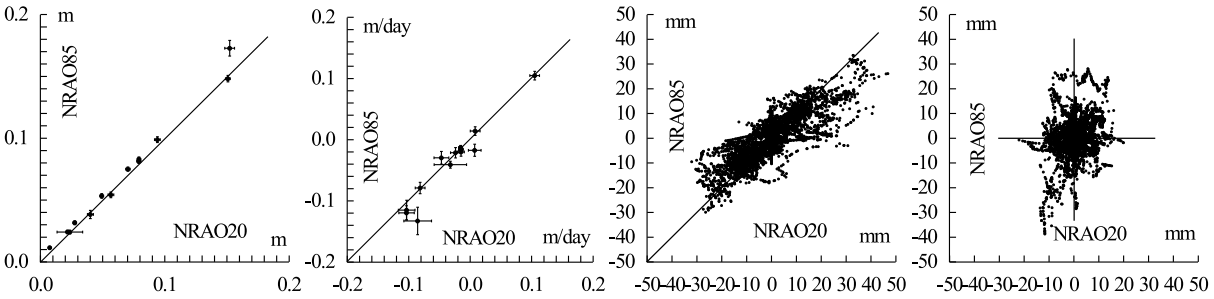

Figure 9: Regression of GLSC-estimates of diurnal wet-delay, wet-rate, wet-signals and clock-signals (from left to right) for NRAO20 and NRAO85 stations located at the same site of NRAO by GLSC-analysis of simultaneous observations

These data shows that the atmosphere over NRAO20 and NRAO85 stations is practicaly common but their clocks are different.

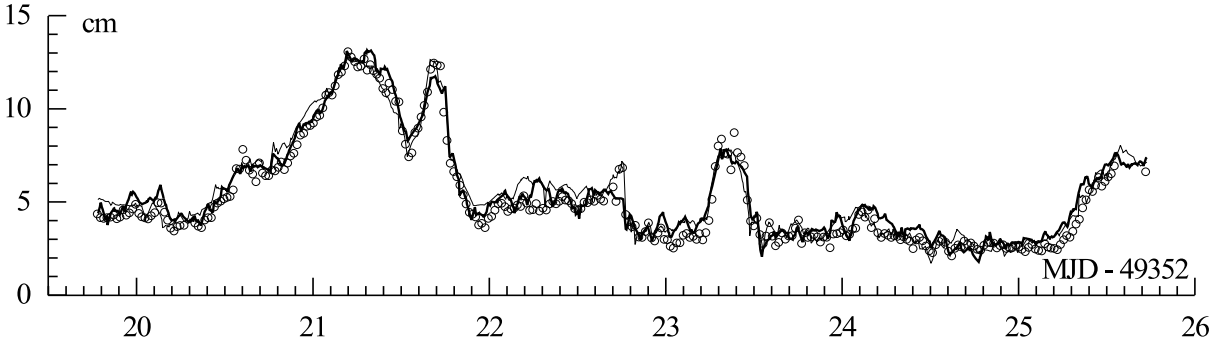

Figure 10: The Onsala total zenith wet-delays including stochastic components derived by GLSC-analysis from six last sessions of CONT94 program shared each onto two sub-sessions (thin and thick lines) in comparison with WVR-measurements (circles).

We can see from Fig. 10 that the GLSC-estimates are not only realiable as they are in agreement with independent WVR-data but also very similar for shared sub-sessions.

Further, the regularizated corrections of both the ICRF-Ext.1 catalogue and IERS(EOP)C04 time-series are demonstrated in Fig. 11. A priori uncertainties of source positions was taken from

the preface of ICRF-Ext.1 catalogue (Gambis, 1999). Analogous values for IERS(EOP)C04 are contained in any IERS Annual Report.

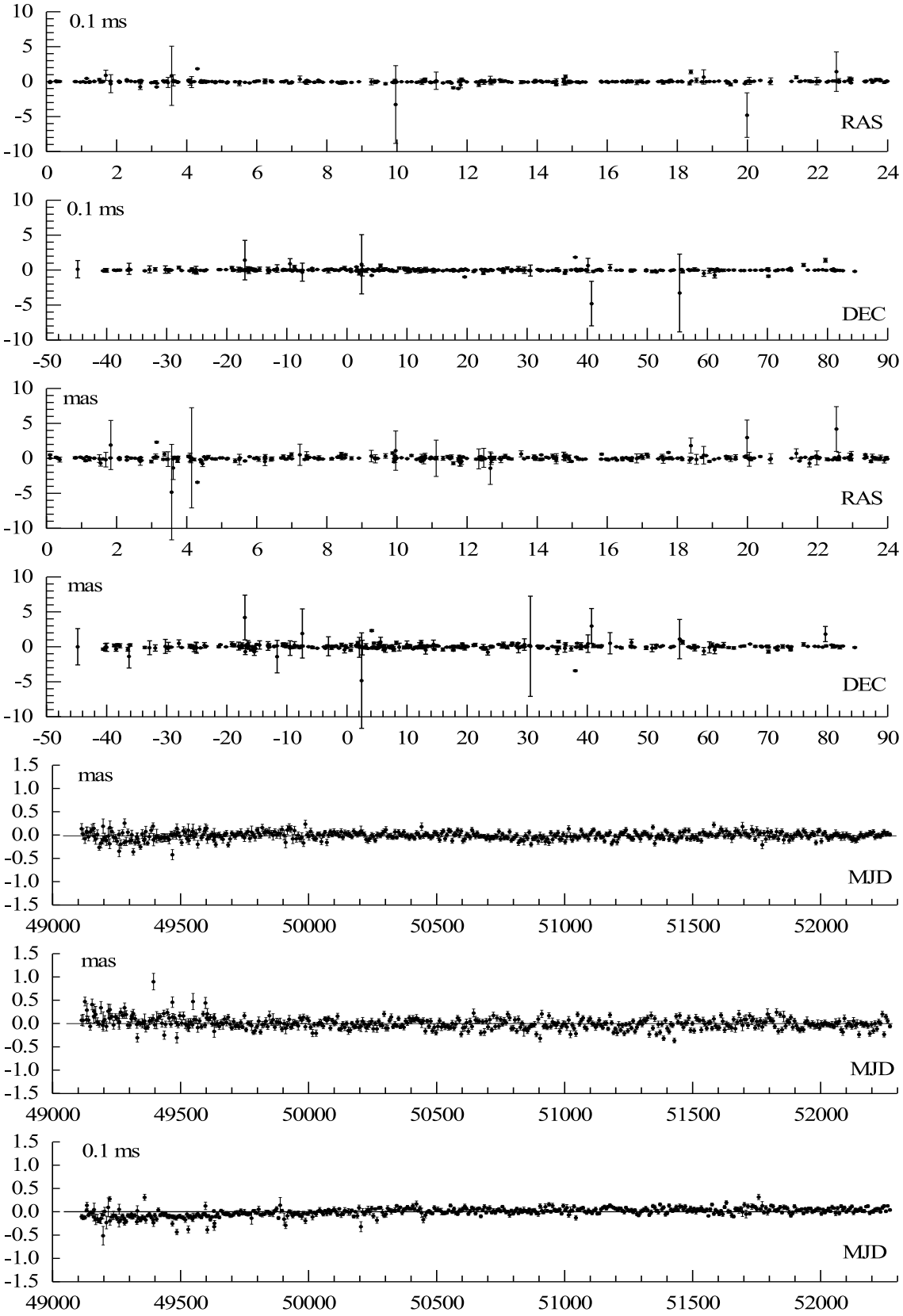

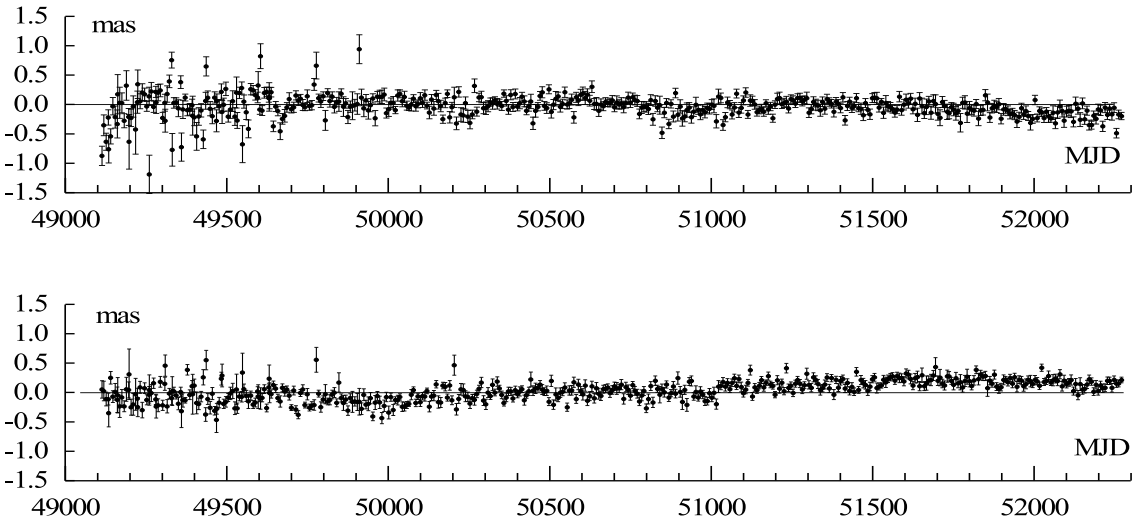

Figure 11: Corrections (up to down) of $\Delta\alpha_\alpha \cos\delta$, $\Delta\alpha_\delta \cos\delta$, $\Delta\delta_\alpha$, $\Delta\delta_\delta$, $\Delta\psi \sin\epsilon$, $\Delta\epsilon$, $\Delta(\mathrm{UT1} - \mathrm{UTC})$, Δx_P and Δy_P.

At present the software QUASAR is ready for global analysis of any amount of VLBI observations by means of GLSC-technique. In what follows the testing and tuning of alternative MLSF and TDKF techniques and introducing of new tranformation from TRS to CRS are needed.

7. REFERENCES

McCarthy D., Petit G., IERS Conventions (2003), `http:/www.iers.org/iers/ products/conv`.

Moritz H., Advanced Physical Geodesy. Moskow, Science, 1983 (in Russian translated).

Gambis D. (ed.). First extension of the ICRF, ICRF-Ext.1, 1998 IERS Annual Report, Chapter VI, 1999, Obs.de Paris, pp. 83 - 128.

Gubanov V.S., Generalized Least-Squares. Theory and Application in Astrometry. SPb, Science, 1997 (in Russian).

Gubanov V.S., Advanced Methods of Astrometrical Data Analysis. Proc. of IAA RAS, issue 6, "Astrometry and Celestial Mechanics", 2001, pp. 102–113.

Gubanov V.S. and Surkis I.F., VLBI Data Processing: Software QUASAR. I. Reduction of observations. Communications of IAA RAS, No.141, 2002, pp. 1–33 (in Russian).

Gubanov V.S., Kozlova I.A. and Surkis I.F., VLBI Data Processing: Software QUASAR. II. Data Analysis Techniques. Communications of IAA RAS, No.142, 2002, pp. 1–36 (in Russian).

Gubanov V.S., Surkis I.F., Kozlova I.A. and Rusinov Yu.L., VLBI Data Processing: Software QUASAR. V. Collocation of 1993-2001 NEOS-A VLBI Data. Communications of IAA RAS, No.145, 2002, 1–36 (in Russian).

Surkis I.F., VLBI Data Processing: Software QUASAR. III. Structure and Functioning Circuit. Communications of IAA RAS, No.143, 2002, pp. 1–65 (in Russian).

Surkis I.F., VLBI Data Processing: Software QUASAR. IV. Operation Control. Communications of IAA RAS, No.144, 2002, 1–36 (in Russian).

IERS CONVENTIONS

D.D. MCCARTHY
U. S. Naval Observatory
Washington, DcC 20392 USA
e-mail: dmc@maia.usno.navy.mil

G. PETIT
Bureau International des Poids et Mesures
Paris, France
e-mail: gpetit@bipm.org

ABSTRACT. The International Earth rotation and Reference system Service (IERS) has implemented the IAU resolutions of the 24th General Assembly in its products. The IERS Conventions now provides an outline of the procedures to be used along with software consistent with those procedures. The Conventions Product Center is provided jointly by the U.S. Naval Observatory (USNO) and the Bureau International des Poids et Mesures (BIPM), who are working on the new edition of the IERS Conventions. The new edition of the conventions has been slightly re-organized with respect to previous issues, and numerous updates have been introduced. The work accomplished or in progress is described.

1. INTRODUCTION

The realization of the International Celestial Reference System (ICRS) requires a set of conventional models and procedures to be used in the analyses of the observational data. The International Earth Rotation Service (IERS) provides these in the IERS Conventions, which contain the recommended procedures not only to define the ICRS but also to derive and interpret the other products of the IERS, such as the International Terrestrial Reference Frame, and the Earth Orientation Parameters.

The IERS Conventions is a publication that is produced by the IERS Conventions Product Center provided jointly by the U.S. Naval Observatory (USNO) and the Bureau International des Poids et Mesures (BIPM). The Product Center provides a web site http://maia.usno.navy.mil/conv2003.html containing the IERS Conventions (2003). This site is to be updated as warranted at approximately annual intervals. In addition the Center produces the material for the IERS Technical Notes that document major changes, and it is expected that this document might be provided at approximately 5-year intervals.

The IERS Conventions (2003) is a continuation of the series of documents begun with the Project MERIT Standards (Melbourne *et al*, 1983) and continued with the IERS Standards (McCarthy, 1989; McCarthy, 1992) and IERS Conventions (McCarthy, 1996). The current issue of the IERS Conventions is called the IERS Conventions (2003). When referenced in

recommendations and articles published in past years, this document may have been referred to as the IERS Conventions (2000).

The celestial system described in the IERS Conventions (2003) is based on IAU (International Astronomical Union) Resolution A4 (1991). It was further refined by IAU Resolution B1 (2000). The definition of time coordinates and time transformations, the models for light propagation and the motion of massive bodies are based on IAU Resolution A4 (1991), further defined by IAU Resolution B1 (2000). In some cases, the procedures used by the IERS, and the resulting conventional frames produced by the IERS, do not completely follow these resolutions. These cases are identified in the document, and procedures to obtain results consistent with the resolutions are shown.

2. COMPONENTS

The IERS Conventions contain descriptions of units, models, software and procedures to be used in deriving and understanding the IERS products. These products assume the use of SI units (Le Système International d'Unitès (SI), 1998) and are generally consistent with the use of Geocentric Coordinate Time TCG as the time coordinate for the geocentric system, and Barycentric Coordinate Time TCB for the barycentric system.

The Conventions describe the conventional concepts that underlie the definition of modern high-precision Celestial and Terrestrial Reference Systems. These have little relationship to the precision of the products but they are likely to affect the accuracy as well as the users interpretation.

Models are provided to describe various physical phenomena. These generally affect precision but might have only a minimal affect on the accuracy. Included also are constants, the numerical values of parameters of common interest. Perhaps the most important is the software that provides practical numerical implementation of the concepts and models.

Finally, the Conventions publication outlines procedures to implement all of the above. The IERS Conventions (2003) does not go so far as to describe standard procedures for data analyses, such as details regarding solution constraints and appropriate spans of data, but future versions may get to that point. These choices affect precision but have little effect on accuracy.

3. CONCEPTS

TBD

4. CONTENTS

The Contents of the document are outlined by the Table of Contents:

The actual contents of the IERS Conventions (2003) available at http://maia.usno.navy.mil/conv2003.html are presented below in outline form.

Chapter 10 - General Relativistic Models for Time, Coordinates and Equations of Motion

Fairhead-Bretagnon Model - Computes the periodic terms of TT. Provided by A. Irwin.

Xhf2002.f routine - Computes TCB-TCG as a function of TT. Provided by W. Harada and T. Fukushima.

HF2002.dat - Parameter file read by Xhf2002.f. Provided by W. Harada and T. Fukushima.

xhf2002.out - Output file of the test driver. Provided by W. Harada and T. Fukushima.

Chapter 11 - General Relativistic Models for Propagation

Appendix - Resolutions from the 24th IAU General Assembly

Glossary - List of acronyms used in the Conventions

In comparison with previous versions the latest version has undergone significant changes. These are outlined below by chapter. The principal contributors are also listed for each chapter.

Chapter 1-General Definitions and Numerical Standards

The chapter has been updated for consistency of notation and concepts with other sections according to IAG (International Association of Geodesy) and IAU working groups. It provides general definitions for topics in other chapters and also the values of numerical standards that are used in the document. It incorporates the previous Chapter 4, which was updated to provide consistent notation and to comply with the recommendations of the most recent reports of the appropriate working groups of the International Association of Geodesy (IAG) and the IAU. It was prepared principally by D. McCarthy and G. Petit with major contributions from M. Burra, N. Capitaine, T. Fukushima, E. Groten, P. M. Mathews, P. K. Seidelmann, E. M. Standish, and P. Wolf.

Chapter 2-Conventional Celestial Reference System and Frame

The chapter, which appeared as Chapter 1 in previous editions has been updated to incorporate the effects of the IAU 2000 24th General Assembly by E. F. Arias with contributions from J. Kovalevsky, C. Ma, F. Mignard, and A. Steppe.

Chapter 3-Conventional Dynamical Reference Frame

Chapter 3 (previously Chapter 2), has been updated to be consistent with notation and concepts of other sections. The conventional solar system ephemeris has been changed to the Jet Propulsion Laboratory (JPL) DE405. It was prepared by E. M. Standish with contributions from F. Mignard and P. Willis.

Chapter 4-Conventional Terrestrial Reference System

Chapter 4 (previously Chapter 3) was rewritten by Z. Altamimi,, C. Boucher, and P. Sillard with contributions from J. Kouba, G. Petit, and J. Ray. It incorporates the new Terrestrial Reference Frame of the IERS (ITRF2000), which was introduced in 2001.

Chapter 5-Transformation Between the Celestial and Terrestrial Systems

The chapter was modified to be consistent with resolutions adopted at the 24th IAU General Assembly and the 2002 IERS Workshop. It was updated principally by N. Capitaine, with major contributions from P. M. Mathews and P. Wallace to comply with the recommendations of the IAU 2000 24th General Assembly. Significant contributions from P. Bretagnon, R. Gross, T. Herring, G. Kaplan, D. McCarthy, Burghard Richter and P. Simon were also incorporated.

Chapter 6-Geopotential

Chapter 6 was updated to include the EGM96 conventional geopotential model and the treatment of tides. V. Dehant, P. M. Mathews, and E. Pavlis were responsible for the revision. Major contributions were also made by P. Defraigne, S. Desai, F. Lemoine, R. Noomen, R. Ray, F. Roosbeek, and H. Schuh.

Chapter 7-Site Displacement

This chapter was updated to be consistent with the geopotential model recommended in Chapter 6. It was prepared principally by V. Dehant, P. M. Mathews, and H.-G. Scherneck. Major contributions were also made by Z. Altamimi, S. Desai, S. Dickman, R. Haas, R. Langley, R. Ray, M. Rothacher, H. Schuh, and T. VanDam. A model for post-glacial rebound is no longer recommended and a new ocean-loading model is suggested. The VLBI antenna deformation has been enhanced.

Chapter 8-Tidal Variations in the Earths Rotation

Changes were made to be consistent with the nutation model adopted at the 24th IAU General Assembly. The model of the diurnal/semidiurnal variations has been enhanced to include more tidal constituents. The principal authors of Chapter 8 were Ch. Bizouard, R. Eanes, and R. Ray. P. Brosche, P. Defraigne, S. Dickman, D. Gambis, and R. Gross also made significant contributions.

Chapter 9-Tropospheric Model

This chapter has been changed to recommend an updated model. It is based on the work of C. Ma, E. Pavlis, M. Rothacher, and O. Sovers, with contributions from C. Jacobs, R. Langley, V. Mendes, A. Niell, T. Otsubo, and A. Steppe.

Chapter 10-General Relativistic Models for Time, Coordinates and Equations of Motion

The chapter has been updated for consistency of notation and concepts with other sections. New software for the TCB-TCG transformation, developed by Harada and Fukushima, has been checked against existing programs and added to the list of such standards. Previously appearing as Chapter 11, it has been updated to be in compliance with the IAU resolutions and the notation they imply. It was prepared principally by T. Fukushima and G. Petit with major contributions from P. Bretagnon, A. Irwin, G. Kaplan, S. Klioner, T. Otsubo, J. Ries, M. Soffel, and P. Wolf.

Chapter 11-General Relativistic Models for Propagation

This chapter (previously Chapter 12), has been updated for consistency of notation and concepts with other sections. It was updated to comply with the IAU resolutions and the notation they imply. It is based on the work of T. M. Eubanks and J. Ries. Significant contributions from S. Kopeikin, G. Petit, L. Petrov, A. Steppe, O. Sovers, and P. Wolf were incorporated.

5. FUTURE

At the BIPM, in collaboration with the IERS Analysis Coordinator and different Product and Analysis centers.

Visiting scientist position + other collaborations possible.

Contributions to determine the most important directions to improve the consistency of IERS combined solutions and how to implement new conventional models/ procedures.

Important topics are, e.g., geocenter motion, impact of using "global" vs. "local" loading models, network effects in the solutions of different techniques...

6. CONCLUSION

The IERS Conventions are the product of the IERS Conventions Product Center. However, this work would not be possible without the contributions acknowledged above. In addition, we would also like to acknowledge the comments and contributions of S. Allen, Y. Bar-Sever, A. Brzeziński, M. S. Carter, P. Cook, H. Fliegel, M. Folgueira, J. Gipson, S. Howard, T. Johnson, M. King, S. Kudryavtsev, Z. Malkin, S. Pagiatakis, S. Pogorelc, J. Ray, S. Riepl, C. Ron, and T. Springer in the compilation of the work.

7. REFERENCES

Le Système International d'Unités (SI), 1998, Bureau International des Poids et Mesures, Sèvres, France.

McCarthy, D. D. (ed.), 1989, *IERS Standards*, IERS Technical Note 3, Observatoire de Paris, Paris.

McCarthy, D. D. (ed.), 1992, *IERS Standards*, IERS Technical Note 13, Observatoire de Paris, Paris.

McCarthy, D. D. (ed.), 1996, *IERS Conventions*, IERS Technical Note 21, Observatoire de Paris, Paris.

Melbourne, W., Anderle, R., Feissel, M., King, R., McCarthy, D., Smith, D., Tapley, B., Vicente, R., 1983, Project MERIT Standards, *U.S. Naval Observatory Circular No. 167.*

MICROARCSECOND MODELS FOR THE CELESTIAL MOTIONS OF THE CELESTIAL INTERMEDIATE POLE (CIP) AND THE CELESTIAL EPHEMERIS (OR INTERMEDIATE) ORIGIN (CEO/CIO)

N. CAPITAINE
SYRTE/UMR8630-CNRS
Observatoire de Paris, 61 avenue de l'Observatoire, 75014, Paris, France
e-mail: capitain@syrte.obspm.fr

ABSTRACT. The Celestial intermediate pole (CIP) and Celestial ephemeris (or intermediate) origin (CEO/CIO) have been adopted by the IAU (c.f. IAU 2000 Resolution B1.8) as the celestial pole and origin, respectively, to be used for realizing the intermediate celestial system between the International Terrestrial System (ITRS) and Geocentric Celestial Reference System (GCRS). Resolution B1.8 has also recommended that the International Earth Rotation and Reference Systems Service (IERS) continue to provide users with data and algorithms for the conventional transformation. The IAU 2000 Resolutions have been implemented in the IERS 2003 Conventions including Tables and routines that provide the celestial motions of the CIP and the CEO with a theoretical accuracy of one microarcsecond after one century using either the classical or the new transformation. This paper reports on the method used for acheiving this accuracy in the positions of the CIP and CIO and on the difference between this rigorous procedure and the pre-2003 classical one.

1. INTRODUCTION

Resolution B1.8 adopted by the IAU in August 2000 has recommended that the transformation between the International Terrestrial System (ITRS) and Geocentric Celestial System (GCRS) be specified by the position of the Celestial Intermediate Pole (CIP) in the GCRS, the position of the CIP in the ITRS and the "Earth Rotation Angle" (ERA). This resolution has also recommended that UT1 be linearly proportional to the ERA, defined as the angle measured along the equator of the CIP between the Celestial Ephemeris Origin (CEO) and the Terrestrial Ephemeris Origin (TEO) through a conventional relationship. This resolution was implemented by the International Earth Rotation and Reference Systems Service (IERS) beginning on 1 January 2003, together with Resolution B1.6 adopting the IAU 2000A precession-nutation model for the position of the CIP in the GCRS and Resolution B1.7 for the definition of the CIP. As required in Resolution B1.6, the IERS is continuing to provide users with data and algorithms for the conventional transformation.

Expressions for the position of the Celestial intermediate pole (CIP) and the Celestial ephemeris origin (CEO) (also called Celestial intermediate origin, CIO) which have been provided in the IERS Conventions 2003 are achieving a theoretical accuracy of 1 microarcsecond after one century. Such an accuracy can be achieved using either the new transformation, or

the classical transformation if this latter follows the rigorous way for taking into account the frame biases, which was not the case for the pre-2003 classical procedure. More details on the procedures and models on which these expressions are based are provided in Capitaine et al. (2003a, 2003b, 2003c).

After having recalled (in Section 2) the definition and use of the CIP and CEO/CIO, we report (Sections 3 and 4) on the accuracy of the models for their celestial motions and compare this accuracy with that obtained when using the pre-2003 classical procedure.

2. DEFINITION AND USE OF THE CIP AND CEO/CIO

The Celestial Intermediate Pole (CIP) has been defined by IAU 2000 Resolution B1.7 as the intermediate pole separating nutation from polar motion explicitly at the 2-day period (i.e. nutations with periods less than 2 days being modeled by their equivalent polar motion). This resolution has recommended that the motion of the CIP in the GCRS be realized "by the IAU 2000A model (Mathews et al. 2002) for precession and forced nutation for periods greater than two days plus additional time-dependent corrections provided by the IERS through appropriate astro-geodetic observations" (*i.e.* through VLBI observations).

The CEO and TEO are the names used in Resolution B1.8 for designating the "non-rotating origin" (Guinot 1979, Capitaine et al. 1986) in the GCRS and ITRS, respectively. In recent IAU discussions they have also been called Celestial and Terrestrial "intermediate" origins, CIO and TIO, for emphazing that they provide together with the CIP the "intermediate" systems (celestial and terrestrial, respectively) between the GCRS and ITRS.

In the new paradigm, the GCRS position of the CIP is provided by the quantities $X(t)$ and $Y(t)$ which are the components of the CIP unit vector in the GCRS (Capitaine 1990). These quantities have been derived from (i) the expressions for the precession-nutation angles referred to the J2000 mean ecliptic, (ii) the corresponding biases (ξ_0, η_0) at J2000, and (iii) the equinox offset at J2000 $d\alpha_0$ (see Figure 1). X and Y are usually called "coordinates" and their numerical expressions are multiplied by the factor $1296000''/2\pi$ in order to provide in arcseconds the value of the corresponding "angles" (strictly their sines) with respect to the z-axis of the GCRS. The classical form of the GCRS to ITRS transformation is written, following a rigorous procedure, as the product of the individual rotation matrices **B** (bias) followed by **P** (precession) then **N** (nutation) and finally **T** (Earth rotation). Elements $(3,1)$ and $(3,2)$ of the resulting matrix $\mathbf{R}_{class}$ provides the classical expression for the GCRS position of the CIP.

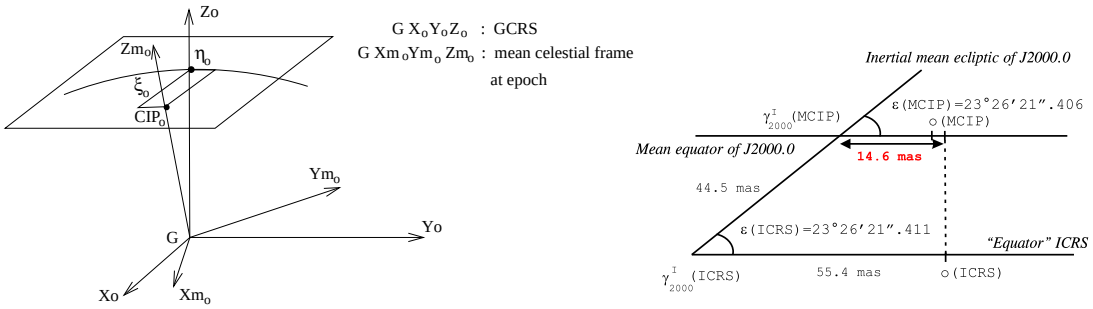

Figure 1: Frame biases between the mean equatorial system at J2000 and the Geocentric celestial reference system (GCRS); celestial pole offsets (left) and equinox offset (right)

Prior to the IAU 2000 definition, UT1 was formally defined by an expression which relates it to mean sidereal time, whereas the new defining relation of UT1 is the IAU 2000 conventional relationship between ERA and UT1. The implementation of this new definition requires using an expression for positioning the CIO in space.

The celestial position of the CIO is provided through a quantity s for the finite displacement of the CIO between epochs t_0 and t with respect to the GCRS x-origin (Capitaine et al. 1986). This computation implements the basic kinematical property of the non-rotating origin when the CIP pole is moving in the GCRS. Other implementations of the kinematical property of the CIO are possible either analytically or numerically (Kaplan 2003, Fukushima 2003b) and the position of the CIO can be referred to other references than the GCRS x-origin, such as the true equinox or the intersection of the CIP meridian or the GCRS zero-meridian with the intermediate equator. The difference GST-ERA for example is the right ascension of the CIO measured from the equinox along the moving equator. It represents the angular distance between the CIO and the equinox which is due to the accumulated precession and nutation in right ascension from J2000 to the epoch t (Aoki &Kinoshita 1983, Capitaine & Gontier 1993).

The IERS has implemented IAU Resolutions in parallel for the CEO/CIO-based transformation and the equinox-based transformation in order (i) to ensure consistency to microarcsecond accuracy between these two procedures and (ii) to ensure continuity on 1st January 2003 between the pre-2003 classical and the post-2003 procedures.

3. MICROARCSECOND MODELS FOR THE CELESTIAL MOTION OF THE CIP

Computation of the IAU 2000 expression for the CIP X, Y coordinates in the GCRS is based either directly on their semi-analytical expression as function of time, or on the elements of the classical rigorous expression of the bias-precession-nutation matrix, $\mathbf{R}_{class}$, both being based on the IAU 2000A precession-nutation (Capitaine et al. 2003a).

The IAU 2000A nutation series, based on the rigid Earth nutation of Souchay et al. (1999) and on the MHB transfer function (Mathews et al. 2002), includes 678 lunisolar terms and 687 planetary terms and provides the direction of the celestial pole in the GCRS with an observed accuracy of 0.2 mas. The Free Core Nutation (FCN), which cannot be predicted rigorously, is not included in the IAU 2000A model, the resulting"noise level" in the derived "celestial pole offsets" being of a fraction of 1 mas. The precession component of the IAU 2000 model is provided by corrections to the IAU 1976 precession of -0.29965"/c in longitude and -0.02524"/c in obliquity and is associated with VLBI estimates for celestial pole offsets at J2000 of $\delta\psi_0 = -41.775$ mas and $\delta\epsilon_0 = -6.8192$ mas. The equinox offset at epoch, $d\alpha_0$ between the x-origin of the GCRS and the mean equinox at J2000, that was omitted in the pre-2003 classical transformation, has also to be considered. The IAU 2000 implementation has used the equinox offset derived from lunar laser ranging observations referred to IERS parameters for Earth's orientation in the GCRS (Chapront et al. 2002).

It should be noted that the pre-2003 VLBI procedures used the IAU 1976 precession and the "total" nutations (*i.e.* the nutations themselves including estimated corrections to the model, plus the contribution of the corrections to the precession rates plus the biases) and omitted the equinox offset. Thus, whereas, there is equivalence to microarcsecond accuracy between the two post-2003 rigorous procedures, there are discrepancies of a few hundred microarcseconds/cy between classical equinox-based pre-2003 procedure and the post-2003 rigorous procedures (Capitaine et al. 2003a). Effects of the VLBI procedure in the estimated X, Y CIP coordinates are shown in Figure 2, regarding the way the precession is considered and the fact that the equinox offset was omitted in the pre-2003 procedure. The differences in X, Y due to the frame biases are: $dX = 153t - 5t^2$; $dY = -372t - 1.7t^2$ and $dX = -1.6t^2$; $dY = -142t$, for the celestial pole offsets and equinox offset at J2000, respectively; the differences due to the way the correction to the precession rates are applied are: $dX = +64t^2$; $dY = -6t^2$.

This shows that besides the improvement in the model for the GCRS position of the CIP due to the use of the IAU 2000A precession-nutation in replacement of the IAU 1976/1980 which has reduced the inaccuracies from a few tens of mas to a few hundred μas, an other improvement

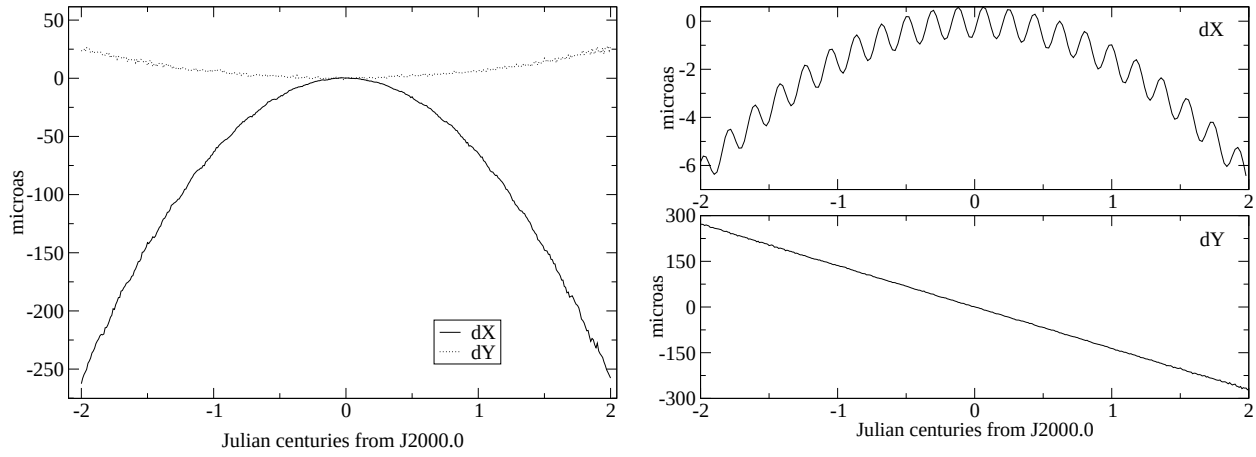

Figure 2: Differences in X and Y between the pre-2003 and post-2003 VLBI procedures (Capitaine et al. 2003a); differences due to precession (left), and to the equinox offset (right)

in the post-2003 expressions comes from the use of a rigorous procedure for taking into account the precession corrections and frame bias that in fact results from the use of the new paradigm as being the "primary" procedure.

Other methods can be used for expressing the GCRS position of the CIP based on different parameters such as the new precession-nutation parameters introduced by Fukushima (2003a), extending those previously considered by Williams (1994) by taking into account the frame biases or the "rotation vector approach", described in Capitaine et al (2003c), that is able to express bias plus precession and nutation.

Note moreover that the IAU 2000 precession which includes only the MHB corrections to the precession rates in longitude and obliquity should be replaced by an improved model which would be dynamically consistent. New precession models have recently been developed that are compatible with IAU 2000 with improved dynamical consistency. The model by Bretagnon et al. (2003) is based on the analytical VSOP87 ecliptic (Bretagnon & Francou 1988), on the SMART97 nutation theory for a rigid Earth (Bretagnon et. al 1998) and on the MHB precession rate in longitude; the model by Fukushima (2003a) is based on an ecliptic fitted to the JPL numerical ephemerides DE405 on a 600-yr interval, on the SF01 nutation theory for a non-rigid Earth (Shirai & Fukushima 2001) and on a quadratic fit to VLBI; the model by Capitaine et al. (2003c) is based on the VSOP87 ecliptic with improved secular terms fitted to DE406 over a 2000-yr interval and on a non-rigid Earth model from Willams (1994) and Mathews et al. (2002); the integration constants have been derived from the MHB estimates with corrections for perturbing effects on the observed quantities. The largest uncertainty in the effects of non-rigidity on precession is the uncertainty in the J2 rate effect (cf. Bourda & Capitaine 2004 and this Volume).

The IAU Working Group on "Precession and the ecliptic", which has been established at the 2003 IAU General Assembly, is in charge of selecting the next precession model to be recommended to the IAU.

4. MICROARCSECOND MODELS FOR THE CELESTIAL MOTION OF THE CEO/CIO

The implementation of the IAU 2000 definition of UT1 has been based on computation of expressions for the celestial positions of the CIO to be used in the transformation between

ITRS and GCRS, once the relationship ERA(UT1) is adopted. This is an important change as compared with the previous procedure in which the GST(UT1) relationship was the primary definition of UT1. A second change is that this new definition has been implemented consistently in the new transformation referred to the CIO and in the classical transformation referred to the equinox.

The determination of the IAU 2000 numerical expressions, linking GST and ERA and locating the CEO, have been performed so that there is no discontinuity in UT1 on 1 January 2003 when changing from the current VLBI procedure to the new one, following the two equivalent options, and in each case compliant with the IAU 2000 precession-nutation (Capitaine et al. 2003b). The CIO-based option uses the quantity providing the GCRS position of the CIO and the equinox-based option uses the equation of the equinoxes providing the position of the equinox w.r.t. the CIO. The polynomial part of $GST_{IAU2000}$ provides the IAU 2000 expression for Greenwich Mean Sidereal Time, GMST, whereas the periodic part provides the complete equation of the equinoxes of which the non-classical part (also called the "complementary terms") replaces the two complementary terms of the IAU 1994 equation of the equinoxes provided in the IERS Conventions 1996 (McCarthy 1996). For practical reasons, the numerical development used for positioning the CIO on the equator of the CIP is for $s + XY/2$ rather than s itself: firstly the former requires fewer terms to reach a given accuracy (Capitaine 1990) and, secondly, there is a helpful similarity between the quantity $s + XY/2$, which equals, up to the 3rd order in X and Y, the GCRS right ascension of the CEO, and the complementary terms in the "complete equation of the equinoxes", which represent the right ascension of the CEO in the mean equatorial frame at J2000.

The differences in the computed UT1 between the post-2003 and pre-2003 procedures due to (i) the frame bias effect already considered in Section 3 regarding its effect in X and Y and (ii) the differences in the expression for the equation of equinoxes (*i.e.* additional periodic terms in the post-2003 expression for the angular distance between the CIO and the equinox) are shown on Figure 3.

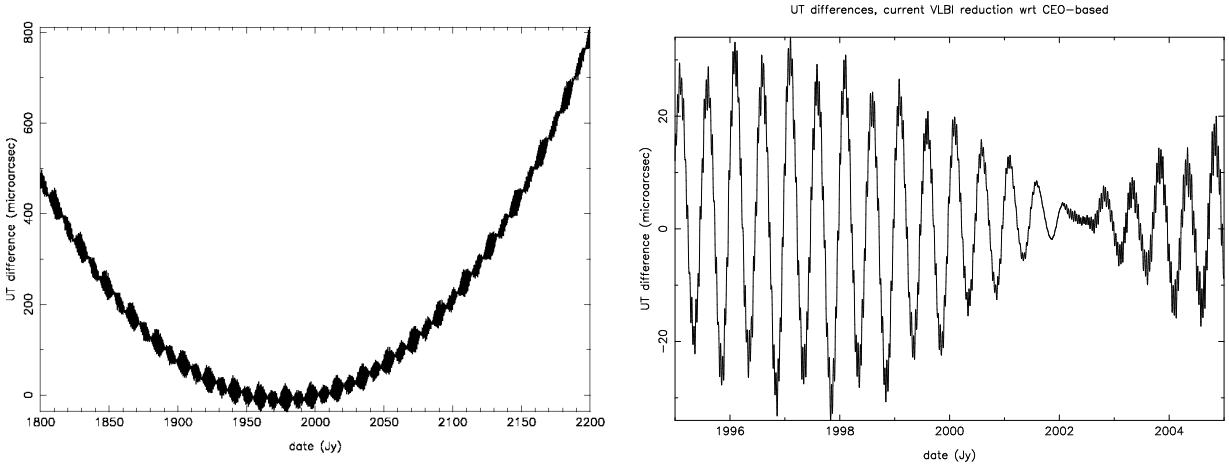

Figure 3: Differences between values of UT1 derived from the pre-2003 and post-2003 VLBI codes (Capitaine et al. 2003b); differences over 4 centuries (left) and five years (right) around J2000

The expected discontinuity in UT1 rate, shown to be unavoidable due to the improved models and the fixed relationship between ERA and UT1, will have an effect on the determination of UT1 less than a few hundreds of microarcseconds over the next century; the corresponding rate variations may reach 5×10^{-15}.

5. REFERENCES

Aoki, S. and Kinoshita, H. 1983, "Note on the relation between the equinox and Guinot's non-rotating origin", *Celest. Mech.***29**, 335.

Bourda G., Capitaine N., 2003, "Temporal variations of the gravity field and Earth's precession", in preparation.

Bretagnon, P. and Francou, G., 1988, "Planetary theories in rectangular and spherical variables VSOP87 solutions," *Astron. Astrophys.***202**, 309.

Bretagnon, P., Francou, G., Rocher, P., and Simon, J.-L., 1998, "SMART97: a new solution for the rotation of the rigid Earth,"*Astron. Astrophys.***329**, 329.

Bretagnon P., Fienga A., Simon J.-L., 2003, "Expressions for precession consistent with the IAU 2000A model. Considerations about the ecliptic and the EOP," *Astron. Astrophys.***400**, 785.

Capitaine, N. and Gontier A.-M., 1993, "Accurate procedure for deriving UT1 at a submilliarc-second accuracy from Greenwich Sidereal Time or from stellar angle," pp. 645–650. *Astron. Astrophys.***275**, 645.

Capitaine, N., Guinot, B., and Souchay, J., 1986, "A Non-rotating Origin on the Instantaneous Equator: Definition, Properties and Use," *Celest. Mech. Dyn. Astr.***39**, 283.

Capitaine N., Chapront J., Lambert S., Wallace P.T, 2003a, Expressions for the CIP and CEO consistent with the IAU 2000A precession-nutation model, *Astron. Astrophys.***400**, 1145.

Capitaine N., Wallace P.T, McCarthy D.D., 2003b, Expressions to implement the IAU 2000 definition of UT1, *Astron. Astrophys.***406**, 1135.

Capitaine N., Wallace P.T, Chapront J., 2003c, Expressions for IAU 2000 precession quantities, *Astron. Astrophys.***412**, 567.

Chapront, J., Chapront-Touzé M., and Francou, G., 2002, 'A new determination of lunar orbital parameters, precession constant and tidal acceleration from LLR measurements," *Astron. Astrophys.***387**, 700.

Fukushima T., 2003a, A new precession formula, *Astron. J.***126**, 494.

Fukushima T., 2003b, "New formulae of relations between GAST, UT1 and ERA" submitted to *Astron. J.*.

Guinot, B., 1979, "Basic Problems in the Kinematics of the Rotation of the Earth," in *Time and the Earth's Rotation*, D. D. McCarthy and J. D. Pilkington (eds), D. Reidel Publishing Company, pp. 7–18.

IERS Conventions (2003), IERS Technical Note 31, D.D. McCarthy and G. Petit (eds).

Kaplan G., 2003, "Another look at Non-rotating Origins," to appear in the Proceedings of Joint Discussion 16, IAU 2003 GA.

Mathews, P. M., Herring, T. A., and Buffett B. A., 2002, "Modeling of nutation-precession: New nutation series for nonrigid Earth, and insights into the Earth's Interior," *J. Geophys. Res.***107**, B4, 10.1029/2001JB000390.

McCarthy D.D.(ed.), 1996 "IERS Conventions (1996)", IERS Technical Note 21, Observatoire de Paris.

Shirai, T., Fukushima, T., 2001,"Construction of a new forced nutation theory of the nonrigid Earth," *Astron. J.***121**, 3270.

Williams, J. G., 1994, "Contributions to the Earth's obliquity rate, precession, and nutation," *Astron. J.***108**, 711.

COMPARISON OF VLBI NUTATION SERIES WITH THE IAU2000A MODEL

Z. MALKIN
Institute of Applied Astronomy
nab. Kutuzova 10, St.Petersburg 191187, Russia
e-mail: malkin@quasar.ipa.nw.ru

ABSTRACT. Three most long and dense VLBI nutation series obtained at the Goddard Space Flight Center, Institute of Applied Astronomy, and U. S.Naval Observatory, containing about 3000 estimates of the nutation angles were used for investigation of systematic differences between observations and IAU2000A model. Bias and secular trends (precession and obliquity rate) were estimated together with main periodical terms for three periods of observations. It is shown that result substantially depends on period of observations used in analysis. Corrections to some IAU2000A nutation terms were also estimated and found to be at the level up to several tens microarcseconds. A new Free Core Nutation model with variable amplitude and period (phase) is developed. Comparison of this model with observations shows better agreement than existing one.

1. INTRODUCTION

New precession-nutation model IAU2000A (MHB2000, Mathews et al., 2002) is officially implemented in the astronomical practice starting from Jan 1, 2003. This model is intended to provide the accuracy at the level of 0.2 mas. Several modern VLBI EOP series provided by the International VLBI Service for Geodesy and Astrometry (IVS) allow us to estimate a disagreement of the IAU2000A model with observations. Those VLBI series are listed in Table 1.

Table 1: Available VLBI nutation series (01 Aug 2003).

Series	Software	Period	Number of points	Number of accepted points
GSF2003C	Calc/Solve	1979–2003	3424	3295
IAAN0307	OCCAM	1979–2003	3233	3091
USN2003A	Calc/Solve	1979–2003	3013	2921
CGS2002A	Calc/Solve	1979–2001	2708	2639
BKG00005	Calc/Solve	1984–2003	2645	2636
AUS00002	OCCAM	1983–2003	1229	1224
SPU0002M	OCCAM	1994–2003	542	532

Three most long, dense and independent nutation series GSF, IAA and USN were selected for detailed analysis. Since only the IAA nutation series provides estimation of celestial pole offset w.r.t. the IAU2000A model, GSF and USN series, containing estimation of celestial pole offset w.r.t. the IAU1976/1980 model, were transformed to the IAU2000A system.

Main results were obtained with averaged series GSF+IAA+USN hereafter referred to as mean series. These four series were compared with the IAU2000A model. The differences between observed nutation series and the model are shown in Figure 1, and spectrum of the differences is presented in Figure 2.

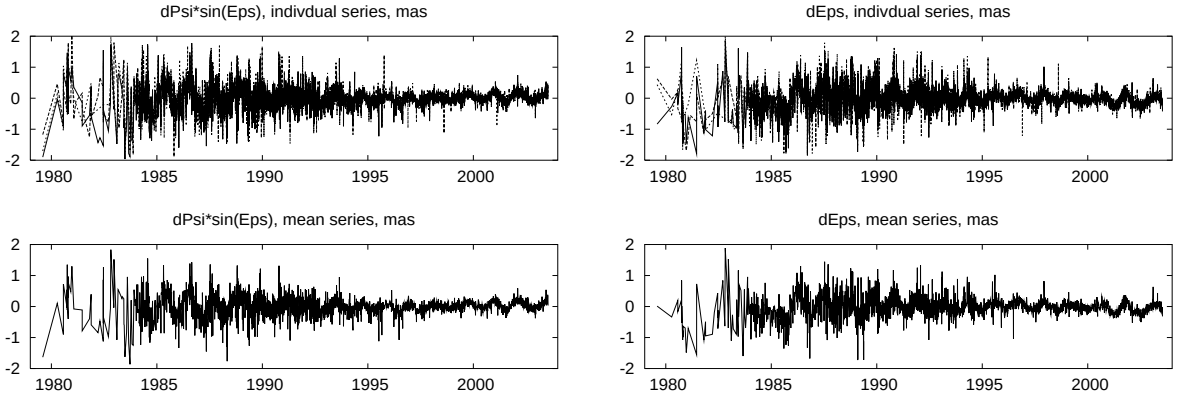

Figure 1: Differences between observed nutation series and the IAU2000A model.

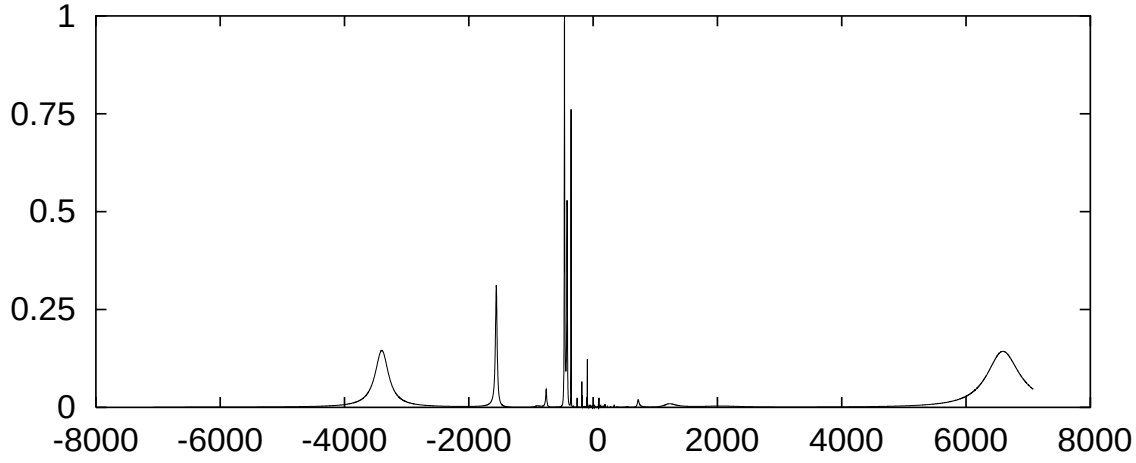

Figure 2: Spectrum of the differences between observed nutation series and the IAU2000A model.

The present investigation of the discrepancies between observations and the model was focused on the following topics.

1. Bias and trend.
2. Corrections to IAU2000A nutation terms.
3. Free Core Nutation (FCN) contribution.

This paper presents some results of this study.

2. BIAS AND RATES

Bias in celestial pole offset, precession constant and obliquity rate were estimated as linear trend along with largest long-period terms 6798.38^d, 3399.19^d, 365.26^d, 182.62^d, 121.75^d. It is well known that the accuracy of the VLBI results had two significant improvement at the epochs *approx*1984.0 and *approx*1990.0 (see e.g. Malkin, 2002). So, bias and rate was estimated for three intervals 1979–2003, 1984–2003 and 1990.0–2003 (in the latter case the term with period 6798.38^d was not included in the adjustment procedure).

The results of computation are presented in Table 2 For more detailed comparison we compute those both for individual and mean series.

Table 2: Bias in $\Delta\psi$ and $\Delta\epsilon$, μas.

Series	1979–2003		1984–2003		1990–2003	
	$\Delta\psi$	$\Delta\epsilon$	$\Delta\psi$	$\Delta\epsilon$	$\Delta\psi$	$\Delta\epsilon$
GSF	-76	$+10$	-84	$+5$	-30	-56
	±23	±9	±23	±9	±9	±4
IAA	$+46$	$+30$	$+38$	$+26$	$+71$	-31
	±23	±9	±24	±9	±10	±4
USN	-65	$+44$	-73	$+39$	$+1$	-30
	±24	±9	±25	±10	±9	±4
Mean	-29	$+30$	-37	$+25$	$+13$	-38
	±22	±8	±22	±8	±9	±4

Table 3: Rate in $\Delta\psi$ and $\Delta\epsilon$, μas/yr.

Series	1979–2003		1984–2003		1990–2003	
	$\Delta\psi$	$\Delta\epsilon$	$\Delta\psi$	$\Delta\epsilon$	$\Delta\psi$	$\Delta\epsilon$
GSF	-7	$+8$	-9	$+7$	$+15$	-8
	±5	±2	±5	±2	±2	±1
IAA	-2	$+5$	-4	$+4$	$+17$	-5
	±5	±2	±5	±2	±2	±1
USN	-14	$+10$	-16	$+9$	$+14$	-9
	±5	±2	±5	±2	±2	±1
Mean	-7	$+8$	-9	$+7$	$+15$	-8
	±4	±2	±5	±2	±2	±1

One can see that there is no evident systematic differences between OCCAM (IAA) and CALC/SOLVE (GSF, USN) results for precession constant and obliquity rate, however such a difference obviously exists for the bias, especially in $\Delta\psi$.

It's remarkable that the results presented here differ substantially, at the level of several tens microarcseconds, from those presented in the previous study (Malkin, 2002). It should be mentioned that both results were obtained using the same software and strategy, and only difference is in VLBI data used in the analysis. Direct comparison of the VLBI series used in previous and present analysis show that the difference (bias) between them also may be as large as several tens microarcseconds. Taking into account well known dependence of VLBI EOP results on station network, CRF realization, software, and other factors (MacMillan and Ma., 2000; Sokolskaya and Skurikhina, 2000), we can conclude that it is hardly possible to obtain the biases and rates with an accuracy better that 10–20 μas and 5–10 μas/yr from the current set of observations.

3. PERIODICAL TERMS

An estimation of the amplitude of the IAU2000A nutation terms have been obtained by Least Squares. The results are shown in Table 4, which includes the same set of harmonics as investigated in (Herring et al., 2002). The estimation was made both for original data and after removing the FCN contribution computed as described in the next section.

Table 4: Corrections to amplitude of nutation terms, μas. Formal errors are about 4 μas.

Period	Original data				After removing FCN			
	$\Delta\psi \sin(\epsilon)$		$\Delta\epsilon$		$\Delta\psi \sin(\epsilon)$		$\Delta\epsilon$	
	sin	cos	sin	cos	sin	cos	sin	cos
6798.38	33	22	−31	−40	30	21	−41	−34
3399.19	21	22	−54	−22	30	24	−49	−13
1615.75	6	−7	−3	45	3	−12	6	46
1305.48	−7	1	4	28	−9	−6	14	15
1095.18	−8	10	7	−5	−11	−2	13	−13
386.00	17	55	−33	6	6	8	4	2
365.26	15	15	−30	13	−4	10	−2	0
346.64	13	3	−14	8	−9	11	−8	1
182.62	−13	−3	−19	−13	−11	1	−11	−12
121.75	−11	−13	−6	−5	−2	−9	−8	−1
31.81	7	1	−2	14	2	−4	−7	8
27.55	10	2	−11	4	17	7	−14	4
23.94	7	−8	2	2	5	−3	5	−4
14.77	−3	0	−7	−1	0	−2	−3	−3
13.78	−14	6	−3	−3	−10	4	−5	−6
13.66	−4	−29	6	0	8	−26	0	9
9.56	2	−8	−2	−2	−3	−9	−3	−4
9.13	−11	17	−2	−10	−14	12	−2	−5
9.12	−11	12	−13	−5	−10	9	−11	1
7.10	−14	20	12	27	9	1	−4	−6
6.86	−3	10	7	−5	4	−1	3	−3

One can see that most of the harmonics with periods close to FCN are affected, as expected. However, evidently due to wide spectrum of the new FCN model, other amplitudes are also influenced. In any case, this effect should be investigated more carefully.

4. FREE CORE NUTATION

To investigate the FCN contribution we used smoothed data to eliminate a noise in the investigated data. Figure 3 shows smoothed differences between observed nutation series and the IAU2000A model. From Figures 1–3 one can see that a signal at the FCN frequency band prevails in the spectrum of the differences, which is also known from previous studies (e.g. Shirai and Fukushima, 2001a).

Several models are proposed for the FCN contribution (e.g. Herring et al., 2002; Shirai and Fukushima, 2001b). All existing models suppose that FCN is an oscillation with constant period of about 430 days and variable amplitude. However, newest investigations (Malkin and Terentev, 2003a, 2003b) show that the FCN period is also variable, which may be explained by variable FCN phase though.

Let us consider how a model with variable amplitude and period (phase) can be used in practice. We can describe the FCN term as

$$\begin{aligned} \Delta\psi \cdot \sin\epsilon_0 &= A(t)\, \sin(\Phi(t))\,, \\ \Delta\epsilon &= A(t)\, \cos(\Phi(t))\,. \end{aligned}$$

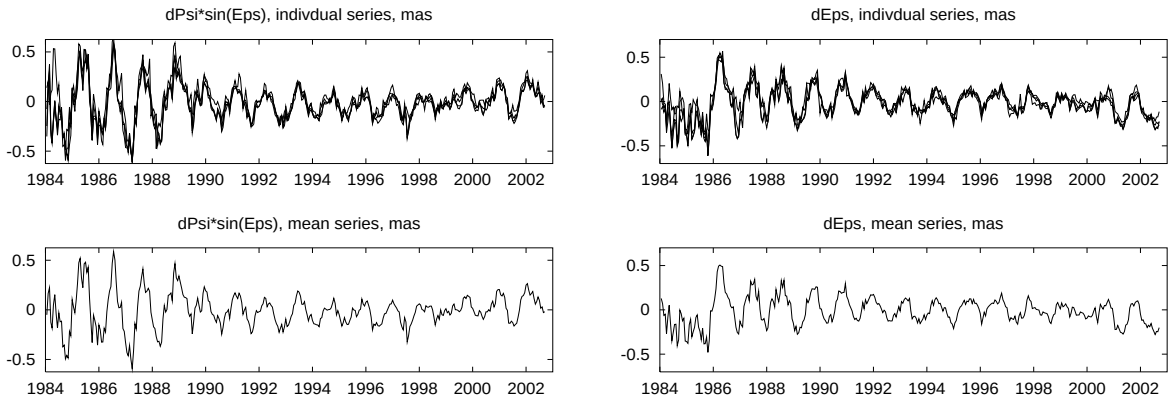

Figure 3: Smoothed differences between observed nutation series and the IAU2000A model.

Mathematically (not geophysically, indeed!), we can suppose three equivalent models for the FCN phase $\Phi(t)$

$$\Phi(t) = \begin{cases} \dfrac{2\pi}{P(t)}\, t + \Phi_0\,, \\ \dfrac{2\pi}{P_0}\, t + \Phi(t)\,, \\ \dfrac{2\pi}{P(t)}\, t + \Phi(t)\,, \end{cases}$$

where P is the FCN period. In other word we can suppose variable period with constant phase, variable phase with constant period, or variable both period and phase. Of course, this is a subject of geophysical consideration, but this doesn not matter for an empirical FCN model using time variations of the FCN parameters found from analysis of the observed data. In practice we can compute $\Phi(t)$ as

$$\Phi(t) = \int_{t_0}^{t} \frac{2\pi}{P(t)}\, dt + \varphi_0\,,$$

where φ_0 ia a parameter to be adjusted. Amplitude variations $A(t)$ can be easily computed from the differences between observed series and model as

$$A(t) = \sqrt{(d\psi * \sin\epsilon)^2 + d\epsilon^2}\,,$$

where $d\psi$ and $d\epsilon$ are the differences in longitude and obliquity at epoch t. Indeed, using such an approach we suppose that all differences in the FCN frequency band can be attributed to the FCN, but this seems to be a good approximation to reality.

Variations of the FCN amplitude $P(t)$ and phase $\Phi(t)$ are shown in Figure 4 along with the corresponding FCN parameters included in the MHB2000 model which is, in fact, also a model with variable phase and amplitude, though this is not stated explicitly (we used the text of the FCN_NUT routine included in the MHB_2000 code to extract the FCN(MHB) amplitude and phase variations). One can see that both models show similar behavior of the FCN parameters, however new approach allow us to get more smooth and predictable functions $A(t)$ and $\Phi(t)$. Comparing these two models one should keep in mind that MHB2000 model is developed only till epoch 2001.4, and after this epoch the difference between models grows rapidly.

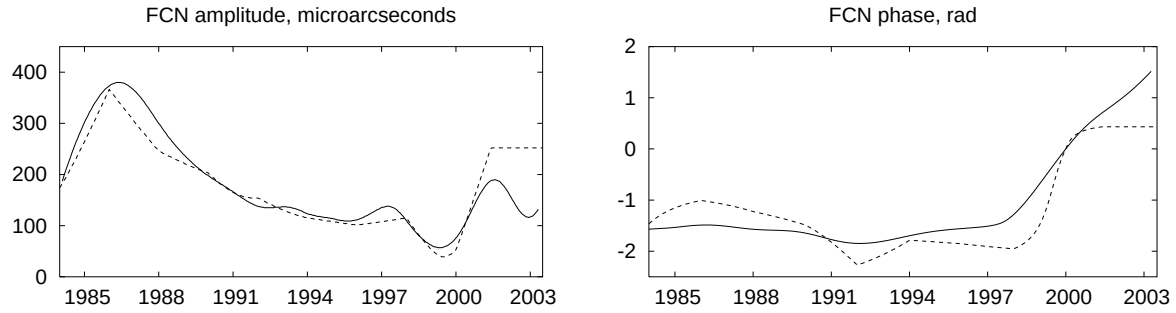

Figure 4: The FCN amplitude and phase variations found in this study (solid line), and a comparison with the MHB2000 model (dashed line).

Figure 5 shows spectra of the differences between observed nutation series and the IAU2000A model computed for raw differences and after removing FCN contribution. One can see that the FCN signal is completely eliminated.

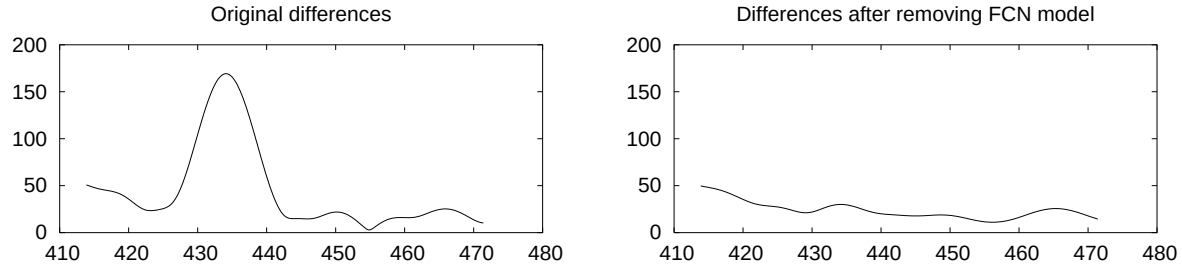

Figure 5: Spectrum of the differences between observed nutation series and the IAU2000A model, period in days, amplitude in μas.

However, the differences between observed nutation series and model have a noise of various origins with the rms compatible with the FCN contribution. To estimate actual contribution of the FCN model to this noise we computed rms of differences between observations and model with three different accounting for the FCN term: no FCN (raw differences), extracting FCN term according to the MHB2000 model, and extracting the FCN term according to new model described here. The results are shown in Table 5. One can see that accounting for the FCN contribution leads to decreasing of differences. Especially interesting is the last part of the table corresponding to period of observations 2002–2003. Using MHB2000 FCN model for this period leads to degradation of differences between observations and the IAU2000A model.

Table 5: WRMS of differences with two FCN models, μas.

Series	All sessions			NEOS			R1R4		
	FCN model			FCN model			FCN model		
	No	MHB	New	No	MHB	New	No	MHB	New
GSF	166	146	138	138	122	120	134	150	102
IAA	170	152	144	140	123	123	138	154	111
USN	161	144	136	138	122	122	136	156	107
Mean	156	136	126	131	113	112	129	146	97

A FCN model with variable period and phase allow us to try a new approach to FCN prediction. We can consider two possibilities. The first one is a prediction of actual FCN contribution, which is developed e.g. in (Brzezinski and Kosek, 2003). Another possibility is to predict functions $A(t)$ and $\Phi(t)$ separately, and then use predictions to construct the FCN contribution using the formulas given above. Figure 6 presents a variant of such a prediction obtained using ARIMA method. It is interesting to compare both approaches of FCN prediction in details.

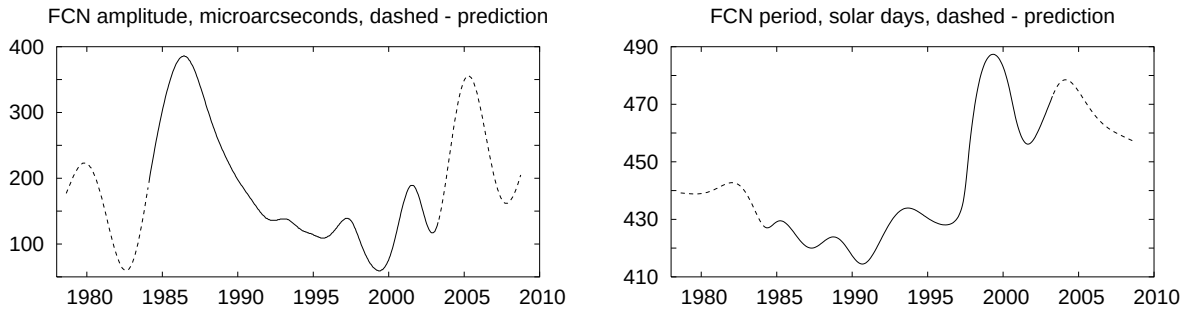

Figure 6: Examples of predictions of the FCN amplitude and phase.

5. CONCLUSIONS

The results of this study allow us to make some conclusions.

1. The IAU2000A model represents the modern VLBI observations with an accuracy at the level of 100–120 μas, i.e. about twice better than intended.

2. Bias between observed and modelled celestial pole offset is found to be at the level 20–30 μas, and, evidently cannot be obtained with an accuracy better that 10–20 μas from the current set of observations. The same can be said about precession constant and obliquity rate which seems to be accurate at the level of several microarcseconds per year, and hardly can be significantly improved using the current set of observations.

3. Free Core Nutation heavily contributes to the differences between the observed nutation series and the IAU2000A model. Latest investigations show that the FCN oscillation has not only variable amplitude, but also variable period or phase. A new FCN model with variable amplitude and phase was found to be in better agreement with observations than existing one.

6. REFERENCES

Brzezinski, A., W. Kosek, 2003: Free core nutation: stochastic modelling versus predictability. This issue.

Herring, T. A., Mathews, P. M., Buffet, B. A., 2002: Modelling of nutation-precession: Very long baseline interferometry results. J. Geophys. Res., **107**, No. B4, 10.1029/2001JB000165.

MacMillan, D., C. Ma., 2000: Improvement of VLBI EOP Accuracy and Precision. In: N. R. Vandenberg, K. D. Baver (eds.), IVS 2000 General Meeting Proc., Koetzting, Germany, Feb 21–24, 2000, 247–251.

Malkin, Z., 2002: A Comparison of the VLBI Nutation Series with IAU2000 Model. In.: IVS 2002 General Meeting Proc., eds. N. R. Vandenberg, K. D. Baver, NASA/CP-2002-210002, 2002, 335–339.

Malkin, Z., D. Terentev, 2003a: Preliminary analysis of the Free Core Nutation from VLBI data. Presented at the 16th Working Meeting on European VLBI for Geodesy and Astrometry, Leipzig, Germany, May 9–10, 2003.

Malkin, Z., D. Terentev, 2003b: Investigation of the Parameters of the Free Core Nutation from VLBI data. Comm. IAA RAS, No 149.

Mathews, P. M., T. A. Herring, B. Buffett, 2002: Modeling of nutation and precession: New nutation series for nonrigid Earth and insights into the Earth's interior. J. Geophys. Res., **107**, No. B4, 10.1029/2001JB000390.

Shirai, T., T. Fukushima, 2001a: Construction of a New Forced Nutation Theory of the Nonrigid Earth. Astron. J., **121**, 3270–3283.

Shirai, T., T. Fukushima, 2001b: Did Huge Earthquake Excite Free Core Nutation? J. Geodetic Soc. Japan, **47**, No 1, 198–203.

Sokolskaya, M., E. Skurikhina, 2000: EOP determination with OCCAM and ERA Packages. In: N. R. Vandenberg, K. D. Baver (eds.), IVS 2000 General Meeting Proc., Koetzting, Germany, Feb 21–24, 2000, 309-313.

THE FIRST RESULTS OF VLBI OBSERVATIONS AT THE SVETLOE OBSERVATORY IN THE FRAMEWORK OF THE IVS OBSERVING PROGRAMS

A. FINKELSTEIN, V. GRATCHEV, A. IPATOV, Z. MALKIN, I. RAHIMOV,
E. SKURIKHINA, S. SMOLENTSEV
Institute of Applied Astronomy
nab. Kutuzova 10, St.Petersburg 191187, Russia
e-mail: amf@quasar.ipa.nw.ru

ABSTRACT. In this paper results of the first 10 geodetic VLBI sessions observed at the Svetloe Radio Astronomical Observatory (SvRAO) of the Institute of Applied Astronomy (IAA) since March 2003 in the framework of the IVS observing programs after installation of Mark 3A terminal in cooperation with NASA. Analysis of observations has been performed at the IAA using OCCAM/GROSS software. The processing of the observations allowed us to determine with high accuracy both the coordinates of the SvRAO and Earth orientation parameters. It is also shown that including Svetloe observatory in the IVS network yields essential improvement of the accuracy of determination of the EOP. Obtained results show high quality of both observations and analysis made at the IAA.

1. INTRODUCTION

Svetloe Radio Astronomical Observatory (SvRAO) was founded by the Institute of Applied Astronomy of the Russian Academy of Sciences (IAA RAS) as the first station of the Russian VLBI network QUASAR. It is located near Svetloe village in the Karelian Neck about 100 km towards North of St.Petersburg, and is primarily intended for regular VLBI observations in the framework of domestic and international programs on astrometry, geodynamics and space geodesy (Finkelstein, 2001).

Until the end of 2002 SvRAO was equipped with only terminal, Canadian S2, with Data Acquisition System developed at the IAA. Using this terminal, SvRAO participated in a number of VLBI programs in collaboration with other VLBI stations in China, Canada and Australia, also with the second IAA VLBI station, Zelenchukskaya, located in the North Caucasus.

In 2002, according to the Agreement between the RAS and NASA, Mark 3A terminal was installed at SvRAO, and since 2003 the observatory started regular VLBI observations in the framework of the IVS (International VLBI Service for Geodesy and Astrometry) astrometry and geodynamics programs. Starting in the regular IVS programs is a result of nearly 15 years of efforts by the IAA, and this is a major milestone for us.

2. VLBI EQUIPMENT OF THE SVRAO

The basic instrument of the SvRAO is a new generation fully steerable radio telescope with homology backup structure. Quasi-paraboloid main dish has diameter of 32 m and focal length of 11.4 m, and the secondary mirror is an asymmetrical modified hyperboloid with the diameter of 4 m. Radio telescope has two operational slewing velocities: fast (azimuth speed $1.5\,^\circ$/s , elevation speed $0.8\,^\circ$/s) and slow (azimuth speed $1.5\,'$/s, elevation speed $0.8\,'$/s). Cable system provides azimuth range $\pm 270^\circ$ of North direction and elevation range (-5° — $+90^\circ$).

The radio telescope is equipped with 5 low-noise cooled receivers with HEMT amplifiers for wavelengths 1.35, 3.5, 6.0, 13 and 18/21 cm for observations in the left and right circular polarizations (Ipatov *et al.*, 1994). To provide the low noise temperature of the "radio telescope — radiometer" system not higher than 50–70 K some input lines of all bandwidth have to be cooled at 20 K. The micro-cryogenic closed circle refrigerators are used for the cooling of low noise amplifiers of all ranges at 20 K.

To be able to switch frequency band and provide multi-band observations quasi simultaneously, the input horns for different wavelengths are located above the circle of 3-meter diameter and the fast switching is achieved by turning of the secondary mirror at certain angle around the radio telescope axis. To maintain simultaneous receiving at the S and X bands in both orthogonal polarizations (to eliminate ionosphere effects), which is essential for realization of astrometric, geodynamical and geodetic programs, the special combined horn has been constructed. The working ranges of intermediate frequencies of these cryo electronic radiometers are 130–480 MHz and 130–890 MHz for X and S bands correspondingly. The noise temperature at the input of cryostat is 15 K and total noise temperatures of "radio telescope — radiometer" system are not higher 50 K for S band and 70 K for X band at the elevations above 20°.

The signal from the radiometer output is transmitted along the phase stable coaxial lines connecting the focal cabin of radio telescope with 14-channel Mark 3A terminal located at the laboratory building. The registration is fulfilled on the magnetic tapes with the use of 24-track tape recorder Honeywell. One tape is provided the tape recording of 18-24 hours of observations depending on program.

Svetloe VLBI site is provided with a qualitative system of time-frequency synchronization, consisting of 4 H-masers with long-time stability about $(3-5)\times 10^{-15}$. One H-maser operates constantly and each other can be switched on during one hour and will achieve all nominal technical parameters during 24 hours. The synchronization of the local time scale with Universal Time is realized with the use of GPS and GLONASS receivers with the accuracy (30–50) ns.

The phase calibration system — generator of picosecond impulses includes two basic units: pulse generator of harmonics on semiconductor diode and circuit producing 1 MHz reference signal with rectangular wavefront from the harmonic signal with the frequency of 5 MHz provided by the H-maser. The measurement of the delay of 5 MHz reference signal in cable system is provided by phase comparator.

Automatic meteorological data system measures atmospheric pressure, direction and velocity of wind, temperature and humidity of air. These data are recorded in log-file of the media.

All systems of the radio telescope are united in general complex with the help of central computer with specialized software, permitting the automatic carrying out of observations. The basis of this software is the Mark IV Field System, Version 9.5.17, being the international standard for VLBI (Himwich, 2000). It was added by site-oriented interface for the control of dish, radiometers and radiometric registration. Software for this interface was developed in Linux media with the use of SNAP language fully integrated in FS media for VLBI and single dish modes.

3. OBSERVATIONS AND RESULTS

The first regular IVS session at Svetloe was observed on March 6, 2003 (Finkelstein *et al.*, 2003). To Sep 1, 2003 Svetloe participated in 14 IVS sessions — 10 R4 sessions (determination of EOP), 3 TRF sessions (improvement of the terrestrial reference frame), 1 EURO session (investigation of crustal deformations in Europe). Four R4 sessions were not correlated in time because of delay in tape delivering due to customs problems. List of sessions and related statistics are presented in Table 1.

Table 1: VLBI sessions observed at Svetloe in March–August 2003.

Session code	Date	Number of stations	Number of sources	Number of scans	Number of observations
R4061	Mar 6	8	36	313	2373
T2015	Mar 18	7	44	348	2079
R4063	Mar 20	8	34	332	2902
R4065	Apr 3	8	44	322	2305
T2016	Apr 8	7	38	231	1067
R4069	Apr 29	8	47	340	2693
EURO68	May 6	9	53	324	5433
T2017	May 20	8	54	542	1985
R4073	May 29	8	54	399	2306
R4075	Jun 12	5	43	203	658
R4079	Jul 10	correlated without Svetloe			
R4081	Jul 24	correlated without Svetloe			
R4083	Aug 7	correlated without Svetloe			
R4085	Aug 21	correlated without Svetloe			
Total		22	94	3354	23801

Schedule files for these sessions were prepared at the NASA Goddard Space Flight Center (GSFC) for the R4 program, and at the Geodetic Institute of the University of Bonn for the T2 and EURO programs.

Correlation of the observations was made at the USNO correlator, except two sessions EURO68 and T2017 which was correlated at the Bonn correlator. The processing factor which is equal to ratio of correlation time to session duration was between 1.0 and 4.2 depending on quality of data and number of stations. The time delay between observations and availability of correlated data was 10–14 days for R4 sessions and ≈2–4 months for T2 and EURO sessions.

During those 10 IVS sessions observed with the participation of SvRAO 23801 observations were obtained, 20596 of them are good, i.e. suitable for scientific analysis. These observations were obtained at 22 VLBI stations, and 113 baselines of length from 99 km (DSS65–YEBES) to 12,496 km (DSS45–YEBES). Station statistics is presented in Table 2.

Scientific analysis of observations has been performed at the IAA using OCCAM/GROSS software (Malkin *et al.*, 2000). The analysis was aimed to compute accurate coordinates of Svetloe radio telescope reference point and the EOP, in accordance with the goal of the corresponding IVS programs. A priori coordinates of the Svetloe radio telescope were obtained from the processing of the GPS observations collected at the permanent GPS station SVTL installed at Svetloe, and geodetic survey on the local geodetic network (Smolentsev *et al.*, 2001). Geocentric coordinates of the Svetloe radio telescope reference point obtained at the IAA are presented in Table 3.

Coordinates are referred to the ITRF2000 at epoch 2003.30. For this computation coordinates of all stations except Svetloe were fixed to VTRF2003 values with only exception of

Table 2: List of participating stations (D – distance from Svetloe, Nsess –number of sessions, Nobs – number of observations, Ngood – number of good observations, Nav – average number of observations per session, Pg – percentage of good observations).

Station	Location	D	Nsess	Nobs	Ngood	Nav	Pg
ALGOPARK	Canada	6256	6	3749	3412	569	91.0
CRIMEA	Ukraine	1811	3	968	779	260	80.5
DSS45	Australia	11734	1	505	401	401	79.4
DSS65	Spain	3192	1	1269	1158	1158	91.3
FORTLEZA	Brazil	8428	7	2359	2099	300	89.0
GGAO7108	USA	6767	2	91	47	24	51.6
GILCREEK	USA, Alaska	5854	5	3658	3446	689	94.2
KASHIM34	Japan	7174	1	608	513	513	84.4
KOKEE	USA, Hawaii	9561	6	2789	2516	419	90.2
MATERA	Italy	2374	9	6183	4973	553	80.4
MEDICINA	Italy	2140	2	2069	1771	886	85.6
NOTO	Italy	2809	1	1420	1227	1227	86.4
NYALES20	Norway, Spitsbergen	2133	6	5103	4585	764	89.8
ONSALA60	Sweden	1080	1	1396	1135	1135	81.3
SESHAN25	China	6761	1	569	492	492	86.5
SVETLOE	Russia	—	10	5671	4866	487	85.8
TSUKUB32	Japan	7141	2	1321	1165	583	88.2
URUMQI	China	4127	2	1116	823	412	73.7
WESTFORD	USA	6269	1	283	204	204	72.1
WETTZELL	Germany	1655	7	4844	4284	612	88.4
YEBES	Spain	3130	2	1427	1100	550	77.1
YLOW7296	Canada	5807	1	204	196	196	96.1

Table 3: Svetloe coordinates at the epoch 2003.30 aligned to ITRF2000.

Analysis center	X, m	Y, m	Z, m
IAA	2730173.850	1562442.667	5529969.064
	±1	±1	±2
VTRF	.850	.668	.071
	±3	±2	±6
MAO	.838	.670	.070
	±2	±1	±3
GSFC	.849	.666	.063
	±1	±1	±2

coordinates of the station Gilmore Creek which was corrected for the jump in station position due to the earthquake happened in November 2002 resulted in station displacement of about 6 cm.

For comparison, coordinates given in the IVS reference system VTRF2003 (Nothnagel, 2003), and those computed at the Main Astronomical Observatory (MAO), Kiev, Ukraina (Bolotin, 2003) are also given in Table 3. New GSFC estimate of Svetloe coordinates obtained and kindly provided by Daniel MacMillan (personal communication) is also included in the Table.

Solutions IAA (present work), MAO and GSFC are obtained from processing of 10–11 observ-

ing sessions, VTRF solution is obtained by means of Helmert transformation of the GSF2002B solution (Nothnagel, 2003), which, in turn, was computed using observations of only one IVS session at Svetloe. For this reason accuracy of the VTRF coordinates of Svetloe is much worse than for other solutions. However, it is the official IVS reference frame.

During the analysis we also computed baseline length for all participated stations. Of course, especially interesting for us were baselines including Svetloe station. They are shown in Table 4.

Table 4: Baseline lengths (E – formal error, R – repeatability).

Baseline Svetloe —	Number of sessions	Length, m	E, m	R, m
ALGOPARK	6	6255567.6332	0.0022	0.0025
CRIMEA	2	1810877.6189	0.0035	0.0049
DSS45	1	11734020.5530	0.0169	
DSS65	1	3192391.5652	0.0034	
FORTLEZA	7	8428008.6707	0.0037	0.0075
GGAO7108	1	6767247.5654	0.1350	
GILCREEK	5	5853689.1323	0.0021	0.0061
KASHIM34	1	7173755.4896	0.0110	
KOKEE	6	9561115.4135	0.0035	0.0061
MATERA	9	2373640.0976	0.0011	0.0019
MEDICINA	2	2139526.9600	0.0024	0.0055
NOTO	1	2808545.4754	0.0031	
NYALES20	6	2133122.9961	0.0011	0.0016
ONSALA60	1	1079812.9364	0.0026	
SESHAN25	1	6760938.2673	0.0103	
TSUKUB32	2	7140832.1563	0.0043	0.0003
URUMQI	2	4127151.1133	0.0043	0.0018
WESTFORD	1	6269171.0929	0.0137	
WETTZELL	7	1654774.8541	0.0010	0.0006
YEBES	2	3129769.6024	0.0043	0.0044
YLOW7296	1	5807450.7252	0.0163	

It should be mentioned that in 2003 station Svetloe was included in the IVS network as tagged along station. i.e supplementary to the regular IVS R4 network. Figure 1 show a typical configuration of the R4 network in 2003. One can see that Svetloe is located near other european stations, and thus does not strengthen substantially the network geometry. So, no significant improvement of the results obtained at the R4 network can be expected after inclusion of Svetloe. Nevertheless, we tried to estimate how it influences the accuracy of EOP results (the main goal of the IVS R4 program).

Estimates of pole coordinates X_p, Y_p, Universal Time $UT1$, and nutation angles $\Delta\psi$ and $\Delta\varepsilon$ were computed both for whole network and for reduced network without Svetloe (Table 5).

Obtained results show that inclusion Svetloe in the IVS network yields substantial improvement in quality of results. Hopefully, planned participation of Svetloe observatory in IVS programs as regular station will allow us to realize more substantial progress in the accuracy of determination of EOP and TRF, and make a valuable contribution to other geodesy and astrometry investigations.

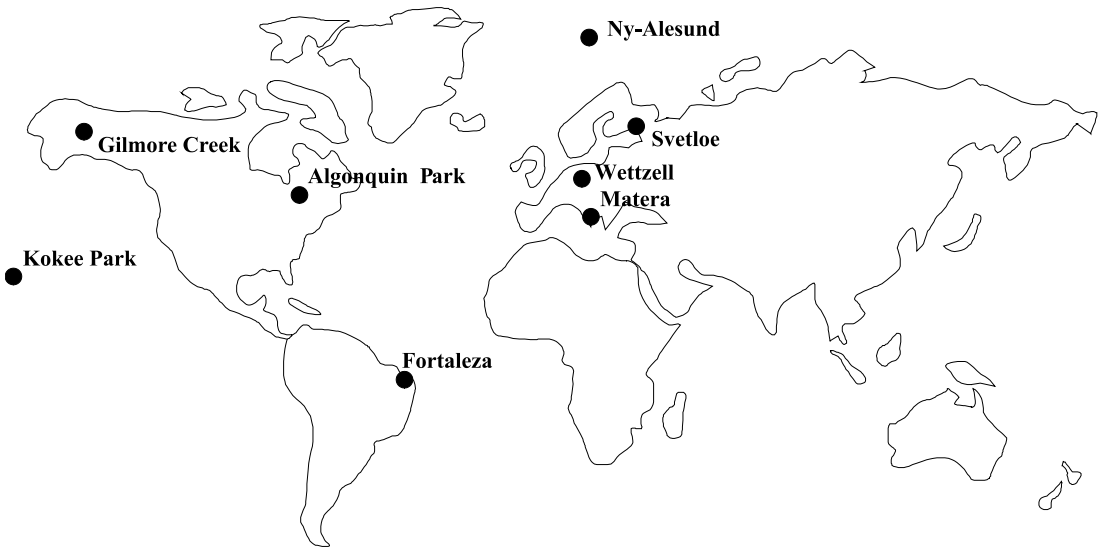

Figure 1: Typical network for IVS R4 experiments.

Table 5: EOP differences with the IERS C04 series (X_p, Y_p — pole coordinates, $UT1$ — Universal Time, X_c, Y_c — celestial pole offset).

EOP	All sessions				R4 (EOP) sessions			
	with Svetloe		w/o Svetloe		with Svetloe		w/o Svetloe	
	bias	wrms	bias	wrms	bias	wrms	bias	wrms
X_p, μas	-233	127	-219	151	-244	74	-224	92
Y_p, μas	378	141	402	148	367	134	390	134
$UT1$, μs	-79	52	-75	53	-87	16	-82	20
X_c, μas	10	37	-2	69	16	27	10	27
Y_c, μas	4	76	-18	95	-11	60	-29	74

Table 6: EOP formal errors (X_p, Y_p — pole coordinates, $UT1$ — Universal Time, X_c, Y_c — celestial pole offset), and other statistics (σ_0 — post-fit rms, C_{max} — maximum correlation between EOP).

EOP	All sessions		R4 (EOP) sessions	
	with Svetloe	w/o Svetloe	with Svetloe	w/o Svetloe
$\sigma(X_p)$, μas	140	169	110	120
$\sigma(Y_p)$, μas	120	146	80	83
$\sigma(UT1)$, μs	56	73	37	44
$\sigma(X_c)$, μas	74	83	60	61
$\sigma(Y_c)$, μas	79	91	63	65
σ_0, ps	44	47	32	34
C_{max}	0.84	0.84	0.64	0.71

4. ACKNOWLEDGMENTS

Authors wish to thank our colleagues Chopo Ma and Ed Himwich (Goddard Space Flight Center), and Brian Corey (Haystack observatory) for fruitful cooperation on VLBI technology and space geodesy being crowned with installation of Mark 3A terminal at the Svetloe observatory and its inclusion in the IVS network. We also grateful to Dan MacMillan (Goddard Space Flight Center) for providing the latest GSFC estimates of Svetloe position.

5. REFERENCES

Bolotin, S., 2003: ftp://cddisa.gsfc.nasa.gov/pub/vlbi/ivsproducts/trf/mao2003a.trf.gz

Finkelstein, A. M., 2001: Radiointerferometric Network QUASAR. Science in Russia, No. 5, 20–26.

Finkelstein A., A. Ipatov, S. Smolentsev, 2002: Obsevatories in Svetloe and Zelenchukskaya of VLBI Network QUASAR. In: Fourth APSGP Workshop, Eds. H. Cheng, Q. Zhihan, 47–57.

Finkelstein, A. M., A. V. Ipatov, S. G. Smolentsev, V. G. Grachev, I. A. Rahimov, Z. M. Malkin, 2003: Highly Accurate Determination of the Coordinates and the Earth's Rotation Parameters Involving the Svetloe VLBI Observatory. Astronomy Letters, 2003, **29**, No 10, 667–673.

Himwich, E., 2000: Introduction to the Field System for Non-Users. In: IVS 2000 General Meeting Proceedings, Eds. N. Vandenberg, K. Baver, 86–90.

Ipatov, A. V., I. A. Ipatova, V. V. Mardyshkin, 1994: In: Progress and Future Observational Possibilities, Eds. T. Sasao, S. Manabe, O. Kameya, M. Iniue, 200.

Malkin, Z., A. Voinov, E. Skurikhina, 2000: Software for Geodynamical Researches Used in the LSGER IAA. In: ASP Conf. Ser., **216**, Astronomical Data Analysis Software and Systems IX, Eds. N. Manset, C. Veillet, D. Crabtree, 632–635.

Nothnagel, A., 2003: VTRF2003: A Conventional VLBI Terrestrial Reference Frame. In: Proc. 16th Working Meeting on European VLBI for Geodesy and Astrometry, Leipzig, Germany, 9–10 May 2003, 195–206.

Smolentsev, S., D. Ivanov, Z. Malkin, 2001: Svetloe Radio Astronomical Observatory. In: 2000 IVS Annual Report, Eds. N. R. Vandenberg, K. D. Baver, 123–126.

ICRF CONSISTENCY CHECK BY COMPARISON OF THE ICRF-Ext.1 WITH THE GAOUA SERIES OF RS CATALOGUES

YA. YATSKIV, A. KUR'YANOVA, S. BOLOTIN
Main Astronomical Observatory
National Academy of Sciences of Ukraine
27 Akademika Zabolotnoho St, 03680 Kiev, Ukraine
e-mail: yatskiv@mao.kiev.ua

ABSTRACT. Main Astronomical Observatory of the National Academy of Sciences of Ukraine (GAOUA is the acronym used by the IERS) is engaged in construction of the ICRF as realized by VLBI. Two different series of catalogues of radio source (RS) positions have been constructed, namely initial catalogues of RSC(GAOUA)YY R NN as resulted from processing the VLBI observations with the SteelBreeze software and combined catalogues of type RSC(GAOUA)YY C NN as resulted from using the so-called Kyiv arc length method for combining initial catalogues provided by various Analysis Centers of the IERS. New initial reference frame RSC(GAOUA)03 R 01 was constructed based on VLBI data from 1979 to 2003 as well as new combined catalogue RSC(GAOUA)03 C 01 was constructed applying the Kyiv arc length method to four initial frames RSC(BKG)03 R 01, RSC(CGS)02 R 01, RSC(GAOUA)03 R 01 and RSC(AUS)03 R 01. Results of comparison between the ICRF-Ext.1, four initial frames, and the combined frame are discussed.

1. INTRODUCTION

Main Astronomical Observatory of the National Academy of Sciences of Ukraine (GAOUA is the acronym used by the IERS) is engaged in construction of the ICRF as realized by VLBI. Two different series of catalogues of radio source (RS) positions have been constructed, namely initial catalogues of RSC(GAOUA)YY R NN as resulted from processing the VLBI observations with the SteelBreeze software and combined catalogues of type RSC(GAOUA)YY C NN as resulted from using the so-called Kyiv arc length method for combining initial catalogues provided by various Analysis Centers of the IERS or the IVS. These catalogues have been used for check of consistency of the ICRF.

2. GAOUA INITIAL CATALOGUES OF RS POSITIONS

Several initial catalogues have been constructed using various versions of the SteelBreeze software (S. Bolotin, 2001). Table 1 gives overview of the GAOUA initial catalogues.

The recent initial catalogue of RS positions RSC(GAOUA)03 R 01 is based upon a solution for all applicable VLBI data since 1979 till July 2003. In total 3,550,143 dual frequency delays acquired on 2,970 astrometric and geodetic sessions have been processed (S. Bolotin, 2003).

Table 1: Statistics of the GAOUA initial catalogues. N is total number of RS positions; N_d is the number of defining RS; σ is internal r.m.s. uncertainty (in mas).

Frame	N	N_d	$\sigma_\alpha * \cos\delta$	σ_δ	Software version
RSC(GAOUA)96 R 01	160	33	0.14	0.21	SteelBreeze-1.0
RSC(GAOUA)97 R 01	129	17	0.21	0.38	SteelBreeze-1.0
RSC(GAOUA)98 R 01	198	55	0.25	0.41	SteelBreeze-1.0
RSC(GAOUA)00 R 01	191	47	0.22	0.39	SteelBreeze-1.2
RSC(GAOUA)03 R 01	1558	211	0.10	0.13	SteelBreeze-2.0

The initial values of RS positions have been taken from the ICRF-Ext.1. Orientation of constructed reference frame was defined by a No-Net-Rotation condition between the ICRF-Ext.1 and the derived catalogue using 35 defining radio sources.

3. GAOUA COMBINED CATALOGUES OF RS POSITIONS

The Kyiv arc length method proposed by Ya. Yatskiv and A. Kur'yanova, 1990, was used for construction of catalogues of type RSC(GAOUA)YY C NN since 1991. This method combines a geometrical arc length calculation with a statistical evaluation of uncertainties of individual and compiled catalogues. The following items explain essentials of the method approach (corresponding mathematical formulae can be found in Kur'yanova A.N. and Yatskiv Ya.S., 1993):

- selection of "basic" catalogues of radio source (RS) positions from set of individual catalogues;
- search for defining RSs common to each selected "basic" catalogues;
- calculation of arc lengths (below simply "arcs") between defining RSs which are common in all "basic" catalogues;
- comparison of calculated arcs for "basic" catalogues, which resulted in evaluation of catalogue weights; determination of mean values of the arcs and "arc minus mean arc" residuals;
- construction of so-called individual "rigid" frames which are based on the arcs between defining RS and on the systems, defined by positions of two selected RSs;
- construction of combined "rigid" frame using the data of previous steps;
- alignment of this combined "rigid" frame to the ICRF and construction of combined reference frame using No-Net-Rotation condition between the combined frame and the ICRF for common defining RSs;
- extension of the reference frame realized by common defining RSs to additional RSs, involved in process of constructing the combined frame.

The eight combined solutions based upon initial catalogues of RS positions provided by IERS and/or IVS were constructed (Y. Yatskiv, O. Molotaj, A. Kur'yanova and V. Tel'nyuk-Adamchuk, 2003).

Table 2 gives some characteristics of the initial reference frames which have been used for construction of recent combined catalogue RSC(GAOUA)03 C 01. Three frames, namely RSC(BKG)03 R 01, RSC(CGS)02 R 01 and RSC(GAOUA)03 R 01 have been used as individual "basic" frames in process of constructing the compiled catalogue of GAOUA type. RS 1606+106 and RS 1130+009 are selected as "basic" sources for defining "rigid" frames.

Table 2: List of VLBI frames under consideration. N is the number of radio sources in the frame; N_b is the number of defining RSs common for the first three catalogues: σ is internal r.m.s. uncertainty (in mas); W is frame weight used for constructing the "rigid" frame.

Frame	N	N_b	$\sigma_\alpha * cos\delta$	σ_δ	W
RSC(BKG)03 R 01	630	161	0.06	0.08	0.38
RSC(CGS)02 R 01	457	161	0.11	0.13	0.14
RSC(GAOUA)03 R 01	1558	161	0.07	0.09	0.48
RSC(AUS)03 R 01	659	161	0.09	0.16	–
RSC(GAOUA)03 C 01	1667	161	0.06	0.08	–

4. COMPARISON OF THE INITIAL FRAMES WITH RSC(GAOUA)03 C 01 and ICRF-Ext.1

Initial and combined catalogues have been compared by using the IERS model:

$$\begin{aligned} A_1 \tan\delta\cos\alpha + A_2 \tan\delta\sin\alpha - A_3 + D_\alpha(\delta - \delta_\circ) &= \alpha_1 - \alpha_2 \\ -A_1 \sin\alpha + A_2 \cos\alpha + D_\delta(\delta - \delta_\circ) + B_\delta &= \delta_1 - \delta_2, \end{aligned}$$

where A_1, A_2, A_3 are rotation angles between two frames under consideration; D_α, D_δ, B_δ represent the systematic effects by three deformation parameters, namely D_α – drift in right ascension as a function of the declination, D_δ – drift in declination as a function of the declination and B_δ – bias in declination.

Only defining sources which are common in the initial frames, RSC(GAOUA)03 C 01 and ICRF-Ext.1 (RSC(WGRF)99 R 01) were used in comparisons. The transformation parameters were evaluated by a least squares fit without weights. The relative global orientation and the deformation parameters between initial catalogues RSC(BKG)03 R 01, RSC(CGS)02 R 01, RSC(GAOUA)03 R 01 and RSC(AUS)03 R 01 (below BKG, CGS, GAOUAr and AUS), combined catalogue RSC(GAOUA)03 C 01 (below GAOUAc) and ICRF-Ext.1 are given in Table 3.

Table 3: Relative orientation between individual frames, combined catalogue and ICRF-Ext.1. N_d is the number of common defining sources, A_1, A_2, A_3 are the rotation angles (in μas), D_α, D_δ are the drifts in right ascension and declination respectively, B_δ is the bias in declination (in μas/deg for the drifts, μas for the biases).

Frames	N_d	A_1	A_2	A_3	D_α	D_δ	B_δ
BKG–ICRF	191	9±29	-17±29	-10±33	-1±1	-1±1	38±25
CGS–ICRF	175	-3±22	16±22	-7±27	-1±1	-1±0	10±21
GAOUAr–ICRF	211	24±30	20±30	-15±35	-1±1	0±1	-28±26
AUS–ICRF	191	138±45	6±46	-85±51	-3±2	-5±1	205±40
GAOUAc–ICRF	211	13±26	5±26	-22±30	-1±1	0±1	5±24

No significant slopes in RA and Dec and biases were detected in any individual frame except RSC(AUS)03 R 01.

Moreover, the constrains applied to align the respective frames including GAOUAc to ICRF have resulted in agreements of frame orientation at a few tens of microarcsecond (see values in Table 3).

Figures 1 and 2 show, for the defining sources which are common to GAOUAc and ICRF, postfit residuals in RA and in Dec as a function of declination, and their normalized residuals in a plane RA – Dec respectively.

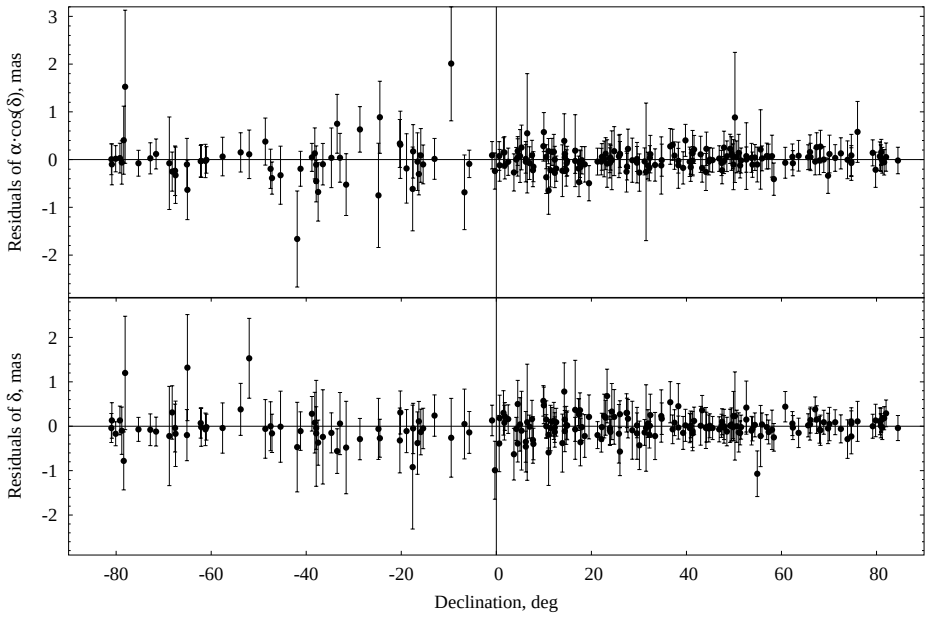

Figure 1: Postfit residuals "GAOUAc–ICRF" against declination for common defining RSs.

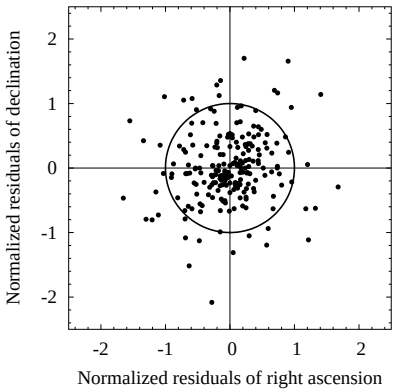

Figure 2: Distribution of normalized residuals "GAOUAc–ICRF" for common defining RSs.

5. ON THE INCONSISTENCIES OF THE GAOUA TYPES OF RS CATALOGUES WITH ICRF-Ext.1

With respect to observational data used for determination of RS positions in ICRF-Ext.1 and RSC(GAOUA)03 R 01 as well as for construction of the combined catalogue RSC(GAOUA)03 C 01 we have to consider that these catalogues are not independent. Thus the comparison between these realizations of the ICRF can not be used as objective quality control.

Nevertheless, we have used the comparison of these three catalogues to determine the so-called "external" estimates of uncertainties for these frames. The following calculations were

made:

a) formal average values of positions of radio sources were derived for different set of individual and combined/compiled catalogues (SO-system);

b) differences $d_{i\circ}$ and $d_{j\circ}$ between positions of i-th and j-th individual frames and SO-system were calculated and used for determination of the coefficient of correlation r_{ij} between i-th and j-th frames.

c) the r.m.s. differences d_{ij} and the correlation r_{ij} between the i-th and j-th frames were used to evaluate the "external" accuracy σ_i of the i-th frame using the following equation

$$d_{ij}^2 = \sigma_i^2 + \sigma_j^2 - 2r_{ij}\sigma_i\sigma_j, \qquad i \neq j$$

Table 4 gives the r.m.s. differences d_{ij}, coefficients of correlation r_{ij} between corresponding frames, and estimated "external" r.m.s. uncertainties σ_i of the ICRF, GAOUAc and GAOUAr frames.

Table 4: "External" estimations of uncertainties of the reference frames. Mean r.s. differences, d_{ij}, correlations, r_{ij}, and the estimated uncertainties, σ_i calculated for all common and for all common defining RSs. Indexes used as follows: 1 - ICRF, 2 - GAOUAc, 3 - GAOUAr.

	r.m.s. differences d_{ij} mas			correlation			uncertainties, mas, on condition $r_{ij} \neq 0$		
	d_{12}	d_{13}	d_{23}	r_{12}	r_{13}	r_{23}	σ_1	σ_2	σ_3
all 584 common RS									
RA	0.54	0.58	0.21	-0.85	-0.89	0.51	0.54	0.06	0.20
Decl	0.61	0.62	0.25	-0.84	-0.86	0.45	0.40	0.23	0.24
211 common defining RS									
RA	0.32	0.34	0.11	-0.86	-0.91	0.57	0.32	0.01	0.12
Decl	0.30	0.38	0.16	-0.73	-0.90	0.37	0.32	0.01	0.19

The data of Table 4 indicate that the internal consistency of the ICRF-Ext.1 could be improved. One of possibility of such improvement is to identify radio sources with large systematic displacements in the ICRF.

Using the set of differences of "Combined frame – ICRF-Ext.1" the large differences in RA and Dec were identified when they were larger than 1 mas (for all common RS) and 0.45 mas (for common defining RS) in three and more catalogues (see Tables 5-6 and 7-8 respectively).

6. CONCLUSIONS

The final conclusions are the following:

1. Constraints applied to align the GAOUA combined catalogues to ICRF have resulted in agreements of frames at a few tens of microarcsecond. No significant slopes and biases in RA and Dec were detected in those of catalogues constructed since 1999.

2. Averaged internal uncertainties of RA and Dec of the GAOUA combined catalogues (since 1999) are less than 0,1 mas and averaged value of the r.m.s. differences of "Combined frame – ICRF" in RA and Dec is about 0,25 mas.

3. The combined catalogue RSC(GAOUA)03 C 01 internally is more consistent as compared with the ICRF-Ext.1.

Table 5: Statistics of large differences in RA for combined catalogues GAOUA and ICRF-Ext.1 – all common RS (Status of the sources: 'D' – defining, 'C' – candidate, 'O' – other radio sources) (in mas).

RS Designation	$\Delta\alpha * \cos\delta$					St
	RSC(GAOUA)					
	98 C 01	99 C 03	00 C 01	01 C 01	03 C 01	
$0138-097$	2.22	1.63	1.64	2.34	2.01	D
$0529+075$	-1.38	–	-1.31	–	-1.01	C
$0823-500$	-1.48	-1.40	-1.32	-1.67	-7.10	C
$1156-094$	1.42	1.33	1.36	1.11	1.02	C
$1323+321$	-10.74	-1.10	–	-2.36	–	C
$1328+307$	–	-1.01	-0.97	-0.98	-1.30	C
$1540-828$	2.04	2.24	2.44	1.01	–	C
$1604-333$	–	–	0.94	1.08	0.75	D
$1733-565$	–	0.86	0.80	1.30	1.55	C
$1740-517$	-2.57	-1.71	-2.46	–	–	C
$1806-458$	-2.76	-1.93	-0.92	–	-1.39	C
$1934-638$	-1.95	-1.99	-2.30	-1.08	–	C
$2128+048$	–	1.05	0.96	1.02	1.18	O

Table 6: Statistics of large differences in RA for combined catalogues GAOUA and ICRF-Ext.1 – common defining RS (in mas).

RS Designation	$\Delta\alpha * \cos\delta$				
	RSC(GAOUA)				
	98 C 01	99 C 03	00 C 01	01 C 01	03 C 01
$0138-097$	2.22	1.63	1.64	2.34	2.01
$0437-454$	-0.54	-0.48	-0.47	-0.44	–
$0537-286$	0.40	0.42	0.46	0.51	0.63
$0733-174$	-0.30	-0.52	-0.50	-0.52	-0.62
$1143-245$	–	-0.79	-0.87	-0.90	-0.75
$1448+762$	0.75	0.84	0.88	0.98	0.58
$1604-333$	–	–	0.94	1.08	0.75
$1727+502$	–	–	-0.53	-0.57	0.88

Table 7: Statistics of large differences in Dec for combined catalogues GAOUA and ICRF-Ext.1 – all common RS (Status of the sources: 'D' – defining, 'C' – candidate, 'O' – other radio sources) (in mas).

RS Designation	$\Delta\delta$ RSC(GAOUA)					St
	98 C 01	99 C 03	00 C 01	01 C 01	03 C 01	
$0259+121$	–	4.70	1.25	1.45	1.40	C
$0440-003$	-1.11	-1.25	-1.08	-1.26	-0.99	D
$0454-463$	–	-6.56	-17.97	-16.73	–	C
$0600+219$	–	–	1.18	1.22	2.27	O
$1156-094$	–	0.97	1.03	1.14	1.17	C
$1402-012$	1.04	0.97	0.94	2.47	2.77	C
$1409+218$	–	1.10	0.99	0.91	–	C
$1718-649$	1.06	1.08	–	1.62	1.32	D
$1951+355$	-2.05	-1.89	-1.79	-1.75	-1.28	C
$2312-319$	-0.98	-1.14	-1.19	-0.79	–	D

Table 8: Statistics of large differences in Dec for combined catalogues GAOUA and ICRF-Ext.1 – common defining RS (in mas).

RS Designation	$\Delta\delta$ RSC(GAOUA)				
	98 C 01	99 C 03	00 C 01	01 C 01	03 C 01
$0039+230$	–	–	0.54	0.53	0.68
$0123+257$	–	-0.47	–	-0.68	-0.57
$0131-522$	–	0.71	0.58	–	1.53
$0440-003$	-1.11	-1.25	-1.08	-1.26	-0.99
$0458+138$	-0.76	-0.97	-0.84	-0.85	-0.38
$0518+165$	0.69	0.56	0.48	0.47	0.37
$0733-174$	–	-0.48	–	-0.51	-0.92
$0812+367$	–	0.72	0.71	0.73	0.54
$0829+046$	–	0.52	0.52	0.47	0.50
$1038+064$	-0.60	-0.62	-0.58	-0.54	-0.46
$1616+063$	–	-0.66	-0.61	-0.60	–
$2059+034$	-1.03	-0.76	-0.66	-0.63	-0.63
$2312-319$	-0.98	-1.14	-1.19	-0.79	-0.48

4. There are several RSs which systematically (for more than three catalogues) exhibit large differences of "Combined frame – ICRF" in RA and Dec (larger than one mas). Three of them are the defining sources, namely 0138-097, 0440-003 and 2312-319, which have to be considered as problem sources to be included in the ICRF.

7. ACKNOWLEDGEMENTS

Celestial reference frames RSC(BKG)03 R 01, RSC(CGS)02 R 01 and RSC(AUS)03 R 01 provided by the International VLBI Service for Geodesy and Astrometry (IVS) were used in this research.

The work has been partly supported by Science and Technology Center of Ukraine (Grant NN - 43) and Grant of Ministry of Education and Science of Ukraine N F7 /256-200/.

8. REFERENCES

Bolotin S.L., 2001. Analysis of VLBI observations. Estimation of parameters, Kinematics and Physics of Celestial Bodies, 17, No. 3, Kiev, pp. 240-248.

Bolotin S. Estimation of the Celestial Intermediate Pole motion in the Terrestrial and Celestial reference frames for VLBI observations on the interval 1979 - 2003, this volume.

IVS: International VLBI Service products available electronically at http://ivscc.gsfc.nasa.gov/service/products.

Kur'yanova A.N., Yatskiv Ya.S., 1993. The compiled catalogue of positions of extragalactic radio sources RSC(GAOUA)91 C 01, Kinematics and Physics of Celestial Bodies, 9, No. 2, pp. 15-25.

Yatskiv Ya.S., Kur'yanova A.N., 1990. A new approach to the construction of a compiled catalogue of positions of extragalactic radio sources. – Inertial Coordinate System on the Sky : Proc. 141th IAU Symp., – Leningrad, Kluwer, pp. 295–296.

Yatskiv Ya., Molotaj O., Kur'yanova A. and Tel'nyuk - Adamchuk V., 2003. Recent compiled catalogue of radio source positions RSC(GAOUA)01 C 01. Proc. Journees Systemes de Reference Spatio-Temporels 2002, Astrometry from Ground and Space, Bucharest (Rumania) (in print).

PULSAR ASTROMETRY: STATE OF THE ART AND PROSPECTS

YU. P. ILYASOV, A. E. RODIN
Pushchino Radio Astronomical Observatory (PRAO) of P.N.Lebedev Physical Institute
Russia, 142290, Moscow region, Pushchino, PRAO
e-mail: ilyasov@prao.psn.ru, rodin@prao.psn.ru

ABSTRACT. Pulsar astrometry is considered to be as an important part of radio astrometry. There are more than 1500 pulsars, which are detected now on the sky. Angular dimensions of pulsars are as small as $10^{-7} \div 10^{-10}$ arcsec. Pulsars can be considered as an extra reference objects in ICRF catalogue and a precise clock regarding to Solar system barycenter. Timing of the millisecond pulsar B1937+21 at PRAO revealed that residuals of its barycentrical pulse Time-of-Arrival (TOA) were no more than 2 microsec (RMS) through 6 years (fractional instabilities $2 \cdot 10^{-14}$ is better than for the best atomic standards). Using timing and VLBI positions of reference pulsars the Eulerian angles from DE200 and ICRF have been defined ($A_x = -4 \pm 2$, $A_y = -13 \pm 3$, $A_z = -19 \pm 5$) mas. It gives good possibilities to link different celestial coordinate systems. Parallax measurements of the nearest pulsars are used for direct measurements of distance to pulsars. Estimation of the GWB density has been made by long-term timing of several millisecond PSR at PRAO as $\Omega_g h^2 < 10^{-6}$ and $\Omega_g h^2 < 10^{-4}$ at low and ultra-low frequency range, respectively

1. INTRODUCTION

After discovery in 1967 of the first pulsars Prof. A. Hewish with colleagues paid attention to the very stable time of repetition their pulses detected by radio telescope. Several weeks they thought that it could be an intelligent signal from an extraterrestrial "Green men". But later on when additional pulsars have been revealed it was clear that it has to be natural object situated in the Galaxy. Now they are identified properly with neutron stars having about 1.5 solar mass and rotating within period from 1.6 ms up to 8 s. Some of them are located in binary systems (binary pulsars). Because of huge magnetic field about $10^{11} - 10^{14}$ Gs the electromagnetic radiation of pulsar comes from the both polar cups of the star. It is well known that apparent pulsar period is decreased slowly due to energy losses (for several "old" pulsars it is estimated as $10^{-17} - 10^{-21}$ s/s). Measuring of a time of arrival (TOA) of pulsar pulses (timing) is one of the main techniques of the pulsar astrometry observations by radio telescope. Combined with coordinate measurement by VLBI technique it means four-dimensional astrometry.

Millisecond pulsars have some advantages against usual (single) pulsars. Its period is short, and its pulse is narrow. That is it important for TOA measurement. Now more than 100 millisecond pulsars are discovered, mostly in binary systems. Therefore millisecond pulsars have reinforced a proposal to use pulsars as excellent time standards and to establish a new pulsar time scale. Later on it was clarified that most millisecond pulsars have very small derivative of pulse period $\dot{P}$ in range $10^{-19} - 10^{-22}$ s/s. Remarkable long-term stability of pulsar period

proves out the possibilities to use these objects as a future astronomical standard precise clocks located in the space and offered common time reference to all terrestrial and space users.

Among fundamental applications of long-term stability is estimation of gravitational waves background (GWB) arisen in the early Universe after the "Big Bang". TOA of pulsar pulses which propagate through curved space-time are affected to variations which can be detected after several years of timing observations. Investigation of timing noise power spectra gives possibility to separate various propagation effects and study physics of interstellar and near pulsar medium, discover planets around pulsars, etc.

Pulsar astrometry department of the PRAO LPI has been conducting timing of usual and millisecond pulsar by using large phased array (LPhA) at Pushchino since 1979 and dish radio telescope RT-64 at Kalyazin since 1995. The basic purpose is to establish a pulsar time scale, link of celestial frames, search of gravitational waves, investigation of pulsar motion in binary systems for testing general relativity. Eulerian angles from DE200 to ICRF have been obtained as following: ($A_x = -4 \pm 2$, $A_y = -13 \pm 3$, $A_z = -19 \pm 5$) mas. Estimation of the energy density of GWB has been obtained as $\Omega_g h^2 < 10^{-6}$ and $\Omega_g h^2 < 10^{-4}$ at low and ultra-low frequency range, respectively.

Importance of pulsar timing array observations both for detection of gravitational waves and for establishment of new astronomical time scale based on high stable rotation of pulsars are confirmed recently by ITU-R in 2002 (Document-7/81-E, 10 Oct. 2002) and IAU Commission 31 in 2003.

2. PULSAR TIMING

The main principles of pulsar timing are presented below. Time of arrival of the Nth pulse at the barycenter of the Solar system is expressed as usual

$$t_N = t_0 + P_0 N + \frac{1}{2} P_0 \dot{P} N^2, \tag{1}$$

where t_N- time of arrival of the Nth pulse to Solar system barycenter (SSB), t_0- reference epoch, P_0- pulsar period at epoch t_0, $\dot{P}-$ derivative of pulsar period at epoch t_0, $N-$ the number of pulses counted from the reference epoch t_0.

Since the observer is not at the SSB the time correction is required. Times of arrival of pulsar pulse to SSB t_N and observer t are related by the following formula

$$t = t_N + \frac{\vec{k} \cdot \vec{r}}{c} - \frac{1}{2cR}[\vec{k} \times \vec{r}]^2 + \Delta_{\rm orb} + \delta t_{\rm rel} + 10^{-2} \frac{DM}{2.41} \frac{1}{f_{\rm obs}^2}, \tag{2}$$

where $c-$ speed of light, $t-$ time of arrival of Nth pulse to observer, $\vec{k}-$ barycentric unit vector to the pulsar, $\vec{r}-$ barycentric radius-vector of the observer, $R-$ distance to pulsar, $\Delta_{\rm orb}-$ delay along the orbit if the pulsar moves in binary system, $\delta t_{\rm rel}-$ relativistic delay which takes into account retardation when pulsar pulse propagates in gravitational field of massive bodies including both planets of the Solar system and companion in binary system, term with dispersion measure DM is dispersive delay for propagation of the pulsar signal at frequency $f_{\rm obs}$ [MHz] through the interstellar medium.

Fitting of the timing parameters includes estimation of t_0, P_0, $\dot{P}$, $\vec{k}$, annual parallax $\pi = 1/R$. Unit vector $\vec{k}$ is not constant and reflects the pulsar position at definite epoch and its proper motion. In the case of two frequency observations there is possibility to directly measure dispersion measure DM. If pulsar moves in the binary system the fitting model includes Keplerian and im some cases post-Keplerian parameters.

Usual single pulsars with periods of order one second are observed with large phased array (LPhA) at frequency 111 MHz. Millisecond pulsars are observed with dish radio telescope RT-64

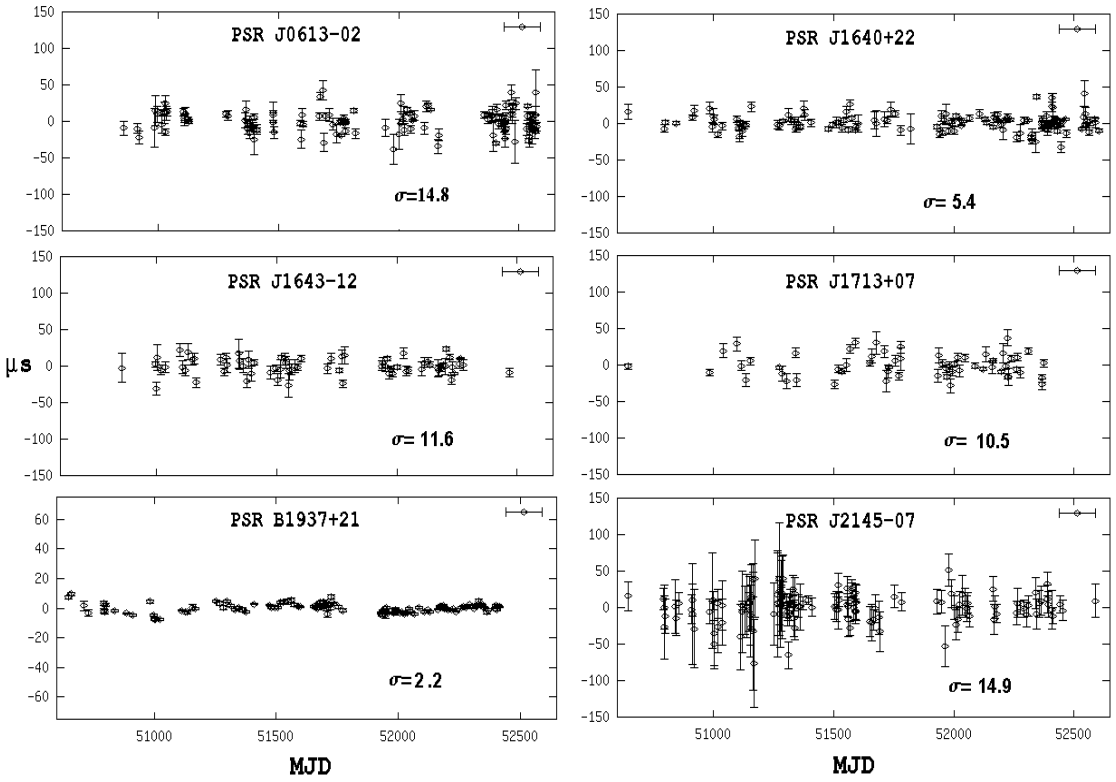

Figure 1: Post-fit timing residuals of six millisecond pulsars.

of Kalyazin Radio Astronomical Observatory (KRAO) at frequency 600 MHz. The residuals of these millisecond pulsars are shown on Fig.1.

Timing data of PSR 1937+21 combined with the similar data from Kashina Space Research Center of Communications Research Laboratory (Japan) at frequency 2.3 GHz (Hanado et al., 2002) allowed to exclude an influence of the interstellar medium. Final RMS of timing residuals for this pulsar is about 2 mcs which corresponds to fractional stability around $1 \cdot 10^{-14}$ at 6 years time interval and shown at Fig.1.

In 1994 an idea that new realization of the ephemeris time (ET) scale based on the motion of a pulsar in the binary system (BPT) had been proposed by Prof. Ilyasov and published in paper (Ilyasov, Kopeikin, Rodin, 1998). It had been proved that fractional stability of BPT may reach 10^{-14} at time interval 10^3 years for short periodic binaries like PSR 1913+16 ($P_b = 7.8$ hours) and $3 \cdot 10^{-12}$ at 20 years for long-periodic binaries like PSR J1713+0747 ($P_b = 68$ days). In the last case fractional stability of BPT is 1.5 order better than the stability of ET based on the motion of the Moon and the Sun. Fractional stability of six millisecond pulsars observed at KRAO are presented at Fig.2.

There exists a problem of the discrepancy between pulsar VLBI and timing positions. This discrepancy occures to arise due to timing noise presented in TOAs (Rodin et al., 1999; Rodin, 2000). The problem is solved by reprocessing timing data by generalized least-square method (LSQ) which takes into account statistical properties of the timing noise or by classical LSQ with additional parameters which describes the noise explicitly.

Pulsar timing observations give a good possibility to estimate energy density of gravitational wave background and search for gravitational waves. In such measurements system "pulsar - observer" is considered as a base of gravitational detector sensitive to perturbations of space-time metrics along the pulsar pulse path. Estimation of energy density of GWB is well developed

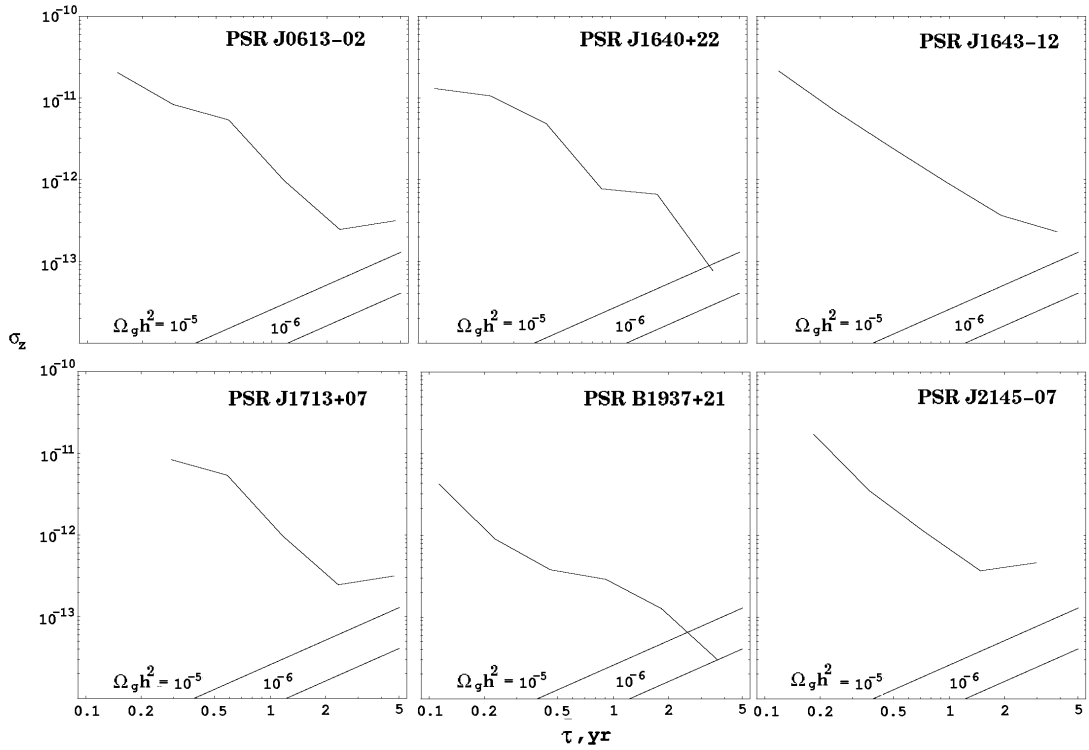

Figure 2: Fractional instabilities σ_z. Theoretical σ_z for $\Omega_g h^2 = 10^{-5}$ and 10^{-6} are presented.

in time domain by using statistics σ_z (Matsakis et al., 1996) at frequency range $10^{-7} - 10^{-9}$ Hz and by variations of derivative of binary period $\Delta\dot{P}_b$ and derivative of projection of semi-major axis to line of sight $\Delta\dot{x}$ at frequency range $10^{-9} - 10^{-11}$ Hz (Kopeikin, 1999). According to σ_z measurements based on timing of PSR 1937+21 the energy density of GWB $\Omega_g h^2 < 10^{-6}$ and according to measurements $\Delta\dot{x}$ and $\Delta\dot{P}_b$ based on the timing of PSR 1640+22 (Potapov et al., 2003) the estimation $\Omega_g h^2 < 10^{-4}$.

3. PULSAR VLBI

Now a lot of pulsars have been observed by VLBI technique. But the most of the observations have been aimed to measure pulsar parallaxes and proper motions. Such measurements are performed by differential VLBI method relative to close reference sources. It is favourable if the reference sources are in the list of the ICRF primary objects. But usually the reference sources are very veak and not in ICRF catalog and appropriate only for differential measurements of parallaxes and proper motion of pulsars. Thus only few pulsars have accurate VLBI positions at milliarcsecond level.

Pulsar astrometry department of PRAO has being conducted pulsar VLBI observations at Kalyazin (Russia) - Kashima (Japan) by absolute method since 1995 (Rodin, Ilyasov, et. al, 1996). The main purpose of this observations is to obtain accurate positions and proper motion. A total of five pulsar positions have been measured (Sekido, 2001) at frequencies 1.4 and 2.3 GHz. There used radio telescope RT-64 at Kalyazin and RT-34 at Kashima. Signal recording has been performed at 32 MHz bandwidth using K4 registrators from CRL on both stations. Gating function has been applied when correlating pulsar data for increasing signal to noise ratio (Rodin, Sekido, 2002).

Eulerian angles from DE200 to ICRF have been calculated on the basis of Russian-Japanese

	Finger et al., 1992	Folkner et al., 1994	Rodin, Sekido, 2001
A_x	1 ± 3	-2 ± 2	-4 ± 2
A_y	-10 ± 3	-12 ± 3	-13 ± 3
A_z	-4 ± 5	-6 ± 3	-19 ± 5

Table 1: Eulerian angles from DE200 to ICRF. Finger et al. and Folkner et al. have used combined VLBI and lunar laser ranging data. Rodin, Sekido have used pulsar VLBI and timing observations.

and other pulsar VLBI observations. Table 1 contains the values of A_x, A_y, A_z calculated at previous epoch by different methods. One can see that there is significant rotation between DE200 and ICRF around z-axis.

4. CONCLUSION

Pulsar astrometry takes an important role in the fundamental astrometry and time metrology, astrophysics and cosmology. Hight stability of pulsar rotational periods and measurement accuracy of TOAs allows to investigate fine effects related with proper pulsar rotation, signal propagation through interstellar medium, interaction of pulsars with other massive bodies, microlensing effects, searching gravitational waves and stochastic background.

High positional accuracy of pulsars gives a possibility to link different celestial systems with milliarcsecond accuracy. It is obvious that as the number of pulsars with well determined positions relative to ICRF is increasing the link accuracy of celestial systems would achieve sub-milliarcsecond level.

It is also possible to consider pulsars as a supplement to extragalactic sources which forms ICRF catalog. Despite their large proper motions pulsars have advantage over quasars due to small angular size unresolved by modern VLBI.

In the field of time metrology timing of several pulsars offers good possibility to establish pulsar time scale independent from TAI scale when it excluded from final TOAs by timing of one pulsar against others. An ensemble of reference pulsars can significantly improve pulsar time scale accuracy (Petit, Tavella, 1996). Since pulsar time scale is valid on relatively long time intervals (10-100 years) it provides natural basis for monitoring usual atomic standards which have comparatively short life time. If to extend the same idea to longer than 100 years time intervals then one needs to monitor pulsars which form pulsar time scale relative to binary pulsar time scale BPT which is stable on very long time intervals 100-1000 years.

Acknowledgements Authors expresses gratitude to Russian Fund of Basic Research (grant No 03-02-16911) and Russian Science and Technology Ministry (Russia-Japan project "Pulsar astrometry").

5. REFERENCES

Finger M.H., Folkner W.M., 1992, in TDA Progress Report 42-109, JPL,Pasadena CA, p.1.

Folkner W.M., Charlot P., Finger M.H., Williams J.G., Sovers O.J., Newhall X.X., Standish E.M., Jr, *Astron. Astrophys.*, **287**, 279 (1994).

Yu.Hanado, Ya.Shibuya, M.Hosokawa, M.Sekido, T.Gotoh, M.Imae, Timing observation of the millisecond pulsar PSR 1937+21 using the Kashima 34 m antenna, Publ. Astron. Soc. Japan, **54**, 305, 2002.

Ilyasov, Yu.P., Kopeikin, S.M. & Rodin, A.E. "A New Astronomical Time Scale Based on the Orbital Motion of Pulsar in a Binary System", Astron. Lett., No 4, 228 (1998).

S.M.Kopeikin, Phys.Rev.D, **56**, 4455, 1997.

D.N.Matsakis, J.H.Taylor, T.M.Eubanks, *Astron. Astrophys.***326**, 924 (1997).

V.Potapov, Yu.Ilyasov, V.Oreshko, A.Rodin, Timing results for the binary millisecond pulsar J1640+2224 on the RT-64 radio telescope in Kalyazin. Astron. Lett., v. 29, No 4, 282 (2003).

A. E. Rodin, Yu. P. Ilyasov, V. V. Oreshko, A. E. Avramenko, B. A. Poperechenko, M. Sekido, M. Imae, Y. Hanado. Pulsar VLBI on Kalyazin (Russia) – Kashima (Japan) baseline. 1996, Proceedings of the TWAA, 10-13 December 1996, Kashima, Japan, p. 265-268.

A. E. Rodin, Yu. P. Ilyasov, V. V. Oreshko, M. Sekido. Timing noise as a source of discrepancy between timing and VLBI pulsar positions. Proceedings of the Colloq. IAU 177, 31 Aug. - 3 Sep. 1999, Bonn, Germany, p.145.

A.E.Rodin, Pulsar Astrometry in presence of the low-frequency noise", PhD Thesis, Lebedev Physical Institute, 2000. (*in Russian*)

A.Rodin, M.Sekido Pulsar astrometry by VLBI and timing, 2001, Chuo University, Tokyo, Radio Science - Communications, Environment, and Energy Conference Digest. p. 47.

A.Rodin, M.Sekido, Pulsar VLBI Observations, Proceedings of the 6th European VLBI Network Symposium, E. Ros, R.W. Porcas, A.P. Lobanov, & J.A. Zensus (eds.), 25-28 June 2002, Bonn, Germany, p. 247.

STATISTICS OF DOUBLE STARS FOR ICRS OPTIC REALIZATIONS

G.A. GONTCHAROV
Pulkovo observatory
Saint-Petersburg, 196140, Russia
e-mail: georgegontcharov@yahoo.com

ABSTRACT. Classification and statistics of visual, spectroscopic, astrometric, interferometric, and photometric non-single stars are given for Hipparcos and Tycho2 based on WDS, CCDM, TDSC, 6^{th} catalogue of visual orbits, 9^{th} catalogue of spectroscopic orbits, and others. Some distinctions between single and non-single stars are emphasized by statistics and kinematics of nearly 20000 Hipparcos stars compiled by us in the Local Stellar System database by completeness of information on position, proper motion, parallax, radial velocity and duplicity. About 1/3 of these stars are non-single ones. They have less space velocities and their dispersions than single stars. Two projects of investigation of non-single stars in optic realizations of the ICRS (such as TAC2, CPC2, AC2000.2, UCAC2, 2MASS, GSC2, USNO B1) are proposed. The statistics of hidden non-singles among the faint stars is obtained after an inspection of images of the sky surveys in comparison with data given in these catalogues [1].

1. GENERAL CLASSIFICATION AND STATISTICS OF NON-SINGLE STARS

A complete and robust classification of stellar pairs by method can be done:

- **Visual pairs** – close pairs on the sky with both components visible. They could be divided by further study into: 1) optical pairs, the results of projections of stars with different parallaxes one near another on the sky, 2) common proper motion (CPM) pairs (usually with separation >20000 AU), 3) fixed pairs (usually with separation <20000 AU), 4) linear pairs with slightly changing separation and/or positional angle and 5) orbital pairs with elliptical motion of the both components.
- **Interferometric pairs** – largely observed by interferometry (see Hartkopf et al. (2003)).
- **Astrometric pairs** – unresolved pairs detected by a variation of photocentre's proper motion (in other words, by its non-linear motion). They can be divided into: 1) delta-mu pairs with proper motion significantly varies from one catalogue to another (they should be considered as astrometric pair candidates until detection of a realistic elliptical motion of the photocentre) (see Wielen et al. (2002)), 2) astrometric pairs, as such, with detected elliptical motion of photocentre giving realistic masses of components (see Gontcharov & Kiyaeva (2002)) and 3) variability-induced movers (VIM) with a specific motion and variation of photocentre (see Hipparcos catalogue description).

[1]Financially supported by the Russian Foundation for Basic Research grant #02-02-16570

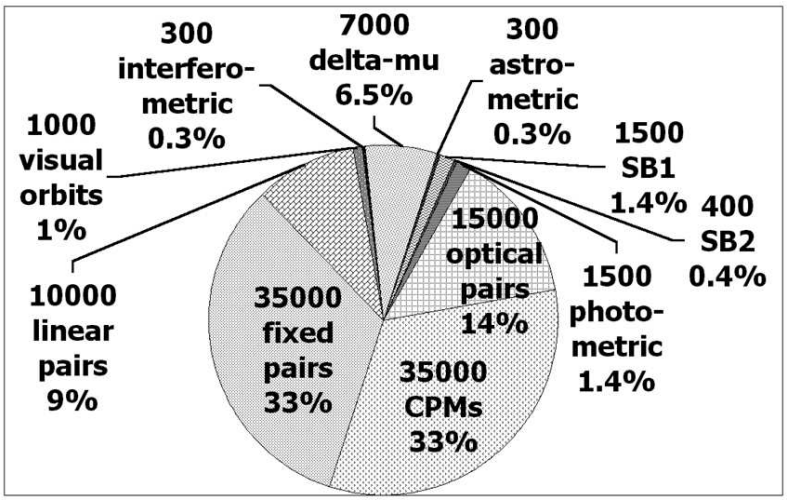

Figure 1: Number and percentage of various classes of non-single stars.

- **Spectroscopic pairs** – with periodic variations of radial velocity due to an elliptical motion. They should be divided into: 1) spectral pairs (long-period SB) with composite spectrum but without motion of lines, 2) SB1 (including exoplanets) with a moving lines of one (brighter) component and 3) SB2 with motion of both sets of lines.
- **Photometric pairs** with specific variability. They include: eclipsing pairs, occultation pairs with a photometric variation in lunar or other occultation and close pairs such as cataclysmic variables and so on.

The current main sources of non-single stars' data are the 6^{th} Catalog of Orbits of Visual Binary Stars by Hartkopf & Mason (2003) with 4865 orbits for 1633 stellar systems (in addition to visual orbits it contains about 300 ones obtained almost purely from speckle-interferometric observations and about 300 purely astrometric orbits; 9^{th} Catalogue of Spectroscopic Binary Orbits by Pourbaix & Tokovinin (2003) with 1895 spectroscopic orbits, about 1500 for SB1 and 400 for SB2; 4^{th} Catalog of Interferometric Measurements of Binary Stars by Hartkopf et al. (2003) with 47000 pairs resolved by interferometry and occultations; Washington Double Star Catalog (WDS) by Mason, Wycoff, & Hartkopf (2003) with over 500000 means of about 100000 visual and astrometric pairs; Tycho Double Star Catalogue (TDSC) by Fabricius et al. (2002) with results for 103259 binaries including 13251 new visual binaries; Catalog of Components of Double and Multiple stars (CCDM) by Dommanget, & Nys (2002) with 105838 components of 49325 visual binaries; ARIHIP catalogue by Wielen et al. (2002) with data for over 7000 delta-mu binaries among Hipparcos stars. One pair can appear in several catalogues. For example, TDSC, CCDM and WDS have many crosses. The total number of cataloged pairs is near 107000. About 92000 of them have no evidence to be optical.

The number and percentage of non-single stars of various classes is presented in Fig. 1. The VIM and spectral pairs are not shown because they are rare. Visual pairs including unrecognized optical, CPM, fixed and linear pairs are about 90% of known pairs. About 92% of known pairs are simple pairs (binaries, or double stars) and 5% – non-hierarchical triples. 32 of 40 nearest stars should be considered as known or suspected members of double and multiple systems (this number is under discussion and tend to be higher in future). The percentage of non-single stars considerably decrease with the distance from the Sun after 100 pc that is seen in Fig. 2. That can be explained by inefficiency of visual and some other methods for detection and separation of distant pairs. 70% of known pairs have magnitude difference of components $< 3^m$ which is a result of an observational selection. 70% of known pairs are in the northern celestial hemisphere

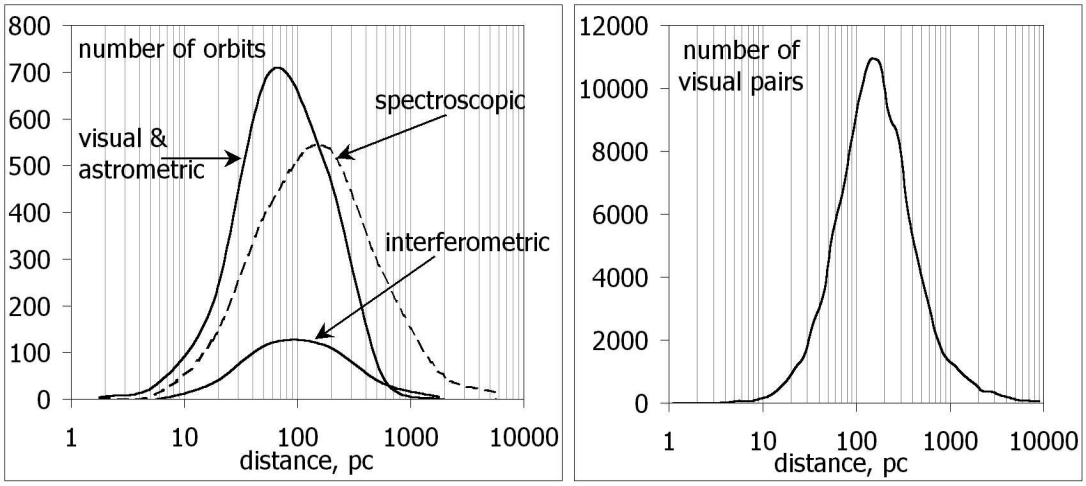

Figure 2: Distribution of known orbits (left) and visual pairs (right) with distance from the Sun.

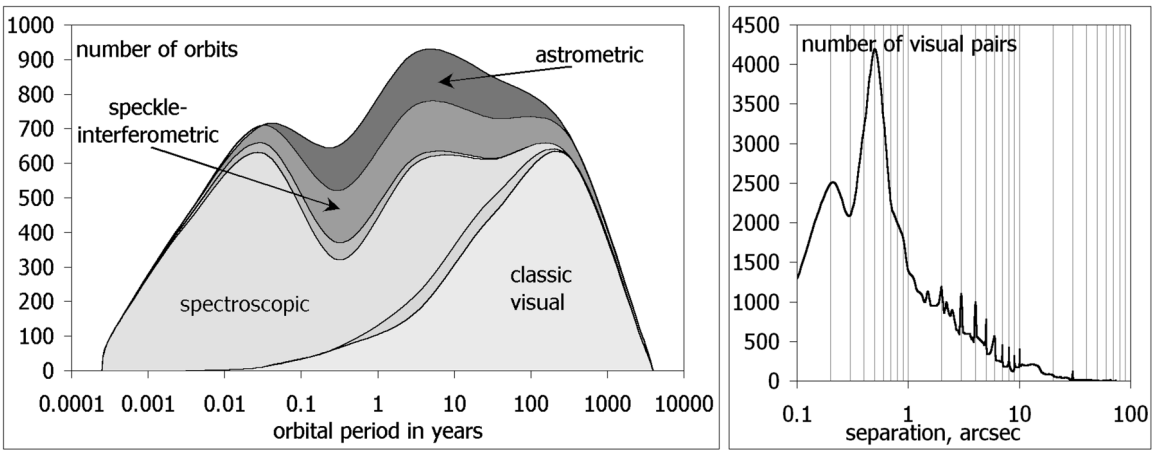

Figure 3: Left:The distribution of known visual, spectroscopic, speckle-interferometric and astrometric orbits with orbital period. Some crosses are seen as wide darker borders of the domains. Some gap at fractions of year can be explained by observational selection due to weather and seasonal periodicity. Right: The distribution of visual pairs with separation (arcsec).

where more observers. Majority of the naked-eye stars (m$< 5.5^m$) and minority of fainter stars are non-singles. The known orbits demonstrate expected distribution with orbital inclination and eccentricity. The current conclusions on complanarity of orbits in multiple systems are controversial. Also there is no clear evidence of a statistical relation between orientation of the orbits and any plane in the Solar system, Gould belt or Galaxy.

For the last decade the distribution of known orbits with orbital period (consequently with semi-major axis) becomes almost normal as shown in Fig. 3. This is a result of the progress in interferometric methods and successful combinations of Hipparcos with ground-based catalogues revealing new astrometric binaries.

2. NON-SINGLE STARS IN THE ICRS REALIZATIONS

Some optical realizations of the ICRS are presented in Tables 1 and 2 (see references).

Brighter components of 1483 visual (91%) and 1447 spectroscopic (76%) orbital pairs are

Table 1: Some optic realizations of the ICRS.

Catalogue	CDS number	Objects	Epoch	Released	Coverage
Hipparcos	I/239	118,218	1991	1997	all sky
ARIHIP	I/286	90,842	1991	2003	all sky
Tycho2	I/259	2,539,913	1991	2000	all sky
TAC2		705,099	1982	2000	-18 +90
CPC2	I/265	274,669	1968	1999	-90 +02
AC 2000.2	I/275	4,621,751	1907	2001	all sky
UCAC2		48,330,571	2000	2003	-90 +40
2MASS	II/246, VII/233	470,992,970	2000	2003	all sky
GSC2.2	I/271	435,457,355	1992	2003	all sky
USNO B1.0	I/284	1,045,913,669	1978	2003	all sky

Table 2: Some properties of optic realizations of the ICRS.

Catalogue	Accuracy	Resolution	Mag limit	Data
Hipparcos	0.001"	∼0.1"	∼14	$\alpha\delta\mu\pi$ V
ARIHIP	0.001"	∼0.3"	∼14	$\alpha\delta\mu\pi$ V
Tycho2	0.06"	∼0.3"	∼14	$\alpha\delta\mu\pi$ V B
TAC2	0.05"	∼3"	6–11	$\alpha\delta$ V B
CPC2	0.05"	∼3"	6–10.5	$\alpha\delta$ ∼B
AC 2000.2	0.3"	∼3"	∼12	$\alpha\delta$ B
UCAC2	∼0.05"	∼3"	8–16	$\alpha\delta\mu$ ∼R
2MASS	∼0.1"	∼2"	∼15	$\alpha\delta$ 3 bands
GSC2.2	∼0.3"	∼2"	∼19	$\alpha\delta$ 2 bands
USNO B1.0	∼0.2"	∼2"	∼21	$\alpha\delta\mu$ 3 bands

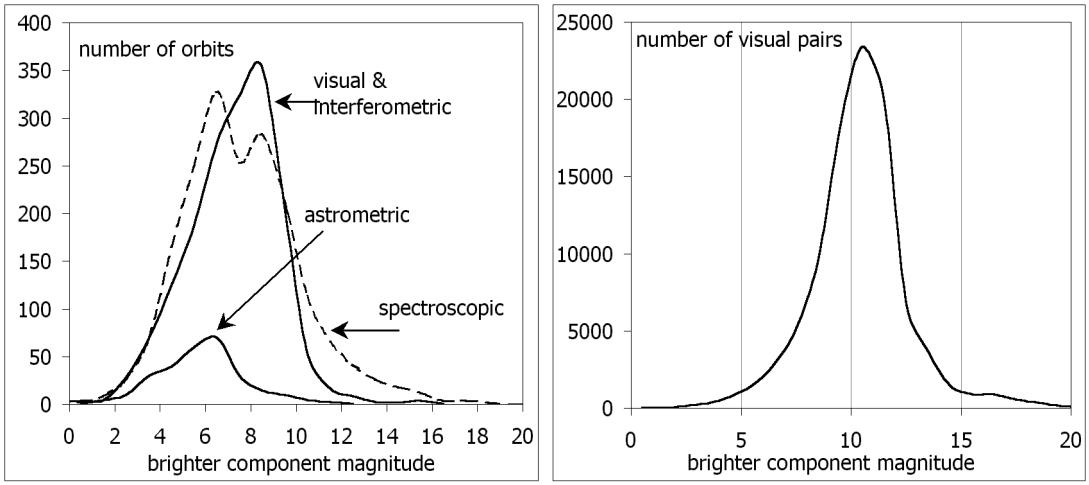

Figure 4: Distribution of known orbits (left) and visual pairs (right) with magnitude of brighter component.

Hipparcos stars. The rest are mainly among Tycho2 stars. Brighter components of nearly 17000 visual and interferometric pairs are Hipparcos stars, and about 53000 ones are Tycho2 stars presented in the TDSC. About 7000 delta-mu binaries and 300 well investigated astrometric binaries are Hipparcos stars. Also about 8000 stars were suspected as non-single stars by the Hipparcos team. Many of them have not proved the duplicity, but some thousands still should be considered as astrometric binary candidates.

Thus, almost all non-single stars of all groups are Hipparcos or Tycho2 stars. The fainter realizations of the ICRS are still mostly unused material in detection of duplicity. It is reflected in the distribution of orbital and visual pairs with magnitude of brighter component in Fig. 4.

The current realizations of the ICRS can be divided into 2 groups with different limiting magnitudes. Two projects to reveal and investigate new non-single stars can be developed with them. The first 6 catalogues in Table 2 together with UCAC2 and some modern observational catalogues such as M2000 (Bordeaux) and CMC12 (La Palma) would give α and δ for at least 4 epochs, as well as μ, π, B, V, R for 2500000 Tycho2 stars. The multiepoch astrometry may reveal thousands non-linearly moving photocentres (astrometric binary candidates). The calculation of color indices and photometric parallaxes to test the reliability of separation-period-mass relations for these pairs would be a next step in evidence of their duplicity. This may be a way to reveal some 1000 new astrometric binaries of $8^m - 12^m$.

Fainter catalogues (UCAC2, 2MASS, GSC2 and USNO B1) can be used in another project: to reveal and investigate visual pairs of $8^m - 16^m$ comparing these catalogues one to another and with the digitized sky surveys. Our inspection of a hundred survey fields of 12'x12' accidentally selected from the Aladin Interactive Sky Atlas at the CDS with nearly 200000 stars from USNO B1 shows that 1) about 15% of the 12^m stars and up to 40% of the $16^m - 18^m$ stars have neighbouring star of Δm$< 3^m$ within 10 arcsec; 2) at least 25% of such satellites of the $8^m - 12^m$ stars are not listed in USNO B1; 3) but nearly 25% other objects near bright stars in USNO B1 are bright images' spikes and other mistakes. Thus, millions uncatalogued visual pairs with separation of 2–10 arcsec are hidden both in the faint catalogues and sky surveys. To reveal those pairs more reliable proper motions, color indices and photometric parallaxes should be obtained in a mutual processing of the catalogues.

3. NON-SINGLE STARS IN THE LOCAL STELLAR SYSTEM DATABASE

To calibrate color indices, photometric parallaxes and other parameters important for further investigations of non-single stars the Local Stellar System (LSS) database of various parameters of 20000 best investigated stars is compiled by us. It is accessible at http://www.astro.spbu.ru/. Single stars and brighter components of pairs are Hipparcos stars. About 1/3 of the stars are non-single ones. The database contains equatorial and galactic spherical coordinates and proper motions, galactic rectangular coordinates X, Y, Z and velocities U, V, W, total space velocity, parallax, radial velocity, B and V magnitudes, $B-V$, absolute magnitude, parameters of duplicity and spectral type. Other parameters to be added. All parameters are inspected, the positions and velocities are recalculated as weighted means from the best sources. Several tests were applied to be sure that the proper motions and radial velocity give us an unbiased system of rectangular components of space velocity. The stars can be divided into 3 groups with different total space velocity, $B-V$ and absolute magnitude: earlier spectral classes (hereafter O-F) with $M < 3.5$ and $B-V < 0.8$, later classes (hereafter G-M) with $M > 3.5$ and red giants (hereafter RG) with $M < 3.5$ and $B-V > 0.8$. O-F stars have comparatively small space velocities whereas G-M and RG with larger velocities are very distinct by M. The percentage of non-singles is 34% for O-F, 31% for G-M and 24% for RG stars.

Detailed statistics, kinematics and calibration of the parameters of the stars will be published elsewhere. Here some distinctions between single and non-single stars are shown. Non-single

Table 3: Velocities and their standard deviations (s.d.) for single and non-single stars of 3 spectral groups in the LSS database. All values in km/s.

Group	Number of stars	U	V	W	s.d. U	s.d. V	s.d. W
O-F singles	6349	-8.9	-16.8	-7.3	38.9	46.5	23.8
O-F non-singles	3272	-9.3	-13.6	-7.4	24.5	21.9	16.8
RG singles	5377	-8.1	-21.4	-7.6	40.8	40.4	25.6
RG non-singles	1685	-6.8	-19.2	-8.3	34.2	29.1	18.7
G-M singles	2337	-12.2	-35.3	-8.2	56.3	54.6	29.0
G-M non-singles	1036	-10.2	-29.9	-9.1	48.2	45.6	25.6

stars have lower mean velocity than singles (29.1 ± 0.5 versus 30.8 ± 0.5 km/s). The standard deviation of the velocities is quite lower for non-single stars. It is presented in Table 3. The V velocity (along galactic rotation) of non-singles is closer to the velocity of the Sun than the one of singles. Fast stars are rare among non-single stars w.r.t. singles: the percentage of non-singles is about 34% at 5 km/s, 25% at 100 km/s and about 10% at >200 km/s.

Single and non-single stars show slightly different HR diagram. The majority of stars in the both groups are main sequence and slightly evolved stars with masses from 0.5 to 5 solar masses. However, the non-singles of the main sequence look systematically brighter and more red than singles whereas the non-singles of the giant branch look brighter and more blue than singles. There are several explanations for this effect (see, for example, Gontcharov et al. (2000)), but the influence of unresolved multiplicity is most evident.

4. REFERENCES

Cutri, R., et al. 2003, 2MASS, http://www.ipac.caltech.edu/2mass/

Dommanget, J., Nys, O. 2002, CCDM, Obs. Royal Belg., http://cdsweb.u-strasbg.fr/viz-bin/Cat?I/274

Fabricius, C. et al. 2002, *Astron.Astrophys.*, 384, 180

Gontcharov, G.A., et al. 2000, IAU 24^{th} General assembly abstracts, Manchester

Gontcharov, G.A., & Kiyaeva, O.V. 2002, *Astron.Astrophys.*, 391, 647

Hartkopf, W.I., & Mason, B.D. 2003, 6^{th} Catalog of Orbits of Visual Binary Stars, USNO, http://ad.usno.navy.mil/wds/orb6/orb6text.html

Hartkopf, W.I. et al. 2003, 4^{th} Catalog of Interferometric Measurements of Binary Stars, USNO & CHARA, http://ad.usno.navy.mil/wds/int4.html

Mason, B.D., et al. 2003, WDS, USNO, http://ad.usno.navy.mil/wds/

Monet, D.G. et al. 2003, USNO B1.0, http://www.nofs.navy.mil/data/fchpix/

Pourbaix, D., Tokovinin, A. 2003, 9^{th} Catalogue of Spectroscopic Binary Orbits, http://sb9.astro.ulb.ac.be/

STScI 2001, GSC2.2, http://www-gsss.stsci.edu/gsc/gsc2/

Urban S., et al. 2001, AC2000.2, http://ad.usno.navy.mil/ac/ac.html

Wielen, R. et al. 2002, Astrometric Catalogue ARIHIP, Astron. Rechen-Inst. Heidelberg, http://www.ari.uni-heidelberg.de/arihip

Zacharias, N., et al. 2003, UCAC2, http://ad.usno.navy.mil/ucac/

acharias, N., Zacharias, M. 1999, *Astron.J.*, 118, 2503,http://www.usno.navy.mil/ad.html

Zacharias, N., et al. 1999, *Astron.J.*, 117, 2895, http://www.usno.navy.mil/ad.html

A NEW APPROACH TO REPRESENTATION OF THE CATALOGUE SYSTEMATIC DIFFERENCES AS APPLIED TO MODERN HIGH PRECISION CATALOGUES

Y.B. KOLESNIK
Institute of Astronomy of the Russian Academy of Sciences
48 Piatnitskaya str., 109019 Moscow, Russia
e-mail: kolesnik@inasan.rssi.ru

ABSTRACT. The shortcomings of the analytical approximation of the catalogue systematic differences by a set of orthogonal basis functions motivated an application of a radically different approach based on the approximation of the systematic differences by the multidimensional smoothing splines. The mathematical basics of the new method are presented and its advantages are demonstrated by comparison of the approximations of the FK5-HIPPARCOS proper motions with both methods.

1. INTRODUCTION

Mignard & Froeschle (2000) and Schwan (2001) published and recommended for general use the systematic differences between FK5 and Hipparcos derived by different methods. The plots of proper motion systematic differences presented by Schwan show the dramatic level of discrepancy between methods reaching up to 2 mas/yr, i.e. of the same order as the systematic differences themselves. The question arises: how can we consider reliable the existing techniques of separation between random and systematic components of catalogue differences after such confusion?

The analytical method was firstly applied to the catalogue astrometry by Brosche (1966), and, in the final form was developed by Bien et al. (1978). It models the three dimensional surface of the systematic component as a series orthogonal functions. The significance of coefficients corresponding to a certain function left in the development is determined with Fischer's test on the basis of a priori chosen significance level. 5% level usually applied. The higher significance level is chosen, less functions are left. In this way, the analytical procedure acts as a low frequency filter with the transfer function completely dependent on the limiting significance level. Since initially the actual character of the systematic component is unknown, application of the same 5% significance level cannot be considered as justifiable.

The other shortcomings of the analytical method have been investigated and outlined by (Taff et al. 1990). They are as follows: the method approximates globally initially unknown 3-dimentional surface; it tracks the differences on the smallest possible scale and then simultaneously globally broadcasts them; the number of dimensions is limited to 3.

2. THE BASICS OF THE MULTIVARIATE SPLINE SMOOTHING TECHNIQUE

The spline approximation is known as an alternative to the analytical method. Its advantages are as follows: 1) it approximates the catalogue differences piecewisely with simple polynomials as the basis functions, so that it is not constrained with a certain a priori chosen global model; 2) it let the smoothing coefficient be flexibly fitted to a desired transfer function; 3) it let the unlimited number of dimensions.

The multidimensional generalization of the ordinary polynomial spline approximation was firstly suggested by Duchon (1976). The mathematical basics of this technique can be found in the textbook Wahba (1990). We consider to model the observed noisy data $(\boldsymbol{x}_i, z_i)$, $i=1,2...N$ with the formal errors σ_i in $d-$dimensional space $x_i \in R^d$with a smooth function $u(\boldsymbol{x}_i)$ so that $z_i = u(\boldsymbol{x}_i)+\varepsilon_i$. The Laplacian smoothing spline (LSS) of degree $2m-1$ is the minimizer $u(\boldsymbol{x}_i)$ of the following expression.

$$S_\lambda(u) = \frac{1}{N}\sum_{i=1}^{N} \sigma_i^{-2}(z_i - u_i)^2 + \lambda J_m(u)$$

where

$$J_m(u) = \sum_{\alpha_1+...+\alpha_d=m} \frac{m!}{\alpha_1!\alpha_2!...\alpha_d!} \iint_{R^d} \left(\frac{\partial^m u(x_1, x_2...x_d)}{\partial x_1^{\alpha_1}...\partial x_d^{\alpha_d}} \right)^2 dx_1...dx_d$$

$\alpha_{1,\quad ...,}\alpha_{\mathrm{d}}$ are $M = \begin{pmatrix} m+d-1 \\ d-1 \end{pmatrix}$ unique combinations of (0,1,. . . ,m).

The integral of the partial derivatives of the function $u(\boldsymbol{x}_i)$ to be derived is the measure of smoothness, and the parameter λ controls the tradeoff between "roughness" of the solution as measured by the second term, and infidelity to the data as measured by the first term.

The smoothing coefficient λ and the order of the partial derivative m are the "turning parameters" of the method. In the procedure of the dynamical fitting of the degree of smoothing an approximation with a certain smoothing parameter yields vectors of a spline function and residuals $\boldsymbol{z}=\boldsymbol{u}(\lambda)+\varepsilon(\lambda)$. Each vector is, in turn, some mixture of the systematic and noisy components: $\boldsymbol{u}(\lambda)=\boldsymbol{u}_s+\boldsymbol{u}_n$ and $\varepsilon(\lambda)=\varepsilon_s+\varepsilon_n$, where $\boldsymbol{u}_s$ and ε_s are systematic components, $\boldsymbol{u}_n$ and ε_n are noisy components. Optimum smoothing corresponds to the case when the noisy component of the spline approximation and the systematic component of the residuals reach minimum $\mathbf{u}_{\mathrm{n}} \rightarrow min$, $\mathbf{r}_{\mathrm{s}} \rightarrow min$. It can be regarded as a statistically justified compromise between an over fitting and an under fitting.

Since the form and character of the real systematics is a priori unknown, the only way to find the optimum smoothing is the analysis of the residuals looking for minimization of its systematic component in the procedure of scanning different λ. In this way, the problem reduces to stochastic filtering.

The cross-validation method was developed especially for appropriate choice of the smoothing coefficient in the spline smoothing technique. It is based on the "one-leave-out" idea (Mosteller & Tukey 1968). The spline approximations $u_{m,\lambda}^{(k)}$is sequentially estimated with k point dropped out. The optimum smoothing corresponds to the minimum of the cross-validation function.

$$V_m^0(\lambda) = N^{-1}\sum_{k=1}^{N} (u_{m,\lambda}^{(k)} - z_k)^2 \sigma_k^{-2} \rightarrow min$$

Ordinary cross-validation applies to symmetric case of equally spaced data and periodic underlaying signal. The generalized cross-validation function (GCVF) was suggested to compensate for effect of nonequally spaced data and possible nonperiodicity of the systematic component by minimizing a certain weighted version of the above expression

$$V_m(\lambda) = N^{-1}\sum_{k=1}^{N} w_k(\lambda)(u_{m,\lambda}^{(k)} - z_k)^2\sigma_k^{-2}$$

$$w_k(\lambda) = \left[(1 - a_{kk}(\lambda))/\frac{1}{N}Tr(I - A_m(\lambda))\right]^2$$

A_m is the hat prediction matrix, I is the singular matrix.

The cross-validation method may be regarded as the form of selection of the optimum rigidity of the underlying systematic component corresponding to the actual noisy component of the data. For this reason, it can viewed also as a kind of stochastic filtering.

3. APPLICATION OF THE SPLINE SMOOTHING FOR APPROXIMATION OF THE CATALOGUE SYSTEMATIC DIFFERENCES

To compare the analytical method to the spline smoothing we approximated the FK5-HIPPARCOS proper motion differences discussed by Schwan (2001). We used for this the coefficients of the analytical development deposited at the Heidelberg web site.

The residual differences are modeled with Laplacian smoothing splines (LSS) in 4-dimentional space as a function right ascension, declination, magnitude m and spectral index γ on positions of the FK5 stars.

$$\Delta_i = u_i\ (\alpha,\ \delta,\ m,\ \gamma) + \varepsilon_i$$

The results of the dynamical fit of the smoothing coefficient are shown in Fig. 1.

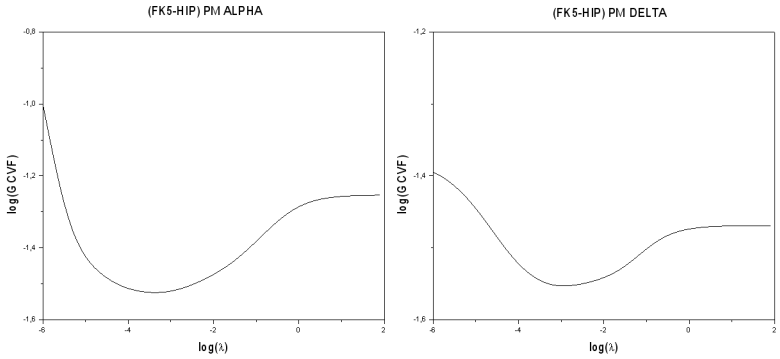

Figure 1: Dynamical fit of the smoothing coefficient λ on the basis of generalized cross-validation method.

Slight magnitude equation in declination and strong color equation in right ascension was found (see Fig. 2) while Schwan does not detect them with the analytical method.

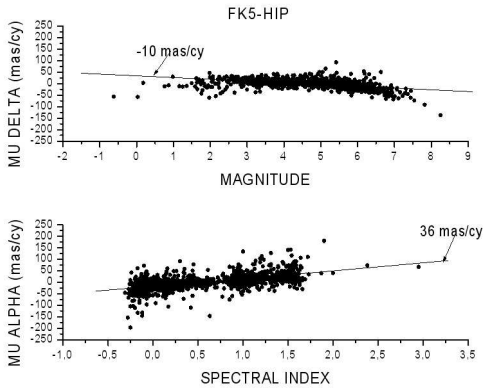

Figure 2: Significant magnitude and color equations of the FK5-Hipparcos proper motion differences.

The analytical and spline approximations of the proper motion differences in right ascension and declination are shown in Fig. 3 and 4. For spline approximation we give the four dimensional representation on positions of FK5 stars as a function of two equatorial coordinates, magnitude and spectral index (bottom) as well as the part of the systematic component depending on right ascension and declination only (in the middle). The general impression is that the analytical approach produces the false periodic systematics while the cross-validation does not detect it. On the other hand, the four dimensional spline representation shows highly irregular character of the systematics, not captured by the analytical approach.

In Fig. 5 the plots of differences between two methods are presented. The order of the differences is within 200 mas/cy in right ascension and 100 mas/cy in declination, i.e. by the order larger than the formal errors of the systematic components. If the present approach based on the dynamical fit of the approximation transfer function is believed statistically more rigorous, the differences are to be attributed to the analytical method.

4. REFERENCES

Bien R., Fricke W., Lederle T., Schwan H., 1978, Veröff. Astron. Rech. Inst. Heidelberg 29.

Brosche P., 1966, Veröff. Astron. Rech. Inst. Heidelberg Nr. 17.

Duchon J., 1976, in W. Schempp and K. Zeller (eds.) Constructive Theory of functions of Several Variables, p.85.

Mignard F., Froeschlé M., 2000, A& A 354, 732.

Mosteller F., Turkey J.F., 1968, Handbook of Social Psychology, vol. 2, Reading, MA, Addison-Wesley, p. 80-203.

Schwan H., 2001, A& A 367, 1078.

Taff L.G., Bucciarelli B, Lattanzi M.G., 1990, ApJ 361, 667.

Wahba G., 1990, Spline models for observational data, SIAM, Philadelphia.

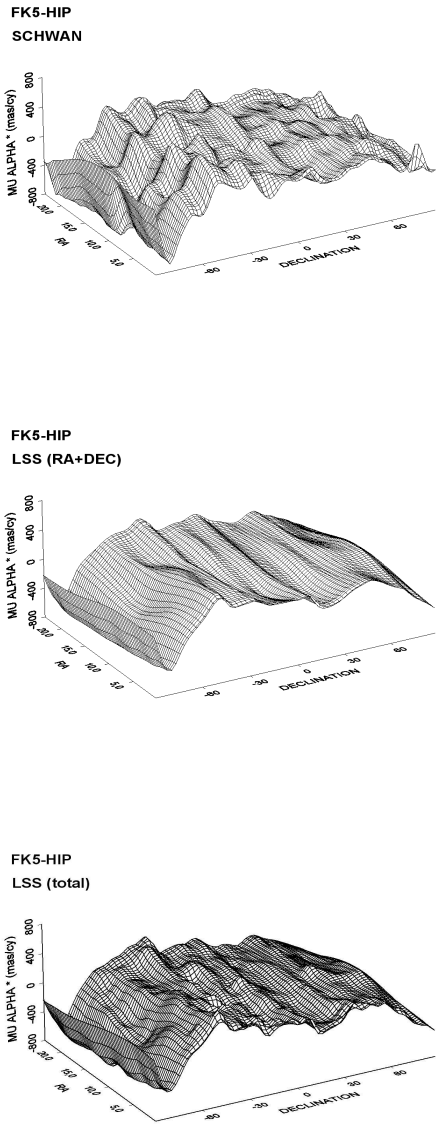

Figure 3: Approximation of the proper motion systematic differences FK5-Hipparcos in right ascension with the analytical method (upper plot) and with the Laplacian smoothing splines (LSS) below.

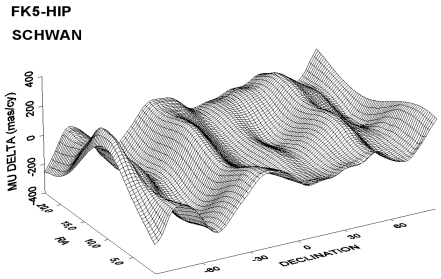

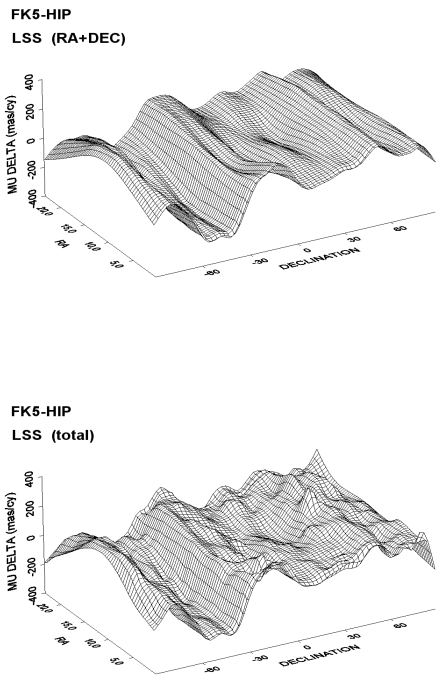

Figure 4: Approximation of the proper motion systematic differences FK5-Hipparcos in declination with the analytical method (upper plot) and with the Laplacian smoothing splines (LSS)below.

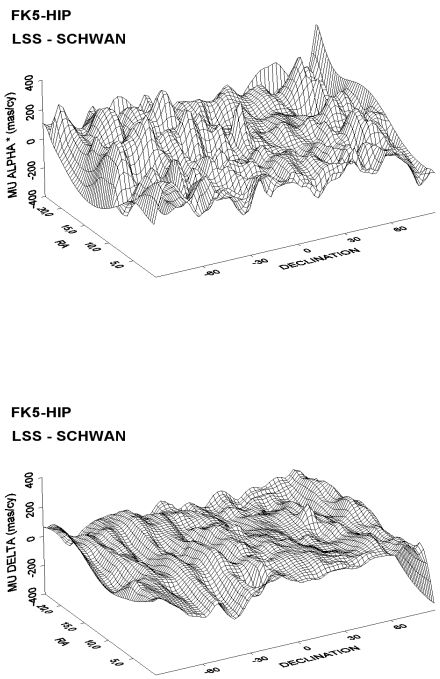

Figure 5: Differences between the multidimensional smoothing spline and the analytical approximations of the FK5-Hipparcos proper motions.

DOES PRECESSION DERIVED FROM FK5-HIPPARCOS AGREE WITH THE VLBI?

V.V. VITYAZEV
Sobolev Astronomical Institute of the SPb University
198904, SPb, Petrodvorets, Universitetsky PR., 28, Russia
Vityazev@venvi.usr.pu.ru

ABSTRACT. Modern determinations based on VLBI observations [1,2] yield the correction $\Delta p = -3.0 \pm 0.1\ mas/y$ to the IAU (1976) value of general luni-solar precession in longitude $p = 5029.0966''/cy$, $J2000.0$. Nevertheless, extensive study of the FK5 spin with respect to HIPPARCOS yields the correction $\Delta p = -1.5 \pm 0.7\ mas/y$ [3,4] which is not consistent with the VLBI. Aiming at the explanation for this fact, the paper presents an examination of the differences FK5-HIPPARCOS treated by different numerical techniques.

It was found that the proper motions of the FK5 in Right Ascension are consistent with the VLBI value of correction to the precessional constant, whereas the proper motions in Declination are not. From this it follows that the precessional correction must be derived only from the differences $\Delta\mu\cos\delta$. To this one should add that the commonly used routines to derive the precessional correction are based on combined solution of the equations for $\Delta\mu'$ and $\Delta\mu\cos\delta$ which assigns to the Declination system the weight three times more than to the R.A. system. It is due to this reason the result comes wrong. At the same time, the differences $\Delta\mu\cos\delta$ taken separately yield the correction $\Delta p = -3.5 \pm 0.1\ mas/y$ which is in good agreement with the VLBI.

1. THE BASICS

The Helmholtz theorem applied to velocity field of stars [5] states that an individual velocity of a star is expressed as the sum of a translation $\bar{V}_0$ (Solar motion)), a divergence characterized by a deformation ellipsoid S, and a spin of the stellar system $\bar{\omega}$:

$$\bar{V} = \bar{V}_0 + grad\ S + \bar{\omega} \times \bar{r}. \tag{1}$$

When the differences FK5-HIPPARCOS are used the only contribution to the difference $\Delta\bar{V}$ is expected from the spin since the Solar motion and the divergence terms vanish. Since the HIPPARCOS catalogue is free from precession and equinox motion, then in the differences FK5-HIPPARCOS the rigid body spin of the stellar system vanishes, and the spin is generated by the FK5 residual precession and non precessional motion of the equinox only:

$$\omega_1 = 0, \tag{2}$$

$$\omega_2 = -\Delta p\ \sin\epsilon, \tag{3}$$

$$\omega_3 = \Delta p\ cos\epsilon - (\Delta\lambda + \Delta e), \tag{4}$$

where ϵ - the tilt of ecliptic.

Thus we see that to find the correction to the constant of precession from the differences in proper motions FK5-HIPPARCOS one needs to solve the next equations of condition:

$$\begin{array}{rcrrr} \Delta\mu\cos\delta & = & -\omega_1\sin\delta\cos\alpha & -\omega_2\sin\delta\sin\alpha & +\omega_3\cos\delta, \\ \Delta\mu' & = & \omega_1\sin\alpha & -\omega_2\cos\alpha, & \end{array} \tag{5}$$

where

$$\begin{array}{rcl} \Delta\mu & = & \mu_{FK5} - \mu_{HIP}, \\ \Delta\mu' & = & \mu'_{FK5} - \mu'_{HIP}. \end{array} \tag{6}$$

2. THE LEAST SQUARES SOLUTION

It is common practice of evaluating the unknowns ω_1, ω_2 and ω_3 from combined solution of equations (5). Nevertheless, the separate solutions are possible too. It is not difficult to show that if the results of separate solutions are $\omega_1^\alpha, \omega_2^\alpha, \omega_3^\alpha$ and $\omega_1^\delta, \omega_2^\delta$, then the combined solution of Eqs. (5) looks like follows:

$$\begin{array}{l} \omega_1^c = \frac{1}{4}(\omega_1^\alpha + 3\omega_1^\delta), \\ \omega_2^c = \frac{1}{4}(\omega_2^\alpha + 3\omega_2^\delta), \\ \omega_3^c = \omega_3^\alpha. \end{array} \tag{7}$$

In other words: *each of ω_i^c is weighted average of ω_i^α and ω_i^δ with predominant contribution of the δ-components.*

From this it follows that the combined solution meets no objection if the systems of $\mu\cos\delta$ and μ' of both catalogues are free from systematic errors. Though the HIPPARCOS catalogue is claimed to have no systematic errors, it is not so in the case of FK5. In such situation the estimates of one-named parameters from separate solutions of equations (5) may differ dramatically giving evidence of large systematic errors in one (or both) systems. Since the result of combined solution is extremely sensitive to the errors of the declination system, the combined solution will give wrong result if the μ_δ system of the FK5 is worse than the $\mu\cos\delta$ system.

2. THE SOLUTION BY VECTORIAL HARMONICS

A new method to solve equations (5) was proposed in [6]. This approach is based on decomposition of the vector field

$$\tilde{\mathbf{V}} = V_\alpha\ \tilde{\mathbf{e}}_\alpha + V_\theta\ \tilde{\mathbf{e}}_\theta,$$

where $\theta = \pi/2 - \delta$, $\tilde{\mathbf{e}}_\alpha$,$\tilde{\mathbf{e}}_\theta$ – unit vectors, on a set of vectorial harmonics $\tilde{\mathbf{T}}_{lm}(\alpha,\theta)$ and $\tilde{\mathbf{S}}_{lm}(\alpha,\theta)$:

$$\tilde{\mathbf{V}}(\alpha,\theta) = \sum_{m=-l}^{m=+l}\sum_{l=1}^{\infty}(t_{lm}\,\tilde{\mathbf{T}}_{lm}(\alpha,\theta) + s_{lm}\,\tilde{\mathbf{S}}_{lm}(\alpha,\theta)). \tag{8}$$

The most attractive feature of this method is the fact that the rigid body rotational field

$$\tilde{\mathbf{V}} = (-\omega_1\cos\alpha\cos\theta - \omega_2\sin\alpha\cos\theta + \omega_3\sin\theta)\ \tilde{\mathbf{e}}_\alpha + (-\omega_1\sin\alpha + \omega_2\cos\alpha)\ \tilde{\mathbf{e}}_\theta \tag{9}$$

is determined only through the coefficients

$$t_{10} = \sqrt{\frac{8\pi}{3}}\ \omega_3, \tag{10}$$

$$t_{11} = \sqrt{\frac{4\pi}{3}}\ (-\omega_1 + i\omega_2). \tag{11}$$

It is this method that was used to find the parameters of mutual orientation and spin of the FK5 and HIPPARCOS [7]. Still, this property of vectorial functions must be treated with caution. Really, if the proper motions in $\alpha-$ and $\theta-$directions are generated by different spins with parameters ω_1^θ, ω_1^α and ω_2^θ, ω_2^α, i.e.

$$\tilde{\mathbf{V}} = (-\omega_1^\alpha \cos\alpha\cos\theta - \omega_2^\alpha \sin\alpha\cos\theta + \omega_3 \sin\theta)\ \tilde{\mathbf{e}}_\alpha + (-\omega_1^\theta \sin\alpha + \omega_2^\theta \cos\alpha)\ \tilde{\mathbf{e}}_\theta, \tag{12}$$

then equation (11) is replaced by

$$t_{11} = \sqrt{\frac{\pi}{12}}\ [-(\omega_1^\alpha + 3\omega_1^\theta) + i(\omega_2^\alpha + 3\omega_2^\theta)]. \tag{13}$$

Now, from (11) and (13) we again get equations (7). This tells us that when the parameters of the spin are different, the vectorial functions have no advantages over the least square combined solution of equations (5). Nevertheless, if both components of proper motions are consistent with a model, the decomposition of proper motions on vectorial functions is promised to be very powerful tool. Recently the application of this method was made to all terms of equation (1). Besides the low order classical terms this approach revealed some higher order harmonics which are beyond the model [12].

2. THE SOLUTION BY SCALAR HARMONICS

Now we are in position to answer the question: which solution is reliable? This requires a more sophisticated method to penetrate into the essence of separate solutions. In this connection we propose to use the decomposition of each components $\Delta\mu\cos\delta$ and $\Delta\mu'$ on a set of the scalar (not vectorial) harmonics

$$\Delta\mu\cos\delta = \sum_{nkl} C_{nkl}\ \ Z_{nkl}(\alpha,\delta), \tag{14}$$

$$\Delta\mu' = \sum_{nkl} C'_{nkl}\ \ Z_{nkl}(\alpha,\delta), \tag{15}$$

where Z_{nkl} are the spherical functions. This technique was proposed by Brosche [8] for representing the systematic differences of two catalogues. Later on, it was elaborated by the author [9,10] for deriving rotation between two reference frames and for kinematical analysis of the proper motions [11]. The main idea of this approach may be explained as follows.

Suppose the decompositions (14) and (15) are made and the coefficients C_{nkl} and C'_{nkl} are derived. It is not difficult to show that in the case of the rigid spin of the frames there are three subsets of the C_{nkl} which are proportional to one of the components $\omega_1, \omega_2, \omega_3$ and two subsets of the C'_{nkl} which are proportional to one of ω_1, ω_2. This means, *and this is the crucial point of the method*, that each of the parameters ω_i may be evaluated at least twice (in the theory as many times as needed). Namely, from $\Delta\mu\cos\delta$ one may derive ω_1 from C_{211}, C_{411}; ω_2 – from C_{210}, C_{410}; ω_3 – from C_{001}, C_{201}, as well as from $\Delta\mu'$ one may calculate ω_1 – via C'_{110}, C'_{310} and ω_2 – via C'_{111}, C'_{311}.

If two estimates of, say ω_1, coincide within the limits of their errors we may be sure that the data contains spin, and this conclusion is made for each sets $\Delta\mu\cos\delta$ or $\Delta\mu'$ independently. We emphasize, that this approach in contrast to commonly used mathematical tools, provides a test that the model is (or not) compatible with the data. It is due to this ability of the scalar harmonics one can make a choice between two alternatives in case when the one-named parameters of equations (5) come different from the separate solutions of these equations.

3. NUMERICAL RESULTS

In this section we present results obtained by solutions of equations (5) from differences $\Delta\mu\cos\delta$ and $\Delta\mu'$ calculated for 1232 stars common to FK5 and HIPPARCOS catalogues.

Table 1: Spin and correction to the precession constant from separate and combined solutions, mas/y, 1232 stars.

	From $\Delta\mu\cos\delta$	From $\Delta\mu'$	From $\Delta\mu\cos\delta$ and $\Delta\mu'$
ω_1	0.32±0.20	-0.56±0.11	-0.32±0.14
ω_2	0.98±0.20	0.48±0.11	0.61±0.14
ω_3	0.80±0.11	-	0.80±0.14
Δp	-2.5± 0.5	-1.2±0.3	-1.5±0.4

The separate and combined solutions are shown in Table (1). From this table one can see that the estimates of the components ω_1 and ω_2 following from separate and combined solutions differ significantly. The values of the correction to the precession constant Δp following from each of solutions are different too, and nothing can be said what solution is preferable. Still, the separate solutions being discordant give evidence that something is wrong and the further analysis is needed.

This more penetrative analysis comes from the scalar harmonics method (Tables 2-3).

Table 2: Spin from $\Delta\mu\cos\delta$ by scalar harmonics, mas/y, 1232 stars.

	n	k	l	First value	n	k	l	Second value
ω_1	2	1	1	0.06 ± 0.21	4	1	1	0.90 ± 0.57
ω_2	2	1	0	**1.39 ± 0.20**	4	1	0	**1.17 ± 0.54**
ω_3	0	0	1	0.62 ± 0.10	2	0	1	3.18 ± 0.34

Table 3: Spin from $\Delta\mu'$ by scalar harmonics, mas/y, 1232 stars.

	n	k	l	First value	n	k	l	Second value
ω_1	1	1	0	-0.58 ± 0.11	3	1	0	-1.02 ± 0.43
ω_2	1	1	1	0.37 ± 0.11	3	1	1	1.89 ± 0.44

Now we see that both estimates of ω_1 and ω_3 derived from either first or second equations (5) are discordant. The same result is stated for ω_2 obtained from $\Delta\mu'$. This is sufficient to make a conclusion that there is no rigid body rotation in the system of μ' of the FK5 with respect to

HIPPARCOS frame. On the contrary, both estimates of ω_2 derived from first equation (5) have good agreement, and this tells us that the only component of the FK5's proper motions suitable for determination of precession is $\Delta\mu\cos\delta$.

4. CONCLUSIONS

It may be argued that the results described above are due to specific properties of the sample under consideration. To see what happens when another sample is taken, we choosed the sample of 512 distant stars which were used by Fricke [13] for deriving the constant of precession IAU 1976. The differences FK5-HIPPARCOS of these stars have been treated in the same way as the sample of 1232 stars. The results are shown in Tables 4, 5 and 6.

Table 4: Spin and correction to the precession constant derived from 512 differences FK5-HIPPARCOS, mas/y.

	From $\Delta\mu\cos\delta$	From $\Delta\mu'$	From $\Delta\mu\cos\delta$ and $\Delta\mu'$
ω_1	0.61±027	-0.68±0.11	-0.35±0.17
ω_2	0.76±0.26	0.53±0.12	0.60±0.17
ω_3	0.85±0.15	-	0.78±0.18
Δp	-1.9± 0.7	-1.3±0.3	-1.5±0.4

Table 5: Spin from 512 differences $\Delta\mu\cos\delta$ by scalar harmonics, mas/y.

		n	k	l	First value	n	k	l	Second value
	ω_1	2	1	1	-0.09 ± 0.38	4	1	1	0.46 ± 0.86
	ω_2	2	1	0	**1.46 ± 0.31**	4	1	0	**1.19 ± 0.65**
	ω_3	0	0	1	0.56 ± 0.21	2	0	1	2.95 ± 0.66

Table 6: Spin from 512 differences $\Delta\mu'$ by scalar harmonics, mas/y.

		n	k	l	First value	n	k	l	Second value
	ω_1	1	1	0	-0.86 ± 0.18	3	1	0	-0.41 ± 0.50
	ω_2	1	1	1	0.68 ± 0.27	3	1	1	1.46 ± 0.69

From these tables we see that the sample of 512 stars gave practically the same results. To this we must add that the situation does not change when the proper motions of the PPM are compared with those of the HIPPARCOS. Indeed, the separate LSM solutions based on 93387 differences PPM-HIPPARCOS, yield $\omega_2 = 1.59 \pm 0.04$ mas/y from $\Delta\mu\cos\delta$ and $\omega_2 = 0.63 \pm 0.02$ mas/y from $\Delta\mu'$. The scalar functions for both estimates of ω_2 from $\Delta\mu\cos\delta$ yield the values 1.43 ± 0.04 mas/y and 3.22 ± 0.15 mas/y. These estimates are discordant, but one must take into account that with respect to spin both hemispheres of the PPM are quite different [3] – and the method of scalar functions reveals this fact.

Summarizing, we can say that the rigid body rotation does exist only in the R.A. proper motions components of the differences FK5-HIPPARCOS and only this system is consistent with the VLBI if the precessional correction is concerned. Returning to the initial sample of 1232 stars we state:

- The Declination system of the FK5 proper motions shows no spin with respect to HIPPARCOS.
- The discordant value $\Delta p = -1.5 \pm 0.7 \;\; mas/y$ is explained by too large weight that the combined solution assigns to the Declination system of proper motions

- The spin of the FK5 with respect to HIPPARCOS exists in the R.A. system of proper motions ONLY.
- This spin gives correction to the precession constant $\Delta p = -3.5 \pm 0.5$ mas/y which is consistent with the result obtained in the VLBI technique.

5. ACKNOWLEDGEMENTS

The author expresses his gratitude to A. Shlyapnikova who made all calculations and appreciates the support of this work by the grant 02-02-16570 of the Russian Fund of Fundamental Research and by the grant of the Leading Scientific School 00-15-96775.

6. REFERENCES

[1] Walter H.G., and Ma C. Correction to the luni-solar precession from very long baseline interferometry, Astron. Astrophys., Vol 284, pp. 1000-1006, 1994.
[2] Chapront J., Chapront-Touze M., Francou G., 1999, A&A 343,642.
[3] *Mignard F., Froeschle F.*, 2000, Global and local bias in the FK5 from the HIPPARCOS data. A&A, 354, pp.732-739.
[4] Zhu Z., Yang T., 1999, AJ 117,1103
[5] Clube S. V. M. Galactic rotation and the precession constant. Mon. Notic. Roy. Astron. Soc. 159, N3. pp.289-314.
[6] *Mignard F., Morando B.*, 1990, Analyse de catalogues stallaires au moyen des harmoniques vectorelles, Journees 90. Systemes de reference spatio-temporels. Paris, pp.151-158.
[7] European Space Agency, The Hipparcos and Tycho Catalogues, "ESA", 1997.
[8] *Brosche P.*, 1966, Representation of systematic differences in positions and proper motions of stars by spherical harmonics, Veroff, des Astron. Rechen-Inst. Heidelberg, N 17, p.1-27.
[9] Vityazev V.V., The ROTOR: a new method to derive rotation between two reference frames. Astron. and Astrophys. Trans., 1994, 4, pp. 195-218.
[10] Vityazev V.V., The ROTOR: Rotation of Frames via Representation of Systematic Differences in Terms of Spherical Functions. – Proc. of IAU Colloquium 165, 1997, Poland, pp. 464-474.
[11] Vityazev V.V., The MOTOR: Stellar kinematics via representation of proper motions by means of orthogonal functions. – Motion of Celestial bodies, Astrometry and Astronomical Reference Frames, Proc. of the JOURNEES 1999, Dresden, 2000, p. 59.
[12] *V. Vityazev, A. Shuksto*, Stellar Kinematics by Vectorial Harmonics, 2003 (in press).
[13] *Fricke W*, 1977, Basic material for the determination of precession and of Galactic rotation and a review of methods and results. – Veroffen Astron. Rechen-Inst., Heidelberg. N 28, p.52.

SCIENTIFIC OBJECTIVES OF A SMALL SIZE CATALOGUE BASED ON THE SPACE-BORN OPTICAL INTERFEROMETRIC MISSION

A.V. BAGROV, Y.B. KOLESNIK
Institute of Astronomy of the Russian Academy of Sciences
48 Piatnitskaya str., 109019 Moscow, Russia
e-mail: abagrov@inasan.rssi.ru, kolesnik@inasan.rssi.ru

ABSTRACT. The Russian space born interferometric mission CELESTA is aimed at construction of the 5000 stars' catalogue of positions and proper motions accurate on the microarcsecond level. The paper presents the arguments for astrometric significance of such a relatively small catalogue.

1. CONCEPTION OF ASTROMETRY FOR THE "CELESTA" MISSION

Space born astrometric mission "CELESTA" is based on the double interferometer-arcmeter OSIRIS (A.A.Boyarchuk et al., 1999). The first step of the mission - foundation of reference system in optical on several brightest stars directly measured in ICRS relatively to its quasars. Positions of "celomer" stars will construct hard frame of triangles, so it will global astrometric frame. The ICRS realization in optic on celomer stars will be presented as set of instant positions of these stars measured in monitoring mode. This will allow to calculate coordinate of any celomer star for any moment with micro-arcseconds accuracy irrelative to nature of its motion.

As the celomer stars are distributed over the whole sky and included to Hipparcos catalogue, their positions may be used for improvement of the Hipparcos proper motions. The rest of the $\sim$5000 stars will be measured in the frame of celomer stars directly tied to the extragalactic reference frame.

The main goals of the mission are as follows:

Establishing Inertial Coordinate Systems in optical with microarcsecond accuracy based on extra Galaxy point-like objects - quasars;

Measuring individual parallaxes of some thousand of stars up to 100 kps for revising the astronomical Distance Scale on the solid basis of direct triangulation;

Providing astrophysics with high precision distances of selected objects.

The main scientific problems to be solved by the OSIRIS project are follows:

A catalogue of positions for $\sim$5000 astronomical objects with sub-millisecond accuracy.

Determination of absolute parallaxes for any type of objects in the Galaxy and, possibly, converting to the determination of parallaxes of extragalactic objects.

Construction of an inertial coordinate system to which the motion of solar system bodies and stars of the Galaxy can be related.

Study of the geometry of the Universe (improvement of the distance scale in the Galaxy and outside of it, study of the galactic rotation) in order to improve the knowledge of the dynamics of the Galaxy (refinement of the value and distribution of its mass including a qualitative estimate of visible and invisible components).

New possibilities allow to solve the following astronomical problems:

Detection of binaries.

Search for dark companions and planets around nearest stars.

Study of the orbital motion in binary and multiple stellar systems.

Study of kinematics and dynamics of stellar clusters.

Determination of motions of the nearest galaxies and the distribution of galaxies in the Universe.

The 4-years working out of the "CELESTA" project finishes stage "A", and the decision of beginning of stage "B" will be done in 2004. The total time of manufacturing astrometric probe and its launching is estimated as 4 years. The duration of the mission is planned to be 5 years and will continue till satellite will be operated. The probe will be low-masses (about 450 kg total) astrometrical satellite, which will be launched to high-altitude elliptical orbit with the apogee 200000-300000 km.

2. NECESSITY OF CHECKING AND IMPROVEMENT OF THE CURRENT REALISATION OF THE ICRS IN OPTICAL

The primary objective of the fundamental astrometry is construction of the distortion free system of the proper motions. The distortions of the Hipparcos system was a priori claimed 0.1 mas for positions and 10 mas/cy for proper motions. The first widely discussed indication that the Hipparcos proper motion system cannot be regarded as an ideally rigid standard is the anomalously small correction to the IAU 1976 precession constant inferred from direct comparison with the ground-based compiled catalogues. The next one is investigation of its systematic differences with respect to the ground-based catalogues. When a large subset of catalogues is incorporated into comparison it is appeared that the Hipparcos system of positions is in dramatic discrepancy with the modern ground-based catalogues as a whole. The level of systematic deviations is by two orders larger then claimed 0.1 mas. It is hard to imagine the source of an error systematically affecting absolutely all ground-based catalogues. When compared with the sequence of the FK catalogues on the 85-year interval it is clearly seen the evolution of the Hipparcos system in time that confirms that the Hipparcos system is not consistent not only with modern catalogues, but with all the catalogues of the 20^{th} century embedded into FK5, FK4 and FK3.

These evidences prove that, since discrepancy of the Hipparcos with respect to ground-based astrometry is not explained, there is still no convincing evidence of the declared high quality of the HIPPARCOS proper motion system in the sense of the global astrometry. This, in turn, leads to the idea that even a small catalogue of several thousands stars directly tied to the extragalactic reference frame during space-born interferometric mission will be of great importance for checking and improving of the HIPPARCOS proper motion system.

3. REFERENCES

Boyarchuk A.A, Bagrov, A.V., Mikisha A.M., et al., 1999, Cosmic Research, Vol.37, No 1, pp. 1-9.

KINEMATICAL TEST OF THE ICRS INERTIALITY

V. V. BOBYLEV
Main Astronomical Observatory of RAS
196140, St. Petersburg, Russia
e-mail: vbobylev@gao.spb.ru

1. THE SYSTEM OF HIPPARCOS AND TRC CATALOGUES

The kinematics of the Hipparcos (ESA, 1997) and TRC (Høg E., *et al.*, 1998) stars has been tested using Ogorodnikov-Milne model (Ogorodnikov, 1965, Clube, 1972). We used the classical approach wihtout parallaxes. This approach allows to use stars with negative parallaxes. The Oort constants $A = 13.7 \pm 0.4$ km/s/kpc, $B = -13.9 \pm 0.3$ km/s/kpc, $C = -3.2 \pm 0.5$ km/s/kpc and vertex deviation $l_{xy} = 7 \pm 1^\circ$ were found using 58675 distant ($r > 0.2$ kpc) Hipparcos stars. The values of the Oort constants A and B are in good agreement with the ones recommended by IAU (1986). The value of the vertex deviation $l_{xy} = 7 \pm 1^\circ$ is in good agreement with the results of different authors, for example, Dehnen and Binney (1998). It was found that the rotation around galactic y-axis of the distant Hipparcos stars occurs with angular velocity $M_{13}^- = -0.36 \pm 0.09$ mas/yr.

On the basis of the TRC the Oort constants were determined as follows: $A = 14.9 \pm 1.0$ km s^{-1} kpc^{-1} and $B = -10.8 \pm 0.3$ km s^{-1} kpc^{-1}. The component of the model above describing the rotation around the galactic y-axis differs noticeably from zero $M_{13}^- = -0.86 \pm 0.11$ mas/yr (TRC stars).

2. CORRECTION TO THE IAU (1976) PRECESSION CONSTANT

The value $M_{13}^- = -0.36 \pm 0.09$ mas/yr can be explained as residual rotation of the Hipparcos (or the ICRS) with respect to the extragalactic inertial frame. One of the causes of this effect is the uncertainty of the luni-solar precession constant adopted during the development of the ICRF (Ma C. *et al*, 1998). With the use of this approach the corrections of the luni-solar precession constant IAU (1976) have been derived as follows: $\Delta p_1 = -3.26 \pm 0.10$ mas/yr. Table 1 gives the corrections to IAU (1976) luni-solar precession constant Δp_1 and ΔE which were found by different authors using different catalogues.

3. MOTION OF THE DISTANT OB-STARS

The value $M_y = -0.36 \pm 0.09$ mas/yr may be of nature not connected with real motions of the stars. Precession of the warp in zx-plane with angular velocity -25 km/s/kpc was proposed by Drimmel et al. (2000). As $M_{13}^- \cdot 4.74 = -1.7$ km/s/kpc, so with $r = 1$ kpc $M_{13}^- \cdot r = -1.7$ km/s, and with $r = 2$ kpc $M_{13}^- \cdot r = -3.4$ /. Fig. 1 gives the components of spatial velocity W of 4250 Hipparcos OB stars (linear velocity on z-coordinate, Drimmel et al. 2000) as a function of galactocentric distance R and velocity of fictitious rotation of the ICRS $M_{13}^- = -0.36$ mas/yr, which can explain inclination of distant OB stars in Fig. 1 (the Solar distance from the Galactic center is $R_\odot = 8.0$ kpc).

Table 1: Corrections to IAU (1976) luni-solar precession constant Δp_1 and ΔE, in mas/yr.

ISSUE	CATALOGUES	Δp_1	ΔE
Miamoto, Sôma (1994)	ACRS	$-2.7_{(0.3)}$	
Rybka et al. (1995)	PPM	$-3.1_{(0.2)}$	$-1.3_{(0.2)}$
Bobylev (1997)	PUL2–PPM	$-2.8_{(0.8)}$	
Ma et al. (1998)	VLBI	$-2.84_{(0.04)}$	
Vityazev (1999)	CGC–HIP	$-3.4_{(1.0)}$	$-3.3_{(1.0)}$
Charpont et al. (2002)	LLR	$-3.02_{(0.03)}$	
Fukushima (2003)	VLBI	$-3.011_{(0.003)}$	

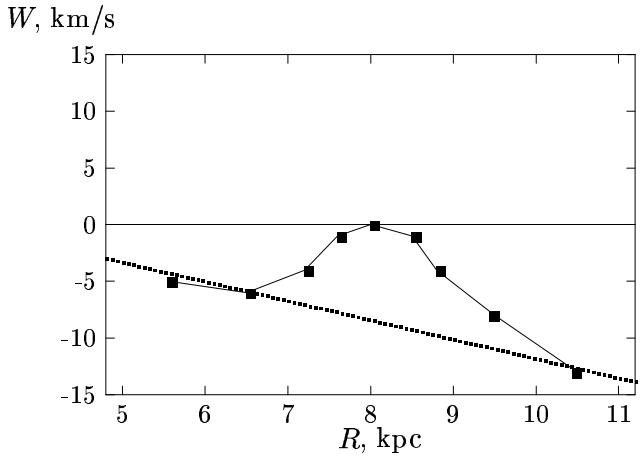

Fig. 1. Residual velocities W of 4250 OB stars as a function of galactocentric distance R by Drimmel et al. (2000). Dotted line corresponds to the vectors of the linear velocities $M_{13}^{-} \cdot r \equiv W$ obtained in this work (zero-point is shifted down).

Acknowledgement. This research has been supported by the Russian Foundation for Basic Research (grant No 02–02–16570).

4. REFERENCES

Bobylev V. V., *JOURNEES 1997*, Eds. J. Vondrák and N. Capitaine (Prague, 1997), p. 91.
Clube S. V. M., *Mon. Not. R. Astr.Soc.*, **159**, 289 (1972).
Chapront J., *et al.*, *Astron. Astrophys.*, **387**, 700 (2002).
Dehnen W. and Binney J. J., *Mon. Not. R. Astr.Soc.*, **298**, 387 (1998).
Drimmel R., *et al.*, *Astron. Astrophys.*, **354**, 67 (2000).
Fukushima T., *Astron. J.*, **126**, 494 (2003).
Høg E., *et al.*, *Astron. Astrophys.*, **333**, L 65 (1998).
Ma C., *et al.*, *Astron. J.*, **116**, 516 (1998).
Ogorodnikov K. F., *Dynamics of Stellar Systems*, (L.: Pergamon Press, 1965).
Rybka S. P., Kinemat. i Fiz. Neb. Tel. **11**, 77 (1995).
The Hipparcos and Tycho Catalogue, ESA SP-1200, (1997).
Vityazev V. V., Dr. Sci. dissertation, St. Petersburg, (1999).

ALL-WAVE ASTROMETRY. BASIC PROBLEMS

A.S. KHARIN
Main Astronomical Observatory, National Academy of Sciences
27 Zabolotnoho Str., Kyiv, Ukraine, 03680
e-mail: kharin@mao.kiev.ua

From ground based or space astronomical practical experience it is known that astrometry as well as astronomy entire can be divided, depending on the range of electromagnetic spectrum where the objects are detected, into the next seven astronomical or astrometrical subsections. They are as follows:
Gamma-ray Astrometry ($\lambda \approx 1.2 \times 10^{-6} \div 0.12\mathring{A}$)
X-ray Astrometry ($\lambda \approx 10^{-5} \div 10^{-2}$ mkm)
Ultraviolet Astrometry ($\lambda \approx 0.01 \div$ 0.4mkm)
Visual optical Astrometry ($\lambda \approx 0.4 \div$ 0.7 mkm)
InfraRed Astrometry (IR) ($\lambda \approx 0.7 \div 350$ mkm)
Submillimetre Astrometry ($\lambda \approx 350$ mkm $\div 1$ mm)
Radio Astrometry ($\lambda \approx 1$ mm $\div 30$ m)

Every of these directions have its specific feature connected with the concrete astronomic or astrometric task, instrumentation (telescopes, sensors, and auxiliary instruments), methods of observations and subsequent processing and, lastly, with special methods of excluding of Earth's atmospheric influences from observations if they are ground-based.

In accordance with these factors the accuracy of astrometrical observations in different electromagnetic ranges is essentially different. The ground based VLBI radio and space optical (HIPPARCOS) observations have the highest accuracy at the level of mas and the Gamma-ray flare sources localization has the lowest accuracy at the level of some arcminutes.

Now International Celestial Reference System (ICRS) is common for two of the above mentioned seven ranges: the Radio and Visual only. But in accordance with the XXII and XXIII IAU GA resolution, the ICRS coordinate system has to be extended to the five electromagnetic wavelengths ranges other then Radio and Visual optics, which is now the most pressing astrometric problem.

There are two ways to solve this problem. First one is to get on the base of the new technology a new more precise observations, as it was proposed in the new space astrometrical and astronomical projects DIVA, GAIA, SIM, RADIOASTRON, ALMA, GHST and some others. But this way may be very long - ten or more years - before the new technology resolution of all these projects will be realized.

The other way is to use method of identification. It is more short and fast and permits to

extend ICRS from Radio and Visual optics to other five spectral divisions if these ones have the objects which have optical or radio counterparts from precise astrometric catalogues that permits to locate these objects.

Now there is a more prospective situation to identify IR sources from catalogues IRAS PSC, DENIS and 2MASS with their optical counterparts from HIPPARCOS or ACT and TYCHO2 that permits to extend the ICRS to IR diapason.

The first version of such an extension has been carried out in Kiev (Kharin, Molotaj, 1999) on the base of CPIRSS (Hindsly and Harrington, 1994). Two level hierarchic IR reference coordinate system has been created. It contains two catalogues. One of them is the first level IR reference catalogue that includes only IR stars which have their optical counterparts from HIPPARCOS and consequently has to represent the ICRS coordinate system. But on our opinion the best representation can be evidently obtained if this first level IR reference catalogue includes additionally the ICRF sources that can be observed in infrared as well.

Because a search had been undertaken to find the radio sources that were observed in infrared also. Firstly the identification of the IRAS PSC stars with their radio counterparts from ISRF were carried out and 31 such sources have been found. Besides the comparison of the Neugebauer list of 179 quasars observed by IRAS satellite in 1983 with the ICRF list (C. Ma, 1998) of 608 candidates has been fulfilled and the extra 55 sources were found. Because 79 IR/Radio sources should be included to the first level IR reference catalogue, compiled in Kiev (Kharin, 2000). Such an addition permits to establish direct connection between the infrared and ICRS coordinate systems.

Acknowledgement. This work was supported by the grant 02.07/00017 of the State Foundation for Basic Research of Ukraine.

REFERENCES

Hindsly R., Harrington R., 1994, *Astron. J.*, **107**, 280-286.111.

Kharin A.S., Molotaj O.A., 1999, *Proc. JOURNEES 1999 & IX Lorman Colloquium*, M. Soffel, N. Capitaine (eds.), Dresden, 55.

Kharin A.S., 2000, *Proc. of the JOURNEES 2000*, N. Capitaine (ed.), Paris, 29-32.

Ma C. et al., 1998, *Astron. J.*, **116**, 516-546.

THE POSITIONS AND PROPER MOTIONS OF 58483 STARS IN THE PULKOVO FIELDS WITH GALAXIES ON THE TYCHO-2 SYSTEM (PUL-3)

M.YU. KHOVRITCHEV, E.V. KHRUTSKAYA, N.M. BRONNIKOVA
Main Astronomical Observatory of RAS
Russia, 196140, Saint-Petersburg, Pulkovskoye chaussee, 65/1
e-mail: deimos@gao.spb.ru

ABSTRACT. A catalogue of positions and proper motions which contains 58483 stars mainly $12^m \div 16.5^m$ (Pul-3) in 146 fields, has been constructed at the Pulkovo observatory. The Pul-3 is based on the results of measurements of the photographic plates with galaxies (Deutsch's plan). All plates were taken using the Pulkovo Normal Astrograph. The Tycho-2 has been used as a reference catalogue. The mean epoch of the Pul-3 is 1963.25. The internal errors of astrometric data of the Pul-3 are $\pm 80\,mas$ for positions and $\pm 5\,mas/yr$ for proper motions.

1. OBSERVATIONS AND ASTROMETRIC REDUCTIONS

The observations were made with Pulkovo Normal Astrograph ($F = 3467\,mm$, $D = 330\,mm$) during the periods from 1935 till 1960 (the first epoch) and from 1969 till 1986 (the second epoch). The exposure times were 1 hour. The majority of stars are in magnitudes range $12^m \div 16.5^m$. The maximal density of stars in the Pulkovo plates is 500 stars per square degree.

The Tycho-2 (Hog E. et. al. 2000) catalogue has been used as a reference catalogue. Only approximate equatorial coordinates of the optical centers of all plates had been known in initial stage of construction of the Pul-3 catalogue and thus recalculation of ones has been done. A six-parameters plate model has been used for astrometric reductions of the plates.

2. THE PUL-3 CATALOGUE CONSTRUCTION

The systematic errors in stars positions depending on coma of the lens and ones as functions of the magnitudes and color indexes (using values B and R from the USNO-A2.0 catalogue) of stars have been revealed in residuals of tangential coordinates of reference stars.

The coma parameters have been determined ($c = 1.6 \pm 0.2\,mas \cdot mm^{-1} \cdot mag^{-1}$ and $mag_0 = 11.3^m \pm 1.2^m$). Magnitude equation and color equation do not depend on plates emulsion but ones strongly depend on declination zone. The considerable magnitude equation corrections have been obtained for stars with $mag < 9^m$ and $mag > 14^m$. The color equation corrections in RA significantly less than ones in DECL. The coefficients of color equations in DECL linearly increase from pole to equator. The more than $50\,mas$ improvement has been made by taking into account of all revealed systematic errors.

Table 1: The estimations of precision of the Pul-3 for different declination zones (internal errors are denoted by ϵ symbol and external errors relative to Tycho-2 are denoted by σ symbol).

declination zone	$\epsilon_\alpha \cos\delta$ mas	ϵ_δ mas	$\epsilon_{\mu_\alpha \cos\delta}$ mas/yr	ϵ_{μ_δ} mas/yr	$\sigma_{\alpha \cos\delta}$ mas	σ_δ mas	$\sigma_{\mu_\alpha \cos\delta}$ mas/yr	σ_{μ_δ} mas/yr
$-5^\circ \div 5^\circ$	90	98	5.5	6.0	141	160	9.2	10.2
$5^\circ \div 15^\circ$	86	86	5.3	5.3	136	159	8.7	10.0
$15^\circ \div 25^\circ$	79	88	4.5	5.1	130	148	9.2	9.1
$25^\circ \div 35^\circ$	85	85	5.1	5.2	154	159	10.2	11.2
$35^\circ \div 45^\circ$	79	78	4.8	4.8	151	157	9.7	10.1
$45^\circ \div 55^\circ$	79	82	4.8	4.9	157	159	11.4	12.5
$55^\circ \div 65^\circ$	77	80	4.9	5.1	162	175	9.9	12.1
$65^\circ \div 75^\circ$	74	78	4.6	4.8	126	142	8.0	9.8
$75^\circ \div 85^\circ$	73	78	4.8	5.1	127	142	8.8	9.9
for full catalogue	80	84	4.9	5.1	142	155	9.2	10.1

The completely corrected equatorial coordinates and new proper motions have been calculated for all stars on each field. The mean epoch of the Pul-3 catalogue is 1963.25. The mean errors of positions and proper motions of the Pul-3 catalogue are presented in Table 1.

The comparisons of the Pul-3 catalogue with Tycho-2 (7588 common stars) and ARIHIP (Wielen R. et. al. 2001)(795 common stars) have been done at the mean epoch of the Pul-3 catalogue. The most systematic differences (Tycho-2 – Pul-3) are within $\pm 10\,mas$ for coordinates and $\pm 0.5\,mas/yr$ for proper motions. The mean differences (ARIHIP – Pul-3) are slight also: $\overline{\Delta\alpha\cos\delta} = +6\,mas$, $\overline{\Delta\delta} = -4\,mas$, $\overline{\Delta\mu_\alpha\cos\delta} = +0.28\,mas/yr$, $\overline{\Delta\mu_\delta} = +0.76\,mas/yr$.

The components of angular velocity vector of rotation of the system of the Pul-3 (Tycho-2 system) relative to the system of the Pul-2 (Bobylev V.V. et. al. 2000) (Pul-2 is a catalogue of absolute proper motions with respect to background galaxies) were obtained from differences of the proper motions (Pul-3 – Pul-2) for more than 50000 mostly faint stars. $\omega_x = -0.76 \pm 0.91\,mas/yr$, $\omega_y = -0.75 \pm 0.74\,mas/yr$, $\omega_z = -2.05 \pm 0.71\,mas/yr$. These results are in good agreement with the similar estimations (Kovalevsky J. et. al. 1997) from (Hipparcos – Lick NPM1) proper motions differences.

The stars from Pul-3 catalogue may be used as reference stars in processing of positional CCD-observations in small fields. The Pul-3 catalogue in combination with modern observations will allow to improve the precision of the proper motions of the faint stars. The Pul-3 is put to CDS, Strasburg, France (I/290).

3. REFERENCES

Hog E. et. al. 2000. The Tycho-2 Catalogue of the 2.5 Million Brightest Stars.*Astron. Astrophys.*. Vol. 355. -P. 27-30.

Wielen R. et. al. 2001. Astrometric catalogue ARIHIP.Veröff. Astron. Rech-Inst. Heigelberg. N. 40. 36 p.p.

Bobylev V.V. et. al. 2000. The catalogue of absolute proper motions of stars Pul-2 – A.N. Deutsch's plan realisation. in proc. "Astrometry, geodynamics and celestial mechanics at threshold of 21 centure." P. 177-178. (in Russian).

Kovalevsky J. et. al. 1997. The Hipparcos catalogue as realisation of extragalactic reference system. *Astron. Astrophys.*, 323, P. 620-633.

COMPARISONS OF THE USNO-B1.0 CATALOGUE WITH PUL-3 AND UCAC1 IN SELECTED FIELDS

M.YU. KHOVRITCHEV, E.V. KHRUTSKAYA
Central Astronomical Observatory of RAS
Russia, 196140, Saint-Petersburg, Pulkovskoye chaussee, 65/1
e-mail: deimos@gao.spb.ru

ABSTRACT. The recently released USNO-B1.0 catalogue which contains more than billion objects, may be widely used in processing of positional CCD-observations with small fields. The goals of this paper are preliminary estimation of the precision and investigation of the systematic errors of astrometric data of USNO-B1.0 by comparing of the USNO-B1.0 catalogue with Pul-3 (northern hemisphere) and UCAC1 (southern hemisphere) catalogues in selected fields. The positional precision of the USNO-B1.0 relative to Pul-3 (epoch 1963.25) and UCAC1 (epoch 2000.0) is inhomogeneous and in average is equal to $0.18''$. Magnitude-dependent systematic errors of the USNO-B1.0 are most significant for stars that are fainter than 15 magnitude.

1. THE RESULTS OF COMPARISONS

The comparison of the USNO-B1.0 (Monet et. al. 2003) with Pul-3 (E.V.Khrutskaya et. al. 2002) catalogue was based on the data of 16 fields (5042 stars, $m \geq 12$). The data for 5 fields from UCAC1 (N.Zacharias et. al. 2000) (16035 stars, $m \geq 12$) were used in comparison of the USNO-B1.0 with UCAC1. The fields radius is 1°. These fields were selected in different zones of RA and DECL. The Tycho-2 stars have been excluded. The mean epoch of USNO-B1.0 positions was about 1980.0 for comparing fields.

The comparison of the USNO-B1.0 catalogue with Pul-3 has been made in the mean epoch of the Pul-3 catalogue. The average differences in coordinates and in proper motions (PUL-3 – USNO-B1.0) are $\Delta\alpha\cos\delta = -0.003''$, $\Delta\delta = -0.038''$, $\Delta\mu_\alpha\cos\delta = -0.7 mas/yr$, $\Delta\mu_\delta = -3.6 mas/yr$. The mean errors of astrometric data of the USNO-B1.0 catalogue (from comparison with PUL-3 for epoch 1963.25) are $\epsilon_\alpha\cos\delta = \pm 0.157''$, $\epsilon_\delta = \pm 0.181''$, $\epsilon_{\mu_\alpha\cos\delta} = \pm 8.6\, mas/yr$, $\epsilon_{\mu_\delta} = \pm 9.2\, mas/yr$.

The systematic differences in coordinates and in proper motions of stars are depended on magnitude and color of ones. The color-dependent systematic errors in positions and proper motions are nonlinear. There are linear dependence on magnitude of differences in RA and in proper motions in RA. These systematic errors are within $\pm 0.1''$ in α and $\pm 4 mas/yr$ in $\mu_\alpha\cos\delta$. The linear dependence on magnitude of differences in DEC is considerable for stars that are fainter than 14 magnitude (Figure 1 (a)). The systematic differences in μ_δ are within $\pm 4\, mas/yr$ and nonlinearly depend on magnitude.

The comparison of the USNO-B1.0 catalogue with UCAC1 has been made on the epoch 2000.0. The average differences in coordinates between UCAC1 and USNO-B1.0 (UCAC1-

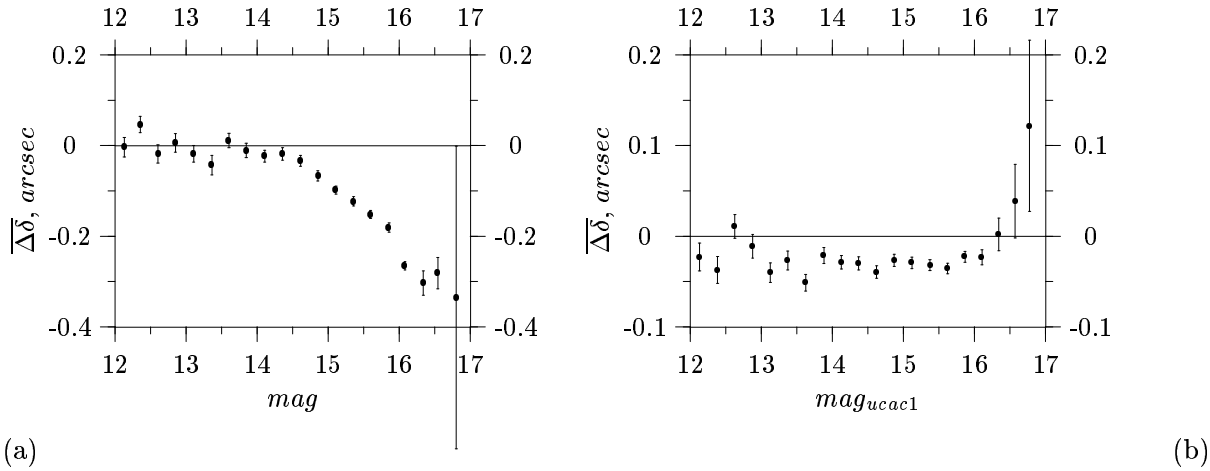

(a) (b)

Figure 1: The systematic differences (PUL-3 – USNO-B1.0)(a) and (UCAC1 – USNO-B1.0)(b) in DEC as functions of stars magnitude.

USNO-B1.0) are $\Delta\alpha\cos\delta = 0.015''$, $\Delta\delta = -0.095''$. The errors of stars coordinates of the USNO-B1.0 relative to UCAC1 for epoch 2000.0 are $\epsilon_\alpha\cos\delta = \pm 0.183''$, $\epsilon_\delta = \pm 0.180''$. The dependencies of the systematic differences in RA and in DECL on magnitude are similar The considerable magnitude-dependent systematic errors have been revealed for faint stars ($> 15^m$)(Figure 1 (b)).

2. CONCLUSIONS

The investigation has shown that the precision of the USNO-B1.0 astrometric data is inhomogeneous. The dependencies of the systematic differences from positions have not been revealed. The individual significant systematic differences in positions ($\geq 0.2'' \div 0.3''$) have been revealed in both comparisons. The values of differences (Pul-3–USNO-B1.0) and (UCAC1–USNO-B1.0) are comparable.

There are magnitude-dependent systematic errors in USNO-B1.0 catalogue. These errors are considerable for stars that are fainter than $14 \div 15$ magnitude.

3. REFERENCES

David G. Monet, Stephen E. Levine, et. al. 2003. The USNO-B catalog. *Astron. J.*125. P.984-993.

E.V.Khrutskaya, M.Ju.Khovritchev, N.M.Bronnikova. 2002. Pul-3: catalogue of positions and proper motions 58239 stars on the ICRS system at the Pulkovo plates with galaxies. Izv. GAO 216. P.336-348. (Russian).

N.Zacharias, S.E.Urban, M.I.Zacharias, et.al. 2000. The first US Naval Observatory CCD astrographic catalog. *Astron. J.*120. P.2131-2147.

TRANSFORMATION BETWEEN ICRS AND ITRS UNDER IAU (2000) RESOLUTIONS

I.I. KUMKOVA[1], M.V. STEPASHKIN[2]
[1] Institute of Applied Astronomy of RAS
10 Kutuzov quay, 191187 St.Petersburg, Russia
e-mail: kumkova@quasar.ipa.nw.ru
[1] St.Petersburg Institute for Informatics and Automatics of RAS
39, the 14th Line, 199178 St.Petersburg, Russia

ABSTRACT. Algorithms of direct and reverse relativistic four dimension transformation of barycentric and geocentric celestial reference coordinate systems (BCRS and GCRS) according to IAU Resolution B1(2000) are developed. It is shown that application of four dimension coordinate systems does not involve any complications for the reduction of observations. Transformation between BCRS and GCRS is considered as a part of the general procedure of linking International Celestial Reference System to International Terrestrial Reference System, provided by the International Earth Rotation Service.

1. INTRODUCTION

The sub-milliarcsecond-level and the microarcsecond-level of precision anticipated for future observational systems demands improved models at all levels of analysis. These improved models require to take into account corrections of General Relativity Theory in data processing. That is why in 1990 at IAU Colloquium N127 (IAU, 1991), IAU recommendations for reference frames and time scales have been formulated in the framework of General Relativity for the first time. In 1991 affirmation of IAU recommendations as Resolution A4 (1991) at the 21th GA IAU and later as Resolution 2 of IUGG (1991) gave the floor for the qualitative change of General Relativity role for ephemeris.

At present according to IAU Resolutions two main practically used coordinate systems are existing. There are ICRS, International Celestial Reference System and ITRS, International Terrestrial Reference System. The time scales of ICRS and ITRS should be respectively TCB (Barycentric Coordinate Time) and TCG (Geocentric Coordinate Time). These scales should be considered as four-dimention relativistic coordinate system, connected by four-dimention relativistic transformation with additional three-dimention rotation of space axes of coordinates. To solve the majority of astronomical tasks it is sufficient to have the only ICRS, ITRS and its practical realization as ICRF and ITRF. However to connect ICRF and ITRF it is necessary to introduce one more local geocentric system with the same time scale TCG, as well as ITRS has, and with the same direction of space axes, as well as ICRS has. Such a system is introduced by IAU Resolution 1.3 (2000) and it is intermediate system between BCRS, Barycentric Celestial Reference System, identified with ICRS, and ITRS and has a title of GCRS, Geocentric Celestial Reference System. The present work is aimed to develop technique for practical

use of BCRS→GCRS and GCRS→BCRS transformations in astrometry taking into account IAU Resolutions (IAU, 2001), specified realization of BCRS and GCRS with TCB and TCG, correspondingly.

2. CALCULATIONS AND RESULTS

To perform transformation from BCRS to GCRS and reverse is necessary to calculate in advance several values, such as vector of Earth's velocity, Solar System bodies potential, function of time and function called relativistic time equation, what has been calculated by integration in numerical as well as analytical form. The algorithm includes determination of a time moment and source coordinates in GCRS, correspondent to the time moment and barycentric source coordinates in BCRS, following to formula of transformation (Brumberg and Groten, 2001)

The reverse transformation is constructed by means of similar tabled values of functions mentioned above but in dependence on argument TCG (in limits of Post-Newtonian accuracy it does not requires any additional calculations). Additional calculations (comparatively to direct transformation) will be needed only in the case of determination of value, defined Earth motion as function of TCG. After the tabled values have been calculated, then source coordinates at the time moment in BCRS are determined by reverse transformation (Brumberg and Groten, 2001)

We carried out calculation following suggested scheme of direct and reverse transformations in two ways (analytical and numerical) for an object, located in point of orbit of geostationary satellite and conditional object, located at the distance of 1 a.u. from barycenter of Solar System. To control of accuracy of transformations, four-dimension object coordinates have been used as initial data for reverse transformation. The reverse transformation resulted again to four-dimension coordinates of the source in BCRS. The comparison of the obtained values and initial numbers, used in direct transformation serves as characteristic of accuracy of calculations. The analysis of performed calculations has shown that accuracy level, what has been initially fixed has been obtained. In the both considered sources (at geostationary orbit and conditional source) in time transformation an error is not manifested up to 10-9, for the coordinate transformation, relative error is less then .

3. CONCLUSIONS

Study of results obtained shows that calculated coordinates by use of suggested technique do not differ from set values at the level of required precision (Post-Newtonian approach taken into account terms of order). Thus, the precision level of the task is reached. Consequently proposed numerical realization for transformation BCRS→GCRS and GCRS→BCRS can be used in data processing.

4. REFERENCES

Brumberg, V.A., Groten, E., 2001, *Astron. Astrophys.*, **367**, 1070-1077.

IAU, 1991, *Proceedings of the 127th Colloquium of the International Astronomical Union. Reference Systems*, Observatory Washington, D.C.

IAU, 2001, *IAU Information Bull.*, **88**, 28-40, (Erata: ibid., **89**, 4, 2001).

A NUMERICAL METHOD FOR THE ANALYSIS OF THE SYSTEMATIC ERRORS IN REFERENCE SYSTEMS FROM NON REGULAR SAMPLES

J.A. LOPEZ [1], F.J. MARCO[1], M.J. MARTINEZ[2]
[1] Departamento de Matemáticas, Universidad Jaume I de Castellón, Castellón Spain
Campus Riu Sec s/n,12071 Castellón Spain.
[2] Departamento de Matemática Aplicada, Universidad Politecnica de Valencia
Camino Vera s/n, 46022 Valencia Spain
e-mail: e-mail:lopez@mat.uji.es, marco@mat.uji.es, martinez@mat.upv.es

ABSTRACT. The main aim of this paper is the analysis of the systematic errors contained in a star catalogue. These errors can be obtained by means of the analysis of the residuals observation minus calculus taken from a set of observated positions in a spatial domaine.
The clasical methods do not work fine if the sample is non homogeneously distributed in the spatial domain. In this paper a new method for the errors analysis from non homogeneous samples is proposed.

1. INTRODUCTION

The main difficulty of this method is the non-ortogonality of the set of functions over the discrete points of the sphere given by the observations because the sample is usualy non-homogeneous. This problem can be aproached using a previous filter by means of a suitable couple composed by a previois smoothing procses and a reconstruction operator.
The smoothing algorithm provide estimators for the values of the $\triangle\lambda(\lambda,\beta)$ and $\triangle\beta(\lambda,\beta)$ from the sample for a lattice over the ecliptic band, and using an exact reconstruction operator until an appropiate order k the error values $(\triangle\lambda, \triangle\beta)$ are reached. The non-ortogonality problem can be solved using this method.
The calculated position of the asteroids can be improved by means of a previous orbital elements correction process. The solution of the normal system obtained from the minimun condition for the residual function provides the values of parameters of the bias model.

2. FILTERING MODEL

Let D be the spherical domain where the observated positions are distributed. In this work the domain D has been token as a band arround the ecliptic $D = \{(\lambda,\beta)|\lambda \in [0, 2\pi]$, $\beta \in [-\beta_{max}, \beta_{max}\}$. Let (α_i, δ_i) be a set of observated positions of minor planets reducted from a star catalogue, and (λ_i, δ_i) their ecliptic coordinates. The differences betwen observated an calculated positions $(\triangle\lambda_i, \triangle\beta_i)$ can be developed [1] by means the series expansions:

$$\triangle\lambda\cos\beta = \sum_{n=0}^{\infty}\sum_{m=0}^{\infty}\epsilon_{n,m}K_{n,m}(\lambda,\beta) \quad \triangle\beta = \sum_{n=0}^{\infty}\sum_{m=0}^{\infty}\eta_{n,m}K_{n,m}(\lambda,\beta)$$

where $K_{n,m}(\lambda,\beta), n, m = 0, 1, ...$ is a suitable orthogonal base of $l^2(D)$ space.
The coeficients of the analytical expansion can be obtained from the minimum condition of the residual function:

$$R(\{\epsilon_{i,j}, \eta_{i,j}\}_{i=1,..,N;j=1,..,M}) = \sum_{i=1}^{NE} \left[r_{\beta_i}^2 + r_{\lambda}^2 \cos^2 \beta_i\right]$$

where NE is the size of the sample.
This method is apropiated if the stars distribution is homogeneous in the spherical domain D. Unfortunately when the sample is token from minor planets observations the sample in non homogeneously distributed in the band D. In this case it is more apropiated [2] take the minimun condition from the integral:

$$R(\{\epsilon_{i,j}, \eta_{i,j}\}_{i=1,..,N;j=1,..,M}) = \int\int_D \left[r_{\beta_i}^2 + r_{\lambda_i}^2 \cos^2 \beta_i\right] d\sigma$$

To evaluate this integral we can discretize the spatial domaine by means of a rectangular lattice. The control volume D_i is determinated by the center of the four adyacent rectangles at the node i (except for the nodes in the boundary) and the values of the $\triangle\lambda$, $\triangle\beta$ is repalced by the mean values:

$$\overline{\triangle\lambda_i} = \frac{1}{V_i}\int\int_{D_i} \triangle\lambda d\sigma, \quad \overline{\triangle\beta_i} = \frac{1}{V_i}\int\int_{D_i} \triangle\beta d\sigma$$

where V_i is the area of the contol volume D_i.
this domain.
The integrals can be calculated from a numerical formulae built for the points of the sample. The values of the $(\triangle\lambda, \triangle\beta)$ can be calculated from a bidimensional reconstruction operator exact until k order in lattice size step h. The bidimensional reconstruction operator can be built as composition of two unidimensional operators [4](Casper, Atkins) one in λ direction and other in β direction.

3. CONCLUDING REMARKS

The clasical method is not appropiated for use a dymamical correction model to study catalogue bias because the sample is not homogeneous in the domain D so the ortogonality of set of basic functions over the sample is not guaranted.
The proposed method developed in this paper is more suitable in these situations.

4. ACKNOWLEDGMENTS

The present work has been partially supported by grants from the Generalitat Valenciana and Fundacion Caja Castellon.

5. REFERENCES

F.J. Marco, M.J. Martínez, J.A. López, 2001, A Comparison of Geometrical and Analytical Methods of Astrometric Correction, *Revista Mexicana de Astronomia y Astrofísica*, **37**, 73–81.

J.A. López, F.J. Marco, M.J. Martínez, 2003, Proposal of a New Computational Method for The Analysis of the Systematic Differences in Star Catalogues, *Proc. of the International Conference of Computational Methods un Sciences and Engineering*, T. E. Simos (Ed.), 391–394.

Casper J. Atkins, H.L., 1993, A Finite Volume Method High Order ENO Scheme for Two-dimensional Hyperbolic Systems, *Journal of Computational Physics*, **106**, 62–76.

A MOTORIZED SYSTEM FOR RAPID DEFLECTION OF VERTICAL DETERMINATION

V. OGRIZOVIĆ
Faculty of Civil Engineering, Department of Geodesy
Bulevar kralja Aleksandra 73/I, 11000 Belgrade, Serbia
e-mail: vukan@grf.bg.ac.yu

ABSTRACT. A specialized motorized system is constructed in order to provide a reliable system for quick astro-geodetic determinations, particularly, astro-geodetic deflections of vertical. The system consists of the following components: (1) A motorized theodolite, (2) a GPS sensor, (3) an atmospheric parameters sensor and (4) a notebook.
The system implements the equal zenith distances method. During the one hour field session, over one hundred of star passes are registered, when using the 45th almucantar. Because of the integration of the system, the result (vertical deflection components) can be calculated right on the spot.

1. INTRODUCTION

Astro-geodetic deflection of vertical components (ξ, η) are used as a control of gravimetric measurements, because they are obtained without assuming the density of the Earth. This motorized system is constructed in order to achieve 0.3" - 0.5" accuracy of the astronomic coordinates (Φ, Λ), within the one hour of a field session. The main requests for the system are the following:

- Creation of the observation program,
- Orientation of the theodolite,
- Placing the instrument in the star's direction,
- Precise time measurement, and
- Logging of the measurements performed during the session.

2. PRINCIPLE OF THE COMMUNICATION

The communication between the system components is organized by a special program written mainly in C++, with interrupts written in Assembler. The registration of the star pass is caught by an interrupt function, logging the notebook oscillator state. The tie between the oscillator state and UTC ticks is established by another interrupt, registering each 1PPS tick sent by the integration box (i.e. GPS sensor).

The hardware integration box consists of:

- GPS sensor with internal power supply (inside the box),
- 1PPS output port (BNC),
- Registration joystick input port (BNC), and
- 3 RS232 I/O ports (DB9).

The 1PPS port is not used here, but it is useful for testing the stability of the GPS sensor oscillator. The registrations of star passes are performed manually, using the joystick input port. One of the serial I/O ports is used for connection with the theodolite. Two other ports, besides the standard I/O facilities (TX and RX pins), use some other pins, in order to establish the tie between 1PPS and the joystick with the integration program, running on the notebook.

3. CONCLUSION

Using this kind of measurement system, one can expect the accuracy of astro-geodetic deflection of vertical components in the range of 0.3" - 0.5", within one hour of field measurement session. During that period, over one hundred of passes can be registered with manual registration.
Since the measurement system is very portable and easy to operate, during the one observation night three to four stations can be visited, if the stations are 5-10 km far away one from another. Due to the characteristics of the equipment and the logging system, the result can be obtained just a few minutes after the session.

4. REFERENCES

GEOCOM Reference Manual, Leica Geosystems, Heerburgg, 1999.

Mueller I. I. Spherical and Practical Astronomy as Applied to Geodesy, Frederik Ungar Publishing Co. New York, 1969.

Murray, C.A. Vectorial Astrometry, J.W. Arrowsmith Ltd. Bristol, 1983.

Ogrizovi'c, V. Prilog primeni novih mernih sistema u astrogeodetskim odredjivanjima, MSc. Thesis, Belgrade, 2002.

FK5-HIPPARCOS: SYSTEMATIC DIFFERENCES WITHOUT ASSUMPTION OF RIGID MUTUAL ROTATION OF THE FRAMES

A. SHLYAPNIKOVA, V. VITYAZEV
Sobolev Astronomical Institute of the SPb University
198904, SPb, Petrodvorets, Universitetsky pr., 28, Russia
Ann@as3597.spb.edu, Vityazev@venvi.usr.pu.ru

ABSTRACT. The first attempt to connect the FK5 and HIPPARCOS frames resulted in deriving six parameters describing the orientation and spin of the FK5 with respect to HIPPARCOS [1]. An extensive study of the rigid body rotaion (RBR) model [2] gave evidence that this model is not compatible with the real differences FK5-HIPPARCOS.

In 2000, Mignard et al.,[3] published tables of the differences FK5-HIPPARCOS smoothed out over the areas of about 230 square degrees. Thus obtained differences include the overall rotation and spin. On the contrary, H. Schwan [4] used strict analytical representation of the differences FK5-HIPPARCOS but eliminated the global rotation and spin from initial data. Both approaches are not free from drawbacks: in case [3] one has not good representation of good data, in case [4] – one has good representation of not good data.

To our mind, to connect the FK5 and HIPPARCOS correctly the RBR model must be discarded. In our paper we present the approximation of systematic differences FK5-HIPPARCOS over a set of orthogonal functions "Legendre-Hermite-Fourier" [5]. No RBR correction were applied to initial differences.

1. RESULTS

We have calculated the differences FK5-HIPPARCOS for positions and proper motions of 1232 stars at the epoch 1991.25 and decomposed them on products of Legendre, Hermite, Fourier polynomials. The coefficients of decomposition (B_j) are given in table 1, where j, p, n, k, l - indexes of decomposition (limiting values p=2, n=10, k=6). The separation of noise from systematic component was made with the probability more than 0.95. The magnitude equation was determined reliably only for $\Delta\alpha\cos\delta$ – (7 harmonics) and for $\Delta\mu_\alpha\cos\delta$ – (2 harmonics). Using our coefficients we calculated the systematic differences for all 1232 selected stars of the FK5.

Analyzing the systematic differences of declinations of stars of FK5 and HIPPARCOS catalogues, we can conclude that equatorial plane of FK5 constitutes a small circle parallel to equator of HIPPARCOS catalogue and displaced by 49.23 ± 2.23 mas in direction to the North Pole. This fact was first stated in [3], the value of displacement being estimated to be ≈ 60 mas. The method of orthogonal decomposition, we used, confirms this estimate.

Table 1: Analytical representation of the FK5-HIPPARCOS systematic difference

Right ascension. Units [mas]																		
j	p	n	k	l	B_j	σ_{B_j}	j	p	n	k	l	B_j	σ_{B_j}	j	p	n	k	l	B_j	σ_{B_j}
1	0	2	0	-1	-25.78	1.99	12	0	5	2	1	-6.72	1.89	23	0	8	4	-1	5.14	1.93
2	0	3	0	-1	21.90	1.93	13	0	7	2	-1	7.33	1.88	24	0	3	5	1	-5.85	1.87
3	0	4	0	-1	-17.87	1.89	14	0	0	3	1	6.33	2.08	25	0	0	6	-1	4.87	2.02
4	0	7	0	-1	-6.13	1.95	15	0	1	3	-1	-8.44	1.96	26	0	2	6	-1	5.79	1.89
5	0	0	1	-1	-16.56	2.03	16	0	1	3	1	-3.57	2.00	27	1	5	0	-1	-10.60	2.11
6	0	1	1	-1	-7.20	2.01	17	0	3	3	1	-8.27	1.96	28	1	6	0	-1	4.95	2.18
7	0	2	1	-1	24.15	1.98	18	0	0	4	-1	-13.21	2.06	29	1	3	1	1	7.14	2.34
8	0	7	1	-1	-6.21	1.88	19	0	1	4	1	8.75	1.95	30	1	7	1	1	4.20	2.23
9	0	7	1	1	6.29	1.94	20	0	3	4	-1	-4.83	1.93	31	1	5	3	1	-4.41	2.41
10	0	0	2	1	11.54	2.13	21	0	4	4	-1	8.79	2.04	32	2	7	4	-1	14.34	4.75
11	0	2	2	1	-7.58	2.03	22	0	5	4	1	-5.79	1.88	33	2	6	5	-1	12.92	4.95
Declination. Units [mas]																		
j	p	n	k	l	B_j	σ_{B_j}	j	p	n	k	l	B_j	σ_{B_j}	j	p	n	k	l	B_j	σ_{B_j}
1	0	0	0	-1	-49.23	2.23	8	0	9	0	-1	10.92	2.02	15	0	5	1	1	6.22	2.07
2	0	1	0	-1	29.74	2.19	9	0	0	1	-1	-17.85	2.23	16	0	0	2	1	-8.04	2.23
3	0	2	0	-1	18.42	2.06	10	0	0	1	1	16.11	2.24	17	0	2	2	1	6.47	2.07
4	0	3	0	-1	-6.92	2.10	11	0	2	1	-1	5.88	2.10	18	0	7	2	1	6.97	2.05
5	0	5	0	-1	-22.36	2.12	12	0	2	1	1	-6.55	2.05	19	0	2	4	-1	7.03	2.10
6	0	7	0	-1	5.90	2.08	13	0	3	1	1	5.58	2.09	20	0	0	6	1	6.16	2.27
7	0	8	0	-1	-6.40	2.05	14	0	4	1	-1	5.16	2.00							
Proper motion in right ascension. Units [mas/y]																		
j	p	n	k	l	B_j	σ_{B_j}	j	p	n	k	l	B_j	σ_{B_j}	j	p	n	k	l	B_j	σ_{B_j}
1	0	0	0	-1	0.46	0.08	7	0	0	1	1	0.24	0.08	13	0	3	5	1	-0.24	0.07
2	0	2	0	-1	-0.67	0.08	8	0	1	1	-1	-0.46	0.08	14	0	9	5	-1	-0.18	0.07
3	0	3	0	-1	0.79	0.07	9	0	2	1	-1	0.41	0.07	15	1	5	0	-1	-0.25	0.08
4	0	4	0	-1	-0.68	0.07	10	0	0	3	-1	0.24	0.08	16	1	3	1	1	0.30	0.09
5	0	6	0	-1	-0.23	0.07	11	0	0	3	1	0.23	0.08							
6	0	7	0	-1	-0.16	0.07	12	0	8	4	-1	0.18	0.08							
Proper motion in declination. Units [mas/y]																		
j	p	n	k	l	B_j	σ_{B_j}	j	p	n	k	l	B_j	σ_{B_j}	j	p	n	k	l	B_j	σ_{B_j}
1	0	0	0	-1	-0.32	0.07	4	0	5	0	-1	-0.53	0.07	7	0	0	1	-1	-0.40	0.07
2	0	1	0	-1	0.50	0.07	5	0	8	0	-1	-0.18	0.07	8	0	0	1	1	-0.30	0.07
3	0	4	0	-1	0.29	0.07	6	0	9	0	-1	0.20	0.06	9	0	2	1	1	-0.28	0.07

2. ACKNOWLEDGEMENTS

The authors appreciate the support of this work by the grant 02-02-16570 of the Russian Fund of Fundamental Research and by the grant of the Leading Scientific School 00-15-96775.

3. REFERENCES

[1] European Space Agency, The Hipparcos and Tycho Catalogues, "ESA", 1997.

[2] Vityazev V., In: Soffel M., Capitaine N. (ed.). Journees 99, Systemes de reference spatio-temporels & Lohrmann-Kolloquium, Observatoire de Paris, Paris, 1999, 14-16.

[3] Mignard F., Froeschle M., A&A, 2000, 354, 732-739.

[4] H. Schwan H., A&A, 2001, 367, 1078-1086.

[5] Bien R., et al., Verrof. Astr. Rech. Inst, 1978, N29.

GPS AND VLBI BASELINE LENGTH VARIATIONS

E. SKURIKHINA[1], N. PANAFIDINA[1], Y. SOKOLOVA[2]
[1]Institute of Applied Astronomy,
nab. Kutuzova 10, St. Petersburg 191187, Russia
e-mail: sea@quasar.ipa.nw.ru
[2]St. Petersburg State University,
Bibliotechnaya sq., 4

1. INTRODUCTION

Observed changes of baseline lengths can be caused by insufficient corrections for observational effects (thermal deformations of VLBI antennas, errors in modeling of tropospheric refraction, etc.) but a number of insufficiently studied or not taken into account properly geophysical effects (atmospheric and snow loading, tides, postglacial rebound, etc.) can result in real changes of baselengths. In this paper we compare baseline length variations derived from GPS and VLBI observations at 6 european stations with long enough observational history.

2. COMPARISON AND RESULTS

Baseline length variations were compared over the period of 1996.0 – 2003.5. VLBI baselengths were computed with the OCCAM package using 24h sessions (Skurikhina, 2000). For more strict account for thermal antenna deformations we used advanced model of this effect (Skurikhina, 2001) which allows to correct observed station position for all types of VLBI mount.

For computation of baseline lengths between european GPS stations we used weekly EPN solutions. These solutions were reprocessed in order to obtain homogeneous coordinate time series since processing strategy with fiducial stations used by EPN can cause a distortion of the network (Malkin and Voinov, 2001). The method of reprocessing is based on deconstraining of the official EPN solutions with further transformation to ITRF2000 (Malkin and Panafidina, 2001). For this study we used 6-parameter Helmert transformation to avoid loss of seasonal geophysical signal in baseline lengths.

One of the most important factor affecting variations of station coordinates is atmospheric loading. We investigated influence of this effect using 3-dimensional atmospheric loading model based on the station displacement time series computed in GSFC. The data were averaged over a week interval corresponding to every GPS week and variations of baselengths were computed from these weekly values.

Results of computation of variations in baseline lengths are presented in the table. Values of rates are in rather good agreement for most baselines but it isn't the case for seasonal variations. Obviously interval of investigation is too short and number of used VLBI observations is too small for many baselines. Also it would be important to verify our results using data obtained from other space geodesy techniques. In this paper we compared the time series spectrums. Ferraz-Mello method of estimation of period from unequally spaced observations (Ferraz-Mello, 1981) was used. The preliminary spectrum analyses showed presence of not only the annual

term in all time series but also a two-year term in GPS and VLBI data. The contribution of atmospheric loading to the annual term depends on station separation and can achieve about one third of the amplitude.

Table 1: Results of analysis of variation of baselengths: baseline length (L), km, number of epochs (N) processed and found in the IVS data base, linear trend (Rate), mm, amplitude of annual term (As), mm, amplitude of semiannual term (Asa), mm.

Base	L	VLBI				GPS				Atmospheric loading		
		N	Rate	Aa	Asa	N	Rate	Aa	Asa	Rate	Aa	Asa
MATE	597	47	–1.8	0.8	1.3	367	–2.3	2.5	0.9	0.0	0.3	0.2
MEDI			±0.2	±0.8	±0.8		±0.1	±0.2	±0.2	±0.0	±0.1	±0.1
MATE	444	25	+0.7	2.4	1.5	356	+2.2	1.7	0.2	+0.0	0.2	0.1
NOTO			±0.4	±1.4	±1.5		±0.1	±0.2	±0.2	±0.0	±0.1	±0.1
MATE	4190	95	-2.4	2.7	2.5	330	–6.2	7.9	2.1	0.0	0.4	0.6
NYAL			±0.5	±0.8	±0.8		±0.4	±0.9	±0.9	±0.0	±0.1	±0.1
MATE	1886	48	–5.2	1.3	0.7	372	–5.1	2.8	1.1	0.1	0.4	0.6
ONSA			±0.5	±1.4	±1.5		±0.1	±0.3	±0.3	±0.0	±0.1	±0.1
MATE	990	154	–3.6	2.2	0.9	372	–3.8	1.7	0.6	0.1	0.5	0.9
WETT			±0.2	±0.5	±0.4		±0.1	±0.2	±0.2	±0.0	±0.1	±0.1
MEDI	893	22	–3.2	3.9	3.5	365	–3.1	3.1	0.5	0.0	0.3	0.3
NOTO			±0.4	±1.4	±1.6		±0.1	±0.2	±0.2	±0.0	±0.1	±0.1
MEDI	3776	55	–2.3	3.2	2.2	339	–5.9	7.4	1.8	–0.3	1.4	0.6
NYAL			±0.4	±1.1	±1.3		±0.4	±0.9	±0.9	±0.1	±0.1	±0.1
MEDI	1429	62	–2.8	1.6	0.9	381	–4.0	2.2	4.3	0.0	1.9	1.2
ONSA			±0.5	±1.7	±1.5		±0.1	±0.3	±9.1	±0.0	±0.1	±0.1
MEDI	522	60	–2.6	0.7	0.6	381	–2.8	0.3	0.4	0.0	0.5	0.5
WETT			±0.2	±0.5	±0.4		±0.1	±0.2	±0.2	±0.0	±0.1	±0.1
NOTO	4580	22	–2.4	2.1	4.8	327	–6.1	8.9	2.0	–0.2	0.4	0.5
NYAL			±0.8	±2.5	±2.5		±0.5	±1.0	±1.0	±0.1	±0.1	±0.1
NOTO	2280	24	–5.0	1.4	2.1	370	–4.9	3.9	1.2	0.1	0.2	0.7
ONSA			±0.3	±1.1	±1.2		±0.2	±0.4	±0.4	±0.1	±0.1	±0.1
NOTO	1371	25	–4.5	1.5	1.0	370	–3.9	2.5	0.6	0.2	0.8	0.6
WETT			±0.4	±1.0	±1.7		±0.1	±0.3	±0.3	±0.1	±0.1	±0.1
NYAL	2387	71	0.6	1.8	2.5	344	–1.3	5.1	1.1	0.0	1.2	1.1
ONSA			±0.5	±1.4	±1.3		±0.3	±0.6	±0.6	±0.0	±0.2	±0.1
NYAL	3283	367	+1.0	2.5	1.1	344	–2.9	6.8	1.6	0.6	0.7	1.2
WETT			±0.1	±0.3	±0.3		±0.3	±0.7	±0.7	±0.1	±0.2	±0.2
ONSA	919	90	–1.0	0.8	0.8	386	–1.4	1.9	0.6	0.1	0.9	0.7
WETT			±0.3	±0.8	±0.8		±0.1	±0.2	±0.2	±0.0	±0.1	±0.1

3. REFERENCES

Malkin Z.M., N. Panafidina, E. Skurikhina, In: proc. 15th Working Meeting on European VLBI for Geodesy and Astrometry, 2001, 116–123.

Malkin Z.M., Voinov A.V., Phys. Chem. Earth (A), 2001, No 6–8, 579–583.

Panafidina N., Malkin Z., In: proc. IAG 2001 Scientific Assembly, 2001

Skurikhina E., In: IVS 2000 General Meeting Proc., 2000, 350–354.

Skurikhina E., In: proc. 15th Working Meeting on European VLBI for Geodesy and Astrometry, 2001, 124–130

Titov O., In: Proc. 13th Working Meeting on European VLBI for Geodesy and Astrometry, 1999, 186–191.

Ferraz-Mello S., The Astronomical Journal Volume 86, 1981

TYCHO-2 AND HIPPARCOS: INTERCOMPARISON OF THE CATALOGUES

A. POPOV, A. TSVETKOV
Sobolev Astronomical Institute of the SPb University
198904, SPb, Petrodvorets, Universitetsky pr., 28, Russia
Aleksey@ap3678.spb.edu; Tsvetkov@ast.usr.pu.ru

ABSTRACT. The Tycho-2 catalogue of position and proper motions of 2.5 millions stars is studied. The statistical and kinematical characteristics are obtained. Unusual blue stars nave been revealed.

1. RESULTS

Among the classical astrometric catalogues [1-4] the Tycho-2 [5-7] keeps an outstanding position since it lists more than one million stars fainter 11^m (Fig. 1). The distribution of stars on magnitude has two maximums. The first one corresponds to $B-V=0.45$, the second one corresponds to $B-V=1.0$ (probably, red giants). Unusual blue stars with $B-V \leq -0.5$ were found. The Hipparcos catalogue does not contain such blue stars in comparison to the Tycho-2.

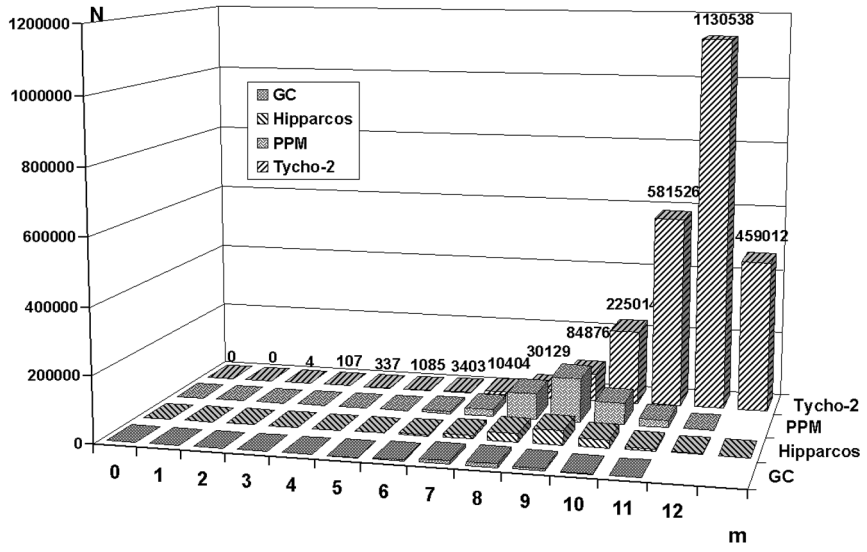

Figure 1: Stellar content of Tycho-2, PPM, Hipparcos and GC catalogues against the magnitude.

The blue stars have a tendency to concentrate in the direction of the Galactic plane, whereas the red stars show more uniform distribution. The same effects are for the Hipparcos stars. However, the Galactic concentration is observed for the most faint stars ($m > 9^m$) regardless their spectral types. It is very interesting that all blue stars with $B - V < -0.5^m$ are generally very faint stars ($m > 11^m$).

The least squares technique was applied for calculating the parameters of the Oort-Linblad and Ogorodnikov-Milne models from several samples of the Tycho-2. The combined and separate solutions were made for equatorial ($|\delta| \leq 15^\circ$) and non equatorial stars for the samples where the correlations between the unknowns have been found to be less than 0.4.

The Oort's parameters for faint stars were compared with the IAU recommended ones. The values of the Oort's parameters significantly depend on the properties of the samples, especially on the magnitude (Table 1) and the color index $B - V$.

Table 1: Dependence of the Oorth's parameters A and B on magnitude

m	A	B
	$km/s \cdot kpc^{-1}$	$km/s \cdot kpc^{-1}$
$(7, 9)$	13.9 $\pm$ 1.0	-11.2 $\pm$ 0.8
$(9, 11)$	14.5 $\pm$ 0.2	-11.1 $\pm$ 0.2
< 11	13.6 $\pm$ 0.1	-10.9 $\pm$ 0.1

The rest of the parameters of the Ogorodnikov-Milne model are insignificant, especially for faint stars. It means that these stars being very distant satisfy the model of plane Galactic rotation.

The main conclusion is that the Tycho-2 contains a lot of more distant stars than the Hipparcos does, and the kinematics of these stars is consistent with the Oort-Linblad model of flat Galactic rotation.

2. ACKNOWLEDGEMENTS

The authors appreciate the support of this work by the grant 02-02-16570 of the Russian Fund of Fundamental Research and by the grant of the Leading Scientific School 00-15-96775.

3. REFERENCES

[1] Bastian U., Roser S. – 1993, PPM Star Catalogue, Vol III-IY, Astron. Rechen-Inst., Heidelberg.

[2] Boss B. – General Catalogue of 33342 stars for the epoch 1950.0,Washington, 1937.

[3]Fricke, W. – Fifth Fundamental Catalogue (FK5). Veroff. Astron. Rechen-Institut,Heidelberg, N 32, 1988.

[4] ESA, FAST, NDAC, TDAC, INCA – The Hipparcos and Tycho Catalogue, ESA SP1200, 1997.

[5] E. Hog, C. Fabricius, V.V. Makarov, S. Urban, T. Corbin, G. Wycoff, U. Bastian, P. Schwekendiek, and A. Wicenec. – The Tycho-2 Catalogue of the 2.5 Million Brightest Stars, *Astron. Astrophys.*, 2000.

6] E. Hog, C. Fabricius, V.V. Makarov, S. Urban, T. Corbin, G. Wycoff, U. Bastian, P. Schwekendiek, and A. Wicenec. – Guide to the Tycho-2 Catalogue, *Astron. Astrophys.*, 2000.

[7] E. Hog, C. Fabricius, V.V. Makarov, S. Urban, T. Corbin, G. Wycoff, U. Bastian, P. Schwekendiek, and A. Wicenec. – Construction and verification of the Tycho-2 Catalogue, *Astron. Astrophys.*, 2000.

THE PROBLEM OF DYNAMICAL REFERENCE SYSTEM CONSTRUCTION AT THE MODERN STAGE

E. I. YAGUDINA
Institute of Applied Astronomy Russian Academy of Sciences
10 Kutuzova emb., 191197, St.-Petersburg, Russia
e-mail: eiya@quasar.ipa.nw.ru

The ICRF now is the fundamental celestial reference frame with the Hipparcos Catalog as the realization of the ICRF at optical wavelengths. Unlike past stellar realizations, which were oriented to the equinox and equator of various reference epochs, the orientation of the ICRF is independent of epoch and will not be changed in the future. The orientation and positions of the ICRF are consistent with the J2000 (FK5) System. The JPL ephemerides (dynamical system) have been oriented onto the ICRF since 1995. According to (Standish, 2003) the notion of dynamical system is no longer " relevant" "since the ICRF is assumed to be inertially founded". The necessity of keeping the dynamical system was discussed a long time ago. As a notion it is conserved and it is necessary to keep in mind another problems like conservation and usage of old observations, historical aspect of non- precessional equinox motion, the problems of mutual orientation of different astronomical systems etc. Especially the problem of mutual orientation of the ICRF and other systems is important even at our times: the link of dynamical and ICRF systems is not reliably known and it is necessary to continue improving of the orientation between different systems. The problem of non-precessional motion of equinox has not only historical aspect: it was suggested in (Vityazev, Yagudina, 2000) that the fictitious motion of the equinox is well correlated with curve $\Delta T = ET - UT$ and can be considered as the first evidence of the irregular rotation of the Earth.

About 18000 optical and radar observations of 35 NEAs and main belt planets have been used to obtain precise asteroids orbits, catalogue orientation parameters and the motion of the dynamical equinox from 1750 till 2002 in Hipparcos system. For obtaining the orientation parameters and equinox motion we collected the observations of 35 minor planets with available radar data. Most of them, 31 planets are NEAs The interval covered by optical observations for this list of objects is more than 90 years, radar measurements are available after 1968. All optical observations were taken from MPC catalogue, radar observations (Doppler and delay) from JPL database 'Small-body astrometric radar observations'. The accuracy of optical observations are of the order of $1''$ for old observations and better than $0.5''$ for observations made after 1960. The precision of Doppler observations varies from 30.0 Hz till 0.1 Hz for the frequency, and from 140 till 0.1 μs for delay. We have discussed similar problems previously, having used 24 NEAs for obtaining the FK5 orientation parameters (Yagudina, 2001). Now, in addition to that we have used the observations of the asteroids with long optical history (such as Iris, Zelinda and others) and for some NEAs (Toutatis, Golevka, etc) the radar observations in the second apparition have been used. Besides, the accuracy of optical observations during the last 4–5 years have increased significantly, the accuracy of CCD observations being about $0.3''$. All this gave us new possibilities for obtaining a more precise solution. All calculations have been performed

Table 1: The dynamical motion for different intervals of time

epoch	Time interval	$d\dot{A}$ $''/cy$	number of observations	Accuracy of optical obs.
2001.8	11 asteroids	-1.034	10252 opt	$1''$
	1900–2000	± 0.079	107 rad	
	23 asteroids	-0.004	6398 opt	$< 1''$
	1950-2000	± 0.001	238 rad	$> 0.5''$
	17 asteroids	-0.003	3150 opt	$< 0.5''$
	1965–2000	± 0.000	181 rad	
	35 asteroids	-0.009	17650 opt	$0.5''$- $1''$
	1900-2002	± 0.001	351 rad	

within the framework of ERA system (Krasinsky and Vasiliev, 1996). The orbits of asteroids have been computed by numerical integration of the relativistic equations of motion taking into account the perturbations from all major planets and the Moon, as well as the Schwarzschild's terms due to the Sun. For calculations of the coordinates of perturbing planets and the Moon the DE200/LE200 ephemerides were used. The way it was fulfilled in previous works the parameters under consideration were the following: among the total parameters of the global solution there are six parameters of the coordinates and velocities corrections for each planet for the standard epoch (they were included in the conditional equations for optical and radar observations), correction to the mean longitude of the Earth, dL, the FK5 equinox correction, dA, the FK5 equator correction, dD, the secular variation of the equinox correction, $d\dot{A}$ (they were included in the conditional equations for only optical data). Several versions of the global solution have been considered. The most interesting results concerning the values of $d\dot{A}$ for different intervals of time on the basis of different number of optical and radar observations are shown at the Table.

We consider that radar observations with refined sets of positional ground-based observations of NEARs and main belt minor planets covering long interval of time can be quite useful for improving the link between Hipparcos and dynamical systems (given by DE ephemerides) and for clarifying the historical problem of motion of dynamical equinox.

REFERENCES

Standish, M. Relating the dynamical frame and ephemerides to the ICRF In: Abstracts of the 25th GA of IAU,16–24 July, 2003.

Vityazev V. V. , Yagudina E. I. The non-precessional motion of the equinox: a phantom or a phenomenon? In: Capitaine N. (ed). Journess 2000, Systemes dereference spatio-temporels, Paris, 18-20 Septembre, 42–47.

Yagudina E. I. The use of radar observations of Near-Earth asteroids in the determination of the dynamical equinox, Celest. Mech., Vol.80,3-4,195–203.

Krasinsky, G.A. and Vasiliev, M.V. ERA: knowledge base for ephemeris and dynamical astronomy, in Wytrzyszczak I.M., Lieske J.H. and Feldman R.A., (eds), Proceedings of IAU Colloquium 165, Poznan, Poland, July 1-5, 1996, 239–244.

NPM2 AND HIPPARCOS PROPER MOTIONS

Z. ZHU
Department of Astronomy, Nanjing University
210093 Nanjing, China
e-mail: zhuzi@nju.edu.cn

ABSTRACT. Comparing the Hipparcos proper motions with those of the Lick NPM2 Catalog, which provides absolute proper motions of objects measured directly relative to external galaxies, we found that the two components of the spin vector, ω_x and ω_y, are apparently less than the value of 0.25 mas yr^{-1} for the uncertainty of the Hipparcos inertiality, while the component ω_z is about three times that value. Inspecting the magnitude- and color-dependent pattern of the proper-motion difference, we found that there is no strong systematics existing in the NPM2 with respect to the Hipparcos proper-motion system.

1. INTRODUCTION

The recent released NPM2 Catalog is the second part of the Lick Northern Proper Motion program (http://www.ucolock.org/~npm/NPM2; Klemola et al. 1987) which contains absolute proper motions, accurate positions, and BV photometry for 232062 stars from 8 magnitude to 18 magnitude in B band. There are 347 NPM2 fields in total covering from +83 degree to −23 degree in declination. The RMS errors of the NPM2 absolute proper motions are about 6 mas yr^{-1} in each coordinate, comparable to the NPM1 errors. The preliminary version of the NPM2 gives 196639 stars, which includes 4395 Hipparcos stars and about 80000 stars in the Tycho-2 Catalogue.

The purpose of this study was to compare the NPM2 proper-motion system with Hipparcos in order to examine the inertiality of the Hipparcos system. In particular, we analyzed the possible sources of systematic errors in the NPM2 system which might infect our solution of the proper-motion systematics.

2. SYSTEMATIC DIFFERENCE IN PROPER MOTIONS

Considering the possible complications arising from the Hipparcos observations of binary, multiple, and suspected non-single systems, we excluded all of these stars found in the Hipparcos Catalogue in our analysis. Thus, only 3768 single stars remain for the analysis, which are common to both NPM2 and Hipparcos catalogues.

In our previous work, we have compared the SPM 2.0 proper motions with those of the Hipparcos (Zhu 2001). In a similar way, the spin vector (ω_x, ω_y, ω_z), which represents the rotational difference between the two frames, are determined by a generalized least-squares method. It is noticed that some proper-motion data, both from the NPM2 Catalog and from the Hipparcos Catalogue, might have large measurement errors. To exclude extremely erroneous

proper motions, the 2.6σ principle is introduced to our procedure. Thus, all stars that contribute large residuals to the solution will be rejected, and then, we obtain a more reliable result. The corresponding spin solution was obtained and is listed in table 1.

Table 1. Systematic differences of the NPM2 and SPM 2.0 relative to the Hipparcos proper-motion system.

	Number of stars	ω_x	ω_y	ω_z
NPM2-HIP	3519	$+0.11\pm0.20$	$+0.19\pm0.20$	$+0.75\pm0.28$
SPM2-HIP	9356	-0.10 ± 0.17	-0.48 ± 0.14	$+0.17\pm0.15$

It is shown that the two components of the spin vector, ω_x and ω_y, are apparently less than the value of 0.25 mas yr^{-1} for the uncertainty of the Hipparcos inertiality, while the component ω_z is about three times that value. The differences between the SPM 2.0 and Hipparcos are not the same as NPM2-HIP, though both the SPM2.0 and NPM2 proper motions were measured directly in an inertial reference system with respect to extragalactic radio sources. A possible reason might be the systematic shift between the NPM2 and SPM 2.0.

In order to examine the magnitude- and color-dependent differences in proper motions between the NPM2 and Hipparcos, we have checked the systematic differences of the proper motions. It indicates that no significant magnitude- and color-depended systematics are found in the NPM2 proper-motion system. It is noticed the magnitude-dependent systematic errors for the brightest NPM2 stars were already removed in the NPM2 reduction. Furthermore, the present range of magnitude is too low to check the magnitude equation of the NPM2 proper-motion system.

3. REMARKS

The Hipparcos Catalogue is a realization of the ICRS system, which was finalized via a specific link program by various observational techniques (Lindegren & Kovalevsky 1995; Kovalevsky et al. 1997). Its proper-motion system is believed to be quasi-inertial to within ±0.25 mas yr^{-1} for all three axes with respect to distant extragalactic objects. The proper motions of the NPM2 Catalog are absolute, measured directly in an inertial reference system, the two proper-motion system should be coincident.

Analyzing the proper-motion differences between the NPM2 and Hipparcos catalogues, we found that components ω_x and ω_y are apparently less than 0.25 mas yr^{-1} in absolute value, while the component ω_z is as large as three times this value. It is confirmed that no significant magnitude- and color-equation is existed in the NPM2 proper motions, compared with the Hipparcos proper motions, in the range from 8 to 12 magnitude.

This work was supported by the National Natural Science Foundation of China (NSFC) and by Nanjing University Talent Development Foundation.

4. REFERENCES

Hanson, R.B., et al. 2003, Lick Northern Proper Motion Program: NPM2 Catalog, http://www.ucolock.org/~npm/NPM2

Klemola, A.R., Jones, B.F., & Hanson, R.B. 1987, *Astron. J.*, 94, 501

Kovalevsky, J., et al. 1997, *Astron. Astrophys.*, 323, 620

Lindegren, L., & Kovalevsky, J. 1995, *Astron. Astrophys.*, 304, 189

Zhu, Z. 2001, *PASJ*, 53, L33

Section II)

ROTATION OF THE EARTH AND OTHER PLANETS: OBSERVATIONS AND MODELS

ROTATION DE LA TERRE ET DES AUTRES PLANÈTES: OBSERVATIONS ET MODÈLES

FREE CORE NUTATION: STOCHASTIC MODELING VERSUS PREDICTABILITY

A. BRZEZIŃSKI, W. KOSEK
Space Research Centre, Polish Academy of Sciences
Bartycka 18A, 00-716 Warsaw, Poland
e-mail: alek@cbk.waw.pl

ABSTRACT. The time series of the celestial pole offsets determined by VLBI contains the free core nutation (FCN) which is a pseudoharmonic oscillation with retrograde period of 430 days and variable amplitude between 0.1 and 0.3 milliarcseconds. This signal is significant at the assumed sub-milliarcsecond level of accuracy therefore needs explanation and modeling. In the first part of this study we recall our earlier results concerning the stochastic modeling of the observed FCN signal. Then we show how the model of the autoregressive process can be applied for prediction of the observed irregular component of nutation and compare results to the extrapolation based on the sinusoidal model of the FCN.

1. INTRODUCTION

The difference between the precession and nutation observed by the *very long baseline interferometry* (VLBI) technique and that predicted by the MHB2000 model (Mathews *et al.*, 2002) contains irregular variations which are significant at the sub-milliarcsecond level of accuracy (see, e.g., Dehant *et al.*, 2003) therefore needs explanation and modeling. There are at least two types of irregular motions:

1. The *free core nutation* (FCN), a pseudoharmonic oscillation with retrograde period of about 430 days and variable amplitude between 0.1 and 0.3 mas (milliarcseconds) as well as variable phase.

2. Atmospheric and nontidal oceanic contributions to nutation which are not strictly harmonic but contain a broad-band variability at the level of 0.1 mas (Bizouard *et al.*, 1998; Petrov *et al.*, 1998).

These irregular motions can be modeled by different methods. Here we will focus attention on the stochastic modeling by the *autoregressive integrated moving-average* (ARIMA) processes. First, we will recall briefly our earlier results on the ARIMA modeling of the FCN, which have been discussed in a series of papers (Brzeziński, 1994; 1996; 2000; Brzeziński and Petrov, 1998; Brzeziński *et al.*, 2002). The ARIMA model is particularly suitable for determination of the parameters of the FCN resonance, the period T, the quality factor Q and the excitation power S needed to maintain the observed free motion. Then, we will consider the possibility of applying this model to predict the future values of the FCN signal. We will also describe first numerical

experiment comparing the autoregressive prediction of the observed time series of the celestial pole offsets to the extrapolation based on the sinusoidal model of the FCN.

2. FREE CORE NUTATION MODE IN EARTH ROTATION

The FCN belongs to the catalogue of the solid Earth modes; see Figure 3 of Eubanks (1993). It influences Earth rotation in two different ways: 1) through resonant enhancement of the amplitudes of those lunisolar nutation waves which are close to the frequency of resonance (indirect effect), and 2) it gives rise to the free oscillation of the pole in response to the irregular excitations, atmospheric, oceanic, etc. (direct effect). In addition, the FCN resonance influences also the tidal gravity variations, but only indirect effect has been detected so far.

2.1. *Observations of the FCN*

The FCN was predicted and explained theoretically already at the end of 19th century (Hough, 1895). Many attempts were made in the past to detect the FCN oscillation in the astrometric observations of Earth rotation, e.g. by Popov (1963), Yatskiv *et al.* (1975), but only the recent measurements by the VLBI have been precise enough both to verify theoretical models of the indirect effect on nutation and to reveal the FCN signal in the celestial motion of the pole (Herring *et al.*, 1986). The FCN oscillation contributes to the time series of the celestial pole offsets which are routinely provided by the International Earth Rotation and Reference Systems Service (IERS). Several series based on the VLBI observations are available from 1979 till now, but for the purpose of tracking the FCN signal it is necessary to reject the data before 1984.

As it can be seen from Figure 1b, the irregular variability of nutation shown in Figure 1a consists mostly of the FCN oscillation which contributes more than 60% to the total power in the series. The period $T = -429.6$ days determined from the *maximum entropy method* (MEM) of spectral analysis (Brzeziński, 1995) agrees quite well with the value $T = -430.2$ days adopted by the MHB2000 model (Mathews *et al.*, 2002), marked in Figure 1b by the vertical line. The amplitude of the FCN varies in time but it does not show any permanent decaying trend. The maximum values, around 0.3 mas, occur before 1990, then become significantly smaller in 1990-ties, and increase again after 2000.

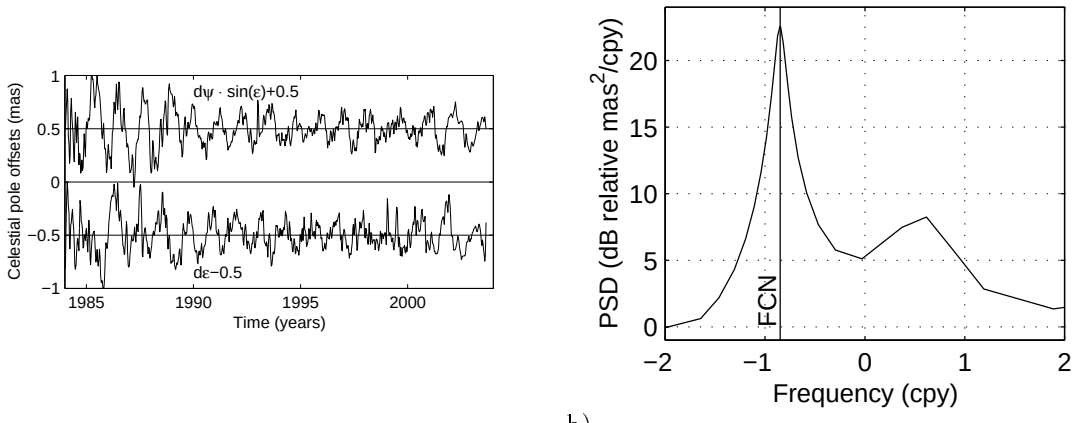

a) b)

Figure 1: Celestial pole offsets observed by the VLBI (IERS combination series C04), after removal of the empirical corrections to the IAU2000 precession/nutation model a) time domain representation, b) frequency domain representation – maximum entropy power spectrum.

2.2. *Modeling of the FCN*

The MHB2000 precession-nutation model adopted as an official IAU standard model and designated as IAU2000 (IERS, 2003), does not include the FCN because it is a free motion that cannot be predicted rigorously. However, the Fortran program `IAU2000A.f` evaluating the nutation model, which is attached to Chapter 5 of the IERS Conventions 2003 (*ibid.*), contains the subroutine `FCN_nut` which can be optionally used in computations. This subroutine implements the FCN model which is recommended by the IERS. The model assumes a constant dissipationless value of the FCN frequency and uses the empirical values of the sine- and cosine-amplitudes (equivalently, the sine- and cosine- amplitudes can be expressed as the amplitude and phase with respect to the selected reference epoch) pre-estimated for the subsequent two-year intervals. The amplitudes are interpolated linearly to the epoch of computation and these are the instantaneous values used to evaluate the FCN signal. In case when the evaluation epoch is larger than the time of the last pre-estimated value, the most recent amplitudes are used in the computation.

An alternative model of the observed FCN signal proposed by Shirai and Fukushima (2001) is a piecewise damped sinusoidal oscillation with a number of the excitation impulses. After assuming the values of the FCN period $T = -431$ days and the quality factor $Q = 15300$, they found that an adequate representation of the FCN signal during the period 1979 to 2000 can be obtained when assuming 4 different excitation epochs: 1989.39, 1994.47, 1994.76 and 1998.99, and determining five complex amplitudes by the least-squares method. This model has a physical explanation, namely it is an implementation of the hypothesis stating that the FCN is excited by large earthquakes.

Another approach for modelling the free oscillations in Earth rotation, originally proposed by Jeffreys (1940) as an adequate representation of the Chandler wobble, is a stochastic modeling by the ARIMA processes. The model assumes that the free signal which is subject to damping, is continuously excited by a certain random process, or a combination of processes. Such excitation corresponds to the retrograde quasi diurnal variation in the atmospheric and oceanic angular momentum driven by the daily solar heating cycle.

The ARIMA modeling of the FCN has been discussed extensively by Brzeziński (1994, 1996, 2000), Brzeziński and Petrov (1998), Brzeziński *et al.* (2002). We proceeded according to the following scheme:

1. Introduce possible simplifications to the equation of motion.
2. Solve equation of motion analytically and perform discretization by applying the trapezoidal rule of integration.
3. Assume equidistant sampling of all variables and introduce simple stochastic models for the excitation process and for the measurement noise.

If the excitation process is modeled as a white noise and the measurement errors as a random walk, then the resulting stochastic model for the observed FCN signal is

$$d_l - \varphi_1 d_{l-1} = v_l - \theta_1 v_{l-1} - \theta_2 v_{l-2}, \tag{1}$$

where $d_l = z_l - z_{l-1}$ is the first difference of the observation $z_l = P_l + n_1$ of nutation, $P_l = d\psi_l \sin\varepsilon_o + i d\varepsilon_l$ denotes the nutation expressed as complex combination of the celestial pole offsets in longitude $d\psi$ and obliquity $d\varepsilon$, with $\varepsilon_o = \varepsilon(\mathrm{J2000})$ and $i = \sqrt{-1}$, n_l is complex measurement noise assumed to be realization of the random walk process, the complex coefficients φ_1, θ_1, θ_2

are known functions of the FCN period T and quality factor Q, and $\{v_l\}$ is a zero-mean sequence of uncorrelated complex-valued random impulses. Eq.(1) describes the ARIMA(1,1,2) model; see, e.g., (Marple, 1987) for theoretical basis. Its parameters can be determined by applying the maximum likelihood algorithm to the time series of observations.

The ARIMA model expressed by eq.(1) which follows from the physics of the FCN, provides the optimum representation in a sense of the criterion of parsimony: it is fully describes by the three complex coefficients φ_1, θ_1, θ_2 and one real coefficient expressing the standard deviation of the driving white noise $\{v_l\}$. An equivalent from the point of view of mathematics, representation of the ARIMA process is provided by the pure *autoregressive* (AR) model

$$z_l - \varphi_1 z_{l-1} - \varphi_2 z_{l-2} - \ldots\ldots - \varphi_p z_{l-p} = v_l. \tag{2}$$

This model involves usually more parameters than the optimum ARIMA counterpart, eq.(1). In case of the nutation time series with a 10-day sampling, shown in Figure 1a, we found the optimum AR order $p = 21$ (see next section for details). It means that the number of parameters increased seven times. But such a pure AR model offers important advantages for our applications. First, there exist simple algorithms for determining its parameters, the coefficients φ_j, $j = 1, \ldots, p$, and standard deviation of the driving noise $\{v_l\}$. In the computations described in the next section we apply the least-squares version of the MEM algorithm to estimate the AR coefficients, with the Akaike *final prediction error* (FPE) criterion for finding the optimum order p; see (Brzeziński, 1995) for computational details. Second, the application of the AR model for prediction is straightforward. One needs only to replace in eq.(2) the unknown future random impulses v_l by their expected values equal to zero. Finally, this model takes into account not only the FCN signal but also other irregular components of the observed time series, such as that expressed by the broad peak at prograde frequencies between 0 and 1 cycles per year, shown in Figure 1b.

3. PREDICTION OF THE IRREGULAR VARIATIONS IN NUTATION

We used in computations the IERS combination series C04 related to the IAU2000 precession-nutation model (file `EOPC04_IAU2000.62-now` downloaded from the following website address `http://hpiers.obspm.fr/eoppc/eop/eopC04`). The series used here contains 7192 daily values of the celestial pole offsets $X = d\psi \sin\varepsilon_o$, $Y = d\varepsilon$, spanning the period between 1984.0 and 2003.7. First, we removed from the input series the model comprising the linear trend and corrections to the important nutation terms. We found by the least- squares fit the following corrections which are in some cases surprisingly large:

		$d\psi \sin\varepsilon_o$	$d\varepsilon$
1-st order polynomial			
	constant (μas)	59 ± 6	32 ± 7,
	slope (μas/yr)	8 ± 1	9 ± 1,
Periodical terms (μas)		retrograde	prograde
	18.6 yr	28 ± 8	68 ± 6,
	9.3 yr	28 ± 6	33 ± 6,
	1.0 yr	5 ± 6	10 ± 6,
	0.5 yr	19 ± 7	9 ± 6.

Then, we smoothed the residual nutation series by the Gaussian filter with full width at a half of maximum equal to 20 days, and interpolated at 10-day intervals, with the first modified Julian date 45710.0. The reduced time series of the nutation residuals, which has a length of 718, is shown in Figure 1a. The MEM power spectrum of $P = X + iY$ computed for the AR

order $p = 21$ (cf. eq.(2)) shows the FCN peak containing more than 60% power of the series. The MEM spectral analysis yields the FCN period of $T = -429.6$ days (Figure 1b), the quality factor $Q = 2995$ and the mean amplitude, that is the square root of the power of oscillation, $A = 179$ μas. If we compute the FCN parameters assuming over the entire time interval 1984.0 to 2003.7 the model comprising both the retrograde and prograde complex sinusoids with a period of 430 days, the result is $A = 107 \pm 6$ μas for the retrograde component and $A = 11 \pm 6$ μas for the prograde one.

Next, we computed the one-year forecasts of the reduced nutation series using two different methods. The first method, designated below as sinusoidal prediction, corresponds to the FCN model recommended by the IERS. It consists in fitting to the last two years of data of the model comprising a sum of the complex sinusoid with a period of -430 days (that describes a uniform circular motion of P in the clockwise direction) and the constant, and then extrapolating this model into the future. Hence, this model allows the time variation of the FCN amplitude and phase while assuming that the motion is purely retrograde. The other method is the AR prediction with the autoregressive coefficients φ_l, eq.(2), estimated by using the last eight years of data. The optimum AR order p was determined as that corresponding to the first local minimum of the FPE value, for which $p \geq 20$.

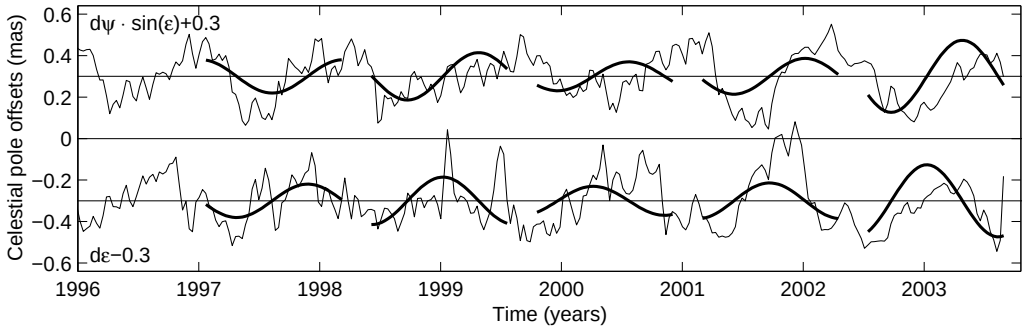

a)

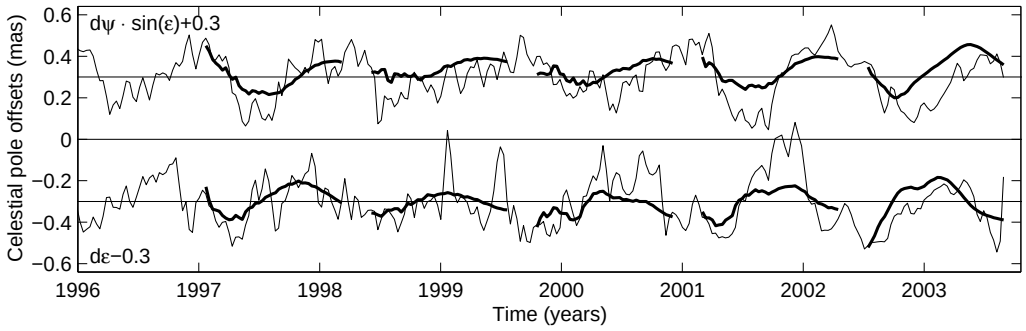

b)

Figure 2: One year predictions (thick line) of the observed nutation residuals (thin line), computed at different starting epochs a) by the extrapolation of the model: constant plus complex sinusoid with a period of -430 days, b) by the use of the autoregressive model.

We considered also the third prediction method assuming constant future values of the series, where the constant was determined as a mean over the last 2.5 years of data that is roughly two full FCN cycles. This model serves us as a reference when estimating the efficiency of the other two methods. The mean prediction error for m days in future was computed as a root mean square difference between prediction and true value, averaged over the whole set of possible starting prediction times. Figure 2 shows sample one-year predictions by the first two

methods, computed for different starting prediction epochs, while the mean prediction errors for m between 10 and 380 days in the future, are compared in Figure 3. For other prediction methods applied to the observations of polar motion see the paper by Kosek *et al.* (this volume) and the references therein.

From the inspection of Figures 2 and 3 we can draw several conclusions. All predictions are generally worse for $Y = d\varepsilon$ which indicates that this component of nutation contains higher noise than the other component $X = d\psi \sin \varepsilon_o$. The mean prediction error of the forecast by constant does not depend on the prediction time, while in case of the sinusoidal model the error increases approximately linearly. As could be expected, the best results are obtained by the AR model. The prediction error growths rapidly for the prediction time m between 10 and 50 days, then increases roughly linearly, and finally becomes almost constant. Again, there is a difference between the X and Y components of nutation. In case of the X component the initial growth of the error is slower, and the stability is reached already for m equal to about 200 days and at the level of 0.10 mas. In case of Y, the corresponding quantities are 270 days and about 0.12 mas. The advantage over the sinusoidal extrapolation is particularly well seen for short and long prediction times. As it can be seen from Figure 2, one reason for better performance of the AR prediction is that the underlying stochastic model does not only attempt to express the FCN but also other fine features of the irregular variability of nutation.

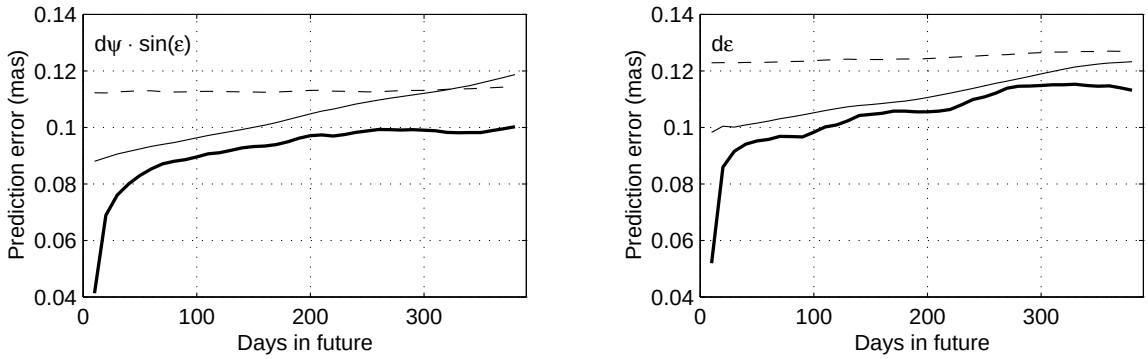

a) b)

Figure 3: The mean prediction error of the observed nutation residuals, assuming the following models: the constant (dashed line), the constant plus complex sinusoid with a period of −430 days (thin solid line) and the autoregressive process (thick solid line).

An important measure of the efficiency of a forecast method is the "predictability" coefficient introduced by Chao (1985)

$$R = 1 - \frac{\sigma_{pred}}{\sigma}\,, \tag{3}$$

where σ_{pred} denotes the estimated mean prediction error (Figure 3), while σ denotes the standard deviation of the series. We replace here σ by the mean error of the prediction by constant, as expressed by the dashed line in Figure 3. For the autoregressive model the predictability takes the following values

days in future	$X = d\psi \sin \varepsilon_o$	$Y = d\varepsilon$
10	63%	58%,
20	39%	30%,
30	32%	25%,
40	29%	23%,
...	...	...,
360	13%	10%,

Hence, in case of the observed celestial pole offsets the predictability is significant only for short prediction lengths. For one-year prediction the efficiency is much lower than in case of polar motion, where it is of the order of 80% to 90%. There are two reasons for such difference: 1) the signal-to-noise ratio is up to 3 orders of magnitude higher for polar motion than for the celestial pole offsets; 2) the FCN is less stable than the Chandler wobble because its dissipation time estimated from observations is several times shorter.

4. SUMMARY AND CONCLUSIONS

Modeling the FCN signal in the time series of the celestial pole offsets observed by VLBI, is an important task of the sub-milliarcsecond astrometry. Its variability (Figure 1) is typical for the randomly excited free oscillator with damping. A similar observation concerning the Chandler wobble led Jeffreys (1940) to the concept of describing the free motion as a realization of the stochastic process, the ARIMA process. We followed this concept and applied the ARIMA model for description of the FCN; see, e.g., (Brzeziński, 1996) for details.

The application of the ARIMA processes in the investigations concerning the FCN offers several advantages. Such model has a good physical explanation since it can be derived directly from the equation of motion. The underlying assumption is that the excitation function behaves as a random process, which is reasonable as far as we consider the influence of the atmosphere and of the nontidal oceanic variability on nutation. The application of the ARIMA model enables determination of the parameters of the FCN mode (Brzeziński and Petrov, 1998) which is independent from the estimation based on the indirect effect (Mathews *et al.*, 2002). The ARIMA model can also be used for the time domain comparison between the FCN signal and the atmospheric and/or oceanic excitation. Unfortunately, such comparisons could not be conclusive so far because we do not have adequate estimates of the atmospheric and oceanic excitation functions (Petrov *et al.*, 1997).

In this research we considered the application of the AR model for prediction of the observed irregular component of nutation including the FCN signal. First computation using the available time series of the celestial pole offsets demonstrated clear advantage of the AR-based prediction over the extrapolation of the sinusoidal model. This advantage is particularly large for short term predictions, up to about 1 month. For longer prediction times, between 1/2 and 1 year, the AR model yields the rms errors of about 0.10 mas for $X = d\psi \sin \varepsilon_o$ and 0.11 mas for $Y = d\varepsilon$.

However, even in case of the AR prediction its efficiency is low. For the prediction length of 10 days, the predictability is (63%,58%) for (X,Y), then it decreases rapidly reaching (32%,25%) for $m = 30$ days, and for $m = 1$ year it takes rather low value of (13%,10%).

Acknowledgments. This research has been supported by the Polish Ministry of Scientific Research and Information Technology under grants No. 5 T12E 039 24 and No. 8 T12E 005 20. Accommodation costs were covered by the Russian Academy of Sciences in frame of bilateral cooperation with the Polish Academy of Sciences.

5. REFERENCES

Bizouard, Ch., Brzeziński, A., and Petrov, S. D., 1998, Diurnal atmospheric forcing and temporal variations of the nutation amplitudes, *Journal of Geodesy*, **72**, 561–577.

Brzeziński, A., 1994, The period and the quality factor of the Free Core Nutation mode determined by the maximum entropy spectral analysis, *Proc. Journées Systèmes de Référence Spatio-Temporels 1994*, edited by N. Capitaine, Paris Observatory, 219–225.

Brzeziński, A., 1995, On the interpretation of maximum entropy power spectrum and cross-

power spectrum in earth rotation investigations, *manuscripta geodaetica*, **20**, 248–264.

Brzeziński, A., 1996, The free core nutation resonance in Earth rotation: observability and modeling, *Proc. Russian Conference "Modern Problems and Methods of Astrometry and Geodynamics"*, edited by A. Finkelstein *et al.*, Inst. of Applied Astronomy of RAS, St. Petersburg, 328–335.

Brzeziński, A., 2000, On the atmospheric excitation of the free modes in Earth rotation, *Proc. Journées 1999 & IX. Lohrmann-Kolloquium, eds. M. Soffel and N. Capitaine*, Paris Observatory, 153–156.

Brzeziński, A., and Petrov, S. D., 1998, Observational evidence of the free core nutation and its geophysical excitation, *Proc. Journées Systèmes de Référence Spatio-Temporels 1998*, edited by N. Capitaine, Paris Observatory, 169–174.

Brzeziński, A., Bizouard, Ch., and Petrov, S. D., 2002, Influence of the atmosphere on Earth rotation: what new can be learned from the recent atmospheric angular momentum estimates? *Surveys in Geophysics*, **23**, 33–69.

Chao, B. F., 1985, Predictability of the Earth's polar motion, *Bull. Géod.,* **59**, 81–93.

Dehant, V., Feissel-Vernier, M., de Viron, O., Ma, C., Yseboodt, M., and Bizouard, Ch., 2003, Remaining error sources in the nutation at the submilliarc second level, *Journal of Geoph. Res.,* **108**, *No. B5*, doi:10.1029/2002JB001763.

Eubanks, T. M., 1993, Variations in the orientation of the Earth, in. D. E. Smith and D. L. Turcotte (eds.), *Contributions of Space Geodesy to Geodynamics: Earth Dynamics, Geodynamics Series, Vol.24*, American Geophysical Union, Washington, D.C., 1–54.

Herring, T. A., Gwinn, C. R., and Shapiro, I. I., 1986, Geodesy by radio interferometry: studies of the forced nutations of the earth, 1. Data analysis, *Journal of Geophys. Res.,* **91**, *No. B5*, 4745–4754.

Hough, S. S., 1895, The oscillations of a rotating ellipsoidal shell containing fluid, *Phil. Trans. R. Soc. London, A, 186*, 469–506.

IERS, 2003, IERS Conventions 2003, eds. D. McCarthy and G. Petit, *IERS Technical Note No. 32*, Verlag des Bundesamts für Kartographie und Geodäsie, Frankfurt am Main, in print (electronic version is available from `http://maia.usno.navy.mil/conv2003.html`).

Jeffreys, H., 1940, The variation of latitude, *Monthly Notices of the Royal Astr. Soc.,* **100**, *No. 3*, 139–155.

Marple, S. L., Jr., 1987, *Digital Spectral Analysis With Applications*, Prentice-Hall, Englewood Cliffs., New Jersey.

Mathews, P. M., Herring, T. A., and Buffet, B. A., 2002, Modeling of nutation-precession: New nutation series for nonrigid Earth, and insights into the Earth's interior, *Journal of Geoph. Res.,* **107**, *No. B4*, doi:10.1029/2001JB000390.

Petrov, S. D., Brzeziński, A., and Bizouard, Ch., 1997, Time domain comparison of the VLBI nutation series and observed changes of the atmospheric angular momentum. *Proceedings Journées Systèmes de Référence Spatio-Temporels 1997*, edited by J. Vondrák and N. Capitaine, Astronomical Institute, Academy of Sciences of the Czech R., 107.

Petrov, S. D., Brzeziński, A., and Nastula, J., 1998, First estimation of the non- tidal oceanic effect on nutation, in. *Proc. Journées Systèmes de Référence Spatio-Temporels 1998*, edited by N. Capitaine, Paris Observatory, 136–141.

Popov, N. A., 1963, Nutational motion of the Earth's axis, *Nature,* **193**, *No.3*, 1153.

Shirai, T., and Fukushima, T., 2001, Construction of a new forced nutation theory of the nonrigid Earth, *Astron. J.*, **121**, 3270–3283.

Yatskiv, Ya. S., Wako, Y., and Kaneko, Y., 1975, Study of the nearly diurnal free nutation based on latitude observations of the ILS stations (I), *Publs. Int. Lat. Obs. Mizusawa,* **10**, *No. 1*, 1–31.

BODY TIDES IN THE EARTH-MOON SYSTEM AND THE EARTH'S ROTATION

G.A. KRASINSKY
Institute of Applied Astronomy of RAS
10 Kutuzov Quay, St.Petersburg, 191187, Russia
e-mail: kra@quasar.ipa.nw.ru

ABSTRACT. Differential equations of rotation of the Earth with the viscous fluid core are presented and applied to explanation of a number of observed effects in the Earth's rotation. The equations take into account some important effects ignored in the adopted theory of the Earth's rotation, namely the effects from the perturbing torques caused by interaction of the potentials, induced by the tidal deformations of the Earth and its fluid core, with the tide arousing bodies (including the dissipative cross interaction of the lunar tides with the Sun and the solar tides with the Moon). Perturbations of this kind could not be accounted in the adopted theory in which only those obtainable by the method of the transfer function are considered. The derived equations explicitly depend on two parameters characterizing the dissipation of energy of the Earth's rotation. These parameters are the effective tidal phase lag δ due to the dissipation by rotation of the Earth as a whole, and the tidal phase lag δ_c due to the dissipation by the differential rotation of the fluid core. The preliminary analysis has shown that the most noticeable of the dissipative effects - the excess of the observed secular obliquity rate compared with predictions of the rigid body model, and the large out-phase amplitudes of the 18.6-year and semi-annual nutations indeed may be explained as the combined effect of these two types of dissipative perturbations.

1. NUTATION IAU 2000 AND ITS DEFICIENCIES

Nutation IAU 2000, recently adopted as an international standard, has significantly improved fitting to the observed positions of the Celestial Pole determined by the VLBI techniques. Dynamical model behind this theory is founded basically on ideas of the work by Sasao, Okubo, and Saito (Sasao et al, 1980) in which the classic method developed by Poincare for the case of the rigid Earth with the fluid core has been generalized to account for effects of elasticity of the mantle (so called SOS model). In rigorous formulation the SOS model describes rotation of the Earth consisting of the elastic mantle and non-dissipative fluid core. When applying this model the dissipative effects of the Earth's rotation are usually treated in a formal way assuming that some constants of the SOS model (for example, the Love number k_2) have imaginary parts and estimating them from the observed positions of the Celestial Pole (see, for instance, Shirai & Fukushima, 2001). Such a semi-empirical approach is equivalent to incorporation of empirical terms into the differential equations of the SOS model. In fact, in order to describe satisfactory the dissipative effects in the nutations, at least five empirical terms must be incorporated. Physical meaning of these empirical parameters is rather uncertain. For instance, if the tidal

phase lag δ is derived from them, its value appears to be roughly inconsistent with the reliable LLR estimate of δ. So the theoretical basis of Nutation IAU 2000 cannot be considered sound enough. Indeed, in (Dehant & Defraign, 1997) it has been shown that the observed out-phase amplitudes of the nutations cannot be satisfactory explained without introducing the empirical terms.

This defficiency arises mainly because of the SOS model (and thus Nutation IAU 2000) accounts only for a part of perturbations caused by the non-rigidity of the Earth, more exactly only for those from the tidal variations of the matrices of inertia of the mantle and the core, the rigid body approximation still being used to model the perturbing torques. In such a simplified approach the resulting perturbations can be expressed in terms of the rigid body nutations and thus it appears possible to present them as a linear differential operator (so called transfer function) applied to the rigid body nutations. However some important perturbations cannot be obtained in this way and that is why they are absent in Nutation IAU 2000. In brief their origin may be explained in the following way. The tidally deformed mantle and the fluid core, while interacting with the perturbing celestial bodies give rise to additional torques which are proportional to the static k_2 and dynamic k_2^d Love numbers, relatively. It is well known that for the elastic Earth the torques of the first type vanish; but that is not the case when the effective tidal phase lag δ is accounted to describe the impact of dissipation of energy by the body tides. The ignored dissipative torques rule evolution of the Earth-Moon system and so are very important. In particular they are responsible for a small (but informative for geophysics) part of the observed obliquity rate unexplainable in the rigid body model. It is easy to see that no secular rate in obliquity can be modeled in the frame of the mentioned above formal considerations of the imaginary parts of parameters of the SOS model. Other observable effects are caused by the ignored torques which are proportional to the dynamical Love number k_2^d and so depend on the differential rotation of the fluid core. These torques contribute on detectable level not only to obliquity rate and out-phase amplitudes of nutations but also to in-phase amplitudes which cannot be neglected but are not obtainable by the method of transfer function.

To derive the rigorous differential equations accounting for such effects, rather tedious analytical manipulations must be carrried out which cannot be presented in the frame of this paper due to the lack of space. Preliminary considerations with more details may be found in our paper (Krasinsky, 2003) available as the file *quasar.ipa.nw.ru/incoming/era/SOSMODEL.ps* by anoinymous FTP.

In the next sections the differential equations for the conventional SOS model as well as for the revised ones are presented (without proves) in the same notations to facilitate their comparison.

2. CONVENTIONAL SOS MODEL OF THE EARTH'S ROTATION

Parameters of the SOS model are so called compliances κ, γ, β. The compliances κ, γ may be expressed in terms of the static k_2 and dynamic k_2^d Love numbers, relatively. Loosely speaking, the dynamic Love number k_2^d scales perturbations in the moments of inertia of the fluid core caused by tides in the mantle, and vice versa. The compliance β can be expressed through a parameter k_2^c which plays part of the Love number of the fluid core. The compliances (or the corresponding Love numbers) may be obtained either theoretically making use of constants of the adopted up-to-date models of the Earth's interior, or from analysis of VLBI data by fitting the rotation theory. Instead of compliances τ, γ, β we here prefer to use the coefficients σ, ν, μ defined by the relations

$$\kappa = e\sigma,\ \gamma = e\frac{\nu}{\alpha},\ \beta = e\frac{\mu}{\alpha},$$

in which the constant α is the ratio of the main moment of inertia of the fluid core to that of the Earth as a whole, and e is the dynamical flattening.

If the 'secular' Love number k_s is defined in the stanard way by the expression

$$k_s = \frac{3Gm_E J_2}{R^3\omega^2} \approx 0.93831,$$

in which G is the gravitational constant, m_E, J_2, R, ω are the mass, the coefficient of the second zonal harmonics of the potential, the mean radius, and the rotational rate of the Earth, then the parameters $\sigma,\ \nu,\ \mu$ may be presented by the relations

$$\sigma = \frac{k_2}{k_s}, \nu = \frac{k_2^d}{k_s},\ \mu = \frac{k_2^c}{k_s}.$$

In these notations the standard SOS equations of the Earth's rotation (see Moritz & Mueller, 1987) may be written in the form

$$\dot{u}(1+e\sigma) - ie\omega(1-\sigma)u + (\alpha+e\nu)(\dot{v}+i\omega v) = L + i\frac{\sigma}{\omega}\frac{\partial L}{\partial t},$$
$$\dot{u} + \dot{v} + iv\omega\left(1 + e_c - \mu\frac{e}{\alpha}\right) = \frac{\nu}{\alpha}\left[L\,(1-e) - \frac{i}{\omega}\frac{\partial L}{\partial t}\right],$$

where at the right parts L is the rigid body torque normalized dividing it by the of main momentum of inertia A, and u, v are complex combinations of the components ω_1, ω_2 and v_1, v_2 of the vectors of angular velocity $\overline{\omega}$ of the mantle and that $\overline{v}$ of the differential rotation of the Earth:

$$\begin{aligned} u &= \omega_1 + i\omega_2, \\ v &= v_1 + iv_2. \end{aligned}$$

The normalized rigid body torque L from the perturbed body is given by the expression

$$L = -ip\omega\xi\zeta,$$

where p is the parameter of the lunar or solar precession

$$p = \frac{3}{2}\frac{mG}{r^3}e,$$

e is the dynamical flattening, $\xi = \rho_1 + i\rho_2,\ \zeta = \rho_3$, and ρ_1, ρ_2, ρ_3 are the ecliptical rectangular coordinates of the geocentric unit vector to the tide arousing body. (In fact the rigid body torque l is the sum of the lunar and solar components: $L = L^1 + L^2$ where $L^k = -ip_k\xi^k\zeta^k$, $p = p_1 + p_2$, p_1, p_2 being parameters of the lunar and solar precession).

The normalized perturbing torque L implicitly depends on the three Euler's angles: the nutation angle θ, the angle of precession ϕ, and the rotational angle ψ. Making use of the Euler's kinematic equations that connect $\dot{\phi}, \dot{\theta}$ with the complex angular velocity u the close system of differential equations arises which presents the dynamical ground of Nutation IAU

2000. In these equations the rotational angle ψ is a known linear function of time and differs from the Greenwich Sidereal Time by the constant $\pi = 3.14..$

3. REVISED SOS EQUATIONS OF THE EARTH'S ROTATION In more rigorous formulation, the SOS equations have to be replaced by the following ones

$$\dot{u}\left(1+\frac{2}{3}e\sigma\right) - ie\omega(1-\sigma)u + \left(\alpha+\frac{2}{3}e\nu\right)(\dot{v}+i\omega v) +$$
$$+iv\sum_{k=1,2}(1-3\zeta_k^2)p_k = L + (\delta+i)\frac{\sigma}{\omega}\frac{\partial L}{\partial t} + L^d + L_c^d,$$
$$\dot{u}+\dot{v}+iv\omega\left[1+e_c-\frac{\mu e}{\alpha}(1+i\delta_c)\right] =$$
$$= \frac{\nu}{\alpha}\left[L\left(1-\frac{2}{3}e\right) - \frac{i}{\omega}\frac{\partial L}{\partial t}\right] + i\delta\frac{\nu}{\alpha}\left[L(1-e) + i\left(\frac{2}{\omega}\right)\frac{\partial L}{\partial t}\right] = 0,$$

in which the normalized dissipative torque L^d consists of the lunar L_1^d and solar L_2^d components caused by the dissipation in the lunar and solar tides, and of the cross interaction torque $L_{1,2}^d$ of these tides

$$\begin{aligned} L^d &= L_1^d + L_2^d + L_{1,2,}^d \\ L_k^d &= -4p_k\epsilon_k\sigma\delta\left[\omega\xi_k\zeta_k + i\left(\zeta_k\frac{\partial}{\partial t}\xi_k - \xi_k\frac{\partial}{\partial t}\zeta_k\right)\right](k=1,2), \\ L_{1,2}^d &= 2\sigma\delta\omega(p_1\epsilon_2+p_2\epsilon_1)(\xi_2\zeta_1+\xi_1\zeta_2), \end{aligned}$$

while L_c^d includes the terms due to the dissipation in the fluid core

$$L_c^d = \nu\delta_c\left[\frac{1}{2}pv(3\cos^2\theta - 2\cos\theta - 1) + ie\left(1-\frac{\nu}{\alpha}\right)L\right],$$

p_1, p_2 being the parameters of the lunar and solar precession, relatively, $\epsilon_1 = p_1/e\omega$, $\epsilon_2 = p_2/e\omega$, and $p = p_1 + p_2$.

These equations explicitly depend on the two dissipative parameters δ and δ_c. The parameter δ is the well-known tidal lag of the Earth as a whole that strongly affects the orbital motion of the Moon being responsible for the evolution of the Earth-Moon system. The parameter δ_c is the phase lag of the tides caused by the differential rotation of the fluid core and it plays important part in the Earth's rotation.

Setting the tidal lags δ, δ_c equal to zero one could expect that the standard and revised systems of the differential equations become equivalent. However it is easy to see that there is no full equivalence: in the revised equation for the variable u the factor $1+2e\sigma/3$ stands in place of the factor $1+e\sigma$ in the SOS equations. The origin of this discrepancy is traced as being due to the incomplete form of the centrifugal tidal potential used in the conventional SOS model in which only the tesseral components of this potential have been accounted for (more details are given in Krasinsky, 2003). Omission of the zonal components leads to minor errors of the second order with respect to e and probably does not deteriorates fitting to observations (though the theoretical interpretation of the results may be distorted indeed).

The rigorous equations show that any attempts to describe the dissipative effects by a formal consideration of imaginary parts of the Love numbers k_2, k_2^d (or of the compliances κ, γ) are of no physical meaning because the functional dependence of equations on the phase lags δ, δ_c

has another structure, excepting the single term in the right part of equation for u which is proportional to the derivative $\partial L/\partial t$. Only this term may be expressed in terms of the imaginary part of the Love number k_2.

4. APPLICATIONS

4.1. PRECESSION AND OBLIQUITY RATE

From the geophysical point of view it seems interesting to interpret the observed value $\dot{\theta}_{obs} = -24.08 \pm 0.017$ mas/cy of the obliquity rate based on VLBI data (see Shirai & Fukushima, 2001). The main part of this value is not the dissipative effect but is the result of omission of some terms in the adopted rigid body nutation, as it has been at first shown in (Williams, 1994). (In fact they are not secular but long periodic terms broken to the time series). In more detail, these terms are due to so called 'tilt' effect of perturbations in the tilt of the lunar orbit to ecliptic (that gives -25.4 mas/cy), and due to direct perturbations from planets with the resulted contribution -1.4 mas/cy, the total effect being -26.8 mas/cy. The value by Williams may be compared with those given by the more recent rigid body models of nutation: -26.5 in SMART97 (Bretagnon et all. 1998) and -27.2 in RDAN97 (Roosbeck & Dehant, 1998). Thus the observed obliquity rate $\dot{\theta}_{obs}$ that has to be explained as the dissipative effect varies in the range:

$$\dot{\theta}_{obs} = 2.7 \div 3.1 \text{ mas/cy}, \tag{1}$$

depending on the applied rigid body model.

From the revised version of SOS equations one can derive the following analytical expressions for the obliquity rate $\dot{\theta}_\delta$ induced by dissipation of the Earth as a whole and the rate $\dot{\theta}_{\delta_c}$ due to the dissipation caused by the differential rotation of the fluid core:

$$\dot{\theta}_\delta = 2p\sigma\delta \sin\theta(\epsilon\cos\theta - 2\tilde{\epsilon}), \tag{2}$$

$$\dot{\theta}_{\delta_c} = p\nu e\left(1 - \frac{\nu}{\alpha}\right)\delta_c \sin\theta\cos\theta, \tag{3}$$

where

$$\epsilon = \frac{p_1\epsilon_1 + p_2\epsilon_2}{p} = 2.04 \times 10^{-5},$$

$$\tilde{\epsilon} = \frac{p_1 n_1\epsilon_1 + p_2 n_2\epsilon_2}{\omega p} = 6.27 \times 10^{-7}.$$

The component $\dot{\theta}_\delta$ of the obliquity rate may be reliably evaluated making use of the estimate $\delta = 0.0376$ based on LLR data,p that gives the positive rates 0.675 mas/cy and 0.153 mas/cy as the impact of the Moon and Sun, relatively, with the total value 0.928 mas/cy. Then the remaining part of the observed obliquity rate (1) must be attributed to the effect of the fluid core:

$$\dot{\theta}_{\delta_c} = 1.8 \div 2.2 \text{ mas/cy}.$$

Applying the theoretical expression (3) we obtain the estimate

$$\delta_c \approx 0.010. \tag{4}$$

Much larger value of δ_c might be anticipated as the following reasoning seems to be plausible. The tidal lag δ of the Earth as a whole, obtained from LLR data, is the weighted sum of the contributions of the mantle and the fluid core. It is known that the dissipation in the mantle is weak and so its contribution to δ is small if any. Thus if only the core were responsible for the tidal lag δ then we could expect that the relation $\delta = \alpha\delta_c$ is valid which would give $\delta_c \approx 0.3$. Note that the derived estimate of δ_c is very sensitive to the ratio ν/α.

4.2. AMPLITUDES OF OUT-PHASE NUTATIONS

From the revised SOS equations it follows that the out-phase amplitudes of the main nutations (18.6 and half year periods) with the sufficient accuracy may be written in the form:

$$\begin{aligned} d\theta^f &= -R_f^{out} \sin\theta_0 d\phi_0^f, \\ \sin\theta d\phi^f &= R_f^{out} d\theta_0^f, \end{aligned}$$

where

$$R_f^{out} = \left[-\nu\delta + \sigma_f\,(\alpha-\nu)\,\delta_c\right] \frac{f}{f+f_c}(1-\alpha)^{-1},$$

and

$$f^c = \omega\left(e_c - \frac{\mu e}{\alpha}\right)(1-\alpha)^{-1}$$

has meaning of frequency of free oscillations of the fluid core in the non-rotating coordinate frame, so called Free Core Nutation, FCN.

In Table 2 the observed in-phase and out-phase amplitudes (in mas) are reproduced from the work (Shirai & Fukushima, 2001) for the three main nutations (including the fortnightly nutation). In this table there are also given the corresponding estimates of δ_c, obtained with the help of the given above analytical expression for the coefficient R_f^{out}. Note that the amplitudes presented in Table 2 are not really observed quantities but the theory-dependent ones because they are obtained by the mentioned above formal method estimating the imaginary parts of the coefficients of the transfer function as solve-for parameters from which the 'observed' out-phase amplitudes have been derived.

Table 1: Observed main nutations and estimates of δ_c.

Period	$d\phi_{in}$	$d\phi_{out}$	δ_c	μ^{dis}	$d\theta_{in}$	$d\theta_{out}$	δ_c	μ^{dis}
6798.38	17206	3.341	0.38	0.09	9205	-1.506	0.47	0.11
182.62	-1317	-1.717	0.46	0.11	579	-0.570	0.44	0.10
13.66	-228	0.286	-	-	98	0.148	-	-

One can see that the four independent estimation of δ_c presented in Table 2 are in a good accordance. They are rather large and marginally out the boundary of the physically meaningful range of this value ($\delta_c < \delta/\alpha \approx 0.35$). The fortnightly amplitudes desagree with the 'observed' ones, but reliability of the last (derived by the semi-empirical method) is disputable.

In the work (Dehant & Defraigne, 1997) it is shown that oceanic tides contribute to the out-phase amplitudes of both the 18.6 year and semi-annual nutations indirectly through action of the fluid core, and as the result about half of the observed values. Hence only the half of the estimated δ_c may be caused by the dissipation in the fluid core. The reduced value

$\delta_c \approx 0.15$ becomes more consistent with the lesser value derived in the previous subsection from the observed obliquity rate (which parameter is not affected by the ocean tides).

5. REFERENCES

Bretagnon, P., Francou, G., Rocher, P, Simon, J. L., 1998, *Astron. Astrophys.*, **329**, 329–338.

Dehant, V., Defraigne, P., 1997, *J. Geophys. Res.*, **102**, No B12, 27569–27687.

Krasinsky, G. A., 2003, Communications of IAA RAS, N 157, 76p.

Moritz, H., Mueller, I. I., 1987, Earth Rotation: Theory and Observation. Unger Publ. Co., New York.

Roosbeck, F., Dehant, V., 1998, *Celest. Mech. Dyn. Astr.*, **70**, 215–253.

Sasao, T. S., Okubo, T., Saito, M., 1980, Proceedings of IAU Symposium 78, E. P. Fedorov, M. L. Smith, and P. L. Bender (eds.), Reidel, 165–183.

Shirai, T., Fukushima, T., 2001, *Astron. J.*, **121**, N 1746, 3270–3283.

Williams, J. G., 1994, *Astron. J.*., **108**, N 2, 711–724.

NEW FORMULAE OF RELATIONS AMONG UT1, GAST, and ERA

T. FUKUSHIMA
National Astronomical Observatory
2-21-1, Ohsawa, Mitaka, Tokyo 181-8588, Japan
e-mail: Toshio.Fukushima@nao.ac.jp

ABSTRACT. By using the latest precession theory of Fukushima and the nutation theory of Shirai and Fukushima, we numerically obtained a new approximation of the quantity $s + XY/2$ and the coefficients of the linear relation between the Earth Rotation Angle and UT1. These are key formulae in the post-2003 IAU formulation to connect the International Celestial Reference Frame and the International Terrestrial Reference Frame. Also we modified the pre-2003 IAU formula converting Greenwich Apparent Sidereal Time (GAST) from/to UT1 so as to be compatible with the modern observation of Earth orientation. The difference from the computation of Capitaine et al. is significant only in the secular components. This is due to the difference in the adopted precession formulae. From the viewpoint of approximation, we prefer the approach of GAST-UT1 relation since it requires the fewer terms in achieving the same degree of approximation.

1. INTRODUCTION

One of the most important procedures in the fundamental astronomy is the transformation between the two representative reference systems, the International Celestial Reference System (ICRS) and the International Terrestrial Reference System (ITRS). At its XXIVth General Assembly at Manchester, the International Astronomical Union (IAU) changed the policy to conduct the transformation. Since the new approach is to be used from 2003, we call the new and the old formulations the post- and the pre-2003 IAU formulations throughout this article.

The precession, the nutation, and the sidereal rotation are tightly connected with each other so that a change of any part of them inevitably induces the appropriate alterations of the others. Recently we developed a new formulation of precession (Fukushima 2003) such that its combination with our previous work on the nutation theory (Shirai and Fukushima 2001) provides a satisfactory agreement with the VLBI observation of celestial pole offsets. Its most significant feature is that not only the lunisolar precession formula but also the planetary precession one is improved. Actually the latter is compatible with the latest planetary/lunar ephemeris, DE405. In the light of the above statement, however, it is far from the completion to update only the theories of precession and nutation, which specify the true equator and equinox of date. Rather requested is a suitable replacement of the procedure of sidereal rotation such that the whole new formulation as a package is compatible with the modern observation of Earth orientations. In this short paper, we report our trials for both the pre- and post-2003 formulations using our new precession and nutation theories.

2. ANOTHER ANGLE TO SPECIFY CEO, q

As Aoki and Kinoshita (1983) clearly stated, Newcomb's definition of UT1 is based on the usage of *departure point* in specifying the longitude origin along the true equator of date. This is no other than the CEO, the Non-Rotating Origin (NRO) on the true equator. The angle s has been mainly used in locating the CEO. On the other hand, Aoki and Kinoshita (1983) provided the analytical expression of q, the angle between the true equinox and the CEO after the correction of the so-called nutation in RA as simply as $(\Delta q - \Delta\psi\cos\epsilon_{\rm A})_{\rm A} = -3.88t + 2.64\sin\Omega + 0.063\sin 2\Omega$ where the unit is mas. The absence of high order trends and mixed secular terms indicates a promising direction. In the below, we develop a new approach to evaluate the angle difference.

The rotational operation converting X, the x-axis of ICRF, to the CEO is expressed by the following five rotation matrices;

$$\mathcal{R}_3(q)(\mathcal{NP})_{\rm NEW} = \mathcal{R}_3(q)\mathcal{R}_1(-\epsilon)\mathcal{R}_3(-\psi)\mathcal{R}_1(\overline{\varphi})\mathcal{R}_3(\overline{\gamma}). \tag{1}$$

Then, the angular velocity vector of the CEO with respect to an inertial reference frame is expressed as

$$\omega_{\rm CEO} = \left(\frac{{\rm d}q}{{\rm dt}}\right)\vec{e}_{\rm P} - \left(\frac{{\rm d}\psi}{{\rm dt}}\right)\vec{e}_{\rm C} - \left(\frac{{\rm d}\epsilon}{{\rm dt}}\right)\vec{e}_{\rm Q} + \left(\frac{{\rm d}\overline{\varphi}}{{\rm dt}}\right)\vec{e}_{\rm N} + \left(\frac{{\rm d}\overline{\gamma}}{{\rm dt}}\right)\vec{e}_{\rm Z}, \tag{2}$$

where $\vec{e}_{\rm A}$ means the unit vector toward a point A. The points additionally used are Z as the ICRF pole, C as the ecliptic pole of date, and P as the equatorial pole of date.

Since the CEO is a non-rotating origin, its inertial motion has no rotational component around P. This is expressed in terms of the angular velocity vector as $\omega_{\rm CEO}\cdot\vec{e}_{\rm P} = 0$. By solving this equation, we derive the differential equation of q as

$$\frac{{\rm d}q}{{\rm dt}} = \frac{{\rm d}\psi}{{\rm dt}}\left(\vec{e}_{\rm P}\cdot\vec{e}_{\rm C}\right) + \frac{{\rm d}\epsilon}{{\rm dt}}\left(\vec{e}_{\rm P}\cdot\vec{e}_{\rm Q}\right) - \frac{{\rm d}\overline{\varphi}}{{\rm dt}}\left(\vec{e}_{\rm P}\cdot\vec{e}_{\rm N}\right) - \frac{{\rm d}\overline{\gamma}}{{\rm dt}}\left(\vec{e}_{\rm P}\cdot\vec{e}_{\rm Z}\right). \tag{3}$$

Noting the fact that $\vec{e}_{\rm P}\cdot\vec{e}_{\rm Q} = 0$ and using the expressions

$$\vec{e}_{\rm P} = \begin{pmatrix} X \\ Y \\ Z \end{pmatrix}, \qquad \vec{e}_{\rm N} = \begin{pmatrix} \cos\overline{\gamma} \\ \sin\overline{\gamma} \\ 0 \end{pmatrix}, \qquad \vec{e}_{\rm C} = \begin{pmatrix} \sin\overline{\varphi}\sin\overline{\gamma} \\ -\sin\overline{\varphi}\cos\overline{\gamma} \\ \cos\overline{\varphi} \end{pmatrix}, \tag{4}$$

we obtain an explicit expression

$$\frac{{\rm d}q}{{\rm dt}} = \left(\frac{{\rm d}\psi}{{\rm dt}}\right)\cos\epsilon - \left(\frac{{\rm d}\overline{\varphi}}{{\rm dt}}\right)\sin\epsilon\sin\psi - \left(\frac{{\rm d}\overline{\gamma}}{{\rm dt}}\right)\left(\sin\epsilon\cos\psi\sin\overline{\varphi} + \cos\epsilon\cos\overline{\varphi}\right), \tag{5}$$

where we used the explicit expressions of the equatorial pole coordinates.

In order to explore an approximate solution of this differential equation, let us ignore the nutation in obliquity when compared with the mean obliquity. Also we assume that the precession in longitude is so small that its cubic and higher order terms are negligible. Further we neglect the difference between two mean obliquities, $\overline{\epsilon}$ and $\overline{\varphi}$, which is small. Then we approximate the right hand side of the above differential equation as

$$\frac{{\rm d}q}{{\rm dt}} \approx \left(\frac{{\rm d}\psi}{{\rm dt}}\right)\cos\overline{\epsilon} - \left(\frac{{\rm d}\overline{\epsilon}}{{\rm dt}}\right)\psi\sin\overline{\epsilon} - \left(\frac{{\rm d}\overline{\gamma}}{{\rm dt}}\right) = \frac{\rm d}{{\rm dt}}\left(\psi\cos\overline{\epsilon} - \overline{\gamma}\right). \tag{6}$$

This is easily integrated and, apart from the constant offset, we obtain an approximate solution $q \approx q^*$ where $q^* \equiv \psi\cos\overline{\epsilon} - \overline{\gamma}$. This is further decomposed into the sum of the secular and the periodic components as $q^* = \overline{q^*} + \Delta q^*$, where $\overline{q^*} = \overline{\psi}\cos\overline{\epsilon} - \overline{\gamma}$ and $\Delta q^* = \Delta\psi\cos\overline{\epsilon}$. The former

is no other than the accumulated precession in RA and the latter is the well-known nutation in RA. Therefore, the angle q^* can be said as the accumulated precession and nutation in RA. Note that q^* contains no large mixed secular terms of high orders.

Now we change the variable to be integrated from q itself to the deviation from this approximate solution as $\delta q \equiv q - q^*$. Then its differential equation becomes

$$\frac{\mathrm{d}\delta q}{\mathrm{dt}} = \left(\frac{\mathrm{d}\psi}{\mathrm{dt}}\right)(\cos\epsilon - \cos\overline{\epsilon}) + \left(\frac{\mathrm{d}(\overline{\epsilon} - \overline{\varphi})}{\mathrm{dt}}\right)\psi\sin\overline{\epsilon} + \left(\frac{\mathrm{d}\overline{\varphi}}{\mathrm{dt}}\right)(\psi - \sin\psi)\sin\overline{\epsilon}$$

$$- \left(\frac{\mathrm{d}\overline{\varphi}}{\mathrm{dt}}\right)\sin\psi\,(\sin\epsilon - \sin\overline{\epsilon}) + 2\left(\frac{\mathrm{d}\overline{\gamma}}{\mathrm{dt}}\right)\left[\sin^2\left(\frac{\epsilon - \overline{\varphi}}{2}\right) + \sin^2\frac{\psi}{2}\sin\epsilon\sin\overline{\varphi}\right]. \qquad (7)$$

All the terms in the right hand side are small in the sense they are of the order of nutation or of the quadratic and higher terms of precessions.

We numerically integrated the transformed equation. The resulting expression of δq seems to contain no significant nonlinear trend nor mixed secular terms judging from its numerical plotting. By using the successive method of harmonic analysis again, we decomposed the integrated δq into a sum of a quintic polynomial of time and some harmonic terms as $\delta q = \overline{\delta q} + \Delta(\delta q)$. Here the secular part is

$$\overline{\delta q} = -3.857532t - 0.108393t^2 - 0.148087t^3 + 0.014484t^4 - 0.000481t^5, \qquad (8)$$

where the unit is mas, t is the time since J2000.0 measured in Julian centuries, and we set the constant term of the secular part be zero for simplicity.

As for the residuals of the decomposition, the rms and the maximum deviation is almost the same as in the case of $s + XY/2$; 0.19 μas and 0.96 μas, respectively. This time, however, this level of precision is realized by the fewer terms. Namely q or δq is more suitable than s or $s + XY/2$ in describing the inertial motion of the location of the CEO. For example, 5 largest terms are enough to approximate δq with the maximum error less than 0.1 mas during the period 1900-2100. While we need 8 terms in expressing $s + XY/2$ at the same level.

Let us return to q itself. We separate it into the sum of the secular and periodic terms; $q = \overline{q} + \Delta q$. Rearranging the approximate formulae of q obtained in the above, we have the final expressions $\overline{q} = \overline{q^*} + \overline{\delta q}$ and $\Delta q = \Delta q^* + \Delta(\delta q)$. In order to obtain the secular part, we evaluated $\overline{q^*}$ for the period 1900-2100 and determined its best-fit polynomial as

$$\overline{q^*} = \overline{\psi}\cos\overline{\epsilon} - \overline{\gamma} = 12.911569 + 4612160.517397t + 1391.650906t^2$$
$$+0.023238t^3 - 0.019475t^4 + 0.000002t^5, \qquad (9)$$

where the unit is mas. Combining this and Eq.(8), we separate the secular part $\overline{q}$ into the linear and nonlinear parts as $\overline{q} = \overline{q}_{\mathrm{L}} + \overline{q}_{\mathrm{NL}}$, where

$$\overline{q}_{\mathrm{L}} = 12.911569 + 4612156.659865t, \qquad (10)$$

and

$$\overline{q}_{\mathrm{NL}} = 1391.542507t^2 - 0.124849t^3 - 0.004991t^4 - 0.000479t^5. \qquad (11)$$

3. RELATIONS AMONG UT1, GMST, AND ERA

The rotation matrix $\mathcal{SNP}$ is written in the post-2003 IAU formulation as $(\mathcal{SNP})_{\mathrm{NEW}} = \mathcal{R}_3(\mathrm{ERA} - s)\mathcal{Q}$. Since the rotation matrix converting the x-axis of the ICRF to the CEO must be the same both in the pre- and the post-2003 IAU formulations, we obtain the identity

$\mathcal{R}_3(-s)\mathcal{Q} = \mathcal{R}_3(q)(\mathcal{NP})_{\rm NEW}$. This means $\mathcal{S}_{\rm NEW} = \mathcal{R}_3({\rm ERA}+q)$. Namely ${\rm GAST}_{\rm NEW} = {\rm ERA}+q$. This relation is separated into those of the secular and periodic parts, respectively, as

$$ {\rm GMST}_{\rm NEW} = {\rm ERA} + \overline{q}, \qquad {\rm EE}_{\rm NEW} = \Delta q. \tag{12} $$

Since the ERA is a linear function of UT1, we split the secular part further as

$$ ({\rm GMST}_{\rm NEW})_{\rm L} = {\rm ERA} + \overline{q}_{\rm L}, \qquad ({\rm GMST}_{\rm NEW})_{\rm NL} = \overline{q}_{\rm NL}. \tag{13} $$

where the subsript L means the linear part and NL does the nonlinear one. We have already obtained the nonlinear part and the periodic part in the previous section.

Now that the relation between the ERA and GMST become clear, there are two ways to fix their relations with the UT1; determining the ERA-UT1 relation first or the GMST-UT1 relation first. Here we take the latter aproach.

Since the nonlinear part is already obtained, we determine the linear part of the GMST-UT1 relation. As was recommended in the IAU 2000 Resolution B 1.8 adopted at the Manchester General Assembly, the continuation of the UT1 in its value and rate must be kept at the transition. Since the polar motion part is unchanged, the condition of continuation is written in the matrix form as

$$ (\mathcal{SNP})_{\rm IERS1997} = (\mathcal{SNP})_{\rm NEW} \tag{14} $$

where the relation must hold in the value and its rate at a certain time. Here the matrix with the subscript IERS1997 is realized by the International Earth Rotation Service (IERS) since 1997.

$$ (\mathcal{SNP})_{\rm IERS1997} = \mathcal{S}_{\rm OBS}\mathcal{N}_{\rm OBS}\mathcal{P}_{\rm A}, \tag{15} $$

This is different from the genuine form in the pre-2003 IAU formulation

$$ (\mathcal{SNP})_{\rm IAU1976} = \mathcal{S}_{\rm A}\mathcal{N}_{\rm A}\mathcal{P}_{\rm A}, \tag{16} $$

in the sense that the observed corrections in the nutation, $\delta\psi$ and $\delta\epsilon$, are added in the sidereal rotation matrix and the nutation matrix as

$$ \mathcal{S}_{\rm OBS} = \mathcal{R}_3\left({\rm GAST}_{\rm A} + \delta\psi\cos\epsilon_{\rm A}\right), \tag{17} $$

and

$$ \mathcal{N}_{\rm OBS} = \mathcal{R}_1\left(-\epsilon_{\rm A} - \Delta_{\rm IAU}\epsilon - \delta\epsilon\right)\mathcal{R}_3\left(-\Delta_{\rm IAU}\psi - \delta\psi\right)\mathcal{R}_1\left(\epsilon_{\rm A}\right), \tag{18} $$

where $\mathcal{P}_{\rm A}$ is the precession matrix of Lieske et al. (1977) and $\Delta_{\rm IAU}\psi$ and $\Delta_{\rm IAU}\epsilon$ are the IAU 1980 nutation.

This convention means that the correction of the precession rate, Δp, of around 3.0 mas/yr, which has been realized by a linear drift in the observed corrections $\delta\psi$, has been already taken into account in determining the UT1 by the IERS 1997 procedure even in the pre-2003 IAU formulation. Therefore, when the precession formulae are replaced by the latest ones including the precession correction, the resulting new GMST-UT1 relation *must* contain the direct contribution of the precession correction. In other words, the numerical coefficients in the linear part of the GMST-UT1 relation would change roughly the same as $\Delta p\cos\epsilon_0 \approx 2.7$ mas/yr when the new precession formulae are applied.

In the previous work (Fukushima 2003), we determined the equinox correction E so as to satisfy the condition

$$ \mathcal{N}_{\rm OBS}\mathcal{P}_{\rm A} = \mathcal{R}_3(E)\left(\mathcal{NP}\right)_{\rm NEW}. \tag{19} $$

The amount of the equinox correction is as small as

$$ E = (+52.403 + 1.452\,t)\ {\rm mas} = (+0.00349353 + 0.00009680\,t)\ {\rm second}, \tag{20} $$

where t is the time since J2000.0 measured in Julian centuries and we reserved superfluous number of digits after the unit conversion for a later use. See Eq.(39) and Table 2 of Fukushima (2003). Then the above condition of continuation is translated as

$$\mathrm{GAST_A} + (\delta\psi)\cos\epsilon_\mathrm{A} = \mathrm{GAST_{NEW}} + E. \tag{21}$$

Since $\delta\psi$ is observbationally determined, this relation must be regarded as a relation to be held in average. In other words, the unknown linear term of $\mathrm{GMST_{NEW}}$ is determined from the observed $\delta\psi$ by a method of weighted least squares. To do this, let us define the quantity

$$\Delta\mathrm{EE} \equiv \mathrm{EE_A} + (\delta\psi)\cos\epsilon_\mathrm{A} - \mathrm{EE_{NEW}}. \tag{22}$$

By conducting a method of weighted linear least squares, we determined the best linear function fitted to the data as

$$(\Delta\mathrm{EE})_\mathrm{L} = -(11.822 \pm 0.011) - (276.542 \pm 0.187)\ \tau \tag{23}$$

where the unit is mas and τ is the time measured since J1990.0 in Julian century. This is rewritten in terms of t measured since J2000.0 in Julian century as

$$(\Delta\mathrm{EE})_\mathrm{L} = (-38.476 - 276.542\,t)\ \mathrm{mas} = (-0.0025651 - 0.0184361\,t)\ \mathrm{second} \tag{24}$$

where we dropped the uncertainties. The weighted rms of the obtained residuals is 0.55 mas.

Then the equation of continuation is rewritten in terms of the secular part as

$$\mathrm{GMST_A}\left(0^\mathrm{h}\mathrm{UT1}\right) + (\Delta EE)_\mathrm{L} = \mathrm{GMST_{NEW}}\left(0^\mathrm{h}\mathrm{UT1}\right) + E. \tag{25}$$

Let us compare the nonlinear part of the both sides. Since the estimated difference ΔEE and the equinox correction E have no nonlinear part, the difference in the nonlinear part is only that in $\overline{q}_\mathrm{NL}$. It is as small as

$$\begin{aligned}(\overline{q}_\mathrm{NL})_\mathrm{A} - (\overline{q}_\mathrm{NL})_\mathrm{NEW} &= \left(5.017483\,t^2 + 0.031791\,t^3 + 0.004999\,t^4 + 0.000543\,t^5\right)\ \mathrm{mas} \\ &= \left(0.00033449887\,T_\mathrm{U}^2 + 0.0000021194\,T_\mathrm{U}^3 + 0.00000033327\,T_\mathrm{U}^4 + 0.0000000362\,T_\mathrm{U}^5\right)\ \mathrm{second}.\end{aligned} \tag{26}$$

After the unit conversion, we again kept more digits than being meningful for the later use. Let us write the linear part of the new GMST as

$$(\mathrm{GMST_{NEW}})_\mathrm{L}\left(0^\mathrm{h}\mathrm{UT1}\right) = A + BT_\mathrm{U}, \tag{27}$$

where A and B are the constants to be determined. Then, the equation to be fitted is rewritten as

$$\begin{aligned}A + B\,T_\mathrm{U} &= \mathrm{GMST_A}\left(0^\mathrm{h}\mathrm{UT1}\right) + (\Delta\mathrm{EE})_\mathrm{L} - E + [(\overline{q}_\mathrm{NL})_\mathrm{A} - (\overline{q}_\mathrm{NL})_\mathrm{NEW}] \\ &= 24110.5423514 + 8640184.7943331\,T_\mathrm{U} + 0.00033449887\,T_\mathrm{U}^2 \\ &\quad + 0.0000021194\,T_\mathrm{U}^3 + 0.00000033327\,T_\mathrm{U}^4 + 0.0000000362\,T_\mathrm{U}^5.\end{aligned} \tag{28}$$

If we write the right hand side formally as $\sum_k a_k T_\mathrm{U}^k$, then the condition of continuation is solved as

$$A = \sum_k (1-k) a_k T_\mathrm{F}^k, \qquad B = \sum_k k a_k T_\mathrm{F}^{k-1} \tag{29}$$

where T_F is the time of fitting. Namely

$$A = 24110.5423514 - 0.00033450\,T_\mathrm{F}^2 - 0.00000424\,T_\mathrm{F}^3 - 0.00000100\,T_\mathrm{F}^4 - 0.00000014\,T_\mathrm{F}^5, \tag{30}$$

$$B = 8640184.7943331 + 0.00066900\,T_{\rm F} + 0.00000636\,T_{\rm F}^2 + 0.00000133\,T_{\rm F}^3 + 0.00000018\,T_{\rm F}^4. \quad (31)$$

Since the ERA is connected to the linear part of GMST, we obtain the relation between ERA and UT1 as a direct byproduct as $\mathrm{ERA_{NEW}} = A + BT_{\rm U} - \overline{q}_{\rm L}$. As another byproduct, we obtain the ratio of rates of the universal and sidereal times as

$$r_{\rm NEW} \equiv 1 + \frac{1}{86400 \times 36525}\left(\frac{\mathrm{dGMST_{NEW}}\left(0^{\rm h}\mathrm{UT1}\right)}{\mathrm{d}T_{\rm U}}\right)$$

$$= r_0 + 2.11993 \times 10^{-13}\,T_{\rm U} + 2.015 \times 10^{-15}\,T_{\rm U}^2 + 4.21 \times 10^{-16}\,T_{\rm U}^3 + 5.7 \times 10^{-17}\,T_{\rm U}^4, \quad (32)$$

where $r_0 \equiv 1 + B/3155760000$.

4. CONCLUSION

By using our precession theory (Fukushima 2003) and nutation series (Shirai and Fukushima 2001), we confirmed that the accumulated precession and nutation in RA, q^*, is a good approximation of q. Then we transformed the differential equation of q into that of $\delta q \equiv q - q^*$. By integrating the transformed differential equation numerically, we obtained δq for the period 1900-2100. Third, by using a successive method of harmonic analysis, we decomposed the quantity δq into a low order polynomial and some periodic and mixed secular terms. By comparing the manner of decrease of the approximation errors with respect to the number of terms, we judge that δq is more suitable than $s + XY/2$ to specify the location of the CEO on the true equator of date.

Then, by using thus-determined formulae of q^* and δq, we determined the new formulas relating Greenwich Apparent Sidereal Timte (GAST), Earth Rotation Angle (ERA), Greenwich Mean Sidereal Time (GMST), Equation of Equinox (EE), and UT1 from the continuation condition that the values and rates of UT1 determined by the pre-2003 IERS procedure and by the new procedure are the same at a certain time of fitting. The resulting formulas are symbolically expressed as

$$\mathrm{GAST_{NEW}} = \mathrm{GMST_{NEW}} + \mathrm{EE_{NEW}}, \qquad \mathrm{ERA_{NEW}} = A + BT_{\rm U} - \overline{q}_{\rm L},$$

$$\mathrm{GMST_{NEW}} = A + BT_{\rm U} + \overline{q}_{\rm NL}, \qquad \mathrm{EE_{NEW}} = (\Delta\psi)\cos\overline{\epsilon} + \Delta(\delta q) \quad (33)$$

where $\overline{q}_{\rm L}$ and $\overline{q}_{\rm NL}$ are the linear and the nonlinear terms of the secular part of q given in the above, respectively, and $\Delta(\delta q)$ is the periodic part of δq.

5. REFERENCES

Aoki, S., Guinot, B., Kaplan, G. H., Kinoshita, H., McCarthy, D. D., and Seidelmann, P. K., 1982, *Astron. Astrophys.*, 105, 359

Aoki, S., and Kinoshita, H., 1983, *Celest. Mech.*, 29, 335.

Capitaine, N., Wallace, P., and McCarthy, D. D., 2003, *Astron. Astrophys.*, 406, 1135.

Fukushima, T., 2003, *Astron. J.*, 126, 494.

Harada, W., and Fukushima, T., 2004, *Astron. J.*, 127, 531.

Lieske, J. H., Lederle, T., Fricke, W., and Morando, B., 1977, *Astron. Astrophys.*, 58, 1.

Seidelmann, P. K., 1982, *Celest. Mech.*, 27, 79.

Shirai, T., and Fukushima, T., 2001, *Astron. J.*, 121, 3270.

Williams, J. G., 1994, *Astron. J.*, 108, 711.

THE HISTORY OF ORLOV'S SESSIONS

A. KORSUN'
Main Astronomical Observatory of National Academy of Sciences of Ukraine
03680 Kiev, Ukraine
e-mail: akorsun@mao.kiev.ua

The Orlov's session in St. Petersburg is fifth such session [1]. The history of these meetings (Orlov's session or conference) began in 1980 the year of the century of the birth of Aleksander Orlov (1880–1954). The 100 anniversary of A. Orlov was mention at the Main Astronomical Observatory of the Ukrainian Academy of Sciences (Kiev) which was founded by A. Orlov in 1944.

The Orlov's conference obtained the international status. The decision was taken to hold such conferences once on six year (this is period of variation of the polar motion) in the cities which were connected with Orlov's scientific activities.

First Orlov's conference "The study of the Earth as a planet by methods of astronomy, geodesy and geophysics" took place on September 29 – October 3, 1980 in Kiev. In Kiev A. Orlov founded the Main Astronomical Observatory and was its Director in 1944–1948, 1951–1952.

The second Orlov conference took place in Poltava, September 29 – October 3, 1986. In Poltava A. Orlov founder the Poltava Gravimetria Observatory in 1926 and he was its director in 1926–1934, 1938–1944.

The 3rd Orlov's conference was held in Odessa (September 7–12, 1992). At the Odessa Astronomical Observatory A. Orlov worked in 1912–1924, and he was its director from 1912. A. Orlov was a professor of the Novorossiisk University in Odessa.

The 4th Orlov's conference was held in Paris as Orlov's session of JOURNEES–98. In Paris A. Orlov worked on probation in Sorbonne and College de France in 1903–1904.

The 5th Orlov's conference also as session is held in St.Petersburg. In St.Petersburg A. Orlov entered the physical and mathematical faculty of the St.Petersburg University in 1898 and he graduated it in 1902. In 1903–1905 A. Orlov send abroad to prepare for professorship. In 1905 he published the first scientific paper "On the determination of correlations to the elements of planetary and cometary orbits". In 1907–1908 A. Orlov worked at the Pulkovo Astronomical Observatory – he observed with zenith-telescope. These observations of latitude variations and their analysis by A. Orlov were very precise for that time. This work put start his research of the polar motion.

In 1915 Orlov defended his Doctor Thesis "Results of the Yur'ev, Tomsk and Potsdam Observations of Luni-Solar Deformations of the Earth" in the St.Petersburg University.

Then main theme of Orlov's wide investigations became the polar motion and analysis the latitude variations. Especially attentions Orlov spared to analysis latitude variations in Pulkovo, which were distinguished by high accuracy.

As mark E. P. Fedorov disciple of Orlov's cause that practically all Orlov's works are noted for novelty and original treatment of astronomical, seismological and geophysical problems topical at that time. They provoked lively discussions and above all they stimulated new theoretical and

experimental investigations including creation of new stations for the observations of latitude variations and terrestrial tides. The ideas proposed by Orlov were further elaborated by his pupils N. Stoyko, J. Vitkovsky, Z. Aksent'eva, N. Popov, E. Fedorov, et al. A. Orlov was founder Ukrainian geodynamics school [2].

E. Fedorov wrote in 1980:

"At the end of the last century a new stage in the study of the Earth began – the planet is regarded as a complex dynamical system that responds to external as well as internal actions. It has became apparent that the observed latitude variations and tidel deformations of the Earth offer a means of determining general mechanical properties of our planet and testing internal structure models. A. Orlov was among those scientists who were the first to realize this possibility".

A. Orlov was founder the Soviet Latitude Service. In 1932 A. Orlov proposed the organization of the Soviet latitude service and also the project of International Latitude Service on parallel $49°36'$. Last project called for the organization of two stations in Blagoveshchensk (USSR) and Winnipeg (Canada) on the Poltava parallel.

In 1941 A. Orlov went to the Far East to organize the Far-East latitude station. Subsequently the Blagoveshchensk Latitude Station organized by his son Boris A. Orlov (1906–1963).

Owing to Orlov's idea the Borovitc latitude station was built in Poland on the parallel of Irkutsk latitude station.

Some methods of study of the polar motion have Orlovs name: method of determination of the mean latitude and method determination the mean pole epoch. By Orlov method were determined the polar coordinates from 1846 to 1969. A. Orlov suggested the original method of the determination of the polar motion from the latitude variations only on one observatory.

The definition for the mean latitude given by A. Orlov was widely discussed and several expression (filters) were proposed for the calculation of the mean latitude. The Orlov's methods widely used in the work of the Soviet Latitude Service (1952–1961) and BIH (1968–1988).

As noted E. Fedorov, A. Orlov in 1953 wrote that the study polar motion over 15–20 years was improved and will have more perfect direction that at present.

In 1958 the book "Latitude Service" by A. Orlov and in 1961 "Selected Works of A. Orlov" in 3 volumes were published.

Lunar crater and asteroid 2627 have name A. Orlov.

In Main Astronomical Observatory of National Academy of Sciences the ideas by Orlov are further elaborated by the pupils his scientific school in the department of Space Geodynamics which was founded by Yaroslav Yatskiv. New methods for the determination of the parameters of Earth rotation (laser ranging, VLBI observations, radio observations of the navigation satellites GPS, GLONASS, etc.) and their analysis were elaborated. Programme complex KIEV-GEODYNAMIKA and STEELBREEZ were created and Department became one of the centres in the International Earth Rotation Service. The satellite ranging station in Kiev was modernized and the work is in progress on creating a fundamental network of stations for observations of the navigation satellites GPS and GLONASS. The investigations of the Department are concerned with a wide range of fundamental and applied problems in astrometry and global geodynamics from the theory of the Earth rotation to the creation of coordinate systems for the Earth and space.

REFERENCES

Korsun', A., 1998, Some stories on the Orlov Conferences, Proc. JOURNEES 1998, Paris, 221.

Yatskiv, Ya., 1998, The Ukrainian Geodynamics School of Alexander Ya. Orlov, Proc. JOURNEES 1998, Paris, 189–194.

EARTH'S RATE OF ROTATION BETWEEN 700 BC AND 1000 AD DERIVED FROM ANCIENT SOLAR ECLIPSES

M. SÔMA[1], K. TANIKAWA[1], K.-A. KAWABATA[2]
[1] National Astronomical Observatory of Japan
Mitaka, Tokyo 181-8588, Japan
e-mail: somamt@cc.nao.ac.jp, tanikawa.ky@nao.ac.jp
[2] Emeritus Professor of Nagoya University
Hanakoganei 4–39–15, Kodaira, Tokyo 187-0002, Japan
e-mail: kawabata-nagoya@jcom.home.ne.jp

ABSTRACT. We analyzed 34 ancient solar eclipses between 700 BC and 1000 AD recorded in China and Japan. From the analysis we have found that the tidal acceleration of the Moon has been constant from 700 BC to the present, and that the TT − UT values had a semi-periodic variation with a period of several hundred years since 700 BC. The nontidal components of TT − UT should be due to the variation of the moment of inertia of the Earth.

1. INTRODUCTION

Stephenson (1997) obtained the values of ΔT = TT − UT from about 720 BC using mainly the ancient solar and lunar eclipses. According to the ΔT curve of his Fig. 14.4, the value of ΔT in the 7th century is between about 4000 and 4500 sec. In Journées 2002 we showed from the solar eclipse records in China and Japan that the ΔT value should have been about 3000 sec in the 7th century. In Sect. 2 we review the discussion about the values in the 7th century based on the solar eclipse records and we also give additional data supporting our ΔT value in the 7th century. In Sect. 3 we show that the tidal acceleration of the Moon obtained from the solar eclipse records from 700 BC to 1000 AD coincides with that derived from the recent lunar laser ranging data. In Sect. 4 we derive the ΔT values between 700 BC to 1000 AD from the same solar eclipse records and show that the ΔT values had a semi-periodic variation with a period of several hundred years since 700 BC.

2. ΔT VALUE IN THE SEVENTH CENTURY

The solar eclipse of 628 April 10 was recorded as "The sun was completely eclipsed" in the Nihongi (Japanese old history book). Nine years later, on 637 April 1, there was another solar eclipse observed in Japan. It was also recorded in the Nihongi, but only recorded as "The sun was eclipsed". If we assume that the ΔT value was 4500 sec at that time as given by Stephenson (1997), the magnitudes of the solar eclipses of the years 628 and 637 become 0.89 and 0.93, respectively, which contradicts the records. In China, solar eclipses of AD 616 and AD 702 were recorded. From these records we concluded that the ΔT value in the 7th century was about 3000 sec.

A lunar occultation of Mars on 681 November 3 was also recorded in the Nihongi as "Mars was occulted". Our calculations showed that actually Mars was not occulted at Asuka, the ancient capital of Japan, but the apparent distance of Mars' center from the lunar limb at the closest approach depends on the adopted ΔT value as follows:

ΔT	Distance
3000 sec	$34''$
4000 sec	$71''$

The Moon's age was 17.3 days and the Moon's phase (fraction of the area of the apparent disk that is illuminated by the Sun) was 95%, but Mars' altitude was 70° above the horizon and Mars' magnitude was -1.4 so that we thought that Mars was bright enough to be seen if it was separated from the bright lunar limb by more than the angular resolution of the naked eye ($40''$ or so), and thus we thought that the observation also showed ΔT should have been about 3000 sec instead of about 4000 sec at that time, but we lacked its definitive evidence.

This year on 2003 July 17 there was a grazing occultation of Mars in Florida, U.S.A., the condition of which was similar to that of the 681 occultation (Moon's age 17.6, Moon's phase 85%, Mars' altitude 50°, Mars' magnitude -1.9). Two people observed it with naked eye. Mars approached from the bright side of the Moon and they lost Mars a couple of minutes after Mars passed by the Moon's cusp. Their observation data were as follows:

Observer	UT	Long.	Lat.	Height	$d_{\rm limb}$	$d_{\rm term}$
	h m s	° ′ ″	° ′ ″	m	″	″
Christopher Stephan	08:22:00	81 03 11 W	27 17 55 N	10	28	35
Richard Coolick	08:20:07	81 49 08 W	26 43 43 N	3	30	38

UT is the time when the observer lost Mars, geodetic coordinates are on 1927 North American Datum and $d_{\rm limb}$ and $d_{\rm term}$ are the apparent distances of Mars' center from the lunar limb and the bright terminator, respectively. Mars' apparent semidiameter was $9''.8$ and Moon's apparent semidiameter was $935''.3$.

The two observers were able to follow Mars until its apparent distance from the bright terminator became less than $40''$, which is almost equal to the angular resolution of naked eye. Thus, the observations confirmed our supposition and they strengthen our result that ΔT was about 3000 sec in the 7th century.

3. TIDAL ACCELERATION OF THE MOON

In order to investigate further the Earth's rate of rotation and the tidal acceleration of the Moon's longitude from the ancient times we have found 34 records of ancient solar eclipses between 700 BC and 1000 AD with descriptions of one of the words of "total", "complete", or "stars were seen" in Chinese and Japanese books. Among these 34 records 4 were found to be the predicted eclipses that cannot be used for our analysis. Remaining 30 records were used in our analysis.

On the tidal acceleration of the Moon versus ΔT plane, we plot an area of the parameters which gives the recorded total/annular eclipses in the capital of the dynasty. Since the tidal acceleration and the ΔT value do not change significantly within a short period of time, we can expect substantially the same values of these parameters for two successive eclipses occurring within a period of, say, 60 years. Fig. 1 shows one of such examples.

The three solar eclipses were recorded in China and it is assumed that these eclipses were observed in Ch'ang-an. The BC 198 Aug 7 eclipse (shown by the bold lines in the figure) was

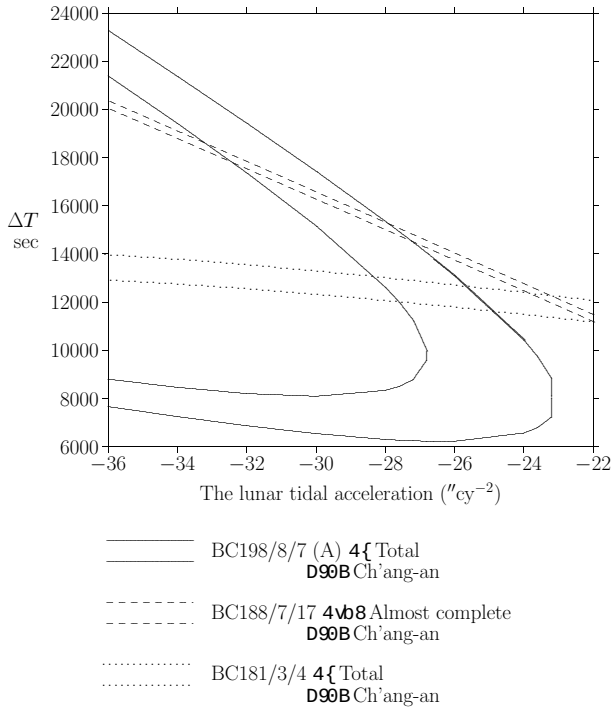

Figure 1: Solar eclipses of 198 BC, 188 BC, and 181 BC The solid lines show the area of the annular phase of the 198 BC eclipse, the broken lines the total phase of the 188 BC eclipse, and the dotted lines the total phase of the 181 BC eclipse.

recorded as "chin". "Chin" usually means total but it was also used for annular eclipses, and in this case the observed eclipse was annular. The BC 188 July 17 eclipse (the broken lines) was recorded as "almost complete". The BC 181 Mar 4 eclipse (the dotted lines) was recorded as "total". Therefore the values of the parameters should be in the common area surrounded by the bold lines and dotted lines and should also be outside the area shown by the broken lines. Hence the tidal acceleration of the Moon can be determined from these eclipse records to be $-(26 \pm 1)''/\mathrm{cy}^2$.

The pair of the solar eclipses of AD 516 and 522 and the pair of those of 616, 628 and 702 also give the result that the tidal acceleration has been $-26''/\mathrm{cy}^2$. The pair of the solar eclipses of 709 BC, 601 BC and 549 BC gives a wider range for the tidal acceleration (see Fig. 2), but it is also consistent with the value of $-26''/\mathrm{cy}^2$ for the tidal acceleration of the Moon. The places and the recorded discriptions for the solar eclipses appearing in the present analysis for the tidal acceleration are given in Table 1.

Since the tidal acceleration $-26''/\mathrm{cy}^2$ of the Moon we obtained agrees with the value obtained from the recent LLR (lunar laser ranging) measurements (Chapront et al. 2002; the value they obtained is -25.858 ± 0.003 ($''/\mathrm{cy}^2$)). It is also consistent with the value -26 ± 2 ($''/\mathrm{cy}^2$) derived from the comparison of the observations of transits of Mercury and lunar occultations of stars covering the period from 1677 to 1973. These facts indicate that the tidal acceleration of the Moon has been constant since 700 BC.

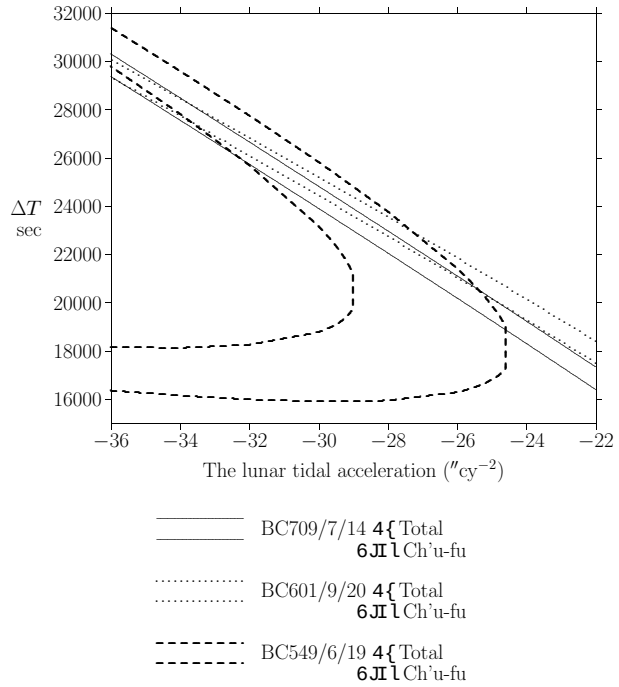

Figure 2: Solar eclipses of 709 BC, 601 BC, and 549 BC. The solid lines show the area of the total phase of the 709 BC eclipse, the dotted lines the total phase of the 601 BC eclipse, and the broken lines the total phase of the 549 BC eclipse.

Table 1. Eclipses used for the tidal acceleration determination.

Date	Place	Description
BC 709 July 14	Ch'u-fu, China	Total
BC 601 Sept 20	Ch'u-fu, China	Total
BC 549 June 19	Ch'u-fu, China	Total
BC 198 Aug 7	Ch'ang-an, China	Total (actually annular)
BC 188 July 17	Ch'ang-an, China	Almost complete
BC 181 Mar 4	Ch'ang-an, China	Total
AD 516 Apr 18	Chien-k'ang, China	Total (actually annular)
522 June 10	Chien-k'ang, China	Total
616 May 21	Lo-yang, China	Total (actually annular)
628 Apr 10	Asuka, Japan	Total
702 Sept 26	Ch'ang-an, China	Almost total

4. PERIODIC VARIATION OF THE EARTH'S ROTAION RATE

Now that we know that the tidal acceleration of the Moon has been $-26''/\mathrm{cy}^2$, we can determine the ΔT values at the times of the recorded solar eclipses using this value for the lunar tidal acceleration. Table 2 shows the solar eclipses we used and the resulting ΔT values.

The obtained ΔT values are shown in Fig. 3. The thick lines indicate that the range was obtained from multiple eclipses and the thin line from single eclipses.

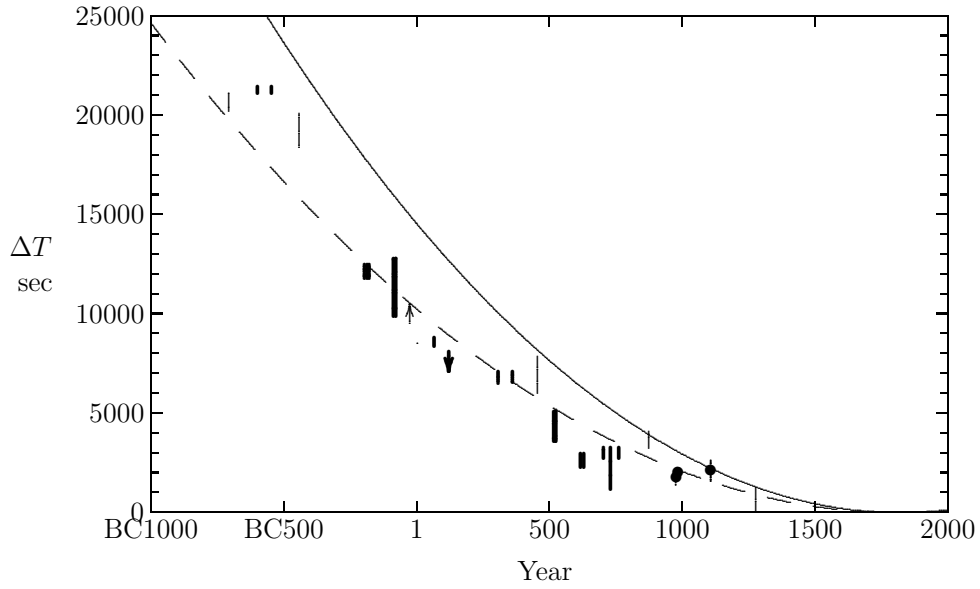

Solid line: tidal effect. Dashed line: parabolic fitting (Stephenson 1997).
•: timed data.

Figure 3: Obtained ΔT values.

The figure clearly shows that the ΔT value had a semi-periodic variation with a period of several hundred years since 700 BC. The nontidal components of ΔT should be due to the variation of the moment of inertia of the Earth.

Suppose that glaciers in polar regions melt and the sea level on the Earth's surface rises by 1 m over 1000 years in a constant rate. Then due to the increase of the Earth's moment of inertia ΔT increases by about 30 minutes. The variation of the sea level due to the variation of atmospheric temperature in the polar regions is a probable cause of the variation of the Earth's rate of rotation in hundreds of years or in a millennium.

5. CONCLUSION

We showed from the ancient solar eclipse records that the tidal acceleration of the Moon has been constant from 700 BC and the ΔT values had a semi-periodic variation with a period of several hundred years since 700 BC. The variation of the sea level due to the variation of atmospheric temperature in the polar regions is a probable cause of the non-tidal components of the variation of the ΔT value.

Table 2. Used Eclipses and Derived ΔT Values.

Date	Description	ΔT/sec		
Single events				
BC 709 July 17	Total	20201	–	21143
BC 444 Oct 24	Stars seen	18375	–	20119
BC 28 June 19	Not complete; Like a hook	9512	<	
AD 2 Nov 23	Total	8510	–	8542
65 Dec 16	Total	8362	–	8810
120 Jan 18	Almost complete		<	8117
454 Aug 10	Total	6027	–	7858
873 July 28	Dark; Total	3237	–	4106
975 Aug 10	Total; Inky darkness	1167	–	4452
Multiple events				
BC 601 Sept 20	Total	21093	–	21466
BC 549 June 19	Total			
BC 198 Aug 07	Total			
BC 188 July 17	Almost complete	11816	–	12471
BC 181 Mar 04	Total			
BC 89 Sept 29	Almost complete; Like a hook	9880	–	12820
BC 80 Sept 20	Almost complete			
AD 306 July 27	Total	6529	–	7120
360 Aug 28	Not complete; Like a hook			
516 Apr 18	Total			
522 July 10	Total	3567	–	5085
523 Nov 23	Venus seen			
616 May 21	Total	2278	–	2959
628 Apr 10	Complete			
702 Sept 26	Almost total; Like a hook			
729 Oct 27	Not complete; Like a hook	2728	–	3254
761 Aug 05	Total; Stars seen			

6. REFERENCES

Chapront J., Chapront-Touzé M., Francou G., 2002, *Astron. Astrophys.*, **387**, 700–709.

Morrison L. V., Ward C. G., 1975, *Mon. Not. R. Astr.Soc.*, **173**, 183–206.

Stephenson F. R., 1997, *Historical Eclipses and Earth's Rotation*, Cambridge University Press.

LA LUNE ET SA ROTATION DE L'ANTIQUITÉ AU XVII^{e} SIÈCLE

M.-P. LERNER, S. DÉBARBAT
SYRTE/UMR 8630, Observatoire de Paris
61 avenue de l'Observatoire, 75014 Paris, France
e-mail: Suzanne.Debarbat@obspm.fr

ABSTRACT. For some two millenia, in the West, an observed phenomenon as ordinary as that of the Moon's face had major theoretical consequences. The fact that the Moon, as seen from the Earth, always has the same appearence, hindered not only the possibility of imagining its rotation upon itself, but furnished one of the observational criteria on which was based the belief in the celestial spheres carrying the heavenly bodies. The dissolution of these spheres made of a fifth essence at the end of the XVIth century, and the advances in celestial cinematics in the following century, were the conditions for the conceptual assimilation of the phenomenon of the Moon's rotation upon itself. At the end of the XVIIth century, Jean-Dominique Cassini (1625-1712) was able to give the duration of the rotation of Mars and Jupiter. It was in this context that he formulated three laws relating to the rotation of the Moon, laws which have since been given his name.

1. INTRODUCTION

La Lune offre un cas idéal pour illustrer le paradoxe suivant : pendant des siècles, le témoignage des sens a constitué un obstacle épistémologique majeur à l'admission d'un fait - la rotation propre de notre satellite - qu'il a même rendu proprement inconcevable[1]. Aristote (-384 – -322) est le principal responsable de ce blocage que les données de l'observation semblaient justifier pleinement, alors que Platon (-427 – -347), sur la base de raisons purement *a priori*, avait accordé à tous les corps célestes, outre les révolutions circulaires qu'ils accomplissent autour de la Terre, un mouvement de rotation propre, celui qui est le plus en rapport avec la nature psychique des astres, que Platon dote d'intelligence et de raison.[2]

[1] Cette communication doit beaucoup à l'excellente étude d'Alan Gabbey qui a pour titre "Innovation and Continuity in the History of Astronomy : The case of the Rotating Moon", dans P. Barker et R. Ariew (éds.), *Revolution and Continuity: Essays in the History and Philosophy of Early Modern Science*, Washington, 1991, p. 95-129; voir aussi M.-P. Lerner, *Le Monde des Sphères*, tome 1, *Genèse et triomphe d'une représentation cosmique*, Paris, 1996.

[2] *Timée*, 34A. Sur ce thème fondamental de la pensée platonicienne, voir l'étude de E. N. Lee, "Reason and Rotation : Circular Movement as the Model of the Mind (Nous) in Later Plato", dans W. H. Werkmeister éd., *Facets of Plato's Philosophy*, Assen 1976, 70-102.

2. LA NON-ROTATION DE LA LUNE SELON LES ANCIENS

Dans le traité *Du ciel*, après avoir postulé que l'éther, ou "premier corps", est la substance dont est composé le ciel, c'est-à-dire toute la région située au dessus des quatre éléments (terre, eau, air et feu) du monde sublunaire et qui s'étend entre la Lune et le firmament, Aristote s'interroge sur la motricité des astres. Comment se déplacent-ils dans le ciel? Etant des corps sphériques, ils peuvent avoir en théorie deux mouvements : soit progression par roulement (*kulisis*), soit rotation (*dinêsis*), deux mouvements qu'Aristote tient pour *exclusifs* l'un de l'autre.

Aristote écarte d'abord le mouvement de rotation. Si les astres toupillaient, ils resteraient dans le même lieu sans changer de place. En effet, dans son mouvement de rotation, la sphère ne change pas de lieu *secundum totum*. Il en va ainsi pour la sphère des étoiles fixes qui tourne sur elle-même, et il doit donc en aller de même pour les parties sphériques du monde que sont les astres : or on les voit se déplacer sur le fond du ciel[3]. De plus, étant de même nature, les corps célestes devraient tous être affectés d'une rotation propre : or seul le Soleil semble tourner sur lui-même lorsqu'on l'observe à son lever et à son coucher. En réalité, ce toupillage n'est pas le fait du Soleil lui-même, mais est dû à l'éloignement de l'astre qui fait littéralement "tourner" notre regard[4].

Aristote élimine ensuite le mouvement de roulement, ou de progression, parce qu'un corps qui roule doit nécessairement accomplir un mouvement de conversion. Cette fois-ci, c'est la Lune qui est convoquée pour rejeter la thèse : ne nous montre-t-elle pas toujours la même face? Or ce qui vaut pour la Lune vaut pour tous les autres astres: il en résulte qu'aucun d'entre eux ne progressera par roulement, ce qui est confirmé par le fait que, à la différence des autres vivants, les astres ne possèdent pas les organes de progression dont la nature, qui ne fait rien en vain, n'aurait pas manqué de les doter s'ils devaient se mouvoir *par eux-mêmes*[5].

La conclusion hâtive tirée de l'observation de la Lune - mais il reste que c'est bien toujours *la même face* de notre satellite que nous *voyons* -, semble avoir empêché Aristote d'imaginer que l'apparence de la Lune qui offre toujours la même face à nos regards, puisse aussi être sauvée par une rotation propre de celle-ci autour de son axe en une période égale à celle de sa révolution autour de la Terre. Conséquence : contre Platon pour qui les astres sont des vivants se déplaçant librement dans le ciel, Aristote a trouvé dans la face inchangée de la Lune une raison empirique très forte pour conforter sa thèse que les planètes, tout comme les étoiles fixes incrustées dans le firmament à l'instar des nœuds dans une planche, sont immobiles dans des sphères qui les emportent autour de la Terre[6].

Le système des sphères concentriques directement emprunté par Aristote aux astronomes Eudoxe (-406?– -355?) et Callippe (-IV^{e} s.), du fait de son incapacité notamment à rendre compte des variations de grandeur apparente des planètes, va être efficacement concurrencé par le système excentro-épicyclique inventé par Hipparque au -II^{e} s., et magistralement élaboré par Ptolémée (100?-170?). Dans ce système - en simplifiant beaucoup - la Lune est solidaire d'un épicycle qui se déplace le long d'un déférent à l'intérieur duquel se trouve située la Terre immobile. Suivant cette hypothèse, un observateur terrestre ne verrait pas toujours la face de la Lune sous la même apparence, mais tantôt orientée dans un sens, tantôt dans le sens inverse. Notons toutefois que, dans l'*Almageste*, Ptolémée ne s'est pas posé la question en ces termes, ni plus tard Copernic (1473-1543) qui, dans le *De revolutionibus*, attache lui aussi la Lune à un épicycle. Dans le corps de leur traité, Ptolémée et Copernic ne considèrent en effet la Lune, et les autres planètes, que comme des points abstraits entraînés par les cercles qui les transportent.

[3] *Physique*, VI 9, 240a 29 *sq.*

[4] M.-P. Lerner, "*Sicut nodus in tabula* : de la rotation propre du soleil au seizième siècle", Journal for the History of Astronomy, 11, 1980, pp. 114-129.

[5] *Du Ciel*, 290a 24-35.

[6] Dans sa monographie *La Lune dans la pensée grecque*, Bruxelles 1973, Claire Préaux passe curieusement sous silence toute cette argumentation d'Aristote relative à l'absence de la rotation propre de la Lune.

3. LA SOLUTION DES MÉDIÉVAUX

Ce sont des auteurs médiévaux - souvent partisans d'un retour à l'astronomie concentrique défendue par Aristote et par son interprète Averroès (1126-1198) -, qui ont posé le problème, et qui ont énoncé la solution qui permettrait de sauver l'apparence de la tache de la Lune, sans pour autant s'y rallier dans la majorité des cas. On trouve l'énoncé de cette solution chez Roger Bacon (1214?-1294) et Richard de Middleton (1249?-1308) au XIII^{e} siècle, chez Lévi ben Gerson, dit Gersonide (1288-1344) et Jean Buridan (1300?-1358?) au siècle suivant, et encore au XVI^{e} siècle chez Giambattista Amico (1502?-1538) et chez Jérôme Fracastor (1478-1555)[7].

Selon Buridan, l'apparence de la tache lunaire vue depuis la Terre serait inchangée si l'on postulait que la Lune effectue une rotation propre autour de son axe dans le même temps que son épicycle accomplit sa révolution autour de la Terre, mais en sens inverse de celui-ci[8]. Ni Buridan, ni les autres auteurs cités n'ont repris à leur compte cette manière de "sauver" la tache de la Lune au motif qu'il faudrait, par voie de conséquence nécessaire, prêter une rotation propre à toutes les planètes - ce dont ils ne voyaient pas de justification rationnelle. Seules exceptions connues à ce refus chez des auteurs médiévaux : Nicole Oresme (1323?-1382)[9], et Albert de Saxe (1316-1390) - lequel invoque précisément le statut cosmologique distinct de la Lune au regard des autres corps célestes, pour admettre qu'elle puisse tourner sur elle-même[10] (Figure 1).

Paradoxalement, la question de la rotation, ou non, de la Lune n'a pas évolué de manière significative jusque vers 1650. Deux auteurs qui se sont intéressés directement aux propriétés physiques de la Lune en tant que corps céleste, à savoir Jean Kepler (1571-1630) et Galilée (1564-1642), n'ont pas pris sur ce sujet la position que l'on aurait pu penser.

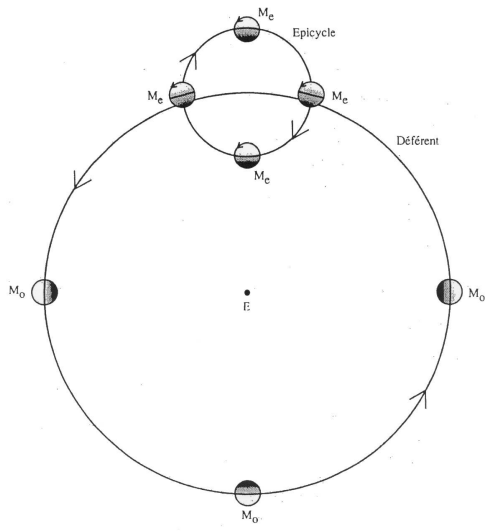

Figure 1: *Modèle épicyclique pour la Lune* (d'après A. Gabbey, art. cité note 1). La Lune (Me) montrera toujours la même face à un observateur situé sur la Terre (E), si elle tourne sur son épicycle dans la même période que celle mise par l'épicycle à parcourir son déférent, mais dans un sens contraire. Sans épicycle, la même face de la Lune (Mo) reste tournée vers la Terre sans rotation propre sur le déférent.

[7] Pour plus de détails, voir M.-P. Lerner, *Le Monde des sphères*, tome 1, pp. 114-115 et notes *ad loc.*

[8] Voir Jean Buridan, *In Metaphysicen Aristotelis Questiones Magistri Ioannis Buridani*, Paris 1518, Lib. XII, Qu. 10, ff. 73-74.

[9] *Le Livre du Ciel et du Monde*, II, 16, éd. A. D. Menut et A. J. Denomy, Madison 1968, pp. 452-461.

[10] *Questiones subtillissimae Alberti de Saxonia in libros de caelo et mundo*, Venise 1492, lib. II, qu. 7, sign. $E4^{v}$, col. 1.

4. LES PRISES DE POSITION DU XVII^{e} SIÈCLE

Dans des écrits remontant à 1609 - ils paraîtront en 1634 sous le titre *Somnium seu Opus posthumum de astronomia lunari* - mais aussi dans le livre IV son *Epitome astronomiae copernicanae* (1620), Kepler rejette résolument l'idée que la Lune tournerait sur elle-même en invoquant l'apparence que nous offre sa tache, absence de rotation que Kepler justifie par le fait que n'ayant pas de satellites à faire tourner autour d'elle - alors que la Terre a sa Lune, Jupiter ses satellites, et le Soleil ses planètes -, il n'y a pas de "raison" que la Lune soit dotée d'un tel mouvement. Et si Kepler a sans aucun doute abandonné l'idée aristotélicienne des sphères porteuses, il trouve une image qui n'en est pas éloignée, au moins du point de vue fonctionnel, pour expliquer les apparences: selon lui, la Lune "tourne autour de la Terre comme si elle était attachée à la Terre par une corde", et c'est pourquoi elle offre toujours le même hémisphère à nos regards, tandis que les Lunaires ont le privilège, eux, de voir le globe terrestre sous toutes ses faces[11]. Quant à Galilée, le premier à avoir vu sur la Lune, grâce à sa lunette, des choses qu'aucun homme n'avait vues avant lui (Figure 2), sa position sur ce sujet ne sera pas des plus claires. En effet, s'il suggère bien dans le *Dialogue sur les deux grands systèmes du monde* (1632) que la Lune devrait tourner sur elle-même si elle était entraînée par un épicycle, il ne dit pas ouvertement s'il retient cette solution[12].

On ne trouve pas davantage chez René Descartes (1596-1650) l'idée de la rotation propre de la Lune. Dans le *Traité du monde* [1633] resté inédit de son vivant, Descartes soutient que la Lune demeure "comme attachée à la superficie de son petit ciel", et qu'elle se trouve empêchée de "tourner derechef autour de son centre"[13]. Plus tard, dans le corps de l'article 152 de la Troisième partie des *Principes de philosophie* (1647, mais la version latine originale date de 1644) intitulé *Pourquoi c'est toujours un même côté de la Lune qui est tourné vers la Terre*, Descartes expliquera que "son autre côté est quelque peu plus solide, et par conséquent doit décrire un plus grand cercle [...]. Et certainement toutes ces inégalités en forme de montagnes et de vallées, que les lunettes d'approche font voir sur celui de ses côtés qui est tourné vers nous, montrent qu'il n'est pas si solide que celui de ses côtés qui est tourné vers nous"[14]. D'après les lois de la mécanique cartésienne appliquée aux mouvements des corps emportés dans un tourbillon, le côté le plus solide de la Lune serait soumis à un *conatus* centrifuge plus grand que celui du côté le plus léger, d'où sa tendance à se "détourner" du centre de son orbite occupé par la Terre.

Dans les années qui suivent la parution des *Principia philosophiae* de Descartes, les prises de position sur le sujet se diversifient, mais sans élaboration conceptuelle notable. En effet, si on constate que des auteurs comme Francesco Fontana (1580-1656), dans ses *Novae coelestium terrestriumque observationes* (1646), et Thomas Hobbes (1588-1679), dans son *De corpore* paru en 1655, postulent bien que la Lune peut en théorie tourner sur elle-même indépendamment de

[11] Voir *Somnium*, trad. angl. par E. Rosen sous le titre *Kepler's Somnium. The Dream or Posthumous Work on Lunar Astronomy*, Madison-London 1967, pp. 77-78; pour l'*Epitome*, voir *Kepler Gesammelte Werke*, éd. M. Caspar *et alii*, Munich 1937 –, vol. 7, p. 319.

[12] *Opere di Galileo Galilei*, Edizione nazionale a cura di A. Favaro, 20 vol., Florence 1899-1919: cf. vol. 7, pp. 89-90; trad. fr. citée par R. Fréreux et F. de Gandt, Point Seuil, Paris 2000, pp. 165-166: "SAGREDO: [...] nous ne voyons jamais plus de la moitié de la Lune, parce qu'elle ne tourne pas sur elle-même, comme elle le devrait pour pouvoir se montrer à nous tout entière. SALVIATI: A moins que ce ne soit le contraire, je veux dire à moins que ce ne soit à cause de sa rotation sur elle-même que nous n'en voyons jamais l'autre moitié; il devrait en être ainsi si la Lune avait un épicycle[...]".

[13] Voir *Le Monde. L'homme*, éd. par A. Bitbol Hespériès et J.-P. Verdet, Paris 1996, ch. 10, p. 40 [= *Œuvres de Descartes*, éd. Adam-Tannery, t. 11, p. 72].

[14] *Principes de philosophie*, III, 152, dans *Œuvres de Descartes*, éd. Adam-Tannery, t. 9, p. 197.

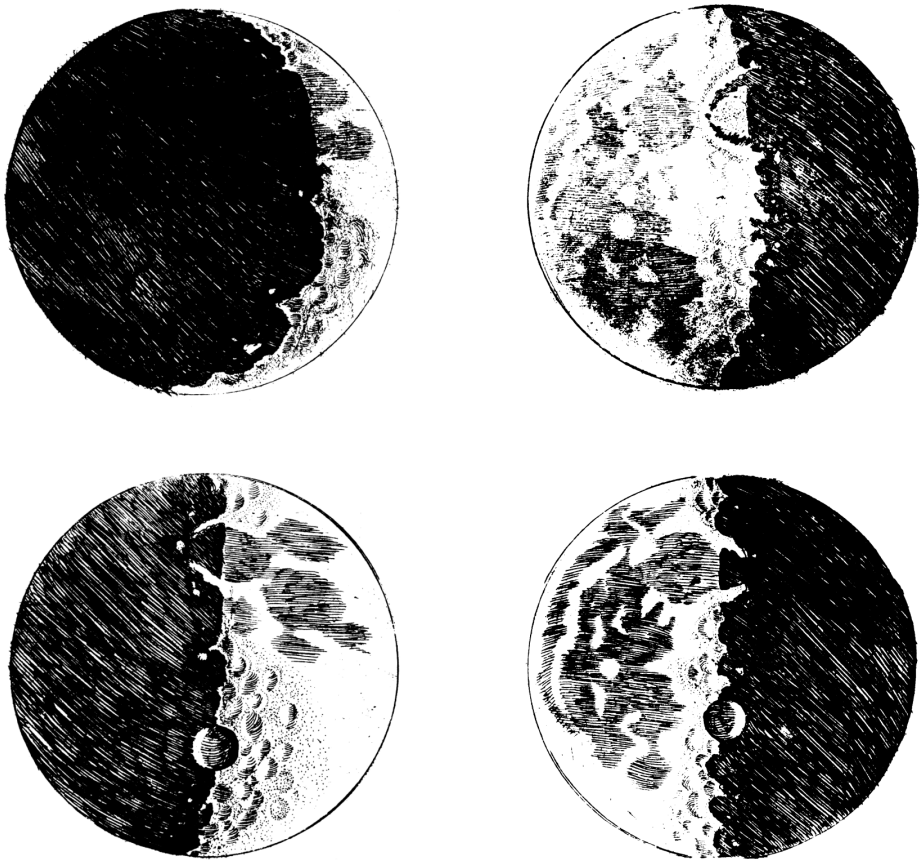

Figure 2: Phases de la Lune d'après les planches gravées dans le *Sidereus nuncius* (Venise 1610), respectivement f. 8r, f. 9v, f. 10r et 10v. En haut, de gauche à droite: Phase en croissant et Phase gibbeuse. En bas, de gauche à droite: Premier quartier et Dernier quartier.
(Document Bibliothèque de l'Observatoire de Paris)

toute mécanique épicyclique, l'idée traditionnelle d'une Lune privée de toute rotation propre est toujours fermement défendue au nom des apparences sensibles par Giambattista Riccioli (1598-1672) dans son *Almagestum novum* publié en 1651 - un ouvrage d'une toute autre autorité dans les milieux astronomiques que ceux que l'on vient de citer[15]. Et l'on sait que Isaac Newton (1643-1727) lui-même, encore dans les années 70 du XVII^{e} siècle, expliquera que la Lune tourne toujours la même face vers la Terre en empruntant à la théorie cartésienne des tourbillons. C'est seulement dans les *Philosophiae naturalis principia mathematica*, c'est-à-dire en 1687, qu'ayant élaboré une mécanique céleste originale, il donnera une explication physique de la rotation propre de la Lune qui sauve en même temps le phénomène complexe de libration[16].

[15] *Almagestum novum astronomiam veterem novamque complectens*, Bologne 1651, tome 1, partie 1, p. 99b.
[16] Sur tout ceci, voir A. Gabbey, art. cit., en particulier pp. 124-129.

5. LES TRAVAUX DES PRÉCURSEURS DE CASSINI

Parmi les raisons qui ont conduit Newton à abandonner sa conception initiale, d'une certaine façon encore prisonnière de l'interdit "aristotélicien" prononcé quelque 2000 ans plus tôt, les observations et calculs de Jean-Dominique Cassini (1625-1712) [= Cassini I] sur la Lune n'ont pas joué un rôle mineur.

Avant d'en venir toutefois à l'énoncé des trois "lois" de Cassini I sur la Lune, il convient de rappeler quelques données plus générales sur l'observation de notre satellite au cours du XVII^{e} siècle.

Pendant cette période, l'intérêt des astronomes pour la Lune est double. D'une part l'utilisation des éclipses du satellite de la Terre se développe grâce à l'augmentation en fiabilité des horloges. Parmi les résultats notables qu'a permis cette précision accrue dans la mesure du temps, on mentionnera la réduction de près d'un tiers de la longitude de la Mer Méditerranée (41°30′ au lieu des 60° que lui avait attribué Ptolémée) à laquelle sont parvenus les observateurs de l'éclipse de Lune du 28 août 1635. On doit ce succès principalement à Nicolas Claude Fabri de Peiresc (1580-1637), Pierre Gassendi (1592-1655) et Joseph Gaultier de La Valette (1564-1647), qui ont su s'attirer les services d'observateurs situés en France (à Paris, Aix, et Digne), en Italie (à Rome et Naples), et ailleurs encore: Alep, Tunis, Le Caire,...

D'autre part, et faisant suite à une proposition d'un certain Sieur de Saint-Pierre[17] auprès de Louise de Kéroualle (1649-1734) transmise au Roi d'Angleterre Charles II, la méthode des distances lunaires, pour la détermination des longitudes à la mer, prenait corps. Ami de Peiresc et de Gassendi, Jean-Baptiste Morin (1583-1656) avait jeté les bases de cette méthode dans son ouvrage de 1647 *La science des longitudes...*[18].

Sur terre, la détermination des longitudes est nécessaire pour l'établissement de cartes précises, la latitude, autre coordonnée locale, s'obtenant facilement par des mesures de hauteur d'étoiles au-dessus de l'horizon. Pour les navigateurs, la connaissance des longitudes est cruciale, et on avait espéré que la découverte des satellites de Jupiter par Galilée en 1610 offrirait un moyen efficace pour déterminer les positions en longitude des navires. Mais il était apparu dès la fin du XVII^{e} siècle qu'il fallait renoncer, en mer, à l'emploi des éclipses des satellites de Jupiter que Cassini I savait parfaitement prédire[19]. La Lune, pour son double rôle, prenait donc une importance capitale : l'instant de ses éclipses étant le même pour tous les points de la Terre d'où elle est visible, la différence des heures locales fournit directement celle des longitudes; quant à la distance qui la sépare d'étoiles dont les positions sont connues, elle se mesure aisément à l'aide d'une arbalestrille.

Les structures de la surface lunaire pouvaient - pensait-on alors - permettre une détermination plus précise des conditions des éclipses. Aussi, après les dessins préliminaires de Galilée, Gassendi et d'autres s'étaient-ils employés à repérer les particularités du relief de la Lune auxquels Riccioli donnait des noms qui ont été conservés de nos jours. Grâce à des objectifs de haute qualité fournis par des opticiens de Rome, Eustachio Divini (1610-1685) et Giuseppe Campani (1635-1715), Cassini I va entreprendre, dès son installation à l'Observatoire de Paris en septembre 1671, une série d'observations qui lui permettent de découvrir, tout d'abord, deux nouveaux satellites à Saturne, la division de l'anneau en 1675 puis, en 1684, deux autres satellites de cette planète. Mais la Lune retient aussi toute son attention pendant cette période: il s'intéresse à la fois aux accidents de sa surface, et à son mouvement dont les irrégularités sont de mieux en mieux mises en évidence par les astronomes. Pour ce faire, ils utilisent des secteurs et des

[17] Cf. *Greenwich Time and the Longitude*, D. Howse, National Maritime Museum in association with Atkearney, Oxford University Press, Oxford, 1997 (1ère édition 1980).

[18] J. Parès, *Jean-Baptiste Morin (1583-1656) et la querelle des longitudes de 1634 à 1647* (thèse Université de Paris I, 1976).

[19] *Ephemerides Mediceorum Syderum ex Hypothesibus & Tabulis Joan. Dominici Cassini. In fol. Bononiae*, in *Le Journal des Sçavans pour l'année 1668*, Paris, 1729, p. 105-107.

quadrants muraux équipés de micromètres mis au point par Adrien Auzout (1622-1691) et Jean Picard (1620-1682) en 1666.

Le mouvement de la Lune ne s'effectue pas avec une période de rotation strictement égale à celle de sa révolution autour de la Terre. Depuis un certain temps déjà, les astronomes avaient observé, de part et d'autre de sa face visible, des portions de globe lunaire faibles, certes, mais non négligeables.

Dans les années 1580-1590, Tycho Brahe (1546-1601) avait mis en évidence - de manière empirique - deux inégalités dans le mouvement de la Lune: la "variation", qui atteint $40'$ et dépend de la différence des longitudes de la Lune et du Soleil; et un autre terme appelé "équation annuelle", qui est une variation du moyen mouvement de la Lune[20].

La première inégalité a pour période la moitié de la lunaison, laquelle régit le retour des phases de la Lune et porte le nom de révolution synodique. La seconde, dont la période est annuelle, se détermine à partir d'un grand nombre d'observations du mouvement de révolution de la Lune autour de la Terre; elle dépend de l'excentricité de l'orbite terrestre, mais c'est par l'observation des éclipses de Lune que Tycho Brahe l'a mise en évidence, le phénomène étant affecté d'une avance ou d'un retard pouvant atteindre 40 minutes d'heure[21].

Le phénomène qui permet de voir, depuis la Terre, environ 59% de la surface lunaire, et appelé "libration", a été étudié principalement par Hevelius (1611-1687) dans sa *Selenographia* (1647)[22] et par Cassini I (Figure 3). Hevelius découvre en 1657, depuis son observatoire de Gdansk, le phénomène qui affecte la longitude céleste de la Lune[23]. Il remarque aussi une anomalie du moyen mouvement de la Lune que, plus tard en 1693, Edmond Halley (1656-1742) étudiera à partir d'éclipses anciennes comparées à celles de son époque[24].

6. LES "LOIS" DE CASSINI

L'ensemble de ces mouvements, déduits d'observations mettant en jeu la Lune, porte à la fois sur sa révolution autour de la Terre et sur son mouvement de rotation sur elle-même. Les observations que conduit Cassini, avec ses objectifs de fort grossissement, lui permettent de faire établir en 1679, à partir d'un ensemble de dessins de structures lunaires recueillis au cours des années soixante-dix du XVII^{e} siècle, une carte la Lune qui est la plus précise jamais faite, et qui le demeurera longtemps. Cassini déduit de l'ensemble de ses observations des lois, sans doute approximatives, mais qui faciliteront à Newton l'établissement d'une première théorie du mouvement de la Lune dans ses *Principia* de 1687[25].

Ces "lois de Cassini" sont au nombre de trois. Cassini en fait état dans *Recueil d'observations...* dans lequel il a inséré *De l'origine et du progrés de l'Astronomie,...* Il indique "De la théorie du soleil on passa à celle de la lune, où l'on fit aussi plusieurs nouvelles découvertes"[26].

Dans cette étude Cassini I rend compte du résultats des observations qu'il a faites à l'Observatoire de Paris depuis de nombreuses années - grâce à des objectifs de fort grossissement (pouvant atteindre, selon Charles Wolf, 600[27]) :

[20] Voir les observations recueillies dans le tome 12 des *Tychonis Brahe Opera Omnia*, éd. J. L. E. Dreyer, 15 tomes, Copenhagen, 1912-1929. Sur la théorie tychonienne de la Lune, voir le chapitre que lui consacre V. E. Thoren dans son *The Lord of Uraniborg. A Biography of Tycho Brahe*, Cambridge 1990, p. 312-333.

[21] Sur toutes ces découvertes, voir A. Danjon, *Astronomie générale*, Blanchard, Paris, 1952 (réimp. 1959 et 1980), p. 277 et 282.

[22] J. Hevelii, *Selenographia: sive, LunæDescriptio ...*, Gedani, 1647, p. 204-272.

[23] J. Hevelii, *Epistolae II. Prior: De Motu Lunae Libratorio*, Gedani, 1654, p. 1-48.

[24] Voir A. Cook, *Edmond Halley*, Oxford, 1998, p. 225-228.

[25] Cf. *Philosophiae Naturalis Principia Mathematica*, London, 1687.

[26] Cassini I ne met de majuscule ni à Soleil, ni à Lune, ni à Terre, alors que Cassini II en mettra. Ce dernier en aurait-il introduit l'usage qui existe de nos jours? Dans les différentes citations de ces astronomes, l'orthographe de l'époque a été conservée.

[27] Ch. Wolf, *Histoire de l'Observatoire de Paris de ses origines à 1793*, Paris, 1902, p. 161-162.

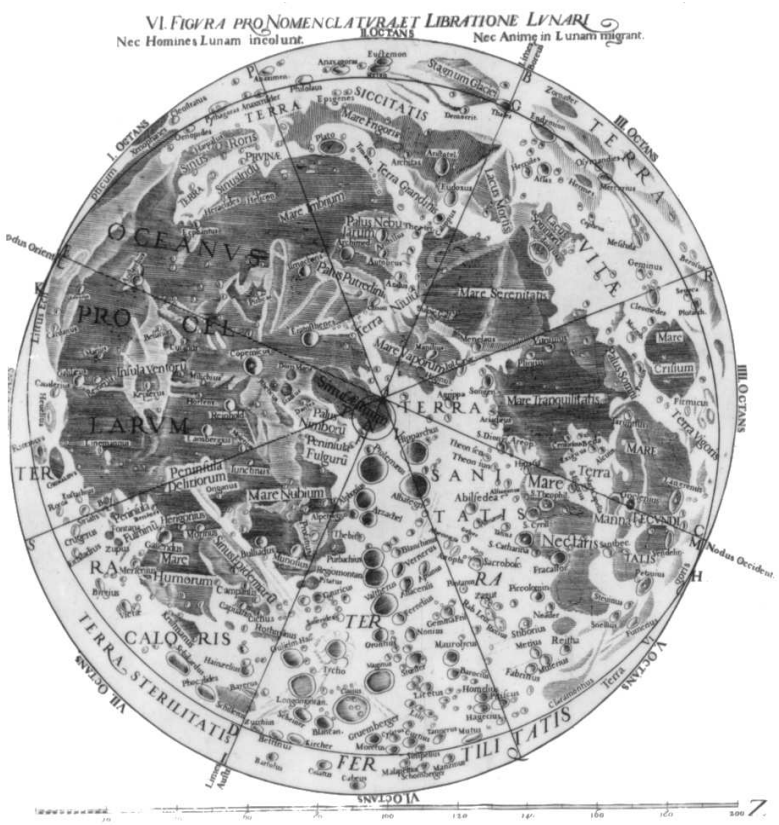

Figure 3: G. B. Riccioli, *Almagestum novum* ..., op. cit. note 15, tome 1, Figure VI, après la page 204. Nomenclature de Riccioli sur la carte de la Lune de Francesco Maria Grimaldi (1618-1663), avec représentation de la libration lunaire. (Document Bibliothèque de l'Observatoire de Paris)

> Pour expliquer cette libration apparente on a trouvé une theorie tres-simple & tres-naturelle. Comme les Coperniciens attribuënt deux mouvemens à la terre, l'un annuel & l'autre journalier ; de mesme on a consideré dans la lune deux mouvemens differens. Par l'un de ces mouvemens dont la révolution s'acheve en 27 jours & un tiers, la lune paroist tourner d'orient en occident sur un axe parallele à celuy de son orbite. L'autre mouvement se fait réellement d'occident en orient sur un axe dont les poles sont éloignez de ceux de l'orbite de la lune transportées dans son globe de sept degrez & demy ; & il a pour colure ou premier meridien le cercle de la plus grande latitude de la lune transportée aussi dans son globe[28].

Puis Cassini I expose les motifs qui l'on conduit à surveiller de manière aussi attentive la surface lunaire:

> Rien ne contribuë davantage à la perfection de la theorie de la lune, que l'observation des éclipses. [..] On a fait une description exacte des taches de la lune, non-seulement pour observer les éclipses

[28] *De l'origine et du progrés de l'Astronomie, et de son usage dans la Géographie et la Navigation* (p. 1-43, en part. p. 34 et 35), dans M. Cassini, *Recueil d'observations faites en plusieurs voyages par ordre de sa Majesté pour perfectionner l'Astronomie et la Géographie, Avec divers Traitez Astronomiques*, Paris, Imprimerire Royale, 1693.

avec plus de facilités & de précision, mais encore pour examiner si dans la suite du temps il n'arrivera point de changement à quelques-unes de ces taches.

Son fils Jacques Cassini (1677-1756) [= Cassini II], publiera en 1740 ses *Elements d'astronomie...* dans lesquels il mentionne à propos de la Lune :

> Par l'observation assidüe des Taches de la Lune, on a reconnu que cette Planete nous présentoit toûjours la même face, avec la seule différence que ses Taches qui conservent entr'elles la même situation, paroissent tantôt s'approcher un peu du bord de son disque apparent, & tantôt s'en éloigner à peu-près de la même quantité[29].

L'observation attentive des taches de la Lune par Cassini I, dans la perspective d'une amélioration de la détermination des longitudes au moment des éclipses de Lune, l'avait conduit à une remarquable description du phénomène. Dans son ouvrage de 1740, Cassini II fournit ensuite, de manière détaillée, les conclusions qu'en tire son père :

> Cette apparence a fait d'abord juger que le globe de la Lune ne faisoit point de révolution autour de son axe, mais qu'il étoit seulement sujet à quelques balancements semblables à ceux que l'on apperçoit dans une boule dont on change le centre de pesanteur, ce qui lui a fait donner le nom de *Librations*.

Puis Cassini II précise de manière très didactique:

> Ces mouvements irréguliers en apparence, & diférents de ceux qu'on a découverts dans la plûpart des autres Planetes qui font leur révolution autour de leur axe, ont donné lieu à mon Pere de juger de cette libration de la Lune étoit produite par la combinaison de deux mouvements, dont l'un est celui de la Lune autour de la Terre, et l'autre est sa révolution autour de son axe. Pour discuter l'effet de ces deux mouvements, il faut considérer qu'il y a dans le globe de la Lune, de même que dans celui du Soleil, un axe qui passe toûjours par les mêmes Taches fixes sur la surface de la Lune, à l'extrémité duquel sont placés deux Poles élevés sur le plan de l'Ecliptique de 87 degrés 1/2, & sur le plan de l'Orbite de la Lune, de 82 degrés 1/2 ; d'où il suit que l'Equateur de la Lune, qui est éloigné de chacun de ces Poles, de 90 degrés, & qui passe aussi toûjours par les mêmes Taches, est incliné à l'Ecliptique, de 2 degrés 1/2, & à l'Orbite de la Lune, de 7 degrés 1/2 (*de nos jours un peu moins de* 7°).

Il poursuit :

> On considérera en second lieu, que les Poles de la Lune sont toûjours dans un grand cercle du globe de cette Planete, parallele au grand cercle qui passe par les Poles de l'Orbite, & par ceux de l'Ecliptique, qu'on peut nommer *Colûre de la Lune*, par la même raison qu'on appelle *Colûre des Solstices*, le grand cercle qui passe par les Poles de l'Equinoxial & l'Ecliptique, à la distance de 90 degrés de l'intersection de ces deux cercles (*l'axe de rotation est perpendiculaire à l'équateur lunaire*).

Enfin, il indique :

> On supposera en dernier lieu, que le globe de la Lune tourne autour de son axe d'Occident en Orient dans l'espace de 27 jours et 5 heures *(de nos jours 27 jours, 7 heures et 43 minutes)* et, par une période égale à celle du retour de la Lune au Nœud de son orbite avec l'Ecliptique. Ce mouvement est analogue à la révolution de la Terre autour de son axe qui se fait d'Occident en Orient, & retourne au même Colûre dans l'espace de 23 heur. 56 minutes *(de nos jours 23 heures, 55 minutes et 4.1 secondes)*.

D'après Cassini II: "Ces hypothèses suffisent pour expliquer toutes les variétés de la libration apparente de la Lune".

[29] *Eléments d'Astronomie*, par Mr Cassini, Paris, Imprimerie Royale, 1740, p. 253-260.

7. CONCLUSION

Les lois de Cassini seront vérifiées à deux reprises au cours du XVIII^{e} siècle. Mayer (1723-1762), astronome à Göttingen mène, en 1748-1749, une série d'observations de plusieurs taches de la Lune qui le conduisent à confirmer les affirmations de Cassini I. Lalande publie, en 1764, de nouvelles observations qu'il a lui-même effectuées et qui entraînent la même conclusion[30].

Plus tard, avec l'accroissement de la précision des instruments d'observation, on constatera que les "lois" de Cassini ont un caractère de première approximation.

Ainsi le nœud ascendant de l'équateur lunaire dans l'écliptique ne coïncide pas rigoureusement avec le nœud ascendant moyen de l'équateur lunaire. En effet, l'inclinaison moyenne de l'équateur lunaire sur le plan de l'orbite subit des fluctuations, non négligeables, mais de très faible amplitude.

Quant à la rotation de la Lune, elle s'effectue autour du petit axe du globe lunaire, axe qui est perpendiculaire au plan de l'équateur lunaire. Et la direction du grand axe, dirigé vers la Terre, peut, elle, s'écarter de quelques centièmes de degré par rapport à la position qui avait conduit Cassini à conclure que l'axe de l'écliptique, celui de l'orbite de la Lune, et celui de son axe de rotation, étaient dans un même plan.

[30] J. N. Nicollet, *Mémoire sur la libration de la Lune*, in *Connaissance des tems pour l'an* 1822, Paris, 1819, p. 228-233.

HIGH-PRECISION NUMERICAL ANALYSIS OF THE RIGID EARTH ROTATION PROBLEM WITH USING A HIGH-PERFORMANCE COMPUTER

G.I. EROSHKIN, V.V. PASHKEVICH
Main Astronomical Observatory of RAS
Pulkovskoe chaussee, 65/1, 196140, St.Petersburg, Russia
e-mails: eroshkin@gao.spb.ru, apeks@gao.spb.ru

ABSTRACT. The present investigation is a development of the previous research on the rigid Earth rotation problem (Eroshkin *et al.*, 2002). The problem is studied numerically by using a high-performance computer Parsytec CCe20. All the calculations are carried out with the quadruple precision. The problem is solved both for the Newtonian case (dynamical case) and for the relativistic case (kinematical case) in which the geodetic perturbations in the Earth rotation are taken into account. Over the whole time interval of the numerical integration the solutions are compared with the corresponding solutions of the semi-analytical theory SMART97 (Bretagnon *et al.*, 1998), corrected in accordance with (Brumberg and Bretagnon, 2000). The behaviour of the secular and periodical terms in the residuals is discussed.

1. INTRODUCTION

In the previous investigation (Eroshkin *et al.*, 2002) a high-precision numerical solution of the rigid Earth rotation problem, accounting for the most essential relativistic perturbations — geodetic perturbations, was constructed by using a personal computer Pentium III 450 MHz. All the calculations were performed with a double precision. The precision of the numerical solution was at the level of several microarcseconds (μas) over the time interval of 1500 years. Such precision was achieved by means of using the regularizing variables, the Rodriges-Hamilton parameters, from which the main part of the secular variation of the angle of the proper rotation was excluded. An important point of the algorithm was a supplementary normalization of the values of Rodrigues-Hamilton parameters evaluated by means of the iterative procedure of the integrator HIPPI (Eroshkin, 2000).

Nevertheless it was considered quite necessary to repeat all the calculations with a quadruple precision in order to verify the earlier obtained results. It is also interesting to construct a numerical solution not only for the relativistic case but also for the Newtonian one. This paper describes the results of the numerical solution of the rigid Earth rotation problem obtained with the use of a high-performance computer Parsytec CCe20, which is a supercomputer of massive-parallel architecture with a separated memory at the Center for Supercomputing Applications of the Institute for High-Performance Computing and Data Bases in St.Petersburg, Russia (http://www.csa.ru/). All the calculations were performed with a quadruple precision. The mathematical model of the present investigation is identical to that used in (Eroshkin *et al.*, 2002). The kinematical solution SMART97 was initially corrected by the change of signs of all the

geodetic terms in the angle of the proper rotation, in accordance with (Brumberg and Bretagnon, 2000). The main purposes of the present research are the verification and improvement of the algorithms of constructing the numerical solutions and additional testing the method of numerical integration HIPPI. The integration of the differential equations is carried out over the time interval from AD 1000 to 3000. It starts from the standard initial epoch January 1, 2000, goes forward to 3000 and then backward to 1000. The numerical integration, carried out forth and back in time, checks a reliability of the method HIPPI. It is performed with 1-day constant step size and with 24-th degree Chebyshev polynomials approximating the right hand sides of the differential equations of the problem.

2. RESULTS

The analysis of the problem is performed over 2000 year time interval from AD 1000 to 3000, with the initial epoch January 1, 2000 (JD=2451545.0). The results of the numerical integration are compared with the semi-analytical solution SMART97 in Euler angles: the longitude of the ascending node ψ (Figures 1a, b), the proper rotation angle ϕ (Figures 2a, b) and the inclination angle θ (Figures 3a, b), (a — Kinematical case, b — Dynamical case). Tables 1–3 contain the results of the least squares adjustment of the behaviours of the discrepancies of the secular character $\Delta_s\psi$, $\Delta_s\phi$, $\Delta_s\theta$ and the secular terms in the corresponding angles of SMART97. In the present paper T denotes the time expressed in thousand Julian years (tjy), counted from the fundamental reference epoch J2000, and the coefficients are expressed in microarcseconds (μas). The correcting polynomials of degree 6 provide the best fitting to the approximating curves.

First of all, it is necessary to notice that Figure 1a and Figure 3a are very similar to the corresponding pictures of Figure 2 of the previous investigation (Eroshkin *et al.*, 2002). However the behaviour of the residuals in the proper rotation angle, depicted in Figure 2a, differs essentially from the corresponding picture in Figure 2 of the previous paper. It is discovered that this discrepancy is connected with the chosen criterion determining the process of the numerical integration. Namely, if HIPPI integrator is used then the convergence of the iterative procedure at every nodal point has to be controlled by the values of the relative errors and not of the absolute ones. The numerical experiments demonstrate that if one uses the relative error control then the results of the quadruple precision integration and double precision integration are quite close over one thousand year time interval.

The comparison of the secular trends in the residuals, corresponding to the kinematical and dynamical cases, depicted in Figures 1–3, is also of interest. The behaviour of the residuals for the angles ψ and ϕ in the kinematical case (Figure 1a and Figure 2a, respectively) is very similar to that in the dynamical case (Figure 1b and Figure 2b, respectively).

From the Tables 1–2 follows that for these angles the essential part of the residuals arises when constructing the dynamical solution SMART97. The geodetic rotations, which are used to derive the kinematical solution of SMART97, introduce relatively small part of the residuals. For the inclination angle θ the behaviour of the residuals in the kinematical and dynamical cases, depicted in Figure 3, differ significantly. Table 3 shows that the basic distinction in the representation of the interpolating curves comes from the quadratic and cubic terms. There is no satisfactory explanation of this phenomenon yet.

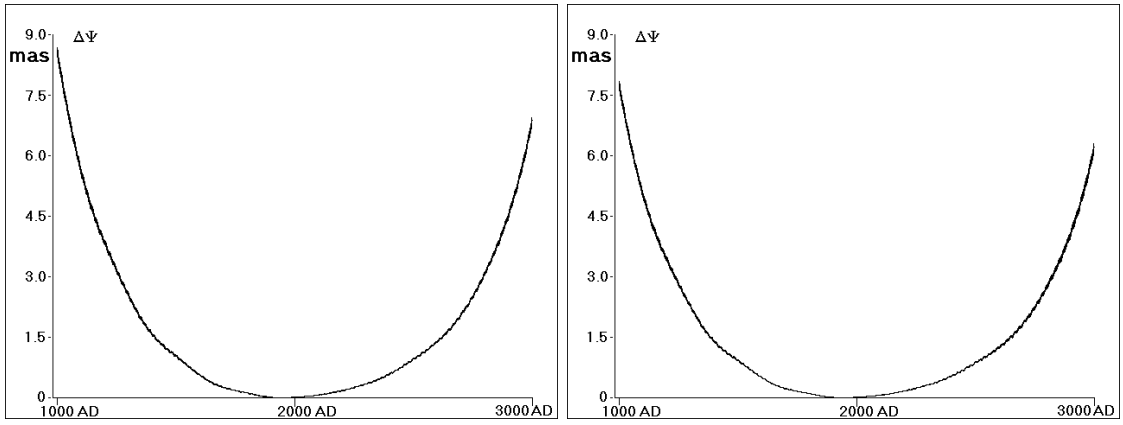

Figure 1: Numerical integration minus solution SMART97 in the angle ψ.

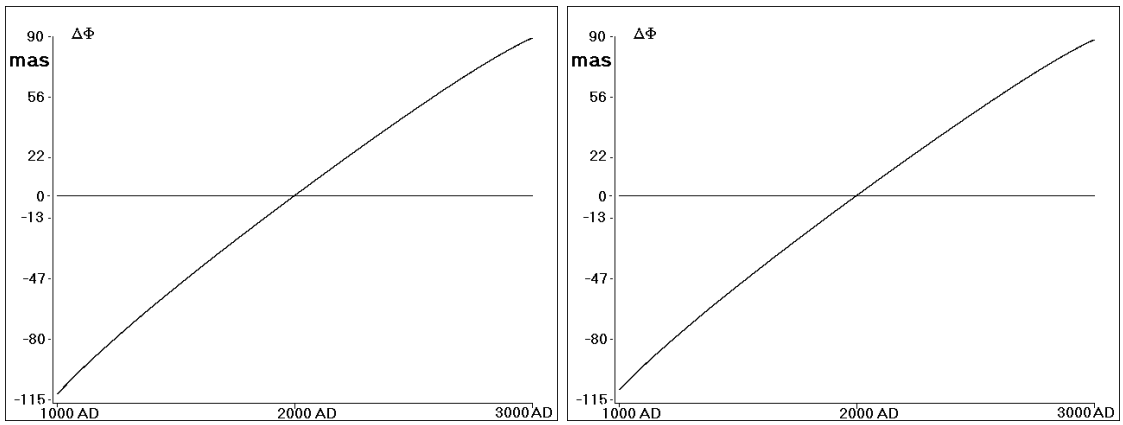

Figure 2: Numerical integration minus solution SMART97 in the angle ϕ.

a) — Kinematical case b) — Dynamical case

Table 1: Secular parts of the angle ψ and interpolating polynomials $\Delta_s\psi$.

	Kinematical case		Dynamical case	
	$\psi_{smart97}(\mu\text{as})$	$-\Delta_s\psi(\mu\text{as})$	$\psi_{smart97}(\mu\text{as})$	$-\Delta_s\psi(\mu\text{as})$
T^0		7.00		6.89
T	50384564881.3693	−206.50	50403763708.8052	−206.90
T^2	−107194853.5817	−3451.30	−107245239.9143	−3180.80
T^3	−1143646.1500	1125.00	−1144400.2282	1048.00
T^4	1328317.7356	−788.00	1329512.8261	−306.00
T^5	−9396.2895	−57.50	−9404.3004	−65.50
T^6		−3415.00		−3421.00

a) — Kinematical case b) — Dynamical case

Table 2: Secular parts of the angle ϕ and interpolating polynomials $\Delta_s\phi$.

	Kinematical case		Dynamical case	
	$\phi_{smart97}(\mu\text{as})$	$\Delta_s\phi(\mu\text{as})$	$\phi_{smart97}(\mu\text{as})$	$\Delta_s\phi(\mu\text{as})$
T^0	1009658226149.3691	6.58	1009658226149.3691	6.53
T	474660027824506304.0000	99598.30	474660027824506304.0000	97991.40
T^2	−98437693.3264	−7182.30	98382922.2808	−6934.40
T^3	−1217008.3291	1066.80	−1216206.2888	1004.00
T^4	1409526.4062	−750.00	1408224.6897	−226.00
T^5	−9175.8967	−30.30	−9168.0461	−37.80
T^6		−3676.00		−3682.00

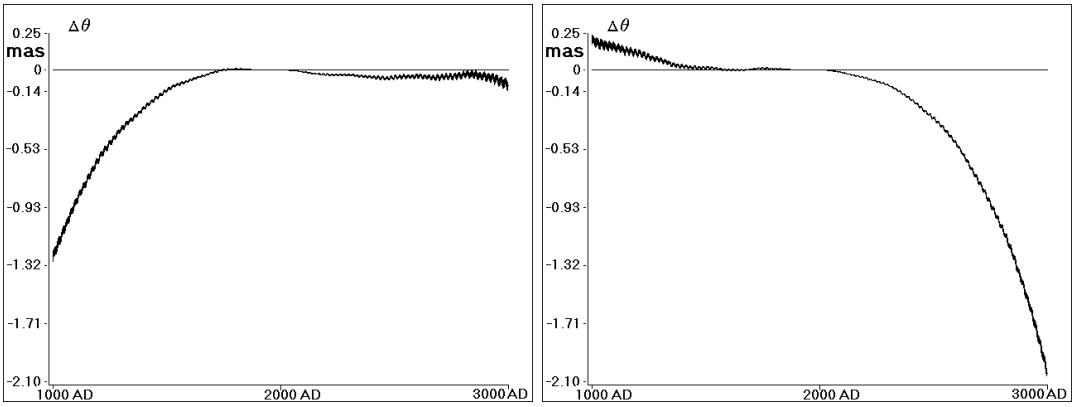

Figure 3: Numerical integration minus solution SMART97 in the angle θ.

a) — Kinematical case b) — Dynamical case

Table 3: Secular parts of the angle θ and interpolating polynomials $\Delta_s\theta$.

	Kinematical case		Dynamical case	
	$\theta_{smart97}(\mu\text{as})$	$\Delta_s\theta(\mu\text{as})$	$\theta_{smart97}(\mu\text{as})$	$\Delta_s\theta(\mu\text{as})$
T^0	84381409000.0000	1.42	84381409000.0000	1.39
T	−265011.2586	−96.61	−265001.7085	−96.73
T^2	5127634.2488	−353.10	5129588.3567	−595.90
T^3	−7727159.4229	771.50	−7731881.2221	−945.10
T^4	−4916.7335	−84.50	−4930.2027	−76.50
T^5	33292.5474	−86.00	33330.6301	−70.00
T^6		−247.50		−247.80

Several harmonics $\Delta_p\psi$, $\Delta_p\phi$, $\Delta_p\theta$ in the residuals are determined by the least squares method with the arguments chosen from the arguments of SMART97 theory. In Tables 4–6 the same harmonics are presented which were determined in (Eroshkin *et al.*, 2002). The standard errors of the coefficients shown in Tables 4–6 have the magnitude of about two orders smaller than the coefficients themselves. The argument $\lambda_3 + D - F$ equals $\Omega + 180^o$; $\lambda_2, \lambda_3, \lambda_4, \lambda_5, \lambda_6$ are the mean longitudes of Venus, the Earth, Mars, Jupiter and Saturn, respectively; D is the difference between the mean longitudes of the Moon and the Sun; Ω is the mean longitude of the ascending node of the lunar orbit; F is the mean argument of the Moon's latitude.

Table 4: The periodical terms $\Delta_p\psi$ and the corresponding harmonics in SMART97.

argument, period		Kinematical case		Dynamical case	
		Coefficients of $\psi_{smart97}(\mu\text{as})$	Coefficients of $-\Delta_p\psi(\mu\text{as})$	Coefficients of $\psi_{smart97}(\mu\text{as})$	Coefficients of $-\Delta_p\psi(\mu\text{as})$
$2\lambda_5 - 5\lambda_6$ 800.9 years	cos	−667.3427	10.05	−667.6674	10.02
	T cos	−291.6144	−5.23	−291.7531	−5.22
	T^2 cos	17.9597	−10.85	17.9848	−10.82
	sin	−512.8209	−0.31	−513.0837	−0.32
	T sin	219.7644	−4.53	219.9043	−4.56
	T^2 sin	98.4238	−3.25	98.4621	−3.24
$3\lambda_2 - 7\lambda_3 + 4\lambda_4$ 302.4 years	cos	−3.4630	−8.46	−3.4630	−8.48
	T cos	0.1067	28.06	0.1067	28.06
	T^2 cos		−41.87		−41.82
	sin	5.1808	2.29	5.1808	2.30
	T sin	0.1046	6.29	0.1046	6.31
	T^2 sin		−27.87		−27.88
$\lambda_3 + D - F$ $(\Omega + 180^o)$ 18.6 years	cos	−439.4833	−0.97	−439.4833	−0.98
	T cos	13416.3947	−27.28	13416.3960	−26.68
	T^2 cos	35849.0443	4.7	35842.8827	2.9
	sin	17280773.3737	−0.08	17280776.3805	−0.07
	T sin	84107.0763	−0.30	84107.0745	−0.37
	T^2 sin	−1178.0123	−5.7	−1178.3901	−5.2

Table 5: The periodical terms $\Delta_p\theta$ and the corresponding harmonics in SMART97.

argument, period		Kinematical case		Dynamical case	
		Coefficients of $\theta_{smart97}(\mu as)$	Coefficients of $\Delta_p\theta(\mu as)$	Coefficients of $\theta_{smart97}(\mu as)$	Coefficients of $\Delta_p\theta(\mu as)$
$2\lambda_5 - 5\lambda_6$ 800.9 years	cos	−237.8839	2.66	−237.9787	2.649
	T cos	214.2387	2.35	214.3301	2.35
	T^2 cos	21.5893	−3.77	21.6003	−3.76
	sin	437.0537	−2.118	437.2269	−2.110
	T sin	106.7941	2.86	106.8398	2.85
	T^2 sin	−61.1330	2.94	−61.1586	2.92
$3\lambda_2 - 7\lambda_3 + 4\lambda_4$ 302.4 years	cos	0.2135	−1.72	0.2135	−1.72
	T cos	−0.0256	−7.37	−0.0256	−7.37
	T^2 cos		2.40		2.42
	sin	0.0549	−2.75	0.0549	−2.752
	T sin	−0.0729	4.19	−0.0729	4.20
	T^2 sin		7.04		7.05
$\lambda_3 + D - F$ $(\Omega + 180^o)$ 18.6 years	cos	−9227885.6279	0.23	−9227886.9315	0.22
	T cos	−9273.2018	0.02	−9273.2018	0.05
	T^2 cos	11.5998	0.95	11.5998	0.87
	sin	32.1530	−0.46	32.1530	−0.46
	T sin	4413.0849	−14.35	4413.0855	−14.02
	T^2 sin	25501.6281	0.74	25499.8022	1.19

Table 6: The periodical terms $\Delta_p\phi$ and the corresponding harmonics in SMART97.

argument, period		Kinematical case		Dynamical case	
		Coefficients of $\phi_{smart97}(\mu as)$	Coefficients of $\Delta_p\phi(\mu as)$	Coefficients of $\phi_{smart97}(\mu as)$	Coefficients of $\Delta_p\phi(\mu as)$
$2\lambda_5 - 5\lambda_6$ 800.9 years	cos	−618.7215	9.16	−618.3585	9.14
	T cos	−269.1674	−4.78	−269.0474	−4.77
	T^2 cos	17.3920	−10.13	17.3622	−10.10
	sin	−474.1121	−0.25	−473.8684	−0.26
	T sin	204.8051	−4.05	204.6460	−4.08
	T^2 sin	90.6361	−3.08	90.6058	−3.07
$3\lambda_2 - 7\lambda_3 + 4\lambda_4$ 302.4 years	cos	−3.1772	−7.97	−3.1772	−7.98
	T cos	0.0979	25.56	0.0979	25.55
	T^2 cos		−37.34		−37.29
	sin	4.7532	2.09	4.7532	2.09
	T sin	0.0959	5.71	0.0959	5.74
	T^2 sin		−25.51		−25.51
$\lambda_3 + D - F$ $(\Omega + 180^o)$ 18.6 years	cos	−403.2789	−0.92	−403.2789	−0.92
	T cos	12309.0477	−24.80	12309.0462	−24.25
	T^2 cos	32869.9705	4.4	32875.6240	2.7
	sin	15852158.3146	0.02	15852155.0374	0.03
	T sin	77184.1368	−0.86	77184.1388	-0.90
	T^2 sin	−1252.4257	−5.5	−1252.0139	−5.0

If one compares the coefficients for Kinematical case, shown in Tables 4–6, with the corresponding quantities in (Eroshkin *et al.*, 2002) then certain differences can be discovered. They have two explanations. Firstly, the signs of all the geodetic terms in the kinematical solution for the proper rotation angle ϕ in SMART97 were changed in accordance with (Brumberg and Bretagnon, 2000). As a result, the coefficients of the harmonic with the argument $2\lambda_5 - 5\lambda_6$ in $\Delta_p\phi$ became essentially smaller. Secondly, in the present investigation the time interval of the adjustment is 2000 years instead of 1500 years, that is 1/3 larger than in the previous work.

As it was previously explained (Eroshkin *et al.*, 2002), the secular and periodical terms determined from the residuals of comparison of the numerical solution and semi-analytical solution SMART97 are the corrections to the corresponding terms of SMART97. As a final step of the present investigation, the kinematical solution SMART97 is modified by adding the secular correction terms from Tables 1–3. The numerical integration is performed anew with the initial conditions determined by the modified kinematical solution SMART97. The results of

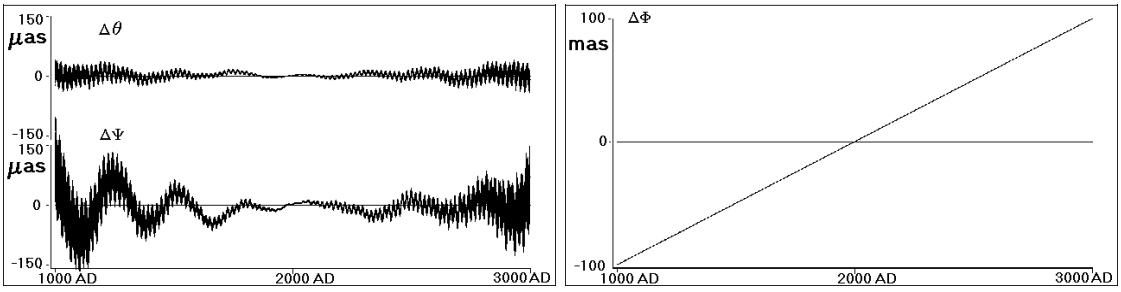

Figure 4: Numerical integration minus kinematical solution SMART97 supplemented by the secular corrections in Euler angles.

comparison of the numerical and modified semi-analytical solutions are presented in Figure 4. The secular trend in the proper rotation angle ϕ does not change practically with respect to that depicted in Figure 2a. In fact, there are differences which can be seen if one compares the polynomial $\Delta_s\phi = 6.62 + 99787.58T - 0.65T^2 - 0.39T^3 + 1.42T^4 + 0.47T^5 - 0.75T^6$, representing the secular behaviour of the residuals in the proper rotation angle from the Figure 4 with the corresponding polynomial from Table 2. This comparison shows that the corrections to the secular terms in the angle of the proper rotation are the real corrections to the second and higher order terms, whereas the linear part of correction is a fictitious one.

It was earlier discovered that the small variation of the initial moment of the numerical integration can change the value of the secular trend. It is quite possible that the reason for this phenomenon is connected with the appearance of the fictitious free nutation (fictitious Euler nutation) in the process of the numerical integration.

3. CONCLUSIONS

The results of the present investigation confirm the validity of the previous study, based on the double precision calculations. The semi-analytical theory of the rigid Earth rotation SMART97, corrected in accordance with the conclusions in (Brumberg and Bretagnon, 2000), represents high-precision semi-analytical solutions of the problem over the time interval of several centuries. The precision of this theory can be improved, for example, numerically by the method proposed by the authors. The time interval of its validity can be also extended in this way.

Acknowledgments. Financial support for this investigation was provided by Russian Foundation for Basic Research, Grants No. 02-02-17611 and No. 03-02-06875. The technical computing support was provided by the Center for Supercomputing Applications at the Institute for High-Performance Computing and Data Bases in St. Petersburg, Russia.

4. REFERENCES

Bretagnon, P., Francou, G., Rocher, P. and Simon, J. L., 1998, *Astron. Astrophys.*, **329**, No.1, 329–338.

Brumberg, V. A. and Bretagnon, P., 2000, *Proceedings of IAU Colloquium 180*, Washington, 293–302.

Eroshkin, G. I., 2000, Book of abstracts *Astrometry, Geodynamics and Celestial Mechanics at the turn of XXIth century*, (eds. A. M. Finkelstein *et al.*), 229–230 (in Russian).

Eroshkin, G. I., Pashkevich, V. V. and Brzeziński, A., 2002, *Artificial satellites*, **37**, No.4, Warszawa, 169–183.

EARTH ORIENTATION PARAMETERS IN 1899–1992 BASED ON THE NEW EARTH ORIENTATION CATALOGUE

C. RON, J. VONDRÁK
Astronomical Institute, Academy of Sciences of the Czech Republic
Boční II 1401, 141 31 Praha 4, Czech Republic
e-mail: ron@ig.cas.cz, vondrak@ig.cas.cz

ABSTRACT. The Earth orientation parameters (EOP), based on optical astrometry observations of latitude and universal time variations and the Hipparcos Catalogue, covering 1899.7–1992.0, were determined in past years at Astronomical Institute in Prague, in close cooperation with the Czech Technical University in Prague, see Vondrák et al. (1998). During the solution it has been discovered that not all Hipparcos stars are suitable for a long-term study; many of them proved to have large errors in proper motions. Recently, the new Earth Orientation Catalogue (EOC) based on the recent star catalogues ARIHIP and TYCHO-2, and also Hipparcos and PPM catalogues, is being prepared by our group. We apply the provisional version of the catalogue to the optical astrometry observations (except for those of the method of equal altitudes) to test the new EOC. The differences of the EOP with respect to the EOP from the solution OA00 (Ron & Vondrák, 2001) are discussed.

1. INTRODUCTION

In the last decade we have used the observations by optical astrometry to derive the Earth Orientation Parameters (EOP) in the International Celestial Reference System (ICRS) which is realized by the reference frame of the Hipparcos Catalogue (ESA, 1997). The solution is described in Vondrák et al. (1998). The last solution denoted as OA00, available at the IERS Product Center as EOP(AICAS) 01 A 01, was described by Ron & Vondrák (2001). The analysis of the residuals proved the insufficient accuracy of some star positions based on the Hipparcos catalogue, caused by errors in proper motions. We corrected about 20% of individual observations by drifts derived from the observations themselves to overcome this imperfection.

Recently, new precise astrometrical catalogues related to ICRS have appeared. The catalogues as ARIHIP (Wielen et al. 2001) or TYCHO-2 (Høg et al., 2000) were derived as combination of the Hipparcos Catalogue (ESA, 1997) with the former ground-based catalogues. Because these catalogues showed to have more reliable proper motion of the stars, we decided to use them in the new determinations of the EOP. Wielen et al. (2001) introduced the star classification – the coefficient K_{ae} called *the astrometrical excellency* – in the scale $0-3$ (the higher the coefficient the better is the star from the astrometrical point of view). We have presented the idea of the new *Earth Orientation Catalogue* (EOC) in Vondrák & Ron (2003). The new catalogue combines the precise star positions of the recent astrometrical catalogues with the

long term series of the optical astrometry observations.

2. SOLUTION OF EOP FROM OPTICAL ASTROMETRY

The following parameters were derived in all preceding solutions:

- for each of the 5-day interval:
  - coordinates of the pole in terrestrial reference frame x, y,
  - universal time differences UT1–TAI (after 1956),
  - celestial pole offsets $\Delta\varepsilon, \Delta\psi \sin\varepsilon$,
- for each instrument:
  - constant, linear, annual and semi-annual deviation in latitude A, A_1, B, C, D, E,
  - constant, linear, annual and semi-annual deviation in universal time A', A'_1, B', C', D', E',
  - rheological parameter $\Lambda = 1 + k - l$ governing the tidal variations of the local vertical.

All observations were recalculated to be related to Hipparcos catalogue, and thus also to ICRS. Due to the relatively short mission of the satellite Hipparcos, the proper motions of the stars that are the components of binaries or multi-star systems were not derived with the sufficient accuracy. For that reason the observations of φ, UT0–UTC and δh had to be corrected. The corrections of individual stars (about 20% of the stars) were derived from the residuals of individual observations with respect to 5-day means of the instrument.

The observation equations lead to the system of normal equations that are singular with defect of matrix equal to 18. Therefore it is necessary to add 18 constraints tying together the parameters $A, \ldots, E'$ and fixing thus the terrestrial reference frame defined by the conventional coordinates of the individual instruments (see Tab. 3) and assuring that projection of seasonal residuals is minimized. The solution is described in details in Vondrák et al. (1998).

3. NEW EARTH ORIENTATION CATALOGUE

The first idea to set up the EOC has been presented by Vondrák & Ron (2003), and first version of the catalogue has been presented at the 25th IAU GA in Sydney (Vondrák & Ron, 2004).

3.1 *The version EOC-0*

In order to assure the most accurate positions and proper motions we searched for the stars first in the catalogue ARIHIP (Wielen et al., 2002) where we found 2995 stars, then in catalogue TYCHO-2 (Høg et al., 2000) with 1250 stars, in Hipparcos catalogue (ESA, 1997) with 146 stars and finally in the PPM catalogue (Roeser & Bastian, 1991, Bastian & Roeser, 1993) with 28 found stars. Only three stars were not found in any of the catalogues and their positions and proper motions were taken from the local catalogue of the instrument.

3.2 *The version EOC-1*

In the first approximation only the observations made in the local meridian (i.e., all observations except those of astrolabes and circumzenithals) were used to improve the catalogue EOC-0. First we derived the positions of the observed stars with respect to the astrometrically excellent stars as follows:

- all available observations of latitude and universal time were re-computed into the reference system of the catalogue EOC-0, using new IAU2000A model of precession-nutation (Mathews et al., 2002);

- the differences of latitude and/or universal time were computed from the mean values of the same night based on astrometrically excellent stars only;
- the differences for the same star at different epochs were subject to linear regression;
- the stars with significant deviations were checked for multiplicity (in the Hipparcos Catalogue), and in a positive case the displacement of the reference point (very often photocenter) from the catalogue entry estimated;
- the individual observations were recomputed with the modified catalogue EOC-0 and the residuals of individual observation with respect to the mean of night (using only the astrometrically excellent stars) were derived again.

Then the combination of the individual observations with original catalogue has been done to improve the positions and proper motions. The time series of observations of a star from all instruments were combined with three virtual observations, corresponding to the catalogue entry. These were chosen so that the weighted linear regression made through these three points returns exactly the same values t_0, σ_0 and σ_μ as given in the input catalogue. If the central epoch is identified with the one of the input catalogue $t_2 = t_0$, $t_1 = t_0 - 90$y and $t_3 = t_0 + 10$y this approach leads to standard deviations of virtual observations at three epochs

$$\sigma_1^2 = 9000\sigma_\mu^2, \qquad \sigma_2^2 = \frac{\sigma_0^2}{1 - (\sigma_0/\sigma_\mu)^2/900}, \qquad \sigma_3^2 = 1000\sigma_\mu^2. \tag{1}$$

The values of σ_i in mas were used to compute the weights of the three virtual observations (each of these 'observed' values being set to zero) as $p_i = (200/\sigma_i)^2$. The weights of all 'real' observations of the same star are all equal to 1, under the assumption that their accuracy is 200mas.

In the preliminary version EOC-1 we used the observations made in local meridian, i.e., all observations except those by the method of equal altitude. The total number of stars observed by these instruments is 3784. The result of the combination of the catalogue EOC-0 with these observations forms the new preliminary version of the catalogue EOC-1.

Medians of standard deviations in positions (mas) and proper motions (mas/y) are shown in Tab. 1 (star denotes the value multiplied by $15\cos\varphi$), separately for the stars that were observed by Hipparcos (HIP) and that were not (not HIP). The third row (other comp.) gives the values for the stars whose reference point is different from the Hipparcos entry.

Table 1: The statistics of the catalogue EOC-1.

Type	n	$\sigma_\alpha^\star$	$\sigma_{\mu\alpha}^\star$	σ_δ	$\sigma_{\mu\delta}$
HIP	3643	0.67	0.51	0.50	0.31
Not HIP	85	8.00	1.40	7.10	1.01
Other comp.	56	7.50	0.90	4.00	0.90

The improvement of EOC-1 with respect to the EOC-0 is demonstrated in Tab. 2, where global characteristics of both catalogues are compared. Median values are displayed again.

4. NEW SOLUTION OF EOP IN THE REFERENCE SYSTEM OF EOC

The new solution of EOP (called OA03) is referred to the preliminary version EOC-1. Because the final version of EOC is not yet prepared, we did not use the observations made by the method of equal altitude (astrolabes and circumzenithals). All observations were re-computed using the

Table 2: The comparison of the catalogues EOC-0 and EOC-1.

Catalogue	n	Ep_α	$\sigma^\star_\alpha$	$\sigma^\star_{\mu\alpha}$	Ep_δ	σ_δ	$\sigma_{\mu\delta}$
EOC-0	4422	1991.25	0.69	0.60	1991.26	0.55	0.57
EOC-1	3784	1991.18	0.68	0.52	1991.10	0.50	0.32

new precession-nutation model IAU2000A (Mathews et al., 2002). The celestial pole offsets with respect to the new model are less than 0.2mas and they are undetectable by the optical astrometry. For that reason we abandoned the determination of the celestial pole offsets in 5-day intervals. The observation equations become simpler and the number of determined unknown parameters decreases significantly. For 5-day intervals we determine only three unknowns (x, y, UT1–TAI) and before 1956 only two (x and y) because the atomic time TAI was not defined yet. The smaller rank of the diagonal matrices for the 5-day intervals led to smaller condition numbers and so to the bigger number of the determined 5-day intervals because it was not necessary to connect so many intervals to assure the diagonal blocks of the normal equations to be positive definite, see Vondrák et al. (1998).

We used the observations of the observatories listed in Tab 3. where the coordinates defining the terrestrial system and the secular drifts of the stations caused by the movements of the lithospheric plates derived from the model NUVEL-1 NNR (DeMets et al., 1994) are shown.

The derived values of the terrestrial coordinates of the pole in the interval 1899.7–1992.0 and the excess of the length of day in the interval 1956.0–1992.0 including their standard deviations in 5-day intervals are shown in Fig. 1.

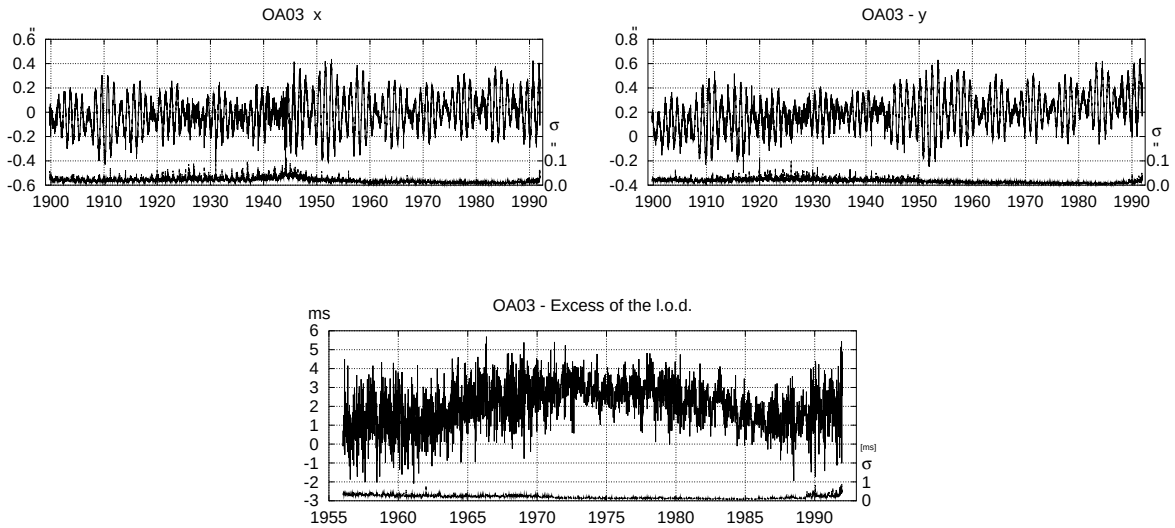

Figure 1: Polar motion at 5-day intervals and excess of the l.o.d. over the nominal value 86400s and their standard errors. The short-periodic tidal variations in l.o.d. ($P < 35$ days) are removed.

Table 3: The coordinates φ_0 and λ_0 of the instruments used in the solution OA03, referred to the mean epoch MJD_0 32000 for the latitude and 43000 for the time observations; $\dot{\varphi}$ and $\dot{\lambda}$ are the secular drifts of the stations, v are the weights used in the solution.

Code	latitude φ_0 ° ' "	$\dot{\varphi}$ ["/cy]	longitude λ_0 ° ' "	dλ [s]	$\dot{\lambda}$ [s/cy]	weights v_φ	v_T
Visual zenith telescopes							
CA	39 08 09.148	+0.061	8 18 44.0			1.19	
CI	39 08 19.427	+0.002	−84 25 00.0			1.04	
GT	39 08 13.289	+0.012	−77 11 57.0			0.85	
KZ	39 08 02.076	+0.001	66 52 51.0			0.72	
MZZ,MZL	39 08 03.709	−0.045	141 07 51.0			0.89	
TS	39 08 10.973	+0.004	63 29 00.0			0.86	
	39 08 11.337	+0.004	63 29 00.0			MJD>18512	
UK	39 08 12.157	+0.025	−123 12 35.0			0.89	
BLZ	44 48 10.444	+0.041	20 30 50.0			0.87	
BK	50 19 09.553	−0.048	127 30 00.0			1.54	
IRZ	52 16 44.313	−0.033	104 20 42.7			0.82	
POL	49 36 13.049	+0.031	34 32 52.0			0.84	
PU	59 46 15.622	+0.034	30 19 39.0			1.02	
PUZ	59 46 15.628	+0.034	30 19 39.0			0.98	
TT	60 24 57.496	+0.040	22 27 00.0			1.95	
VJZ	52 05 56.207	+0.041	21 00 00.0			0.66	
Photoelectric transit instruments							
IRF	52 16 44.0		104 20 42.0	−0.0061	+0.0084		0.85
KHF	50 00 00.0		36 13 58.0	+0.0039	+0.0083		0.85
NK	46 58 18.0		31 58 28.0	+0.0086	+0.0078		0.95
PUF,PUG	59 46 18.0		30 19 38.0	+0.0009	+0.0096		1.24
PUH							
WHF	30 32 28.9		114 20 41.4	+0.0176	+0.0060		0.76
Photographic zenith tubes							
MZP,MZQ	39 08 02.736	−0.045	141 07 52.0	−0.0032	−0.0005	0.72	0.74
OJP	49 54 55.145	+0.044	14 47 09.0	+0.0107	+0.0072	1.20	1.28
PIP	−35 20 40.563	+0.036	−57 17 09.0	+0.0373	−0.0005	1.82	1.79
RCP,RCQ	25 36 47.098	+0.008	−80 22 56.0	+0.0026	−0.0027	1.17	1.05
WA	38 55 17.263	+0.012	−77 03 56.0			1.28	
W,WGQ	38 55 17.308	+0.012	−77 03 56.0	+0.0018	−0.0044	0.97	0.85
MS	−35 19 17.486	+0.182	149 00 19.0	+0.0316	+0.0049	1.00	0.86

Table 4: The comparison of statistics of the solutions OA00 and OA03.

	OA00	OA03
number of observations	4447400	3262496
number of unknowns	29809	16285
number of 5-day intervals	6693	6715
number of instruments	41	27
standard deviation σ_0	$\pm 0.188''$	$\pm 0.177''$
mean square difference wrt IERS C04 (1962-1992)	$\pm 0.047''$	$\pm 0.050''$

5. CONCLUSIONS

The new catalogue shows significant improvement with respect to all of the catalogues used so far in the derivation of the Earth orientation parameters. The improvement can be seen both in version EOC-0 (that only takes over the best from the current catalogues) and EOC-1 (where the catalogue EOC-0 is combined with observations of the 33 instruments observing in the local meridian). The best improvement is achieved in proper motions in declination, thanks to a long history of latitude observations. The final solution of EOC is under preparation.

In the new solution of the Earth orientation parameters OA03 only the observations with the instruments working in the local meridian (VZT, PTI, PZT) were used, in the reference system of the catalogue EOC-1. In contrast to the solution OA00 the new model of precession-nutation was used, and therefore we abandoned the determination of the celestial pole offsets. The results of the solution OA03 even with the less number of used observations (73%) with respect to OA00 are comparable with this solution.

Acknowledgements. This project is supported by the grant No. A3003205 awarded by the Grant Agency of the Academy of Sciences of the Czech Republic.

6. REFERENCES

Bastian U., Roeser S., 1993, Positions and Proper Motions – South, *Astron. Rechen-Inst.* Heidelberg.

DeMets C., Gordon R. G., Argus D. F., Stein S., 1994, Effect of recent revisions to the geomagnetic reversal time scale on estimates of current plate motions, *Geophys. Res. Let.*, **21**, 2191–2194.

ESA, 1997, The Hipparcos and Tycho Catalogues, *ESA SP-1200.*

Høg E., Fabricius C., Makarov V. V., et al., 2000, The Tycho-2 Catalogue of the 2.5 million brightest stars, *Astron. Astrophys.*, **355**, L27–L30.

Mathews P. M., Herring T. A., Buffet B. A., 2002, Modelling of nutation–precession: New nutation series for nonrigid Earth, and insights into Earth's interior, **107**, (B4), 10.1029/2001JB00390.

Roeser S., Bastian U., 1991, Positions and Proper Motions – North, *Astron. Rechen-Inst.*, Heidelberg.

Ron C., Vondrák J., 2001, On the celestial pole offsets from optical astrometry in 1899–1992, In: N. Capitaine (ed.) *Proc. Journées 2000 Systèmes de référence spatio-temporels*, Paris, 201–202.

Vondrák J., Pešek I., Ron C., Čepek A., 1998, Earth orientation parameters 1899.7–1992.0 in the ICRS based on the Hipparcos reference frame, *Publ. Astron. Inst. Acad. Sci. Czech R.*, **87**, 56 pp.

Vondrák J., Ron C., 2003, An improved optical reference frame for long-term Earth rotation studies, In: N. Capitaine & M. Stavinschi (eds.) *Proc. Journées 2002 Systèmes de référence spatio-temporels*, Bucharest, 49–55.

Vondrák J., Ron C., 2004, Earth Orientation Catalogue – An improved reference frame, In: R. Gaume, D. McCarthy & J. Souchay (eds.) *IAU XXV, Joint Discussion 16: The ICRS Maintenance and Future Realizations*, in print.

Wielen R., Schwan H., Detbarn C., et al., 2001, Astrometric Catalogue ARIHIP containing stellar data selected from the combination catalogues FK6, GC+HIP, TYC2+HIP and from the Hipparcos Catalogue, *Veröff. Astron. Rechen-Inst. Heidelberg*, No. 40, Kommissions-Verlag G. Braun, Karlsruhe.

IMPACT OF THE ADDITION OF THE OCEAN TO THE ATMOSPHERIC EXCITATION OF POLAR MOTION ON VARIABILITY OF SPECTRA AND CORRELATION WITH POLAR MOTION

B. KOLACZEK, J. NASTULA
Space Research Centre of the Polish Academy of Sciences
Bartycka 18a, 00-716 Warsaw, Poland
e-mail: kolaczek@cbk.waw.pl

ABSTRACT. Impact of the addition of the ocean to the atmospheric excitation of polar motion on variability of spectra of polar motion and correlation with polar motion is investigated. Variations of the seasonal and subseasonal spectra of the atmospheric and joint atmospheric plus oceanic excitation functions of polar motion and their time variations are computed by the Fourier Transform Function and compared. These spectra are very similar. Correlations between geodetic and either atmospheric or joint atmospheric plus oceanic excitation functions are computed in four spectra bands range from 10 to 500 days. In all cases correlation coefficients for joint atmospheric plus oceanic excitation functions are higher and more stable than for atmospheric excitation function.

1. INTRODUCTION

Atmosphere and ocean have been shown to excite variations in polar motion at intraseasonal, seasonal and interannual periods (Brzeziëski, 2003;Gross et al, 2003; Nastula and Ponte, 1999; Ponte at al., 1998; Ponte and Ali, 2002). Adding oceanic angular momentum (OAM) to atmospheric angular momentum (AAM) increases a correlation coefficient with the observed by geodetic techniques excitation of polar motion, but there is still significant discrepancy between modeled excitation and the observed. Here emphasis is placed on the aspect of time variability of spectra and correlation coefficient. We are interested in results of adding the OAM to AAM on spectra and correlation coefficient with the observed data.

2. DATA

In the analyses we use the following series of data:

-Geodetic polar motion, IERS CO4 (IERS 2001) with the sampling interval 1 day and the data span: 1982.0 - 2002.0,

-Geodetic polar motion, combined solution COMB2002 of Gross (2003), with the sampling interval 12 hours and the data span: 1962 to 2003,

- Reanalyses Atmospheric Angular Momentum (AAM,) with the sampling interval 6 hours and the data span: 1948 to 2003 (Kalnay et al., 1996),

- Ocean Angular Momentum MIT model -P98 (Ponte et al., 1998) with the sampling interval 5 days and data spam 1985.0-1996.3,

- Ocean Angular Momentum ECCO JPL model - GO3 (Gross et al., 2003) with the sampling interval 1 day and the data spam 1980.0-2000.2.

3. ANALYSES

We analyse influences of Ocean Angular Momentum - OAM on the spectra of polar motion and their time variations. Correlations between geodetic polar motion excitation function computed from polar motion with polar motion excitation functions of different OAM models and AAM as well were studied also.

3.1 SPECTRA

Spectra of geodetic, atmospheric and join atmosperic+oceanic excitation functions of polar motion were computed by the Fourier Transform function. In this case the IERS C04 pole coordinates were used to compute the geodetic excitation function. All three spectra seen in Figure 1 have the same character. In all these spectra there are the oscillations with periods of about 40, 50, 60, 120, 180 days. These oscillations in the spectra of combined series of AAM+OAM are the most energetic ones. It means that the AAM and OAM variations play in concert in this part of spectra.

The time variable spectra of the AAM and AAM+OAM excitation functions of polar motion were computed by the Fourier Transform Band Pass Filter - FTBPF (Kosek, 1995) in three spectra ranges 20-90, 90-230, 230-500 days (Fig. 2). For these computations P98 OAM Model was used. Time variations of the most energetic oscillations with periods of 360, 180, 120, 60, 40 days are similar in both cases. 5-6 years oscillations of amplitudes of these oscillations is seen. The short period oscillations with periods of 40 and 60 days seem to be a little stronger in the case of the OAM+AAM excitation functions than in the case of the AAM excitation function alone.

3.2 CORRELATIONS

In order to check impact of OAM excitation function of polar motion on variations of polar motion correlations between the geodetic excitation functions of polar motion and AAM as well as AAM+OAM excitation functions were computed for two different models of OAM, P98 and GO3. In this case the COMB2002 pole coordinates data are used. Computed correlations in 4 different spectra ranges are shown in Fig. 3 and Table 1.

Table 1: Correlation between time series of geodetic excitation and either atmospheric of joint atmospheric and oceanic excitation. Complex correlation is expressed by its magnitude. Spectral range 10 - 90 days.

Series	Correlation		
	χ_1	χ_2	$\chi_1 + i\chi_2$
Period,	1988.0 $\longrightarrow$ 1996.3		
P98+AAM	0.73	0.80	0.78
G03+AAM	0.78	0.86	0.84
AAM	0.55	0.71	0.67

Correlations between geodetic and AAM+OAM excitation functions are very high and in

the case of the annual and semiannual range of spectra correlations coefficients are higher than in the case of GEOD/AAM. For period ranges 150-90, 90-10 days correlation coefficients are slightly lower from previous ones and more variable. Their variability is not so strong as in the case of AAM alone.

It is known from previous studies (Kolaczek et al., 2003) that the correlations between geodetic and AAM excitation functions are disturbed by El Niño/ La Niño phenomena. One can notice that the correlation between AAM+OAM and geodetic excitation functions of polar motion is not so sensitive on El Niño/ La Niña impacts.

4. CONCLUSIONS

Analyses show the similarity of the spectra of seasonal and subseasonal variations of polar motion excitation functions of AAM and combined AAM plus OAM.

There are high correlations between geodetic and combined atmospheric plus oceanic excitation functions of polar motion in period ranges from 10 - 500 days. The coefficients of the correlation between geodetic and combined atmospheric plus geodetic excitation functions are always higher and more stable then in the case of correlation between atmospheric and geodetic excitation functions.

Acknowledgments. This work has been partly supported by the Polish National Commitee for Scientific Research (KBN), the grant No. 5 T12E 039 24.

5. REFERENCES

Brzezinski, A., 2003, Oceanic excitation of polar motion and nutation: an overview. In: *IERS Technical Note No. 30*, B. Richter. (ed.), Verlag des Bundesamts für Kartographie und Geodäsie, 144–149.

Gross R. S., Fukumori, I., and Menemenlis, D., 2003, Atmospheric and oceanic excitation of the Eath's wobble during 1980-2000, *J. Geophys. Res.*, 108(B8), in press.

IERS, Annual Report, 2001, Verlag des Bundesamts für Kartographie und Geodäsie, Frankfurt am Main 2002.

Kalnay, E., 1996, The NCEP/NCAR 40-year Reanalysis Project, *Bull. Amer. Meteor. Soc.*, 77, 437–471.

Kolaczek, B., Nastula, J., and Salstein, D., 2003, El Nino-related variations in atmopshere-polar motion interactions, *J. Geodynamics*, Special Issue Earth Rotation and Episodic Processes, **36**, No 3, 397–406.

Kosek, W., 1995, Time Variable Band Pass Filter Spectrum of real and complex-valued polar motion series, *Artificial Satellites. Planetary Geodesy*, **30**, 1, 27–43.

Nastula, J., and Ponte, R. M., 1999, Further evidence of oceanic excitation of polar motion, *Geophys. J. Int.*, **139**, 123–130.

Ponte, R. M., and Stammer, D., 1999, Role of ocean currents and bottom pressure variability on seasonal polar motion, *J. Geophys. Res.*, **104**, 23, 393–409.

Ponte, R. M., Stammer, D., and Marshall, J., 1998, Oceanic signals in observed motions of Earth's pole of rotation, *Nature*, **391**, 476–479.

Rogers, J. C., 1984, The association between the North Atlantic Oscillation and the Southern Oscillation in the Northern Hemisphere, *Mon. Weather Rev.*, **112**, 1999–2014.

Ponte, R. M., and Ali, A. H., 2002, Rapid ocean signals in polar motion and length of day, *Geophys. Res. Lett.*, **29**, 10.10129/2202GL015312.

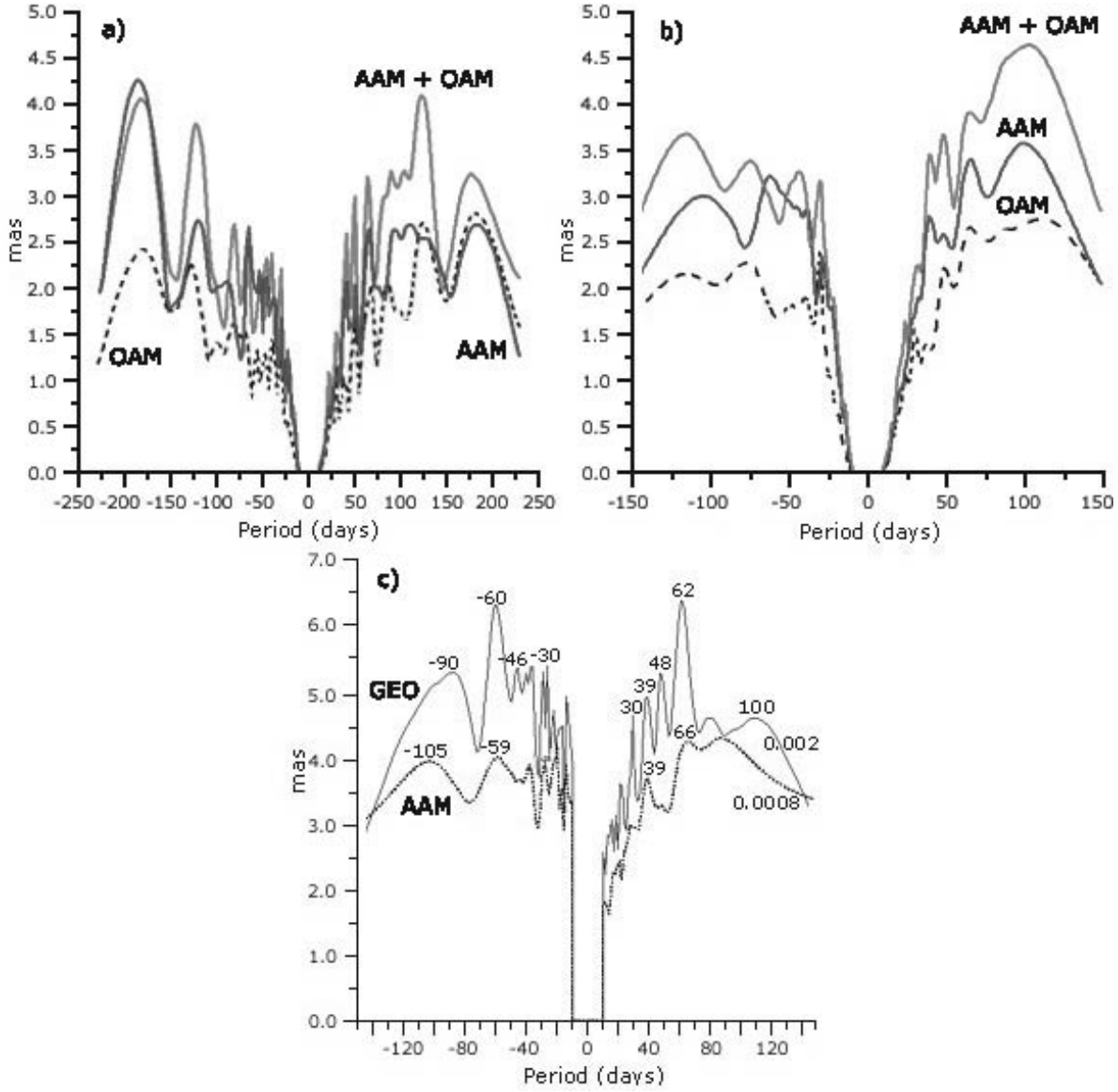

Figure 1: Spectra of the atmospheric (AAM), oceanic (OAM), and atmospheric plus oceanic (AAM + OAM) excitation functions computed by FTBPF with (a) the parameter $\lambda = 0.006$ (b) the parameter $\lambda = 0.015$. (c) The FTBPF amplitude spectrum of the geodetic excitation functions (GEO) pole coordinates and AAM excitation function computed with the parameters $\lambda = 0.002$, and $\lambda = 0.0008$, respectively.

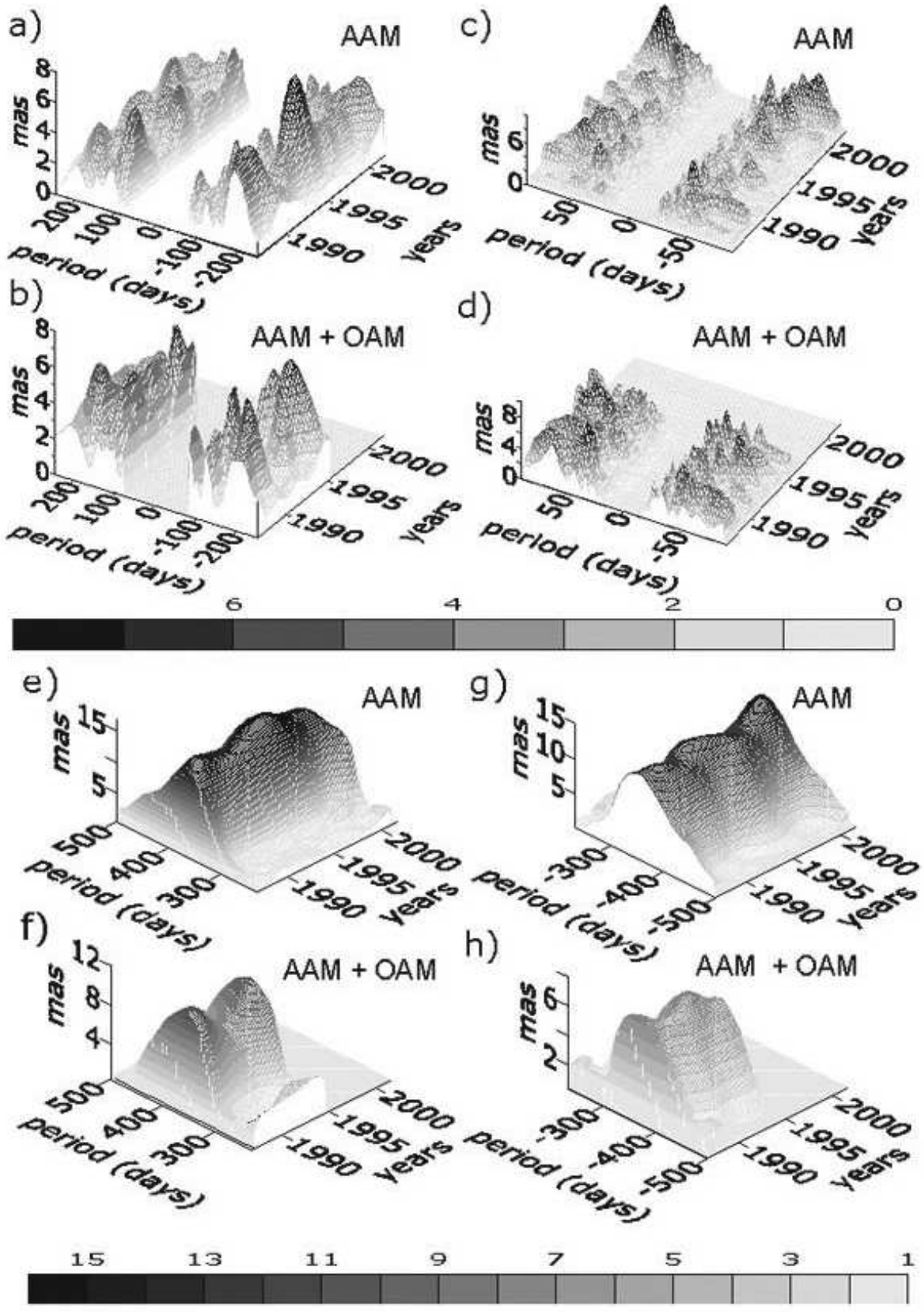

Figure 2: Time variable spectra of the AAM (a),(c),(e),(g) and of the AAM + OAM (b),(d),(f),(h)computed by the FTBPF with; (a)-(d) $\lambda = 0.006$; (e)-(h) $\lambda = 0.003$, in the three spectra bands with period renges: 10–90, 90–230 and 230–500 days.

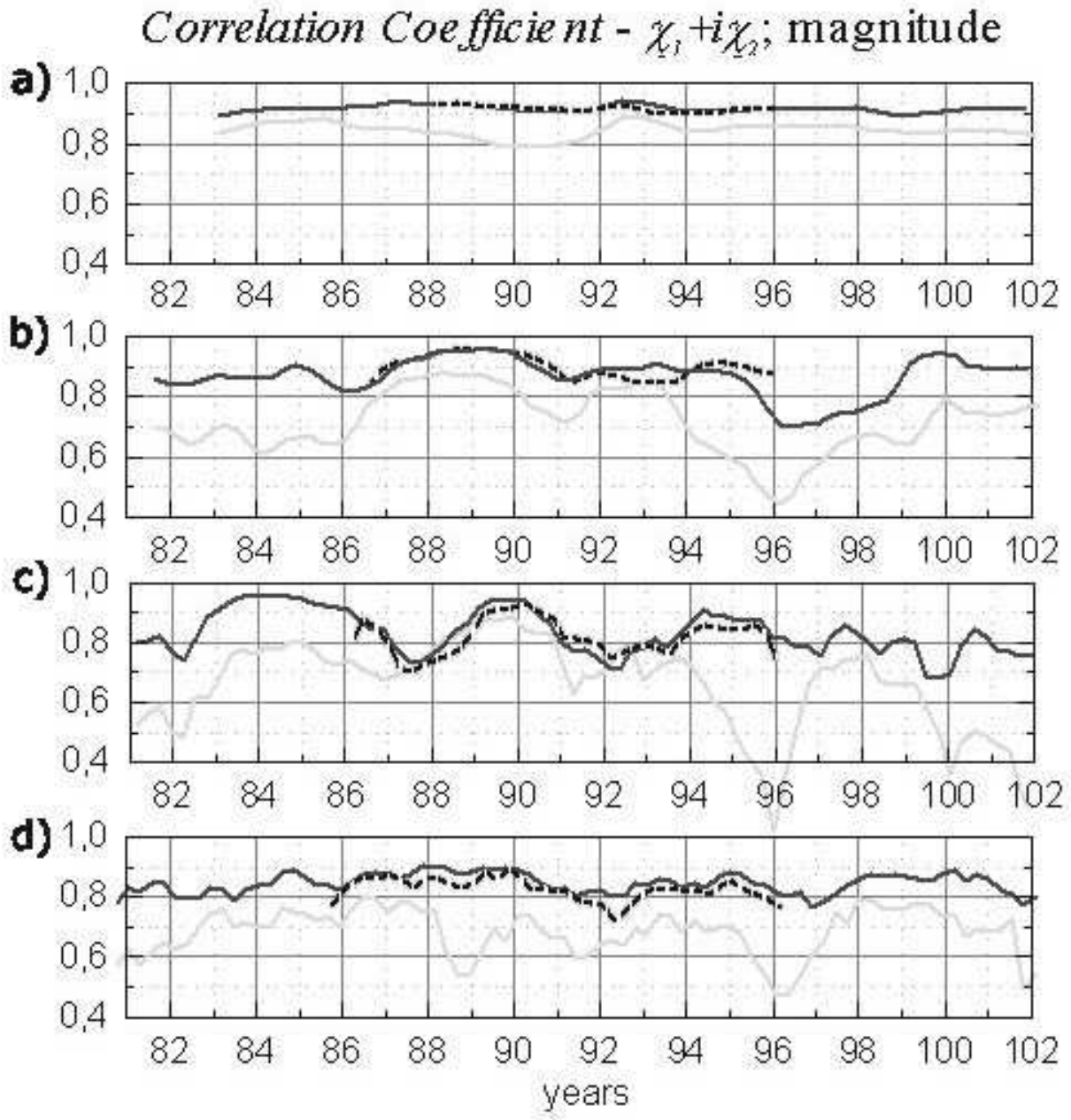

Figure 3: Correlation coefficients between the complex — valued equatorial components of geodetic (GEO) and either atmospheric or joint atmospheric and oceanic excitation functions for polar motion filtered by the Butterworth filter (a) 450-230 days, (b) 230-150 days, (c) 150–90 days, (d) 90–10 days intervals, starting each 100 days of a year since 1962, computed over (a) 2190 days, (b) 1095 days, (c) 730 days, (d) 540 days. Comparison is shown for the OAM P98 (dotted line), OAM G03 (black line), AAM (gray line)

INTERACTIVE EARTH ROTATION THROUGH THE WEB

CH. BIZOUARD
SYRTE/UMR8630-CNRS
Observatoire de Paris, 61 avenue de l'Observatoire, 75014 Paris, France
e-mail: christian.bizouard@obspm.fr

ABSTRACT. On the WEB site of the Earth Orientation Center (http://hpiers.obspm.fr/eop-pc) we propose a panel of interactive tools devoted to the study of the Earth rotation : selection and plots of the Earth Orientation Parameters (EOP), numerical analysis of these parameters, real time Earth rotation matrix, comparison of EOP series, and analysis of the geophysical excitation in the Earth rotation fluctuations.

1. INTRODUCTION

One task of the Earth Orientation Center located at the Paris Observatory is to archive various set of Earth Orientation Parameters obtained thourough the world, to validate them, and then to provide by combination a reference series (C04). Whereas pure numbers can satisfy engineer only interested in getting the matrix from the ground to the frame where the satellite orbits are computed, physicist or astronomer need graphical representation and numerical analysis for investigating the astronomical or physical process underlying the Earth rotation variability. For the user it is quite a waste of time to extract time series from the WEB, and then to process them by his own numerical and graphical means. Actually, such tools have been set up on the web site of the Earth Orientation Center, http://hpiers.obspm.fr/eop-pc, thank to the dynamical language PHP and Apache Server. Following sections are devoted to the description and potentiality of these tools.

2. DRAWING OF THE EOP

Our first endeavour has been focused on the selection and the graphical representation of the EOP, first of all, the reference combined series C04. Presently it is possible to draw any time series : combined, operational, long term EOP time series, between two selected dates, with choice of the format of the date (civil date / modified julian date / besselian year). The considered cases are the following :

- polar motion x time series
- polar motion y time series
- polhody (x,-y)
- UT1 - UTC

- UT1 - TAI
- Excess of the lenght of day (LOD)
- Earth rotation rate (only for reference combined series C04)
- Nutation offset in longitude $d\psi$ time series, with respect to IAU 1980 nutation model
- Nutation offset in longitude $d\varepsilon$ time series, with respect to IAU 1980 nutation model
- Nutation offsets $(d\psi \sin \varepsilon_0, d\varepsilon)$ in the mean equatorial plane
- Nutation offset dX time series, with respect to IAU 2000 nutation model
- Nutation offset dY time series, with respect to IAU 2000 nutation model
- Nutation offsets (dX, dY) in the mean equatorial plane

These EOP parameters can also be printed on the WEB browser rather than drawed. An useful option allows the user to remove from the length of day the well modeled contribution of the zonal lunisolar tides.

3. COMPARISON OF EOP SERIES

One important task of our service is to provide comparison of the operational EOP series with respect to the combined series C04 (standard deviation, bias). Now this comparison has been extended to any kind of series, long term or operational, and time interval for the comparison can be chosen. The differences between series can be either plotted or submitted to FFT or least square fit of any harmonic component and polynomial trend.

4. NUMERICAL ANALYSIS OF THE EOP

Numerical analysis of the EOP is presently available through the WEB. It is restricted to long term series (at least 3 years of data), including the combined C04 series. The proposed tools are the following : data selection, data plotting, spectral analysis, periodogram, least squares fit of any harmonic component and plynomial, Vondrak filtering, Singular Spectral Analysis. The implementation of these tools is based upon an interface toward FORTRAN and C executables, especially the C library MIMOSA developped by S. Lambert.

5. ROTATION MATRIX

For practical purposes or tests we provide the rotation matrix from the terrestrial frame to the celestial frame including a prediction of 6 months. Such tool is of primary interest for geodesy or orbitography. We provide also derived parameters, especially the component of the instantaneous rotation vector within the crust or the celestial reference frame. It is possible possible to set independently polar motion, UT1-UTC and nutation offsets to zero, as well to include diurnal and semidiurnal effect associated the oceanic tides.

6. EXCITATION OF THE EARTH ROTATION

Among all the users, geophysicist will have particular interest in the interactive comparison the atmospheric angular momentum to the total excitation found in polar motion, length-of-day

and nutation. The time interval can be selected, but also the Chandler frequency, the Free Core Nutation frequency, and their respective quality factors, which are critical parameters for computing the equatorial excitation functions.

7. CONCLUSION

To our knowledge interactive tools on WEB for studying the Earth rotation were not available. By a few "clicks" they provide a clear and flexible representation of the phenomena involved in the Earth rotation, as well as fast numerical analysis and intercomparison of the involved time series. This is also a easy way to watch at the last fluctuations of the Earth rotation, and to detect possible episodic effects. We hope to design far more sophisticated tools in the near future.

Aknowledgements : our thanks to J. B. Nguyen, who has set up Appache Server, T. Carlucci for his advises in PHP programming, and S. Lambert for making available the library MIMOSA.

8. REFERENCES

http://hpiers.obspm.fr/eop-pc
http://php.net

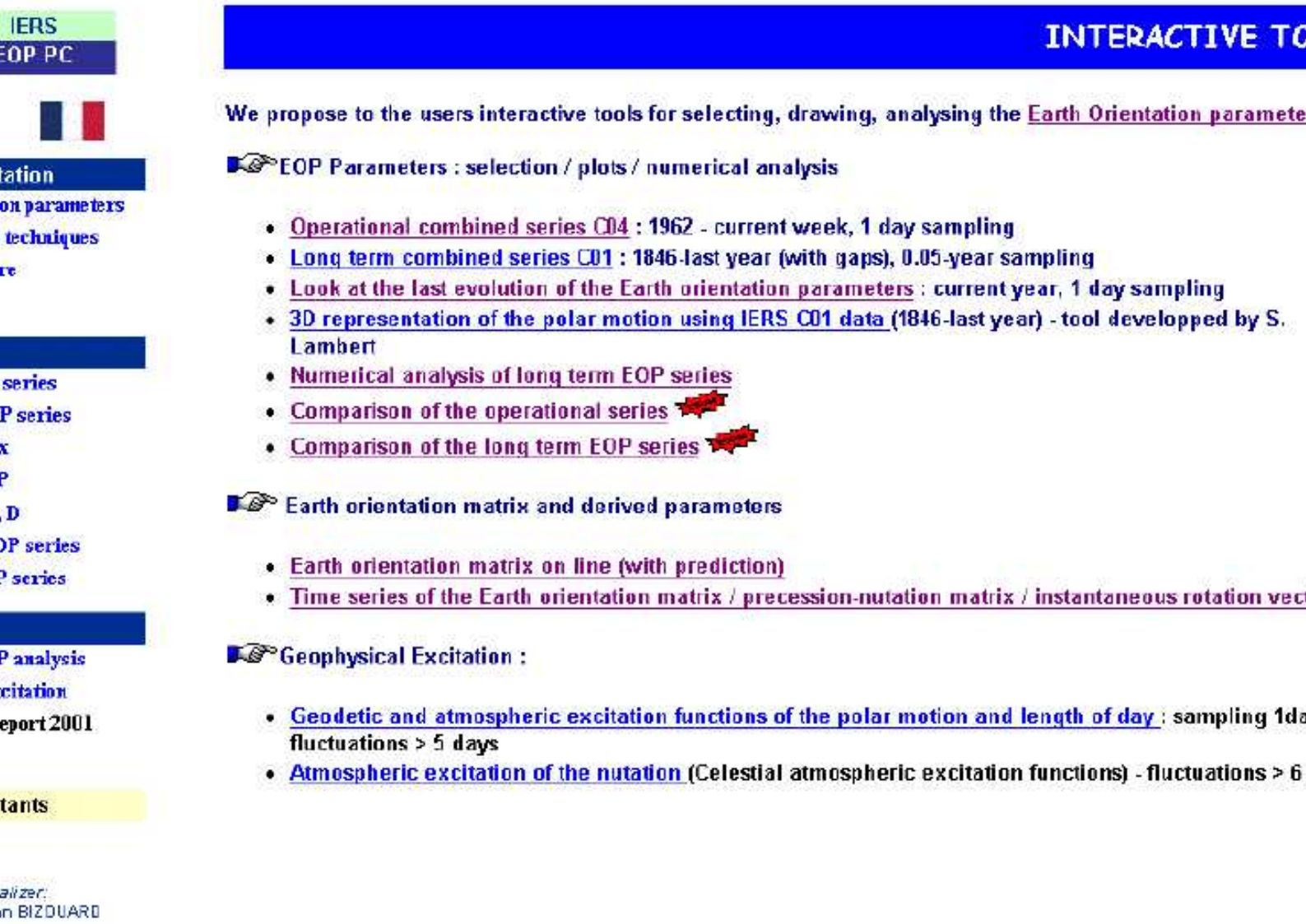

Figure 1: http://hpiers.obspm.fr/eop-pc: Interactive tools.

NEAR REAL-TIME IERS PRODUCTS

W.H. WOODEN, T.J. JOHNSON, M.S. CARTER, A.E. MYERS
U.S. Naval Observatory
Washington, DC 20392, U.S.A.
e-mail: whw@usno.navy.mil

ABSTRACT. Earth orientation parameters (EOP), which relate the terrestrial reference system to the celestial reference system, are critical to modern navigation and space applications. The Rapid Service/Prediction Center (RS/PC) of the International Earth Rotation and Reference Systems Service (IERS) produces EOP for those users who reduce data collected in the very recent past (require rapid service) or who operate in real time (require predictions). The IERS Bulletin A and its associated data files constitute the near real-time IERS products which meet these users' needs. This paper discusses the RS/PC's current combination and prediction process, recent improvements to the process, accuracy of the current solutions, and planned improvements.

1. INTRODUCTION

Accurate knowledge of Earth orientation parameters (EOP) is needed for a variety of high-precision applications including modern navigation, astronomy, geodesy, communications, and timekeeping. The EOP provide the time-varying alignment of the Earth's terrestrial reference frame with respect to the celestial reference frame. The U.S. Naval Observatory (USNO) operates the Rapid Service/Prediction Center (RS/PC) for the International Earth Rotation and Reference Systems Service (IERS). The RS/PC produces the IERS Bulletin A on a rapid turnaround basis, primarily for real-time users and others needing the highest quality EOP information before the IERS final (Bulletin B) values are available. Bulletin A and its associated standard and the daily rapid EOP data files constitute the near real-time IERS products. Bulletin A includes polar motion (x,y), universal time (UT1-UTC), and the celestial pole offsets ($\delta\psi, \delta\varepsilon$ and dx, dy) and predictions of these parameters. Two versions of Bulletin A are prepared, a daily and a weekly. Long-term stability and consistency with the other IERS products is achieved by aligning Bulletin A with the IERS final (Bulletin B) series, which is produced by the IERS Earth Orientation Center at the Paris Observatory in France.

The observational estimates of EOP from the IERS Technique Centers, especially their rapid and preliminary series, are key contributions to the Bulletin A. USNO's ability to function as the RS/PC is enhanced by its active involvement in the Technique Centers. As an Associate Analysis Center of the International GPS Service, USNO has the opportunity to examine ways to improve the contribution of GPS observations to EOP. As an Operations Center, Correlator, and supporter of observing stations within the International VLBI Service, USNO is intimately involved in all aspects of the collection of VLBI observations and understanding their impact on EOP.

In an effort to improve the accuracy of near real-time EOP, the RS/PC has continued to modify its combination and prediction procedures. This paper highlights recent changes since the summary of the process given by Luzum et al. (2001).

2. COMBINATION AND PREDICTION PROCESS

The combination and prediction process contains five major steps: data preparation, combination, prediction, product generation, and dissemination. To a great extent this process has been automated. The contributed observations used in the preparation of the Bulletin A are available at ftp://maia.usno.navy.mil/bulla-data.html. The contributed analysis results are based on data from Very Long Baseline Interferometry (VLBI), Satellite Laser Ranging (SLR), the Global Positioning System (GPS) satellites, Lunar Laser Ranging (LLR), and meteorological predictions of variations in Atmospheric Angular Momentum (AAM).

The data preparation consists of retrieving each of the data types (either automatically or manually), preprocessing the data (e.g., doing unit conversions, reformatting, etc.), and applying the biases and rates for each data type. Each of the data types are processed in turn: VLBI data (24-hr and Intensive sessions), GPS data (EOP and UTGPS), SLR data, and AAM data.

The combination program calculates polar motion (x, y), UT1-UTC, length of day (LOD), and nutation offsets ($\delta\psi, \delta\varepsilon$). For polar motion, UT1-UTC, and LOD, known signals are removed (e.g., zonal solid Earth tides), the data are sorted by time and a cubic-spline fit to the data is determined, the fit is used to determine the daily solution, data for the fit and residual plots are written to files, the known signals are added back into the daily solution, and the final data file is updated. For the nutation offsets, VLBI 24-hour session data are read in, weights applied, the 1980 nutation theory is subtracted from the observations, the data are sorted by date and a cubic fit is determined, the fit is used to determine daily solution, data for fit and residual plots are written to files, and $\delta\psi$ and $\delta\varepsilon$ offsets are written to the final data file.

For polar motion $\sim$400 days' worth of data are used in the prediction routine. The prediction is based on an extrapolation of an annual and semiannual ellipse and a Chandler circle fit to the last 400 days of x and y data and the rate of the last observed polar motion observation. For UT1-UTC $\sim$365 days' worth of data are used. The auto-regressive integrated moving average (ARIMA) is used. For the nutation offsets, the predictions of $\delta\psi$ and $\delta\varepsilon$ are based solely on VLBI data. If no new data are available, a new prediction of these nutation angles cannot be determined. Therefore, the length of the prediction into the future for $\delta\psi$ and $\delta\varepsilon$ can and does vary in the daily solution files.

Additional details on the processing and prediction techniques are given by Wooden and Johnson (2003).

3. IMPROVEMENTS TO THE PROCESS

The most recent improvements to the process include the enhanced GPS UT1-like quantity that improves UT1-UTC combination results at solution epoch, the introduction of AAM UT1-like quantity that improves UT1-UTC prediction, the addition of USNO and IVS-combination data to VLBI data sets, the automated VLBI data retrieval and updating, the automated weekly SLR data retrieval and updating, and the compliance with IAU 2000 resolutions with respect to the production of new nutation series, dX and dY. The analysis of GPS orbit planes performed at USNO to produce a UT1-like quantity, UTGPS, is described by Kammeyer (2000). The introduction of the AAM UT1-like quantity that improves UT1-UTC prediction is given by Johnson et al. (2003). A careful evaluation of the USNO and IVS Combination 24-hour VLBI data sets clearly indicated that the robustness of the solution, especially for the nutation angles, would be significantly improved. As a consequence, these data sets were introduced into the combination solution in January 2003. The data processing software was modified in February

Figure 1. Differences Between Bulletin A Daily Solutions and the Earth Orientation Parameters available in Bulletin B and C04

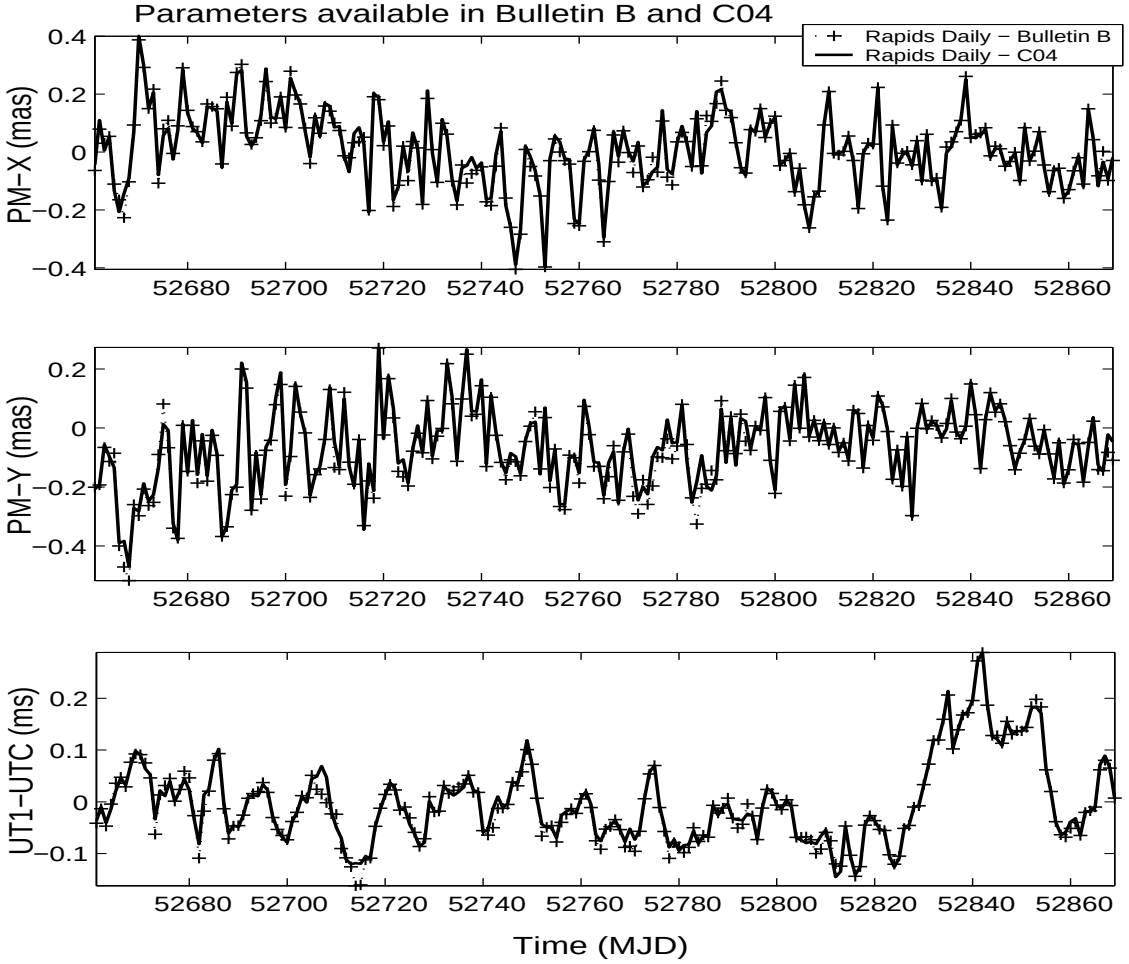

2003 to enable the editing of all data types used in the polar motion and UT1 combination solutions, including the nutation software. In July 2003 the processing software was modified to do automated SLR data retrieval and updating. Near the end of 2002, USNO prepared for the implementation of the IAU 2000 resolutions by creating a dX and dY series with respect to the IAU 2000A Precession/Nutation theory. Additional files that contain the dX and dY series were created and implemented in Bulletin A as of 1 January 2003.

4. ACCURACY

The accuracy of the near real-time IERS products is assessed by comparing the daily Bulletin A to the IERS C04 and the Bulletin B series. Figure 1 shows these comparisons from the beginning of 2003. The agreement for the x and y components of polar motion is relatively good. The large difference in UT1-UTC is a result of the lack of VLBI data due to problems with the observing network in late-June and July. The figure highlights the criticality of VLBI observations for UT1-UTC determination. If current prediction accuracies are to be maintained, VLBI observations must be retained as part of the EOP determination and prediction process.

Table 1 gives the statistics of the differences between the Bulletin A solution and the Bulletin B and C04 solutions for 2002 and 2003. For 2003 the UT1-UTC numbers in parentheses are the differences when the extended period without VLBI data is excluded. Although the mean differences in the y-component are somewhat larger, the overall agreement for 2003 is better than that for 2002. The uncertainty of the x-component of polar motion is 20 percent smaller,

Table 1. Comparisons of Daily Bulletin A Solutions to Bulletin B and C04 for Years 2002 and 2003

Year	Daily Bulletin A - Bulletin B Mean (mas or ms)	Daily Bulletin A - Bulletin B Std. Dev. (mas or ms)	Daily Bulletin A - C04 Mean (mas or ms)	Daily Bulletin A - C04 Std. Dev. (mas or ms)
2002				
PM-X	0.01	0.15	0.02	0.15
PM-Y	-0.04	0.14	-0.03	0.13
UT1-UTC	-0.012	0.060	-0.015	0.057
2003				
PM-X	0.01	0.12	0.01	0.12
PM-Y	-0.06	0.12	-0.05	0.12
UT1-UTC	-0.002	0.072*(0.047)	-0.001	0.071*(0.043)

*Includes values during an extended period without VLBI (late June and July).

the y-component is 8-15 percent smaller, and the UT1-UTC uncertainty is 20-25 percent smaller.

5. FUTURE IMPROVEMENTS

There are several areas of research being pursued to improve the accuracy of our near real-time IERS products. As was mentioned earlier, a dX and dY series with respect to the IAU 2000A Precession/Nutation Theory was created and implemented in Bulletin A on 1 January 2003 in order to be in compliance with the IAU 2000 resolutions. However, the new theory is not fully implemented in our processing. Our near-term goal is to complete the replacement of the old IAU 1980 Nutation Theory with the new IAU 2000A Nutation Theory. Another effort is to improve and standardize the techniques used in estimating the rates and biases that are applied to the different analysis center data products. The goal is to improve the consistency of data handling and to decrease the time required to add updated data sets into our process. A third research area is to examine the weighting applied to the data from different analysis centers to improve the high frequency signal content of the combination. Finally, different prediction methods are being investigated to quantify the potential improvement in current prediction accuracies.

Acknowledgments. It is a pleasure to acknowledge the contribution of agencies and individuals that provide Earth orientation data to the IERS. In addition the helpful comments and assistance of James Rohde and Drs. Dennis McCarthy and Victor Slabinski are gratefully acknowledged.

6. REFERENCES

Johnson, T. J., Luzum, B. J., Ray, J. R., 2003, Improved Near-term UT1R Predictions Using Forecasts of Atmospheric Angular Momentum, *Journal of Geodynamics*, in press.

Kammeyer, P., 2000, A UT1-like Quantity from Analysis of GPS Orbit Planes, *Celest. Mech. Dyn. Astr.*, **77**, 241–272.

Luzum, B.J., Ray, J. R., Carter, M. S., Josties, F. J., 2001, Recent Improvements to IERS Bulletin A Combination and Prediction, *GPS Solutions*, 4, No. 3, 34–40.

Wooden, W. H., Johnson, T. J., 2003, Rapid Service/Prediction Centre, *IERS Annual Report 2002*, 46–53.

COMPARISON OF POLAR MOTION PREDICTION RESULTS SUPPLIED BY THE IERS SUB-BUREAU FOR RAPID SERVICE AND PREDICTIONS AND RESULTS OF OTHER PREDICTION METHODS

W. KOSEK[1], D.D. McCARTHY[2], T.J. JOHNSON[2] and M. KALARUS[1]
[1]Space Research Centre, Polish Academy of Sciences, Warsaw, Poland
[2]US Naval Observatory, Washington DC, USA
E-mail: kosek@cbk.waw.pl

ABSTRACT. In this paper, four different methods for the prediction of x, y pole coordinates are investigated. We examined the accuracies of autocovariance (AC), least-squares extrapolation (LS), a least-squares extrapolation and autoregressive combination (LS+AR), and a least-squares extrapolation and neural networks combination (LS+NN) in predicting pole position. The most accurate prediction is the combination of the least-squares extrapolation and the autoregressive prediction of the least-squares extrapolation residuals applied to the complex-valued pole coordinates data. The problem of any prediction method of pole coordinates data in the polar coordinate system is a significant prediction error of the integrated angular velocity.

1. INTRODUCTION

The current prediction method of polar motion data carried out in the IERS Rapid Service/Prediction Center, called in this paper the USNO prediction, is the least-squares extrapolation of a Chandler circle, and annual and semiannual ellipses fit to the last 400 days of the combined pole coordinate data (McCarthy and Luzum 1991, IERS 2003a). The differences between this LS extrapolation and the last observed pole position determined in the USNO combination and the rate reported by the IGS in their rapid series are used to adjust the curve. The polar motion prediction errors for a few days in the future are several times greater than their determination error, which is of the order of 0.1 mas. The main reasons for poor accuracy prediction of pole coordinate data are irregular amplitude and phase variations of short period oscillations with periods less than one year (Kosek 2000) and irregular phase and amplitude variations of the annual oscillation (Kosek *et al.* 2001, 2002). The two biggest maxima of the annual oscillation phase and amplitude preceded the two biggest El Niño events in 1982/83, 1997/98 (Kosek *et al.* 2001, 2002). We examined the abilities of the AC, LS, LS+AR, and LS+NN techniques to predict the x, y pole coordinates. In this paper the polar motion predictions were computed directly from the x, y pole coordinate data or from the predictions of the radius and angular velocity in the polar coordinate system (Kosek 2002, 2003).

2. DATA

The analysis used the USNO pole coordinate data resulting from combination of observational data in the years 1973 - 2003.8 with a sampling interval of 1-day (IERS 2003a), the IERS EOPC01 and EOPC04 pole coordinate data in the years 1846 - 2002 and 1962 - 2003.8 with the sampling intervals of 0.05 years and 1-day, respectively (IERS 2003b). To create one pole coordinate data file the EOPC01 data were interpolated with a 1-day sampling interval before 1962 and these interpolated data were extended from 1962 to 1976 by the EOPC04 data and by the USNO pole coordinate data after 1976.

3. AUTOCOVARIANCE, AUTOREGRESSIVE AND NEURAL NETWORKS PREDICTIONS

The biased autocovariance estimations of a stationary and equidistant complex-valued time series z_t, $t = 1, 2, ..., n$ and of the same time series extended by the first AC prediction point z_{n+1} are given be the following formulae:

$$\hat{c}_{zz}^{(n)}(k) = \frac{1}{n} \sum_{t=1}^{n-k} z_t \overline{z}_{t+k}, \quad for \;\; k = 0, 1, ..., n-1 \tag{1}$$

$$\hat{c}_{zz}^{(n+1)}(k) = \frac{1}{n+1} \sum_{t=1}^{n-k+1} z_t \overline{z}_{t+k} \quad for \;\; k = 0, 1, ..., n \tag{2}$$

The first predicted value is determined by the principle that the autocovariance of the extended time series coincide as closely as possible with the autocovariance estimated from the given series and it is expressed by the minimum condition (Kosek 1993, 1997, 2002; Kosek *et al.* 1998):

$$R(z_{n+1}) = \sum_{k=1}^{n-k} |\hat{c}_{zz}^{(n)}(k) - \hat{c}_{zz}^{(n+1)}(k)|^2 = min, \tag{3}$$

The solution of the ensuing equation $\partial R(z_{n+1})/\partial z_{n+1} = 0$ yields the first prediction value:

$$z_{n+1} = \sum_{k=1}^{n-k} \overline{\hat{c}}_{zz}^{(n)}(k) z_{n-k+1} / \hat{c}_{zz}(0). \tag{4}$$

The second prediction point can be computed in the same way after the first one is added at the end of the time series. The following predictions are computed in a similar fashion.

In the AR prediction method the complex-valued autoregressive coefficients were computed using the Brzeziński (1994, 1995) algorithm, which is the modification of the Barrodale and Erickson (1980) algorithm for the maximum entropy coefficients of a real-valued time series. The optimum autoregressive order was estimated by AkaikeTs goodness-of-fit criterion: $\sigma_M(n + M + 1)/(n - M - 1)$, in which M is the optimum autoregressive order, n is the number of data and σ_M is the variance of the residuals.

In time series prediction by neural networks (NN) the main problem is to design the structure of the network and effectiveness of the training algorithm (Schuh *et al.* 2002). In this investigation the NN Toolbox of Matlab 5.3, in which the topology of the network consisted of two layers, was used. The input and hidden layers include 4 neurons with radial basis (*radbas*) transfer function and 2 neurons with linear (*purelin*) transfer function, respectively (Kalarus and Kosek 2003). This NN was generated using the *newff* Matlab function, which creates a feed-forward backpropagation network. The fastest and optimal method of training the NN

using Matlab function *trainlm* was used which updates weight and bias values according to the Levenberg-Marquardt optimization (More 1978).

4. POLAR MOTION PREDICTION IN THE POLAR COORDINATE SYSTEM

To predict the x, y pole coordinate data in the polar coordinate system, the observed data were first transformed to the radius and angular velocity (Kosek and Kalarus 1993). The first prediction points of the radius and angular velocity were transformed back to the Cartesian coordinate system using linear intersection formulae (Kosek 2002, 2003). To compute the radius it is necessary to compute the mean pole. The mean pole was computed using an Ormsby (1961) low pass filter and predicted by the LS method (Kosek 2003).

In order to compute predictions of the radius and angular velocity the AC prediction and the combination of the LS prediction with the autoregressive prediction of the LS extrapolation residuals (LS+AR) were applied. In the AC prediction the last 40 years of the radius and angular velocity time series were used. In the LS+AR prediction the LS model which consists of six oscillations with periods of 2220 days (6.1 years), 1200, 650, 310, 200 and 130 days (Kosek and Kalarus 2003) was fit to the last 35 years of the radius and angular velocity data and then the autoregressive coefficients were estimated from the last six years of the radius and angular velocity LS extrapolation residuals. The differences between the AC and LS+AR methods and USNO's combination solution for the x, y pole coordinates and their corresponding radius and angular velocity estimates are shown in Figure 1.

The mean prediction errors of the radius, integrated angular velocity, as well as the x and y pole coordinate data are shown in Figure 2. It can be noticed that the problem of prediction of pole coordinate data in the polar coordinate system is the significant error in the prediction of the integrated angular velocity. The prediction errors of the radius are smaller than those of the integrated angular velocity.

5. POLAR MOTION PREDICTION IN THE CARTESIAN COORDINATE SYSTEM

In the LS+AR prediction the LS extrapolation model of the Chandler circle, annual and semiannual ellipses and a bias was fit to the last ten years of the complex-valued pole coordinate data. The complex-valued autoregressive coefficients were computed from the last 870 days (twice the Chandler period) of the complex-valued LS extrapolation residuals.

To predict the x, y pole coordinate data by the combination of the LS and NN prediction methods (LS+NN) the LS model which consists of the linear trend as well as the Chandler and annual oscillations was computed from the beginning of the IERS EOPC04 data to the starting prediction epoch. The LS polar motion extrapolation residuals were interpolated with a 10 day sampling interval to reduce the computation time of training the NN. The pattern of training the NN was equal to 100 days in order to compute the first prediction point (Kalarus and Kosek 2003).

In the LS+AR and LS+NN prediction methods, the polar motion prediction is the sum of the LS extrapolation model and the AR or NN predictions of the LS extrapolation residuals. The differences between the LS+AR and LS+NN predictions of the x, y pole coordinate data and their future values at different starting prediction epochs are shown in Figure 3. It can be noticed that the prediction errors of the LS+AR prediction method are smaller than for the USNO and LS+NN prediction. The mean prediction errors of the x and y pole coordinate data in 1984-2003.7 for the USNO, LS+AR and LS+NN prediction methods are shown in Figure 4. Usually the mean prediction errors of the LS+AR prediction are less than for the USNO prediction in x and y. The mean prediction errors of the LS+NN prediction are less than for

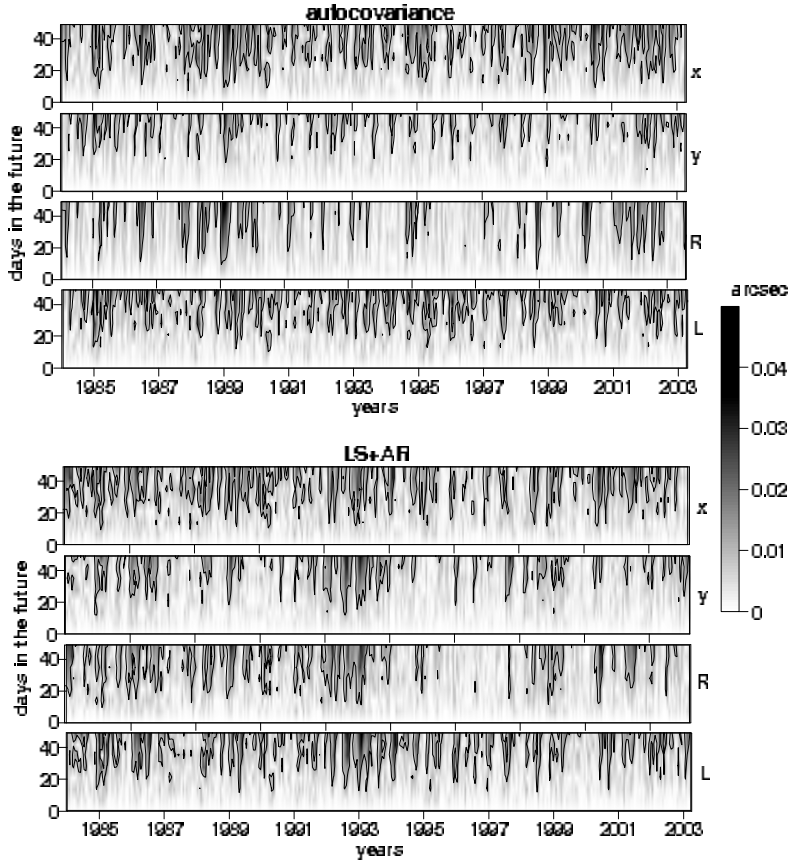

Figure 1: The absolute values of the difference between the pole coordinate data (x, y), radius R, integrated angular velocity L and their AC and LS+AR predictions computed at different starting prediction epochs in the polar coordinate system (contour lines at 0.01 arcsec).

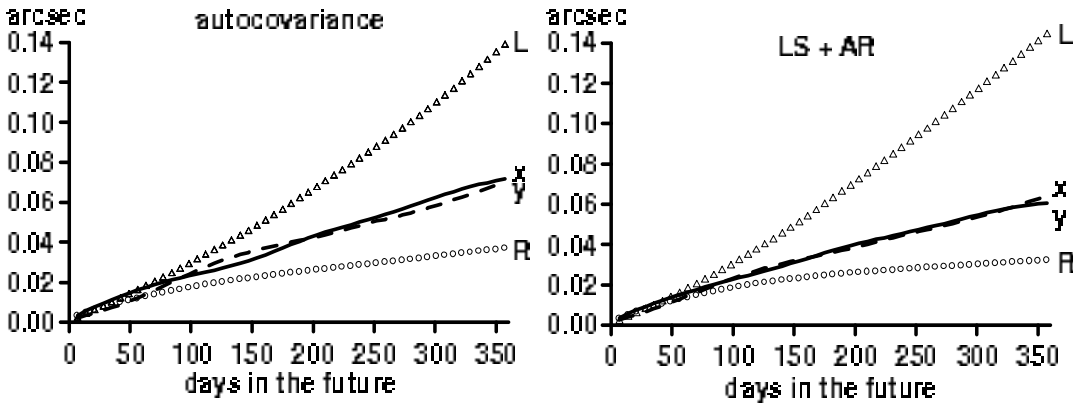

Figure 2: The mean prediction errors in 1984-2003.8 of the radius R (circles), integrated angular velocity L (triangles) and x (solid line), y (dashed line) pole coordinate data for the AC and LS+AR prediction methods applied in the polar coordinate system.

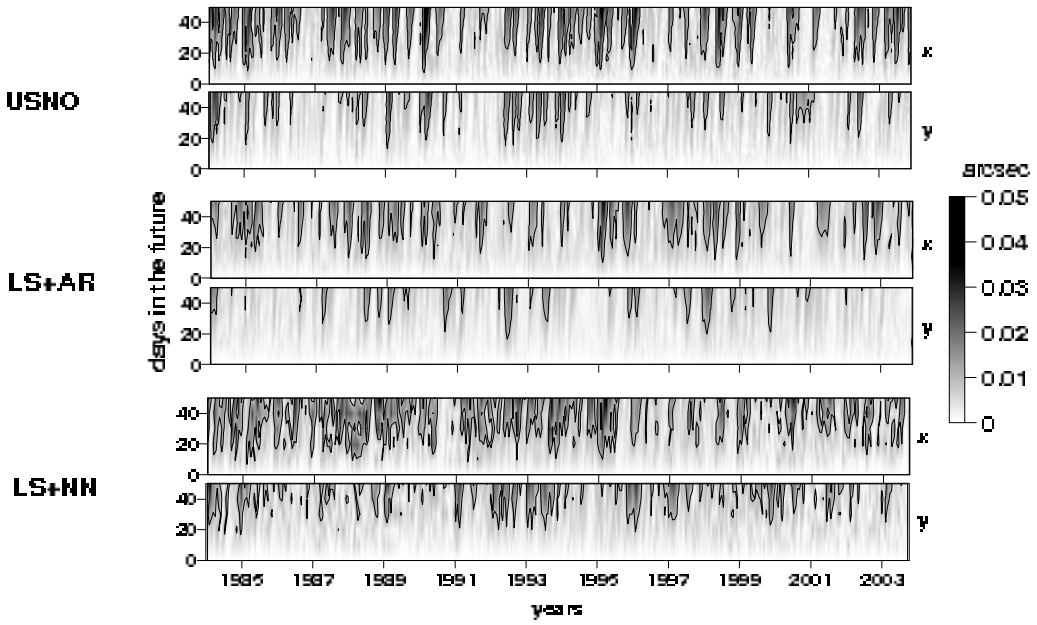

Figure 3: The absolute values of the difference between the x, y pole coordinate data and their USNO, LS+AR and LS+NN predictions computed at different starting prediction epochs (contour lines at 0.01 arcsec).

the UNSO prediction for prediction lengths greater than 30 to 40 days in x and for prediction lengths greater than 100 days in y. The mean prediction errors of the LS+AR and LS+NN predictions are of the same order for x and are less for the LS+AR prediction than for the LS+NN prediction in y for prediction lengths less than 100 days.

6. CONCLUSIONS

The problem of any prediction method of pole coordinate data in the polar coordinate system is the error in the prediction of the integrated angular velocity. The prediction errors of pole coordinate data using the combination of the LS+AR prediction method are smaller than for the USNO prediction. For predictions of less than 40 days into the future only the LS+AR out performs USNO, while for predictions greater than 100 days both LS+AR and LS+NN will

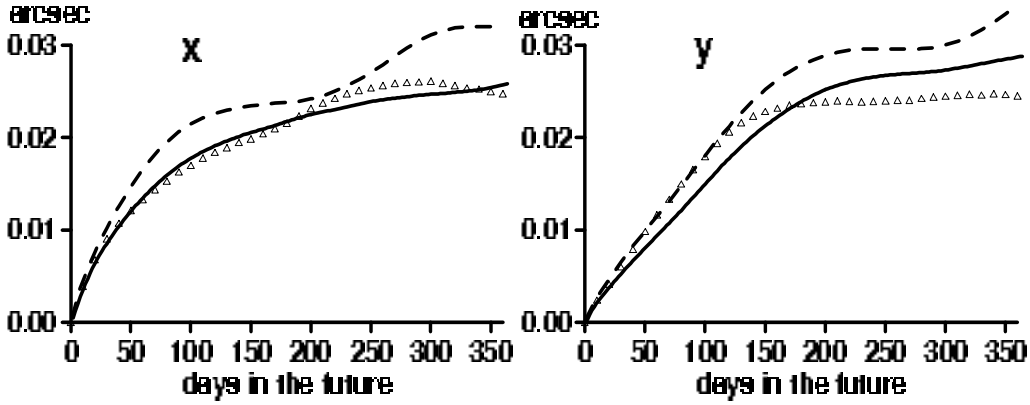

Figure 4: The mean prediction errors of the x and y pole coordinate data in 1984-2003.8 for the USNO (dashed line), LS+AR (solid line) and LS+NN (triangles) prediction methods.

perform better in both the x and y pole coordinate.

Acknowledgments. This paper was supported by the Polish Committee of Scientific Research project No 8 T12E 005 20 under the leadership of Dr. W. Kosek. The authors thank Prof. A. Brzeziński for the algorithm for the maximum entropy coefficients of complex-valued time series and Dr. W. Popiński for the autoregressive prediction procedures of complex-valued time series.

7. REFERENCES

Barrodale, I., and Erickson, R. E., 1980, Algorithms for least-squares linear prediction and maximum entropy spectral analysis - Part II: Fortran program, *Geophysics*, **45**, 433–446.

Brzeziński, A., 1994, Algorithms for estimating maximum entropy coefficients of the complex-valued time series, *Allgemeine Vermessungs-Nachrichten*, Heft **3**/1994, 101–112, Herbert Wichman Verlag GmbH, Heidelberg.

Brzeziński, A., 1995, On the interpretation of maximum entropy power spectrum and cross-power spectrum in earth rotation investigations, *manuscripta geodaetica*, **20**, 248–264.

IERS, 2003a, IERS Annual Report 2002, 3.5.2 Rapid Service/Prediction Centre, 46–53.

IERS, 2003b, The Earth Orientation Parameters, http://hpiers.obspm.fr/eop-pc/.

Kalarus, M., and Kosek, W., 2003, Prediction of Earth orientation parameters by artificial neural networks, submitted to *Artificial Satellites - Journal of Planetary Geodesy.*

Kosek, W., 1993, The Autocovariance Prediction of the Earth Rotation Parameters, *Proc. 7th International Symposium "Geodesy and Physics of the Earth" IAG Symposium No. 112*, Potsdam, Germany, Oct. 5-10, 1992, H. Montag and Ch. Reigber (eds.), Springer Verlag, 443–446.

Kosek, W., 1997, Autocovariance Prediction of Short Period Earth Rotation Parameters, *Artificial Satellites, Journal of Planetary Geodesy*, **32**, 75–85.

Kosek, W., McCarthy, D. D., Luzum, B., 1998, Possible Improvement of Earth Orientation Forecast Using Autocovariance Prediction Procedures, *Journal of Geodesy*, **72**, 189–199.

Kosek, W., 2000, Irregular short period variations in Earth rotation, *IERS Technical Note*, **28**, 61–64.

Kosek, W., McCarthy, D. D., and Luzum, B. J., 2001, El Niño impact on polar motion prediction errors, *Studia Geophysica et Geodaetica*, **45**, 347–361.

Kosek, W., McCarthy, D. D., Luzum, B. J., 2002, Variations of annual oscillation parameters, El Niño and their influence on polar motion prediction errors, *Proc. Journees 2001, Systemes de Reference Spatio-Temporels*, Brussels, 24-26 Sep. 2001, 85–90.

Kosek, W., 2002, Autocovariance prediction of complex-valued polar motion time series, *Advances of Space Research*, **30**, 375–380.

Kosek, W., 2003, Polar motion prediction by different methods in polar coordinate system, *Proc. Journees 2002, Systemes de Reference Spatio-Temporels*, Bucarest, 25-28 Sep. 2002.

Kosek, W., Kalarus, M., 2003, Time-frequency analysis and prediction of polar motion radius and angular motion, *Artificial Satellites – Journal of Planetary Geodesy*, **38**, No 2, 41–54.

McCarthy, D. D., and Luzum, B. J., 1991, Prediction of Earth Orientation, *Bull. Geod.*, **65**, 18–21.

More, J. J., 1978, The Levenberg-Marquardt algorithm implementation and theory, *Numerical Analysis, ser. Lecture Notes in Mathematics*, G. Watson (ed.), **630**, New York: Springer-Verlag, 105–116.

Ormsby, J. F. A., 1961, Design of Numerical Filters with Application to Missile Data Processing, *J. Assoc. Compt. Mach.*, **8**, 440–466.

Schuh, H., Ulrich, M., Egger, D., Muller, J., and Schwegmann, W., 2002, Prediction of Earth orientation parameters by artificial neural networks. *Journal of Geodesy*, **76**, 246–258.

GENERALIZED MEAN OF INDIVIDUAL EOP SERIES BY LEAST-SQUARES COLLOCATION TECHNIQUE

YU.L. RUSINOV
Institute of Applied Astronomy of RAS
10, Kutuzov quay, 191187, St.Petersburg, Russia
e-mail: rusinov@quasar.ipa.nw.ru

ABSTRACT. To obtain combined solution of the Earth orientation parameters, least-squares collocation method is used. Auto- and crosscovariance functions of signals were calculated. The result corrections achive ± 0.25 mas of arc for polar motion and nutation, and ± 0.02 msec for UT1 – UTC.

1. INTRODUCTION

At present observations of the Earth orientation parameters (EOP) are carried out using different observation techniques. The main part of them are VLBI, VLBI-intensives, SLR, LLR and GPS. Every observational program has different set of EOP, different time steps or nonequidistant, properly errors, etc. Therefore combined solution of EOP is needed. This solution has to be equidistant and take into account possible correlations between observational series. The existing reference system IERS (EOP) C04 which is obtained using Allan variance analysis of the difference between series without any reference to combined series (Gambis, 2001). This solution does not take into account possible correlations in observational series and between different observational series, that will be demonstrated in this paper.

At 1997 Prof. Gubanov in his monography (Gubanov, 1997) demonstrated that least-squares collocation technique may be applied to improvement of combined solution of EOP. This method gives two different algorithms of estimation: least-squares collocation and generalized average. The former is used in case of we know reference covariance function and the latter used otherwise. The stochastic approach developed at (Moritz, 1987) allows to takes into account possible correlations in observational series and between each others.

2. STRUCTURE OF OBSERVATIONS

There are two types of observational series that are used to calculate combined solution EOP(IERS)C04: longterm and operational available at `http://hpiers.obspm.fr/eop-pc/` Longterm series are updated on this WWW every year. Almost all observations are covers time interval since 1993 up to 2002. Two last years until now are covered by operational EOP series. They are updated a weekly twice. In order to remove low frequency harmonics, e.g. Chandler wobble in polar motion, annual and semiannual components in EOPs, etc. from observational series, time series of differences between observational series and improved reference system were calculated and values of EOP were resulted on the observational time lags by lin-

ear interpolation. These differences have linear shift which is due to tidal variations, tectonics movement etc. and white noise which is due to random errors of observations. This trend was calculated and removed from all differences. Let us consider set of observational series in more details.

The time series of polar motion are produced by GPS, VLBI and SLR data centers. The GPS series have 1 day time step and reduced to the midnight of the date. The long term GPS series are calculated by Universitaet Bern GeoForschung Zentrum, and Jet Propulsion Laboratory. The operational GPS series are obtained by the same data centers and some others, but the others series were observed on too short time interval. VLBI time series are calculated by Bundesamt fuer Kartographie und Geodaesie, Goddard Space Flight Center, Institute of Applied Astronomy, Observatoire de Paris and Shangai Observatory. These series are not equidistant and have to be interpolated. The SLR observational series are produced by Space Geodesy Centre, Central Laboratory for Geodesy Analysis, Institute of Applied Astronomy and Glavniy Observatorya Ukraine.

UT1 – UTC is observed by the same Data Centers as polar motion, but there is VLBI-intensive observation technology that calculate only UT1 – UTC. These series have 1 day time step and short series can be processed in combined solution. More detailed descriptions of these series are available on the IERS web-site. The VLBI-intensive programs carry out every day observations, but these are have more low accuracy and precision than other programs. But intensive series need to be interpolated anyway because time lags of observations do not coincide with time lags of EOP(IERS)C04 system.

The observations of nutation are carried out by VLBI techniques only. Because on the IERS website files with observations are sorted by Data Analysis Center, therefore one observational file may contains some different EOPs. These observations are carried out with varying time lags, therefore time step between two observations in the same series may be from 1 day upto 7 days and interpolation is demanded in order to reduce to equidistant time lags.

3. TIME SERIES INTERPOLATION BY LEAST-SQUARES COLLOCATION

Let us consider the problem of observations interpolation onto equidistant time grid. On input we have many time series, everywhere have its proper observation program. Some of these programs have time step approximately equal to 1 day, any others — 3 days or 7 days. In general almost all correspond time series are not equidistant, but in order to obtain combined solution we have to reduce these series to uniform time lags. This problem may be solved by interpolation procedure. There are many interpolation techniques, such as polynomial interpolation, interpolation by rational function, spline interpolation, etc. These techniques process series, but the least-squares collocation makes interpolation of statistical characteristic of series — autocovariance function.

Let us consider more detail the least-squares collocation (LSC) technique for individual series. We have to evaluate signal vector $\boldsymbol{s}$ from observational vector $\boldsymbol{l}$, that has random white noise $\boldsymbol{r}$

$$\boldsymbol{l} = \boldsymbol{s} + \boldsymbol{r} \tag{1}$$

If signal and noise does not correlate between each other and we know autocovariance matrix of noise $\boldsymbol{Q}_{rr}$ that problem can be solved by main formula of LSC (Gubanov, 1997)

$$\hat{\boldsymbol{s}} = \boldsymbol{Q}_{sl}\boldsymbol{Q}_{ll}^{-1}\boldsymbol{l}, \tag{2}$$

where $\boldsymbol{Q}_{ll}$ — autocovariance matrix of individual data. Matrices $\boldsymbol{Q}_{ll}, \boldsymbol{Q}_{sl}$ can be estimated from autocovariance function of process

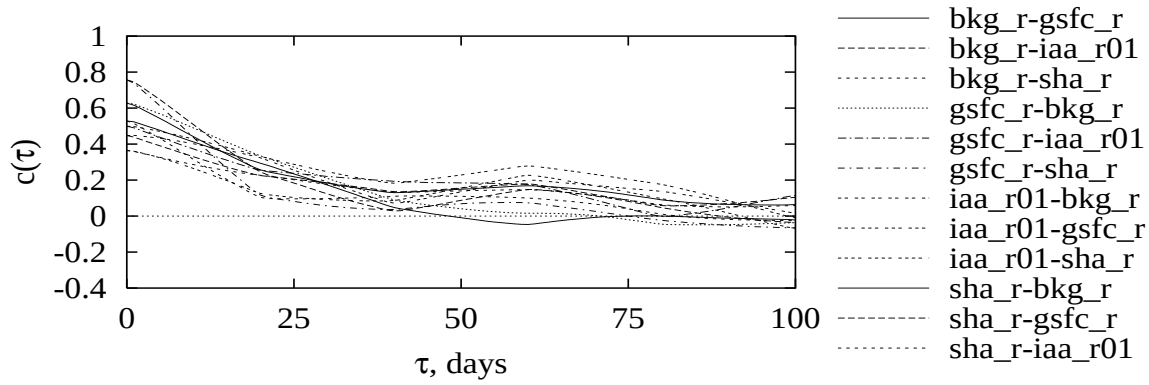

Figure 1: Some cross-correlation functions for X-coordinate of pole.

$$\boldsymbol{Q}_{sl} = \begin{pmatrix} q(t'_0 - t_0) & q(t'_0 - t_1) & \dots & q(t'_0 - t_n) \\ q(t'_1 - t_0) & q(t'_1 - t_1) & \dots & q(t'_1 - t_n) \\ \dots & \dots & \ddots & \dots \\ q(t'_{n'} - t_0) & q(t'_{n'} - t_1) & \dots & q(t'_{n'} - t_n) \end{pmatrix}, \tag{3}$$

$$\boldsymbol{Q}_{ll} = \begin{pmatrix} q(t_0 - t_0) & q(t_1 - t_0) & \dots & q(t_n - t_0) \\ q(t_0 - t_1) & q(t_1 - t_1) & \dots & q(t_n - t_1) \\ \dots & \dots & \ddots & \dots \\ q(t_n - t_1) & q(t_n - t_1) & \dots & q(t_n - t_n) \end{pmatrix} + \sigma_n^2 \boldsymbol{I}, \tag{4}$$

$$\tag{5}$$

where t_0, t_1, ..., t_n — time lags of input data, t'_0, t'_1, ..., $t'_{n'}$ — time lags of output data, σ_n^2 — noise dispersion, $q(\tau)$ — estimations of autocovariance function of signal. If signal $\boldsymbol{s}$ and noise $\boldsymbol{r}$ does not correlate with each other then covariation matrix between signal and observations $\boldsymbol{Q}_{sl}$ is equal to matrix of signal autocovariation $\boldsymbol{Q}_{ss}$. problem. As we can improvable time series and reference system. differences by equal to zero that is

4. OBTAINING COMBINED SOLUTION BY GENERALIZED AVERAGE ALGORITHM

Interpolated and filtered series were interpreted as vectors $\boldsymbol{l}_k$. If values of cross-correlation functions near $\tau = 0$ are approximately equal to zero for any pair of observational series then the reference system IERS (EOP) C04 is not need of any improvement, but this is not take place in real processing. At Figs. 1–5 some cross-correlation functions between individual series are presented.

Because we do not know apriory covariance function of corrections to reference system EOP (IERS) C04 therefore we have to average by generalized average algorithm (Moritz, 1987, Gubanov, 1997 pp.97–106). The stochastic corrections to reference system EOP (IERS) C04 can be calculated by formula

$$\hat{\boldsymbol{s}} = \left(\sum_{i=1}^{m} \sum_{j=1}^{m} \tilde{\boldsymbol{Q}}_{ij} \right)^{-1} \left(\sum_{i=1}^{m} \sum_{j=1}^{m} \tilde{\boldsymbol{Q}}_{ij} \boldsymbol{l}_i \right), \tag{6}$$

where $\boldsymbol{l}_i$ are vectors of individual interpolated and filtered series, block-matrices $\tilde{\boldsymbol{Q}}_{ij}$ may be built from auto- and crosscovariation functions between series $\boldsymbol{l}_i$ and $\boldsymbol{l}_j$. After that we have

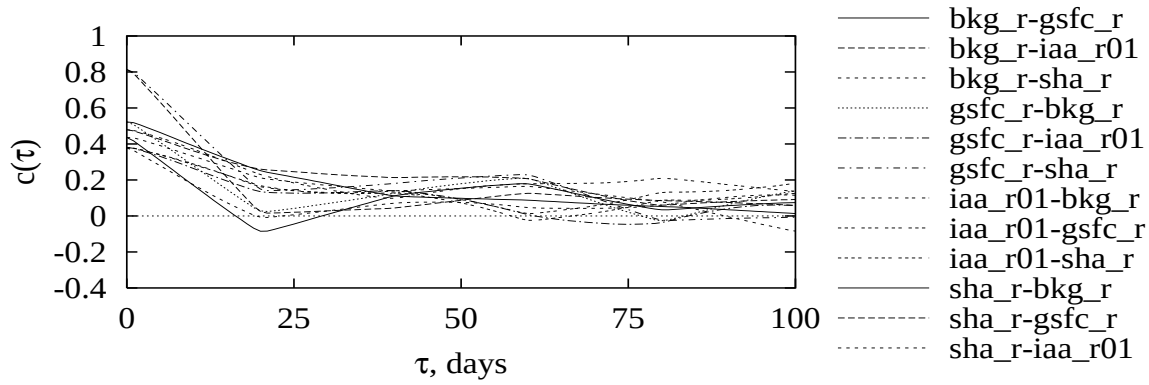

Figure 2: Some cross-correlation functions for Y-coordinate of pole.

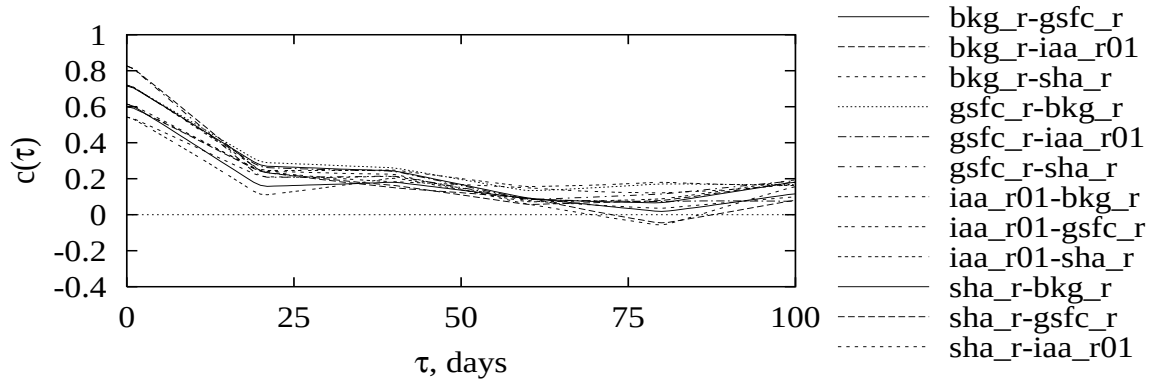

Figure 3: Some cross-correlation functions for UT1 – UTC.

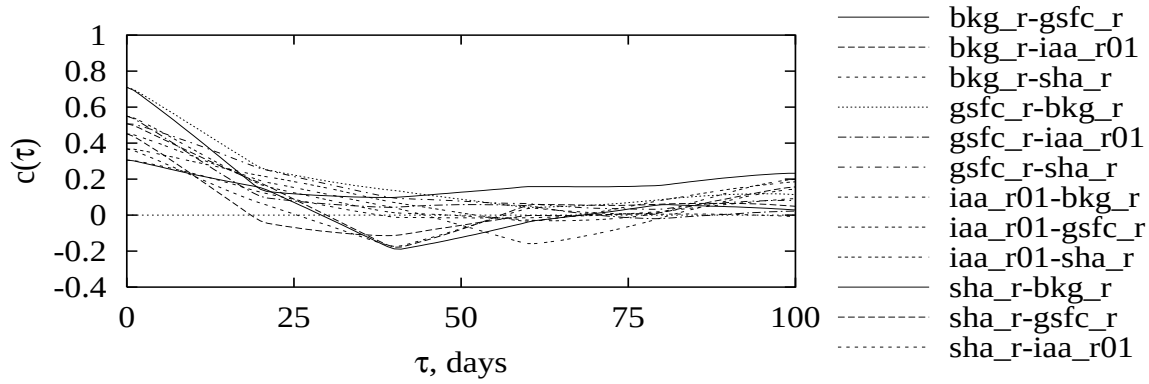

Figure 4: Some cross-correlation functions for $d\Psi$.

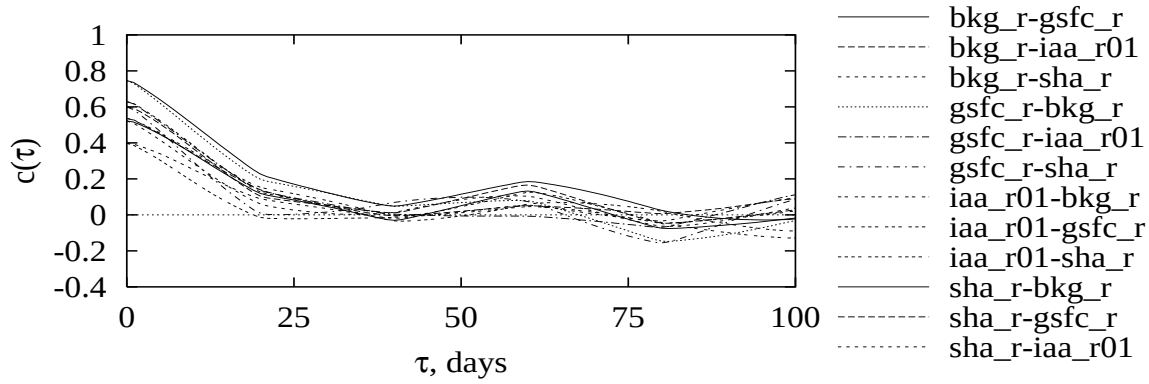

Figure 5: Some cross-correlation functions for $d\epsilon$.

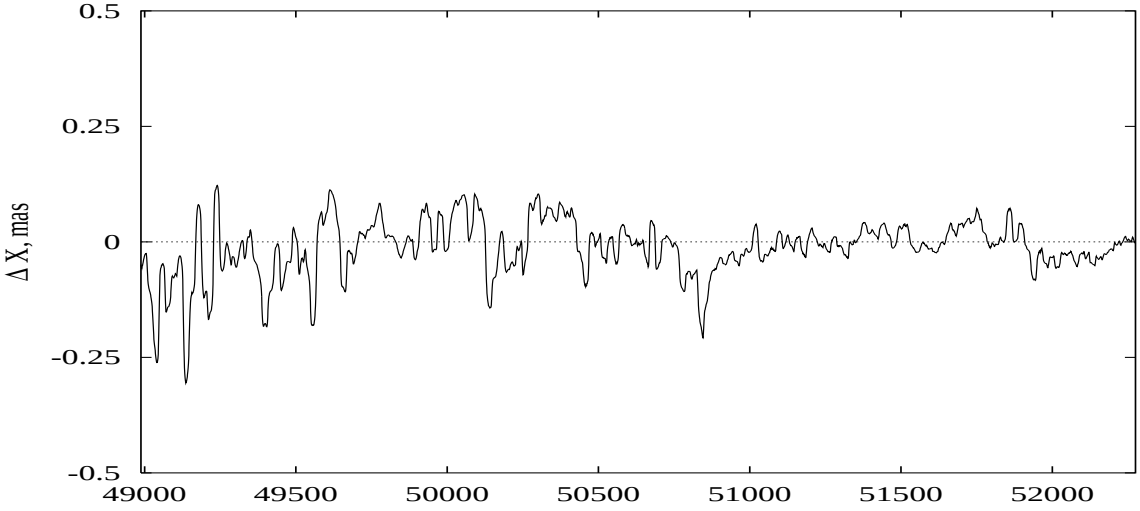

Figure 6: Corrections to reference system EOP (IERS) C04 for X-coordinate of pole.

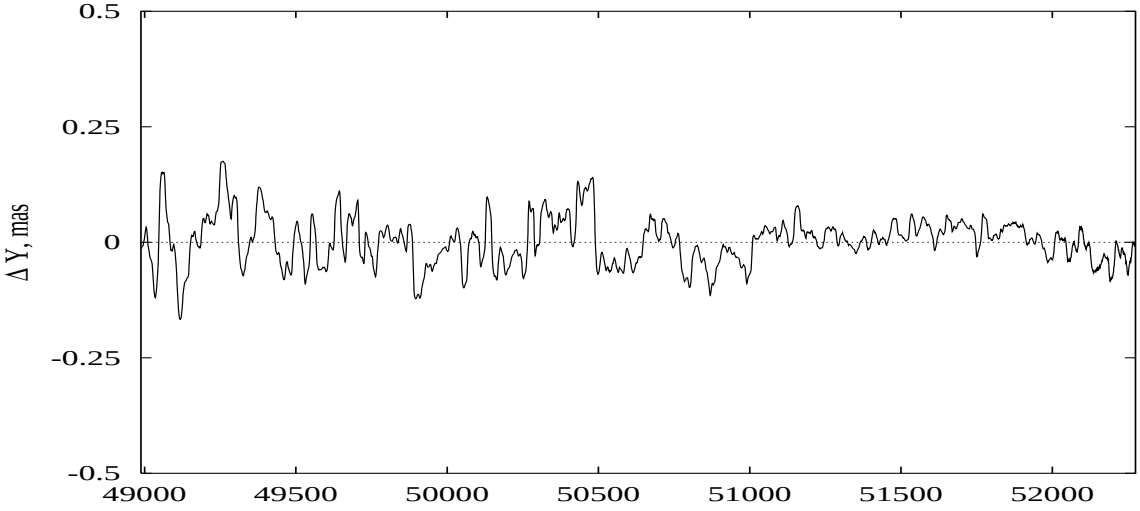

Figure 7: Corrections to reference system EOP (IERS) C04 for Y-coordinate of pole.

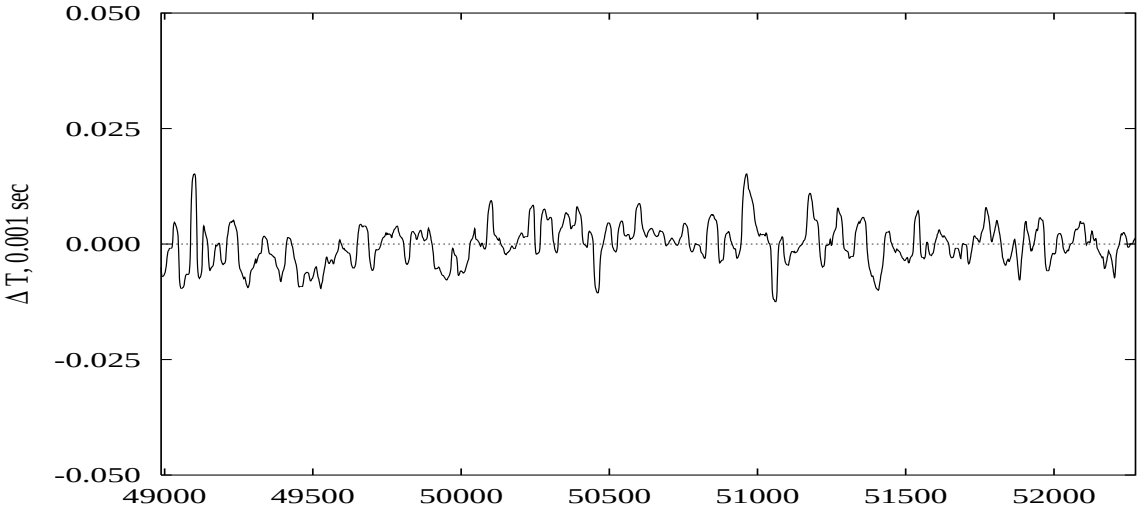

Figure 8: Stochastic corrections to reference system EOP (IERS) C04 for UT1 – UTC.

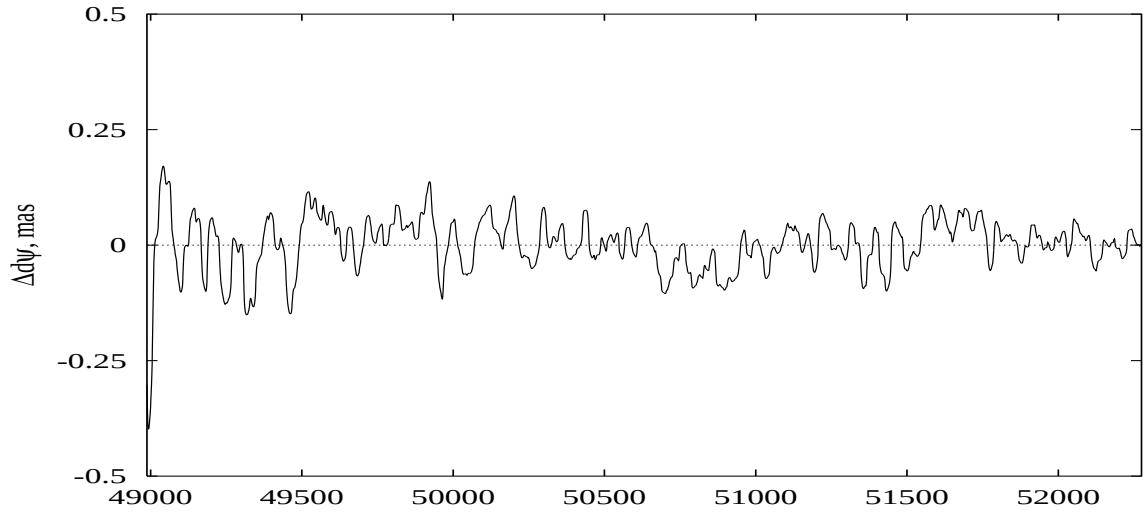

Figure 9: Stochastic corrections to reference system EOP (IERS) C04 for $d\Psi$.

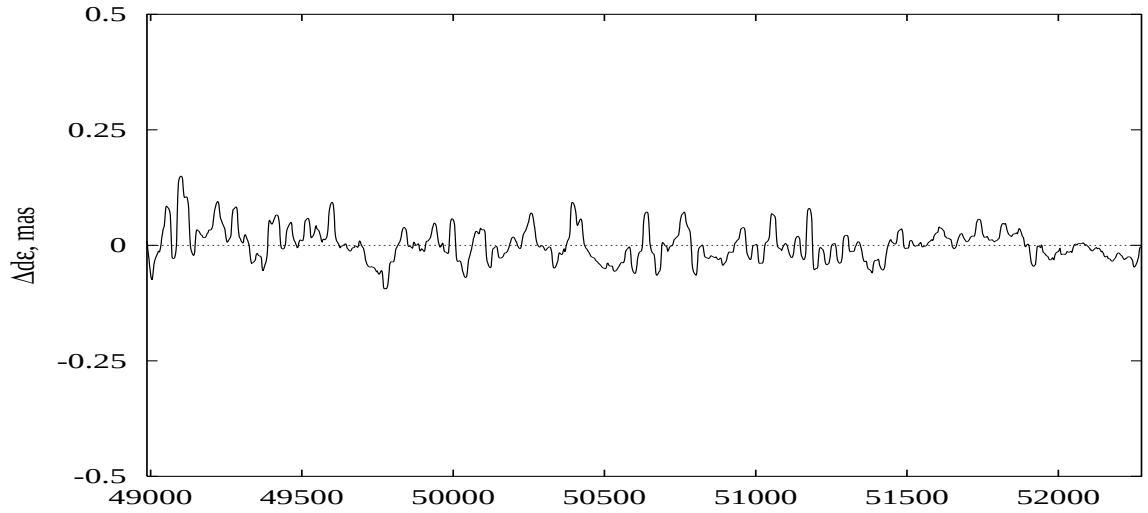

Figure 10: Stochastic corrections to reference system EOP (IERS) C04 for $d\epsilon$.

built general covariance matrix of data $\boldsymbol{Q} = [\boldsymbol{Q}_{ij}]$ and its inverse matrix $\boldsymbol{Q}^{-1} = \tilde{\boldsymbol{Q}} = [\tilde{\boldsymbol{Q}}_{ij}]$. Thus using matrices $\tilde{\boldsymbol{Q}}_{ij}$ and vectors $\boldsymbol{l}_j$ we can obtain stochastic corrections using generalized average algorithm. These stochastic corrections to series EOP (IERS) C04 are available at Figs. 6–10.

Acknowledgments. This activity is supported financially by Russian Foundation of Basic Research (grant 03-02-17591).

5. REFERENCES

Gambis D., 2001, Allan Variance analysis applied to Earth orientation Analysis, *Adv. Space Research.*

Gubanov V. S., 1997, Generalized least-squares. Theory and application in astrometry, Saint-Petersburg, Russia, In Russian.

Moritz H., 1987, Averaging two functions. Bull. Geodesique, **61**, N 1, 21–40.

IAU2000: COMPARISON WITH THE VLBI OBSERVATIONS AND OTHER NUTATION THEORIES

S.L. PASYNOK
Sternberg State Astronomical Institute
13, Universitetskij pr., 119992, Moscow, Russia
e-mail: pasynok@sai.msu.ru

ABSTRACT. The modern nutation theories of the nonrigid Earth predict the nutation amplitudes with very high precision and the differences between main amplitudes sets of these theories are small. Therefore complete comparison of the theories impossible without estimation of the differences between theoretical nutation angles and VLBI observations. This comparison for modern nutation series (IAU2000 (Mathews et.al.(2002)), GF99(Getino and Ferrandiz (2000)), HJL2001 (Huang et.al. (2001)) and ZP2003 series (Zharov and Pasynok (2003))) were made.

The IVS *.ngs files for VLBI observations from 1980 to 2002 and package OCCAM5.0 (Titov and Zarraoa (2001)) were used for calculation of corrections for theories. As results the corrections to the nutation angles $\Delta\varepsilon$ and $\sin\varepsilon_0\Delta\psi$ for each theory were obtained. The IAU2000 theory (without FCN) achieves the best accuracy.

The main term of the differences between theory and observations is the free core nutation (FCN). This term is different for each theory.

1. INTRODUCTION

The 4 modern nonrigid nutation theories were selected for analysis: IAU2000a, GF99, ZP2003, HJL2001. The theories IAU2000a and GF99 are now well known. The ZP2003 has specific atmospheric account and more detailed analysis of the conservation low. This theory differs from ZP2002 (Zharov and Pasynok (2002)) by the elastic nonlinear term in tidal potential. The HJL2001 theory uses the numerical integration method.

The modern nutation theories of the nonrigid Earth predict the nutation amplitudes with very high precision and the differences between main amplitudes sets of these theories are very small (see Table 1).Therefore complete comparison of the theories impossible without estimation of the differences between theoretical nutation angles and VLBI observations.

The IVS *.ngs files for VLBI observations from 1980 to 2002 and package OCCAM5.0 (Titov and Zarraoa(2001)) were used for calculation of corrections for theories. Original package was modified but the processing core of the OCCAM5.0 was not changed: only new nutation theory were included and new interface was created.

The processing VLBI observation for every theory was uniform: every *.ngs file was processed with the every theory as the start approximation. The observable additions to the theoretical

Table 1: The nutation amplitudes for the main nutation term (18.6 years) in *mas*.

Theory	S0psi	C0eps
IAU2000	-17206.416	9205.233
GF99	-17206.393	9205.018
ZP2003	-17206.366	9205.162
HJL2001	-17206.271	9205.147

Table 2: The correlation between FCN for nutation theories for $\delta\psi$ nutation angle.

	IAU2000	**GF99**	**ZP2003**	**HJL2001**
IAU2000	1	0.40	0.61	0.22
GF99	0.40	1	0.28	0.03
ZP2003	0.61	0.28	1	0.37
HJL2001	0.22	0.03	0.37	1

nutation angles were determined. The results were clipped at the 1 mas wrms error level.

2. NUMERICAL RESULTS

The differences between theoretical and observational nutation angles are plotted on the Fig. 1 and Fig. 2 (gray line). The solid black lines are running average of these differences. These lines are determined mainly by the free core nutation(FCN). As we see this term is different for each theory, especially for $\delta\psi$ angle (see Table 2).

The wrms of differences between theories and observations are shown in the Table 3. But for more clear comparison it is convenient to introduce the approximation quality coefficient according to:

$$K \equiv \frac{\sqrt{\frac{1}{2}\left((\delta\varepsilon_{IAU2000})^2 + (\sin\varepsilon_0\delta\psi_{IAU2000})^2\right)}}{\sqrt{\frac{1}{2}\left((\delta\varepsilon)^2 + (\sin\varepsilon_0\delta\psi)^2\right)}}$$

The approximation quality coefficients for theories are shown in the Table 4.

Table 3: The wrms of the nutation theories(μas).

Theory abbreviation	$\Delta\varepsilon$	$\sin\varepsilon_0\Delta\psi$
IAU2000	218	171
GF99	232	173
ZP2003	230	204
HJL2001	288	223

Table 4: The approximation quality coefficient.

Theory abbreviation	K
IAU2000	1
GF99	0.96
ZP2003	0.90
HJL2001	0.76

Table 5: The wrms of the differences between nutation theories for $\delta\varepsilon(\mu as)$.

	IAU2000	**GF99**	**ZP2003**	**HJL2001**
IAU2000	0	128	143	186
GF99	128	0	183	175
ZP2003	143	183	0	160
HJL2001	186	175	160	0

It is interesting to compare the wrms of the differences between theories and observations and wrms of the differences between different theories (rms of the differences between theories which were weighted using observations weights). The comparison of the Table 3 with Table 5 and Table 6 shows that differences between any theory and observations and differences between this theory and other theory are similar.

The every theory achieves the best accuracy only with the it's own precession rate and pole biases (Table 7). It is interesting that differences between these parameters for different theories are much more then internal accuracy of any theory (Table 8).

3. CONCLUSIONS

The brief conclusions from numerical results are following.

1. The best approximation is provided by IAU2000 theory($K = 1$). But GF99, ZP2003, HJL2001 are very close to it ($0.76 < K < 0.96$). Thus, all theories provide good approximation of the VLBI observations.

2. From the statistical point of view the differences between theories are negligible small. (Because of time of the VLBI observations is short (approximately 1 main nutation period) and the wrms of the differences between theories are approximately the same as the differences between any theory and VLBI observations).

3. The theories predict the different precession rate corrections and pole biases. Therefore

Table 6: The wrms of the differences between nutation theories for $\delta\psi(\mu as)$.

	IAU2000	**GF99**	**ZP2003**	**HJL2001**
IAU2000	0	115	282	271
GF99	115	0	317	305
ZP2003	282	317	0	331
HJL2001	271	305	331	0

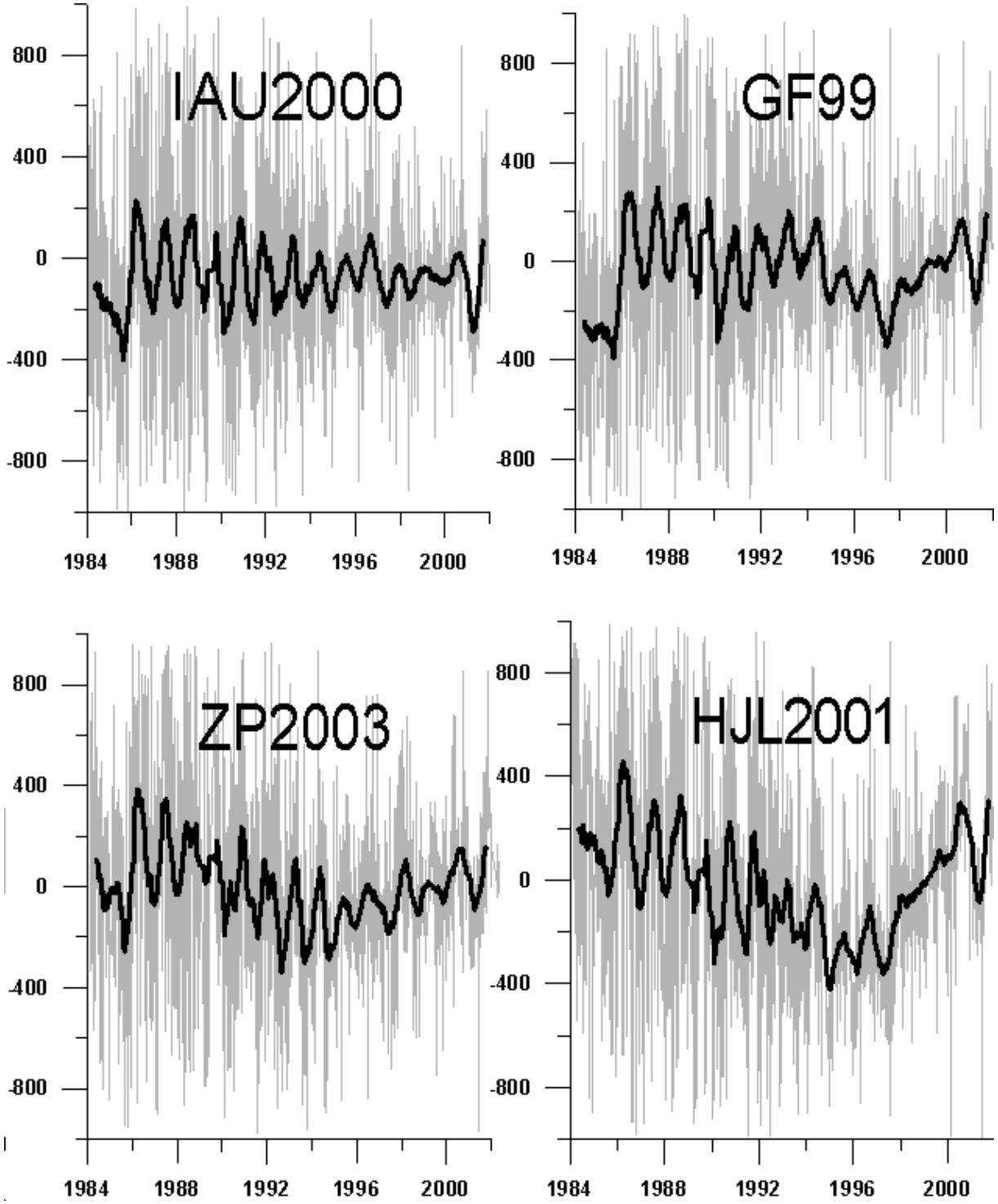

Figure 1: Differences between theories and observations for $\delta\varepsilon$ nutation angle in μas(gray line). The black line is the running average of this differences which mainly determined by FCN.

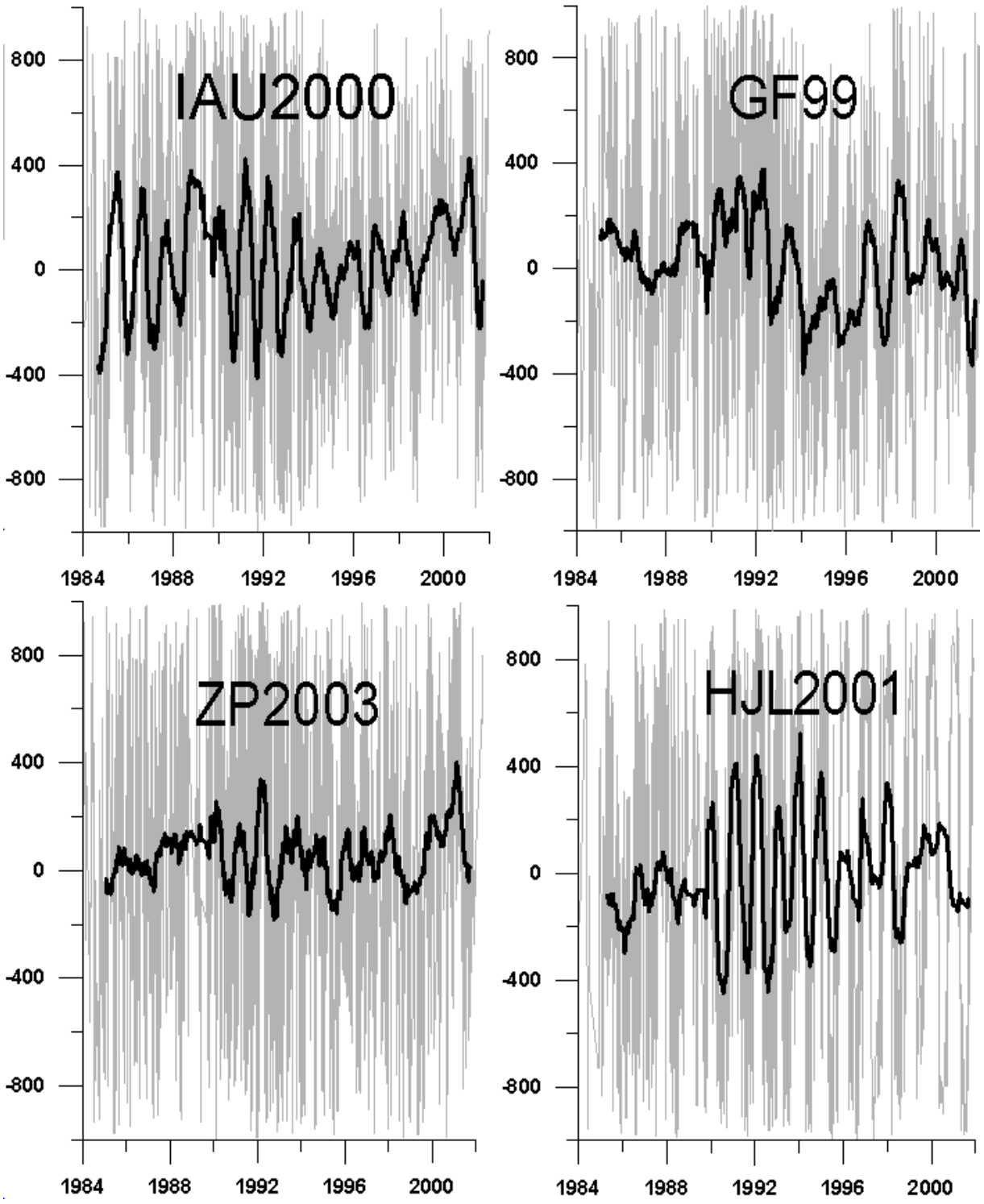

Figure 2: Differences between theories and observations for $\delta\psi$ nutation angle in μas(gray line). The black line is the running average of this differences which mainly determined by FCN.

Table 7: The precession rate corrections and pole biases.

	IAU2000	**GF99**	**ZP2003**	**HJL2001**
$\delta\psi_A("/c)$	-0.2996	-0.3001	-0.3115	-0.3050
$\delta\varepsilon_A("/c)$	-0.0252	-0.0282	-0.0226	-0.0249
$\xi_0(")$	-0.016617	-0.017129	-0.015873	-0.017196
$\eta_0(")$	-0.006819	-0.005390	-0.006838	-0.005192

Table 8: The accuracy of the precession rate corrections and pole biases.

	External (between different theories)	**Internal (IAU2000)**
$\delta\psi_A("/c)$	0.010	0.00040
$\delta\varepsilon_A("/c)$	0.003	0.00010
$\xi_0(")$	0.001	0.00001
$\eta_0(")$	0.001	0.00001

the more correct theory can be determined with time. The monitoring of the differences between the best nutation theories and VLBI observations is needed for determination of the most correct theory.

4. The FCN term is different for each theory. Therefore it can be describe correctly until the most correct theory will be determined. From the statistical point of view the time of the VLBI observation have to be equal to at least 3 main nutation periods for this purpose.

The author deeply thanks Zharov V.E. for discussions. This work has been supported by the Russian Foundation for Basic Researches (grants 01-02-16529 and 02-05-39004).

4. REFERENCES

Huang, C. L., Jin, W. J., Liao, X. H., 2001, *Geophys. J. Int.*, **146**, 126–133.

Getino, J., Ferrandiz, J. M., 2000, In: *Proceedings of IAU Colloquium 180*, 236–241.

Mathews, P. M., Herring, T. A., Buffet, B. A., 2002, *J. Geophys. Res.*, **107(B4)**, 10.1029/2000JB000390.

Titov, O., Zarraoa, N., OCCAM5.0: Users Guide.

Zharov, V. E., Pasynok, S. L., 2002, Theory of nutation of the non-rigid Earth with the atmosphere, In: *Proceedings of Proc. of Journess 2002*, (in press).

DETERMINATION OF EOP FROM COMBINATION OF SLR AND VLBI DATA AT THE OBSERVATIONAL LEVEL

N.V. SHUYGINA
Institute of applied astronomy of RAS
10 Kutuzov quay, 191187 St.Petersburg, Russia
e-mail: nvf@quasar.ipa.nw.ru

ABSTRACT. Time series of Earth orientation parameters (EOP) are commonly obtained independently from the processing of high accuracy modern observations such as VLBI, SLR, LLR, and GPS. This paper is devoted to an attempt of determination of EOP series from the joint analysis of SLR and VLBI measurements at the observation level. We used laser ranges to geodetic satellites LAGEOS, LAGEOS 2, and Etalon 1&2. All range measurements are taken from the Crustal Dynamics Data Informational System (CDDIS) and European Data Center (EDC). VLBI observations of distant quasars are obtained from the NEOS-A campaign. Processing of these measurements is performed in two steps. On the first stage the short arc technique with the arc length of 7 days is applied to all SLR measurements to adjust orbital parameters along with coefficients to the radiation pressure reflectance model and along track acceleration terms. All these parameters are considered to be non-stochastic. For VLBI measurements zenith component of troposphere delay and its gradients in horizontal and vertical directions are adjusted as stochastic signals on each day of observation. Both coordinates of quasars and site coordinates are considered to be accurately known and are not improved. It is very important that both SLR and VLBI observations are processed by the same program package, using the same astronomical constants and models for different kinds of measurements.

On the second stage SLR and VLBI observations are mixed to determine corrections to variables mentioned above along with all five Earth rotation parameters. Kalman filtering procedure is used to solve the system of conditional equations. Combining SLR and VLBI measurements on the short one day arc makes it possible to get standard deviations of parameters 1.5 times smaller to compare with that obtained by means of each technique separately. Applying Kalman filtering method to the longer observational time span of 7 days allows us to derive EOP variations with subduinal periods.

1. INTRODUCTION

Satellite laser ranging as well as very long baseline interferometry is the most useful techniques used to derive geodynamic information. Now a number of program packages are developed to process observation of different kinds. It is obvious that all these packages consist basically of similar procedures and routines, and only a small fraction of them is specific for each package. It is clear that it is possible to construct a universal program package for any type of ephemeris applications. It is the programming system ERA (Ephemeris Research in Astronomy) that is intended to process different types of high precision observations (Krasinsky, 1997). The use

of the ERA system permits us to obtain Earth orientation parameters from the combination of SLR and VLBI data at the observational level. In particular, mixing SLR measurements of LAGEOS 1 & 2 and Etalon 1 & 2 satellites with the VLBI observations of quasars we can improve all parameters of Earth rotation.

2. DATA ANALYSIS

The data analysis was performed using the software, which is basically follows the IERS Conventions 1996 (McCarthy, 1996). The dynamical model for LAGEOS-type satellites includes the following perturbations:

- Gravitational perturbations due to the Sun, the Moon and planets (JPL DE403 planetary ephemeredes);
- Newtonians terms caused by the non-geodetic motion of the Earth (coupling of the external mass action and the Earth quadrupole moment effect) - indirect acceleration due to the oblateness of the Earth;
- Newtonian perturbing acceleraion due to the Earth's non-sphericity. The Earth gravity field is calculated according to the EGM model truncated to the 20-th degree and order with the following values for the coefficients $\overline{C}_{20}, \overline{C}_{21}, \overline{S}_{21}$ and their rates:

$$\begin{array}{rrrr} & & \dot{\overline{C}}_{20} = & 1.162 \times 10^{-11}/\text{year}, \\ \overline{C}_{21} = & -0.187 \times 10^{-9}, & \dot{\overline{C}}_{21} = & -1.300 \times 10^{-11}/\text{year}, \\ \overline{S}_{21} = & 1.195 \times 10^{-9}, & \dot{\overline{S}}_{21} = & 1.100 \times 10^{-11}/\text{year}. \end{array} \tag{1}$$

- The changes in the geopotential coefficients $\overline{C}_{21}, \overline{S}_{21}$ due to the dynamic polar motion according to the formulas:

$$\begin{aligned} \Delta\overline{C}_{21} &= K_f \overline{C}_{20}\sqrt{3}(x_p(t) - \overline{x}_p(t)), \\ \Delta\overline{S}_{21} &= -K_f \overline{C}_{20}\sqrt{3}(y_p(t) - \overline{y}_p(t)), \end{aligned} \tag{2}$$

where

$K_f = 0.331$;

$\overline{x}_p, \overline{y}_p$ – mean values of $x-$ and $y-$ pole coordinates at the epoch $t_0 = 2000.0$ which are calculated according to formulas:

$$\begin{aligned} \overline{x}_p(t) &= \overline{x}_p(t_0) + \dot{\overline{x}}_p(t_0)(t - t_0), \\ \overline{y}_p(t) &= \overline{y}_p(t_0) + \dot{\overline{y}}_p(t_0)(t - t_0), \end{aligned} \tag{3}$$

with the following numerical values of the mean coordinates and their rates:

$$\begin{aligned} \overline{x}_p(t_0) &= 0.054\text{mas}, \quad \dot{\overline{x}}_p(t_0) = 0.00083\text{mas/year}, \\ \overline{y}_p(t_0) &= 0.357\text{mas}, \quad \dot{\overline{y}}_p(t_0) = 0.00395\text{mas/year}. \end{aligned} \tag{4}$$

- Perturbations due to the direct solar radiation pressure;
- Along-track empirical acceleration (the coefficient is considered to be a solve-for parameter for each orbital arc);
- Relativistic terms (Schwarzschild terms, Lense-Thirring terms due to the Earth rotation, quadrupole terms).

3. OBSERVATIONS AND RESULTS

Laser ranges to geodetic satellites LAGEOS, LAGEOS 2, and Etalon 1&2, and VLBI observations of extragalactic objects obtained within the NEOS–A program were used to derive Earth orientation parameters. Determination of EOP from the joint processing of these measurements was performed by means of two different statistical methods — standard least squares procedure and Kalman filtering method. In both cases short arc technique with the arc length of 7 days was applied to all SLR measurements to adjust orbital parameters along with coefficients to the radiation pressure reflectance model and along track acceleration terms. All these parameters are considered to be non-stochastic. For VLBI measurements zenith component of troposphere delay and its gradients in horizontal and vertical directions are adjusted as stochastic signals on a day of observation. Covariation functions for these parameters were calculated on the basis of the model of troposphere (Stotskii, 1992) and "random walk" procedure for clock modeling described in (Vasilyev, 1999). Neither coordinates of quasars nor site coordinates are not improved in these cases.

Table 1: Corrections to the EOP and their formal uncertainties obtained from different sets of observations.

EOP	VLBI	VLBI+ L1+L2	VLBI+ L1+L2+E1+E2	SLR
x_p (mas)	-0.326	-0.001	0.023	0.099
	86	44	43	86
y_p (mas)	0.034	0.204	0.208	0.202
	84	31	30	82
UT1-UTC (ms)	0.026	0.017	0.015	
	5	4	4	
$d\psi$ (mas)	-0.260	-0.190	-0.182	
	143	133	130	
$d\epsilon$ (mas)	0.240	0.187	0.227	
	72	67	65	

In the first case the SLR and VLBI observations are mixed to determine corrections to variables mentioned above along with all five Earth rotation parameters in the frame of the weighted least squares method. Table 1 illustrates corrections to the Earth orientation parameters to compare with the EOP(IERS) C 04 and their formal uncertainties obtained from different sets of observations (pure VLBI observations or VLBI measurements combined with SLR observations of different satellites — LAGEOS (L1), LAGEOS 2 (L2), Etalon 1 (E1), and Etalon 2 (E2)) on a day period of time. It is clear that combining SLR and VLBI measurements on the short one day arc allows us to get standard deviations of pole coordinates smaller to compare with those obtained by means of each technique separately.

At the second stage Kalman filtering procedure is used to solve the system of conditional equations. Applying the Kalman method to the combination of VLBI and SLR data on the period of one month permits us to derive continuous set of Earth orientation parameters on the whole period with high resolution. Table 2 shows root mean square and formal uncertainties of this one-month EOP set as compared with that of EOP(IERS) C 04.

One can see that both *rms* and formal uncertainties of celestial pole coordinates obtained

Table 2: Formal uncertainties and root mean square residuals of determination of the EOP on 28 days period.

EOP	VLBI+SLR		VLBI		SLR	
	rms	formal	rms	formal	rms	formal
x_p (mas)	0.16	0.06	0.07	0.13	0.23	0.07
y_p (mas)	0.20	0.05	0.16	0.13	0.27	0.06
UT1-UTC (ms)	0.013	0.007	0.011	0.007		
$d\psi$ (mas)	0.27	0.20	0.18	0.22		
$d\epsilon$ (mas)	0.23	0.10	0.24	0.11		

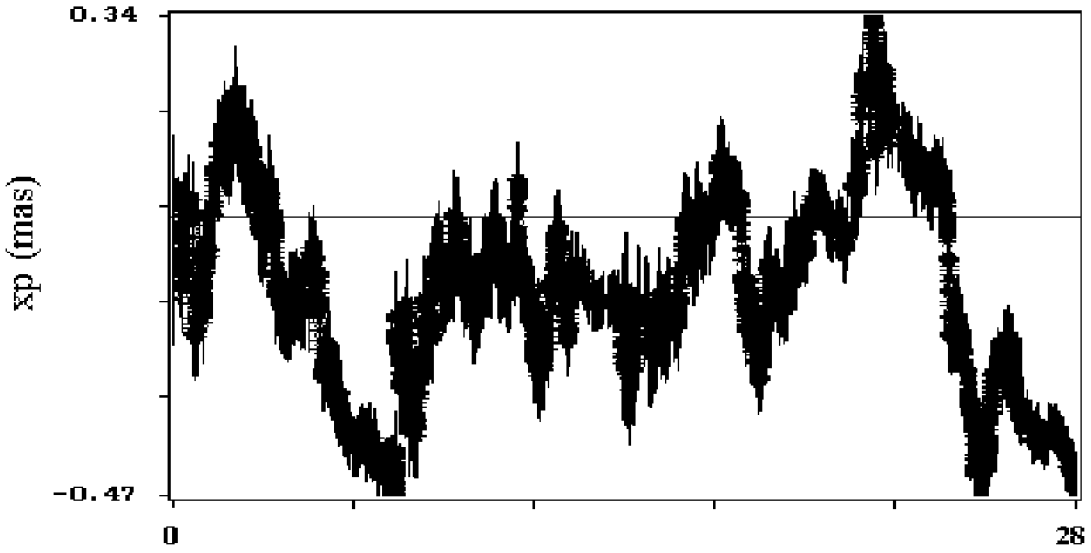

Figure 1: Differences of x_p and EOP(IERS) C 04 derived by means of Kalman filtering.

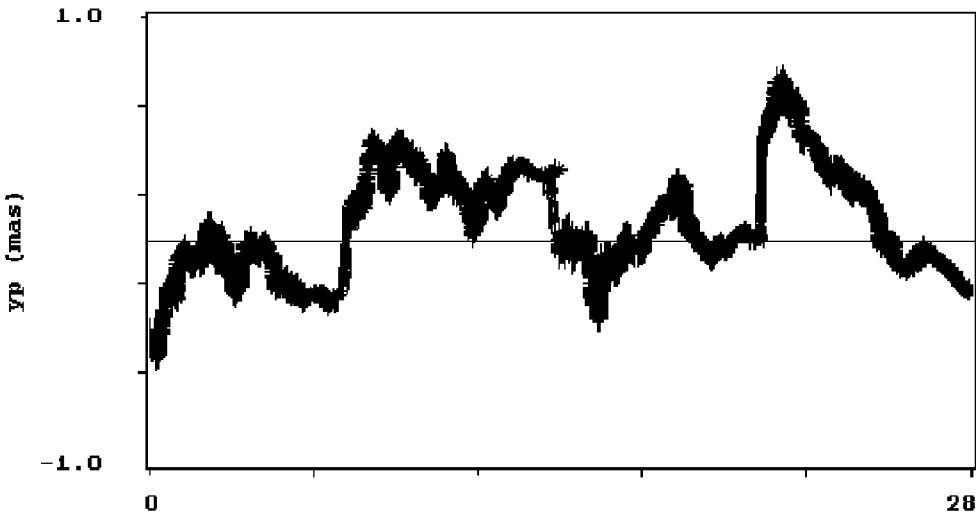

Figure 2: Differences of y_p and EOP(IERS) C 04 derived by means of Kalman filtering.

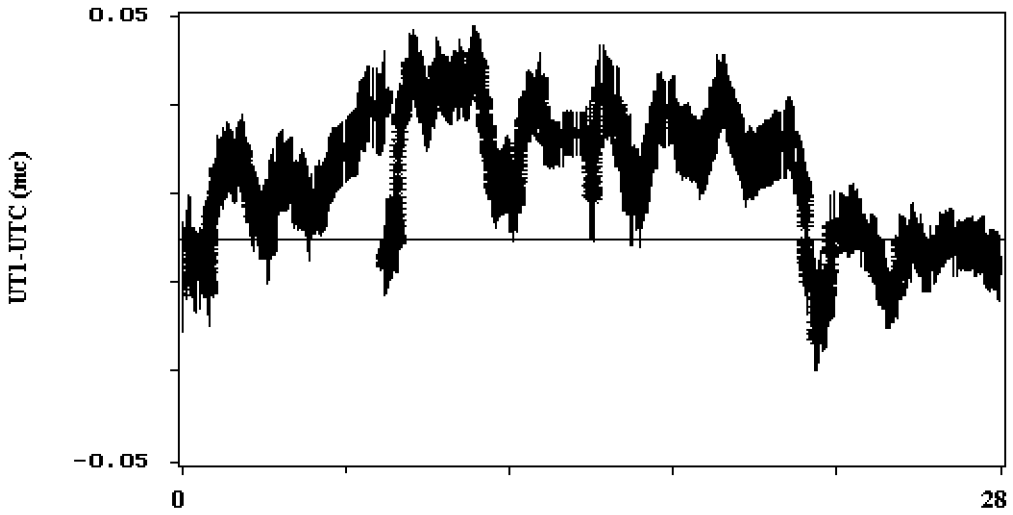

Figure 3: Differences of UT1–UTC and EOP(IERS) C 04 derived by means of Kalman filtering.

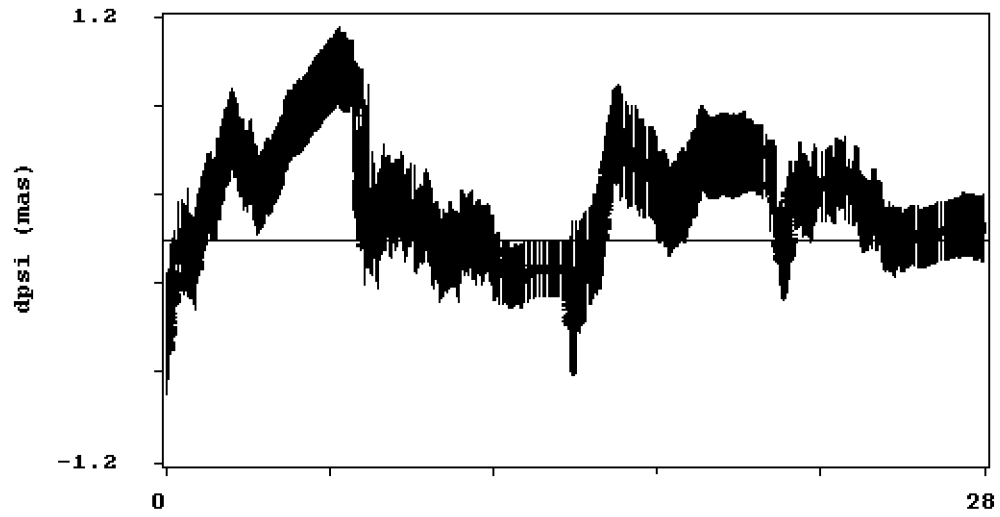

Figure 4: Differences of $d\psi$ and EOP(IERS) C 04 derived by means of Kalman filtering.

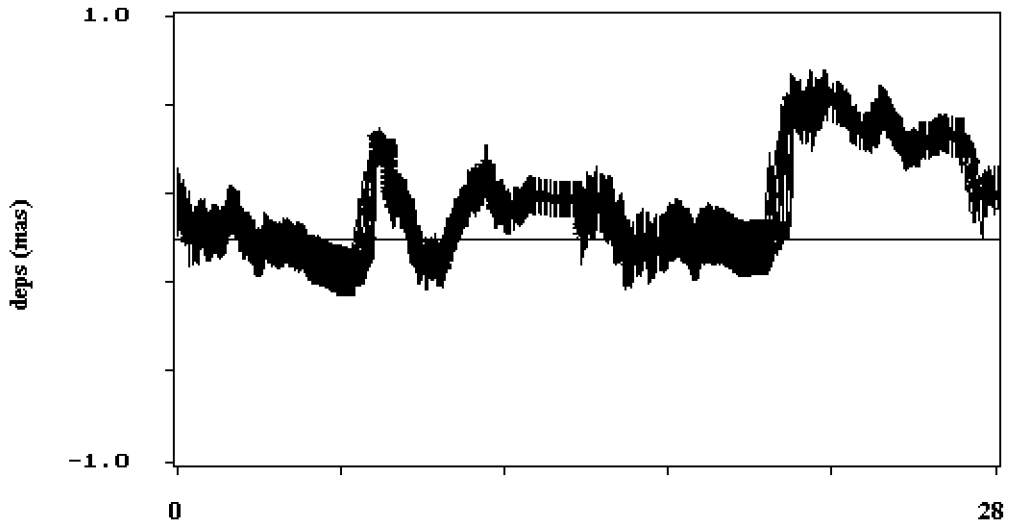

Figure 5: Differences of $d\epsilon$ and EOP(IERS) C 04 derived by means of Kalman filtering.

from combination of SLR and VLBI data are not better then that of derived from each technique separately. But an attaching SLR observations to the VLBI measurements gives us the possibility to determine celestial pole ofsets on the whole period of time (Figures 1–5 illustrate differences between x_p, y_p, UT1–UTC and EOP(IERS) C 04 values derived by means of Kalman filtering procedure).

4. CONCLUSIONS

- It is very important that both SLR and VLBI observations are processed by the same program package, using the same astronomical constants and models for different kinds of measurements;
- Processing both VLBI and SLR observations permits us to obtain all five Earth orientation parameters on the whole time span;
- Application of stochastic estimation to combine observational data allows us to determine continuous set of EOP with high time resolution.

5. REFERENCES

McCarthy, D. D., (ed.)., 1996, IERS Conventions 1996, *Technical Note 21.*

Andersen, P. H., 2003, Combination of the VLBI, GPS and SLR observations at the observation level, *Proc. EGS-AGU-EUG Joint Assembly 2003*, Nice, France, 386.

Shuygina, N. V., 2000, Determination of the Earth rotation parameters from the Lageos SLR and VLBI data, *Proc. Journees 1999 and IX Lohrmann-Kolloquium: Motion of celestial bodies, astrometry and reference frames*, M. Soffel, N. Capitaine (eds.), 214–216.

Yaya, P., 2002, Combination of geodetic techniques to determine the Earth orientation parameters, *Proc. Journees 2001 Influence of geophysics, time and space reference frames on Earth rotation studies*, N. Capitaine (ed.), 46–50.

Stotskii, A. A., 1992, Path length fluctuation through the Earth troposphere: turbulent model and data of observations, *Proc. of the specialist meeting on microwave radiometry and remote sensing applications*, Westmaster R. (ed.), 256–261.

Krasinsky, G. A., Vasilyev, M. V., 1997, ERA: knowledge base for ephemeris and dynamical astronomy, *Proc. IAU Coll. No. 165*, Poznan, Poland, I. M. Wytrzyszczak, J. H. Lieske, R. A. Feldman (eds.), 239–244.

Vasilyev, M., 1999, Real time autonomous orbit determination of GEO satelliteusing GPS, **ION–GPS–99**, Nashville, USA, 451–457.

ON THE USE OF DORIS DATA FOR DETERMINATION OF THE EOP AND GEOCENTER MOTION

S.P. KUZIN, N.A. SOROKIN, S.K. TATEVIAN
Institute of Astronomy of RAS (INASAN)
48, Pyatnizkaya st., 119017, Moscow, Russia
e-mail: statev@inasan.ru

ABSTRACT. This paper presents results of the global DORIS network processing, carried out at the INASAN Analysis Center with the use of measurement data from the "old" satellites (SPOT2 +SPOT4 + TOPEX/POSEIDON) having onboard DORIS receivers for the time period April, 1999 - June,2002. Data analysis was performed with the use of GIPSY/OASIS2 software. The free-network approach for a simultaneous estimation of orbital parameters, station coordinates and Earth's orientation parameters has been applied. Time series of weekly values of Geocenter motion are in good agreement with the results of IGN/JPL analysis center. A regression analysis and a simultaneous estimation by the least square method, have been used for an estimation of the constant term ,linear trend, semi-annual and annual amplitudes and phase of the original time series. Time series of the "geocenter motion" are obtained by the "geometric" method with the use of Helmert transformation of the coordinates of all DORIS stations to the ITRF2000.

The DORIS system was developed by CNES and IGN to meet science and operational user requirements in very precise orbit determination and high accuracy location of ground beacons for point positioning. The main features of the DORIS system are the high accuracy of the Doppler measurements, worldwide and homogeneous distribution of ground beacons, excellent orbital coverage. DORIS data are also relatively simple to process, and this makes DORIS a good technique for the purpose of operational determination of site positions and polar motion. More detailed description of the methods used at the INASAN Analysis Center for DORIS data processing has been described in our previous works [Kuzin S. P. and S. K. Tatevian, 2000; 2002]. The station coordinates are estimated on daily basis using three satellites (SPOT2, SPOT4, TOPEX). In addition to station coordinates, we estimate simultaneously the orbital parameters and several other parameters (EOP, tropospheric corrections, clock drifts offsets) with a free-network approach and weakly constraining the apriori station coordinates to a 100 meters sigma. Then daily solutions are combined into weekly solutions, projected (removing of the indetermination due to loosely definition of the terrestrial reference frame) and transformed to a well defined reference frame using 7 parameters of Helmert transformation. The results of the transformation operation provide simultaneously the coordinates (and full-covariance matrix) and also the estimated 7 parameters of the transformation. Three translations parameters and scale factor are more significant as compared with 3 rotational ones as they can provide information on possible physical variations of the geocenter due to different seasonal mass re-

distribution in the Earth system and due to unstability of the unit of the length that is usually biased by unmodelled effects (ionospheric correction).

We have recomputed DORIS data from all operating beacons of the DORIS network for the period 11.04.1999–01.06.2002 (3 years 2 months, 164 weeks). The data for the satellites having manoeuvres during the processing periods were deleted. All weekly solutions were derived in the same reference frame (ITRF2000) with an accuracy depending on a quality of the DORIS solution itself and on the accuracy of the adopted reference system at the epoch of measurements. Time series of weekly DORIS solutions for coordinates of about forty DORIS stations were obtained. In a whole a repeatability of station coordinates are estimated at the level of 30 mm and standard deviations 1.5–5.0 cm. It can also be seen that besides systematic drift, there are temporal variations depending on the site location and the type of equipment.

Time series of weekly geocenter variations with respect to ITRF00 are shown at Fig.1 for the same time period as stations coordinates. The data have been analysed through the harmonical analysis in order to determine short and long-periodic signals. A constant term and the trend have been estimated in order to express the time series in a common reference frame. For the annual and semiannual variations of the geocenter the amplitudes and phases (refer to 1993.0) are presented in the table 1.

Table 1: Annual and semiannual amplitudes and phases of geocenter variations.

Component	**Annual**		Semiannual		**Trend**
	A, mm	***Phase, deg***	***A, mm***	***Phase, deg***	***mm***
X	5.5 ± 0.2	112.6 ± 5.5	1.3 ± 0.2	157.9 ± 22.6	-1.7 ± 0.1
Y	4.1 ± 0.3	345.8 ± 7.9	6.1 ± 0.5	190.9 ± 3.4	-0.8 ± 0.1
Z	11.5 ± 0.5	322.3 ± 19.1	6.4 ± 2.7	177.6 ± 25.4	1.7 ± 0.7
S (scale)	0.3 ± 0.5	278.1 ± 11.0	0.6 ± 0.05	170.4 ± 6.5	-0.02 ± 0.01

Annual and semiannual phases are referred to 1993.0

The obtained values are comparable in amplitudes with the results from previous DORIS geocenter analysis [C.Boucher, P.Sillard, 1999]. The phases are different. The greater amplitude for z may be caused by the dominance of seasonal mass redistributions between the northern and southern hemisphere [H. Montag, 1999]. Additionally to the annual and semiannual signals several other more shorter periods (a fortnight and of one to four months) were found and it must be noted that the amplitudes of some short-periodic signals are comparable with the amplitudes of the semiannual signals.

SUMMARY

Center of mass variations must be properly accounted for in the realization of the tracking station locations within the reference frame, that is especially important for the altimeter measurements of sea-level and plate tectonics studies. Geocenter motions as determined using DORIS data, are of the order of 7-10 mm in each coordinate, but secular trends in the geocenter components may be more carefully surveyed for long-term measurements of sea-level change and some other geophysical phenomena.

Due to relatively simple technique of data processing, DORIS is a good technique for the purpose of operational determination of the polar motion. But as the satellites, having on board DORIS systems, are not specially dedicated to the geodynamic studies, the best precision on polar motion now is in the range of 0,5-0,8 milliarcseconds. Improvements in the accuracy of

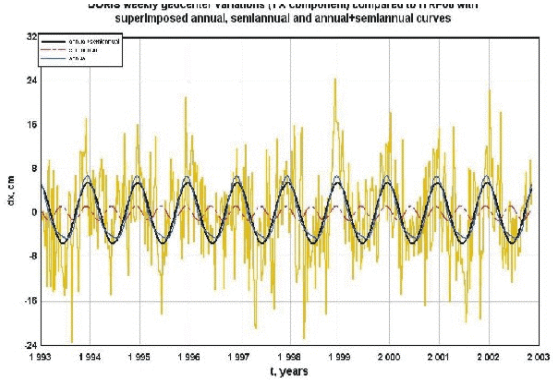
superImposed annual, semiannual and annual+semiannual curves
dX, cm
t, years

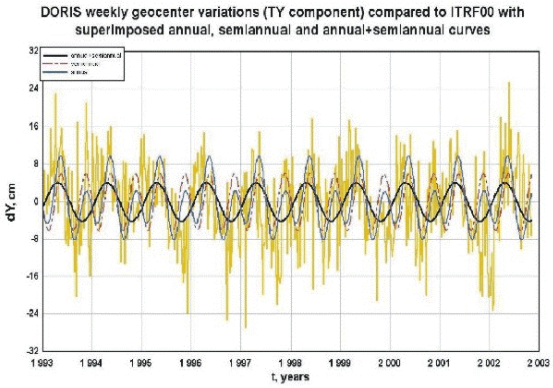
DORIS weekly geocenter variations (TY component) compared to ITRF00 with
superImposed annual, semiannual and annual+semiannual curves
dY, cm
t, years

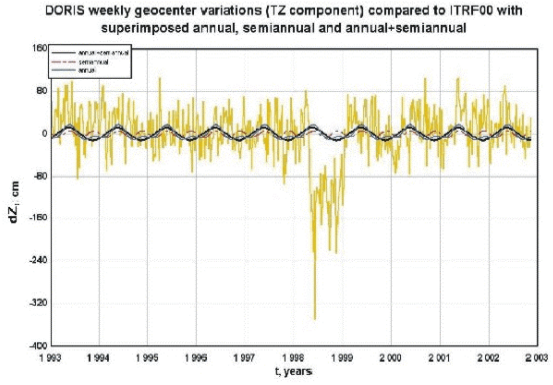
DORIS weekly geocenter variations (TZ component) compared to ITRF00 with
superimposed annual, semiannual and annual+semiannual
dZ, cm
t, years

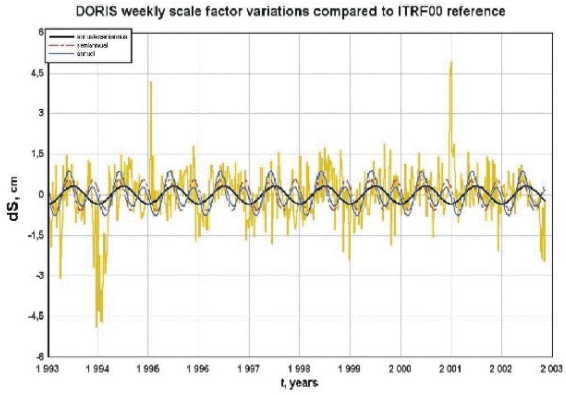
DORIS weekly scale factor variations compared to ITRF00 reference
dS, cm
t, years

the DORIS polar motion monitoring are anticipated with the launch of new spacecrafts equiped with new receivers, which will provide lower measurement noise and better accuracy of orbital parameters.

Our investigations will be continued for the analysis of more longer time series of stations coordinates, EOP and geocenter variations.

REFERENCES

Kuzin, S. P., Tatevian, S. K., 2000, DORIS data analysis at the Institute of Astronomy of RAS, *Proceedings of "DORIS DAYS"*, May 1–3, 2000, Toulouse, France.

Kuzin, S. P., Tatevian, S. K., 2002, On computation of weekly DORIS solutions for 1999-2001 time period, *Proceedings of the IDS workshop*, Biarritz, France, June 13–14, 2002.
http : *//ids.cls.fr/html/report/ids_workshop_*2002*/programme.html*.

Boucher, C., Sillard, P., 1999, Synthesis of submitted geocenter time series, *IERS Technical Note 25*, IERS Analysis Campaign to Investigate Motions of the Geocenter, J. Ray (ed.), April 1999.

Montag, H., 1999, Geocenter motions derived by different satellite methods, *IERS Technical Note 25*, IERS Analysis Campaign to Investigate Motions of the Geocenter, J. Ray (ed.), April 1999.

VARIATIONS OF $\bar{C}_{21}, \bar{S}_{21}$ GEOPOTENTIAL COEFFICIENTS FROM SLR DATA OF LAGEOS SATELLITES

I.S. GAYAZOV
Institute of applied astronomy of RAS
10 Kutuzovskaya quay, 191187 St.Petersburg, Russia
e-mail: gayazov@ipa.nw.ru

ABSTRACT. SLR data of Lageos 1 and Lageos 2 satellites on 8-year time span have been processed to analyse long-term variations of $\bar{C}_{21}, \bar{S}_{21}$ geopotential coefficients. The first-degree harmonic coefficients $\bar{C}_{10}, \bar{C}_{11}, \bar{S}_{11}$ which are equivalent to the geocenter offsets and the corrections to $\bar{C}_{20}$ coefficient were also included in 10-day solutions together with orbital parameters and along-track accelerations of satellites. The aim of the work was to verify the adequacy of the dynamic pole tide formulation in the latest issue of IERS Conventions. Monthly averaged values of corrections to $\bar{C}_{21}, \bar{S}_{21}$ coefficients does not show explicit long-term variations. The analysis also allowed to determine corrections to the linear model based on the mean rotational pole path of the Earth.

1. INTRODUCTION

Determination of the geopotential coefficients $\bar{C}_{21}$ and $\bar{S}_{21}$ is essential for relating the Earth gravity field to the reference coordinate system. Monitoring of these coefficients can also provide with important information about the Earth core-mantle dynamics (Wahr,1987), (Wahr, 1991), (Greiner-Mai and Barthelmes, 2001), but for a long time the accessibility of their variations from satellite observations was not obvious (Gegout and Cazenave, 1993). A number of investigations of last years devoted to analysis of temporal variations of the geopotential contain results on coefficients $\bar{C}_{21}, \bar{S}_{21}$ as well (Cheng et al, 1997), (Eanes et al, 1997), (Pavlis, 2002).

In this connection it should be particularly mentioned the analysis by the research group from CSR of Texas university (Eanes et al, 1997), where the temporal variations of the second-degree geopotential coefficients were determined from SLR data of Lageos satellites. It was found that the $\bar{C}_{21}$ and $\bar{S}_{21}$ time series on 5-year time interval have a variability correlated to polar motion. This result could be explained by errors in the nominal model of the Earth rotational deformations. We were interested in analysing this effect since the following innovations have been made by IERS:

1) The formulation of mean $\bar{C}_{21}, \bar{S}_{21}$ coefficients and the rotational deformations of the Earth has been revised in IERS Conventions 2000 (McCarthy, 2000);

2) New geopotential model EGM96 (Lemoine et al., 1998) has been released and recommended by IERS Conventions instead of JGM3.

2. DATA ANALYSIS

It is expected that the implementation of the new satellite projects based on new observation techniques will result in essential increasing the accuracy of the geopotential coefficients up to level of 10^{-12}. However, this optimistic prognosis concerns mainly the coefficients in high-frequency area. As for the lowest degree harmonic coefficients first results from GRACE project (GRACE, 2003), (Reigber et.al., 2003) show (Table 1), that the accuracy of their determination is not better than in models derived by traditional satellite geodesy methods.

Table 1. Errors of low-degree harmonic coefficients in the recent gravity models (units: 10^{-10}).

l m	EGM-96 (GSFC, NIMA)	GGM01-GRACE (CSR)	EIGEN-GRACE (GFZ)
2 0	0.36	2.65	3.11
2 1	-	0.77	1.57
2 2	0.54	0.85	1.26
3 0	0.18	0.45	0.44
3 1	1.40	0.64	0.52
3 2	1.11	0.90	0.71
3 3	0.95	1.24	0.69

Thus, the analysis of laser observations of geodynamic satellites on long time intervals can be still considered as a reasonable tool for determination of low-degree harmonic coefficients of the geopotential and their variations.

GRAPE program package (Gayazov et al, 2000) developed at the IAA for processing GPS and SLR data has been used for the data analysis. All dynamic and kinematic models in this package follow the IERS Conventions (McCarthy, 2000). Coefficients of the gravity model EGM96 (Lemoine et al, 1998) up to degree and order (20 x 20) were taken into account in orbital calculations. For accounting the ocean tide effects on satellite orbits the combination of EGM96S and GOT99.2b (Ray R., 1999) models has been used. Considering that the short-term tides are given more accurately in the GOT99.2b model, we used it for diurnal and semidiurnal tides, whereas the long-term ocean tide coefficients were taken from EGM96S model. Fixed IERS C04 series for Earth rotation parameters and ITRF2000 station coordinates were used in all calculations.

Lageos 1 and Lageos 2 laser observations on 8-year time span from 49800 MJD to 52800 MJD have been processed. The data analysis was performed in the following two steps:

1) adjustment of parameters for 10-day orbital arcs;

2) forming the series of 30-day averages of harmonic coefficients and their analysis.

The set of free parameters for each orbital arc included:

– Initial state vectors of satellites;

– Along-track accelerations;

– 6 harmonic coefficients ($\bar{C}_{10}, \bar{C}_{11}, \bar{S}_{11}, \bar{C}_{20}, \bar{C}_{21}, \bar{S}_{21}$).

Including of the first-degree coefficients to the set of adjusted parameters is natural, because they are responsible for translation of the gravity field to the Earth fixed system, while $\bar{C}_{21}$ and $\bar{S}_{21}$ coefficients determine its orientation.

The model values of coefficients $\bar{C}_{21}, \bar{S}_{21}$, were calculated according to IERS Conventions

$$\begin{aligned} \bar{C}_{21}(t) &= \bar{C}_{21}(t_0) + \dot{\bar{C}}_{21}(t - t_0) + \Delta\bar{C}_{21}(RD) + \Delta\bar{C}_{21}(TD), \\ \bar{S}_{21}(t) &= \bar{S}_{21}(t_0) + \dot{\bar{S}}_{21}(t - t_0) + \Delta\bar{S}_{21}(RD) + \Delta\bar{S}_{21}(TD), \end{aligned}$$

where mean values of coefficients are determined by

$$\begin{aligned} \bar{C}_{21}(t) &= -2.23 \cdot 10^{-10} - 0.337 \cdot 10^{-11}(t - t_0), \\ \bar{S}_{21}(t) &= 14.48 \cdot 10^{-10} + 1.606 \cdot 10^{-11}(t - t_0), \end{aligned}$$

for the reference epoch $t_0 = 2000.0$ and t is time in years. Terms with RD and TD refer to rotational and tidal deformations correspondingly. Different components of these coefficients give rise to various perturbations in satellite orbits. The characteristic values of orbital perturbations for Lageos satellites are given in Table 2.

Table 2. Perturbations in Lageos orbits due to $\bar{C}_{21}, \bar{S}_{21}$ coefficients.

Components in $\bar{C}_{21}, \bar{S}_{21}$	Periods	Amplitudes
Constant, linear	1 d	10–12 cm
Long-term (rotational deformations)	1 d	5–6 cm
Short-term (lunar and solar tides)	10–6000 d	up to 500 m

When analysing the observations on 10-day orbital arcs we intended to use the sensitivity of short-term perturbations to linear and long-term components of the coefficients and determined corrections to their model values.

3. RESULTS

Common characteristics of 10-day arc solutions are summarised in Table 3.

Table 3. Summary of SLR data analysis.

Number of observations per arc	1500 - 5000
RMS of SLR data residuals	2 - 6 cm
Formal errors of determined coefficients	$(1 - 5) \cdot 10^{-11}$

Figures 1 and 2 present monthly averages of determined corrections to $\bar{C}_{21}, \bar{S}_{21}$ coefficients and results of their spectral analysis. As it could be seen from Fig. 2, there are no dominating peeks in the vicinity of chandler period. It can be considered as a result of adequate accounting the effect of rotational deformations according to the latest IERS Conventions.

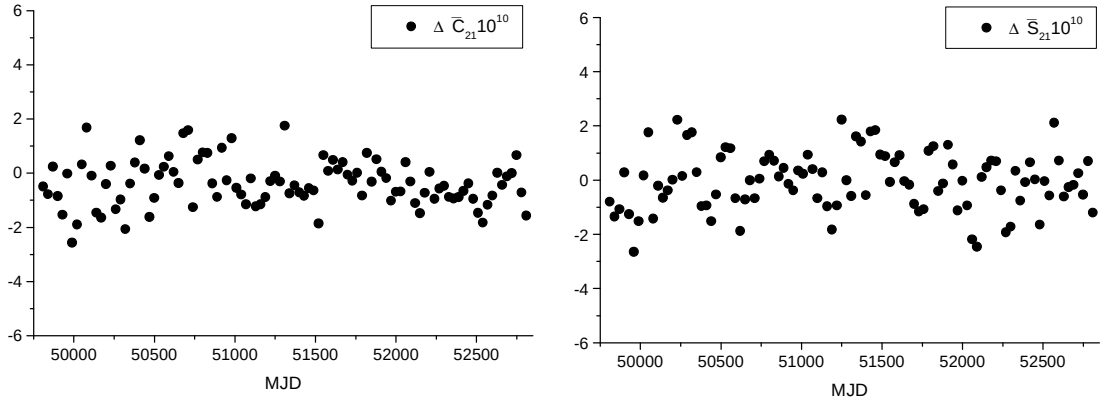

Figure 1: Monthly averages of corrections to $\bar{C}_{21}, \bar{S}_{21}$. coefficients

Averaging results on the 8-year time interval we have found the following corrections to the mean coefficients at epoch 2000.0

$$\begin{aligned} \Delta\bar{C}_{21}(2000.0) &= (-4.1 \pm 0.8) \cdot 10^{-11}, \\ \Delta\bar{S}_{21}(2000.0) &= (-0.5 \pm 1.0) \cdot 10^{-11}, \end{aligned}$$

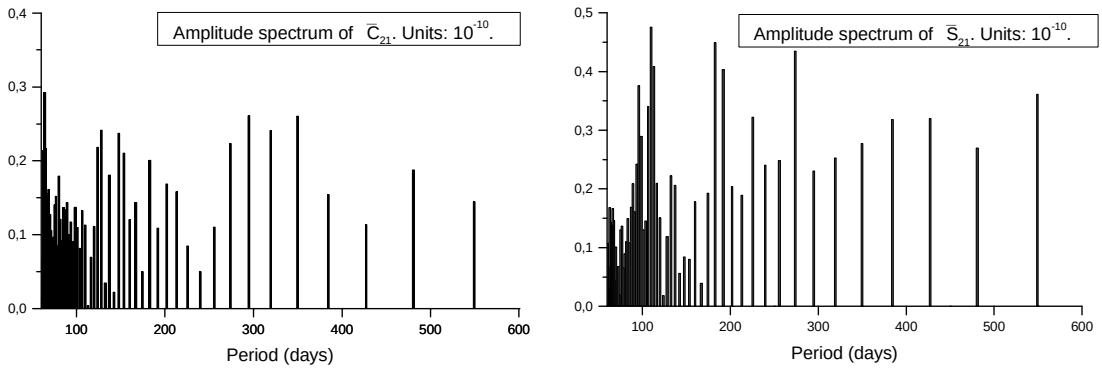

Figure 2: Amplitude spectra of $\Delta\bar{C}_{21}$ and $\Delta\bar{S}_{21}$.

and to their rates

$$\begin{aligned}\Delta\dot{\bar{C}}_{21} &= (-0.26 \pm 0.23) \cdot 10^{-11}\ y^{-1},\\ \Delta\dot{\bar{S}}_{21} &= (+0.08 \pm 0.29) \cdot 10^{-11}\ y^{-1}.\end{aligned}$$

Obtained coefficients as compared with other recent results are presented in Fig. 3.

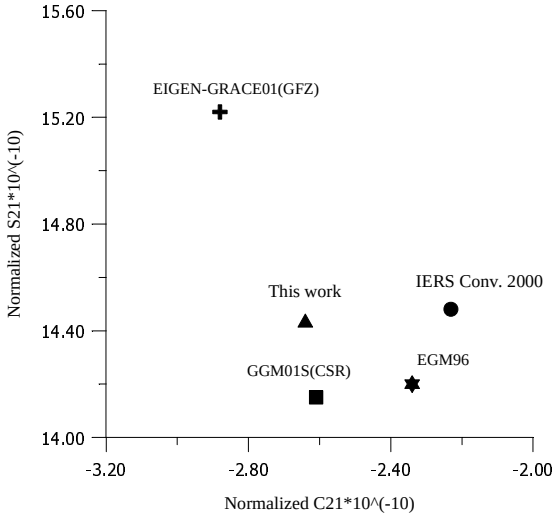

Figure 3: Comparing results for $\bar{C}_{21}, \bar{S}_{21}$ coefficients.

It should be mentioned that the coefficients $\bar{C}_{21}, \bar{S}_{21}$ derived from the satellite motion analysis correspond to the mean figure axis but not to the mean rotation pole. Using the relation between mean pole coordinates and $\bar{C}_{21}, \bar{S}_{21}$ (McCarthy, 2000) we transformed our coefficients to linear trends in the mean figure axis. They are shown in Fig. 4 against the background of mean rotation pole path from IERS Conventions. The significant difference in X-coordinate of the figure axis can be analysed in further investigations.

We also present here results for the geocenter offsets T_x, T_y, T_z. They were calculated from our series of harmonic coefficients $\bar{C}_{11}, \bar{S}_{11}, \bar{C}_{10}$ using the following well known relations

$$\begin{aligned}T_x &= \sqrt{3} R_e \bar{C}_{11},\\ T_y &= \sqrt{3} R_e \bar{S}_{11},\\ T_z &= \sqrt{3} R_e \bar{C}_{10},\end{aligned}$$

where $R_e = 6.378 \cdot 10^9$ mm.

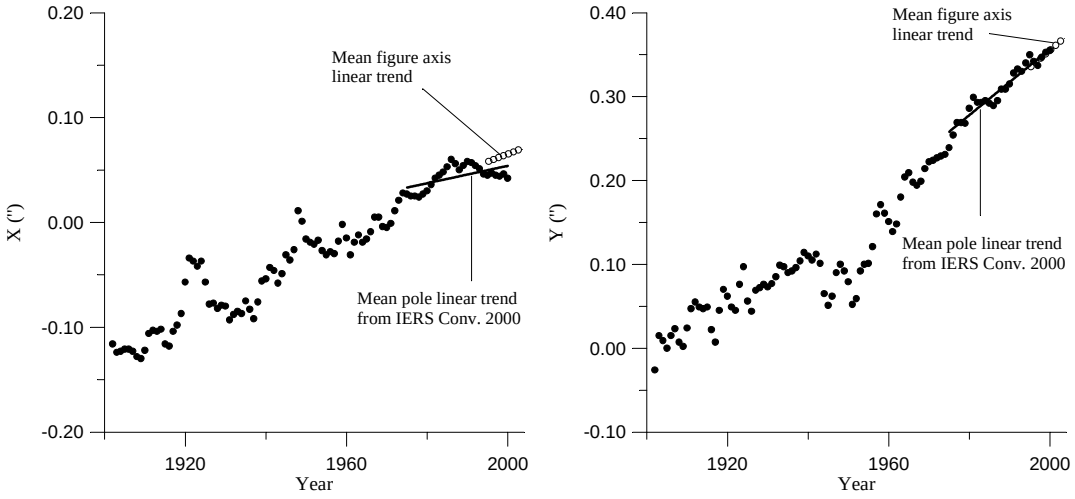

Figure 4: Coordinates of the determined mean figure axis and the IERS mean pole.

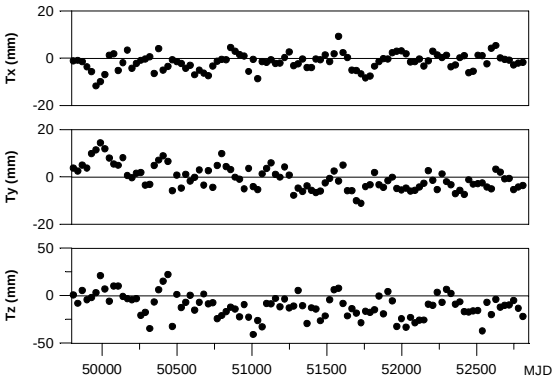

Figure 5: Geocenter offsets.

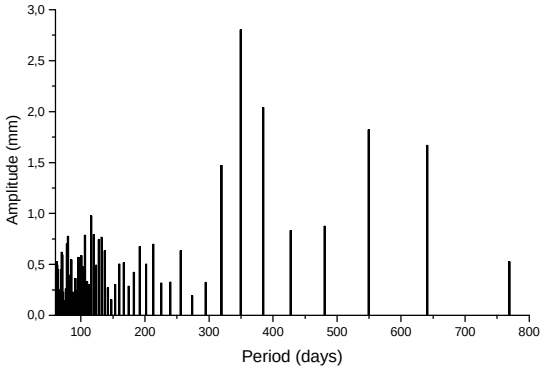

Figure 6: Amplitude spectrum of T_x.

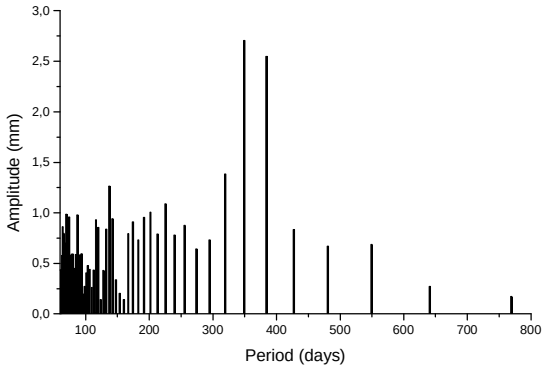

Figure 7: Amplitude spectrum of T_y.

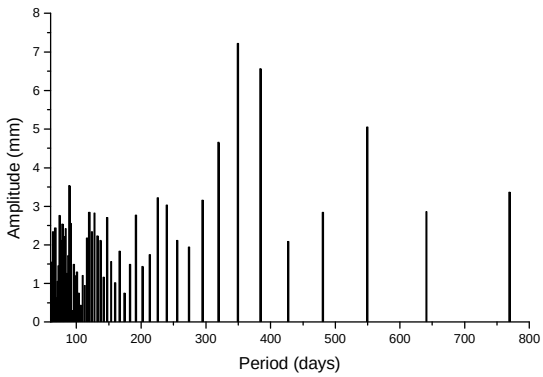

Figure 8: Amplitude spectrum of T_z.

Monthly averaged geocenter offsets are presented in Fig. 5 and their amplitude spectra are shown in Fig. 6 - 8. Amplitudes of annual period found from this analysis are 2.5 ± 0.4 mm, 2.8 ± 0.5 mm, 7.1 ± 1.6 mm for T_x, T_y, T_z correspondingly. They are in good agreement with other results obtained during the geocenter motion analysis campaign (Ray J., 1999).

4. REFERENCES

Cheng, M. K., Shum, C. K., Tapley, B. D., 1997, Determination of long-term changes in the Earth's gravity field from satellite laser ranging observations, *J. Geophys. Res.*, **102**, 22377–22390.

Eanes, R., et al., 1997, Observations of zonal and Non-zonal Mass Redistribution using SLR, *Suppl. EOS Transact.*, **78**, N 46.

Gayazov, I. S., Keshin, M. O., Fominov, A. M., 2000, GRAPE software for GPS data processing: first results of ERP determinations, IGS Network Workshop 12-14 July 2000, Oslo, Extended abstracts.

Gegout, P., and Cazenave, A., 1993, Temporal variations of the Earth gravity field for 1985–1989 derived from Lageos, *Geophys. J. Int.*, **114**, N 2, 347–359.

GRACE Gravity Model GGM01, 2003, Internet http://www.csr.utexas.edu /grace/.

Greiner-Mai, H., and Barthelmes, F., 2001, Relative wobble of the Earth's inner core derived from polar motion and associated gravity variations., *Geophys. J. Int.*, **144**, N 1, 27–36.

Lemoine, F. G., et al., 1998, The Development of the Joint NASA GSFC and National Imagery and Mapping Agency (NIMA) Geopotential Model EGM96, NASA/TP-1998-206861, GSFC.

McCarthy, D. D. (ed.)., 2000, IERS Conventions 2000, Internet http://maia.usno.navy.mil/conv2000.html.

Pavlis, E. C., 2002, EOP from laser ranging to LAGEOS and ETALON satellites, Presented at IERS Workshop on Combination Research and Global Geophysical Fluids, Munich, Germany, Nov.18-21.

Ray, R. D., 1999, A global ocean tide model from Topex/Poseidon altimetry: GOT99.2, NASA Tech. Memo. 209478, GSFC. FTP server ftp://geodesy.gsfc.nasa.gov/dist/ray/GOT99.2b.

Ray, J. (ed.)., 1999, IERS Analysis Campaign to Investigate Motions of Geocenter, IERS Technical Note 25.

Reigber, Ch., et al., 2003, First EIGEN Gravity Field Model based on GRACE Mission Data Only (in prep. for GRL), Internet http://www.gfz-potsdam.de/grace/.

Wahr, J. M., 1987, The Earth's C_{21} and S_{21} gravity coefficients and the rotation of the core, *Geophys. J. R. Astron. Soc.*, **88**, 265–276.

Wahr, J. M., 1990, Corrections and update "The Earth's C_{21} and S_{21} gravity coefficients and the rotation of the core", *Geophys. J. Int.*, **101**, 3, 709–711.

NEW APPROACH TO DEVELOPMENT OF MOON ROTATION THEORY

J.M. FERRANDIZ[1], YU.V. BARKIN[1,2]
[1] Alicante University, Department of Applied Mathematics. Spain
E-mail: jm.ferrandiz@ua.es
[2] Sternberg Astronomical Institute, Moscow, Russia

The external shell of the Moon (its mantle) is considered as non-spherical, rigid layer. Inner shell is liquid core, which occupies ellipsoidal cavity of the Moon. The motion of two-layer Moon is considered in gravitational fields of the Moon and Sun. For study we use combination of two methods. First method was developed earlier and applied for study of interaction in the Earth core-mantle system due to Moon and Sun attraction and was applied in Earth rotation theory (Ferrandiz, Barkin, 2001). Another method is an analytical method of construction of the resonant rotational motion of synchronous satellites and Mercury, considered as non-spherical rigid bodies. This method have been applied to construction of analytical theory of Moon rotation (Barkin, 1989) and here we modified this method with purpose to apply it to study of resonance rotation of two-layer Moon.

Main resonant properties of the Moon motion are described by Cassini's laws (Cassini, 1693) and studied by the famous scientists on the base of rigid and non-spherical Moon models. And here in first we have been obtained and formulated these laws and their generalization for two-layer Moon model. New fine resonant effect was studied and perturbations of the first and second order have been described in analytical form. Our purpose also was to obtain evaluations of periods of free core nutation for some model of the Moon. Canonical equations of motion in Andoyer and Poincare variables were constructed for considered problem in form the more convenient for application of mentioned methods. Force function of considered mechanical system (we take into account second and third harmonics) was constructed. Obtained results illustrate important phenomena of core-mantle interaction of the Moon.

Generalized Cassini's laws for two-layer model of the Moon were described as specially-constructed generating solution on the base of average equations of the first order. They consist additional regularities to classical Cassini's laws connected with liquid core.

1. Vectors of angular velocities and angular momentums of the core and Moon coincide with its polar axis of inertia.

2. The mantle-core system of the Moon rotates as one rigid body about polar axis of inertia in direction of its orbital motion with constant angular velocity equal to mean orbital motion with respect to geocentric ecliptic reference system connected and rotated with mean node of lunar orbit on ecliptic plane. One from the equatorial axes of inertia in mean motion is oriented to the Earth centre.

3. Mean ascending node of the lunar orbit on ecliptic coincides with mean descending node of general plane orthogonal to vectors of angular momentums of the core and Moon, to angular velocity of the Moon. This plane coincides with lunar equator. Normal to ecliptic plane, to equator plane, vectors of angular momentums of the Moon and its core, vector angular velocity

of the Moon are situated in one plane orthogonal to ecliptic plane.

4. Angular momentums of the Moon and its core (and also angular velocity of the Moon) form constant angle with normal to ecliptic plane which equal $\rho = 1^{o}32'48''$ and it is determined from equation (12), (13) in dependence from precession of lunar orbit plane, from fine resonant properties of perturbations in translatory-rotary motion of the Moon and from dynamical oblatenesses of the Moon.

On the next step we have analyzed frequencies of free oscillations of core-mantle system of the Moon. On the base of known data about Moon structure (we have used model of axisymmetrical lunar core of Williams et al. (2003)) we have been obtained the following model values (evaluations) of moments of inertia of the Moon and its core:A=0.393751244, B=0.39384103, C=0.3940000;A_c=0.000236211, C_c=0.000236258(1 unit=mR^2,m and R is a mass and a mean radius of the Moon). Corresponding periods of oscillations were determined on the base of analytical formulae of a developed theory. They are equal:T_1=53855 days and T_2=0.99980095 T_F (T_F=27.212231 days is a sinodic period). Last period determines long period of relative oscillation of the core and mantle T_r=136683 days. The mentioned periods are equal:T_1=147.5 years, T_r=374.2 years. Difference in periods of rotational motion and free oscillation for the Moon consists 7.800 min. For the Earth system this difference consists 4.464 min.

A new effect of a splitting of vectors of angular momentums of the Moon and its core has been established in result of analysis of the role of third harmonic of the force function. The small mutual inclination of angular momentum vectors of the mantle and liquid core (angular splitting in 0.0327 arcsec) was discovered and described analytically.

Developed method let us consecutively determine constant and pure conditionally-periodic perturbations of the first, second and more higher orders for all Poincare variables. Analytical formulae for perturbations in rotation of two-layer Moon were obtained for Andoyer and Poincare variables and their amplitudes were evaluated. General scheme of construction of perturbations of second and higher orders was described. Next stage presents a more difficult problem on construction of solution in neighborhood of discussed in this paper solution. For rigid model of the Moon last problem has been solved earlier and perturbations (including perturbations of the fifth order) were constructed (Barkin, 1989).

Barkin's work was accepted by grant SAB2000-0235 of Ministry of Education of Spain and partially by grants AYA2001-0787 and ESP2001-4533.

REFERENCES

Barkin, Yu. V., 1989, Dynamics of system of non-spherical celestial bodies and rotation theory of the Moon, *Doctoral dissertation*, Moscow State University, Moscow, 412 p.

Cassini, J. D., Traite de l'origine et du progress de l'astronomie, Paris.

Ferrandiz, J. M., Barkin, Yu. V., 2001, Dynamics of the rotational motion of the planet with the elastic mantle, liquid core and with the changeable external shell, *Proc. of Intern. Conf. "AstroKazan-2001", Astronomy and geodesy in new millennium (24-29 September 2001)*, KSU: Publisher "DAS", 123–129.

Williams, J. G., Boggs, D. H., Ratcliff, J. T., Dickey, J. O., 2003, Lunar rotation and the lunar interior, *Lunar and Planetary Science*, XXXIV, 1161.pdf.

MERCURY RESONANT ROTATION

YU.V. BARKIN[1,2], J.M. FERRANDIZ[2]
[1] Sternberg Astronomical Institute, Moscow, Russia
E-mail: barkin@sai.msu.ru
[2] Alicante University, Department of Applied Mathematics
E-mail: jm.ferrandiz@ua.es

Present significance of the study of rotation of Mercury considered as a core-mantle system arises from planned Mercury missions. New high accurate data on Mercury's structure and its physical fields are expected from BepiColombo mission (Anselmi et al., 2001). Investigation of resonant rotation of Mercury, begun by Colombo G. (1966), will play here main part.

New approach to the study of Mercury dynamics and the construction of analytical theory of its resonant rotation is suggested. Within these approach Mercury is considered as a system of two non-spherical interacting bodies: a core and a mantle.The mantle of Mercury is considered as non-spherical, rigid (or elastic) layer. Inner shell is a liquid core, which occupies a large ellipsoidal cavity of Mercury. This Mercury system moves in the gravitational field of the Sun in resonant traslatory-rotary regime of the resonance 3:2. We take into account only the second harmonic of the force function of the Sun and Mercury. For the study of Mercury rotation we have been used specially designed canonical equations of motion in Andoyer and Poincare variables, more convenient for the application of mentioned methods. Approximate observational and some theoretical evaluations of the two main coefficients of Mercury gravitational field J_2 and C_{22} are known. From observational data of Mariner-10 mission were obtained some first evaluations of these coefficients: $J_2 = (8 \pm 6) \cdot 10^{-5}$ (Esposito et al., 1977); $J_2 = (6 \pm 2) \cdot 10^{-5}$ and $C_{22} = (1.0 \pm 0.5) \cdot 10^{-5}$ (Anderson et al., 1987). Some theoretical evaluation of ratio of these coefficients has been obtained on the base of study of periodic motions of the system of two non-spherical gravitating bodies (Barkin, 1976). Corresponding values of coefficients consist: $J_2 = 8 \cdot 10^{-5}$ and $C_{22} = 0.33 \cdot 10^{-5}$. We have no data about non-sphericity of inner core of Mercury.

There are also some evaluations of moments of inertia Mercury and its core: $C/(mR^2) = 0.35, C_m/C = 0.5 \pm 0.07$ (Peal, 1996). Here C and C_m are the moments of inertia of the full Mercury and of its core, m and R is a mass and a mean radius of Mercury.

Based on two methods, we consider the rotation of Mercury in the gravitational field of the Sun. First method of perturbation has been effectively applied to the construction of a rotational theory of the Earth for its models as two or three layer celestial body moving in gravitational fields of the Moon, Sun and planets in wide set of papers ranging in 1999–2001 years of Ferrandiz J. M. and Getino J.(2001). Another method is an analytical method of construction of the resonant rotational motion of synchronous satellites and Mercury, considered as non-spherical rigid bodies. This method has been applied earlier to construction of an analytical theory of rotation of the Moon considered as rigid non-spherical body (Barkin, 1989). Here we modified these methods to apply them to the study of the resonant rotation of a two-layer Mercury. By this we use very effective for the application of perturbation methods and dynamical geometrical

illustration the canonical equations in Andoyer and Poincare variables. Main resonant properties of Mercury motion were been described first as generalized Cassini's laws (Colombo, 1966). But Colombo and some another scientists considered Mercury as rigid non-spherical body sometimes taking into account tidal deformation. Here we have been obtained and formulated these laws and their generalization for a two-layer model of Mercury.

1. Vectors of angular velocities and angular momentums of the core and Moon coincide with its polar axis of inertia. 2. The mantle-core system of Mercury rotates as one rigid body about polar axis of inertia in direction of its orbital motion with constant angular velocity equal 3/2 from the mean orbital motion of Mercury. 3. Mean ascending node of the Mercury orbit on invariable (ecliptic) plane coincides with the mean descending node of the general plane orthogonal to vectors of angular momentums of the core and Mercury. 4. Angular momentums of Mercury and its core make a constant small angle with the normal to ecliptic plane which depends from dynamical oblatenesses of Mercury, from a precession velocity of Mercury orbit plane and oth.

On the next step we have evaluated frequencies of free oscillations of core-mantle system of Mercury. Based on the mentioned data about Mercury (Barkin, 1976) we have been obtained the following model values of moments of inertia of Mercury and its core: A=0.3499534, B=0.3499667, C=0.35; A_c=0.1749767, C_c=0.175000 (1 unit=mR^2, m and R is a mass and a mean radius of Mercury). Here we used model values for moments of inertia of the core using also some analogy with axysimmetrical model of the core of the Moon from the paper Williams et al.(2003). Corresponding periods of free oscillations were determined on the base specially constructed equations of developed theory. They are equal: T_1=260543$\cdot T_{rot}$ days and T_2 = 0.999468$\cdot T_{rot}$ (T_{rot}=58.6462 days is a period of Mercury rotation). Last period determines long period of relative oscillation of the core and mantle T_r=302 years. The mentioned period T_1=713 years.

Algorithm of calculations of perturbations of first and high order in Mercury resonant rotation in neighborhood of Cassini-Colombo motion have been developed.

Barkin's work was accepted by grant SAB2000-0235 of Ministry of Education of Spain and partially by grants AYA2001-0787 and ESP2001-4533 is also acknowledged.

REFERENCES

Anderson J. D., Colombo G., Esposito P. B., Lau E. L., Trager G. B., 1987, The mass, gravity field and ephemeris of Mercury, *Icarus*, 337–349.

Anselmi A., Scoon G. E. N., 2001, BepiColombo, ESA's Mercury Cornerstone mission, *Planetary and Space Science*, **49**, 1409–1420.

Barkin Yu. V., 1976, About plane periodic motions of a rigid body in gravitational field of a sphere, *Astron. J.*, **53**, 1110–1119 in Russian.

Barkin Yu. V., 1987, An analytical theory of the lunar rotational motion, *Proc. Int. Symp. "Figure and Dynamics of Earth, Moon and Planets"* (September 1986, Prague), Monograph series of VUGTK, Prague, 657–677.

Colombo G., 1966, Cassini's second and third laws, *Astron. J.*, **71**, 891.

Esposito P. B., Anderson J. D., Ng A.T.Y., 1977, Experimental determination of Mercury's mass and oblateness, *Space Res.*, **17**, 639–644.

Getino J., Ferrandiz J. M., 2001, Forced nutations of a two-layer earth model, *Mon. Not. R. Astr.Soc.*, **322**, N 4, 785–799.

Peal S. J., 1996, Characterizing the core of Mercury, *LPS XXVII*, 1168.

TEMPORAL VARIATIONS OF THE GRAVITY FIELD AND EARTH PRECESSION–NUTATION

G. BOURDA, N. CAPITAINE
SYRTE - UMR8630/CNRS, Observatoire de Paris
61 avenue de l'Observatoire - 75014 Paris, France
e-mail: Geraldine.Bourda@obspm.fr

1. INTRODUCTION

Due to the accuracy now reached by space geodetic techniques, the temporal variations of a few Earth gravity field coefficients can be determined. Such variations result from Earth oceanic and solid tides, as well as from geophysical reservoirs masses displacements and post-glacial rebound. They are related to variations in the Earth's orientation parameters through their effect in the inertia tensor. We use (i) time series of the spherical harmonic coefficients C_{20} ($C_{20} = -J_2$) of the geopotential and also (ii) ΔC_{20} models for removing a part of the geophysical effects. The series were obtained by the GRGS (Groupe de recherche en Géodésie Spatiale, Toulouse) from the orbitography of several satellites (e.g. LAGEOS, Starlette, CHAMP) from 1985 to 2002 (Biancale et al., 2000). In this preliminary approach, we investigate how these geodesic data can influence precession-nutation results.

2. DATA AND METHOD

From the C_{20} variation series, we can derive the corresponding variations of the dynamical flattening H, according to : $\Delta H = -M\ R_e^2\ \frac{\Delta C_{20}}{C}$, where M is the mass of the Earth, R_e its mean equatorial radius and C its principal moment of inertia. The ΔH series obtained in this way are mostly composed of an annual, semi-annual and 18.6-year terms. In order to investigate the influence of the variations in dynamical flattening on the precession-nutation, we integrate the following precession equations (Williams 1994, Capitaine et al. 2003 = P03) based on the observed ΔH series :

$$\begin{aligned} \sin\omega_A \frac{d\psi_A}{dt} &= (r_\psi\ \sin\epsilon_A)\ \cos\chi_A - r_\epsilon\ \sin\chi_A \\ \frac{d\omega_A}{dt} &= r_\epsilon\ \cos\chi_A + (r_\psi\ \sin\epsilon_A)\ \sin\chi_A \end{aligned} \quad (1)$$

where r_ψ and r_ϵ are the total contributions to the precession rate, respectively in longitude and obliquity, depending on the factor H.

3. COMPUTATION AND RESULTS

We use the precession equations (1) and the software GREGOIRE (Chapront, 2003), together with the ΔC_{20} data, to compute the effects in precession nutation. We find differences in the coefficients of the polynomial development of the precession angle ψ_A, depending on the ΔC_{20} contribution and the J_2 rate implemented (J_2 rate = $\dot{J}_2$). The results are composed of a

polynomial part and a periodic part (i.e. Fourier and Poisson terms) discussed in the next paragraph. The effect due to the J_2 rate (i.e. effect on the t^2 term of ψ_A) can be taken into account using a series from 1985 to 1998 (Bourda and Capitaine, 2004). In Table 1, our results rely on ΔC_{20} data from 1985 to 2002 and then do not take into account this effect.

Table 1: Polynomial expression for ψ_A (up to degree 3) : (1) P03 and (2) Difference of our computation (influence of the ΔC_{20} *residuals*, obtained with various H constant parts) with respect to P03.

		t	t^2	t^3
(1) *P03*		*5038".481507*	*-1".079007*	*- 0".001140*
(2) Difference of our	geodetic H constant part	0".413188	-0".001667	0".2 10^{-6}
computation w.r.t P03	VLBI H constant part	0"	-0".001579	0".5 10^{-6}

Table 2: Periodic contribution for the t^0 term of ψ_A, for different ΔC_{20} contributions; in microarcseconds.

	Period	cos	sin
Residuals	Annual	-1	1
	Semi-annual	-	1
Solid Earth tides	18.6-yr	-2	120
TOTAL	18.6-yr	4	105

4. DISCUSSION

The precession rate (i.e. term in t in the ψ_A development) derived from the C_{20} obtained by space geodetic techniques is smaller than the one obtained by VLBI (see Table 1). The difference is about 400 mas/c, i.e. $\simeq 10^{-4}$ $\times$ the precession rate value (this corresponds to a constant part of $-2.6835\ 10^{-7}$ in the H value). Dehant and Capitaine (1997) already mentioned such a discrepancy relative to the IAU 1976 precession. Considering an error of about 10^{-10} in the ΔC_{20} data, we deduce an error of about 0.5 mas/c in the precession constant, which means that the difference obtained above is significant. In the future, several causes for this discrepancy will be investigated, such as the effect of the violation of hydrostatic equilibrium.

Then, the H variations coming from the *residuals* (i.e. ΔC_{20} data without atmospheric, oceanic tides or solid Earth tides ΔC_{20} models) observed by space geodetic techniques involved effects on the precession angle of about 1 μas or less (see Table 2). We also observed that the oceanic and atmospheric contributions were negligible. The principal periodic change, is due to the ΔC_{20} solid Earth Tides 18.6-yr variation, and is about 120 μas (in sine).

For further studies, the Earth model has to be improved by considering (i) a refine Earth model, with core-mantle couplings and (ii) a reliable J_2 rate value.

5. REFERENCES

Biancale, R., Lemoine, J.-M., Loyer, S., Marty, J.-C., Perosanz, F., 2002, private communication of the C20 data.

Bourda, G., Capitaine, N., 2004, Precession nutation and space geodetic determination of the Earth's variable gravity field, submitted to *Astron. Astrophys.*

Capitaine, N., Wallace, P. T., Chapront, J., 2003, Expressions for the IAU 2000 precession quantities, *Astron. Astrophys.*, **412**, 567–586.

Chapront, J., 2003, Gregoire software, Notice, Paris Observatory.

Dehant, V., Capitaine, N., 1997, On the precession constant: values and constraints on the dynamical ellipticity; link with Oppolzer terms and tilt-over-mode, *Celest. Mech. Dyn. Astr.*, **65**, 439–458.

Williams, J. G., 1994, Contributions to the Earth's Obliquity rate, Precession and Nutation, *Astron. J.*, **108 (2)**, 711–724.

A NEW FORMULATION OF THE DAMPING EFFECT IN EARTH'S AND MARS' FREE POLAR MOTION

M. FOLGUEIRA[1], J. SOUCHAY[2]
[1] Instituto de Astronomía y Geodesia (UCM-CSIC)
Facultad de CC. Matemáticas. Universidad Complutense de Madrid
Plaza de Ciencias, 3, Ciudad Universitaria, 28040 Madrid, Spain
e-mail: martafl@mat.ucm.es
[2] Observatoire de Paris, SYRTE, UMR 8630 du CNRS
61 avenue de l'Observatoire, 75014 Paris. France
e-mail:Jean.Souchay@obspm.fr

ABSTRACT. In this paper, we undertake firstly an extension of Kubo's procedure (1991) for the torque-free rotational motion of a triaxial and non-rigid body, neglecting therefore the external forces and taking into account only the deformation caused by the centrifugal force due to the rotation. Then, the straightforward application of such extension to the axially and elastic Earth and Mars is demonstrated.

The results are shown in terms of Andoyer's variables and its canonically conjugate variables since the corresponding variational equations expressed in terms of these variables seem to be more convenient and permit to separate clearly the different aspects considered in the study of the free polar motion, that is to say, the triaxiality, elasticity and time lag.

Finally, and from our mathematical modelling of the problem, a detailed discussion of the damping of the free polar motion is presented for a better understanding of the Chandler wobble and its maintenance in presence of such dissipation.

1. ANALYTICAL SOLUTION FOR THE FREE POLAR MOTION OF A DEFORMABLE BODY

We have considered an Hamiltonian formulation to express the analytical solution for the free polar motion of an elastic and triaxial body. The explicit form of such solution is:

$$l = -l_1 t + l_2 \sin(2l_1 t) \tag{1}$$

$$J = J_0 \times \exp\{-J_1 t - J_2 \cos(2l_1 t)\} \tag{2}$$

where the coefficients l_i and J_i are the general form:

$$l_1 = \frac{C_0\Omega}{\bar{A}}\left[\frac{C_0-\bar{A}}{C_0} - \rho\cos\delta\right] \quad ; \quad l_2 = \frac{C_0\Omega\varepsilon}{2\bar{A}l_1}$$

$$J_0 = 0.''5\times\exp\left\{\frac{C_0\Omega\varepsilon}{2\bar{A}l_1}\right\} \quad ; \quad J_1 = \frac{C_0\Omega\rho}{\bar{A}}\sin\delta \quad ; \quad J_2 = \frac{C_0\Omega\varepsilon}{2\bar{A}l_1} \tag{3}$$

and being A_0, B_0 and C_0, the principal moments of inertia of a rigid body, $\bar{A} = \frac{A_0+B_0}{2}$, ε a triaxial parameter, ρ an elastic parameter and δ the phase shift.

From the above equations, we can deduced that in addition to the classical Chandlerian component of the polar motion, an oscillation exists, with frequency twice the frequency of the Chandler wobble and an amplitude proportional to the triaxial coefficient. The tables 1 and 2 show how the phase shift, responsible of the damping effect, combined with parameters related to the triaxiality and elasticity are influencing to the polar motion.

$\delta(^\circ)$	l_1	l_2	$J_0\times10^5$	J_1	J_2
0	0.01425	-0.00277	0.24174	0.0	-0.00277
1	0.01425	-0.00277	0.24174	0.00011	-0.00277
5	0.01427	-0.00276	0.24174	0.00056	-0.00277

Table 1: Variations of the coefficients l_1, l_2, J_0, J_1 and J_2 for the Earth with changing δ. The units are in radians.

k	$\delta(^\circ)$	l_1	l_2	$J_0\times10^5$	J_1	J_2
0.15	0	0.02862	-0.037289	0.23353	0.0	-0.03729
0.15	1	0.02862	-0.037288	0.23353	0.00008	-0.03729
0.15	5	0.02863	-0.037267	0.23354	0.00038	-0.03727
			———			
0.25	0	0.02568	-0.041553	0.23254	0.0	-0.04155
0.25	1	0.02568	-0.041551	0.23254	0.00013	-0.04155
0.25	5	0.02571	-0.041509	0.23255	0.00064	-0.04151

Table 2: Variations of the coefficients l_1, l_2, J_0, J_1 and J_2 for Mars with changing δ and the love number k. The units are in radians.

Acknowledgments. The research was carried out in the Department of *"Systèmes de Référence Temps Espace" (SYRTE)*, Paris Observatory, under a finantial support of Paris Observatory, France (M. Folgueira). She also wants to thank to the Junta de Castilla y León (Spain)(VA072/02).

2. REFERENCES

Kubo Y., 1991, Solution to the rotation of the elastic Earth by method of rigid dynamics, *Celest. Mech.*, **50**, 165–187.

Lambeck K., 1988, Geophysical Geodesy. The slow deformations of the Earth, *Oxford Science Publications.*

Souchay J., Folgueira M., Bouquillon S., 2002, Effects of the triaxiality on the rotation of celestial bodies: application to the Earth, Mars and Eros, *Earth, Moon and Planets (accepted).*

VARIATIONS OF THE SECOND ORDER HARMONICS OF GEOPOTENTIAL FROM THE ANALYSIS OF THE ETALON SLR DATA FOR 1992–2001

T.V. IVANOVA, N.V. SHUYGINA
Institute of Applied Astronomy of RAS
10, Kutuzov quay, 191187 St.Petersburg, Russia
e-mail: itv@quasar.ipa.nw.ru, nvf@quasar.ipa.nw.ru

The paper is devoted to study of the second order harmonics of the geopotential from analysis of satellite laser ranging to Etalon 1&2. All available observations for 1992–2001 are taken from the Crustal Dynamics Data Informational System (CDDIS) and the European Data Center (EDC). Each measurement represents a normal point produced from two-way ranges averaged on 2-minute interval. A total number of approximately 10-year period of Etalon1&2 observations is about 46000 for each satellite. These observational data were analysed by means of the problem-oriented programming system for ephemeris astronomy ERA (Ephemeris Research in Astronomy) (Krasinsky and Vasilyev 1996), which is basically follows the IERS Conventions. Initial site positions were taken from ITRF2000 solution. Transformation from the Terrestrial Reference Frame to Celestial Reference Frame is carried out using IAU (1976) precession, IAU (1980) nutation, celestial pole offsets and Earth rotation parameters taken from EOP (IERS) C04 series.

The main aim is to estimate the in-phase amplitude of K_1 tidal wave in the tesseral harmonics C_{21}, S_{21} which manifest themselves as sinusoidal oscillations $\Delta C_{21}, \Delta S_{21}$ with the period of one sidereal day, given in IERS Conventions 2003 (McCarthy 2003) for the normalized coefficients $\overline{C}_{21}, \overline{S}_{21}$ in the form

$$\left(\Delta\overline{C}_{21}\right)_{K_1} = K_1 \sin(S+\pi)\,, \qquad \left(\Delta\overline{S}_{21}\right)_{K_1} = K_1 \cos(S+\pi)\,, \tag{1}$$

where

$$K_1 = 471.8 \times 10^{-12}, \tag{2}$$

S being the Greenwich Mean Siderial Time. This wave is caused by the differential rotation of the Earth's fluid core and so is very informative for geophysics.

The data analysis has been performed into two steps. The whole time span was divided into 21-day arcs. It turned out that 21-day interval is the optimal period of time for which there are sufficient number of normal points. At the first step six coordinates and velocities, along-track acceleration and reflectance coefficients were adjusted by the least-squares data fitting (Ivanova and Shuygina 2002). At the second step simultaneously with these parameters the K_1 amplitude and the correction to C_{20} have been estimated. The last values are regarded as global parameters for the time interval of one year, while the orbital parameters are considered as the local ones on each arc.

Corrections to C_{20} were determined over 10 intervals of a year. Averaging all the corrections we have obtained:

$$\Delta C_{20} = (-4.0 \pm 2.2) \times 10^{-10}. \tag{3}$$

Estimating K_1 a smoothing procedure was applied. We separated the whole time span of 10 years into 1-year intervals with subsequent displacement of each interval on a 21-day arc. The obtained 155 estimates are shown in Figure 1, where the error bars are 3.5σ values determined by the least-squares solutions.

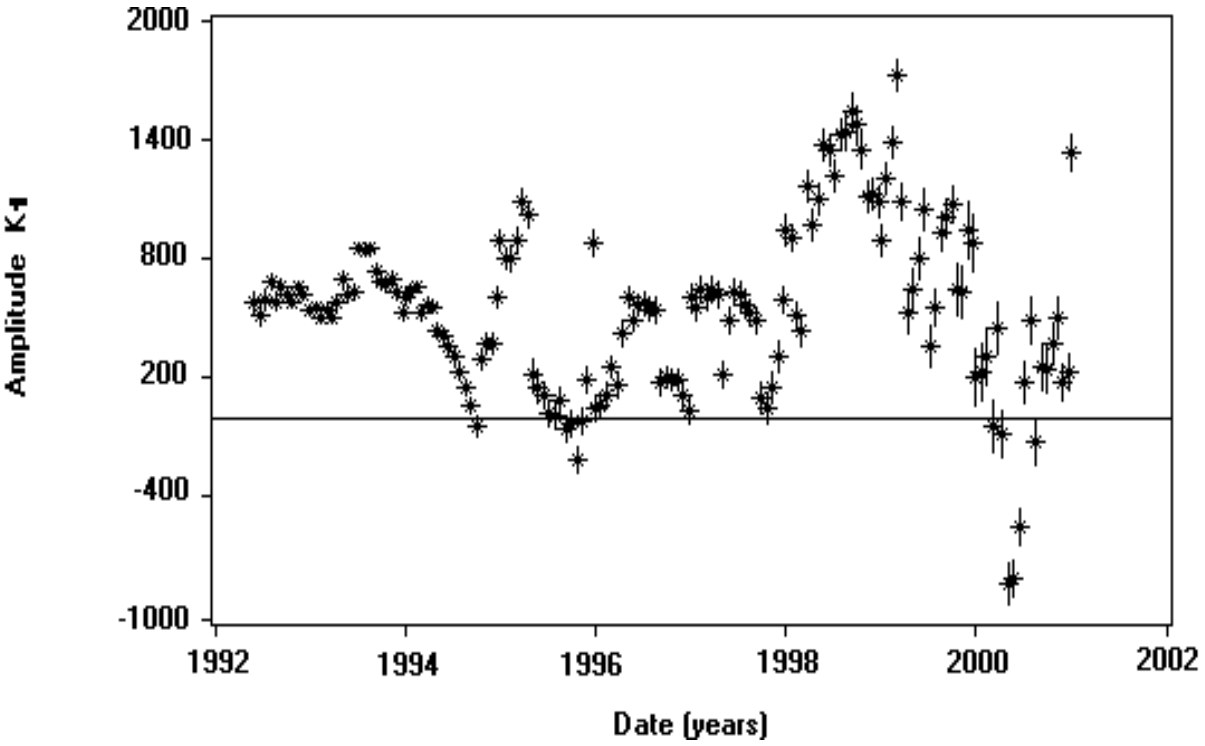

Figure 1: $K_1 \times 10^{12}$ amplitude estimated for 1992 - 2001 years.

It should be paid attention to the increase of the error bars to the end of the time span interval. The most likely cause of that is the deterioration of technical and physical characteristics of satellites with time.

After averaging we have obtained the following estimate of the K_1 amplitude:

$$K_1 = (557.9 \pm 25.1) \times 10^{-12} \tag{4}$$

which has to be compared with IERS value (2). One can see that the estimated K_1 amplitude is slightly different from that recommended by IERS Conventions. More precise determination of this difference is the problem of further investigation.

REFERENCES

Krasinsky G. A., Vasilyev M. V., 1996, ERA: knowledge base for ephemeris and dynamical astronomy, *In: Proceedings of IAU Colloquium 165*, 239.

McCarthy D. D., 2003, IERS Conventions 2003, *IERS Technical Note*, **32**.

Ivanova T. V., Shuygina N. V., 2002, Analysis of SLR observations of the Etalon geodetic satellites, *IAA Transactions*, **8**, 90.

MOTION OF THE EARTH'S POLE

L.D. AKULENKO, S.A. KUMAKSHEV, YU.G. MARKOV
Institute for Problems in Mechanics of the Russian Academy of Sciences
pr. Vernadskogo, 101-1, 119526 Moscow, Russia
e-mail: kumak@ipmnet.ru

Using approximate methods of nonlinear mechanics, we construct a theoretical model of the polar motion that satisfies the astrometric data of the IERS. This model is shown to rationally explain the observed characteristics of a complicated oscillatory process executed by the angular-velocity vector with respect to a coordinate system associated with the Earth. In this report we substantiate the possibility of constructing a simple dynamic model using the methods of celestial mechanics. The realization proposed for the first-approximation model involves a small number of parameters determined from observations and makes it possible to reliably (from the statistic standpoint) interpret essential characteristics of the pole trajectory and give a reasonably accurate prediction from one to a few years.

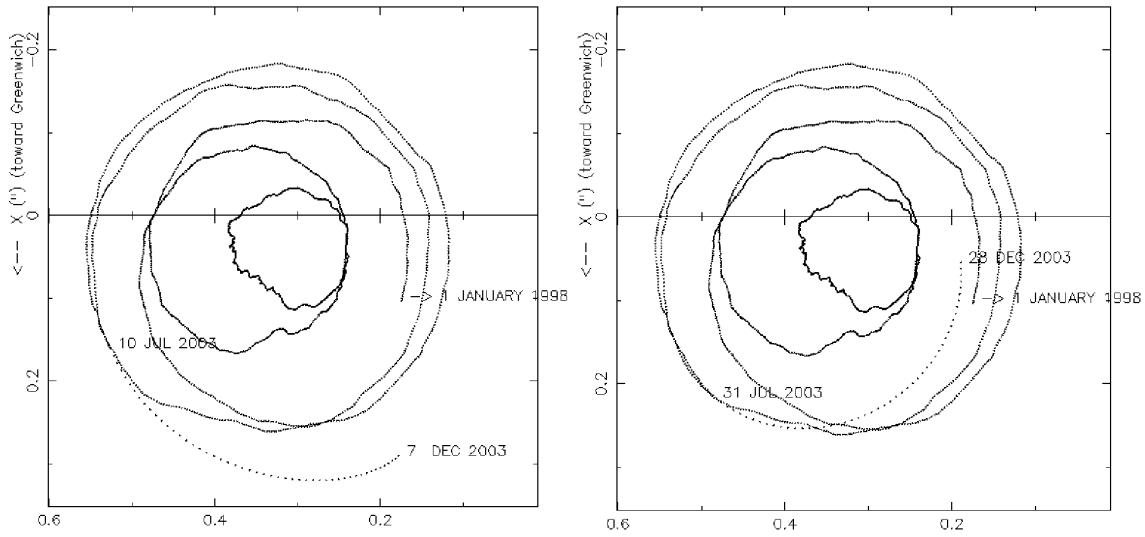

Figure 1: 100-dayes prediction (in dots) from the EOP Product Center.

The authors believe that the annual nutation oscillations can be explained and calculated on the basis of additionally taking into account the daily gravitational tides occurring in the deformable Earth. The simultaneous analysis of the Euler dynamic and kinematic equations for the inertia tensor deformed with the daily period in the coordinate system associated with me Earth, with allowance for the orbital motion and the figure-axis inclination to the ecliptic plane, makes it possible to establish the presence of the solar moment-of-force action with an annual period relative to the equatorial axes of inertia. The necessary value of the amplitude for this action attains $M_h = 10^{20}$ kg m^2 s^{-2} and leads to a relative variation of principal central

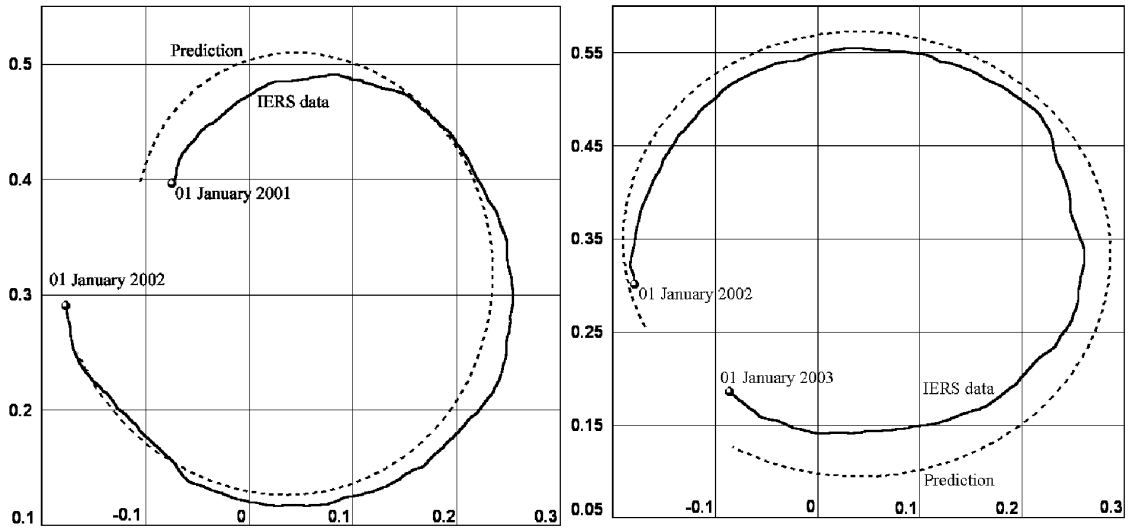

Figure 2: The prediction maded two-years (in dots) ago [1] and the real polar motion.

moments of inertia on the order of 10^{-5}. The effect of the lunar gravitational-force moment is less by a factor of 20, which is explained by a substantial difference in frequencies for eigenmodes and external actions.

We cearried out numerous calculations for verifying the efficiency ofthe model by the interpolation in time intervals from 2 to 20 years and the prediction of the trajectory for 1–5 years. The results obtained testify to the satisfactory accuracy for the interpretation of observations and for the prediction of the pole trajectory by a very simple theoretical first-approximation model. This model admits its natural refinement and complication by taking into account accessory factors to which we can also assign random perturbations.

Here on the figure 1 two variants with the 100-dayes prediction of the polar motion are depicted by dots. They were taken from the site of the EOP Product Center (http://hpiers.obspm.fr /eoppc/eop/eopc04/eopc04-xy.gif). As one can see the used algorithm of prediction is unstable and produce a rather big error.

The proposed by authors model in more details was published two years ago in (Akulenko et al., 2002) together with the prediction. On the figure 2 the comparison of two-years prediction by the above model and the real polar motion is depicted. The prediction was given at once (see for details (Akulenko et al., 2002)) and here for convenience divided into two parts. Each of them is equal to one year. As one can see this prediction is in the rather good agreement with the real data.

REFERENCES

Akulenko L. D., Kumakshev S. A., Markov Yu. G., 2002, Motion of the Earth's Pole, *Doklady Fiziki*, **47**, N 1, 78–84 (in Russian).

INFLUENCE OF EARTH'S ROTATION RATE AND DEFORMATIONS ON PRECESSION-NUTATION

S. LAMBERT
SYRTE - UMR8630/CNRS, Observatoire de Paris
61 avenue de l'Observatoire, 75014 Paris, France
e-mail: sebastien.lambert@obspm.fr

ABSTRACT. In this study, we investigate, first, the couplings between axial and equatorial components appearing when developping the dynamical equations of the Earth rotation at the second order, and second, the effects of variations of the dynamical ellipticity, giving rise to changes in the gravitational lunisolar torque and therefore in precession-nutation. We provide the computation of these effects for a refined Earth model with elastic mantle and decoupled liquid core.

1. COUPLING BETWEEN EARTH'S ROTATION RATE AND ORIENTATION

The equatorial motion of the instantaneous Earth rotation vector $\omega = \Omega(m_1 + im_2)$ in the terrestrial frame is given by the general Euler-Liouville equation which is developped to the second order :

$$\dot{m} - i\frac{C-A}{A}\Omega(1+m_3)m + \frac{\dot{c}+i\Omega c}{A} = \frac{\Gamma}{A\Omega} \tag{1}$$

where $c = c_{13} + ic_{33}$ is the non-diagonal element of the deformation part of the inertia tensor and Γ is the equatorial tidal torque expressed in the terrestrial frame computed from the expression Γ' in the celestial frame by the relation :

$$\Gamma = \Gamma' e^{-i\Phi} \tag{2}$$

in which Φ is the sidereal rotation angle.

Variations of Euler's angles are related to the instantaneous vector of rotation by the Euler's kinematical relations :

$$\begin{aligned} \dot{\theta} + i\dot{\Psi}\sin\theta &= -\Omega m e^{i\Phi} \\ \dot{\Phi} + \dot{\Psi}\cos\theta &= \Omega(1+m_3) \end{aligned} \tag{3}$$

Equations (1), (2) and (3) show two couplings between the axial and the equatorial components of the rotation vector of the Earth. One coupling comes from the product $m \times m_3$ in the left hand side. Another coupling is in the torque Γ which is expressed in the terrestrial frame and is affected by the rotation of angle Φ which depends on quantity m_3. Equation (1) can be solved analytically for a simplified Earth model in order to check the effects of these couplings. It appears to be negligible, at the level of a few microarcseconds.

2. VARIATIONS OF THE DYNAMICAL ELLIPTICITY

The tidal gravitationnal torque is derived from the sectorial part of the lunisolar potential ϕ (Sasao et al. 1980) in the celestial reference frame :

$$\Gamma' = \Gamma'^{(1)} + \Gamma'^{(2)} = -i\Omega^2(C-A)\phi - i\Omega^2(\delta C - \delta A)\phi \tag{4}$$

where $\Gamma'^{(1)}$ is the first-order part of the torque, depending on the lunisolar potential ϕ and on the mean moments of inertia of the Earth, and $\Gamma'^{(2)}$ is the second-order part of the torque, including the zonal deformations of the Earth :

Assuming that the trace of the inertia tensor is constant, let $\delta(2A+C) = 0$, we have :

$$\delta C - \delta A = \frac{3}{2}\delta C \tag{5}$$

The second order torque leads to the main effect on nutation angles. We implemented it considering variations of the dynamical ellipticity as given in the IERS Conventions 2003. In fact, it provides variations for the LOD induced by zonal tides which can be easily converted into variations of axial moment of inertia :

$$\frac{\delta C}{C} = \frac{\delta LOD}{\overline{LOD}} = -m_3^z \tag{6}$$

where the subscript z indicates that these rotation rate variations come from zonal tides. $\overline{LOD}$ is the duration of the mean solar day (86400 s).

3. NUMERICAL RESULTS

For the calculation we use the lunisolar potential computed from the lunar theory ELP2000 (Chapront-Touzé & Chapront 1983) and the solar system semi- analytical solution VSOP87 (Bretagnon & Francou 1988), and the use of the GREGOIRE software package developped by J. Chapront (Paris Observatory) and allowing manipulation of large Poisson's series. We develop the Earth model in order to include a liquid core. The main periodical effect is found on the 18.6- year nutation which amplitude should be changed by 208 μas in longitude and -10 μas in obliquity. The contribution to the precession rate in longitude is -5 mas per century. More details can be found in Lambert & Capitaine (2004).

4. REFERENCES

Bretagnon, P., Francou, G., 1988, *Astron. Astrophys.*, 202, 309.

Chapront-Touzé, M., Chapront, J., 1983, *Astron. Astrophys.*, 124, 50.

IERS Conventions 2003, to be published, D. D. McCarthy G. Petit (eds.).

Lambert, S., Capitaine, N., 2004, submitted to *Astron. Astrophys.*.

Mathews, P. M., Herring, T. A., Buffett, B. A., 2002, *J. Geophys. Res.*, 107 B4, 10.1029.

Sasao, T., Okubo, S., Saito, M., 1980, *Proc. of IAU Symposium 78*, E. P. Federov, M. L. Smith, P. L. Bender (eds.), D. Reidel, Hingham, Mass., 165.

THE DEFINITION OF THE FORCED NUTATIONS BY THE FINITE ELEMENT METHOD

M.V. LUBKOV
Poltava Gravimetrical Observatory of National Academy of Sciences of Ukraine
Myasoyedova 27/29, 36029 Poltava, Ukraine
e-mail: pgo@poltava.ukrtel.net

ABSTRACT.

It is presented the variational finite element approach for modelling EOP. As for approbation of this approach it has made the definition of the luni-solar forced nutation of the simplified dynamical earth model. Three main nutation terms, obtaining according to presented above method from PREM-model of the Earth, have compared with respective data of Molodensky and Wahr.

1. THE FORMULATION OF THE PROBLEM

Let us consider, that Earth is two axes ellipsoid of revolution, has absolutely rigid inner core, stratificated liquid outer core, and also has elastic isotropic nonhomogenous mantle and crust. Liquid core can oscillate relatively the mantle. The Earth is the self-gravitating, hydrostatically prestressed body. It rotates around own axis, taking under influence from the luni-solar attraction. The influence of an ocean and atmospheric loads not takes into account.

We shall neglect the flattening and the rotational effects in the elastic shell, as they are vanishing small, and shall take into account influence of relative, Euler, Coriolis, centrifugal forces on the elliptical liquid core. Then, using operation for eliminating static meanings of the stress tensor in the elastic shell and static pressure in the liquid core, obtained from hydrostatically equilibrium conditions of the Earth, come to the equilibrium equation in the elastic shell and to the motion equation in the liquid core relatively tidal actions, presented in Tisserand reference system (X,Y,Z) of the mantle:

$$0 = grad(V_e + V_1 + u_R g(R)) - div\vec{u}\, grad W_g + \frac{1}{\rho} div\hat{P}_1; \tag{1}$$

$$\ddot{\vec{u}} + 2\vec{\Omega} \times \dot{\vec{u}} = grad[V_e + V_1 + u_R g(R) + (1 + \frac{\sigma}{\Omega}\phi)] - 2\frac{\sigma}{\Omega}\frac{\partial \phi}{\partial z}\vec{e}_z - \frac{1}{\rho} grad p_1. \tag{2}$$

Where $V_e = K(xz\cos\sigma t + yz\sin\sigma t)$ - tesseral part of tidal wave potential; $\phi = -\Omega^2\varepsilon(xz\cos\sigma t + yz\sin\sigma t)$ - changing of centrifugal potential due to nutation; $V_1 = kV_e$ - potential due to tidal deformations; W_g - self-gravitating potential; ρ - density; ε - polar motion radius of the tidal wave, σ - frequency of the tidal wave; R - radius of the earth point; u_R - radial displacement component; $g(R)$ - gravity acceleration; $\hat{P}_1$ - changing stress tensor, due to tidal shell deformation; p_1 - tidal pressure changing in the liquid core, k - Love number.

Let us assume that vibrations into liquid core are results from the forced tidal frequency σ. Make up Lagrang functionals for the elastic shell and for the liquid core respectively in the displacement form in the cylindrical coordinate system (z, r, φ), where axis r coincides with the Tisserand axis Z:

$$E_1 = \pi \iint_{F_s} [c_1(\varepsilon_{zz}^2 + \varepsilon_{rr}^2 + \varepsilon_{\varphi\varphi}^2) + 4c_2\varepsilon_{zr}^2 + 2c_3(\varepsilon_{zz}\varepsilon_{rr} + \varepsilon_{zz}\varepsilon_{\varphi\varphi} + \varepsilon_{rr}\varepsilon_{\varphi\varphi})]rdzdr -$$
$$-\pi \iint_{F_s} [2(1+k)Krw + w(\frac{\partial w}{\partial z}\cos\alpha + 2\frac{\partial u}{\partial z}\sin\alpha)g(R) + 2w(w\cos\alpha + 2u\sin\alpha) \times \quad (3)$$
$$\times g_R'\cos\alpha - 2w(\frac{\partial w}{\partial z} + 2(\frac{\partial u}{\partial r}))g(R)\cos\alpha + 2(1+k)Kzu + u(2\frac{\partial w}{\partial r}\cos\alpha + \frac{\partial u}{\partial r}\sin\alpha) \times$$
$$\times g(R) + 2u(2w\cos\alpha + u\sin\alpha)g_R'\sin\alpha - 2u(2\frac{\partial w}{\partial z} + \frac{\partial u}{\partial r} + \frac{u}{r})g(R)\sin\alpha]\rho rdzdr;$$

$$E_2 = \pi \iint_{F_s} [c_4(\varepsilon_{zz}^2 + \varepsilon_{rr}^2 + \varepsilon_{\varphi\varphi}^2) + 2c_4(\varepsilon_{zz}\varepsilon_{rr} + \varepsilon_{zz}\varepsilon_{\varphi\varphi} + \varepsilon_{rr}\varepsilon_{\varphi\varphi})]rdzdr -$$
$$-\pi \iint_{F_s} [\sigma(\sigma + 2\Omega)w^2 + \sigma^2u^2]\rho rdzdr - 2\pi \iint_{F_s} [\Omega(\Omega+\sigma)\varepsilon w + \Omega(\Omega-\sigma)\varepsilon u]\rho rdzdr + \quad (4)$$
$$+\pi \iint_{F_s} [2(1+k)Krw + w(\frac{\partial w}{\partial z}\cos\alpha + 2\frac{\partial u}{\partial z}\sin\alpha)g(R) + 2w(w\cos\alpha + 2u\sin\alpha)g_R'\cos\alpha +$$
$$+2(1+k)Kzu + u(2\frac{\partial w}{\partial r}\cos\alpha + \frac{\partial u}{\partial r}\sin\alpha)g(R) + 2u(2w\cos\alpha + u\sin\alpha)g_R'\sin\alpha]\rho rdzdr;$$

Here $c_1 = \frac{\lambda+4\mu}{3}$; $c_2 = \mu$; $c_3 = \frac{\lambda-2\mu}{3}$; $c_4 = \frac{\lambda}{3}$;λ, μ - Lame coefficients; ε_{ij} - strain tensor components; w, u - displacement components along axes z, r respectively; F_s - meridian cross section area of the Earth; $\cos\alpha = \frac{z}{R}$; $\sin\alpha = \frac{z}{R}$.

2. THE FINITE ELEMENT METHOD RESOLVING PROBLEM

For resolving system of the equations (1, 2), taking into account rigidity of the inner core and absence of the surface earth loads, let us apply the finite element method, based on the variational Lagrang principal in the displacement form, which tends to resolving system of the variational equations such as:

$$\delta E_1(u_i) = 0; \qquad \delta E_2(u_i) = 0. \quad (5)$$

For resolving system of the equations (5), used 8-node isoparametric quadrilateral curve finite element.

In this short presentation we omit the finite element procedure of resolving these variational equations, we are only present meanings of the main nutation terms, defining according to described above method from PREM-model of the Earth, and also the respective data of Molodensky(1961) and Wahr(1981).

	Dynamical model	Molodensky	Wahr
18,6 year: $\Delta\Theta$	9",2052	9",2044	9",2025
$\Delta\Psi\sin\Theta$	-6", 8454	-6", 8441	-6", 8416
Semiannual:$\Delta\Theta$	0", 5713	0", 5719	0", 5736
$\Delta\Psi\sin\Theta$	-0", 5229	-0", 5232	-0", 5245
Fortnightly:$\Delta\Theta$	0", 0968	0", 0972	0", 0977
$\Delta\Psi\sin\Theta$	-0", 0893	-0", 0899	-0", 0905

HIGH-FREQUENCY VARIATIONS OF THE EARTH ROTATION FROM THE VLBI AND GPS OBSERVATIONS

L.V. ZOTOV
Sternberg Astronomical Institute
13 Universitetskij pr., Moscow, Russia
e-mail: tempus@lnfm1.sai.msu.su

ABSTRACT. High frequency variations of UT1-UTC in diuarnal and subdiurnal frequency band were detached with use of Panteleev's filter from the series of the Earth Orientation Parameters (EOP) estimations provided by the Center for Orbit Determination (CODE), which is a part of the International GPS Service (IGS). This series with 1-hour resolution is available in the time span from 02.01.1995 to 14.02.1998. The comparison of the UT1-UTC variations with Ray's model, recommended by the International Earth Rotation Service (IERS) for ocean tidal effect calculation, showed existence of regions of disagreement, where the differences reach a level of 150 microseconds. Periodograms of differences contain harmonics with frequencies from 3 to 11 cycles per day and residual energy in diuarnal and semidiurnal frequencies. All these effects we found artificial rely upon the analysis of errors, information about the IGS network (Rothacher et al., 2001) and from the comparison with the independent estimations of the high frequency EOP variations derived from the weekly VLBI observations. For this the OCCAM 5.0 package with some modifications was used.

1. RESULTS OF ANALYSIS

The Center for Orbit Determination, provided the series of Earth Orientation Parameters estimations with 1-hour resolution in the interval from 02.01.1995 to 14.02.1998. High frequency variations of the UT1-UTC were detached from these series using Panteleev's filter (Panteleev, Tchesnokova, 2003) and were compared with Ray's model of influence of the global ocean tides on the rotation of the Earth. The results of comparison are represented by Fig. 1. The regions of disagreement up to 150 microseconds can be seen. The analysis of errors of CODE-series (Fig. 2) reinforced by the information upon the IGS network (Rothacher et al., 2001) allowed us to conclude, that some of this regions (at least in September 1997, MJD 50700) are connected with changes in the number of IGS observing stations.

Power spectrum estimates (Fig. 3) of the differences between CODE EOP and Ray's model contain some residual energy with periods of about 12 and 24 hours, which can be connected with an orbital resonance (GPS satellites period is close to 12 h). In the spectra there also present some harmonics with periods from 3 to 11 cycles per day.

For comparison the high-frequency EOP estimations were independently derived from the weekly VLBI observations (Fig 4). For this the OCCAM 5.0 software package was used (Titiov, Schuh, 2000).

Figure 1: High-frequency CODE UT1-UTC comparison with R.Ray's model.

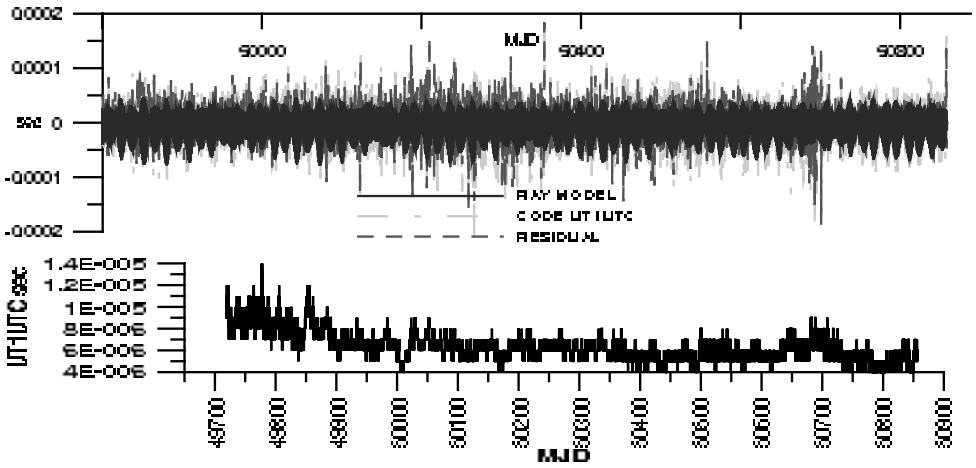

Figure 2: Errors of CODE UT1-UTC estimations.

Figure 3: UT1-UTC residual spectra (left) and Ray's model spectral components (right).

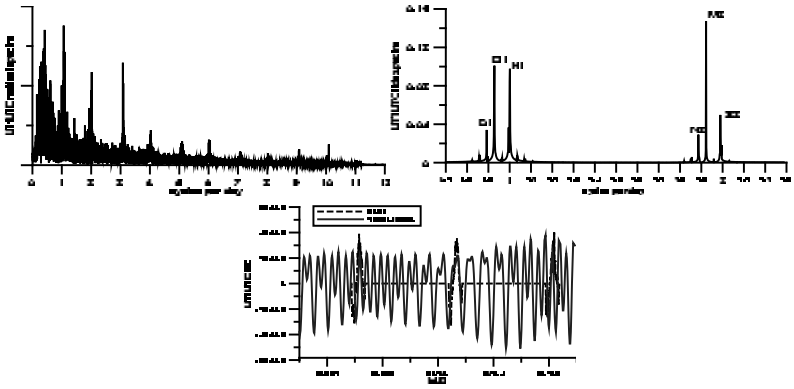

Figure 4: UT1-UTC estimations from VLBI in comparison with Ray's model, September 1997.

We came to the conclusion, that most of the effects described above, observable in the satellites data, have an artificial cause.

This work was supported by the RFBR grunts 01-02-1659, 02-05-39004.

2. REFERENCES

Zharov V. E., Gambis D., Bizouard Ch., 2000, Diurnal and sub-diurnal variations of the Earth rotation, *IERS TN 28*, Observatoire de Paris, 5.

Rothacher M., Beutler G., Weber R., Hefty J., 2001, High-frequency variations in Earth rotation from Global Positioning System data, *J. Geophys. Res.*, **106**, 13, 771-13, 778.

Panteleev V. L., Tchesnokova T. S, 2003, Mathematical models of the gravimetrical data processing, *Geology and Prospecting*, Moscow.

Titov O., Schuh H., 2000, Short period in Earth rotation seen in VLBI data analysed by the least-squares collocation method, *IERS TN 28*, Observatoire de Paris, 33.

Section III)

PLATE TECTONICS, CRUSTAL DEFORMATIONS AND GEOPHYSICAL FLUIDS

PLAQUES TECTONIQUES, DÉFORMATIONS CRUSTALES ET FLUIDES GÉOPHYSIQUES

ATMOSPHERIC, NON-TIDAL OCEANIC AND HYDROLOGICAL LOADING INVESTIGATED BY VLBI

H. SCHUH[1], G. ESTERMANN[1,2]
[1)]Institute of Geodesy and Geophysics, Vienna University of Technology
Gusshausstr. 27-29, 1040 Wien, Austria
e-mail: harald.schuh@tuwien.ac.at
[2)]now at: Research School of Earth Science,
The Australian National University, Canberra, Australia

ABSTRACT. Today, the small deformations associated with the response of the Earth to atmospheric and hydrological loading are of growing interest. These effects cause site- dependent vertical displacements with ranges up to ± 30mm due to atmospheric pressure variations and due to mass redistribution in surface fluid envelopes, in particular in continental water reservoirs (soil moisture, snow cover, and groundwater). Models of site displacements based on new global and regional databases of soil moisture and snow depths are now available and also models exist for non-tidal ocean loading. The NEOS-A VLBI sessions and also the extremely precise CONT sessions (two continuous weeks in 1994 and in 2002) are used to investigate how the effects influence the results of high precision VLBI measurements. Main emphasis is put on the repeatability of station heights and of baseline lengths. Small improvements are achieved when applying the considered loading models but are still not clearly above the significance level. This yields to the conclusion that the global loading models are not yet precise enough in some regions of the Earth and that other uncorrected influences disturb the VLBI measurements.

1. INTRODUCTION

The temporal redistribution of oceanic, atmospheric, and hydrological masses perpetually loads and deforms the Earth's crust. Surface displacements, due to atmospheric mass circulation, are dominated by the effects of synoptic scale systems (1000-2000 km wavelength) having periods of less than two weeks. Peak-to-peak vertical displacements of 10 to 20mm are common at mid-latitudes (Rabbel and Zschau, 1985; van Dam and Wahr, 1987; Manabe et al., 1991). The effects are larger at higher latitudes due to the larger pressure variability found there.

While surface displacements are largest for atmospheric pressure variations with periods of one to two weeks, annual signals are also existing having amplitudes between 0.5 and 3mm. At annual periods, variations in continental water storage become important, too.

Tidal and non-tidal motions of oceanic mass also contribute to the deformation spectrum at points on the Earth's surface. Variations in bottom pressure driven by uncompensated changes in sea surface heights can induce vertical deformations at coastal sites of up to 12mm with periods of approximately one month.

For all of these loading signals, the vertical deformations are larger than the horizontal ones by factor 3 to 10. Given the amplitude of the loading induced vertical crustal motion, it is

necessary to evaluate the effects of loading on when interpreting geodetic data. Loading effects caused by the redistribution of surface masses have been observed in high-precision geodetic data for some time now (see for example, van Dam and Herring, 1994; van Dam et al., 1994; MacMillan and Gipson, 1994; Sun et al., 1995; Haas et al., 1997; Scherneck et al., 2000; and van Dam et al., 2001). As the results of space geodetic measurements are more and more being interpreted in terms of geodynamic processes (plate tectonics, post-glacial rebound, sea level rise, etc.) it is becoming necessary to remove loading effects from the geodetic data.

2. MODELS USED FOR LOADING COMPUTATIONS

A brief description of the various approaches for modeling loading displacements is given by Schuh et al. (2003). All loading models need two ingredients:

- the input data in terms of global mass variations;
- the computation of the corresponding displacements using one of the various approaches and based on different Earth models and geodynamic parameters.

For further details see the paper mentioned above. Here, only one example for loading deformations will be given: hydrological loading due to soil moisture. At annual periods, variations in continental water storage are significant. The modeled vertical displacements have ranges of up to 30mm, with root-mean-square values as large as 8mm.

Several new global models exist for soil moisture that were used for our study. These include

- Huang et al. (1996);
- Global Soil Wetness Project (GSWP), (Douville et al., 1999);
- Milly et al. (2002).

All models provide $1° \times 1°$ gridded data of soil water in the upper layer of the ground (usually the top 2 meters) that were interpolated to the position of the ground stations. The GSWP and Milly models provide also snow depth variability.

The annual displacements of Algonquin Park from each of these models are shown in Fig. 1 covering a total range of 3mm. There is about a 2mm peak-to-peak difference in the annual component determined using the Huang model versus the Milly model. Current geodetic techniques can determine annual crustal motions to at least this accuracy, indicating that we may be able to use these techniques to refine the long-wavelength models of soil moisture variability.

3. INVESTIGATION OF LOADING EFFECTS BY VLBI

Considering the accuracies of a few mm that are going to be achieved by high precision global geodetic measurements, it becomes quite clear, that loading displacements have to be taken into account when analyzing space geodetic data.

3.1. VLBI DATA ANALYSIS

In the investigations reported here, all NEOS-A sessions (weekly VLBI measurements, each 24h with 5-7 stations) from January 1996 to December 2001 were analyzed and also the CONT02 session covering a continuous period of 15 days in October 2002. In a first solution following the standard procedure of VLBI analysis no a-priori loading corrections were applied. In the least-squares fit a free network solution was done for each 24h VLBI session to determine baseline lengths; then a second solution was carried out, constraining the horizontal coordinates to

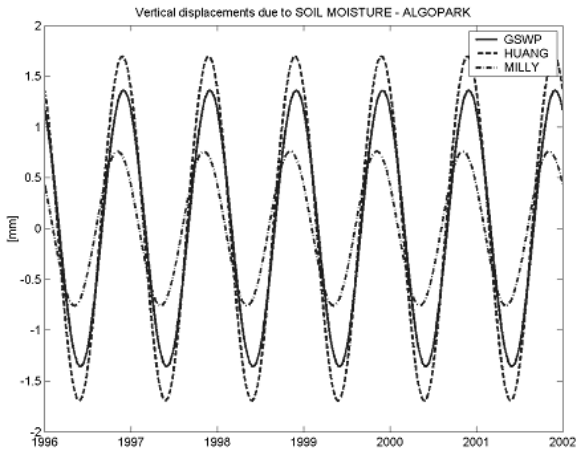

Figure 1: Vertical displacements due to soil moisture

ITRF2000 and estimating the vertical coordinates (i.e. station heights), only. These two solutions will be called 'reference' in the following sections. The VLBI Software package OCCAM (V 5.1) was used for the analysis of the VLBI data. It has been developed by European VLBI groups since 1983 and is applied by six IVS Analysis Centers (three operational Analysis Centers). It can be applied under MS/DOS and Unix or Linux and is a very flexible VLBI program (Titov et al., 2001).

3.1.1. VLBI STATION HEIGHTS AND BASELINE LENGTHS

Now, the VLBI analyses were repeated with a-priori loading corrections applied. Again all NEOS-A sessions from January 1996 to December 2001 were analyzed. The station heights and baseline lengths were determined and compared with the results of the first, uncorrected 'reference' solution by computing the scatter around the mean station heights and around straight-lines fitted to the baseline lengths. Figures 2 and 3 represent the number of VLBI sessions with improved repeatabilities. Improvements of the station heights and baseline lengths when correcting for loading effects were obtained in 64% of all combinations of loading models treated here. The average positive improvement is 3 to 4% never exceeding 13%. If the improvement is negative, i.e. if the results became worse, it is less than 1% on the average.

Considering all of the stations there is not one combination of the loading models that seems to be superior to the others. From this, it can be concluded that the existing mass loading models that were used for this study still have deficiencies on several regions of the globe.

CONT02 was a VLBI sessions observing 15 days continuously in October 2002. The goal of the CONT02 campaign was to acquire the best possible state-of-the-art VLBI data over a two-week period to demonstrate the highest accuracy of which VLBI is capable.

For these sessions only displacements due to atmospheric loading computed by H.-G. Scherneck were available (Scherneck, 2000). As for the NEOS-A sessions, the station heights and baseline lengths were determined. The results of the first 'uncorrected' version were compared with the VLBI results where the atmospheric loading displacements were applied a priori. For these analyses the tropospheric mapping function NMF (Niell, 1996) was used first. Then the computations were repeated with the new tropospheric mapping function IMF (Niell, 2001) in order to test the influence of the chosen mapping function when investigating atmospheric loading.

Improved repeatabilities of the station heights and baseline lengths when correcting for loading effects were obtained in about 75% of all combinations of loading models treated here. The repeatabilities improve at an average of 11% when applying the atmospheric loading displace-

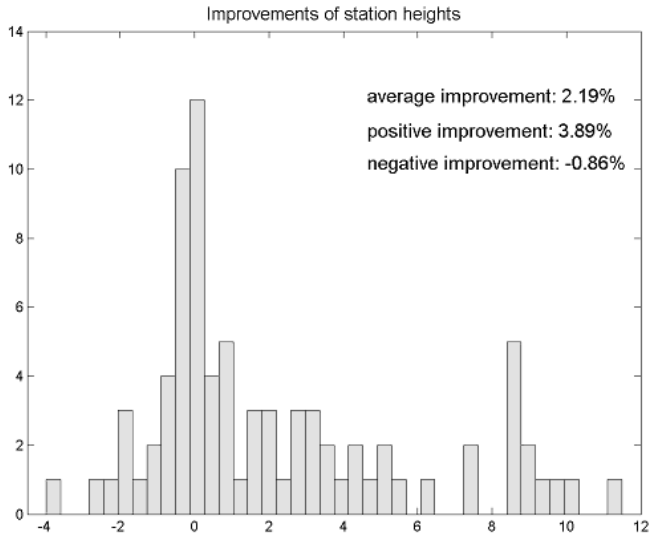

Figure 2: NEOS-A Sessions: Improvements of repeatabilities of station heights

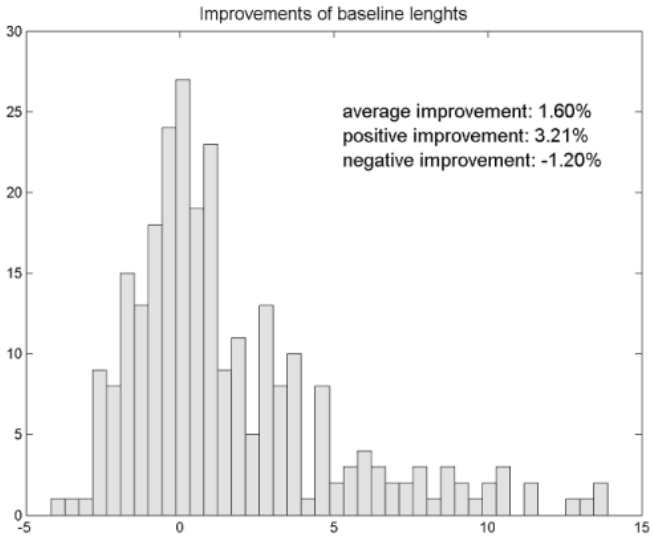

Figure 3: NEOS-A Sessions: Improvements of repeatabilities of baseline lengths

ments and using the NMF. When using the IMF the repeatabilities improve even by 17% on the average.

The results of this investigations are summarized in Tab. 1, which includes the statistics of the continuous session in January 1994 CONT94. It is evident that in particular for the very precise CONT- sessions it is worth applying loading corrections to improve the quality of the geodetic results.

4. CONCLUSIONS

Non-tidal loading effects are in the range of +10 to 30mm and should be corrected when analyzing space geodetic data which are intended to reach an accuracy of a few mm. So far, only weak correlation between VLBI station heights and modeled radial loading displacements (<0.3) can be observed (see Schuh et al., 2003). When applying a-priori corrections due to loading the scatter around the mean station heights and the baseline lengths decreases for most of the

	NEOS-A		CONT 94		CONT 02	
	%	∅	%	∅	% NMF/IMF	∅ NMF/IMF
Baseline lengths	64	3,3	71	12	71/75	3,7/5,2
Station heights	64	3,9	43	25	75/75	10,7/16,8

Table 1: Percentage [%] of improved baseline lengths and station heights and average positive improvements [∅].

stations. The improvements is the bigger the more precise the VLBI observables are and the better the tropospheric refraction is modeled. However, it is obvious, that further improvements of loading models are needed, in particular by using better global models for snow and soil moisture.

5. REFERENCES

Douville, H., Bazile, E., Caille, P., Giard, D., Noilhan, J., Peirone, L., Taillefer, F., 1999, Global Soil Wetness Project: Forecast and assimilation experiments performed at Météo-France, *J. Meteor. Soc. Jap.*, **77**, 305–316.

Haas, R., Scherneck, H.-G., Schuh, H., 1997, Atmospheric loading corrections in geodetic VLBI and determination of atmospheric loading coefficients, *In: Proceedings of the 12th Working Meeting on European VLBI for Geodesy and Astronomy*, Honefoss, Norway, 12-13 September 1997, B. R. Pettersen (ed.), 111–121.

Huang, J., van den Dool, H., Georgakakos, K. P., 1996, Analysis of Model-Calculated Soil Moisture over the United States (1931-1993) and Application to Long-Range Temperature Forecasts, *Journal of Climate*, **9**, No.6, 1350–1362.
http://www.cpc.ncep.noaa.gov/soilmst/paper.html

MacMillan, D. S., Gipson, J. M., 1994, Atmospheric pressure loading parameters from very long baseline interferometry observations, *J. Geophys. Res.*, **99**, 18081–18087.

Manabe, S., Sato, T., Sakai, S., Yokoyama, K., 1991, Atmospheric loading effect on VLBI observations, *In: Proceedings of the AGU Chapman Conference on Geodetic VLBI: Monitoring Global Change*, NOAA Tech. Rep. NOS 137 NGS 49, 111–122.

Milly, P. C. D., Shmakin, A. B., Dunne, K. A., 2002, Global Modeling of Land Water Balances: The Land Dynamics Model (LaD), *Journal of Hydrometeorology*, **3**, 283–299.

Niell, A. E., 1996, Global mapping functions for the atmosphere delay at radio wavelengths, *J. Geophys. Res.*, **101**, No. B2, 3227–3246.

Niell, A. E., 2001, Preliminary evaluation of atmospheric mapping functions based on numerical weather models, *Phys. Chem. Earth*, **26**, 475–480.

Rabbel, W., Zschau, J., 1985, Static Deformations and gravity changes at the Earth's surface due to atmospheric loading. *J. Geophys.*, **56**, 81–99.

Scherneck, H.-G., 2000, HGS Air Pressure Loading.
http://www.oso.chalmers.se/ hgs/apload.html

Scherneck, H.-G., Haas, H., Laudati, A., 2000, Ocean Loading Tides, *For, In and From VLBI. Proc. First IVS General Meeting*, Kutzting, N. Vandenberg, K. Baver (eds.), 257–262.

Schuh, H., Estermann, G., Crétaux, J.-F., Bergu-Nguyen, M., van Dam, T., 2003, Investigation of atmospheric and hydrological loading by space geodetic techniques, *International Workshop on Satellite Altimetry for Geodesy, Geophysics and Oceanography*, Wuhan, Sept. 2002, Springer, IAG Series (in press).

Sun, H. P., Ducarme, B., Dehant, V., 1995, Effect of the atmospheric pressure on surface displacements, *J. Geodesy*, **70**, 131–139.

Titov, O., Tesmer, V., Boehm, J., 2001, Version 5.0 of the OCCAM VLBI software, User Guide, *AUSLIG Technical Reports 7*, AUSLIG, Canberra.

van Dam, T. M., Blewitt, G., Heflin, M.B., 1994, Atmospheric Pressure Loading Effects on GPS Coordinate Determinations, *J. Geophys. Res.*, **99**, 23939–23950.

van Dam, T. M., Herring, T. A., 1994, Detection of Atmospheric Pressure Loading using Very Long Baseline Interferometry Measurements, *J. Geophys. Res.*, **99**, 4505–4517.

van Dam, T. M., Wahr, J. M., Milly, P. C. D., Shmakin, A. B., Blewitt, G., Lavallee, Larson, K., 2001, Crustal displacements due to continental water loading, *Geophys. Res. Lett.*, **28(4)**, 651–654.

van Dam, T. M., Wahr, J. M., 1987, Displacements of the Earth's Surface Due to Atmospheric Loading: Effects on Gravity and Baseline Measurements, *J. Geophys. Res.*, **92**, 1281.

INFLUENCE OF THE ATMOSPHERIC AND OCEANIC CIRCULATION ON THE PLATE TECTONICS

N.S. SIDORENKOV
Hydrometcenter of Russia
11-13 Bolshoi Predtechensky per., 123458 Moscow, Russia
e-mail: sidorenkov@rhmc.mecom.ru

ABSTRACT. The non-tidal irregularities of the Earth rotation are mainly due to the exchange between the angular momentum of the solid lithosphere and its fluid environment - the atmosphere and the hydrosphere. This exchange occurs due to the moments of the frictional forces and pressure forces pushing on mountain ranges. Special Bureau for the Atmosphere carries out the monitoring of the exchange of the angular momentum by both the momentum approach (i.e., by the evaluation of the effective functions of the atmospheric and oceanic angular momentum), and the torque approach (i.e., the evaluations of the torque resulting from the wind and current stresses and pressures).

Calculations of the friction and pressure momentum forces are performed for the entire Earth surface as a whole. However, the lithosphere is cracked on a set of the lithosphere plates. The lithosphere plates can move in the horizontal direction under the effect of the friction and pressure (acting on mountain ranges) forces. Therefore, when calculating the torque, it is necessary to carry out the integration not only for the entire Earth surface but also separately for every lithosphere plate.

The estimations of the orders of magnitudes of the atmospheric and oceanic forces effecting on a separate plate and of the stresses of the interaction between plates are given in this paper. The mechanical action of the atmosphere and ocean on the lithosphere plates is likely to be an initial cause of earthquakes. The empirical facts which evidence for the benefit of this conclusion are given.

A mathematical model of the movement of the lithosphere plates under the effect of the frictional and pressure forces is formulated. Two equations describing the horizontal movement of the plate's center of gravity and one equation describing the rotation of the plate around the vertical axis are used. The algorithm of calculation of the movement of the lithosphere plates is constructed.

1. INTRODUCTION

It is well known that seasonal variations in the Earth rotation are determined by the redistribution of the angular momentum between the atmosphere and the Earth. When the moment of the atmosphere is increasing then the moment of the Earth is decreasing and vice versa. This regularity is well seen on next graph where the time series of the angular momentum of the atmosphere is compared with the time series of the angular momentum of the Earth (Fig.1).

Thus, the non-tidal irregularities of the Earth rotation are mainly due to the exchange

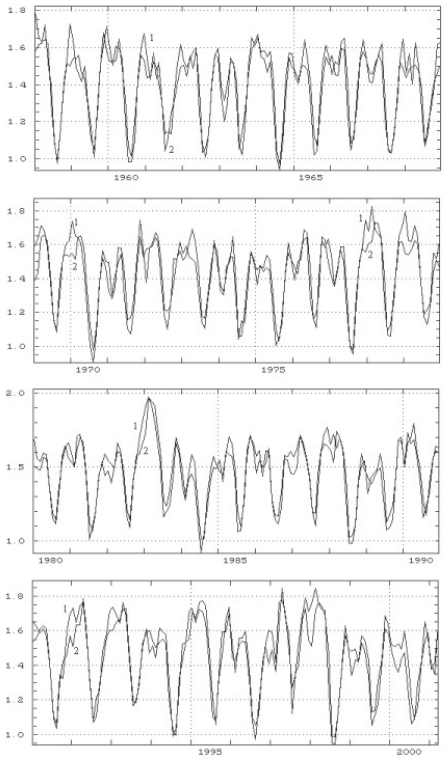

Figure 1: The angular momentum of the atmosphere (1) and the angular momentum of the Earth (2).

between the angular momentum of the solid lithosphere and its fluid environment - the atmosphere and the hydrosphere. This exchange occurs due to the moments of the frictional forces and pressure forces pushing on mountain ranges. Special Bureau for the Atmosphere carries out the monitoring of the exchange of the angular momentum by both the momentum approach (i.e., by the evaluation of the effective functions of the atmospheric and oceanic angular momentum), and the torque approach (i.e., the evaluations of the torque resulting from the wind and current stresses and pressures).

Calculations of the friction and pressure momentum forces are performed for the entire Earth surface as a whole. However, the lithosphere is cracked on a set of the lithosphere plates. The atmosphere and ocean are acting on the lithosphere plates, and only then this action is being transmitted to the Earth. What is the result of the atmospheric action on the lithosphere plates? Let's recollect, that under the lithosphere, there is a layer of the lower viscosity - an asthenosphere in which the lithosphere plates are capable to float. Continents are frozen in to the oceanic plates, and they may passively move with them (Trubitsyn and Rykov 1998; Trubitsyn, 2000). The lithosphere plates float in the asthenospherical substratum. On the decade time scale, the lithosphere plates can move in the horizontal direction under the effect of the friction and pressure (acting on mountain ranges) forces. Plates in motion under the action of the friction stresses and pressure, which the atmosphere and ocean produce on the exterior surface of the plate. The viscous cohesive force with the asthenosphere on the soles and end faces of the plates decelerates their moving, but the exterior forces overcome this resistance. Therefore, when calculating the torque, it is necessary to carry out the integration not only for the entire Earth surface but also separately for every lithosphere plate. The moment of forces effecting on an individual plate, determines the vector of the movement of the plate.

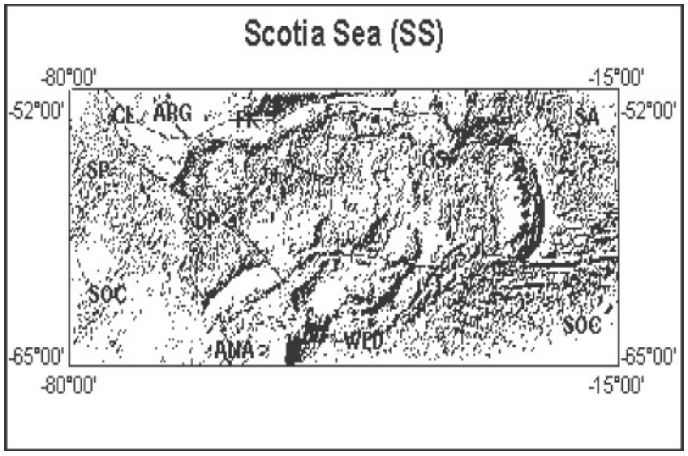

Figure 2: Westerly atmospheric winds and oceanic currents have broken down lithosphere bridge the South America – Antarctic Peninsula and have shifted its to the east by 1500 km. The color map can be looked on the site
http://walrus.wr.usgs.gov/infobank/gazette/html/regions/ss.html.

2. EVIDENCES

A good example of this is the situation in the Drake Passage (Fig.2). Strong westerly winds dominate in the 40°–50°th S. They generate the powerful Antarctic Circumpolar Current (ACC) in the Southern Ocean. The South America, Antarctic Peninsula and the underwater lithosphere present a barrier for ACC. Westerly atmospheric winds and oceanic currents have replaced this barrier downstream and have shifted this lithosphere bridge to the east by 1500 km. This process resulted in the formation of the Scotia Sea (South-Antilles hollow). It is bordered along perimeter by the remains of the lithosphere bridge in the form of the South-Antilles ridge and numerous islands, the arc of the South Sandwich Islands being the principal of them. This ridge, at the drifting in the eastward stream, has crumpled the oceanic lithosphere and has formed the deep South-Sandwich trench.

Let us present one more evidence for the benefit of our hypothesis. The atmospheric circulation has a remarkable feature at the latitudes of 35°N and 35°S, the wind direction alters to the opposite one. Easterly winds predominate in the tropical belt between these latitudes, and westerly winds – in the moderate and high latitudes. According to this, the stress of friction on the surface of the lithosphere is directed in two opposite sides. Therefore, the maximum stress in the lithosphere should concentrate near the latitudes of 35°N and 35°S. These bands should exhibit an increased seismic and tectonic activity. Really, in the Northern hemisphere, in this band, continuous mountain ranges are extending through the Mediterranean Sea, Middle East, Iran, Pamir, Tibet, Japan and USA. Here, earthquakes and eruptions of volcanoes occur most frequently. In the Southern Hemisphere, the band of the sign change of the wind direction over the water surface of the World Ocean. Therefore, the seismic and tectonic processes do not manifest themselves.

3. ESTIMATIONS

Now let us estimate the order of magnitudes of the atmospheric and oceanic forces effecting on a separate plate and of the stresses of the interaction between plates. At the common

wind velocity (u = 10 m/s) the friction stress τ on the surface of the plate is $\tau = c\rho u^2 = 0.004 \times 1.27 kg \cdot m^{-3} \times (10 m \cdot s^{-1})^2 = 0.5$ N/m ^{2}, the area of the plate is $\approx 2 \cdot 10^{13}$ m ^{2}; therefore, the total atmospheric force effecting on a separate plate, is equal $\approx 1 \cdot 10^{13}$ N. Under the effect of this force the plate interacts with the circumjacent plates through the frontal contacts. The interaction takes place only at the sites of adhesion of plates, and the area of contacts may be small. The total atmospheric force concentrates on this small area. Therefore, the stresses may reach such high values ($10^6 - 10^7$ N/m ^{2}), at which the discontinuity and displacement of plates from each other occur. The discontinuity triggers the seismic waves. Thus, the mechanical action of the atmosphere and ocean on the lithosphere plates controls relative movements of the lithosphere plates and can cause the earthquakes and volcanic activity.

There is a substantial body of publications in which close correlations between seismicity and variations of the atmospheric indices (Sytinsky, 1985), seismicity and fluctuations in the Earth rotation (Zharov et al., 1991; Gorkavyi et al., 1994a, 1994b; Barsukov, 2002) are found. Our hypothesis explains these correlations. The atmospheric and oceanic circulation is the initial cause of both the whole class of earthquakes and the variations in the Earth rotation. Note that the variations in the Earth rotation are very small ($\frac{\delta\omega}{\omega} \approx 10^{-8}$) and do not affect the geophysical processes (Sidorenkov, 2002).

Thus, the research results and observations confirm the hypothesis about the movement of the lithosphere plates under the impact of the atmospheric and oceanic circulation on the decade time scale. The total effect of the movement of all lithosphere plates is interpreted by geophysists as the decade fluctuations of the Earth rotation.

4. MODEL

Our hypothesis can be mathematically described similarly to the Trubitsyn's model of the mantle convection with floating continents (Trubitsyn, 2000).

It is known that the motion of a rigid body is defined by the motion of its center of masses and by the rotation with respect to the center of masses. To deduce the differential equations of the plate motion, we use the theorem of the movement of the center of masses of the plate:

$$m\frac{d\vec{V}_{0i}}{dt} = \vec{F}_i, \tag{1}$$

and the theorem of the angular momentum:

$$\frac{d\vec{H}_i}{dt} = \vec{L}_i, \tag{2}$$

where m is the mass of the plate; $\vec{V}_{0i}$ is the instantaneous velocity vector of the center of masses; $\vec{H}_i$ is the angular momentum of the plate; $\vec{F}_i$ is the external force; and $\vec{L}_i$ is the total force moment (torque), which is the sum of the moments q_i of forces σ_j applied to separate elements of the plate surface

$$q_k = \varepsilon_{ijk}(x_i - x_{i0})\sigma_j. \tag{3}$$

The angular momentum of the plate may be determined

$$H_i = I_{il}\omega_l. \tag{4}$$

Here I_{ik} is the moment of inertia tensor of the plate,

$$I_{ik} = \int \rho[(x_l - x_{l0})^2\delta_{lj} - (x_i - x_{i0})(x_k - x_{k0})]dv. \tag{5}$$

Let us consider only the horizontal movement of the center of masses of the plate and its rotation around of the vertical axis. In this case, the equations (1-2) are reduced to the system of three equations:

$$m\frac{du_1}{dt} = \int\int(-p\delta_{1j} + \tau_{1j} + f_{1j})n_j ds; \tag{6}$$

$$m\frac{du_2}{dt} = \int\int(-p\delta_{2j} + \tau_{2j} + f_{2j})n_j ds; \tag{7}$$

$$I_{33}\frac{d\omega_3}{dt} = \int\int \varepsilon_{ij3}(x_i - x_{0i})(-p\delta_{jk} + \tau_{jk} + f_{jk})n_k ds. \tag{8}$$

Here, x_i are the coordinates of an arbitrary point of the continent; x_{i0} are the coordinates of the instantaneous center of masses of the plate; δ_{ij} is the Kronecker symbol (equal to 1 at $i = j$ and 0 at $i \neq j$); ε_{ijk} is the Levy-ЦCivita symbol, which is equal to 0 (if any two indexes coincide) or 1 (at an even transposition of indexes with respect to (1, 2, 3)) and -1 (if this transposition is uneven); p is pressure; τ_{jk} are the friction stresses of the atmosphere and ocean on the exterior surface of the plate; f_{jk} are viscous stresses of the asthenosphere on submerged surface of the plate; n_j is the unit vector of the outward normal to the surface of the plate; ds is absolute value of an elementary surface area of the solid continent.

Taking into account that:

$$\frac{dx_1}{dt} = u_1, \frac{dx_2}{dt} = u_2, \frac{d\varphi}{dt} = \omega_3, \tag{9}$$

we can, using the given magnitudes coordinates of the center of masses of the plate $x_1(t)$, $x_2(t)$, $\varphi(t)$ and values $p(t)$, $\tau_{ij}(t)$ end $f_{ij}(t)$, calculate the linear velocities $u_1(t)$, $u_2(t)$ of the translational motion and the angular velocity $\omega_3(t)$ of the rotation of a plate. Equations of motion (6-8) are necessary to write out for each plate.

The model allows us to calculate the linear velocities $u_1(t_1)$ and $u_2(t_1)$ of the translational horizontal motion of the plate's center of masses and the angular velocity $\omega(t_1)$ of the rotation of the plate around the vertical axis. This is made using the values of the frictional $\tau_{ij}(t_1)$ and the pressure $p(t_1)$ forces of the atmosphere and the ocean and the force $f_{ij}(t_1)$ of the interaction with the viscous asthenosphere, applied to the submerged surface of the plate, calculated for the moment t_1. Knowing these velocities and initial coordinates of the plate $x_1(t_1)$, $x_2(t_1)$, $\varphi(t_1)$ it is possible to find its position in the subsequent instant $t_2 = t_1 + \Delta t$: $x_1(t_2) = x_1(t_1) + u_1(t_1)\Delta t$, $x_2(t_2) = x_2(t_1) + u_2(t_1)\Delta t$, $\varphi(t_2) = \varphi(t_1) + \omega_3(t_1)\Delta t$. Then, using new values $\tau_{ij}(t_2)$, $p(t_2)$ and $f_{ij}(t_2)$, we calculate $u_1(t_2)$, $u_2(t_2)$ and $\omega_3(t_2)$, and determine the position of a plate for the following instant t_3. The calculations are performed up to the final moment of time. The time step depends on the discretization of calculations of the friction and pressure forces of the atmosphere and the ocean.

5. SUMMARY

Under the effect of the atmospheric and oceanic forces, the plates interact with the circumjacent plates through the frontal contacts. The stresses may reach such high values (10^6-10^7 N/m^2) at which the discontinuity and displacement of the plates from each other occur, that trigger the earthquakes. Relative movements of the lithosphere plates create the Earth's main earthquake and volcanic zones.

When calculating the moments of friction forces and pressure, the integration of the atmospheric and oceanic forces should be performed not only for the entire Earth surface but

also separately for every lithosphere plate. The algorithm of calculation of the movement of lithosphere plates is developed.

*Acknowledgments.*The investigation was carried out under a financial support of the Russian Foundation for Fundamental Research, Grant No 02-02-16178.

6. REFERENCES

Barsukov O. M., 2002, Godichnye variazii seismichnosti i skorosti vrashenija Zemli [Yearly variations of seismicity and velocity of the Earth rotation], *Fizika Zemli*, No 4, 96–98. [In Russian with English text In *Izvestiya, Physics of the Solid Earth*, **38**, No. 4].

Gorkavy N. N., Levitzky L. S., Taidakova T. A., Trapeznikov Ju. A., Fridman A. M., 1994, O vyjavlenii trech component seismicheskoi aktivnosti Zemli [About detection of three components of a seismic activity of the Earth], *Fizika Zemli*, No. 10, 23–32. [In Russian with English text In *Izvestiya, Physics of the Solid Earth*, **30**, No. 10].

Gorkavy N. N., Trapeznikov Ju. A., Fridman A. M., 1994, O globalnoi sostavljajuchei seismicheskogo prozessa i ee svjazi s nabludaemymi osobennostjami vrachenija Zemli [About global component of the seismic process and its connection with observable singularities of the Earth's rotation], *Dokl. Ross. Akad. Nauk*, **338**, No. 4, 525–527, [In Russian].

Sidorenkov, N. S., 2002. Fizika nestabilnostey vrashenija Zemli [Physics of the Earth's rotation instabilities], Moscow, Nauka, 384 pp., [In Russian with English summary and contents].

Sytinsky A. D., 1985, Svjaz seismichnosti Zemli s solnechnoi aktivnostju i atmosfernymi processami [Connection of seismicity of the Earth with solar activity and atmospheric processes], *Thesis of the doctor of physical and mathematical sciences*, Leningrad, Arctic and Antarktic research institut, 206 pp, [In Russian].

Trubitsyn V. P., Rykov V. V., 1998, Global Tectonics of Floating Continents and Oceanic Lithospheric Plates, *Dokl. Ross. Akad. Nauk*, **359**, No. 1, 109–111, [In Russian].

Trubitsyn V.P., 2000, Principles of the Tectonics of Floating Continents, *Izvestiya, Physics of the Solid Earth*, **36**, No. 9, 708–741.

Zharov V. E., Konov A. S., Smirnov V. B., 1991, Variazii parametrov vrashenija Zemli i ich svjaz s silneishimi zemletrjasenijami mira [Variations of parameters of the Earth rotation and their connection with the strongest earthquakes of the world], *Astronomicheskii Zhurnal*, **68**, No. 1, 187–196. [In Russian with English text in *Astronomy Reports*, **35**, No. 1].

NEW MODELS FOR REDUCTION OF THE VLBI DATA

V.E. ZHAROV
Sternberg State Astronomical Institute
13, Universitetskij pr., 119992, Moscow, Russia
e-mail: zharov@sai.msu.ru

ABSTRACT. For improvement of accuracy of the VLBI reduction new models of motion the VLBI stations due to atmospheric loading were developed. New models of the atmospheric radio refraction and tropospheric delay are based on numerical integration of the index of refraction depending on the local surface pressure, temperature and the partial pressure of water vapor.

1. INTRODUCTION

One of the methods to improve the accuracy of radio interferometry is development of new models for the delay and delay rate observables. The delay and delay rate models are the sum of components: geometry of baseline and source, clock and the atmosphere. The model of the station motion due to atmospheric loading and nutation theory (geometry components) were improved and used in the ARIADNA software. Atmospheric loading was computed by convolving a Green's function with the surface atmospheric pressure distribution.

Model of motion of each the VLBI station is represented as sum of annual, semi-annual and semi-diurnal components. In addition to this deterministic signal the vertical site displacement is corrected for the local pressure anomaly.

Effects of the atmosphere on the radio wave propagation are the atmospheric radio refraction and additional tropospheric delay. New model of the atmospheric radio refraction which is more precise at low elevation angles was implemented. The developed algorithm was used for calculation of the additional tropospheric delay. Instead of use of the mapping functions the path length through the troposphere was calculated by the numerical integration of the index of refraction which depends on the surface pressure, temperature and the partial pressure of water vapor.

2. DISPLACEMENT DUE TO THE ATMOSPHERIC LOADING

Effects of atmospheric loading can be computed by convolving a Green's function with distribution of surface atmospheric pressure. Green's function describe the response of an elastic Earth to a point load on its surface.

The vertical u_v and tangential u_θ displacement can be written as Farrell's elastic Green's functions (Farrell, 1972):

$$u_v = \frac{m(\theta,\lambda)}{M} R \sum_n h'_n P_n(\cos\psi), \tag{1}$$

$$u_\theta = \frac{m(\theta,\lambda)}{M} R \sum_n l'_n \frac{\partial P_n(\cos\psi)}{\partial\psi}, \tag{2}$$

where $m(\theta,\lambda)$ is mass of a point load with co-latitude θ and longitude λ; M, R are mass and radius of the Earth, h'_n, l'_n are the loading numbers, ψ is the arc between load and point of measurement of surface displacement. Mass of load can be found from local pressure $p(\theta,\lambda)$:

$$m(\theta,\lambda) = \frac{1}{g}[p(\theta,\lambda) - \overline{p(\theta,\lambda)}]ds,$$

where g is the gravitational acceleration, $\overline{p(\theta,\lambda)}$ is mean surface pressure over a region with square equals to ds.

Components of horizontal displacement in the eastern u_e and northern u_n directions are equal to

$$u_e = -u_\theta \sin\varphi, \quad u_n = -u_\theta \cos\varphi, \tag{3}$$

where φ is azimuth of load from a point of measurement.

Total displacement in point of measurement can be found by summation of u_v, u_e, u_n for different $m(\theta,\lambda)$ over the Earth's surface.

Displacements of each VLBI station were computed using four times daily global surface pressure values on a $5° \times 5°$ grid. The NCEP spherical harmonic coefficients data were used. The coefficients can be found on site of the SBA (SBA, 2003) :

$$p(\theta,\lambda) = (2-\delta_{0m}) \sum_{m=0}^{M} \sum_{n=m}^{N+J} (a_n^m \cos m\lambda - b_n^m \sin m\lambda) P_n^m(\cos\theta),$$

where δ_{0m} is the Kronecker delta function, and $J = 0$ or M depending on whether the truncation is triangular or rhomboidal, respectively. Surface displacements are calculated using an Earth model in which the oceans respond as an inverted barometer to atmospheric pressure loading.

As example the vertical, eastern and northern displacement of Fortaleza station due to the atmospheric loading are shown on left part of Fig.1 and correspondence of displacement and local pressure (right part).

The largest variation (peak-to-peak) in the radial displacement are of order of 10 mm and occur on different timescales: from 12 hours to 1 year. It corresponds pressure variations over a point of measurement of order of 20–30 mbar. Horizontal displacements have amplitude of order of 1 mm. Main period of variations is equal to 1 year. Semi-diurnal displacements are observed for equatorial stations.

Model of vertical displacement is represented by sum of three terms and additional term that corresponds a linear regression with coefficient k of local pressure variations ΔP and displacement (right upper plot on Fig.1). Only periodic terms are included in model of horizontal displacement because there are no correlations with local pressure variations:

$$u_r = \sum_{i=1}^{3} [(a_r)_i \cos(Arg_i) + (b_r)_i \sin(Arg_i)] + k\Delta P,$$

$$u_{e,n} = \sum_{i=1}^{3} [(a_{e,n})_i \cos(Arg_i) + (b_{e,n})_i \sin(Arg_i)],$$

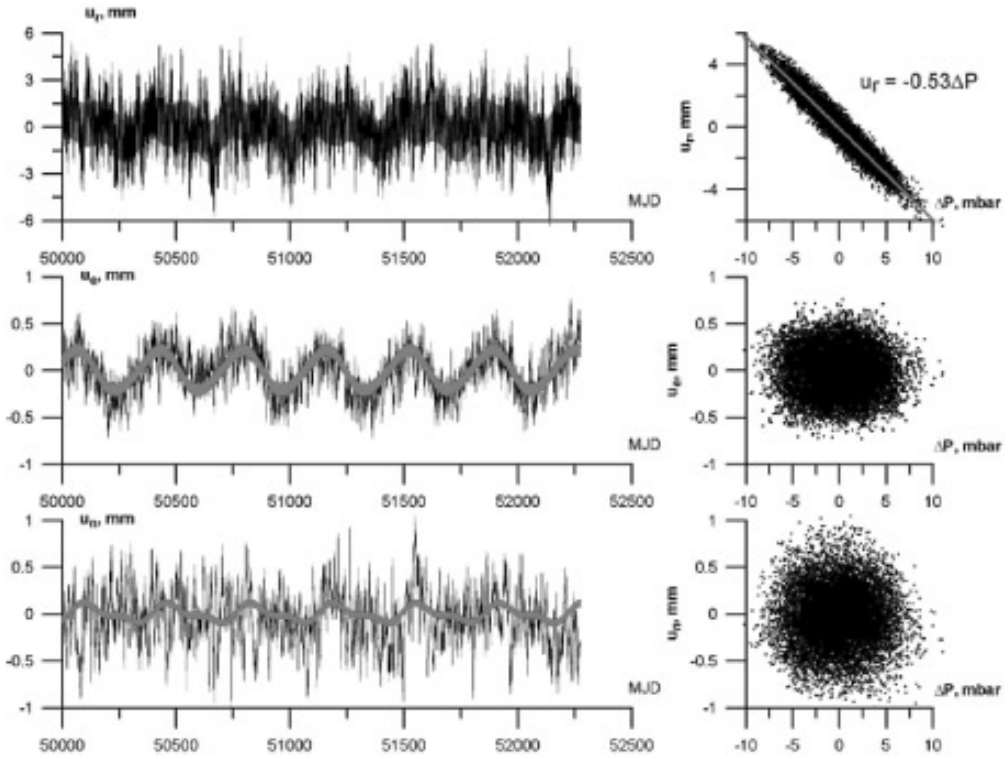

Figure 1: Displacement of Fortaleza station.

where $Arg_i = 2\pi/T_i\Delta t$, $T_1 = 1$ year, $T_2 = 1/2$ year,$T_3 = 1/2$ day,$\Delta t = MJD - 44239.0$ (Jan.1 1980).

Coefficients k, $(a_r)_i, (b_r)_i$, $(a_{e,n})_i, (b_{e,n})_i$, $i = 1, 2, 3$ were calculated for each VLBI station and can be sent by author on request.

3. TROPOSPHERIC DELAY AND REFRACTION

In order to calculate tropospheric delay and refraction the model of standard atmosphere is used. In spherical symmetric atmosphere the additional signalTs path between two layers with radius S_1 and S_2 is

$$S = \int_{S_1}^{S_2} (n-1)\sec\theta ds,$$

where n is the index of refraction and θ is zenith angle of the observed source. As shown by Murray (1983) the index of refraction for radio waves depends on density of air ρ and density of water vapour ρ_w:

$$S = S_d + S_w = \int_{S_1}^{S_2} \beta_d \rho \sec\theta ds + \int_{S_1}^{S_2} (\beta_w - \beta_d)\rho_w \sec\theta ds,$$

where β_w, β_d are parameters depending on the surface pressure, temperature and the partial pressure of water vapor.

For $\theta = 0°$ we have zenith tropospheric delay Z_d or Z_w and for $\theta \neq 0°$ we can write:

$$S = Z_d + \Delta Z_d + Z_w + \Delta Z_w = Z_d\Big(1 + \frac{\Delta Z_d}{Z_d}\Big) + Z_w\Big(1 + \frac{\Delta Z_w}{Z_w}\Big) = Z_d \cdot F_d + Z_w \cdot F_w, \qquad (4)$$

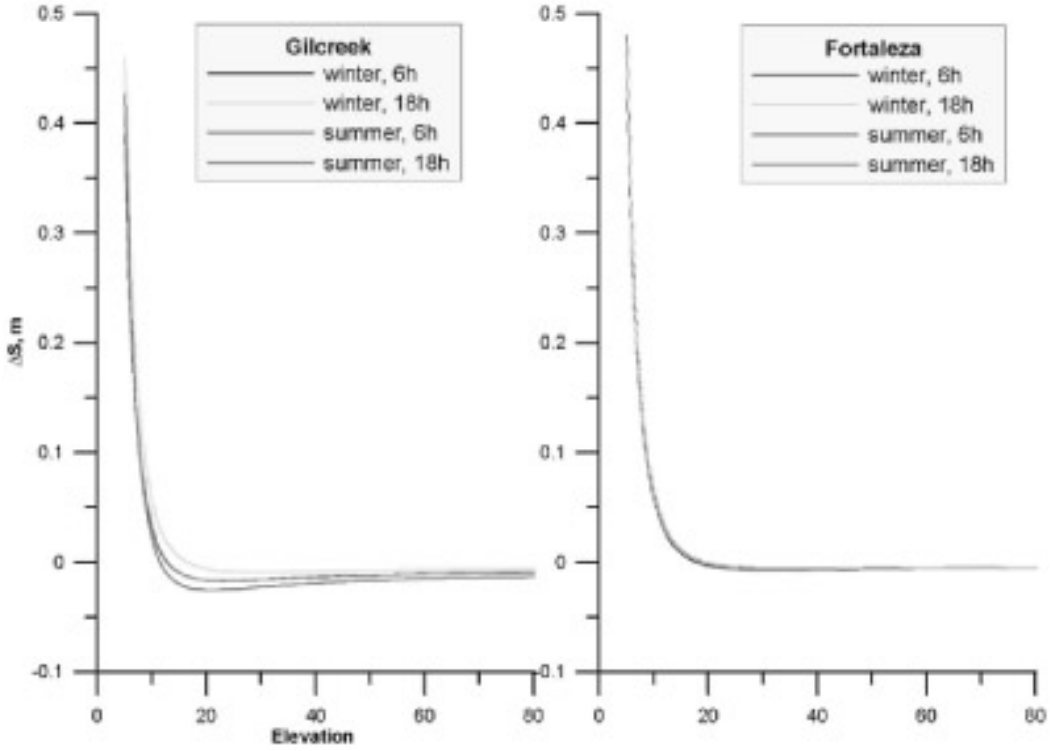

Figure 2: Tropospheric delay differences (direct calculation minus the Niell's mapping functions) for Gilcreek and Fortaleza stations.

where F_d, F_w are the mapping functions. Tropospheric delay was written in form (4) in order to compare results with traditional approach when delay in the troposphere is calculated as product of zenith delay and the mapping function.

Tropospheric delay was calculated by numerical integration of the index of refraction depending on the local surface pressure, temperature and the partial pressure of water vapor. Difference of tropospheric delay that was obtained by numerical integration and by calculation of the Niell's mapping functions is shown on Fig. 2 for equatorial (Fortaleza) and northern (Gilcreek) stations.

One can see from Fig.2 that there is diurnal variation of tropospheric delay for Gilcreek. Amplitude of this variation can reach 2-3 cm for elevation angles in range $10° \div 30°$.

Radio refraction Δz in spherical symmetric atmosphere is equal to

$$\Delta z = \int_{\theta_0}^{\theta_1} \frac{d\ln n}{d\ln s}\left(1 + \frac{d\ln n}{d\ln s}\right)^{-1} d\theta,$$

where θ_0 is apparent zenith angle of the source, θ_1 is zenith angle of the source when the atmosphere is absent, s is the length of radio wave path. The empirical model used in CALC software was compared with values Δz (Fig. 3).

There is significant difference for low elevation angles between two models: for angles $< 10°$ this difference can reach $150 \div 200$ arcsec.

3. CONCLUSIONS

New models of displacements of the VLBI sites were calculated. Tropospheric delay and radio refraction were calculated by numerical integration of the index of refraction depending on the local surface pressure, temperature and the partial pressure of water vapor.

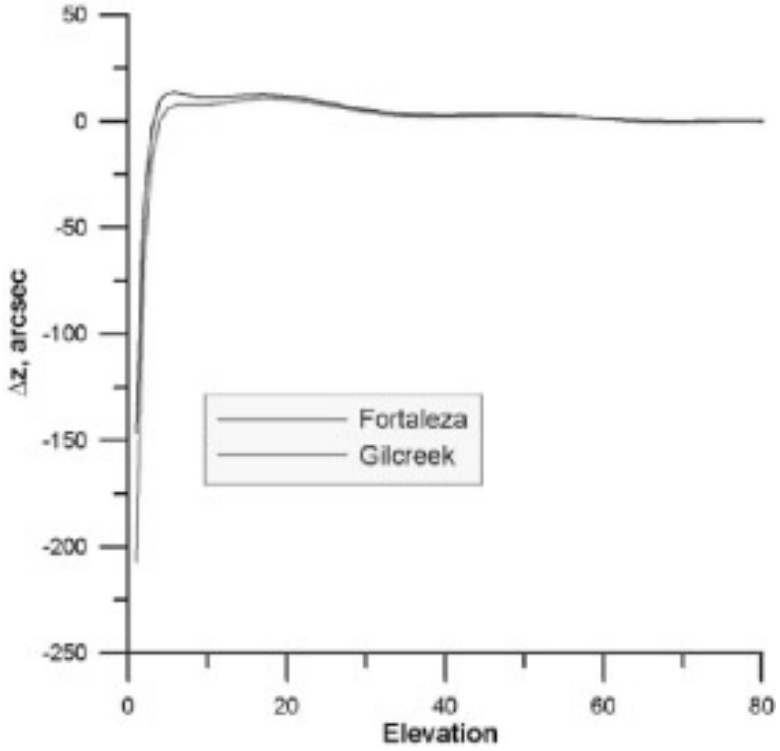

Figure 3: Radio refraction differences (direct calculation minus empirical model used in CALC software) for Gilcreek and Fortaleza stations.

This work was supported by the Russian Foundation for Basic Research (grants 01-02-16529 and 02-05-39004).

4. REFERENCES

Farrell, W. E., 1972, *Rev. Geophys. Space Phys.*, **10(3)**, 761–797.
Murrey C. A., 1983, *Vectorial Astrometry*, Adam Hilger Ltd, Bristol.
SBA, http://ggfc.u-strasb.fr/pub/sba/sba/html.

TIDAL VARIATIONS FROM LOCAL ASTROMETRIC EOP SETS

V. GORSHKOV, N. SHCHERBAKOVA, N. MILLER, E. PRUDNIKOVA
Main Astronomical Observatory of RAS
65/1 Pulkovskoe sh., 196140, St.Petersburg, Russia
e-mail: vigor@gao.spb.ru

In this paper the material of Pulkovo database was used for the investigation of tidal variations in different regions. The part of this data (1899.7-1992.0) was used for recalculation EOP in international work (Vondrak et al., 1998). Since 1) nearly ten years of observations were added, in some of these sets new systematic (refraction reductions) were included, 2) the new precession-nutation model IAU2000A (Convention, 2000) was taken into consideration, 3) the new model of diurnal tidal oceanic perturbations of EOP and sub-diurnal geopotential perturbations of polar coordinates was appeared, 4) tidal variations of the Earth rotation in frequency region from 5 days to 18.6 years were improved.

The above-mentioned models were used by IERS software tools (Bizouard, 2002). The ICRS (HiC) was used for processing all observational sets.

The combination of Love's numbers $\Lambda = 1 + k - l$ was estimated by diurnal and semi-diurnal variations of vertical (generally by O_1 and M_2 waves) and k was estimated by the tidal variations of the Earth rotation (M_m and M_f waves). The model equation is

$$r(t) = kv(t) + \Lambda w(t) + \epsilon(t). \quad (1)$$

The polyharmonic functions of tidal irregularity of the Earth rotation $v(t)$ and variation of vertical $w(t)$ were taken from (Vondrak et.al., 1998), $\epsilon(t)$ is the noise component, $r(t)$ is observed residuals from EOP(IERS)C01 and C04 (UT1R-UTC, X,Y). The using (UT1R-UTC) suggests the including of 41 short-periodic terms of tidal variations of the Earth rotation up to 35 days. The M_m (27.53 day) and M_f (13.66 day) waves were excluded from (UT1R-UTC) to be evaluated from the observations by the model (1). The influence of the above-mentioned sub-diurnal oceanic loads (71 terms) and luni-solar perturbations (10 terms) on EOP was taken into account.

Table 1: Love's number.

Ins.	PUF	PUG	PUH	RIG	NIK	IRK	PUZ1	PUZ2
ϕ_0	59.8^o	59.8^o	59.8^o	56.9^o	47.0^o	52.3^o	59.8^o	59.8^o
λ_0	30.3^o	30.3^o	30.3^o	24.0^o	32.3^o	104.3^o	30.3^o	30.3^o
Span	62.0-71.4	71.2-85.4	71.9-03.5	79.4-87.0	74.0-92.4	79.0-99.9	04.8-41.5	48.8-95.0
k	0.28±.16	0.20±.14	0.18±.12	0.30±.18	0.20±.10	0.16±.11	-	-
Λ	1.14±.49	1.10±.44	1.06±.35	1.31±.64	1.24±.36	1.20±.36	1.25±.61	0.89±.34

The tools for calculation of Λ and k were least-squares method (LSM) solution of conventional equations (1) for each instrument, spectrum analysis (FFT) and singular spectrum analysis (SSA) in soft realization from (Goliandina et al., 2001). SSA was used together with FFT for low frequency filtration. The main usage of two-dimensional (2D) realization of SSA was in joint analysis of $r(t)$-sets with chosen tidal harmonic component. This approach permits to investigate the dynamics of the probable instability of this component in sets.

The principal results evalueted by LSM are given in the table. The heterogeneity of sets has some influence on the SSA results, so any conclusions about dynamics of regional elastic properties of the Earth by astrooptical EOP sets could not be done.

Irregular 5-7 years variations of the Earth rotation velocity (LOD)were revealed as a by-product of this research. The most significant errors in UT0-UTC (catalog, instrumental and refraction origin) cannot excite systematic errors of 5-7 years variations. But in the astrometric EOP data by the best instruments (Vondrak et al.,1998) these variations are presented with amplitude about 100 msec from 1984 (when astrometric tools have stopped participation in the EOP determination) up to the end of the realization (1992). It may be only if global EOP sets are not uniform or/and if new observational means cannot register the reaction of some geophysical process on LOD.

Two sets of LOD in disposal of IERS database were investigated by SSA (C04(IERS)EOP and LOD from 1832 to 1997 (Gross, http://hpiers.obspm.fr/)). The residuals of LOD variations after the reconstruction by the first main components (99.3% of set power) show the presence of quasi-periodical variations with amplitude about 0.15 msec in both sets (fig. 1a).

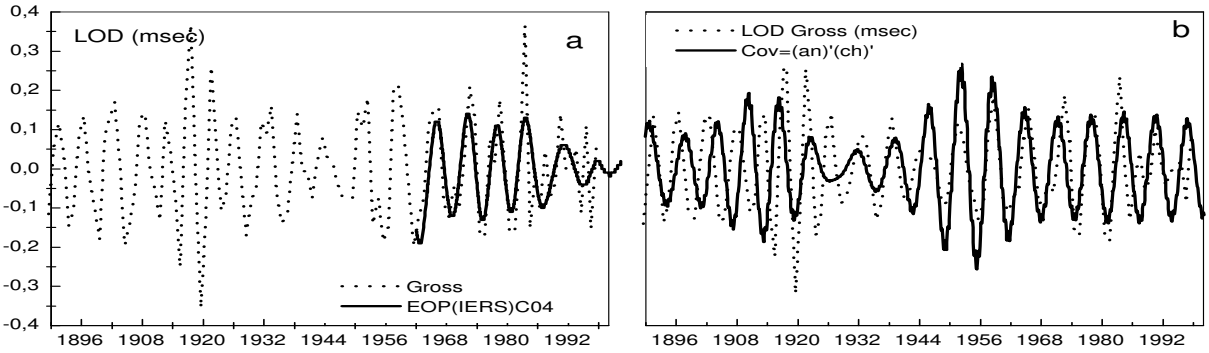

Figure 1: a) The residuals of LOD sets after subtraction of reconstructed decadal variation.
b) The residuals of LOD and function COV describing phase relation of annual and chandler pole oscillation.

There is more important fact of significant correlation of LOD and phase relation of annual and chandler polar motion. When these oscillations are in phase - the LOD is increasing (fig. 1b) and vice versa. This correlation is especially evident after the attenuation of chandler wobble in 1920. The character of the LOD variations as a whole (the damping of amplitude and the phase change) are similar to polar motion dynamics. This can be consequence of geophysical linking of these processes (Gorshkov et al.,2002) or presence of mutual reason of modulation.

REFERENCES

Bizuard Ch., 2002, http://hpiers.obspm.fr/eop-pc/.

IERS Convention 2000, http://maia.usno.navy.mil/conv2000.html.

Goliandina N., Nekrutkin V., Zhigljavsky A., 2001, (http://vega.math.spbu.ru/), *Analysis of Time Series Structure. SSA and Related Techniques*, 305.

Gorshkov V., Vorotkov M., 2002, Dynamics of polar motion and longperiodic Earth rotation variations, *Izv. GAO*, **216**, 415–425 (in Russian).

Vondrak J., Pesek I., Ron C., Cepec A., 1998, Earth orientation parameters 1899-1992 in the ICRS based on the HIPPARCOS reference frame, *Publ. Astr. Inst. Acad. Science of Czech*, Rep.87.

ON EXPEDIENCY OF CREATION IN EURASIA NETWORK OF UNIFIED POINTS OF JOINT ASTRONOMICAL, GEODETIC AND GEOPHYSICAL DETERMINATIONS OF THEIR POSITION CHANGES

A. GOZHY
Poltava Gravimetrical Observatory of NAS of Ukraine
Myasoyedova 27/29, 36029 Poltava, Ukraine
e-mail: pgo@poltava.ukrtel.net

1. INTRODUCTION

Nowadays in astronomy, geodesy and geophysics the high-precise determination of very small temporal changes of spatial and geophysical parameters is a very important scientific and practical problems. The quantities of these changes are commensurable with quantities of proper motions of observation points and with quantities of determination errors. To obtain high accuracy of separate determinations of such very small quantities, it is necessary to have special network of unified points of joint observations by different methods.

2. ORDERED, JOINT, UNIFIED AND REPEATED DETERMINATIONS

By ordered complex of unified points of joint astronomical, geodetic and geophysical determinations or observations(JAGGD points or JAGGO points) we mean such regional or global network of points of determinations, where on each point the same combination of methods of astronomical, geodetic and geophysical determinations of point position and other values are used. By points of joint determinations we mean points, where various results of observations can be reduced to the same geometrical centre of point on each epoch. By unified determinations we mean such ones, which are executed by the same programs and methods, in unified buildings and by unified instruments etc. On JAGGD point the different types of observations are expedient to execute not permanently, but in separate series, which are periodically repeated without changes of programs and methods of observations.

3. APPROXIMATE COMPLEX OF METHODS OF OBSERVATIONS AND OBJECTS OF DETERMINATIONS ON JAGGD POINTS

Minimal necessary set of determination methods in JAGGD points ought to consist high-precise determinations of: 1) geodetic coordinates by GPS-method and geometric levelling; 2) astronomical coordinates by means of a specially created zenith tube or prismatic astrolabe; 3) gravity values by means of a gravimeter; 4) gravity direction by means of a specially created instrument; 5) terrestrial surface inclination by means of a tiltmeter; 6) point proper movements by independent of basic determination methods; 7) changes of external conditions of observations. It is possible to increase scientific and practical potentialities and importance of JAGGD points network by organizing on its basis interferometric observations.

4. OVERCOMING THE MAIN OBSTACLE FOR CREATION OF JAGGD POINTS NETWORK

Minimal set of JAGGD cannot be organized at any of the already existing points for separate astronomical, geodetic and geophysical observations. The main obstacle for direct use of already existing points of separate observations is substantial difference in external conditions where determinations are carried out. Astronomical and geodetic observations are executed on the Earth surface, and geophysical ones are executed in closed underground chambers and mines. The only type of building which is suitable for JAGGD is deep vertical mine (DVM). Just DVM may be adapted for execution of different observations in and over it. DVM are very convenient also for placing of deep fundamental coordinate centres in it.

5. PECULIARITIES OF EQUIPMENT OF DVM SUITABLE FOR JAGGD POINTS CREATION

For creation of JAGGD point we need DVM with the following peculiarities. It should be build on ledge bed-rocks in ecologically safe place. It should be have complete isolation from groundwater, hardening from action of unfavorable exterior weather requirements, convenience of operation. Its depth should be about 25–50 m and inner diameter about 3–5 m. On the bottom of DVM there should be basic observation pillar with geometrical centre to which should be reduced the results of all kinds of determinations. Gravimetric, tiltmetric and other geophysical determinations should be executed directly on the pillar. In the mine entrance vicinity the additional geometrical centres should be situated. Results of all on-surface observations (geodetic, astronomical, meteorological) should be related to these centres. Between the additional centres and the main centre a simple geometrical connection should exist. On-surface entrance to DVM could be designed as astronomical pavilion with symmetrically opening roof. Topographical conditions in DVM vicinity should be favorable for executing of all types of observations on JAGGD point.

6. EXPEDIENCY OF CREATION OF UNIFIED JAGGD POINTS NETWORK IN EURASIA

In geophysics the creation of in-depth points network for only one type of determination (gravimetric, tiltmetric, seismometric or others) is quite expedient. In geodesy and practical astronomy the creation of only in-depth coordinate centres network is quite expedient also. And certainly the creation of a unified in-depth JAGGD points network is some more expedient because those points are simultaneously standard astronomical-geodetic coordinate points, and universal geophysical stations, and unique laboratories for geodynamic investigations. The creation of JAGGD points network will help to : study of the Earth figure evolution, verify geophysical hypotheses about nature of the Earth figure changes, bring together and generalize study of the Earth's figure and study of the Earth's rotation, determine all combinations of Love numbers from observations only in one point, make high-precise coordinate connection of maps of various geophysical fields to high-precise terrestrial coordinate systems and study temporal changes of parameters of those fields, compare results of geophysical determinations in terrestrial and space conditions, study temporal changes of geoid's figure, determine length of arcs between zeniths of separate pairs of JAGGD points and length of connecting them chords, study nature and predict rise of anomalous geophysical phenomena. The creation of unified in-depth JAGGD points network in Eurasia will be a huge step to creation of a global network of such points and to complex solution of global geophysical and geodetic scientific and practical problems. To study of many global geophysical and geodynamical phenomena several hundreds of unified in-depth JAGGD points will contribute more than thousands of modern diverse observations of change of different spatial and geophysical parameters.

Section IV)

SOLAR SYSTEM DYNAMICS

DYNAMIQUE DU SYSTÈME SOLAIRE

NUMERICAL EPHEMERIDES OF PLANETS AND THE MOON — EPM AND IMPROVEMENT OF SOME ASTRONOMICAL CONSTANTS

E.V. PITJEVA
Institute of Applied Astronomy of RAS
10 Kutuzov quay, St.Petersburg, 191187, Russia
e-mail: evp@quasar.ipa.nw.ru

ABSTRACT. The current state of the last version of the planet part of EPM (**E**phemerides of **P**lanets and the **M**oon) ephemerides whose origin dates back to the 1970s, is presented. Ephemerides of the planets and the Moon have been numerically integrated in the PPN metric over a 125-year time interval (1886–2011). The dynamical model of EPM2003 ephemerides includes mutual perturbations from the nine planets, the Sun, the five most massive asteroids, the Moon, lunar physical libration, perturbations from other 296 asteroids, as well as perturbations from the solar oblateness and the massive asteroid ring with constant mass distributions in ecliptic plane. EPM2003 ephemerides have resulted from a least squares adjustment to observational data totaling more than 280000 position observations (1913–2003) of different types. The set of different astronomical constants have been obtained from accurate radiometic observations. The angles of the rotation between EPM2003 and the ICRF are (in mas): $\varepsilon_x = 4.5 \pm 0.8$, $\varepsilon_y = -0.8 \pm 0.6$, $\varepsilon_z = -0.6 \pm 0.4$. The two versions of EPM2003 ephemerides have been constructed in TDB and TCB time scales as the independent variables of the equations.

1. DYNAMIC MODELS OF PLANETARY MOTION OF DE AND EPM EPHEMERIDES

The current state of the last version of the planet part of EPM (**E**phemerides of **P**lanets and the **M**oon) ephemerides, whose origin dates back to the 1970s, is presented. At the same time, to ensure space flights the construction of numerical planetary ephemerides was undertaken by several groups in the USA and Russia. For comparison, I'll further consider our EPM ephemerides created first at the Institute of theoretical astronomy and later at the Institute of applied astronomy as well as well-known DE ephemerides of JPL.

Common to all DE/LE and EPM ephemerides is a simultaneous numerical integration of the equations of motion of the nine major planets, the Sun, the Moon and the lunar physical libration performed in the Parameterized Post-Newtonian metric for the harmonic coordinates $\alpha = 0$ and General Relativity values $\beta = \gamma = 1$.

The various ephemerides differ slightly in

- the modelling of the lunar libration,
- the reference frames,

- the accepted value of the solar oblateness,
- the modelling of the perturbations of asteroids upon the planetary orbits,
- the sets of observations to which ephemerides are adjusted.

Some characteristics of DE118/LE62, DE200/LE200, DE403/LE403, DE405/ LE405, EPM87, EPM98, EPM2000, EPM2003 ephemerides are given in Table 1. The detailed description and comparison of DE and EPM ephemerides are given in the paper by Pitjeva (2001).

Table 1. Ephemerides DE and EPM.

Ephemeris	Interval of integration	Ref. frame	Mathematical model	type	Data number	interval
DE118	1599→2169	FK4	Integrating of	optical	44755	1911-79
(1981)			Sun,Moon,9 planets	radar	1307	1964-77
⇓		⇓	+perturbations	spacecraft	1408	1971-80
DE200		dynamic.	from 3 asteroids	LLR	2954	1970-80
		frame	(Keplerian ellipses)	total	50424	1911-80
EPM87	1700→2020	FK4	Integrating of	optical	48709	1717-80
(1987)			Sun,Moon,9 planets	radar	5344	1961-86
			+perturbations	spacecraft	–	–
			from 5 asteroids	LLR	1855	1972-80
			(Keplerian ellipses)	total	55908	1717-86
DE403	−1410→3000	ICRF	Integrating of	optical	26209	1911-95
(1995)			Sun,Moon,9 planets	radar	1341	1964-93
⇓	⇓		+perturbations	spacecraft	1935	1971-94
DE404	−3000→3000		from 300 asteroids	LLR	9555	1970-95
			(mean elements)	total	39057	1911-95
EPM98	1886→2006	DE403	Integrating of	optical	–	–
(1998)			Sun,Moon,9 planets	radar	55959	1961-95
			5 астер.+ perturb.	spacecraft	1927	1971-82
			from 295 asteroids	LLR	10000	1970-95
			(mean elements)	total	67886	1961-95
DE405	1600→2200	ICRF	Integrating of	optical	28261	1911-96
(1997)			Sun,Moon,9 planets	radar	955	1964-93
⇓			+perturbations	spacecraft	1956	1971-95
DE406	−3000→3000		from 300 asteroids	LLR	11218	1969-96
			(integrated)	total	42410	1911-96
EPM2000	1886→2011	DE405	Integrating of	optical	–	–
(2000)			Sun,Moon,	radar	58076	1961-1997
			9 planets,	spacecraft	24587	1971-1997
			300 asteroids	LLR	13500	1970-1999
				total	96163	1961-1999
EPM2003	1886→2011	ICRF	Integrating of	optical	44490	1913-2003
(2003)			Sun,Moon,	radar	58076	1961-1997
			9 planets,	spacecraft	164193	1971-2002
			301 asteroids,	LLR	14612	1970-2001
			asteroid ring	total	281371	1913-2003

In the past ephemerides have been aligned onto the FK4 reference frame, then onto the dynamical equator and equinox and now ephemerides are oriented onto the **I**nternational **C**elestial **R**eference **F**rame (ICRF). Starting with DE405 a nonzero value of the solar oblateness

$J_2 = 2 \cdot 10^{-7}$ obtained from some astrophysical estimates was accepted for integrating.

A serious problem in the construction of planetary ephemerides arises due to the necessity to take into account the perturbations caused by minor planets. In DE200 and our more previous versions the perturbations from only three or five biggest asteroids were accounted for. The experiment showed that the fitting of these ephemerides to the Viking lander data is poor. The perturbations from 300 asteroids have been taken into account in the ephemerides DE403, DE405, and EPM ephemerides starting with EPM98. Masses of many of these asteroids are quite poorly known, and as shown by Standish and Fienga (2002), the accuracy of the planetary ephemerides deteriorates due to this factor. Masses of few most massive asteroids which more strongly affect Mars and the Earth can be estimated from observations of martian landers and spacecraft orbiting Mars. The five of 300 asteroids proved to be double and their masses are known now. The masses of Eros(433) and Mathilda(253) have been derived by perturbations of the spacecraft during the NEAR flyby. Unfortunately, the classical method of determining masses of asteroids for which close encounters occur is limited by uncertainty in masses of the large asteroids, perturbations by others, unmodeled asteroids, and a quality of observations. Perhaps, masses of many asteroids will be obtained by high accuracy observations during the GAIA mission, but it will not be soon. So at present masses of the rest of 301 asteroids have been estimated by the astrophysical method. The latest published diameters of asteroids based on infrared data of IRAS (**I**nfra **R**ed **A**stronomical **S**atellite) and MSX (**M**idcourse **S**pace **E**xperiment), as well as observations of occultations of stars by minor planets and radar observations have been used in this paper. The mean densities for C,S,M taxonomy classes have been estimated while processing the observations.

At the several meters level of accuracy the orbit of Mars is very sensitive to perturbations from many minor planets. These objects are mostly too small to be observed from the Earth, but their total mass is large enough to affect the orbits of the major planets. The major part of these celestial bodies moves in the asteroid belt and their instantaneous positions may be considered homogeneously distributed along the belt. Thus, it seems reasonable to model the perturbations from the remaining small asteroids (for which individual perturbations are not accounted for) by computing additional perturbations from a massive ring with a constant mass distribution in the ecliptic plane (Krasinsky et al., 2002). Two parameters that characterize the ring (its mass and radius) are included in the set of solution parameters.

Thus, the dynamical model of EPM2003 ephemerides includes the following perturbations: mutual perturbations from the nine planets, the Sun, the five most massive asteroids, the Moon, lunar physical libration, perturbations from other 296 asteroids, as well as perturbations from the massive asteroid ring and from the solar oblateness.

The lunar-planetary integrator embedded into the program package (Krasinsky and Vasilyev, 1997) ERA-7 (**ERA**: **E**phemeris **R**esearch in **A**stronomy) has been used. Numerical integration of the equations of motion in the barycentric coordinate frame of J2000.0 was carried out by the Everhart method over a 125-year time interval (1886–2011).

2. PROCESSING THE RADAR AND OPTICAL DATA

EPM2003 ephemerides have resulted from a least squares adjustment to observational data totaling more than 280000 position observations (1913–2003) of different types including radiometric observations of planets and spacecraft, CCD astrometric observations of the outer planets and their satellites, meridian transits and photographic observations. Data used for the production of ephemerides were taken from databases of the JPL website (http:/ssd.jpl.nasa.gov/iau-comm4/) created and kept by Dr. Standish, the database of optical observations of Dr. Sveshnikov and extended to include Russian radar observations of planets (on the website of IAA http: //www.ipa.nw.ru/ PAGE/DEPFUND/LEA/ENG/englea.htm).

Radar observations have been reduced for relativistic corrections, the effects of propagation of electromagnetic signals in the Earth troposphere and in the solar corona as well as reduction for the topography for ranging of planet surfaces. Special mention should be made of the uniqueness of the extremely precise observations of the martian Viking (1976-1982), Pathfinder landers (1997) and MGS (Mars Global Surveyor) data (1998-2002) which are free from uncertainties due to planetary topography that do remain in radar ranging despite the modeling of topography. The positions of the landers are computed taking into account the precession, nutation and estimated seasonal terms of the Mars rotation.

The part of MGS data obtained during 1998 was carried out at superior solar conjunction unlike the later MGS data of 1999-2002. Although the frequency was high (the X-band), while the minimum impact parameter (p) was $p = 15.89R_\odot$ for the date 27.04.1998, the effect of the solar corona delay was considerable. When these data were excluded from the fitting the residuals for them were calculated with the obtained ephemerides, their rms appeared to be as large as 150 m which value greatly exceeded the a priory errors. These residuals decreased after reduction for the solar corona with different values of parameters of the corona model for different parts of MGS observations. A simple model of the solar corona was used:

$$N_e(r) = \frac{A}{r^6} + \frac{B + \dot{B}t}{r^2},$$

where $N_e(r)$ is the electron density.

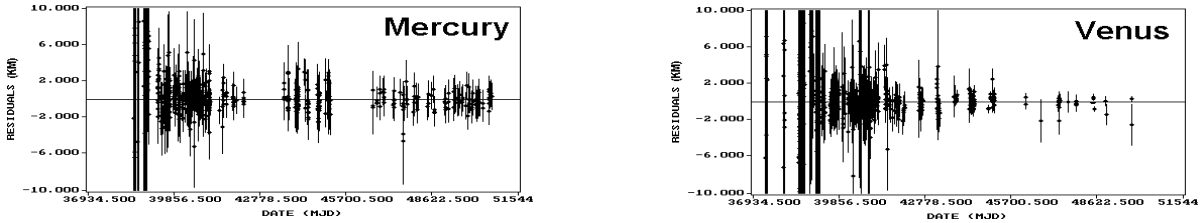

Figure 1: Ranging residuals 1960–2000 for Mercury and Venus, the scale ±10 km.

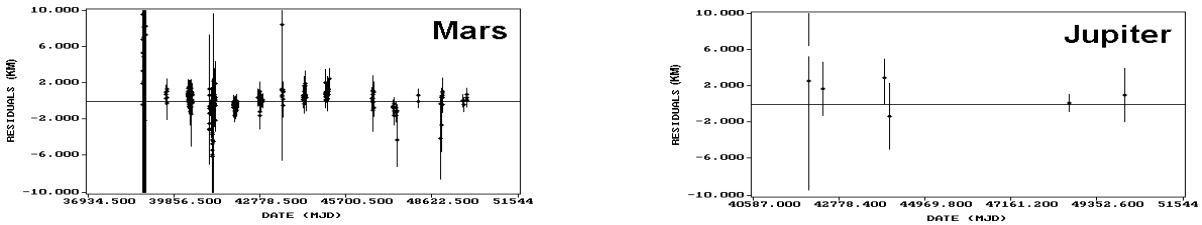

Figure 2: Ranging residuals for Mars (1960–2000) and Jupiter (1970–2000), the scale ±10 km.

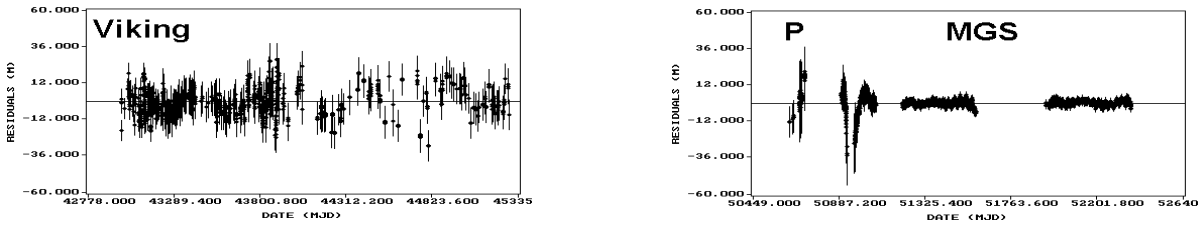

Figure 3: Ranging residuals of Viking (1976–82); Pathfinder, MGS (1997–2002), the scale ±60 m. The result was better when apart from the B coefficient, its time variation was also included. For the remaining MGS data of 1999-2002 the solar corona delay was modeled with another

value of the B coefficient.

The residuals of all radiometric data are shown in Fig. 1–3. The rms residuals of ranging for the Mercury are 1.4 km, for Venus and Mars are 0.7 km, for Viking and Pathfinder are 8 m, MGS (1998) are 7 m, MGS (1999–2002) are less 2 m. For the MGS observations even far away from the solar conjunction there still remains a signature at the a priory errors level. The reason for this is unclear, maybe the removal of the orbit of the MGS spacecraft was insufficiently accurate.

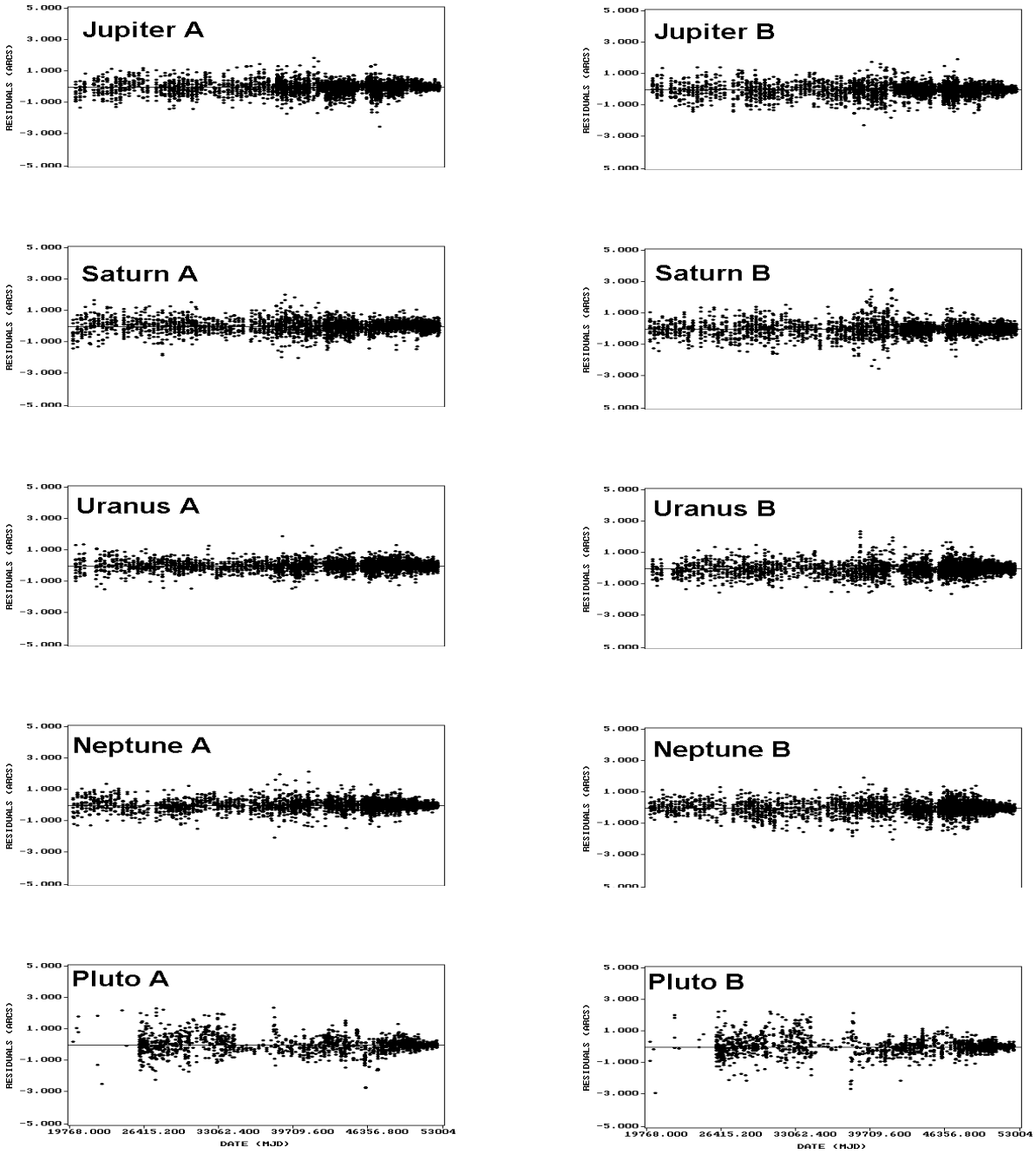

Figure 4: Residuals of the outer planets 1913–2003 in $\alpha \cos \delta$ (A) and in δ (B), the scale $\pm 5''$.

The observations of satellites of Jupiter and Saturn are of great importance for optics, as they are more accurate than the observations of their parent planets and practically free from the phase effect. CCD data, obtained at Flagstaff observatory, whose observational program started

in 1995 and is still being continued are the most accurate. All these positions are referenced to ICRF, using reference stars taken from ACT or Tycho-2 catalogues. Another group of high accuracy data is photographic observations of satellites of Jupiter, Saturn, as well as Uranus and Neptune planets obtained at Nikolaev observatory during 1962–1998. They are referenced to the ICRF system by a special method which has given good results for minor planets. Combination of the satellite data from Flagstaff and Nikolaev has been successfully used to improve the planet ephemerides. Residuals of all the observations of the outer planets are shown in Fig. 4. Unfortunately, observations of Pluto are mainly photographic and have quite poor accuracy and their rms are worse.

3. ORIENTATION OF EPM2003 ONTO ICRF

Ephemerides EPM were oriented onto the **I**nternational **C**elestial **R**eference **F**rame (ICRF). The most precise optical data of the outer planets and their satellites, obtained at Flagstaff, Nikolaev, La Palma) have already been referenced to the ICRF. The remaining optical observations, referenced to different catalogues, at first were transformed to the FK4 systems by Sveshnikov. Then they were referenced to the FK5 using known formulae (see as the example Standish et al., 1995), and were finally transformed to the ICRF using the values of the three angles of the rotation between the HIPPARCOS and FK5 catalogues, J2000 in mas (Mignard, 2000):

$$\varepsilon_x = -19.9,\ \varepsilon_y = -9.1,\ \varepsilon_z = 22.9.$$

Orbits of the four inner planets (with the exception of angles of the orientation) are determined entirely by the ranging observations of planets and spacecraft. The system of these planets was oriented to the ICRF by the including the ICRF-base VLBI measurements of spacecraft (Magellan in orbit about Venus and Phobos on its approach to Mars) in the adjustment, in the same way that has been done by Standish (1998b) for DE405. The angles of the rotation between the EPM ephemerides and the ICRF reference frame were obtained (in mas):

$$\varepsilon_x = 4.5 \pm 0.8,\ \varepsilon_y = -0.8 \pm 0.6,\ \varepsilon_z = -0.6 \pm 0.4.$$

4. RESULTS OBTAINED

The formal standard deviations of orbital elements of planets are shown in the Table 2. Note that the uncertainties, given in this paper, are formal standard deviations; realistic error bounds may be an order of magnitude larger.

Table 2. The formal standard deviations of elements of the planets.

planet	a [m]	$\sin i \cos\Omega$ [mas]	$\sin i \sin\Omega$ [mas]	$e\cos\pi$ [mas]	$e\sin\pi$ [mas]	λ [mas]
Mercury	0.205	3.472	3.630	0.350	0.304	0.901
Venus	0.338	0.662	0.652	0.042	0.044	0.202
Earth	0.169	—	—	0.001	0.001	—
Mars	0.783	0.004	0.009	0.001	0.001	0.004
Jupiter	627	2.471	2.246	0.322	0.372	1.108
Saturn	4425	3.498	4.299	4.068	3.242	3.675
Uranus	41030	4.156	6.602	5.355	3.470	9.610
Neptune	516808	4.286	9.107	15.626	19.617	38.857
Pluto	3821864	7.716	15.567	92.264	37.804	91.196

where a - the semi-major axis, i - the inclination of the orbit, Ω - the ascending node, e - the eccentricity, π - the longitude of perihelion, λ - the mean longitude. The value of the astronomical unit has been obtained:

$$\text{AU}=149597870693.3 \pm 0.1 \text{ m}.$$

The parameters of Mars rotation, masses of Ceres, Pallas, Vesta, Iris, Bamberga, Juno, densities of C,S,M classes of asteroids, the estimation of the total mass of the main asteroid belt, the solar quadrupole moment, parameters of PPN formalism β and γ have been estimated in the fitting process to all the observations. Table 3 – 6 demonstrates some of these values.

Table 3. The parameters of the Mars rotation.

$\dot{V}$ [^{o}/day]	I_q [^{o}]	$\dot{I}_q$ [$''$/year]	Ω_q [^{o}]	$\dot{\Omega}_q$ [$''$/year]
350.891985294	25.1893930	-0.0002	35.437685	-7.5844
± 0.000000012	±0.0000053	±0.0007	± 0.000021	± 0.0015

The value of precession constant for Mars is close to the recent value obtained from the data of the Viking, Pathfider landers and MGS radio tracking (Yoder et al., 2003):

$$\dot{\Omega}_q = [-7.''597 \pm 0.''025(10\sigma)]/\text{year}$$

Table 4. Masses of Ceres, Pallas, Juno, Vesta, Iris, Bamberga.
in $(\text{GM}_i/\text{GM}_\odot)\cdot 10^{-10}$

(1)Ceres	(2)Pallas	(3)Juno	(4)Vesta	(7)Iris	(324)Bamberga
4.749	1.036	0.142	1.358	0.052	0.051
±0.007	±0.003	±0.003	±0.001	±0.001	±0.001

Table 5. The solar quadrupole moment, the radius and the mass of the asteroid ring, the total mass of the main asteroid belt.

J_2 10^{-7}	R_{ring} AU	M_{ring} $10^{-10}\text{M}_\odot$	M_{belt} $10^{-10}\text{M}_\odot$
2.5±0.3	3.07±0.07	3.38±0.35	15.1±2.0

Table 6. Progress in the determination of the parameters of PPN formalism and $\dot{G}/G$.

year	β	γ	$\dot{G}/G(10^{-11}\text{yr}^{-1})$
1985	0.76±0.12	0.87±0.06	4.1 ±0.8
1994	1.014±0.070	1.006±0.037	0.28 ±0.32
2003	1.0002±0.0001	0.9999±0.0001	0.003 ±0.008

Along with the planetary ephemerides the improved ephemerides of the orbital and rotational motions of the Moon have been fitted by processing the 1979-2001 LLR observations by Krasinsky (2002) where the last version of this theory accounting for a number of subtle selenodynamical effects is described.

For further details regarding the masses of asteroids, the full set of used observations and etc. the reader is referred to the paper (Pitjeva, 2003).

5. THE CONVERSION FROM THE TDB TO TCB TIME SCALE EPHEMERIDES

For correlation and comparison with the wide-spread JPL DEs ephemerides the EPMs ephemerides were created up to now in TDB time scale, close to T_{eph} (Standish, 1998a) used for the DEs ephemerides. To be consistent with IAU resolutions, ICRS should be treated as

four-dimensional reference frame with TCB time scale in which planetary ephemerides should be constructed. Although the conversion to TCB time scale could not and did not allow greater accuracy of ephemerides and adjusted parameters, users processing the VLBI and Earth satellite observations must have TCB ephemerides, so the two versions of EPM ephemerides are constructed for TDB and TCB time scales.

In accordance with the recommendations of literature (see, for example, Brumberg and Groten, 2001) the values of masses GM_i and initial coordinates of all celestial bodies involved in integration for the date JD=2448800.5 were multiplied by the factor $(1+L_B)$ for the construction of EPM2003 ephemerides in the TCB time scale. Because EPM ephemerides are very close to DE405 ephemerides the value $L_B = 1.55051976772 \cdot 10^{-8}$, obtained for relationship between TCB and TDB of DE405 ephemerides (IERS Conversions, 1996) has been used.

Thus, the following modifications must be done for the conversion from the TDB to TCB time scale ephemerides:

- the integration epoch:
  $\mathrm{date}(TCB) = (\mathrm{date}(TDB) - 2443144.5) * L_B + \mathrm{date}(TDB)$
- positions: $x_i(TCB) = x_i(TDB) * (1 + L_B)$
- masses: $GM_i(TCB) = GM_i(TDB) * (1 + L_B)$
  $L_B = 1.55051976772 \cdot 10^{-8}$

This version involves the same numerical values in terms of TCB and TDB for the unit of length (AU) in km and for any velocities including the speed of light. At the XXV IAU General Assembly, Dr. Standish proposed another, more complicated version of conversion to TCB ephemerides retaining the same numerical value in SI units for the heliocentric constant $GM_\odot$ in terms of TDB and TCB. This situation is rather confusing. In any case, some official recommendation should be adopted (see Brumberg and Simon, 2004).

6. REFERENCES

Brumberg V. A., Groten E., 2001, *Astron. Astrophys.*, **367**, 1070–1077.

Brumberg V. A., Simon J.-L., 2004, in the same issue.

Krasinsky G. A., Vasilyev M. V., 1997, *in: Proceedings of the IAU Coll.165, Dynamics and Astrometry of Natural and Artificial Celestial Bodies*, I. M. Wytrzyszczak, J. H. Lieske, R. A. Feldman (eds.), Dordrecht, Kluwer, 239–244.

Krasinsky G. A., Pitjeva E. V., Vasilyev M. V., Yagudina E. I., 2002, *Icarus*, **158**, 98–105.

Krasinsky G. A., 2002, *Communication of IAA RAN*, **148**, 27p.

Mignard F., 2000, *in: Towards models and constants for sub-microarcsecond astrometry*, Johnston K. J., McCarthy D. D., Luzum B. J., Kaplan G. H. (eds.), U.S. Naval Observatory, Washington DC, USA, 10–19.

Pitjeva E. V., 2001, *Celest. Mech. Dyn. Astr.*, 2001, **80**, N 3/4, 249-271.

Pitjeva E. V., 2003, *Communication of IAA RAN*, **155**, 19p.

Standish E. M., Newhall XX, Williams J. G., Folkner W. M., 1995, *Interoffice Memorandum*, **314.10–127**, 22p.

Standish E. M., 1998a, *Astron. Astrophys.*, **336**, 381–384.

Standish E. M., 1998b, *Interoffice Memorandum*, **312.F-98-048**, 18p.

Standish E. M., Fienga A., 2002, *Astron. Astrophys.*, **384**, 322–328.

Yoder C. F., Konoplev A. S., Yuan D. N., Standish E. M., Folkner W. M., 2003, *Science*, **300**, Issue 5617, 299–303.

NEW HARMONIC DEVELOPMENT OF THE EARTH TIDE-GENERATING POTENTIAL

S.M. KUDRYAVTSEV
Sternberg Astronomical Institute of Moscow State University
13, Universitetsky Pr., Moscow, 119992, Russia
e-mail: ksm@sai.msu.ru

EXTENDED ABSTRACT. *(The complete paper is published in the Journal of Geodesy, 2004,* **77***, 829-838)*

Doodson (1921) first performed an accurate representation of the Earth tide-generating potential (TGP) by harmonic series. Subsequent expansions were done by Cartwright and Tayler (1971), Cartwright and Edden (1973), Büllesfeld (1985), Xi (1987, 1989), and Tamura (1987, 1995). The latest and to date most accurate harmonic developments of the TGP have been made by Hartmann and Wenzel (1994, 1995) and Roosbeek (1996).

The classical representation of the Earth TGP generated by external attracting bodies (the Moon, Sun, planets) at an arbitrary point P on the Earth's surface at epoch t is

$$V(t) = \sum_j \mu_j \sum_{n=2}^{\infty} \frac{r^n}{r_j^{n+1}(t)} P_n\left(\cos\psi_j(t)\right) \tag{1}$$

where V is the value of the TGP at P; r is the geocentric distance to P; μ_j, r_j are, respectively, the gravitational parameter and geocentric distance to the j^{th} body; ψ_j is the angle between P and the j^{th} body as seen from the Earth center; P_n is the Legendre polynomial of degree n.

The expression (1) is expanded in our study as

$$V(t) = \sum_{n=2}^{\infty}\sum_{m=0}^{n} V_{nm}(t) = \sum_{n=2}^{\infty}\sum_{m=0}^{n} \left(\frac{r}{R_E}\right)^n \bar{P}_{nm}\left(\sin\varphi'\right)\left[C_{nm}(t)\cos m\theta^{(A)}(t) + S_{nm}(t)\sin m\theta^{(A)}(t)\right] \tag{2}$$

where

$$C_{nm}(t) = \frac{1}{2n+1}\sum_j \frac{\mu_j}{R_E}\left(\frac{R_E}{r_j(t)}\right)^{n+1} \bar{P}_{nm}\left(\sin\delta_j(t)\right)\cos m\alpha_j^{(A)}(t) \tag{3}$$

$$S_{nm}(t) = \frac{1}{2n+1}\sum_j \frac{\mu_j}{R_E}\left(\frac{R_E}{r_j(t)}\right)^{n+1} \bar{P}_{nm}\left(\sin\delta_j(t)\right)\sin m\alpha_j^{(A)}(t) \tag{4}$$

and R_E is the mean Earth equatorial radius; $\alpha_j^{(A)}(t)$, $\delta_j(t)$ are, respectively, the instantaneous right ascension and declination of the j^{th} body referred to the true geoequator of epoch t with an origin point A - that being the projection of the mean equinox of date; $\theta^{(A)}(t)$ is the local sidereal time at P reckoned from the same point A - so that it is related to the Earth fixed east longitude (from Greenwich) λ of P simply as

$$\theta^{(A)}(t) = \lambda + GMST \tag{5}$$

($GMST$ is Greenwich Mean Sidereal Time defined by a well-known expression by Aoki et al., 1982); φ' is the geocentric latitude of the point P; and $\bar{P}_{nm}$ is the normalized associated Legendre function related to the unnormalized one P_{nm} as

$$\bar{P}_{nm} = N_{nm} P_{nm} \tag{6}$$

where

$$N_{nm} = \sqrt{\frac{\delta_m (2n+1)(n-m)!}{(n+m)!}}$$

and

$$\delta_m = \begin{cases} 1, & if \quad m = 0 \\ 2, & if \quad m \neq 0. \end{cases}$$

The classical expression for the TGP (1) has to be completed by some additional terms reflecting the main effect of Earth's flattening (Wilhelm 1983; Dahlen 1993; Hartmann and Wenzel 1995; Roosbeek 1996) which can be re-written as follows

$$V^{fl}(t) = \frac{r}{R_E} \left(\bar{P}_{10} \left(\sin \varphi' \right) C_{10}(t) + \bar{P}_{11} \left(\sin \varphi' \right) \left[C_{11}(t) \cos \theta^{(A)}(t) + S_{11}(t) \sin \theta^{(A)}(t) \right] \right) \tag{7}$$

where

$$C_{10}(t) = \sqrt{\frac{15}{7}} \frac{\bar{J}_2}{R_E} \sum_j \mu_j \left(\frac{R_E}{r_j(t)} \right)^4 \bar{P}_{30} \left(\sin \delta_j(t) \right) \tag{8}$$

$$C_{11}(t) = \sqrt{\frac{10}{7}} \frac{\bar{J}_2}{R_E} \sum_j \mu_j \left(\frac{R_E}{r_j(t)} \right)^4 \bar{P}_{31} \left(\sin \delta_j(t) \right) \cos \alpha_j^{(A)}(t) \tag{9}$$

$$S_{11}(t) = \sqrt{\frac{10}{7}} \frac{\bar{J}_2}{R_E} \sum_j \mu_j \left(\frac{R_E}{r_j(t)} \right)^4 \bar{P}_{31} \left(\sin \delta_j(t) \right) \sin \alpha_j^{(A)}(t) \tag{10}$$

$\bar{J}_2$ is the normalized value for the dynamical form-factor of the Earth ($\bar{J}_2 = J_2 / N_{20}$).

The coefficients $C_{nm}(t)$, $S_{nm}(t)$ contain information about instantaneous positions of the attracting bodies at every epoch t at which one calculates the TGP value $V(t) + V^{fl}(t)$. Angles $\alpha_j^{(A)}(t)$ and $\delta_j(t)$ in expressions (3), (4), (8)-(10) are reckoned along and from the true geoequator of the epoch t, so the relevant values for the coefficients $C_{nm}(t)$, $S_{nm}(t)$ fully take into account the effects of both precision and nutation in obliquity. Because of the choice for the origin point A nutation in longitude is not included to the values for $C_{nm}(t)$, $S_{nm}(t)$. Otherwise, one would have to repeatedly take the same effect into account in (5), i.e. substitute there Greenwich True Sidereal Time for Greenwich Mean Sidereal Time, what is more complicated. (When expanding (1) to (2) one gets just differences $\theta^{(A)}(t) - \alpha_j^{(A)}(t)$ between the local sidereal time at P and the right ascension of every perturbing body.)

Having harmonic expansions for $C_{nm}(t)$, $S_{nm}(t)$ one can further calculate the time-dependent values of the TGP at an arbitrary point $P(r, \phi', \lambda)$ on the Earth's surface by using relations (2), (5) and (7). The tidal acceleration along the Earth radius (or "the gravity tide") is obtained as the radial derivative of the TGP

$$g(t) \equiv \frac{\partial \left(V(t) + V^{fl}(t) \right)}{\partial r} = \sum_{n=2}^{\infty} \frac{n}{r} \sum_{m=0}^{n} V_{nm}(t) + \frac{1}{r} V^{fl}(t). \tag{11}$$

In our work the coefficients $C_{nm}(t)$, $S_{nm}(t)$ have been directly expanded to finite second-order Poisson series of the following form

$$C_{nm}(t) \left[S_{nm}(t) \right] \approx \sum_{k=1}^{N} \left[\left(A_{k0}^c + A_{k1}^c t + A_{k2}^c t^2 \right) \cos \omega_k(t) + \left(A_{k0}^s + A_{k1}^s t + A_{k2}^s t^2 \right) \sin \omega_k(t) \right] \tag{12}$$

where A^c_{k0}, A^c_{k1},...,A^s_{k2} are constants, and $\omega_k(t)$ are some pre-defined arguments which are assumed to be forth-degree polynomials of time

$$\omega_k(t) = \nu_k t + \nu_{k2} t^2 + \nu_{k3} t^3 + \nu_{k4} t^4. \tag{13}$$

For that we first calculated numerical values for the coefficients $C_{nm}(t)$, $S_{nm}(t)$ of the TGP expansion according to (3), (4), (8)-(10) at every six hours within 1000-3000. The latest JPL long-term ephemeris DE/LE-406 (Standish, 1998) was employed as a source of the Moon, Sun and planets coordinates. When calculating the coefficients we used values for the planetary gravitational parameters from Standish (1998) and values for $\bar{J}_2$ and R_E from the IERS Conventions (McCarthy and Petit, 2003). (The value for the latter constant which further has to be used in (2) and (7) along with expansions of the coefficients is 6378136.3 m.)

The arguments (13) in expansion (12) were selected as follows. From Simon et al. (1994) we took complete fourth-order polynomial expressions for mean longitude of the ascending node of the Moon Ω, for Delaunay variables D, l', l, F (mean elongation of the Moon from the Sun, mean anomaly of the Sun, mean anomaly of the Moon, and mean longitude of the Moon subtracted by Ω, respectively), and for mean longitudes of Venus, Jupiter, Mars, Saturn and Mercury. (As Hartmann and Wenzel (1994) showed the attraction of other planets is negligible when calculating the TGP.) The set of arguments of the Moon, Sun and planets motion referred to the mean ecliptic and equinox of date was chosen using the latest value of the precession constant. Then we approximately evaluated a spectrum of the tabulated numerical values of $C_{nm}(t)$, $S_{nm}(t)$ at numerous combinations of multipliers of the arguments' frequencies by using classical FFT procedure. After that, every wave in the spectrum which had a preliminary amplitude exceeding or equal to minimum level $10^{-8} m^2/s^2$ was expanded to Poisson series by using the improved technique of spectral analysis (Kudryavtsev, 2004). Analysis proves that only coefficients $C_{nm}(t)$, $S_{nm}(t)$ of degree $n \leq 6$ have amplitudes increasing the chosen minimum level. The total number of waves included in the final spectrum of the TGP, named KSM03, is equal to 26,753 - what is the total sum of all N in expansions (12) made for every coefficient.

The complete set of coefficients of KSM03 development of the TGP can be found at http://lnfm1.sai.msu.ru/neb/ksm/tgp/coeff.zip. (The description of the data format is done in file http://lnfm1.sai.msu.ru/neb/ksm/tgp/readme.pdf.)

The accuracy of KSM03 expansion of the Earth TGP has been checked by computation of the gravity tide values (11) at a mid-latitude station. As the latter we choose Black Forest Observatory (BFO) Schiltach: $r = 6366836.9$ m, $\phi = 48.3306°$N, $\lambda = 8.3300°$E at which Hartmann and Wenzel (1995) and Roosbeek (1996) also computed the tidal gravity by using their expansions of the TGP. First, we calculated the total tidal gravity at that station by means of strict expressions (2)-(4) and (7)-(11) where the Moon, Sun and planets spherical coordinates were computed using the most precise JPL ephemeris DE/LE-405 (Standish, 1998). The gravity tides at BFO were calculated at every hour within the whole time span covered by that ephemeris, 1600-2200. Then we calculated the gravity tides at the same point and at the same set of epochs by using KSM03 expansion of the TGP and compared the results with the exact values. The maximal deviation between the two sets of data at any epoch within the whole time span of six hundred years length does not exceed 0.39 nGal (1 nGal=$10^{-11} m/s^2$). The corresponding r.m.s. difference between the data over the same interval is less than 0.025 nGal. It exceeds the accuracy of any previously made harmonic development of the TGP in time domain by a factor of at least three.

The work was supported in part by grant 02-02-16887 from the Russian Foundation for Basic Research.

REFERENCES

Aoki, S., Guinot, B., Kaplan, G. H., Kinoshita, H., McCarthy, D. D., Seidelmann, P. K., 1982, The new definition of Universal Time, *Astron. Astrophys.*, **105**, 359–361.

Dahlen, F. A., 1993, Effect of the Earth's ellipticity on the lunar tidal potential, *Geophys. J. Int.*, **113**, 250–251.

Büllesfeld, F. J., 1985, Ein Beitrag zur harmonischen Darstellung des gezeitenerzeugenden Potentials, Deutsche Geodätische Kommission, Reihe C, Heft 314, München.

Cartwright, D. E., Tayler, R. J., 1971, New computation of the tide generating potential, *Geophys. J. R. Astron. Soc.*, **23**, 45–74.

Cartwright, D. E., Edden, A. C., 1973, Corrected tables of tidal harmonics, *Geophys. J. R. Astron. Soc.*, **33**, 253–264.

Doodson, A. T., 1921, The harmonic development of the tide generating potential, *Proc. R. Soc. Lond. A*, **100**, 305–329.

Hartmann, T., Wenzel, H.-G., 1994, The harmonic development of the Earth tide generating potential due to the direct effect of the planets, *Geophys. Res. Lett.*, **21**, 1991–1993.

Hartmann, T., Wenzel, H.-G., 1995, The HW95 tidal potential catalogue, *Geophys. Res. Lett.*, **22**, 3553–3556.

Kudryavtsev, S. M., 2004, Improved harmonic development of the Earth tide-generating potential, *J. of Geodesy*, **77**, 829–838.

McCarthy, D. D., Petit, G. (eds.), 2003, IERS Conventions (2003), *IERS Tech Note*, **32**, Verlag des Bundesamts für Kartographie und Geodäsie, Frankfurt am Main.

Roosbeek, F., 1996, RATGP95: a harmonic development of the tide-generating potential using an analytical method, *Geophys. J. Int.*, **126**, 197–204.

Simon, J.-L., Bretagnon, P., Chapront, J., Chapront-Touzé, M., Francou, G., Laskar, J., 1994, Numerical expressions for precession formulae and mean elements for the Moon and planets, *Astron. Astrophys.*, **282**, 663–683.

Standish, E. M., 1998, JPL Planetary and Lunar Ephemerides DE405/LE405, JPL IOM 312.F-98-048, Pasadena.

Tamura, Y., 1987, A harmonic development of the tide-generating potential, *Bll. Info. Marées Terrestres*, **99**, 6813–6855.

Tamura, Y., 1995, Additonal terms to the tidal harmonic tables, In: *Proceed. of the 12th Int. Symp. on Earth Tides*, Science Press, Beijing/NewYork, 345–350.

Wilhelm, H., 1983, Earth's flattening on the tidal forcing field, *Geophys. J. Int.*, **52**, 131–135.

Xi, Q. W., 1987, A new complete development of the tide-generating potential for the epoch J2000.0, *Bull. Info. Marées Terrestres*, **99**, 6766–6812.

Xi, Q. W., 1989, The precision of the development of the tidal generating potential and some explanatory notes, *Bull. Info. Marées Terrestres*, **105**, 7396–7404.

STABILITY OF EQUATORIAL SATELLITE ORBITS

V. MIOC, M. STAVINSCHI
Astronomical Institute of the Romanian Academy
Str. Cuţitul de Argint 5, RO-040558 Bucharest, Romania
e-mail: vmioc@aira.astro.ro, magda@aira.astro.ro

ABSTRACT. We study satellite orbits lying in the equatorial plane of a planet via the geometric methods of the theory of dynamical systems. To model the planetary gravitational potential, we expand it to the sixth zonal harmonic. The motion equations are regularized by means of McGehee-type transformations of the second kind. Naturally considering the motion to be collisionless and escapeless, we take into account the whole interplay among field parameters, total-energy level and angular momentum. This gives rise to various phase-portraits. In the most general case as regards the changes of sign of parameters, we meet: saddles generating simple or double homoclinic loops, double loops inside one loop of a larger double loop, centers surrounded by periodic and quasiperiodic trajectories, heteroclinic orbits, etc. Of course, less general cases lead to simpler phase portraits. Every type of phase orbit is translated in terms of physical motion. Such qualitative results are useful to the analysis of circumplanetary motion of major or infinitesimal satellites, rings, etc.

1. INTRODUCTION

Consider a planet that presents mass-distribution symmetry with respect to an axis. The equatorial motion of a satellite in the gravitational field of such a planet will be governed by the potential

$$U(\mathbf{q}) = \sum_{n=1}^{7} a_n / |\mathbf{q}|^n ,$$

where $\mathbf{q}$ is the radius vector of the satellite with respect to the mass centre of the planet and a_n are real parameters. We consider $a_1 > 0$ (the Newtonian term), $a_2 = 0$, $a_3 < 0$, as in the general planetary case in the solar system. To obtain the most general situations, we considered the whole sign interplay among $a_4 - a_7$.

Since we deal with satellites, we naturally consider the motion to be free of collision and escape. Collisionless dynamics is possible only for $a_7 < 0$, while escapeless dynamics is possible only for negative energy levels. To regularize the motion equations, we use the coordinates introduced by McGehee (1974). To identify the stability zones, we resort to the reduced 2D phase space, describing all possible phase curves, and using a foliation by the constant angular momentum. The stable orbits are either circular (relative equilibria) or noncircular (periodic and quasiperiodic); see Figure 1. The initial data that lead to quasiperiodic trajectories have

positive Lebesgue measure.

2. BASIC EQUATIONS

Modelling the motion of a satellite in the considered field, the associated two-body problem can be reduced to a central-force problem. The planar motion of the satellite with respect to the planet is described by the Hamiltonian $H(\mathbf{q},\mathbf{p}) = |\mathbf{p}|^2/2 - \sum_{n=1}^{7} a_n/|\mathbf{q}|^n$, where $\mathbf{q} = (q_1,q_2) \in \mathbf{R}^2 \setminus \{(0,0)\}$, $\mathbf{p} = (p_1,p_2) \in \mathbf{R}^2$ are the configuration vector and the momentum vector of the satellite, respectively. The problem admits the first integrals of angular momentum ($q_1p_2 - q_2p_1 = L = \text{constant}$) and of energy ($H(\mathbf{q},\mathbf{p}) = h/2 = \text{constant}$).

To regularize the motion equations, we apply the following sequence of McGehee-type transformations (McGehee 1974; see also Mioc and Stavinschi 2001, 2002):

$$\begin{aligned} r &= |\mathbf{q}|, \\ \theta &= \arctan(q_2/q_1), \\ \xi &= \dot{r} = (q_1p_1 + q_2p_2)/|\mathbf{q}|, \\ \eta &= r\dot{\theta} = (q_1p_2 - q_2p_1)/|\mathbf{q}|, \end{aligned} \tag{1}$$

which introduce standard polar coordinates,

$$\begin{aligned} x &= r^{7/2}\xi, \\ y &= r^{7/2}\eta, \end{aligned} \tag{2}$$

which scale down the velocity components, and a Sundman-type rescaling of time $d\tau = r^{-\alpha}dt$, $\alpha \in \mathbf{N}$. (This last transformation does not interest us in what follows.)

In this way we obtain regular equations of motion. Under the transformations (1)−(2), the angular momentum integral and the energy integral become respectively

$$y = Lr^{5/2}, \tag{3}$$

$$x^2 + y^2 = hr^7 + 2\sum_{n=1}^{7} a_n r^{7-n}, \tag{4}$$

whereas the singularity at $r = 0$ was replaced by the collision manifold $M_0 = \{(r,\theta,x,y) \mid r = 0, \theta \in S^1, x^2 + y^2 = 2a_7\}$ pasted on the phase space.

One sees that, for $a_7 < 0$, the motion is collisionless (see the expression of M_0). Also, by (4), that escape ($r \to \infty$) is not possible for $h < 0$. We shall hence study the motion within the framework of these two assumptions.

One could ask: why using McGehee-type coordinates to collisionless motion? On the one hand, the dynamics in these coordinates appears very simple. On the other hand, they will serve as a basis for a next investigations including collision and escape.

The regularized equations of motion do not contain θ explicitly, so we can factorize the flow by S^1. Next, we eliminate y between (3) and (4). In this way the phase-space dimension was reduced from 4 to 2. The energy integral in the (r,x)-plane will read

$$x^2 = f(r) = hr^7 + 2a_1r^6 - L^2r^5 + 2a_3r^4 + 2a_4r^3 + 2a_5r^2 + 2a_6r + 2a_7,$$

where we took into account the fact that $a_2 = 0$.

We shall describe the phase-space structure for negative energy levels, analyzing the behaviour of the function $x = \pm\sqrt{f(r)}$. Since $f(r) = x^2$, it must be nonnegative, so we have to consider only the regions on the real line where this condition is fulfilled. Also since r is a distance,

we consider only the positive roots of $f(r)$. We also shall consider, for the same purpose, the positive roots of the polynomial $\tilde{f}(r) = df(r)/dr = 7hr^6 + 12a_1r^5 - 5L^2r^4 + 8a_3r^3 + 6a_4r^2 + 4a_5r + 2a_6$.

To deal with the most general case, we suppose that $f(r)$ has six changes of sign (the maximum possible) for $h < 0$, $a_1 > 0$, $a_3 < 0$, $a_7 < 0$. This entails a maximum of six positive roots (according to Descartes' rule) for $f(r)$, and five positive roots for $\tilde{f}(r)$.

3. PHASE-SPACE STRUCTURE

The phase-space structure for the considered case is plotted in Figure 1.

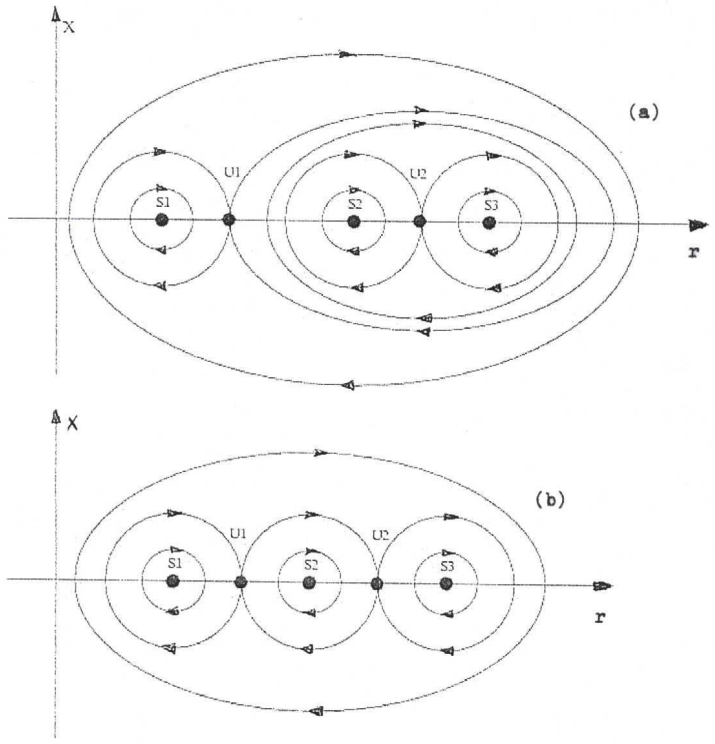

There exists a critical energy level h_c that creates, along with the interplay of the field parameters, three different phase portraits. The foliation performed by making $|L|$ increase points out a great variety of phase orbits, as well as bifurcations (corresponding to critical values of L) concretized by relative equilibria: three centres S (stable circular orbits) and two saddles U (unstable circular orbits).

Figure 1a plots the case $h < h_c < 0$. The inner saddle U_1 generates a double homoclinic loop, whose outer "petal" shelters another double homoclinic loop, generated by the outer saddle U_2.

There are three kinds of quasiperiodic and periodic orbits. The ones that correspond to phase curves surrounding all equilibria have significant eccentricities. The ones that correspond to phase curves lying inside the outer loop generated by U_1, but outside the double loop of U_2, have smaller eccentricities. By comparison, the quasiperiodic and periodic orbits situated inside the double loop of U_2 have smaller eccentricities, but we can say nothing about the eccentricities of such orbits lying inside the inner loop of U_1. All these orbits are stable.

The figure corresponding to the case $h_c < h < 0$ is wholly similar to Figure 1a, but inverted left-right.

Figure 1b plots the case $h = h_c$. The two saddles U_1 and U_2 generate: an inner homoclinic

loop (U_1), an outer homoclinic loop (U_2), and two heteroclinic trajectories that link U_1 and U_2. There are two kinds of quasiperiodic and periodic orbits. The ones that correspond to phase curves surrounding all equilibria have significant eccentricities. The ones that correspond to phase curves lying inside the separatrices have smaller eccentricities. All these orbits are stable.

4. CONCLUDING REMARKS

To search for stability regions in our problem, we described the phase portraits for the whole interplay among field parameters (with the restrictions $a_1 > 0$, $a_2 = 0$, $a_3 < 0$, $a_7 < 0$), energy level (restricted to $h < 0$), and angular momentum.

The most important features of the model are:

4.1. There exist cases ($h < h_c$, $h > h_c$) in which two double homoclinic loops (one sheltered in one "petal" of another) associated to two saddles create five zones of stable quasiperiodic and periodic orbits (Figure 1a). There also exist cases ($h = h_c$) in which there are four zones of stable quasiperiodic and periodic orbits (Figure 1b).

4.2. The sets of quasiperiodic and noncircular periodic orbits have positive Lebesgue measure. Indeed, choosing initial data on such an orbit, and considering the foliations performed, in a neighbourhood of this point there exists an open set of initial data that lead to the same kind of orbit.

4.3. The role of the angular momentum is of the same importance as that of the energy. It creates bifurcations within the same energy level.

4.4. Our results were obtained for the maximum number of changes of sign of $f(r)$ and $\tilde{f}(r)$. Simpler mathematical situations entail simpler phase portraits.

4.5. Such qualitative are useful to analyze the stability of the circumplanetary motion of major or infinitesimal satellites, rings, etc.

Acknowledgments. The paper was done within the framework of the grant 18/2003 of the Romanian Academy.

5. REFERENCES

McGehee, R., 1974, *Invent. Math.*, **27**, 191.
Mioc, V., Stavinschi, M., 2001, *Phys. Lett. A*, **279**, 223.
Mioc, V., Stavinschi, M., 2002, *Phys. Scripta*, **65**, 193.

IMCCE PLANETARY SOLUTION: OVERVIEW AND PROSPECTS

A. FIENGA, J.-L. SIMON
IMCCE/Observatoire de Paris
77 av. Denfert-Rochereau, Paris, France
e-mail: fienga@imcce.fr simon@imcce.fr

ABSTRACT. The VSOP solutions of the planetary motions are analytical solutions of the planets of the solar system, from Mercury to Neptune. These solutions have to give highly accurate ephemerides on long time intervals, about several thousand years for the inner planets and 1000 years of the outer planets. VSOP2002 (Bretagnon, 2002), the last unfinished VSOP version processed by P.Bretagnon, will be presented and its current accuracy will be discussed. A new analytical solution, VSOP2003, based on VSOP2002, is under development: Pluto perturbations based on the new analytical description of its motion (Simon 2003) are added, we introduce the developments of the mean short periods based on TOP (Simon, 2000), perturbations of the 300 asteroids are added with a one angular parameter model. In parallel, numerical solutions are also under development. Compared to VSOP solutions, these solutions will give more accurate positions and velocities of planets over shorter periods of time. Two types of solutions are considered: i) one follows the JPL integrator and algorithm. Its current status of development as well as the accuracies achieved by this version under process will be given during the talk. ii) one is based on the symplectic integrators developed by Laskar and Robutel (2001). It will be very accurate on short period of time (ten years) but also on very long period of time (several millions of years).

1. OVERVIEW

The VSOP solutions of the planetary motions are analytical solutions of the planets of the solar system, from Mercury to Neptune. These solutions have to give highly accurate ephemerides on long time intervals, about several thousand years for the inner planets and 1000 years of the outer planets. The perturbations are written as Poisson series of the mean mean longitudes λ. The main VSOP versions are the following: i) VSOP82 (Bretagnon, 1982), fitted to the JPL numerical integration, DE200 (Newhall et al, 1983) and written with elliptical variables, ii)VSOP87 (Bretagnon and Francou, 1988), built on VSOP82 in Cartesian and spherical variables and given in several reference frames, iii)VSOP200x (Moisson 2000, Moisson et Bretagnon 2001, Bretagnon, 2002). This last version was built in a relativistic frame, took into account the perturbations of Ceres, Pallas, Vesta, Iris and Bamberga, and it was fitted on DE403 (Standish et al, 1995). This version improved the VSOP82/87 with a factor 10 on small intervals of time. P.Bretagnon was still working on a new improved VSOP200x solution. In the following, we will call the last version of VSOP200x leaved by P.Bretagnon, VSOP2002.

The current accuracy of VSOP2002 will be discuss next. For Mercury, Venus and the Earth, the comparison to DE403 indicate an improvement of VSOP82 about a factor 40, and an improvement of the Moisson's solution about a factor 5. For the outer planets, the differences

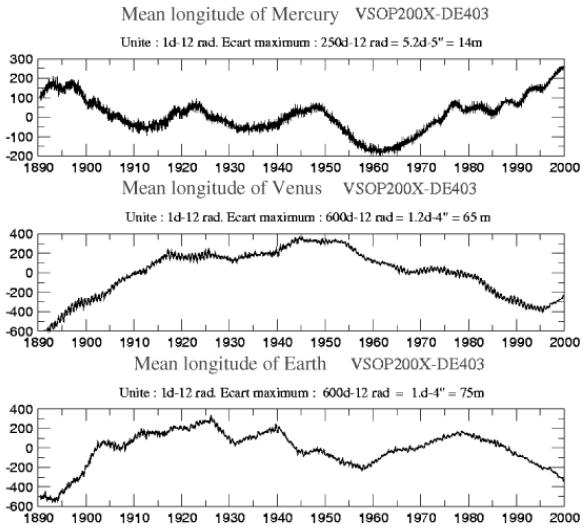

Figure 1: Differences, over [1890, 2000], between VSOP200X and DE403 for the mean longitudes of Mercury, Venus and the Earth-Moon Barycenter

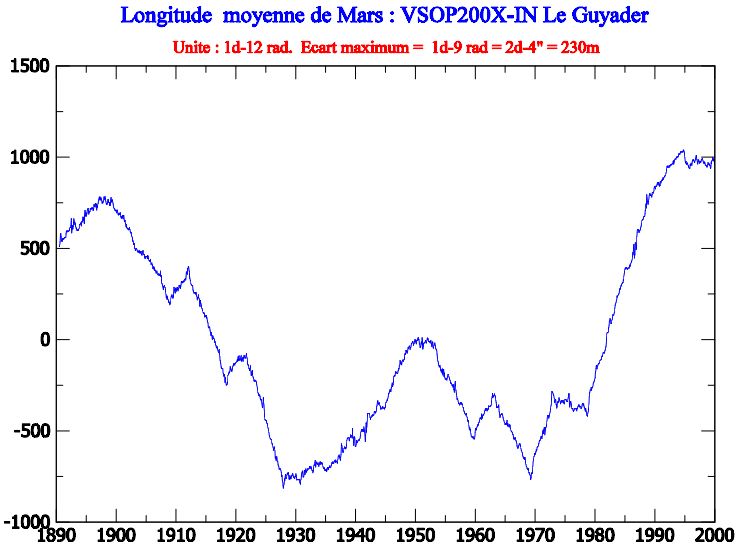

Figure 2: Differences in Mars mean longitudes, over [1890, 2000], between VSOP200X and a numerical integration without the 297 asteroides of DE403.

between VSOP2002 and DE403 are smaller than 750m for Jupiter and 3.5km for Saturn. It is an improvement of a factor 40 compared to VSOP82 and a factor 3 compared to VSOP200x. For Uranus and Neptune, the differences with DE403 are important because Pluto is not included in the solutions. Over 6000 years, the differences for the inner planets between VSOP2002 and an internal numerical integration show an improvement of VSOP82 of about a factor 10 to 100, depending of the planet. For the outer planets, the differences are important. They are induced by a bad behaviour of mean short periods as Poisson series of mean mean longitudes. An improvement of these terms in using the TOP theory (Simon, 2000) would be possible.

2. PROSPECTS

Based on these remarks, a new solution, VSOP2003, is under development.i) Pluto perturbations based on the new analytical description of its motion (Simon 2003) will be added, ii)

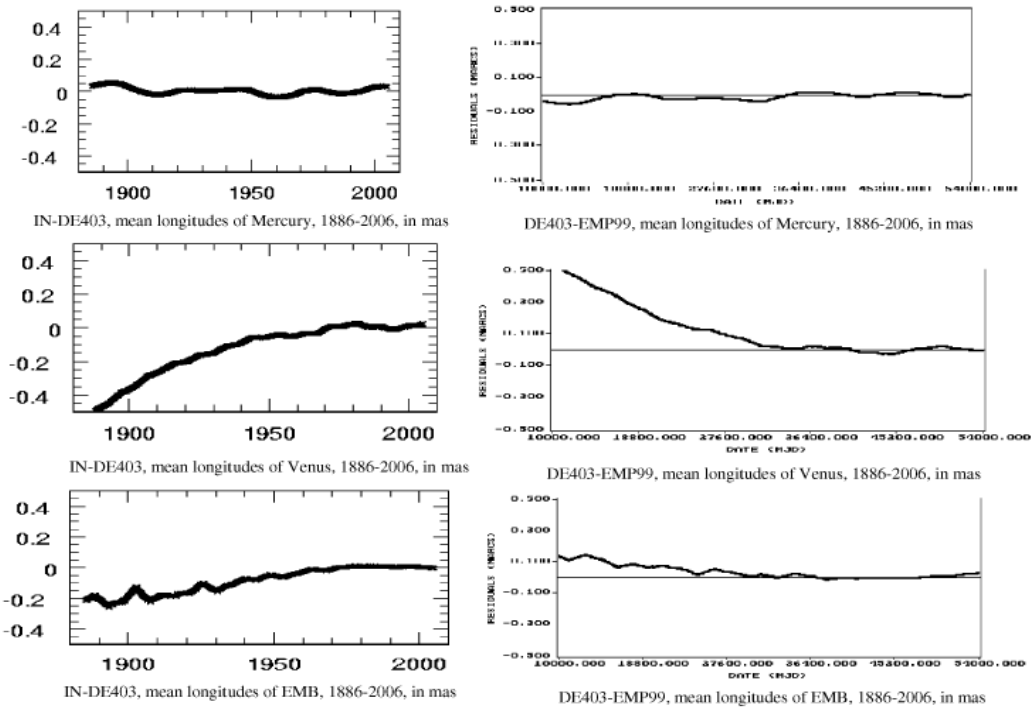

Figure 3: Comparisons between our new numerical integration and the EMP99 solution (Pitjeva 2001) for Mercury, Venus and the Earth-Moon barycenter (EMB).

In parallel, numerical solutions are under development. Compared to VSOP solutions, these solutions will give more accurate positions and velocities of planets over shorter periods of time. Two types of solutions are considered: i) one follows the JPL integrator and algorithm. It is based of the Moshier program (Moshier, 1992), and its current status is the following: the integration is done in a relativistic frame, perturbations of 300 asteroids are included, and it is fitted to DE403. This version will be used as tests for VSOP and a second, more accurate and more efficient numerical integrator, presented next. Accuracies achieved by this version under process will be given during the talk. ii) one is based on the symplectic integrators developed by

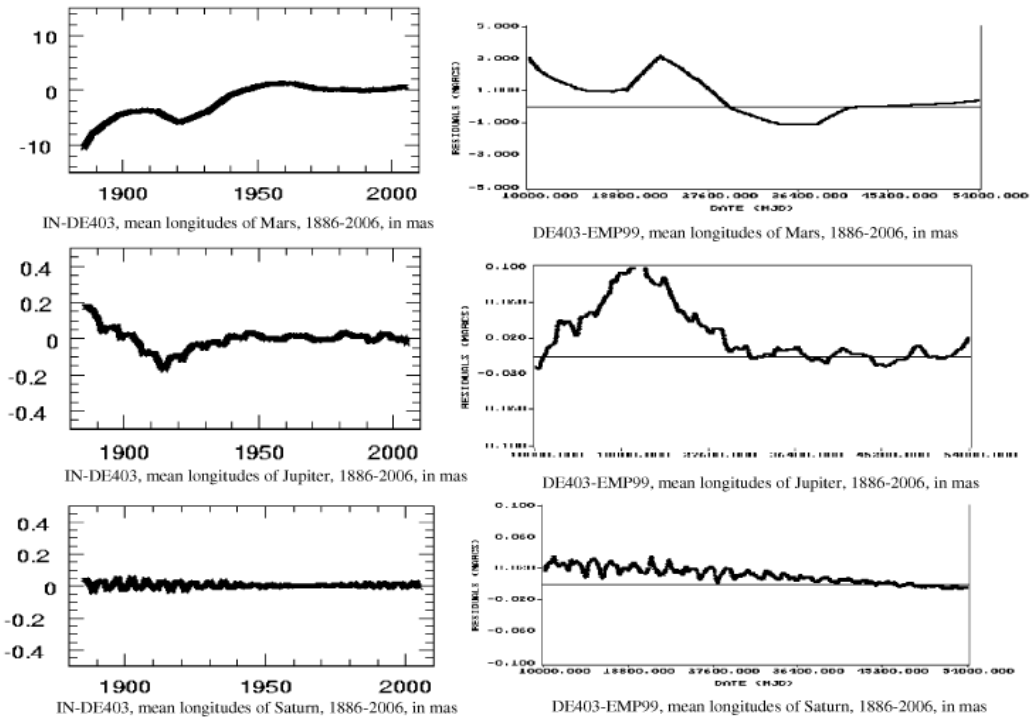

Figure 4: Comparisons between our new numerical integration and the EMP99 solution (Pitjeva 2001) for Mars, Jupiter and Saturn.

Laskar and Robutel (2001). The version will be tested versus the previous solution. It will be very accurate on short period of time (ten years) but also on very long period of time (several millions of years). It will also be stabler and more CPU efficient.

3. REFERENCES

Bretagnon, P., 1982, *Astron. Astrophys.*, **114**, 278.

Bretagnon, P., Francou, G., 1988, *Astron. Astrophys.*, **202**, 309.

Bretagnon, P., 2002, *private communication.*

Laskar, J., Robutel, Ph., 2001, *Celest. Mech. Dyn. Astr.*, **80**, 205.

Moisson, X., 2000, Integration du mouvement des planetes dans le cadre de la relativite generale, *These de doctorat de l'observatoire de Paris.*

Moisson, X., Bretagnon, P., 2001,

Moshier, S. L., 1992, *Astron. Astrophys.*, **262**, 613.

Newhall, X X, Standish, E. M., Williams, J. G., 1983, *Astron. Astrophys.*, **125**, 150.

Pitjeva, E. V., 2001, *Celest. Mech. Dyn. Astr.*, **80**, 249.

Simon, J. L., 2000, NSTBDL S076, 77.

Simon, J. L., 2003, IMCCE Journees scientifiques, to be published.

Standish, E. M., Newhall, X X, Williams, J. G., Folkner, W. F., 1995, JPL planetary and lunar ephemerides, DE403/LE403, JPLIOM **314**, 10.

CHARACTERISTICS OF EROS 433 ROTATION

J. SOUCHAY
SYRTE - Observatoire de Paris
77 avenue Denfert-Rochereau, F-75014, Paris, France
e-mail: Jean.Souchay@obspm.fr

ABSTRACT. This paper summarizes the contents of recent analytical studies related to the rotation of the asteroid Eros 433 (Souchay et al.,2003; Souchay and Bouquillon,2004). Thanks to the very accurate observational data obtained by the intermediary of the probe mission NEAR (Near Earth Asteroid Rendez-Vous) and detailed by Miller et al.(2002), it is possible to determine with an exceptional accuracy the ephemerides of the rotation of the asteroid, and more specifically the values of the coefficients of precession and nutation. After explaining the parametrization of the problem and the way of calculation, we give the principal results, which enable to modelize Eros' rotation both for long-term (100 years) and very short term (a few hours).

1. INTRODUCTION

As any celestial body, the rotation of Eros can be separated into two independent parts, which must be combined each together : one is the free motion of rotation, i.e., the rotation when not considering any perturbing body, and the other is the forced motion, i.e., the motion caused by the gravitational torque exerted by any external celestial body (Sun, planet, satellite etc...). In the case of Eros, we only consider here the perturbation caused by the Sun. Concerning the free motion, two rotation modes for celestial bodies can be found : one is a rotation along the shortest axis, which generally corresponds to the axis around which the moment of inertia is maximum , the other is along the longest axis, generally with minimum moment of inertia. These modes are respectively called *short axis modes* and *long-axis modes*. Exhaustive studies about these two kinds of rotational free modes can be found, for instance in Kinoshita (1972), starting from an Hamiltonian based theory. The short axis mode is ordinary stable and secularly stable, whereas the long-axis mode is ordinary stable but secularly unstable. In case of dissipation, the long axis mode becomes unstable, whereas the short-axis mode remains stable. Notice that in the solar system, a major part of asteroids undergoes a short-axis rotational mode, although long-axis modes have been found, for example in the case of Toutatis (Burns and Safronov, 1973, Harris,1994) Therefore, although no clear information can be reached from the NEAR's exploration to know if Eros free motion belongs to the first or the second of the categories above, we can assume with no doubt that Eros undergoes a short-axis rotational mode. Therefore we will consider in the following that Eros' rotational motion is around the axis of maximum moment of inertia C, quoted as the *axis of figure*, thus applying the usual terminology available for the planets. Another fundamental bu unknown parameter (in fact this parameter is known only for the Earth) which plays a large place in the rotational mode is the value of the angle (called

here J) between the axis of figure and the axis of rotation (see Kinoshita,1977), and which is one of the two parameters enabling us to determine what is called for the Earth, the *polhodie* or polar motion. We can consider that this angle is very close or equal to 0, which is adequate to a condition of minimum of energy.

In order to compute the gravitational torque exerted by the Sun on Eros, which depends on the latitude and the longitude of the Sun with respect to a reference system related to the asteroid, we need to know its orbital osculating elements, which can be found for instance from the MPCORB (Minor Planet Centre Orbit Database). Eros has a semi-major axis close to Mars' one ($a = 1.4583145 A.U.$), and its orbit has a relatively high excentricity ($e = 0.2228487$). This explains why the asteroid can be considered as a Near Earth Asteroid, its perihelion distance being of the order of 1.13 A.U. Notice that the values above have been obtained at 2002, June 5th. Eros' inclination is : $i = 10°.83019$, and its mean motion is $n = 3.5677539 rd/y$, which corresponds to an orbiting period of roughly 1.76 year. All these elements are subject to dramatic changes, due to the possibility of becoming very close to the Earth as well as to Mars.

2. THE NEAR PROBE : A PRECIOUS DATA FOR THE ROTATION

After some technical problems, the NEAR probe was finally inserted into an orbit around Eros, starting from February 14, 2000. A set of several techniques, as radiometric tracking data, optical imaging and laser data, led to very precious and accurate informations about parameters which are fundamental to elaborate ephemerides of the rotation of the celestial object : these are the shape, gravity field and rate of rotation, as well as the location of the polar axis at a given instant (Miller et al.,2002).

For instance, it was possible to elaborate a shape model at 180th. degree order (Zuber et al.,2000), and to determine the gravity field of the asteroid as a combination of spherical harmonics at the order 15 (Miller et al.,2002). It was also shown in this last paper that the very small offset between the center of figure and the center of mass indicates that the asteroid has a very uniform density ($\pm$ 1%) on a large scale. The rotation rate was measured with a precision of $\pm 0.00023°/d$, that is to say roughly $1"/d$, whereas the equatorial coordinates α and δ of the pole have been obtained with a precision respectively of $\pm 0.003°$ and $\pm 0.005°$, which gives a global precision for the orientation of the pole in the space of roughly 25" (Miller et al.,2002; Konopliv et al., 2002).

Eros belongs to S-Class asteroids, which can be generally found in the inner part of the main asteroid belt and its albedo is moderate (the geometric value is 0.27). The absolute magnitude of Eros, which means the magnitude at 0° phase angle and 1 AU from the Sun and the Earth, is 11.16.Eros' mass could be estimated to $6.6904 \pm 0.003 \times 10^{15} kg$, corresponding to a volume of $2503 \pm 25 km^3$. This gives an equivalent mass per volume unit equal to $2.67 g/cm^3$ Eros is a very irregular body, with a large variation of the distances from the center of mass to the surface, with 3.19 km as the minimum value, and 17.67 km as the maximum one. The Eros' moments of inertia, which play a fundamental role in the rotation, have been determined at the 4^{th} digit. Their normalized values are : $A = 17.09 km^2; B = 71.79 km^2$ and $C = 74.49 km^2$. As a consequence the dynamical ellipticity, which characterized the flattening of the object in a dynamical point of view, is : $H_d = \frac{2C-(A+B)}{2C} = 0.40341$. This is by two orders of magnitude larger than the dynamical ellipticity of telluric planets as the Earth or Mars. At last the rotation period, which is also fundamental for the determination of the constant of precession and of the coefficients of nutation, is 5.27025547 h.

3. THE PARAMETRIZATION OF EROS'ROTATION

As we are concerned here with the motion of Eros' figure axis in space and by analogy with the case of the Earth, a natural reference frame for the parametrization of this motion should be built from a basic plane and an origin on this plane, which are the Eros orbital plane (E) and the ascending node of (E) with respect to the Eros equator. By analogy with the Earth, this point can be called Eros' vernal equinox, written as γ_{Eros}. For sake of commodity, the basic plane (E) Eros' orbital plane for a given epoch, and not of the date, as it is conventionally the case for the Earth.

In order to determine the mean value of Eros'obliquity ε^0, we have to calculate the coordinates of both the unit vector parallel to the figure axis $\vec{f}$ and the unit vector $\vec{o}$ perpendicular to the orbital plane . The most suitable way to do that is to calculate the coordinates of $\vec{f}$ and $\vec{o}$ with respect to an ecliptic reference system. The equatorial coordinates of the figure axis $\vec{f}$ are given by Miller et al.(2002) : $\alpha_f = 0^h 45^{mn} 28^{sec}$, $\delta_f = 17°.227$. Through the classical transformations between equatorial coordinates and ecliptic coordinates we obtain easily the ecliptic rectangular coordinates of the unit vector $\vec{f}$ along the figure axis : $\vec{f} = (0.936397, 0.290552, 0.1968248)$. In another way, the ecliptic coordinates of $\vec{o}$ are obtained through the orbital parameters i and Ω: $\vec{o} = (\sin i \sin\Omega, -\sin i \cos\Omega, \cos i) = (-0.1550278, -0.1061713, 0.9821883)$. Therefore, the obliquity ε can be obtained from one among the two formulas below, involving vectorial and scalar products: $\vec{o} \times \vec{f} = \vec{w} \sin\varepsilon \qquad \vec{o} \cdot \vec{f} = \cos\varepsilon$ where $\vec{w}$ is the unit vector along the direction of the descending node N' of Eros orbit (E^0) with respect to Eros true equator. Choosing this way of calculation, Souchay et al.(2003) have shown that Eros' mean obliquity at the reference epoch (J2002) is $\varepsilon = 89°.008 \approx 89°0'29"$, which means that Eros' figure axis is nearly aligned with Eros orbital plane, in a similar manner as for Uranus.

4. FREE ROTATIONAL MOTION

Eros free rotational motion can be studied from Hamiltonian formalism (Kinoshita,1991), involving such parameters as e and D defined in the following way :

$$e = \frac{1}{2}\Big(1/B - 1/A\Big)D \qquad 1/D = \frac{1}{C} - \frac{1}{2}\Big(\frac{1}{A} + \frac{1}{B}\Big) \tag{1}$$

The very large value of e leads to the use of specific approximated formula for the determination of $n_{\tilde{l}}$ and $n_{\tilde{g}}$ (Kinoshita,1991) which are the frequencies of the polar motion and of the proper angle of rotation, respectively defined from a meridian origin.

$$n_{\tilde{l}} = \frac{G}{D}\sqrt{1-e^2} \times \left[1 - \frac{1}{2(1-e)}j^2\right] + O(j^4) \approx \frac{G}{D}\sqrt{1-e^2} \tag{2}$$

$$n_{\tilde{g}} = \frac{1}{2}(1/A + 1/B)G + \frac{G}{D}(1 - \sqrt{1-e^2}) \times \left[1 + \frac{1}{2}\sqrt{(1+e)/(1-e)}j^2\right] + O(j^4)$$

$$\approx \frac{1}{2}(1/A + 1/B)G + \frac{G}{D}(1 - \sqrt{1-e^2}) \tag{3}$$

Where G is the amplitude of the angular momentum. Notice that $l + g = \Phi$ is the rotation angle, whose the rate has been determined with a remarkable precision (about 2"/day) by Miller et al.(2002), who set the value : $n_{\tilde{l}} + n_{\tilde{g}} = \dot{\Phi} = 28.612732 rd/d$ With the ratio $n_{\tilde{l}}/n_{\tilde{g}} = 1/7.59160$ deduced from the preceding equations, we finally obtain : $n_{\tilde{l}} = -4.3407869 rd/d$ and $n_{\tilde{g}} = 32.953519 rd/d$.

Therefore it is possible to modelize completely the free rotational motion, at the condition that the angle J is known, which is not the case. As an example Souchay and Bouquillon (2004) gave the curve of the free motion for a value $J = 1$".

5. FORCED MOTION : PRECESSION AND NUTATION

Long periodic variations

The method to calculate the coefficients of nutation and precession is taken from Kinoshita(1977и and has been applied extensively for the Earth (Souchay et al.,1999)

Finally, the expressions of the nutations in longitude and in obliquity are given by the following formulas :

$$\Delta\psi = \frac{K\cos I}{2}\times\left[\left(3e+\frac{27}{8}e^3+C[\frac{e}{2}-\frac{e^3}{12}]\right)\frac{\sin M}{\dot{M}}\right.$$
$$+\left(\frac{9}{2}e^2+\frac{7}{2}e^4+C[-1+\frac{5}{2}e^2-\frac{41}{48}e^4]\right)\frac{\sin 2M}{2\dot{M}}+\left(\frac{53}{8}e^3+C[-\frac{7}{2}e+\frac{123}{16}e^3]\right)\frac{\sin 3M}{3\dot{M}}$$
$$\left.+\left(\frac{77}{8}e^4+C[-\frac{17}{2}e^2+\frac{115}{6}e^4]\right)\frac{\sin 4M}{4\dot{M}}-C\frac{845}{48}e^3\frac{\sin 5M}{5\dot{M}}-C\frac{533}{16}e^4\frac{\sin 6M}{6\dot{M}}\right]$$
$$-S(\frac{e}{2}-\frac{e^3}{24})\frac{\cos M}{\dot{M}}+S(1-\frac{5}{2}e^2+\frac{37}{48}e^4)\frac{\cos 2M}{2\dot{M}}$$
$$+S(\frac{7}{2}e-\frac{123}{16}e^3)\frac{\cos 3M}{3\dot{M}}+S(\frac{17}{2}e^2-\frac{115}{6}e^4)\frac{\cos 4M}{4\dot{M}}$$
$$\left.+S\frac{845}{48}e^3\frac{\cos 5M}{5\dot{M}}+S\frac{533}{16}e^4\frac{\cos 6M}{6\dot{M}}\right] \qquad (4)$$

$$\Delta\varepsilon = -\frac{K\sin I}{2}\times\left[(-\frac{e}{2}+\frac{e^3}{24})\frac{C\cos M}{\dot{M}}+(\frac{e}{2}-\frac{e^3}{12})\frac{S\sin M}{\dot{M}}\right.$$
$$+(1-\frac{5}{2}e^2+\frac{37}{48}e^4)\frac{C\cos 2M}{2\dot{M}}-(1-\frac{5}{2}e^2+\frac{41}{48}e^4)\frac{S\sin 2M}{2\dot{M}}$$

$$+(\frac{7}{2}e-\frac{123}{16}e^3)\times\frac{(C\cos 3M-S\sin 3M)}{3\dot{M}}+(\frac{17}{2}e^2-\frac{115}{6}e^4)\times\frac{(C\cos 4M-S\sin 4M)}{4\dot{M}}$$
$$\left.+\frac{845}{48}e^3\times\frac{(C\cos 5M-S\sin 5M)}{5\dot{M}}+\frac{533}{16}e^4\times\frac{(C\cos 6M-S\sin 6M)}{6\dot{M}}\right] \qquad (5))$$

Where M is Eros' mean anomaly, I the obliquity, and with $K = \frac{3n^2}{\omega_3}\times H_d$ With $H_d = 2C - A - B/2C$. We thus get the numerical value for K : $K = 30404".165/cy$. C and S are terms dependent on slow orbital parameters which can be taken as constant terms for a long time span (Souchay et al.,2003)

We can notice that because of the large value of the eccentricity ($e \approx 0.222$) the sub-harmonics of M remain relatively large, whereas in the case of the nutation of the Earth, for which the eccentricity is small ($e \approx 0.0167$) the corresponding amplitudes decline very fastly.

The Oppolzer terms, which make the difference between the nutations for the axis of angular momentum and the axis of figure have been calculated ion detail by Souchay et al. (2003), and

are very small, so that we can assimilate the nutation of the axis of figure to that of the angular momentum.

Finally, we obtain the following numerical results for the nutation respectively in longitude $\Delta\psi$, and in obliquity$\Delta\varepsilon$.

$$\Delta\psi = 0".590\sin M + 0".042\cos M - 0".192\sin 2M - 0".166\cos 2M - 0".128\sin 3M$$
$$-0".087\cos 3M - 0".054\sin 4M - 0".035\cos 4M - 0".024\sin 5M$$
$$-0".014\cos 5M - 0".008\sin 6M - 0".005\cos 6M \quad (6)$$
$$\Delta\varepsilon = 2".420\sin M - 4".054\cos M - 9".614\sin 2M + 16".037\cos 2M - 5".073\sin 3M$$
$$+8".464\cos 3M - 2".052\sin 4M + 3".424\cos 4M - 0".853\sin 5M$$
$$+1".423871\cos 5M - 0".299905\sin 6M + 0".500370\cos 6M \quad (7)$$

Notice the very large ratio (roughly 27) of the leading amplitude in obliquity, with respect to the leading amplitude in longitude, which is explained by the value very close to 90° of Eros obliquity, and which is the contrary of what happens for the Earth. Moreover, the leading amplitude with respect to the same effect of the Sun on the nutation of the Earth, is also much larger (16" instead of 0.5"). This is due to the large value of Eros' dynamical ellipticity H_d.

Eros' precession is calculated by integrating the constant part of the potential. It is given by the following expression, at the $4^{th.}$ order of the eccentricity :

$$\dot{\psi} \approx K \times \left[1 + \frac{3}{2}e^2 + \frac{15}{8}e^4\right]\cos I \quad (8)$$

We thus obtain the numerical value : $\dot{\psi} = 2".840133/y$. We can thus observe that this rate, which represents the displacement of the mean Eros equinox along the orbit plane, is very small in comparison with the Earth, because of the value of the obliquity I, close to 90°. Thus, according to this precession rate, the Eros equinox accomplishes one revolution in more than 450 000 years, to be compared with the 26 000 years precession cycle for the Earth.

The curve of the figure axis given analytically in this paper has been compared with that given by Miller et al., and the agreement is fairly good (Souchay et al.,2003)

Short periodic variations

The short periodic variations of Eros'rotation are coming from the fact that the asteroid has a strongly triaxial shape. This results in terms in the potential exerted by the Sun with rate close to 2ω, where ω is Eros'rotational rate (Kinoshita,1977;Souchay et al.,1999). These terms have been computed by Souchay and Bouquillon (2004), and the related coefficients of the nutation $\Delta\psi$ are listed in the table 1 below. The coefficients in obliquity are exactly the same with inversion of the sine and cosine parts. The combination of the Fourier terms with close periods leads both for $\Delta\psi$ and $\Delta\varepsilon$ to a beating with amplitudes oscillating between 0 and 0".02.

Table 1: Coefficients of the high-frequency forced nutation in longitude $\Delta\psi^f_{forced}$ of Eros. ω is the argument for the sidereal Eros'rotation, and M is Eros' mean anomaly.

2ω	0.0846	0.0000	$2^h38^{mn}06^s$
$2\omega - M$	0.4890	-0.2610	$2^h38^{mn}08^s$
$2\omega + M$	-0.4182	-0.2517	$2^h38^{mn}05^s$
$2\omega - 2M$	-3.4287	2.0655	$2^h38^{mn}10^s$
$2\omega + 2M$	3.3211	1.9900	$2^h38^{mn}03^s$
$2\omega - 3M$	-2.7241	1.6361	$2^h38^{mn}11^s$
$2\omega + 3M$	2.6271	1.5746	$2^h38^{mn}02^s$
$2\omega - 4M$	-1.4715	0.8831	$2^h38^{mn}13^s$
$2\omega + 4M$	1.4636	0.8489	$2^h38^{mn}00^s$
$2\omega - 5M$	-0.7662	0.4592	$2^h38^{mn}15^s$
$2\omega + 5M$	0.7357	0.4409	$2^h37^{mn}58^s$
$2\omega - 6M$	-0.3236	0.1937	$2^h38^{mn}16^s$
$2\omega + 6M$	0.3100	0.1858	$2^h37^{mn}57^s$

6. REFERENCES

Burns J. A., Safronov, V. S., 1973, Asteroids nutation angles, *Month. Not. R. Astron. Soc.*, **165**, 403-411.

Harris A. W., 1994, Tumbling Asteroids, *Icarus*, **107**, 209-211.

Kinoshita, H., 1972, First-order Perturbations of the Two Finite Body problem, *Publ. Astr. Japan*, **24**, 423-457.

Kinoshita, H., 1977, Theory of the rotation of the rigid Earth, *Celest. Mech.*, **15**, 277-326.

Kinoshita, H., 1991, Analytical expansions of torque-free motions for short and long axis modes, *Celest. Mech.*, **53**, 365-375.

Konopliv, A. S., Miller, J. K., Owen, W. M., Yeomans, D. K., Jon, D. G., Garmier, R., Barriot, J. P., 2002, A Global Solution for the Gravity Field, Rotation, Landmarks, and Ephemeris of Eros, *Icarus*, **160**, 289-299.

Miller, J. K, Konopliv, A. S., Antreasian, P. G., Bordi, J. J., Chesley, S., Helfrich, C. E., Owen, W. M., Wang, T. C., Williams, B. G., Yeomans, D. K., 2002, Determination of shape, gravity, and rotational state of asteroid Eros 433, *Icarus*, **155**, 3-17.

Souchay, J., Loysel, B., Kinoshita, H., Folgueira, M., 1999, Corrections and new developments including crossed-nutation and spin-orbit coupling effects, *Astron. Astroph. Suppl. Ser.*, **135**, 111-131.

Souchay, J., Kinoshita, H., Nakai, H., Roux, S., 2004, A precise modeling of Eros433 rotation, *Icarus*, in press.

Souchay, J., Bouquillon, S., The high frequencies variations of Eros' rotation, *Astron. Astrophys.*, subm.

Zuber, M. T., Smith, D. E., Cheng, A. F., Garvin, J. B., Oded Aharonson, Cole, T. D., Dunn, P. J., Guo, Y., Lemoine, F., Neumann, G. A., Rowlands, D., Torrence, M. H., 2000, The Shape of 433 Eros from the NEAR-Shoemaker Laser Rangefinder, *Science*, **289**, 2097-2101.

CCD-OBSERVATIONS OF GALILEAN SATELLITES OF JUPITER DURING THEIR MUTUAL OCCULTATIONS AND ECLIPSES IN 2003 AT PULKOVO OBSERVATORY

I.S. IZMAILOV, M.YU. KHOVRITCHEV, E.V. KHRUTSKAYA, T.P. KISELEVA
Main Astronomical Observatory of RAS
65/1 Pulkovskoye chaussee, 196140, St.Petersburg, Russia
e-mail: melon@gao.spb.ru

ABSTRACT. CCD-observations of mutual events in the system of Galilean satellites of Jupiter were made with Pulkovo 26-inch Refractor. The results of astrometric and photometric CCD-observations have been obtained for 19 and 20 events correspondingly. The internal accuracy of the moments of maximal phase of the events is $0.5\,sec \div 4.8\,sec$ for photometric observations and $0.7\,sec \div 7\,sec$ for astrometric observations. The agreement between the moments of maximal phase of the events determined from astrometric and photometric observations is within $10\,sec$. The minimal distances between satellites obtained from astrometric observations of occultations are $0.05'' \div 1''$ with accuracy $0.01'' \div 0.02''$. The differences between observational and ephemerides moments of the maximal phase of the events are within $2\,sec \div 24\,sec$.

1. INTRODUCTION

The CCD-observations of mutual events (occultations and eclipses) in the system of Galilean Satellites of Jupiter were made during the period from January till April 2003 at Pulkovo observatory with 26-inch Refractor and CCD ST-6. The description of the parameters of CCD ST-6 and the methods and programs of observations were presented in paper Izmailov I.S. et. al. 1998. The observations were made accordance to the ephemerides of mutual events calculated by N.V.Emelianov. The experience of such observations have been collected in 1997 during previous campaign of accumulated observations of mutual events (N.V. Emelianov et al. 2000).

The 20 photometric observations of 10 occultations and 10 eclipses have been done. Photometric observations were accompanied by astrometric observations (19 events). From 100 to 1000 CCD-frames were used for each photometric observations of occultations and eclipses. The moments of time were determined in the time scale UTC with accuracy $0.05\,sec$. The time delay between neighboring CCD-frames is less than 10 sec. The time of exposures for each frame was about of $0.1sec$. The combination of yellow and blue filters with effective wave length $550\,nm$ was used for observations.

2. THE RESULTS OF PHOTOMETRIC OBSERVATIONS

The light curves present changing with time of sums or differences of magnitudes of satellites during occultations or eclipses. It have been represented using Gaussian model:

$$m(t) = \exp\left(-a(t - T_0)^2 - b\right) + c.$$

Parameter a characterizes the duration of the event, parameter b shows the maximal decreasing of brightness and c is a free parameter.

The parameters of the model were determined using gradient algorithm of the nonlinear least-squares method.

Table 1 and Figures 1, 2 present the results of 11 most successful observations. The others 8 of ones require further investigations.

Table 1: The results of photometric CCD-observations of the mutual events of Jupiter's Galilean satellites.

date/event	$T_0 \pm \sigma_{T_0}$	T_1	T_2	$\Delta m_{max} \pm \sigma_m$
	$h\ m\ s$	$h\ m\ s$		
0106 2E1	23 32 50.879 ± 00.657	23 25 30.815	23 40 10.942	0.676 ± 0.022
0110 2O1	19 26 24.578 ± 04.966	19 17 20.195	19 35 28.961	0.254 ± 0.045
0203 4O1	17 12 12.794 ± 00.676	17 09 27.472	17 14 58.116	0.597 ± 0.023
0203 2O3	23 31 18.518 ± 00.977	23 24 18.508	23 38 18.529	0.285 ± 0.006
0203 2E3	23 39 43.847 ± 01.096	23 32 12.275	23 47 15.419	0.254 ± 0.005
0218 4E3[1]	20 48 37.401 ± 02.155	20 41 35.689	20 55 39.113	0.567 ± 0.028
0306 1O2[2]	19 47 41.088 ± 02.100	19 46 21.140	19 49 01.036	0.331 ± 0.055
0315 3E4	22 14 43.936 ± 00.787	22 07 05.318	22 22 22.554	0.994 ± 0.016
0320 1O2	23 52 21.334 ± 00.946	23 50 59.892	23 53 42.776	0.163 ± 0.018
0326 2E1[3]	20 40 44.675 ± 04.810	20 39 32.469	20 41 56.880	0.215 ± 0.048
0421 1O2	21 29 04.764 ± 00.725	21 27 37.407	21 30 32.121	0.210 ± 0.021

The first two symbols in date field denote month and the last two symbols denote day. The occultations are denoted by "O" symbol and eclipses are denoted by "E" symbol. The names of satellites are denoted by digits: 1 – Io, 2 – Europe, 3 – Ganymede, 4 – Callisto.

T_0 – moment of the maximal phase of the event (UTC),
T_1 and T_1 – moments of beginning and ending of the event,
Δm_{max} – maximal decreasing of brightness,
σ_{T_0} and σ_m – errors of T_0 and Δm_{max}.

Remarks for few results in Table 1:
1 – observations have been made through holes between clouds,
2 – the transparent clouds was covering the sky during observations,
3 – strong wind during observations.

The values σ_m and σ_{T_0} were estimated in accordance to:

$$\sigma_m = \sqrt{\frac{\sum_{i=1}^{n}(mag_i - m(t_i))^2}{n-4}}, \quad \sigma_{T_0} = \sigma_m \cdot \left(\sum_{i=1}^{n}\left(\frac{\partial m(t)}{\partial T_0}\Big|_{t=t_i}\right)^2\right)^{-1/2}.$$

Here n is number of separate measurements of the satellites magnitudes and mag_i is the sum or the difference of satellites magnitudes at the moment t_i.

The value Δm_{max} was calculated using expression:

$$\Delta m_{max} = |m(T_0) - c| .$$

The assumption $m(T_{1,2}) = c + \sigma_m$ was used for calculation of the moments of beginning and ending of the events (T_1 and T_2).

3. THE RESULTS OF ASTROMETRIC OBSERVATIONS

The astrometric observations were started before the events and finished after the events. The whole period of observations of one event was 1 - 1.5 hours. The moments of minimal distances, the minimal distances and relative velocities of satellites for the occultations with their errors were determined. The errors of minimal distances are within $0.01'' \div 0.02''$, the errors of determination of the moments of minimal distances are within $0.7\,sec \div 7\,sec$. The minimal distances are within $0.05'' \div 1''$ (Kiseleva T.P. et. al. 2002).

The results of astrometric observations of occultations are presented in Table 2 (the lines without date and the denotations of the events contain the RMS errors of all values listed in previous line). T_0 is the moment of minimal distances; r_0 is the minimal distances; X, Y - are the components of r_0 in RA and DECL; V_x, V_y are the components of relative velocities of satellites; N is the number of CCD-frames in series.

It would be desirable to emphasize, astrometric observations of occultations allow to determine the parameters of occultations (moments of the maximal phase, minimal distances) also in the case when the photometric observations were not made successfully (for example, the observations at 7.01, 17.01, 15.02, 25.03, 01.04 in Table 2).

Table 2: The results of astrometric CCD-observations of mutual occultations.

Data and Events	T_0 h m s	N	r_0 arcsec	X arcsec	Y arcsec	V_x arcsec/h	V_y arcsec/h
01 07 2O1	01 25 15.858	197	1.0270	0.3419	0.9684	-4.9956	1.7634
	±7.285		±0.0083	±0.0107	±0.0080	±0.0155	±0.0115
01 16 4O2	00 43 58.148	300	0.4907	-0.1546	-0.4657	-12.5194	4.1570
	±2.887		±0.0094	±0.0107	±0.0092	±0.0025	±0.0022
02 03 4O1	17 12 02.918	149	0.0479	-0.0152	-0.0454	-27.3507	9.1727
	±0.972		±0.0072	±0.0079	±0.0072	±0.0230	±0.0210
02 03 2O3	23 30 49.057	110	0.3334	0.1058	0.3162	-11.6509	3.8977
	±1.238		±0.0023	±0.0044	±0.0020	±0.0032	±0.0014
02 15 2O1	19 15 56.453	238	1.0943	-0.3243	-1.0451	-16.4691	5.1112
	±0.875		±0.0044	±0.0041	±0.0044	±0.0109	±0.0116
03 06 1O2	19 47 42.557	136	0.3506	0.1040	0.3348	31.7936	-9.8765
	±0.835		±0.0115	±0.0072	±0.0118	±0.0188	±0.0310
03 20 1O2	23 52 15.444	103	0.4524	0.1333	0.4323	30.2036	-9.3120
	±0.858		±0.0076	±0.0075	±0.0076	±0.0225	±0.0228
03 25 2O3	20 47 57.791	157	0.7415	-0.2022	-0.7133	-16.0298	4.5449
	±1.148		±0.0102	±0.0044	±0.0105	±0.0143	±0.0343
04 01 2O3	23 55 34.990	62	0.9353	-0.2591	-0.8987	-16.3076	4.7015
	±4.250		±0.0216	±0.0199	±0.0217	±0.0210	±0.0230
04 21 1O2	21 29 05.551	246	0.3621	0.1062	0.3462	25.5804	-7.8438
	±0.785		±0.0048	±0.0059	±0.0047	±0.0214	±0.0171

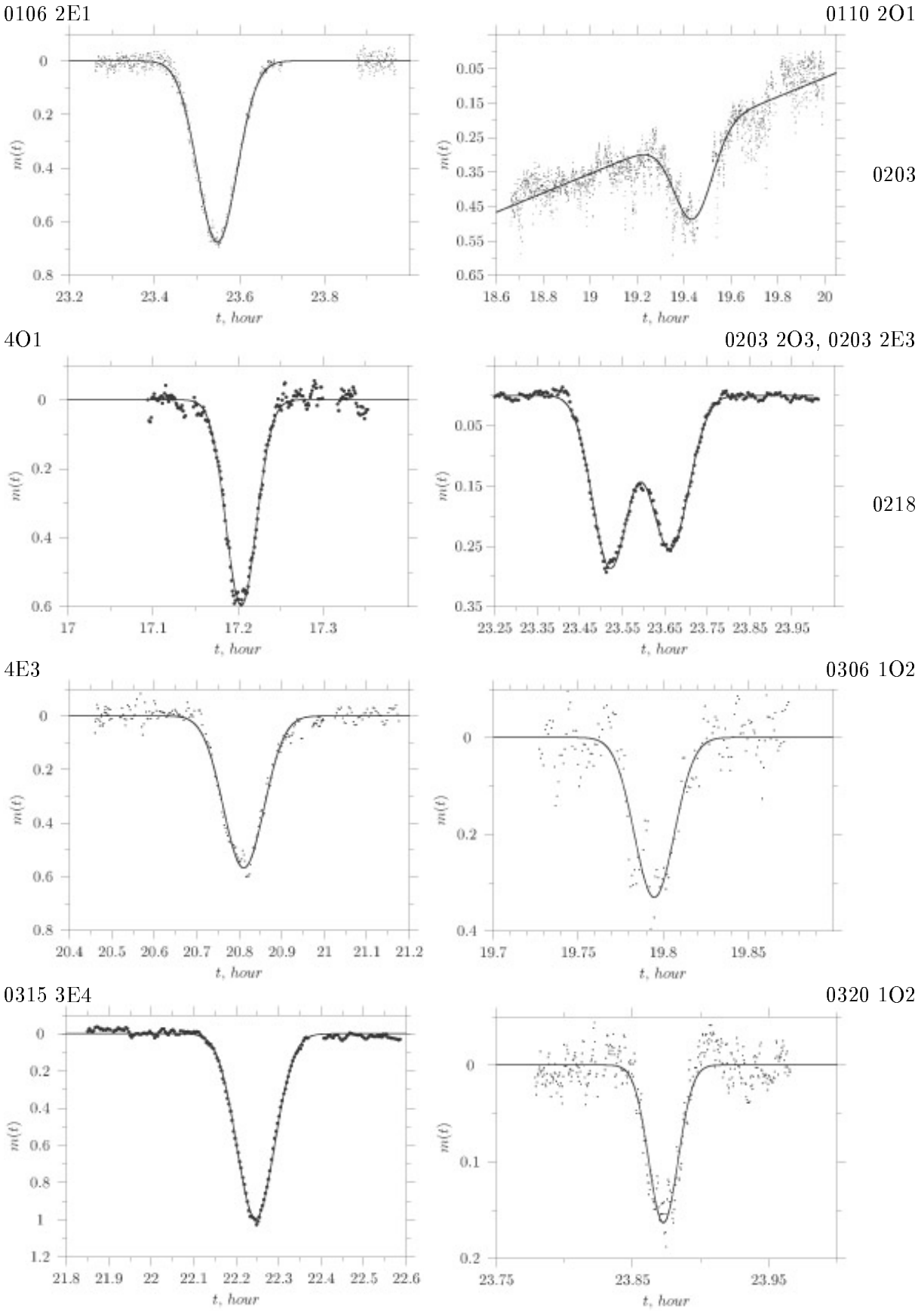

Figure 1: The light curves that have been derived from the results of photometric CCD-observations.

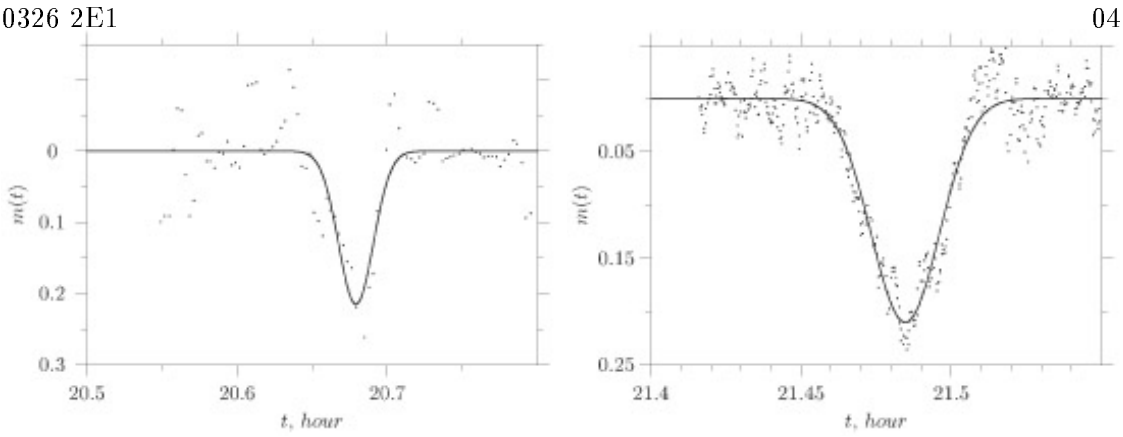

Figure 2: The light curves that have been derived from the results of photometric CCD-observations.

5. CONCLUSIONS

The agreement between results of astrometric and photometric determination of the moments of the maximal phase of occultations is in the limits of 10 *sec*. The comparison of moments of events derived from photometric observations with the ephemerides are presented in Table 3.

Table 3: The comparison of the moments of mutual events with the ephemerides.

Data	Events	(O - C)T_0 s
01 06	2E1	-7.121
02 03	4O1	+23.794
02 03	2O3	+14.146
02 03	2E3	-0.792
02 18	4E3	-1.600
03 06	1O2	-6.912
03 15	3E4	+13.436
03 20	1O2	-7.166
03 26	2E1	-7.325
04 21	1O2	-12.236

The Table 3 demonstrates that the accuracy of moments of events is equal to $\pm 12.0 sec$. This value corresponds to relative angular distances between two satellites less than $0.107''$. It testifies about small errors of observations and ephemerides.

The astrometric and photometric observations of mutual events in the system of Galilean satellites may be used for the improvement of the theories of motions of satellites, for the construction of the model of events and to the more accurate definition of sizes and figures of satellites.

Acknowledgments. This work was carried out with supporting of Russian Foundation for Basic Research, project N 01-02-17018.

6. REFERENCES

Izmailov, I. S., Kiselev, A. A., Kiseleva, T. P., Khrutskaya, E. V., 1998, Using a CCD Camera in Pulkovo Programs of Observations of Binary and Multiple stars and Satellites of Major Planets with 26-inch Refractor, *Astronomy Letters*, **24**, 5, 665–672.

Emelianov, N. V., et al., 2000, Mutual positions of the Galilean satellites of Jupiter from photometric observations during their mutual occultations and eclipses in 1997, *Astron. Astrophys., Supplement Series*, **141**, 433–447.

Kiseleva, T. P., Izmailov, I. S., Mozhaev, M. A., 2002, The observations of close approachments and occultations of stars by asteroids with 26-inch refractor at Pulkovo observatory, *Izvestia GAO*, **216**, 181–184.

PHOTOMETRIC OBSERVATIONS OF THE MUTUAL EVENTS OF THE GALILEAN SATELLITES OF JUPITER MADE AT NIKOLAEV ASTRONOMICAL OBSERVATORY IN 2002–2003

J-E. ARLOT[1], G.K. GOREL[2], L.A. HUDKOVA[2], A.V. IVANTSOV[2], EU.S. KOZYREV[2]

[1] Institut de mecanique celeste (IMCCE) of Observatoire de Paris
UMR 8028 du CNRS, 77 avenue Denfert-Rochereau, F-75014, Paris, France
e-mail: arlot@imcce.fr

[2] Research Institute Nikolaev Astronomical Observatory
vul. Observatorna 1, Mykolaiv, 54030, Ukraine
e-mail: gudkova@mao.nikolaev.ua

ABSTRACT. For the first time at Nikolaev during 2002–2003 there have been made CCTV observations of the mutual phenomena of the Galilean satellites. Guide-telescope of the Zone Astrograph (D=0.115 m, F=2.0 m) and CCTV-camera with 1/3" diagonal have been used for the observations. During the entire period of the observations there were obtained 22 TV series of mutual events (9 occultations and 13 eclipses). Preliminary photometric processing of FITS frames of one event was made with the help of STARLINK software. Analysis of light curve has shown a threshold of detected flux drop nearly 0.1 magnitude.

1. INTRODUCTION

Occultations and eclipses of satellites by each other are usually called as mutual phenomena or events in the systems of Jupiter satellites or other outer planet satellites that can be observed from the Earth. Such events occur in the system of Galilean satellites of Jupiter every 6 years, when the Earth and the Sun go through the common plane of the satellites orbits (Arlot, 2002). From the observational point of view these events are characterized with a small drop of magnitude, which take place in a short time. As a rule maximum brightness fall doesn't exceed one magnitude.

Fast photometry of these events became possible in the last decades only due to a wide spread of cameras with CCD sensors. Such observations make it possible to determine precise moments of maximum magnitude drop that can be equivalent to position observation of satellites with accuracy to 1 mas (Arlot, 2002). Moreover these observations give a vast material for astrophysical research.

2. THE OBSERVATIONS

Photometrical observations of mutual phenomena in the system of Galilean satellites of Jupiter in PHEMU03 campaign were made in Nikolaev Astronomical Observatory at the first time. From October 28, 2002 till June 5, 2003 according to the ephemeride of the Institut de

mecanique celeste et de calcul des ephemerides
(*http* : *//www.imcce.fr/ephem/ephesat/en/visiphemu_formulaire_eng.html*) there should be 128 events in the geographical conditions of Nikolaev for our instrumental possibilities. Weather conditions allowed us to get only 22 events, among them 9 occultations and 13 eclipses (observers were Hudkova L.A., Ivantsov A.V., Gorel G.K.).

Telescope-guide (D=0.115 m, F=2.0 m) of Zone Astrograph with a television 1/3" CCD camera fixed at it was used to observe the mutual phenomena. An ordinary TV-tuner was used for 8-bit A/D conversion of TV frames. Field of view 7'x 9' of such a system has allowed to record at least one reference satellite simultaneously with event. All records were made without any filter.

Time moments in UTC with necessary accuracy were provided by time service of Nikolaev Observatory. Software under OS Windows, written by Kozyrev Eu.S., uses standard library avicap32.dll for video capture and allows to record observational moments for every frame with the accuracy of 1 ms by means of syncronometer. The frequency of records was from 1 to 4 frames per second that depended on the duration of the event. The mean record of one event had about 3000 frames in length.

Video series of dark and flat field frames were additionally recorded every observational night. For extinction correction the records of stars like the Sun spectral class (Khaliullin et al., 1985) were made at different zenith distances in the beginning and at the end of every observation of mutual phenomena.

3. PRE-PROCESSING AND ANALYSIS

Processing of CCD frames is making with STARLINK software
(*http* : *//www.starlink.rl.ac.uk*) which allows for astronomer to inspect and transform frames.

For presentation of observations made in Nikolaev there were processed 3038 frames of occultation (J4OJ1) on December 16, 2002. The French ephemerides of this event gives magnitude drop in 0.36, duration of the event was 395 seconds and the place of the satellites was at 3.8 planet radiuses from Jupiter.

A study of dark frames allowed us to remove noise pattern that was present at all frames. As far as the work with flat-fielding and Jupiter background is still continuing, their corrections were not made for. The results given below were got by the aperture photometry with growth curves applying to every object to find an optimal aperture radius.

In Fig. 1 one can see: (a) magnitude change of J2 versus time (in seconds) with arbitrary zeropoint (background), standard error is 0.081; (b) the same change, but for J3, standard error is 0.067. The change of the magnitude difference between J2 and J3 is present in Fig. 2a, standard error is 0.094. Given errors are in such agreement, when there is no correlation between magnitude measurements of J2 and J3 on the same frame as you can see in Fig. 2b. A small difference between standard errors for magnitude measurements of two reference satellites may be caused by the not uniform background close to the satellites and the complexity of processing such frames. The figures show that magnitude measurements with arbitrary zeropoint in such a processing are more accurate than relative ones.

Also this fact confirms Fig. 3 where you can see the change of magnitude for phenomena in time: a) relatively to the J3 and b) relatively to the background. Presented results give the less detectable magnitude change in 0.1 magnitude, and testify about the necessity to improve method of the processing that will be a subject of our further work.

Acknowledgments. Astronomers of Nikolaev Astronomical Observatory would like to thank Institut de mecanique celeste et de calcul des ephemerides, especially Dr. J.-E. Arlot for financial support for the grant in the PHEMU03 campaign. Besides, we acknowledge the software pro-

a) b)

Figure 1: Change of Jupiter satellites magnitude of with time (in seconds) for a) J2 (Europe) and b) J3 (Ganimed).

a) b)

Figure 2: a) Change of magnitude difference between J2 and J3 with time (in seconds) and b) correlation between magnitude measurements of J2 and J3.

a) b)

Figure 3: The changes of magnitude for phenomena with time relatively to the a) J3 and b) background.

vided by the Starlink Project, which is run by CCLRC on behalf of PPARC. The authors thank Dr. Malcolm Currie from the Quick Programming Service (Starlink) whose suggestions on FITS format and discussions on data processing were useful.

4. REFERENCES

Arlot, J.-E., 2002, Presentation of the Galilean Satellites of Jupiter and of their Mutual Phenomena, *http://www.imcce.fr/Phemu03/ntph01_eng.html*.

Khaliullin, Kh., Mironov, A. V., Moshkalyov, V. G., 1985, A New Photometric WBVR System, *Astrophysics and Space Science*, **111**, 291.

ASTROMETRIC OBSERVATIONS OF URANUS IN 2002 WITH THE NORMAL ASTROGRAPH AT PULKOVO

N.M. BRONNIKOVA, T.A. VASIL'EVA
Main Astronomical Observatory of RAS
65/1, Pulkovskoye chaussee, 196140, St.Petersburg, Russia
e-mail: bron@gao.spb.ru

ABSTRACT. 22 positions of Uranus are given. The plates were taken with the normal astrograph at Pulkovo in 2002. The reference stars are taken from catalogue Tycho-2. The average (O-C) are as follows: $(O-C)_\alpha = -0.014^s \pm 0.005^s$, $(O-C)_\delta = -0.''410 \pm 0.''092$ from the comparison with the ephemeris DE200. The errors of one position are equal to $\pm 0''.35$ for α and $\pm 0''.43$ for δ.

1. RESULTS

The photographic astrometric observations of the Uranus with the Normal Astrograph at Pulkovo have been carried out from 1919 to 1974 until the planet was get over the zone of the large negative declinations. As a rule 3 – 4 plates were taken with the expositions 6 minutes in the year with the diaphragm 0.5 D. The observations 1919 – 1969 have been treated by V.V.Lavdovsky (Lavdovsky V.V. 1971) again using the Yale catalogues as a reference. In 1989 the plates taken from 1968 to 1974 have been treated too. The catalogue FOCAT-S was used (Bronnikova N.M, et al. 1989).

In 2002 it was decided to regenerate the observation of Uranus with the Normal Astrograph although the conditions of the observations was no enough favorable. From August 3 to December 3 have been taken 22 plates with the diaphragm. For increasing of the accuracy of the determination of the positions of the Uranus we were taken 3 – 4 images on the each plate. Sometimes it was obtained two plates at one night. The stellar brightness of Uranus did not attenuated.

The plates were measured with "Ascorecord". The reference stars were taken from catalogue Tycho - 2. The reduction carried by the method six constants. Every image was treated separately to estimate the internal error of one observation of one plate.The comparison of the obtained position with the ephemeris DE200 and DE405 using the programm EPOS (L'vov, et.al. 1999)were carried out.

The errors of one observation for one plate with three or more images are equal to $0.''04$ – $0.''48$ for right ascension and $0.''10$ – $0.''80$ for declination depending on the conditions of the observations, the quality of the images of the Uranus, the reference stars and the quality of the plates. Some plates were very foggy.

All position obtained with one plate were obtained as the average. In the end we were obtained 22 geocentric equatorial positions of the Uranus at the epoch and equinox J2000.0. In the table the data of the observations (UTC), (O-C) for the ephemeris DE200 and name of

the observers are given (Br–N.M. Bronnikova, Bb–V.V. Bobylev, Dm–A.A. Dement'eva, Na–N.V. Narizhnaya)

The mean errors of one position are equal to $\pm 0.''35$ for right ascension and $\pm 0.''43$ for declination .

In the work (Chanturia, et.al. 2002) 105 positions of the Uranus taken with DAZ in Abastumani in 1987-1994 were obtained. The catalogue PPM was used as a reference. The mean $(O-C)_\alpha = -0.''262$, $(O-C)_\delta = -0.''234$. The errors of one observation are $\pm 0.''200$ for α and $\pm 0.''245$ for δ. The observations were taken with week of the brightness of Uranus and at the zenith of distances $65° - 66°$.

Table 1: Geocentric equatorial coordinates of Uranus in 2002.

Date (UTC)			α_{2000}			δ_{2000}			$(O-C)_\alpha$	$(O-C)_\delta$	Observer
			h	m	s	°	'	"	s	"	
2002	08	03.961641	21	59	40.084	-13	05	10.91	-0.022	+0.10	Br
2002	08	10.928843	21	58	37.889	-13	10	48.49	-0.012	+0.16	Br
2002	08	10.941827	21	58	37.754	-13	10	49.35	-0.030	-0.06	Br
2002	08	12.931400	21	58	19.618	-13	12	28.14	-0.025	-1.03	Br
2002	08	12.942654	21	58	19.551	-13	12	24.44	+0.011	-0.78	Br
2002	08	15.923312	21	57	52.156	-13	14	55.18	-0.012	-0.43	Br
2002	08	15.932315	21	57	52.051	-13	14	55.81	-0.033	-0.62	Br
2002	08	18.914584	21	57	24.536	-13	17	22.64	-0.017	-0.15	Br
2002	08	18.925260	21	57	24.452	-13	17	22.96	-0.001	+0.07	Br
2002	08	27.893836	21	56	01.726	-13	24	41.45	-0.038	+0.10	Br
2002	08	29.906178	21	55	43.464	-13	26	17.89	+0.044	+0.15	Dm
2002	09	02.878146	21	55	07.628	-13	29	25.90	-0.027	-0.61	Br
2002	09	02.888649	21	55	07.542	-13	29	26.17	-0.019	-0.39	Br
2002	09	08.867112	21	54	15.268	-13	33	58.04	-0.016	-0.73	Br
2002	09	10.832032	21	53	58.644	-13	35	23.80	-0.027	-0.57	Bb
2002	09	10.846576	21	53	58.537	-13	35	24.76	-0.013	-0.90	Bb
2002	09	10.856618	21	53	58.441	-13	35	25.24	-0.024	-0.95	Bb
2002	09	11.850211	21	53	50.142	-13	36	07.89	-0.030	-0.88	Br
2002	09	25.822398	21	52	03.847	-13	45	07.80	-0.052	-0.50	Bb
2002	11	29.659032	21	50	43.061	-13	49	53.58	+0.036	+0.21	Na
2002	11	30.623818	21	50	47.904	-13	49	26.58	+0.021	-0.16	Br
2002	12	03.653023	21	51	04.242	-13	47	55.68	-0.026	-1.04	Br

The means (O–C) relatively DE200 are $-0.014^s \pm 0.005^s$ for RA and $-0.''410 \pm 0.''092$ for DECL. Ones relatively DE405 are $-0.013^s \pm 0.005^s$ for RA and $-0.''403 \pm 0.''092$ for DECL.

2. REFERENCES

Bronnikova, N. M., Dement'eva, A. A., Ryl'kov, V. P., et.al., 1989, *Izv. GAO*, **206**, 23–25, (in Russian).

Lavdovsky, V. V., 1971, *Izv. GAO*, **189-190**, 144–175, (in Russian).

L'vov, V. N., Smekhacheva, S. I., Tsekmejster, S. D., 1999, Gaidence for Users, GAO RAN, St.Petersburg, (in Russian).

Chanturiya, S. M., Kisseleva, T. P., Emelianov, N. V., 2002, *Izv. GAO*, **216**, 349–362, (in Russian).

INTERNAL STRUCTURE MODELS OF MARS

H. ZHANG
Department of Astronomy, Nanjing University
22nd Hankou Road, Nanjing, P.R.China
jupiter@nju.edu.cn

ABSTRACT. Mars Global Surveyor(GMS) presents more precise data, which enable us to understand further the internal structure by modelling Mars. An inverse approach of the problem of modelling the interiors of Mars is proposed. The internal structure with a pure core is recommended according to the elementary calculations.

1. INTRODUCTION

The parameters to directly constrain the internal structure models are the mean density and dimensionless mean moment of inertia of the body. More precise geodetic data, such as polar moment of inertia, are provided by the Mars Global Surveyor tracking data. These data enable us to understand the internal structure by modelling Mars. The following table lists some parameters of Mars(Table 1). R denotes the mean radius, GM product of universal gravitational constant G and mass M, C/MR^2 the polar moment of inertia, and k_2 the second Love number of Mars.

Table 1: Some parameters of Mars.

Parameters	Values	Reference
R(km)	3389.92	Bills and Ferrari(1978)
GM(km^3/s^2)	42823.716 ± 0.0002	Smith et al.(2001)
C/MR^2	0.3650 ± 0.0012	Yoder et al. (2003)
k_2	0.153 ± 0.017	Yoder et al. (2003)

An inverse approach of the problem of modelling the interiors of Mars is proposed. But thermal corrections are not considered. For a real body, it is in the hydrostatic and thermodynamic equilibriums. An improved model, in which the hydrostatic and hydrostatic equilibriums are taken into considered, should be constructed in the future.

2. INTERIORS OF MARS

Three-layer models are considered in detail, which consist of the outer shell, the mantle and the central core. The mantle and the core are assumed to be in the hydrostatic equilibrium. And the equations of state for the mantle and the core can be derived from the empirical bulk moduli, respectively. Bulk moduli of the major silicates (olivine, orthopyroxene, clinopyroxene,

plagioclase) are in the range 1-1.3Mbar at normal conditions; and for a pure Fe core, bulk moduli is 1.66Mbar (Kuskov and Kronrod, 2001). Since bulk moduli for an Fe-FeS core is unknown, the values of bulk moduli for an Fe-FeS core is adopted as those for a pure Fe core. Therefore, the Emden equations of the mantle and the core can be expressed, respectively(cf. Zhang and Zhang, 2001). As regards the outer shell, the density is treated as a constant parameter (2.96g/cm^3) and the thickness is assumed to range between 50 and 100 km (Zuter et al., 2000; Turcotte et al., 2002).

With the appropriate imposed boundary conditions, the Emden equation for the core can be numerically solved from the center outwards and the Emden equation for the mantle from the surface inwards. According to the continuity of pressure at the core-mantle boundary, a possible size of the core can be determined.

3. RESULTS

Two groups of models are constructed, from which four typical models are picked out and displayed in Table 2. The first two refer to an Fe-FeS core with the density of 5.15g/cm^3 and the other two refer to a pure Fe core with the density of 8.00g/cm^3. In the tables, ρ_c denotes the central density of the core, p_c the central pressure, r_c the radius of the core, r_m the size of the mantle, ρ_m the mean density of the mantle, h the size of the outer shell, ρ_s the mean density of the outer shell, I/MR^2 the dimensionless mean moment of inertia and $\bar{\rho}$ the calculated mean density of Mars.

Table 2: Internal Structure Models of Mars.

		Mars-01	Mars-02	Mars-03	Mars-04
Core	ρ_c(g/cm^3)	5.15	5.15	8.00	8.00
	$p_c(kbar)$	370	380	470	475
	r_c(km)	2134.4	2168.21	1480.46	1473.77
Mantle	r_m(km)	1205.58	1121.71	1859.46	1816.15
	ρ_m(g/cm^3)	3.213	3.324	3.463	3.504
Outer Shell	h(km)	50	100	50	100
	ρ_s(g/cm^3)	2.96	2.96	2.96	2.96
Total	I/MR^2	0.3661	0.3652	0.3653	0.3549
	$\bar{\rho}$(g/cm^3)	3.93314	3.93309	3.93303	3.93311

The following conclusions can be given from the above calculations.

- If Mars has an Fe-FeS core, it can own a larger core, whose size can reach 2168km. However, the core radii of the models with a pure Fe core are around 1480km, which are similar to the results provided by Yoder et al.(2003).
- The model with a pure Fe core may have a smaller dimensionless mean moment of inertia than that with an Fe-FeS core.
- The central pressure is about 375kbar for the model with an Fe-FeS core.But for the model with a pure Fe, the central pressure is about 470kbar.
- For the same density of the core and the same thickness of the outer shell, the core size of the model increases and the mean density of the mantle decreases as the central pressure p_c increases.
- The Love number k_2 of Mars is larger than 0.1, which indicates a solid core. The models with a pure core are more reasonable.

Acknowledgments. This work is supported by the National Natural Science Foundation of China.

4. REFERENCES

Bills, B. G., Ferrari, A. J., 1978, *J. Geophys. Res.*, **83**, 3497.
Kuskov, O. L., Kronrod, V. A., 2001, *Icarus*, **151**, 204.
Smith, D. A., Zuber, M. T., Neumann, G. A., 2001, it Science, **294**, 2141.
Turcotte, D. L., et al., 2002, *J. Geophys. Res.*, **107**, 1.
Yoder, C. F., et al., 2003, *Science*, **300**, 299.
Zhang, H., Zhang, C. Z., 2001, *Chin. J. Astron. Astrophys.*, **3**, 275.
Zuber, M. T., et al., 2000, *Science*, **287**, 1788.

COMPARISON OF KYIV DATABASE OF LUNAR OCCULTATION

L. KAZANTSEVA[1], L. KISLYUK[2]
[1] Astronomical observatory of Taras Shevchenko Kyiv National University
3 Observatorna str., 04053 Kiev, Ukraine
e-mail:likaz@observ.univ.kiev.ua
[2] Main Astronomical Observatory of NAS of Ukraine
27 Akademika Zabolotnoho str., 03680 Kiev, Ukraine
e-mail:kislyuk@mao.kiev.ua

ABSTRACT. Description of computer database of the results of lunar occultation observations collected at the Astronomical Observatory of the Kyiv National University is given. The results of processing the database materials as well as the same results taken from other databases were investigated by means of spectral and correlation analysis of uniform temporal series. Dependence of findings from change of the input parameters (system of astronomical constants, lunar ephemeris, reference star catalogue) were analyzed. When analyzing the Kyiv database the presence of some periodicities in O-C values that were found out by other investigators have been confirmed.

1. INTRODUCTION

The Kiev Database of Lunar Occultations (KDLO) includes complete data for more than 25000 observations of these phenomena observed during 1963-2003[1]. Almost 2/3 of these data have not been processed before and they have not been included yet to the world banks. Besides total occultations KDLO consits of data concerning 59 observations of grazing occultations (411 times) and 33 occultations of planets by the Moon (316 times). Majority of observations were made visually. Only approximately 2% of all observations were obtained using photoelectric and CCD equipments. Mean timing accuracy of them lies between 0.06 and 0.09 s. Almost 70 % of observations of occultations were made with dark limb of the Moon. 590 observers from 78 sites of Ukraine, Russia, Georgia, Belorus', Moldova, Lithuania, and Uzbekistan took part in observations. There are the following advantages of the KDLO: using the same type of time recording devices; reducing the occultation timings to the UTC scale through the uniform Time Service; positions of observers are given in the same Geodetic System.

2. ANALYSYS OF THE OBSERVATIONAL DATA AND REZULTS OF PROCESSING

On the level of input data the results of observations from KDLO are compatible with the similar data of the world banks [2,4,6]. Processing of the observational data were made by means of conventional 3-stage methods [3,6]. On each stage the results of processing were compared to the results of another authors which differ from one another with using different input data (system of astronomical constants, Lunar Ephemeris and charts of lunar profile as well as the

reference star catalogue). At the first stage for each observation the difference between the observed and calculated angular distance from the star to the lunar limb, $(O-C) \equiv \Delta\sigma$, were obtained. These values were compared with the analogues data from different series of lunar occultation data. All the data have practically normal distribution of values and similar standard deviations. At the second stage equations being formed for each observation were combined into systems on lunations and years. As a result of solving these equations series of values of (O-C) corrections to ecliptical coordinates of the Moon $(\Delta L, \Delta B)$ were obtained which were analysed by means of spectral and correlation analysis as the uniform temporal series. We found out some periodical terms in (O-C) values. The same periodicities are present in other considered series of lunation solutions. The greatest amplitude have the terms which correspond to periods of changing the Delaunay arguments (F, d, l_M, l_S) and longitude of node of the Moon's orbit,Ω. Earlier many investigators (E.Brown, 1923; L.V.Morrison and F.McBain Sadler, 1969; M.Soma, 1985; C.Jordi and G.Rossello, 1990) noted to presence of these periodicities. It was considered that the most of the periodic terms are caused with inaccuracies of astronomical constants, star positions, the Moon's motion theory and the Moon's profile charts. However it is impossible to understand why these periodicities are remained (true, with lesser amplitude) when we use modern high-precision mentioned input parameters. At the third stage main corrections were obtained solving the equation system for the whole set of data. Results obtained for the KDLO data as well as the [5] results are given in table 2 for comparison. They are practically the same within the errors of determination.

Comparison of two series of solutions of equation systems

Corrections	Soma 2000	KDLO
To the lunar ecliptic longitude	$-83.5 \pm 3mas$	$-101 \pm 27mas$
To the right ascension system of the stars	$-32.8 \pm 19mas$	$+9 \pm 34mas$
Rotation of the star's coordinates		
around the equinox	$-3.6 \pm 6mas$	$-12 \pm 11mas$
Rotation of the Hipparcos reference frame	$+0.67 \pm 0.42mas/yr$	$+1.2 \pm 0.65mas/yr$
	$+0.22 \pm 0.09mas/yr$	$+0.11 \pm 0.15mas/yr$
	$-4.57 \pm 1.29mas/yr$	$-3.2 \pm 2.2mas/yr$

We conclude that the KDLO is compatible with the similar data of the world bank from the point of view of its accuracy and duration of observation time period.

3. REFERENCES

Kazantseva L. V., Osipov A. K., 2002, *Kinem.Phys.Cel.Bodies* **18**, 179–187.
Morrison L. V., 1978, *Greenwich Obs. Bull.*, No 183, 14 p.
Morrison L. V., 1979, *Mon. Not. Astr. Soc.*, No 187, 41–82.
Morrison L. V., Appleby G. M., White M. T., 1984, *Greenwich Obs. Bull.*, No 192, 12 p.
Soma M., 2000, *Proceeding of IAU Colloquim 180*, 115–119.
Report of lunar occultation observations, 2003, *ILOC*, No 21, 1–8.

EVOLUTION OF A TWO-PLANETARY REGULAR SYSTEM ON A COSMOGONIC TIME SCALE

K.V. KHOLSHEVNIKOV[1], E.D. KUZNETSOV[2]
[1] Sobolev Astronomical Institute, St.Petersburg State University
28, Universitetsky pr., 198504, St.Petersburg, Stary Peterhof, Russia
e-mail: kvk@astro.spbu.ru
[2] Astronomical Observatory, Urals State University
51, Lenin pr., , Ekaterinburg, Russia
e-mail: Eduard.Kuznetsov@usu.ru

ABSTRACT. For the planetary three-body problem we use Jacobian coordinates, introduce two systems of osculating elements, construct the Hamiltonian expansions in the Poisson series in all elements. Further we construct the averaged Hamiltonian by the Hori — Deprit method with accuracy upto second order with respect to the small parameter, the generating function, change of variables formulae, and right-hand sides of averaged equations. The averaged equations for the Sun – Jupiter – Saturn system are integrated numerically at the time-scale of 10 Gyr. The motion turns out to be almost periodical. The low and upper limits for averaged eccentricities are 0.016, 0.051 (Jupiter), 0.020, 0.079 (Saturn), and for averaged inclinations to the ecliptic plane are 1.3°, 2.0° (Jupiter), 0.73°, 2.5° (Saturn).

1. AVERAGED PLANETARY THREE-BODY PROBLEM

This work continues researches beginning in (Kholshevnikov, Greb, & Kuznetsov 2001; 2002). We consider the planetary three-body problem the Sun – Jupiter – Saturn. We use Jacobian coordinates as best-fitting. Small parameter μ is equal to 10^{-3}. Let us represent the Hamiltonian as a sum of the unperturbed part h_0 and the perturbed one μh_1. The Hamiltonian h_0 depends on semi-major axes only. The Hamiltonian h_1 may be thought of as a constant factor having dimension of velocity squared and a dimensionless part h_2.

The disturbing function h_2 is presented as Poisson series $h_2 = \sum A_{kn} x^k \cos ny$, where x are positional elements, y are angular ones, A_{kn} are numerical coefficients, k and n are multi-indices. The summation is taken over non-negative k_s and integer n_s, $s = 1, ..., 6$. We obtain limits of the Poisson series summation ensuring the Hamiltonian accurate up to μ^σ.

We use two systems of osculating elements. The first system is close to the Keplerian one. In the second system denominators arising in a process of averaging transforms are extremely simple. On the other hand, it has a deficiency, mixing several elements of all planets.

The rational version of the Poisson series processor PSP (Brumberg 1995; Ivanova 1995) is used to construct the expansion of disturbing Hamiltonian h_2 into Poisson series. The expansion of disturbing Hamiltonian is processed up to μ^2. The summation is taken over $k_1 + \cdots + k_6 \le 6$, $|n_s| \le 15$ $(s = 1, \ldots, 6)$. For each of the osculating elements system two variants of the expansion are constructed. The first variant deals with numerical values of parameters (masses, mean

values of semi-major axes, ...) corresponding to the system the Sun – Jupiter – Saturn. The second one deals with their litteral expressions depending on parameters of the system. The expansions with numerical data contain 61086 terms. The expansions with litteral parameters contain 182744 terms for the first system and 183227 terms for the second one.

The Hori – Deprit method (Lie transforms method) is used to construct the averaged Hamiltonian $H(X, Y)$. This method is based on Poisson brackets that allows us to use non-canonical elements writing down the Poisson brackets in the corresponding system of phase variables (Kholshevnikov & Greb 2001). The Hamiltonian $h(x, y)$ is averaged over the fast variables. The averaged Hamiltonian H is presented by power series in the small parameter μ upto μ^2. For calculations we use the rational version of the echeloned Poisson series processor EPSP (Ivanova 2001). Transformations are made for both systems of elements with numerical parameters. Two approximations of Hori — Deprit method are made. The generating function, change of variables formulae between averaged and osculating systems, and right-hand sides of averaged equations of motion are obtained.

2. BEHAVIOUR OF THE SUN — JUPITER — SATURN SYSTEM ON 10 Gyr

The averaged equations are integrated numerically at the time-scale of 10 Gyr. The equations for slow variables are integrated by Everhart and Runge-Kutta high order methods. The equations for fast variables are integrated by spline interpolation method. Accuracy of integration is detected by computation of integrals of energy and area.

The motion turns out to be almost periodical. The low and upper limits for averaged eccentricities are 0.016, 0.051 (Jupiter), 0.020, 0.079 (Saturn), and for averaged inclinations are 1.3°, 2.0° (Jupiter), 0.73°, 2.5° (Saturn). Evolution of the ascending nodes longitudes with respect to the ecliptical plane and the arguments of pericentre turns out to be secular. Evolution of the ascending node longitudes depends on the base plane. Difference between the ascending nodes longitudes of Jupiter and Saturn with respect to Laplace plane is equal to 180° exactly.

Estimates of the Liapunovian Exponents for the system the Sun – Jupiter – Saturn are obtained. The corresponding Liapunovian Time turns out to be 14 Myr (Jupiter) and 10 Myr (Saturn).

Our results are qualitatively in agreement with ones obtained by (Laskar 1994; Murray, & Dermott 1999; Ito, & Tanikawa 2002).

Acknowledgments. This work was partly supported by the RFBR, Grant 02-02-17516, Program *Universities of Russia*, Grant UR.02.01.027, and the Leading Scientific School, Grant NSh-1078.2003.02.

3. REFERENCES

Brumberg, V. A., 1995, Analytical techniques of celestial mechanics, Springer, Heidelberg.

Ito, T., Tanikawa, K., 2002, *In: Proc. IAU 8 Asian-Pacific Regional Meeting*, **II**, 45.

Ivanova, T. V., 1995, *In: IAU Symp. 172, Dynamics, ephemerides and astrometry of the solar system*, S. Ferraz-Mello, B. Morando, J. -E. Arlot (eds.), Kluwer Academic Publishers.

Ivanova, T., 2001, *Celest. Mech. Dyn. Astr.*, **80**, 167.

Kholshevnikov, K. V., Greb, A. V., Kuznetsov, E. D., 2001, *Solar System Research*, **35**, 243.

Kholshevnikov, K. V., Greb, A. V., 2001, *Solar System Research*, **35**, 457.

Kholshevnikov, K. V., Greb, A. V., Kuznetsov, E. D., 2002, *Solar System Research*, **36**, 68.

Laskar, J., 1994, *Astron. Astrophys.*, **287**, L9.

Murray, C. D., Dermott, S. F., 1999, *Solar system dynamics*, Cambridge university press.

THE DETERMINATION OF COORDINATES OF SATURN BY OBSERVATIONS OF IT'S SATELLITES WITH 26-INCH REFRACTOR AT PULKOVO

T.P. KISELEVA, O.A. KALINICHENKO, M.A. MOZHAEV
Main Astronomical Observatory of RAS
65/1, Pulkovskoye chaussee, 196140, St.Petersburg, Russia
e-mail: melon@gao.spb.ru

ABSTRACT. The results of determination of coordinates of Saturn from the observations of it's satellites without measuring the images of the planet are presented. 25 positions of Saturn have been determined from photographic observations with 26-inch refractor at Pulkovo in 1994–2003. The accuracy of Saturnian coordinates estimated by comparison of observational data with the theory DE405 is about ± 0.15" for both right ascension α and declination δ.

1. INTRODUCTION

Regular CCD and photographic observations of eight major satellites of Saturn with the aim of determination of relative positions of satellites are carried out at Pulkovo observatory with the 26-inch refractor. The results of observations are reduced by the "scale-trail" method [1] and are characterized by high inner and external accuracy. For photographic observations the inner standard error of one relative position of pair of satellites is equal to ± 0.06", and the external one is ± 0.12" [2]. For CCD observations the errors are ± 0.01" and ± 0.14" correspondingly. The "scale-trail" method does not require reference stars for the determination of relative positions of satellites. But the presence of at least one reference star with accurate position in the small field of view of telescope allows us to determine the coordinates of the planet without measuring it's image on the plate or CCD-frame. The problem may be solved if accurate coordinates of some reference star and theoretical cronocentric coordinates of satellite are known. The precision of coordinates of Saturn in this case is conditioned by precision of theory of motion of satellites, precision of coordinates of reference stars and errors of observations. The errors of theory of motion plays the main part because the errors of coordinates of stars in cosmic catalogues Hipparcos and Tycho-2 are small enough, not exceeding 0.1", and the errors of measurements are the same. The errors of theories of motion of different satellites do not exceed 0.1" - 0.2". Such method of determination of coordinates of Saturn has essential advantage since it does not require measurement of images of planet distorted by phase, rings and other atmospheric factors. Systematic errors of positions of Saturn caused by that factors run up to 0.4" in δ [2].

2. RESULTS

In this papier we present the results of our photographic observations of Saturnian satellites in 1994–2003. 25 positions of Saturn on 25 photographic plates have been determined by measuring satellites and stars of Hipparcos or Tycho-2 catalogues without measurement of images of Saturn.

From 1 to 6 stars and from 1 to 6 satellites were used on each plate and mean values were taken. Method of 6 constants was used for 5 plates, but 20 plates were reduced by the "scale-trail" method. The differences of positions of satellites and stars were determined. The cronocentric coordinates of satellites were taken from Harper and Taylor's ephemerides. Combining these values with coordinates of stars from Tycho-2 or Hipparcos catalogues we were able to calculate the topocentric coordinates of Saturn. The equatorial topocentric coordinates of Saturn (right ascension α and declination δ) at the epoch 2000 are presented in the Table 1.

Table 1: Topocentric coordinates of Saturn.

N of plate	Date (UTC)			α_{2000}			δ_{2000}			$(O-C)_\alpha$	$(O-C)_\delta$
				h	m	s	°	'	"	s	"
19690	1994	08	09.007930	22	52	04.650	-09	18	24.26	-0.005	-0.12
19988	1995	08	27.986915	23	36	55.330	-05	01	25.64	-0.015	-0.35
20107	1995	10	15.809035	23	23	55.805	-06	25	29.56	+0.016	+0.05
20108	1995	10	15.830485	23	23	55.516	-06	25	31.02	+0.010	+0.23
20109	1995	10	21.855919	23	22	41.950	-06	32	36.20	-0.008	-0.03
20110	1995	10	21.878699	23	22	41.690	-06	32	37.46	-0.010	-0.23
20751	1998	11	10.803692	01	50	54.728	+08	28	23.58	-0.002	+0.06
20752	1998	11	10.826522	01	50	54.322	+08	28	21.86	-0.022	+0.28
20953	1999	11	18.864532	02	44	20.014	+13	10	34.77	+0.010	-0.23
20963	2000	02	10.692300	02	37	31.753	+13	01	02.36	+0.009	+0.04
21117	2001	02	16.756527	03	30	41.797	+16	58	52.99	-0.002	+0.15
21202	2001	08	28.961833	04	52	18.131	+20	45	09.33	-0.006	+0.06
21214	2001	09	01.027415	04	52	56.053	+20	45	48.50	0.000	0.00
21215	2001	09	01.053163	04	52	56.351	+20	45	48.95	0.000	+0.13
21227	2001	09	20.100971	04	55	20.425	+20	47	12.48	+0.008	+0.06
21241	2001	10	23.026501	04	52	57.741	+20	39	46.39	+0.020	-0.10
21263	2002	02	01.769459	04	26	15.323	+19	59	15.03	+0.021	-0.04
21375	2002	12	10.945572	05	43	13.787	+22	03	34.60	+0.018	-0.32
21380	2003	02	01.826670	05	27	32.908	+22	02	10.32	+0.015	+0.04
21381	2003	02	04.925570	05	27	04.880	+22	02	26.10	+0.002	-0.19
21384	2003	02	15.747327	05	26	02.192	+22	03	52.56	+0.014	-0.01
21386	2003	02	20.752281	05	25	52.109	+22	04	48 43	+0.005	+0.04
21387	2003	02	21.742356	05	25	51.545	+22	05	00.53	-0.006	-0.11
21392	2003	03	02.711277	05	26	08.312	+22	07	09.02	+0.010	-0.08
21396	2003	03	04.793896	05	26	17.779	+22	07	43.26	+0.002	-0.01

The mean value of error in results depending on 4 satellites (measuring and theories) is about ± 0.07" for both α and δ. The comparison of coordinates of Saturn with DE405 ephemerides gives the following mean results: $(O-C)_\alpha = +0.003^s$, mean $(O-C)_\delta = -0.04$". The analysis of accuracy of Saturnian coordinates on the basis of (O-C) gives the following estimates: $\sigma_\alpha \cos\delta = \pm 0.15$", $\sigma_\delta = \pm 0.16$". From the results obtained we can conclude, that this method of determination of precise coordinates of far planets may be used for both photographic and CCD observations.

Acknowledgments. This work was carried out with the support of Russian Founddation for Basic Research, project N 01-02-17018.

3. REFERENCES

Kiselev A. A., 1989, Theoretical Foundations of Photographic astrometry, Moscow, Nauka.

Kiseleva T. P., Izmailov I. S., Kalinitchenko O.A., 2002, Astrometry of Saturnian satellites on the basis of photographic and CCD observations with 26-inch Refractor at Pulkovo observatory in 1995–2000, *Izvestia GAO at Pulkovo*, N 216, 174–180.

KLENOT – PRACTICAL USE OF SOLAR SYSTEM DYNAMICS IN FOLLOW-UP ASTROMETRY OBSERVATIONS OF SMALL SOLAR SYSTEM BODIES

M. KOČER, J. TICHÁ, M. TICHÝ
Kleť Observatory
Zátkovo nábřeží 4, 370 01 České Budějovice, Czech Republic
e-mail: kocer@klet.cz, www: http://www.klet.cz/

ABSTRACT. The KLENOT project is a project of the Kleť Observatory, Czech Republic, devoted to astrometric observations of Near Earth objects, distant objects and comets.

The improved effort of the large NEO surveys resulting in an increasing number of newly discovered NEOs calls for continuous follow-up astrometry to secure an accurate orbit determination of discovered bodies first in discovery opposition and then during next apparitions. Considering this urgent need of astrometric follow-up, the fact that many of these targets are fainter then magnitude $m_V = 20.0^m$ and our results and experience in minor planet and comet CCD astrometry done at Kleť since 1993, we decided to bring into operation a new 1-m class facility working on a permanent basis - the KLENOT telescope. The regular observing of the telescope started in March 2002 (the MPC code 246).

We discuss here methods and techniques we use for follow-up astrometry. Some of the practical results are also mentioned.

1. KLENOT PROJECT

Kleť Observatory Near Earth and Other Unusual Objects Observations Team (and Telescope) project goals:

- Confirmatory observations of newly discovered fainter NEO candidates
  Some of new search facilities produce discoveries fainter than $m_V = 20^m$ (for example 1.8-m Spacewatch II, 1.2-m Palomar/NEAT) which need a larger telescope for confirmation and early follow-up. A 1-m class telescope is also very suitable for confirmation of very fast moving objects and our larger FOV enables to search for NEO candidates having a larger ephemeris uncertainty.

- Follow-up astrometry of poorly observed NEOs
  It is necessary to observe newly discovered NEOs in a longer arc during the discovery opposition when they get fainter. Special attention is given to "virtual Impactors" and PHAs, target of future space missions or radar observations. On the other hand, it is necessary to find and use an optimal observing strategy to maximize orbit improvement of each asteroid.

- Recoveries of NEOs in the second opposition
  For the determination of reliable orbits it is required to observe asteroids in more then one

opposition. If the observed arc in a discovery apparition is long enough, the chance for a recovery in the next apparition is good. If the observed arc at single opposition is not so good, we plan to search along the line of variation. For this purpose a larger field of view is an advantage.

- Follow-up astrometry of other unusual objects (Centaurs and transneptunian objects)
- Detection of cometary features of a newly discovered objects
- Search for new asteroids
- Follow-up of Gamma-ray burst (GRB) optical counterparts

2. KLENOT TELESCOPE

The KLENOT telescope (1.06-m f/3) was built using an existing dome and infrastructure of the Kleť Observatory. The original mounting was upgraded and the optoelectronical control system was added. The telescope is equipped by CCD camera Photometrics Series 30 (chip SITe 003B 1024×1024 pixels, pixel size 24 microns, liquid nitrogen cooling) so that the final field of view of the telescope is 33 x 33 arcminutes. The limiting magnitude is $m_V = 22^m$ for 180-sec exposure time in standard weather condition.

3. TECHNOLOGY

A special software package has been developed for the KLENOT project at the Kleť Observatory using a combination of programs running both on Linux and Windows platforms. The system consists of web-based observation planing tools (program `ephem`), data-acquisition, CCD camera control and data processing tools (programs `blink`, `astrometry`, `residua` and `orbit`).

4. RESULTS

The regular observations of the KLENOT project started in March 2002. By September 2003 14.720 astrometric positions of Solar System objects has been obtained (and published to MPC); 4303 of them have been observations of NEAs (412 Atens, 2420 Apollos, 1471 Amors) and 755 have been observations of comets. Other important results of the KLENOT project are recoveries of 12 NEAs, recoveries of comets `C/2003 A1`, `C/2003 A2` and `100P` as well as the discovery of Apollo-type asteroid `2002 LK`.

Acknowledgments. This work has been sponsored by The Grant Agency of the Czech Republic Reg. No. 205/98/0266, The 2000 NEO Shoemaker Grant of The Planetary Society, and The Grant Agency of the Czech Republic Reg. No. 205/02/P114.

5. REFERENCES

Tichá, J., Tichý, M., Kočer, M., 2002, KLENOT - Kleť Observatory Near Earth and Other Unusual Objects Observations Team and Telescope, *ESA SP-500: Asteroids, Comets, and Meteors: ACM*, 793–796.

Sekanina, Z., Chodas, P. W., Tichý, M., Tichá, J., Kočer, M., 2003, Peculiar Pair OF Distant Periodic Comets C/2002 A1 and C/2002 A2 (LINEAR), *Astron. J.*, **591**, Issue 1, L67–L70.

PRECISE POSITION OF SATURN OBTAINED FROM A STELLAR OCCULTATION BY TETHYS

M. SÔMA[1], T. HAYAMIZU[2], T. SETOGUCHI[3], T. HIROSE[4]
[1] National Astronomical Observatory of Japan
Mitaka, Tokyo, Japan
e-mail: somamt@cc.nao.ac.jp
[2] Sendai Space Hall
Sendai-City, Kagoshima-Pref., Japan
e-mail: uchukan@bronze.ocn.ne.jp
[3] Japanese Occultation Information Network
Yoshida-Cho, Kagoshima-Pref., Japan
e-mail: set@bronze.ocn.ne.jp
[4] International Occultation Timing Association
Shimomaruko, Ota-Ku, Tokyo, Japan
e-mail: thirose@cam.hi-ho.ne.jp

ABSTRACT. A stellar occultation of a 9.1 magnitude star by Saturn's satellite Tethys was observed on 2002 Dec. 15 in Japan and in Europe. From them a precise position of Tethys relative to the star was obtained, and using orbital theories of Tethys around Saturn a precise position of Saturn was obtained. This paper gives a preliminary results of the analysis.

1. INTRODUCTION

The occultation of TYC 1310-02435-1 (9.1 mag) by Saturn's satellite Tethys on 2002 Dec. 15 (early morning of Dec. 16 in Japan Standard Time) was originally predicted by David Herald in Australia about a year before the event. He predicted that the event would be visible in the southern part of China, the Sahara Desert in Africa, etc. However, just 4 days of the event Jan Manek, a member of the International Occultation Timing Association (IOTA) in Czech Republic recalculated the prediction, and found that the event would be visible in Japan and in Europe. Based on this prediction the occultation was detected by 7 observers in Japan and 2 in Europe.

The observations provide a very precise position of Tethys with respect to the star, and hence a very precise position of Saturn with respect to the star at the time of the occultation.

2. OBSERVATIONS AND ANALYSIS

The observations were made by the following people:

Positive video observations:
Mitsuru Kashiwagura, Hiromi Hamanowa, Hideo Takashima, Katsuhiko Kitazaki, Eisaku Katayama (Japan)

Positive visual observations:
Akira Yaeza, Akie Hashimoto (Japan), Vitali S. Nevski (Belarus), Wojciech Burzynski (Poland)
Negative observations:
Pic du Midi Observatory (France), Rui Goncalves (Portugal), Oscar Canales Moreno (Spain), Ricard Casas (Spain), Hilari Pallares Albalat (Spain), Carles Schnabel (Spain), F. Izquierdo (Spain)

The observations fit very well with the diameter 1060 km of Tethys which was obtained by the Voyager spacecrafts. The results of our preliminary analysis are as follows:
Geocentric position of Tethys relative to the Tycho-2 positions of the occulted star TYC 1310-02435-1 for the epoch of 2002 Dec. 15 $18^{\rm h}\ 58^{\rm m}\ 00^{\rm s}$ TT is
R.A. $05^{\rm h}\ 51^{\rm m}\ 33^{\rm s}.9493 \pm 0^{\rm s}.0001$ and Dec. $+22^\circ\ 03'\ 31''.687 \pm 0''.002$.
By taking into account the accuracy of the Tycho-2 positions of the star, the accuracies of the position with respect to ICRF become $\pm 0^{\rm s}.0015$ and $\pm 0''.026$, respectively.

The theories of the motion of Tethys around Saturn by Harper & Taylor (1993) and by Dourneau (1987, 1993) were used to obtain the positions of Saturn. The resulting corrections to the JPL DE405 positions of Saturn for the epoch of 2002 Dec. 15 $18^{\rm h}\ 58^{\rm m}\ 00^{\rm s}$ TT are
$\Delta\alpha = +0^{\rm s}.0106$ and $\Delta\delta = +0''.036$ via Harper & Taylor (1993), and
$\Delta\alpha = +0^{\rm s}.0080$ and $\Delta\delta = +0''.079$ via Dourneau (1987).
Hence the mean corrections to the JPL DE405 position of Saturn with respect to ICRF are
$\Delta\alpha = +0^{\rm s}.009 \pm 0^{\rm s}.001$ and $\Delta\delta = +0''.06 \pm 0''.02$.

Details of the observations and analysis will be published elsewhere.

3. CONCLUSION

From the observation of a stellar occultation by Tethys a precise position of Saturn at the time of the occultation was obtained.

4. REFERENCES

Harper D., Taylor D. B., 1993, *Astron. Astrophys.*, **268**, 326–349.
Dourneau G., 1987, Doctoral Thesis, 1993, *Astron. Astrophys.*, **267**, 292–299.

Section V)

RELATIVITY AND TIME

TEMPS ET RELATIVITÉ

THE BCRS AND THE LARGE SCALE STRUCTURE OF THE UNIVERSE

M. SOFFEL, S. KLIONER
Lohrmann Observatory,
Dresden Technical University,
01062 Dresden, Germany

ABSTRACT. The BCRS is presently defined for an isolated solar system by ignoring effects from cosmology. Various problems that arise if one tries to match the BCRS with a cosmological metric that describes the expansion of the universe are discussed. An approximate solution for the BCRS with cosmological constant Λ is given.

1. THE BCRS AND COSMOLOGY

According to IAU-Resolution B1.3 the BCRS with coordinates $(t, \mathbf{x})$ is defined by a metric tensor of the form

$$\begin{aligned} g_{00} &= -1 + \frac{2w}{c^2} - \frac{2w^2}{c^4} + \mathcal{O}(c^{-5}) \\ g_{0i} &= -\frac{4}{c^3} w^i + \mathcal{O}(c^{-5}) \\ g_{ij} &= \delta_{ij} \left(1 + \frac{2}{c^2} w \right) + \mathcal{O}(c^{-4}) \,. \end{aligned} \tag{1}$$

Here, the gravito-electric potential w generalizes the usual Newtonian gravitational potential U and the gravito-magnetic potential w^i describes gravitational effects resulting from moving gravitational sources. The order symbols in Eq.(1) indicates that the validity of the metric tensor is restricted to the first post-Newtonian approximation of Einstein's theory of gravity. In that approximation, using the harmonic gauge condition, the field equations read

$$\begin{aligned} \left(-\frac{1}{c^2} \frac{\partial^2}{\partial t^2} + \nabla^2 \right) w &= -4\pi G\sigma + \mathcal{O}(c^{-4}) \,, \\ \nabla^2 w^i &= -4\pi G\sigma^i + \mathcal{O}(c^{-2}) \,. \end{aligned} \tag{2}$$

Here σ and σ^i are the gravitational mass and mass current density, respectively. Mathematically they are related to the energy-momentum tensor $T^{\mu\nu}$ by

$$\sigma = \frac{1}{c^2} \left(T^{00} + T^{ss} \right) \,, \quad \sigma^i = \frac{1}{c} T^{0i} \,. \tag{3}$$

For the present definition of the BCRS spacetime is assumed to be asymptotically flat, i.e.,

$$\lim_{\substack{r\to\infty \\ t=\text{const}}} g_{\mu\nu} = \text{diag}(-1,+1,+1,+1)\,. \tag{4}$$

This condition assumes that all kinds of gravitational sources outside the solar system, as well as the vacuum energy (or cosmological constant) that pervades every volume element of our universe, are ignored.

As is well known the (averaged) global mass-energy distribution on large cosmic scales determines the global geometry of the universe as well as its global dynamical development. For a description of the universe on large scales the so-called "cosmological principle" is of great value. This principle says that on very large scales our universe is homogeneous and isotropic. Mathematically the Robertson-Walker metric follows from this principle. For a flat space in suitable coordinates $(T, \mathbf{X})$ this metric takes the form

$$ds^2 = -c^2\, dT^2 + a^2(T)\, d\mathbf{X}^2\,, \tag{5}$$

where $a(T)$ is the cosmic scale factor. Such a cosmic metric has profound consequences for astrometry: it describes cosmic red shift effects due to the expansion of the universe and leads to various distance measures like parallax distance, luminosity distance, angular diameter distance or proper motion distance that differ from each other (Weinberg, 1972). The question of empirical validity of the cosmological principle has been investigated in detail in recent years (Lahav, 2000 and references quoted therein). Up to scales of order of some 100 Mpc the universe is obviously very clumpy and dominated by a hierarchical structure (our galaxy (0.03 Mpc), the local group (1-3 Mpc), the local supercluster (20-30 Mpc)). Deep red shift surveys like the 2dF Galaxy Redshift Survey show distinct structures like the great wall with dimension of $150\times 70\times 5$ Mpc. On scales larger than about 100 Mpc the cosmological principle, however, seems to be satisfied well. Further support comes from studies of the anisotropies of the Cosmic Microwave Background Radiation (CMBR), especially the data from the Wilkinson Microwave Anisotropy Probe WMAP. The data show (Lahav, 2000) that for scales larger than about $1000/H$ Mpc (H is the the Hubble constant in units of 100 km/s/Mpc) density fluctuations $\delta\rho/\rho$ are smaller than 10^{-4}. Thus the Robertson-Walker metric can be justified empirically for such large spatial scales. Theoretically one expects such a metric to result from some spatial averaging procedure (unfortunately such a rigorous averaging algorithm has not yet been worked out for Einstein's theory of gravity) and the question is what kind of signatures of this cosmic metric can be found locally, e.g., on solar-system scales.

The WMAP data just mentioned also contributes significantly to the present cosmological standard model. According to that model the age of our universe is about 13.7 billion years, the Hubble constant $H_0 = (71 \pm 4)$ km/s/Mpc and the total density parameter Ω that determines the global geometry of the universe is about 1, i.e. our universe is practically flat (which is also implied theoretically from the inflation scenario). More specifically the contribution to Ω from luminous matter is about 0.04, from dark matter 0.23 and from the vacuum energy 0.73.

2. RELATING THE BCRS WITH A COSMOLOGICAL METRIC

Due to the hierarchical structure of our cosmic neighbourhood one might extend the hierarchy of astronomical reference systems from the GCRS and the BCRS to some "GaCRS" (galactic celestial reference system), some "LoGrCRS" (local group celestial reference system) etc. In such a hierarchy each system will contain tidal forces due to effects from the external matter. Nevertheless, at a certain scale cosmologiocal effects can no longer be ignored and the expansion of the universe has to be taken into account.

Theoretically one faces the problem how to match a local metric such as the one defining the BCRS with the Robertson-Walker metric that describes the gravitational physics on large cosmic scales. As a first step in the present paper we considered the vacuum energy only. The vacuum energy can be described by a cosmological constant Λ. We started with the following ansatz for the local metric

$$\begin{aligned} g_{00} &= -1 + \frac{2}{c^2}\, w(t,\mathbf{x}) - \frac{2}{c^4}\, w^2(t,\mathbf{x}) + \mathcal{O}(c^{-5}), \\ g_{0i} &= -\frac{4}{c^3}\, w^i(t,\mathbf{x}) + \mathcal{O}(c^{-5}), \\ g_{ij} &= \delta_{ij}\left(1 + \frac{2}{c^2}\, w'(t,\mathbf{x})\right) + \mathcal{O}(c^{-4}). \end{aligned} \tag{6}$$

Since the constant Λ is very small ($\Lambda \approx 2 \cdot 10^{-52}\,\mathrm{m}^{-2}$) we neglect all terms $\mathcal{O}(\Lambda\, G)$ (G being the Newtonian gravitational constant). In this approximation and implying the gauge condition $w_{,t} + w^i{}_{,i} = \mathcal{O}(c^{-2})$ the field equations read

$$w_{,ii} - \frac{1}{c^2} w_{,tt} = -4\,\pi\, G\, \sigma + c^2\, \Lambda, \tag{7}$$

$$w^i{}_{,jj} = -4\,\pi\, G\, \sigma^i. \tag{8}$$

Denoting w_σ a potential satisfying

$$w_\sigma{}_{,ii} - \frac{1}{c^2} w_{\sigma,tt} = -4\,\pi\, G\, \sigma, \tag{9}$$

one gets

$$w = w_\sigma + \frac{1}{6}\, c^2\, \Lambda\, x^i\, x^i, \tag{10}$$

$$w' = w_\sigma - \frac{1}{12}\, c^2\, \Lambda\, x^i\, x^i. \tag{11}$$

Note that for positive values of Λ the vacuum yields a repulsive gravitational force. Potential w_σ denotes the contribution of ordinary solar system matter and the remaining terms describe the influence of the overall vacuum energy in the universe. In our local coordinates at this level of approximation the cosmological constant leads to a static cosmic tidal-like term that grows quadratically with coordinate distance r ($r^2 = x^i\, x^i$). Looking at orders of magnitude one finds that these cosmic tidal terms are completely negligible in the solar system (see also Cooperstock et al., 1998). Only at cosmic distances where the cosmic red shift are not negligible they play a role.

It is important to note that there exists a well-known exact solution of the Einstein field equations with cosmological term called the Schwarzschild-de Sitter solution:

$$ds^2 = -Ac^2 dT^2 + A^{-1} d\rho^2 + \rho^2(d\theta^2 + \sin^2\theta d\varphi^2), \tag{12}$$

$$A = 1 - \frac{2m}{\rho} - \frac{1}{3}\,\Lambda\,\rho^2, \tag{13}$$

where m is the Schwarzschild radius (normalized mass) of a spherically symmetric body embedded in the de Sitter universe with cosmological constant Λ. In the limit $\Lambda = 0$ this solution

coincides with the Schwarzschild solution in the Schwarzschild standard coordinates. In the limit $m = 0$ Eq. (12) describes the de Sitter cosmological solution (empty static universe with cosmological constant Λ). This well-known metric can be transformed into isotropic form which, neglecting terms of order $\mathcal{O}(m\,\Lambda)$, coincides with the metric (6) potentials with (10) for the case of a spherically symmetric mass distribution. On the other hand the same metric (12)–(13) can be transformed into the form (Robertson, 1928)

$$
\begin{aligned}
ds^2 &= g_{00}\,c^2\,dT^2 + g_{RR}\,d\mathbf{X}^2, && (14)\\
g_{00} &= -\left(\frac{1-\frac{m}{2\,a_\Lambda\,R}}{1+\frac{m}{2\,a_\Lambda\,R}}\right)^2, && (15)\\
g_{RR} &= a_\Lambda^2(T)\left(1+\frac{m}{2\,a_\Lambda\,R}\right)^4, && (16)\\
a_\Lambda(T) &= \exp\left(\sqrt{\frac{\Lambda}{3}}\,c\,T\right), && (17)
\end{aligned}
$$

which can be though of as a perturbed Fermi-Walker solution (5). This form of the metric can be used to match the BCRS metric (6) with (10) to the Robertson-Walker metric. Indeed, at the cosmic distances where the Λ terms in (10) play a role, the non-spherical part of the local potential w_σ and the local vector potential w^i can be neglected, and the rest can be directly matched to (14)–(17). This matching and further details will be published elsewhere.

The general Robertson-Walker metric (5) with arbitrary $a(T)$ can be also transformed in what we can call "local coordinates". Indeed, the transformation

$$
\begin{aligned}
t &= T + \frac{1}{2c^2}\,a\,\dot{a}^2\,R^2 + \mathcal{O}(R^4), && (18)\\
\mathbf{x} &= a(t)\,\mathbf{X}\left(1+\frac{1}{4\,c^2}\,\dot{a}^2\,R^2 + \mathcal{O}(R^4)\right) && (19)
\end{aligned}
$$

brings the metric (5) into the form

$$
ds^2 = \left(-1+\frac{1}{c^2}\,\frac{\ddot{a}}{a}\,R^2 + \mathcal{O}(R^4)\right)c^2\,dt^2 + \left(1+\frac{1}{2\,c^2}\,\left(\frac{\dot{a}}{a}\right)^2 R^2 + \mathcal{O}(R^4)\right)d\mathbf{x}^2. \qquad (20)
$$

The same procedure can be done to any order of R. In the limit of de Sitter universe the function $a(T)$ is defined by (17) and (20) coincides with the Schwarzschild-de Sitter metric and with the BCRS metric with Λ in the corresponding limits. The fact that local coordinates exist also for general Robertson-Walker metric fosters the hope that the BCRS can be also matched to the Robertson-Walker universe in the general case. Details will be published elsewhere.

We might finally ask about the contribution of visible and dark matter to the spacetime metric and formulate the 'Local Expansion Hypothesis': the cosmic expansion induced by ordinary (visible and dark) matter occurs on all length scales, i.e., also locally. The question whether this hypothesis is true or not has a long history and one must confess that this fundamental problem so far has no satisfying solution. If we forget about the Λ-term the famous Einstein-Strauss solution (Einstein, Strauss, 1945, Bonnor, 2000), where a pure static Schwarzschild solution without mass-energy inside of some spherical vacuole can be matched exactly to a global Robertson-Walker metric indicates that this hypothesis might be wrong. It has been argued that such a solution is unstable and cannot be generalized to situations of less symmetry but nevertheless the sign of warning is clear. This also indicates that the transition from the local metric to the

cosmic one cannot be studied by looking at a single spherically symmetric density inhomogeneity; one rather has to study theoretically a basically clumpy universe, defining some suitable spatial averaging procedure and then study the limit of larger and larger scales. Likely the inhomogeneity scale determined by the two-point correlation function will also theoretically indicate the validity of the cosmic Robertson-walker metric.

In conclusion let us summarize that if one is interested in cosmology, radial coordinates of remote objects (e.g., quasars) should be defined with respect to a metric which turns into a cosmological metric (e.g. the Robertson-Walker one) in the limit of very large barycentric distances. Several possibilities to construct such a metric have been sketched above. The implications of such a "local cosmological" metric on the processing of astrometrical data should be further investigated.

3. REFERENCES

W. Bonnor, Class.Quan.Grav. **17**, 2739 (2000)

F. Cooperstock, V. Faraoni, D. Vollick, Ap.J. **503**, 61 (1998)

A. Einstein, E. Straus, Rev.Mod.Phys. **17**, 120 (1945)

First Year Wilkinson Microwave Anisotropy Probe (WMAP) Observations; papers in: Ap.J.S., **148** (2003)

O. Lahav, Proc.of the NATO ASI, Isaac Newton Institute, Cambridge, July 1999; ed. R. Critenden, N. Turok; Kluwer

H.P. Robertson, Philosophical Magazine, 5, 835–848 (1928)

R.C. Tolman, *Relativity, Thermodynamics and Cosmology*, Clarendon Press, Oxford, 1934

S. Weinberg, Gravitation and Cosmology, Wiley (1972)

RELATIVISTIC INDIRECT THIRD–BODY PERTURBATIONS IN THE SMART EARTH'S ROTATION THEORY

V.A.BRUMBERG† and J.–L.SIMON‡

† Institute of Applied Astronomy
10, Kutuzov quay, 191187 St. Petersburg, Russia
e-mail: brumberg@quasar.ipa.nw.ru

‡ Institut de mécanique céleste et de calcul des éphémérides
77, av. Denfert–Rochereau, 75014 Paris, France
e-mail: Jean-Louis.Simon@imcce.fr

ABSTRACT. In neglecting by very small relativistic direct third–body perturbations it is possible to use formally Newtonian equations of the Earth's rotation in DGRSC, dynamically non–rotating geocentric ecliptical reference system with Terrestrial time TT as the time argument. To obtain relativistic indirect third–body perturbations in the SMART theory of the Earth's rotation one can use the relativistic formulae expressing the DGRSC position vectors referred to TT in terms of the VSOP BRSC (barycentric ecliptical reference system) position vectors referred to Barycentric dynamical time TDB. Then the right–hand members become functions of TT alone and one can use the standard SMART iteration techniques to obtain the relativistic contributions into three Euler angles relating ITRS and DGRSC.

1. INTRODUCTION

SMART97 (Bretagnon et al. 1997, 1998, 2003) represents the most accurate semi–analytical theory of rotation of the rigid Earth constructed so far. In the recent years Pierre Bretagnon, the principal author of this theory, was extending it for the case of the non–rigid Earth (Bretagnon 2002) using the transfer function of Mathews et al. (2002). SMART97 is a purely Newtonian theory. Bretagnon was going also to convert it into relativistic theory (Bretagnon and Brumberg 2003) but his death broke off this work. The aim of the present paper is to continue it.

One may find in literature relativistic equations of the Earth's equations of different type in dependence on adopted Earth's model (see Brumberg 1998; Klioner and Soffel 1998, 1999 and references therein). Instead of dealing with such complicated equations we prefer to start with by taking into account in SMART97 the relativistic indirect third–body perturbations as proposed by Bretagnon and Brumberg (2003). In doing so, we neglect by very small direct relativistic third–body perturbations. It enables us to retain the formally Newtonian differential equations of the Earth's rotation and to get the relativistic extension of SMART97 solution by applying in the right–hand members of these equations the four–dimensional transformation between geocentric and barycentric quantities. It leads to the main relativistic terms in the

Earth's rotation problem called by us the relativistic indirect third–body perturbations.

All expressions below are given in the post–Newtonian approximation within c^{-2} accuracy.

2. RS HIERARCHY

2.1 Barycentric and geocentric reference systems

We use below the hierarchy of relativistic reference systems (RSs) constructed in (Brumberg et al. 1996; Brumberg 1997; see also the detailed exposition by Bretagnon and Brumberg 2003) and illustrated by Fig. 1.

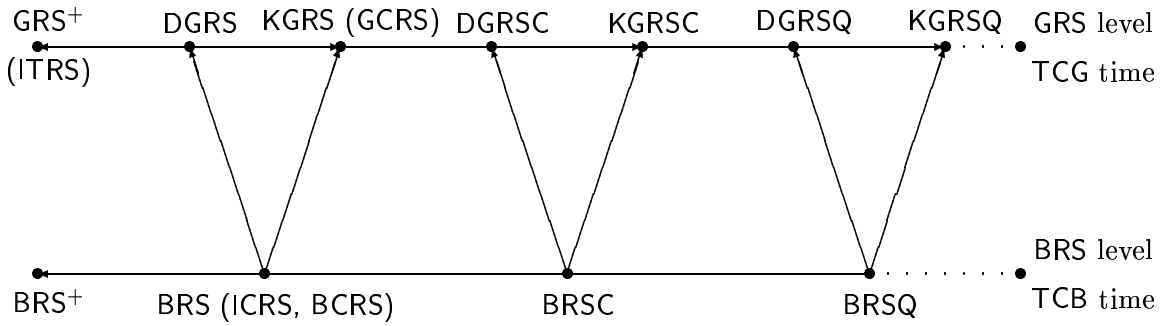

Figure 1: Barycentric and Geocentric Reference Systems (RSs)
B — barycentric, G — geocentric, C — ecliptical, Q — equatorial,
D — dynamical, K — kinematical, $^+$ — rotating (BBG, 1996);
ICRS — International Celestial RS, ITRS — International Terrestrial RS (IERS);
BCRS — Barycentric Celestial RS, GCRS — Geocentric Celestial RS (IAU 2000)

The four reference systems of the barycentric (B) level referred to the barycentric coordinate time t =TCB (or to TDB in practice) are related by means of

$$[\mathrm{BRS}^+] = P(t)[\mathrm{BRSC}] = P(t)P_C[\mathrm{BRS}] = P(t)P_C P_Q^T[\mathrm{BRSQ}]. \tag{1}$$

[ ] means here and below a triplet of the corresponding spatial coordinates.

The corresponding reference systems at the geocentric (G) level referred to the geocentric coordinate time u =TCG (or to TT in practice) are related by means of

$$[\mathrm{GRS}^+] = \hat{P}_1(u)[\mathrm{DGRSC}] = \hat{P}_1(u)P_C[\mathrm{DGRS}] = \hat{P}_1(u)P_C P_Q^T[\mathrm{DGRSQ}], \tag{2}$$

$$[\mathrm{GRS}^+] = \hat{P}_0(u)[\mathrm{KGRSC}] = \hat{P}_0(u)P_C[\mathrm{KGRS}] = \hat{P}_0(u)P_C P_Q^T[\mathrm{KGRSQ}]. \tag{3}$$

Kinematically (K) or dynamically (D) non–rotating GRSs are distinguished by subscript q, i.e. $q = 0$ for K versions and $q = 1$ for D versions. K and D versions of GRSs are related by means of

$$[\mathrm{KGRS}] = (E - c^{-2}F)[\mathrm{DGRS}], \qquad [\mathrm{KGRSC}] = (E - c^{-2}F_C)[\mathrm{DGRSC}],$$
$$[\mathrm{KGRSQ}] = (E - c^{-2}F_Q)[\mathrm{DGRSQ}] \tag{4}$$

and

$$\hat{P}_1(u) = \hat{P}_0(u)(E - c^{-2}F_C). \tag{5}$$

Here F stands for the geodetic rotation matrix (its expression vanishing for J2000.0 is given by Bretagnon and Brumberg 2003) whereas F_C and F_Q represents its analogues for the ecliptical (C) and equatorial (Q) GRSs, respectively, i.e.

$$F_C = P_C F P_C^T, \qquad F_Q = P_Q F P_Q^T. \tag{6}$$

The constant rotation matrices P_C, P_Q used in this paper are taken in accordance with DE403, i.e.

$$P_C = D_1(\varepsilon) D_3(\chi), \qquad P_Q = D_3(\chi) \tag{7}$$

where $\varepsilon = 23^\circ 26' 21.40928''$, $\chi = -0.05294''$. The slightly different values are proposed in (Bretagnon 2002; Bretagnon et al. 2003) for future analytical planetary ephemerides. The problem of consistency of the existing analytical and numerical planetary and lunar theories as well as of the Earth's rotation theory with the hierarchy of relativistic reference systems is not still completely solved.

Operations with rotation matrices are often replaced by operation with rotation vectors by using the relationships of the type

$$F^i = \tfrac{1}{2}\varepsilon_{ijk} F^{jk}, \qquad F^{ij} = \varepsilon_{ijk} F^k, \qquad \varepsilon_{ijk} = \tfrac{1}{2}(i-j)(j-k)(k-i). \tag{8}$$

$\hat{P}(u)$ represents the Earth's rotation matrix relating DGRSC and terrestrial matrix ITRS (designated here also as GRS$^+$). Since SMART97 is supposed to be constructed in DGRSC three Euler angles, $\underset{1}{\psi}$, $\underset{1}{\theta}$, $\underset{1}{\varphi}$, of matrix $\underset{1}{\hat{P}}(u)$ may be regarded as dynamical Earth orientation parameters (EOP). The analogous Euler angles $\underset{0}{\psi}$, $\underset{0}{\theta}$, $\underset{0}{\varphi}$, of matrix $\underset{0}{\hat{P}}(u)$ relating KGRSC and ITRS may be regarded as kinematical EOP. One has

$$\underset{q}{\hat{P}}(u) = D_3(\underset{q}{\varphi}) D_1(-\underset{q}{\theta}) D_3(-\underset{q}{\psi}) \qquad (q = 0,\ 1), \tag{9}$$

D_i being the elementary rotation matrices. The dynamical and kinematical Euler angles are related by the formulae

$$\underset{1}{\varphi} - \underset{0}{\varphi} = -\frac{c^{-2}}{\sin\theta}\left(F_C^1 \sin\psi + F_C^2 \cos\psi\right), \qquad \underset{1}{\theta} - \underset{0}{\theta} = c^{-2}\left(F_C^1 \cos\psi - F_C^2 \sin\psi\right),$$

$$\underset{1}{\psi} - \underset{0}{\psi} = c^{-2}\left[F_C^3 - \frac{\cos\theta}{\sin\theta}\left(F_C^1 \sin\psi + F_C^2 \cos\psi\right)\right] \tag{10}$$

(in the post–Newtonian approximation there is no need to distinguish between Newtonian and relativistic values in the relativistic right–hand members). These relationships have been actually used in SMART. In taking into account only the geodesic precession and nutation in narrow sense, one has $F_C^1 = F_C^2 = 0$ and, hence, $\underset{1}{\varphi} = \underset{0}{\varphi}$, $\underset{1}{\theta} = \underset{0}{\theta}$.

Note that to get the designations of the original papers on SMART (Bretagnon et al. 1997, 1998) one should put $\psi = -\psi$ and $\theta = -\omega$.

To complete the discussion of the RS hierarchy of Fig. 1 let us note that the Earth's rotation matrix relating GCRS and ITRS is determined in our notation as $T = \underset{0}{\hat{P}}(u) P_C$. The Earth's rotation in BRS may be described by the rotation matrix $P(t^*) = \underset{0}{\hat{P}}(u)$ where t^* is the solution of the relativistic time equation

$$u = t^* - c^{-2} A(t^*) \tag{11}$$

with the time function determined by

$$\dot{A}(t) = \tfrac{1}{2}\mathbf{v}_E^2 + \bar{U}_E(t, \mathbf{x}_E), \qquad \bar{U}_E(t, \mathbf{x}_E) = \sum_{A \neq E} \frac{GM_A}{r_{EA}} \tag{12}$$

with initial condition $A(t_0) = 0$, t_0 being the 1977 Origin (see the detailed discussion by Bretagnon and Brumberg 2003). However, rotating system BRS^+ is not used in practice.

2.2 Relativistic extension of SMART97 by using RS hierarchy

It is assumed that VSOP theories are constructed in BRSC with TDB as a time argument while SMART97 is considered in DGRSC with TT as a time argument. Therefore, in treating SMART in the relativistic framework the values of masses should be adequately adjusted taking into account that $(GM)_{\mathrm{TDB}}$ coefficients in VSOP and $(GM)_{\mathrm{TT}}$ coefficients in SMART are related by

$$(GM)_{\mathrm{TT}} = (1 + L_C)(GM)_{\mathrm{TDB}} \tag{13}$$

with the value of $L_C = 1.480826855667 \times 10^{-8}$ obtained with the VSOP solution (Bretagnon and Brumberg 2003). But this mass–adjustment is not made in the present work aimed to evaluate the influence of the relativistic indirect third–body perturbations. Indeed, the main perturbation factors in the right–hand members of the DGRSC equations of the Earth's rotation, are due to the action of the Sun (S) and the Moon (L). Initially, these right–hand members contain geocentric position vectors $\mathbf{w}_A$ for $A = S, L$. As proposed in (Bretagnon and Brumberg 2003) these geocentric vectors are to be expressed by virtue of BRSC↔DGRSC transformation in terms of BRSC quantities as follows:

$$w^i_A(u) = z^i_A(u) - z^i_E(u) + c^{-2}\big[\Lambda^i(t^*, \vec{r}_{AE}) + \mathbf{v}_E \mathbf{r}_{AE} v^i_{AE}\big], \tag{14}$$

with $\mathbf{x}_E$, $\mathbf{v}_E$, $\mathbf{x}_A$, $\mathbf{v}_A$ denoting BRSC coordinates and velocities of the Earth and the disturbing body, respectively, $\mathbf{r}_{AE} = \mathbf{x}_A - \mathbf{x}_E$, $\mathbf{v}_{AE} = \vec{v}_A - \mathbf{v}_E$ and

$$\Lambda^i(t, \mathbf{r}_{AE}) = \tfrac{1}{2}\mathbf{v}_E \mathbf{r}_{AE} v^i_E - q\varepsilon_{ijk} F^j r^k_{AE} + \bar{U}_E(t, \mathbf{x}_E) r^i_{AE} + \mathbf{a}_E \mathbf{r}_{AE} r^i_{AE} - \tfrac{1}{2}\mathbf{r}^2_{AE} a^i_E\,, \tag{15}$$

$\mathbf{a}_E$ being BRSC acceleration of the Earth. The moment t^* means here

$$\mathrm{TDB}^* = \mathrm{TT} + c^{-2} A_p \tag{16}$$

if time function $A(t)$ is represented in TDB as

$$A(t) = c^2 L_C t + A_p(t). \tag{17}$$

The function z^i_E representing the BRSC position of the Earth in terms of TCG or TT is given in our case by

$$(1 - L_C) z^i_E(\mathrm{TT}) = x^i_E(\mathrm{TDB}^*) = x^i_E(\mathrm{TT}) + c^{-2} A_p v^i_E + \ldots\,. \tag{18}$$

The function z^i_A is determined by the same formula by replacing E for A. The power–trigonometric time series for all functions occurring here are tabulated in (Bretagnon and Brumberg 2003).

Functions $x^i_E(\mathrm{TT})$, $x^i_A(\mathrm{TT})$ represent just VSOP series of the argument TDB taken for the moment TT. Therefore, they are expressed in terms of 11 fundamental arguments (mean longitudes of eight major planets and Delaunay arguments D, F, l of the lunar theory) representing now linear functions of TT. One more fundamental argument ϕ (the linear part of the expression for the Euler angle φ) is specific for SMART solution. In such a way, the right–hand members of the DGRSC equation of the Earth's rotation become functions of TT and may be solved by iterations just in Newtonian case (Bretagnon et al. 1997, 1998). In result we get the solution taking into account relativistic indirect third–body perturbations. Based on the dynamical solution for $\underset{1}{\psi}$, $\underset{1}{\theta}$, $\underset{1}{\varphi}$ one finds by means of (10) the kinematical solution $\underset{0}{\psi}$, $\underset{0}{\theta}$, $\underset{0}{\varphi}$ and then the astrometric Earth's rotation matrix $T = \underset{0}{\hat{P}}(u) P_C$ including now the main relativistic corrections.

3. RIGHT–HAND MEMBERS

Computation of the right–hand members of the Earth's rotation equations in the SMART theory (Bretagnon et al. 1997, 1998) is based on the VSOP series for $\mathbf{x}_{(C)A}(\mathrm{TDB})$ where (C) indicates

the ecliptical system BRSC and A stands for the body A ($A = E$ for the Earth, $A = S$ for the Sun, $A = L$ for the Moon, etc.). In the original SMART theory referred to TDB the geocentric coordinates of the Sun and the Moon in DGRSC are treated just as the differences of the corresponding BRSC coordinates $\mathbf{x}_{(C)S} - \mathbf{x}_{(C)E}$ and $\mathbf{x}_{(C)L} - \mathbf{x}_{(C)E}$ referred to TDB. In the present work the equations of the Earth's rotation are referred to TT with using $\mathbf{w}_{(C)A}$(TT) for the geocentric coordinates of the Sun ($A = S$) and the Moon ($A = L$). Considering the smallness of the planetary perturbations in the Earth's rotation problem all disturbing planets may be treated just as in the Newtonian case, i.e. by putting $\mathbf{w}_{(C)A}(\mathrm{TT}) \approx \mathbf{x}_{(C)A}(\mathrm{TDB}) - \mathbf{x}_{(C)A}(\mathrm{TDB})$ and TT≈TDB.

Starting from the VSOP values $\mathbf{x}_{(C)A}$(TDB) for $A = E$, S, L and the ICRS coordinates of the Earth $\mathbf{z}_E$(TT) resulted from the data of (Bretagnon and Brumberg 2003) we compute successively the series for the solar BRSC coordinates $\mathbf{z}_{(C)S}$(TT), for the lunar BRSC coordinates $\mathbf{x}_{(C)L}(\mathrm{TDB}) - \mathbf{x}_{(C)E}(\mathrm{TDB})$ and $\mathbf{z}_{(C)L}(\mathrm{TT}) - \mathbf{z}_{(C)E}(\mathrm{TT})$, and finally for the solar DGRSC geocentric coordinates $\mathbf{w}_{(C)S}$(TT) and for the lunar DGRSC geocentric coordinates $\mathbf{w}_{(C)L}$(TT). All series are presented in the compact form adopted presently in VSOP, i.e.

$$x^i_A(t) = \sum_\alpha t^\alpha \left[\sum_k X^\alpha_{ik} \cos(\psi^\alpha_k + \nu^\alpha_k\, t) \right] \tag{19}$$

The time argument t is in fact either TDB or TT. The fundamental trigonometric arguments of the semi–analytical SMART series are given in Appendix A.

4. FINAL EXPANSIONS

Having got the relativistic coordinates $\mathbf{w}_{(C)A}$(TT) ($A = S$, L) we perform iterations as described in (Bretagnon et al. 1997, 1998) to obtain the solution with taking into account the main relativistic indirect third–body perturbations. This solution is compared with the Newtonian SMART solution based on the Newtonian luni–solar coordinates $\mathbf{x}_{(C)A}(\mathrm{TDB}) - \mathbf{x}_{(C)E}(\mathrm{TDB})$ ($A = S$, L). Since in the Newtonian theory there is no difference between TT and TDB we may just compare the coefficients of the series (19) for both solutions. The differences between the dynamical Euler angles $\underset{1}{\psi}$, $\underset{1}{\theta}$, $\underset{1}{\varphi}$ (relating ITRS and DGRSC) in the Newtonian (N) and relativistic solutions demonstrate the influence of the indirect relativistic third–body perturbations. The dynamical Euler angles for both (Newtonian and relativistic) versions are converted by means of (10) into the kinematical Euler angles $\underset{0}{\psi}$, $\underset{0}{\theta}$, $\underset{0}{\varphi}$ (relating ITRS and KGRSC) also for the Newtonian (N) and relativistic solutions. The differences between the dynamical and kinematical Euler angles for the relativistic solution (evidently, within the post–Newtonian approximation the similar differences for the Newtonian version are practically the same) exposed in Appendix B (Tables (1)–(3)) improve the corresponding values given in (Bretagnon et al. 1997). The differences between the kinematical Euler angles in the Newtonian and relativistic solutions (Tables (4)–(6) of Appendix B) differ only slightly from the corresponding differences between the dynamical angles (this discrepancy reveals only in terms of the third and higher power of time). For the sake of completeness, we reproduce also the series for the geodesic rotation vector $\mathbf{F}_C$ (Tables (7)–(9) of Appendix B).

Let us note once again that the Newtonian and relativistic SMART solutions are distinguished just with respect to the employed luni–solar coordinates as stated above. When converting from DGRSC to KGRSC both these solutions are transformed practically in the same manner as prescribed by the geodesic rotation (10). Newtonian solutions in DGRSC and KGRSC are differ by relativistic terms caused by the mutual rotation of reference systems not affecting the Newtonian nature of the solution itself.

The final expansions show that the differences in the Euler angles for the Newtonian and relativistic solutions are of the order of 35 μas over 20 yrs (cf. the precision of SMART97 of 2 μas) and 150 μas over 100 yrs (cf. the precision of SMART97 of 12 μas). Therefore, the relativistic indirect third–body perturbations found here are within the accuracy of SMART97 theory and may be used to improve this theory.

5. OPEN QUESTIONS

Before concluding this paper we would like to mention some points of possible confusion due to the lack of rigorous astronomical definitions.

1. The main astronomical reference systems ICRS and GCRS being now well defined (IAU 2001) it is necessary that the orientation of the reference systems underlying the existing ephemerides such as DE, LE, EPM, VSOP, ELP, SMART, etc., be rigorously related with these fundamental RSs. The constant rotation matrices P_C, P_Q relating ICRS with BRSC and BRSQ, respectively, just illustrate the adjustment of the VSOP RS (BRSC) to ICRS.

2. The geodesic rotation vector $\mathbf{F}$ is given by its first order derivative (see, e.g., Bretagnon and Brumberg 2003) but no one IAU resolution specifies the arbitrary constant involved in integrating this equation. In our work we imply the condition $\mathbf{F} = 0$ for J2000.0 as suggested in (Bretagnon and Brumberg 2003).

3. In spite of the IAU definition of the epoch J2000.0 with respect to TT the existing planetery and lunar theories often make use of the epoch J2000.0 with respect to TDB.

4. The use of AS (astronomical system of units) in BRS and GRS needs to be specified as well. In using 'practical' time scales TDB (or else $\mathrm{T_{eph}}$) and TT instead of 'theoretical' time scales TCB and TCG one has to deal with the scaling factors $(1 - L_B)$ and $(1 - L_G)$ for the coordinates $\mathbf{x}$, $\mathbf{w}$ and mass–coefficients GM, $G\hat{M}$ in BRS and GRS, respectively (Brumberg et al. 1998). L_G is now fixed by the IAU Resolution B1 (2000) as a defining constant. By contrast, L_B and L_C related by means of $1 - L_B = (1 - L_C)(1 - L_G)$ depend on specific planetary theories. Within the currently employed approximation $M = \hat{M}$ one has (13). The AS unit of time $d = 1\,\mathrm{day} = 86400s$ is defined directly by its relationship to the SI unit of time. The AS unit of mass is defined as the mass of the Sun M_S. The AS unit of length AU is defined by the condition $k = \sqrt{G} = 0.01720209895$ provided that the units of measurement are d, M_S and AU. This definion involves the relationship with the SI unit of length

$$AU = \left(\frac{GM_S d^2}{k^2}\right)^{1/3} . \tag{20}$$

in form $1\,AU = \chi$ m. The defining relation (20) results from the Kepler's third law in standard designations $n^2a^3 = GM_S$. To distinguish between TDB and TCB values let us mark TDB values by the asterisk *. One has (in SI units)

$$a^* = (1 - L_B)a\,, \qquad v^* = v\,, \qquad (GM_S)^* = (1 - L_B)(GM_S), \qquad n^* = (1 - L_B)^{-1}n \tag{21}$$

with the third Kepler's law $n^{*2}a^{*3} = (GM_S)^*$. In astronomical units there results

$$n^2a^3 = GM_S\,\chi^3\,, \qquad n^{*2}a^{*3} = (GM_S)^*\,\chi^{*3} \tag{22}$$

where $1(AU)_{\mathrm{TDB}} = \chi^*$ m. Hence,

$$\left(\frac{\chi^*}{\chi}\right)^3 = \left(\frac{n^*}{n}\right)^2 \left(\frac{a^*}{a}\right)^3 \frac{M_S}{M_S^*}\,. \tag{23}$$

Therefore, the standard AS values $d = 1$ day, $M_S = 1$, $AU = 1$ correspond to BRS with TCB. When using BRS with TDB there results $d^* = (1 - L_B)d = (1 - L_B)$ day and one has to choose between two currently used options.

First option:

$$M_S^* = (1 - L_B)M_S = (1 - L_B)\,, \qquad AU^* = (1 - L_B)AU = (1 - L_B)\,, \qquad \chi^* = \chi \tag{24}$$

(the unit of mass $= (1 - L_B)$ solar mass of AS TCB, the unit of length $= (1 - L_B)$ astronomical units of length of AS TCB, all formulae (21) are valid both in SI and AS units, the same numerical value of the AS unit of length in m both for TDB and TCB).

Second option (based on E.M.Standish comments at the GA IAU 2003):

$$M_S^* = M_S = 1\,, \qquad AU^* = AU = 1\,, \qquad \chi^* = (1 - L_B)^{1/3}\,\chi \tag{25}$$

resulting to

$$\frac{a^*}{\chi^*} = (1 - L_B)^{2/3}\,\frac{a}{\chi}\,, \qquad \frac{v^*}{\chi^*} = (1 - L_B)^{-1/3}\,\frac{v}{\chi} \tag{26}$$

or just

$$a^* = (1 - L_B)^{2/3}\,a\ [\mathrm{AU}], \qquad v^* = (1 - L_B)^{-1/3}\,v\ [\mathrm{AU/day}] \tag{27}$$

(the unit of mass $= 1$ solar mass of AS TCB, the unit of length $= 1$ astronomical units of length of AS TCB, formulae (21) are valid only in SI units to be replaced by (27) in AS units, the same numerical value of the heliocentric constant GM_S in SI units both for TDB and TCB).

6. CONCLUSION

The relativistic indirect third–body perturbations considered in this paper contribute within 35μas accuracy in the Euler angles determining the Earth orientation parameters (relating ITRS with DGRSC or KGRSC). Therefore, they are indeed of practical importance for the SMART solution. Using the formalism of (Bretagnon and Brumberg 2003) it is possible to compute the rotation vector $\mathbf{A}$ of GCRS→ITRS transformation for the Newtonian and relativistic SMART solutions and to find explicitly the relativistic contributions in the components of this vector. Denoting the triplet of the ITRS spatial coordinates by $\mathbf{y}$ we may represent the GCRS→ITRS in form

$$\mathbf{y} = T\,\underset{0}{\mathbf{w}} \tag{28}$$

$$T = \underset{0}{\hat{P}}(u)P_C\,. \tag{29}$$

or

$$T = D_3(\underset{0}{\varphi})D_1(-\underset{0}{\theta})D_3(-\underset{0}{\psi})D_1(\varepsilon)D_3(\chi)\,. \tag{30}$$

Introducing the rotation vector A one may use the rotation formula

$$T = R(\mathbf{A}), \qquad R(\mathbf{A})\mathbf{x} = \mathbf{x} - \sin a(\hat{\mathbf{A}} \times \mathbf{x}) + (1 - \cos a)[\hat{\mathbf{A}} \times (\hat{\mathbf{A}} \times \mathbf{x})] \tag{31}$$

where $a = |\mathbf{A}|$ is the rotation angle, $\hat{\mathbf{A}} = \mathbf{A}/a$ is the unit vector along the rotation axis, $\mathbf{x}$ is an arbitrary coordinate vector. Vector A is given in (Bretagnon and Brumberg 2003) in three forms corresponding to 'dynamical' representation with three Euler angles, 'classical kinematical' representation (precession/nutation, diurnal rotation and polar motion) and modern 'kinematical' representation involving the non–rotating origin. The first representation in terms of $\underset{0}{\psi}$, $\underset{0}{\theta}$, $\underset{0}{\varphi}$ is most closely related with the SMART solution. Evaluating the variation $\delta\mathbf{A}$ between the relativistic and Newtonian values of $\mathbf{A}$ one may find the influence of the relativistic terms on

the GCRS→ITRS transformation (see (A.24), (A.25) in Bretagnon and Brumberg 2003). This work is now in progress.

Numerical values exposed in this paper are given mainly for the illustration purposes. The complete expansions involved in the Newtonian and relativistic SMART solutions may be available in the electronic form by request to the second author .

7. REFERENCES

Bretagnon, P.: 2002, *Trans. Inst. Appl. Astron.* **8**, 33

Bretagnon, P. and Francou, G.: 1988, *Astron. Astrophys.* **202**, 309

Bretagnon, P. and Brumberg, V.A.: 2003, *Astron. Astrophys.* **408**, 387

Bretagnon, P., Rocher, P., and Simon, J.L.: 1997, *Astron. Astrophys.* **319**, 305

Bretagnon, P., Francou, G., Rocher, P., and Simon, J.L.: 1998,*Astron. Astrophys.* **329**, 329

Bretagnon, P., Fienga, A., and Simon, J.-L.: 2003, *Astron. Astrophys.* **400**, 785

Brumberg, V.A.: 1991, *Essential Relativistic Celestial Mechanics*, Hilger, Bristol

Brumberg, V.A.: 1996, In: N.Capitaine, B.Kolaczek, and S.Debarbat (eds.), *Earth Rotation, ReferenceSystems in Geodynamics and Solar System* (Journées 1995), Warsaw, 29

Brumberg, V.A.: 1997, In: I.M.Wytrzyszczak, J.H.Lieske, and R.A.Feldman (eds.), *Dynamics and Astrometryof Natural and Artificial Celestial Bodies*, Kluwer, 439

Brumberg, V.A.: 1998, *Trans. Inst. Appl. Astron.* **3**, 152 (in Russian)

Brumberg, V.A., Bretagnon, P. and Guinot, B.: 1996, *Celes. Mech. & Dyn. Astron.* **64**, 231

Brumberg, V.A., Bretagnon, P., Capitaine, N. et al.: 1998, In: J.Anderson (ed.), *Highlights of Astronomy*, **11A**, 194

IAU: 2001, *IAU Information Bull.* **88**, 28 (Errata: ibid., **89**, 4, 2001).

Klioner S.A. and Soffel M. 1998, In: J.Andersen (ed.)*Highlights of Astronomy* **11A**, 173

Klioner S.A. and Soffel M. 1999, In: J.Henrard and S.Ferraz–Mello (eds.), *Impact ofModern Dynamics in Astronomy*, Kluwer, 435

Mathews, P.M., Herring, T.A., and Buffet, B.A.: 2002, *J. Geophys. Res.* **107**, B4

APPENDIX

A. Fundamental arguments

As stated above, the expansions of the present paper have 12 trigonometrical arguments as follows:

$$
\begin{aligned}
\lambda_1(t) &= 4.40260867435 + 26087.9031415742\,t\,,\\
\lambda_2(t) &= 3.17614652884 + 10213.2855462110\,t\,,\\
\lambda_3(t) &= 1.75347029148 + 6283.0758511455\,t\,,\\
\lambda_4(t) &= 6.20347594486 + 3340.6124266998\,t\,,\\
\lambda_5(t) &= 0.59954632934 + 529.6909650946\,t\,,\\
\lambda_6(t) &= 0.87401658845 + 213.2990954380\,t\,,\\
\lambda_7(t) &= 5.48129370354 + 74.7815985673\,t\,,\\
\lambda_8(t) &= 5.31188611871 + 38.1330356378\,t\,,\\
D(t) &= 5.19846640063 + 77713.7714481804\,t\,,\\
F(t) &= 1.62790513602 + 84334.6615717837\,t\,,\\
l(t) &= 2.35555563875 + 83286.9142477147\,t\,,\\
\phi(u) &= 4.89496121282 + 2301216.7536515365\,u\,.
\end{aligned}
$$

The mean longitudes of eight major planets $\lambda_i(t)$ are referred to ICRS (to the reference system of of DE403 in practice). Therefore, their constant parts are those given in (Bretagnon et al. 1998). Their frequencies are also issued from (Bretagnon et al. 1998) but without taking into account the precession. The Delaunay arguments $D(t)$, $F(t)$, $l(t)$ of the lunar theory are taken from (Bretagnon et al. 1998). Originally, these arguments are functions of t =TDB but in accordance with (18) they are used here just as the linear functions of u =TT. The last argument, $\phi(u)$, representing the linear part of the Euler angle φ of the Earth's rotation is taken from (Bretagnon et al. 1998) as well. All values here and below are given using the astronomical unit as the unit of length (1 AU=149597870.691 km as in DE403) and 1000 Julian years (365250 Julian days) as the unit of time (tjy).

B. Final expansions

This Appendix contains the initial terms of the final series described in Section 4. All series are presented in form of (19). The data in the 6–column Tables 1–9 read: ordinal number of the term, components of the trigonometric argument (mean longitudes of eight major planets from Mercury to Neptune, arguments D, F, l of the lunar theory and the Earth's rotation angle ϕ) given to show the physical meaning of the term, coefficient X, the phase angle ψ of the argument, the frequency ν of the argument and exposant α of power of t. The time argument t is either TDB or TT as indicated explicitly. The negative components of the trigonometric arguments are underlined. The coefficients of the series in Tables 1–6 are given in radians. The coefficients of the series in Tables 7-9 for $\mathbf{F}_C$ are given in arcseconds to facilitate their comparison with our previous results and the results of other authors. The coefficient of the term No. 11 in Table 9 corresponds to geodesic precession. The truncation level is 0.1E-11 over 1000 yrs in Tables 1–3, 0.5E-11 over 100 yrs or 0.1E-9 over 1000 yrs in Tables 4–6, and 0.1E-7 arcsecond over 1000 yrs in Tables 7–9.

Table 1. Differences $\underset{1}{\psi} - \underset{0}{\psi}$ (TT) (GRSC)

1	001000000000	.742300349 − 09	.466926087 + 01	.628307585 + 04	0
2	000000000000	.397739929 − 10	.000000000 + 00	.000000000 + 00	0
3	001000001$\underline{1}$00	.145708061 − 10	.252987892 + 01	.337814272 + 03	0
4	002000000000	.930524508 − 11	.462564700 + 01	.125661517 + 05	0
5	00002$\underline{5}$000000	.203878362 − 11	.709948865 + 00	.711354700 + 01	0
6	000000000000	.930785387 − 04	.000000000 + 00	.000000000 + 00	1
7	001000000000	.474945452 − 10	.260332598 + 01	.628307585 + 04	1
8	001000001$\underline{1}$00	.355965693 − 11	.960586737 + 00	.337814272 + 03	1
9	002000000000	.116661765 − 11	.259734787 + 01	.125661517 + 05	1
10	000000000000	.244280065 − 06	.314159265 + 01	.000000000 + 00	2
11	001000001$\underline{1}$00	.299152471 − 10	.417657693 + 01	.337814272 + 03	2
12	001000000000	.203316536 − 11	.956674751 + 00	.628307585 + 04	2
13	002000000000	.172295028 − 11	.340748453 + 01	.125661517 + 05	2
14	000000000000	.365594907 − 08	.314159265 + 01	.000000000 + 00	3
15	001000001$\underline{1}$00	.117386023 − 10	.261099272 + 01	.337814272 + 03	3
16	002000000000	.121017860 − 11	.500979962 + 01	.125661517 + 05	3
17	000000000000	.579411556 − 08	.000000000 + 00	.000000000 + 00	4
18	001000001$\underline{1}$00	.269183168 − 11	.106628445 + 01	.337814272 + 03	4
19	000000000000	.388062532 − 10	.314159265 + 01	.000000000 + 00	5
20	000000000000	.247036977 − 10	.314159265 + 01	.000000000 + 00	6

Table 2. Differences $\underset{1}{\theta} - \underset{0}{\theta}$ (TT) (GRSC)

1	001000001$\underline{1}$00	.631723382 − 11	.410068897 + 01	.337814272 + 03	0
2	000000000000	.322968763 − 11	.000000000 + 00	.000000000 + 00	0
3	00002$\underline{5}$000000	.957304138 − 12	.524343393 + 01	.711354700 + 01	0
4	000000000000	.473867892 − 10	.000000000 + 00	.000000000 + 00	1
5	001000001$\underline{1}$00	.154310985 − 11	.252997314 + 01	.337814272 + 03	1
6	000000000000	.947355383 − 08	.000000000 + 00	.000000000 + 00	2
7	001000001$\underline{1}$00	.883496788 − 11	.569290077 + 01	.337814272 + 03	2
8	000000000000	.228920555 − 07	.314159265 + 01	.000000000 + 00	3
9	001000001$\underline{1}$00	.216768803 − 11	.418750886 + 01	.337814272 + 03	3
10	000000000000	.653596505 − 10	.314159265 + 01	.000000000 + 00	4
11	000000000000	.184605964 − 09	.000000000 + 00	.000000000 + 00	5
12	000000000000	.179171613 − 11	.314159265 + 01	.000000000 + 00	6

Table 3. Differences $\underset{0}{\varphi} - \underset{1}{\varphi}$ (TT) (GRSC)

1	001000001$\underline{1}$00	.158810048 − 10	.567147813 + 01	.337814272 + 03	0
2	000000000000	.103746803 − 10	.314159265 + 01	.000000000 + 00	0
3	00002$\underline{5}$000000	.213211607 − 11	.376137398 + 01	.711354700 + 01	0
4	000000000000	.191527491 − 10	.000000000 + 00	.000000000 + 00	1
5	001000000000	.423492232 − 11	.466929724 + 01	.628307585 + 04	1
6	001000001$\underline{1}$00	.387872333 − 11	.409816916 + 01	.337814272 + 03	1
7	000000000000	.265537808 − 06	.000000000 + 00	.000000000 + 00	2
8	001000001$\underline{1}$00	.274735254 − 10	.104917664 + 01	.337814272 + 03	2
9	002000000000	.164479145 − 11	.278147098 + 00	.125661517 + 05	2
10	000000000000	.388849875 − 08	.000000000 + 00	.000000000 + 00	3
11	001000001$\underline{1}$00	.115340467 − 10	.575444761 + 01	.337814272 + 03	3
12	002000000000	.116412840 − 11	.185998408 + 01	.125661517 + 05	3
13	000000000000	.631104235 − 08	.314159265 + 01	.000000000 + 00	4
14	001000001$\underline{1}$00	.265593077 − 11	.420628407 + 01	.337814272 + 03	4
15	000000000000	.380544861 − 10	.000000000 + 00	.000000000 + 00	5
16	000000000000	.267916561 − 10	.000000000 + 00	.000000000 + 00	6

Table 4. Differences $\underset{0}{\psi_N} - \underset{0}{\psi}$ (TT) (KGRSC)

1	00 1 000001$\underline{1}$00	.231266586 − 10	.252922703 + 01	.337814272 + 03	0
2	0010$\underline{19}$03000000	.759550646 − 11	.284970036 + 01	.980309527 + 00	0
3	00 1 000001$\underline{1}$00	.780322332 − 08	.959162770 + 00	.337814272 + 03	1
4	00 2 000000000	.115291472 − 08	.365346519 + 00	.125661517 + 05	1
5	00 2 000002000	.199920367 − 09	.447910095 + 01	.167993695 + 06	1
6	00 2 000002$\underline{2}$00	.188795275 − 09	.191827564 + 01	.675628545 + 03	1
7	00 1 000001$\underline{1}$00	.190446025 − 08	.568655793 + 01	.337814272 + 03	2
8	00 2 000000000	.562966495 − 09	.194262028 + 01	.125661517 + 05	2
9	00 0 000000000	.117110967 − 09	.000000000 + 00	.000000000 + 00	2
10	00 0 000000000	.382641250 − 09	.314159265 + 01	.000000000 + 00	3
11	00 1 000001$\underline{1}$00	.234166521 − 09	.420126686 + 01	.337814272 + 03	3
12	00 2 000000000	.137527571 − 09	.352339649 + 01	.125661517 + 05	3
13	00 0 000000000	.250403635 − 08	.000000000 + 00	.000000000 + 00	4

Table 5. Differences $\underset{0}{\theta}_N - \underset{0}{\theta}$ (TT) (KGRSC)

1	001000001100	.123517565 − 10	.410001583 + 01	.337814272 + 03	0
2	001000001100	.416734462 − 08	.252995484 + 01	.337814272 + 03	1
3	002000000000	.499381069 − 09	.507773508 + 01	.125661517 + 05	1
4	001000001100	.101645481 − 08	.965285401 + 00	.337814272 + 03	2
5	000000000000	.323583375 − 09	.314159265 + 01	.000000000 + 00	2
6	002000000000	.243819609 − 09	.373329495 + 00	.125661517 + 05	2
7	000000000000	.859605900 − 08	.314159265 + 01	.000000000 + 00	3
8	001000001100	.124723404 − 09	.577801150 + 01	.337814272 + 03	3

Table 6. Differences $\underset{0}{\varphi} - \underset{0}{\varphi}_N$ (TT) (KGRSC)

1	00 1 000001100	.212112060 − 10	.567081957 + 01	.337814272 + 03	0
2	0010190300000	.265955171 − 11	.625381360 + 00	.980309527 + 00	0
3	00 1 000001100	.715812097 − 08	.410075543 + 01	.337814272 + 03	1
4	00 2 000000000	.105778263 − 08	.350693917 + 01	.125661517 + 05	1
5	00 2 000002000	.183423115 − 09	.133750830 + 01	.167993695 + 06	1
6	00 2 000002200	.173274092 − 09	.505986832 + 01	.675628545 + 03	1
7	00 1 000001100	.174700634 − 08	.254497058 + 01	.337814272 + 03	2
8	00 2 000000000	.516512839 − 09	.508421183 + 01	.125661517 + 05	2
9	00 0 000000000	.107461963 − 09	.314159265 + 01	.000000000 + 00	2
10	00 0 000000000	.340588092 − 09	.000000000 + 00	.000000000 + 00	3
11	00 1 000001100	.214853535 − 09	.105831374 + 01	.337814272 + 03	3
12	00 2 000000000	.126190931 − 09	.381968078 + 00	.125661517 + 05	3
13	00 0 000000000	.250626807 − 08	.314159265 + 01	.000000000 + 00	4

Table 7. $c^{-2}F_C^1$(TT) (GRSC) (coefficients in arcseconds)

1	00 1000001100	.130302301 − 05	.410074370 + 01	.337814272 + 03	0
2	00 0000000000	.666116309 − 06	.000000000 + 00	.000000000 + 00	0
3	00 0025000000	.197458153 − 06	.524343393 + 01	.711354700 + 01	0
4	0813000000000	.335755401 − 07	.214693239 + 01	.262983048 + 02	0
5	03 5000000000	.274317722 − 07	.418857071 + 01	.775522617 + 03	0
6	00 1000000100	.213556899 − 07	.338135431 + 01	.906177374 + 05	0
7	00 1000000100	.155700142 − 07	.615764243 + 01	.780515857 + 05	0
8	00 0020000000	.113693032 − 07	.572693663 + 01	.105938193 + 04	0
9	00 0000000000	.956621901 − 05	.000000000 + 00	.000000000 + 00	1
10	00 1000000000	.311750820 − 07	.466912341 + 01	.628307585 + 04	1
11	00 0000000000	.195442531 − 02	.000000000 + 00	.000000000 + 00	2
12	00 1000000000	.137268118 − 07	.454103182 + 01	.628307585 + 04	2
13	00 0000000000	.601796456 − 03	.000000000 + 00	.000000000 + 00	3
14	10 0000000000	.520765790 − 05	.314159265 + 01	.000000000 + 00	4
15	10 0000000000	.192780654 − 06	.314159265 + 01	.000000000 + 00	5

Table 8. $c^{-2}F_C^2$(TT) (GRSC) (coefficients in arcseconds)

1	00	1000001100	.130305083 − 05	.567154555 + 01	.337814272 + 03	0
2	00	0000000000	.851215459 − 06	.314159265 + 01	.000000000 + 00	0
3	00	0025000000	.174934562 − 06	.376137398 + 01	.711354700 + 01	0
4	0813000000000		.326128037 − 07	.373005969 + 01	.262983048 + 02	0
5	03	5000000000	.267920049 − 07	.260932664 + 01	.775522617 + 03	0
6	00	1000000100	.213538259 − 07	.181060019 + 01	.906177374 + 05	0
7	00	1000000100	.155685742 − 07	.144520895 + 01	.780515857 + 05	0
8	00	0020000000	.114422842 − 07	.415710213 + 01	.105938193 + 04	0
9	00	0000000000	.140865733 − 05	.000000000 + 00	.000000000 + 00	1
10	00	1000000000	.347458181 − 06	.466925775 + 01	.628307585 + 04	1
11	00	0025000000	.129546311 − 07	.461641251 + 01	.711354700 + 01	1
12	00	0000000000	.217843218 − 01	.000000000 + 00	.000000000 + 00	2
13	00	1000000000	.232329482 − 07	.252863427 + 01	.628307585 + 04	2
14	00	0000000000	.158568418 − 03	.314159265 + 01	.000000000 + 00	3
15	10	0000000000	.121552283 − 04	.314159265 + 01	.000000000 + 00	4
16	10	0000000000	.105689498 − 06	.000000000 + 00	.000000000 + 00	5

Table 9. $c^{-2}F_C^3$(TT) (GRSC) (coefficients in arcseconds)

1	001000000000	.153110555 − 03	.466926126 + 01	.628307585 + 04	0
2	000000000000	.624062608 − 05	.000000000 + 00	.000000000 + 00	0
3	002000000000	.191850004 − 05	.462609811 + 01	.125661517 + 05	0
4	000000001000	.371707163 − 06	.486077422 + 00	.777137714 + 05	0
5	004830000000	.174492597 − 06	.283203731 + 01	.352311373 + 01	0
6	001010000000	.207986602 − 06	.585127088 + 01	.575338489 + 04	0
7	022000000000	.127215510 − 06	.441820021 + 01	.786041939 + 04	0
8	011000000000	.912767135 − 07	.613529387 + 01	.393020970 + 04	0
9	001001000000	.788781114 − 07	.559096259 + 01	.606977676 + 04	0
10	001200000000	.531395177 − 07	.358258491 + 01	.398149002 + 03	0
11	000000000000	.191988304 + 02	.000000000 + 00	.000000000 + 00	1
12	001000000000	.944199242 − 05	.267808013 + 01	.628307585 + 04	1
13	002000000000	.236615606 − 06	.263508345 + 01	.125661517 + 05	1
14	004830000000	.222412262 − 07	.153676866 + 01	.352311373 + 01	1
15	000025000000	.113644375 − 07	.884980375 − 01	.711354700 + 01	1
16	000000000000	.134870204 − 03	.314159265 + 01	.000000000 + 00	2
17	001000000000	.399915448 − 06	.107231782 + 01	.628307585 + 04	2
18	002000000000	.170005184 − 07	.867218932 + 00	.125661517 + 05	2
19	000000000000	.181895781 − 04	.314159265 + 01	.000000000 + 00	3
20	001000000000	.132810927 − 07	.584295983 + 01	.628307585 + 04	3
21	100000000000	.252135692 − 06	.000000000 + 00	.000000000 + 00	4

A NEW REALIZATION OF TERRESTRIAL TIME

G. PETIT
Bureau International des Poids et Mesures
92312 Sèvres France
e-mail: gpetit@bipm.org

ABSTRACT. Terrestrial Time TT is a time coordinate in a geocentric reference system. It is realized through International Atomic Time TAI, which gets its stability from some 200 atomic clocks worldwide and its accuracy from a small number of primary frequency standards (PFS) which frequency measurements are used to steer the TAI frequency. Because TAI is computed in "real-time" and has operational constraints, it does not provide an optimal realization of TT. The BIPM therefore computes another realization TT(BIPM) in post-processing, which is based on a weighted average of the evaluations of TAI frequency by the PFS. The procedures to process PFS data have been recently updated and we consequently propose an updated computation of TT(BIPM). We use all recently available data from new Cs fountain PFS and a revised estimation of the stability of the free atomic time scale EAL on which TAI is based. The performance of the new realization of TT is discussed and is used to assess the accuracy of recent PFS measurements.

1. INTRODUCTION

Terrestrial Time TT was defined by Recommendation IV of Resolution A4 of the International Astronomical Union, adopted at its XXIst General Assembly (1991). The scale unit of TT is chosen to agree with the SI second on the rotating geoid and its origin is defined by the following relation to TAI : TT = TAI + 32.184 s on 1977 January 1^{st}, 0 h TAI. International Atomic Time TAI, the time scale established by the BIPM, is a realization of Terrestrial Time TT, i.e. a coordinate time of a geocentric reference system. TAI gets its stability from some 200 atomic clocks kept in some 50 laboratories worldwide and its accuracy from a small number of primary frequency standards (PFS) developed by a few metrology laboratories. The scale interval (unit) of TAI is based on the SI second, i.e. the period associated with an hyperfine transition of the cesium atom, as it is realized by these primary frequency standards. To be more specific, in the computation of TAI, a free-running time scale, EAL, is first established from a weighted average of some 200 atomic clocks, then the frequency of EAL is compared with that of the primary frequency standards using all available data processed with the algorithm presented in [Azoubib et al. 1977], and a frequency shift (frequency steering correction) is applied to EAL to ensure that the frequency of TAI is accurate. Changes to the steering correction are designed to ensure accuracy without degrading the long-term (several months) stability of TAI, and these changes are announced in advance in the BIPM monthly Circular T. Uncertainty in the frequency of TAI originates from uncertainties in the PFS evaluations and in the links between each PFS and TAI, and from instabilities in the time scale used to connect the PFS

evaluations which are carried out at different times. Procedures to estimate these uncertainties and to report the results in BIPM publications have been updated in 2000 [Petit 1999]. It is notable that, at present time, the three sources of uncertainty in TAI (time scale instabilities, uncertainties in PFS frequency and in frequency transfer techniques) contribute each at a level which is close to, or slightly below, 1×10^{-15} in fractional frequency.

Because TAI is computed in "real-time" every month and has operational constraints (e.g. no correction for a mistake discovered many days after the publication), it does not provide an optimal realization of TT. The BIPM therefore computes another realization TT(BIPM) in post-processing [Guinot 1988], which is based on a weighted average of the evaluations of TAI frequency by the PFS. Several versions have been computed in the 1990s, the latest of which is TT(BIPM99) (see ftp://62.161.69.5/pub/tai/scale/). Over the last ten years important improvements have been achieved (see section 2) and, since 1999, twelve different primary frequency standards have provided evaluations of the TAI frequency, including five Cs fountain clocks for which all systematic frequency shifts have been estimated with a relative uncertainty close to 1×10^{-15}. Therefore a new realization of TT(BIPM) has been computed and some of its applications are described in section 3.

2. EVOLUTION OVER 10 YEARS: 1993-2003

We examine here the progresses realized over the last decade, mainly in what concerns the stability of the ensemble time scale EAL and the accuracy of TAI. Substantial improvements have also taken place in time transfer but these have little effects on the long-term intervals (one month and above) in which we are interested here. We choose to consider a period starting around 1993, when the first commercial clocks of a new generation were introduced.

Improvements in the stability of EAL have mainly resulted from two sources: the improvement of the clocks themselves and the changes in the weighting scheme that were introduced to better take advantage of the quality of the clocks in the ensemble average. There were three main changes in the decade: From 05/1995, the variance below which the maximum weight is attributed to a clock was decreased. From 01/1998, the maximum weight of a clock was set to a fixed value (0.7%). From 01/2001, the maximum weight was set to 2/N, where N is the number of weighted clocks (typically 220), then it was set to 2.5/N from 07/2002. We therefore distinguish four periods to describe the stability of EAL, each of them representing an improvement over the previous one (see Petit 2003).

Many progresses in primary frequency standards and some change in the treatment of their data have occurred over the decade: First, following Recommendation S2 (1996) of the CCDS, a frequency correction for the black-body radiation shift has been applied to all primary frequency standard results. The main effect is a global change in the frequency of TT which has been taken into account since TT(BIPM96). However the most notable events have been the introduction of new types of primary standards: First optically pumped PFS in 1995, then Cs fountains. The first fountain data were reported in 1995 but such data have been regularly available only since the end of 1999. A side effect has been the notable increase in the number of different PFS available during a given year: from about two per year in the early 1990s, the number increased to nearly 10 per year in the 2000s.

3. THE NEW REALIZATION TT(BIPM2003) AND SOME APPLICATIONS

Basic features of the new procedure for computing TT(BIPM) are the following:

*All PFS measurements reported back to 1992 have had their associated uncertainty values updated in accordance to the new procedure [Petit 1999].

*The frequency of EAL with respect to the PFS is then estimated for each month since 1993 with the usual procedure [Azoubib et al. 1977] but with new estimations for the stability model of EAL as mentioned in Section 2. This best estimate represents f(EAL-TT).

*The series of monthly values f(EAL-TT) is slightly smoothed (low pass filter with a cutting frequency around 2 yr^{-1}) so as to include possible yearly signatures in the smoothed frequencies (EAL-TT). It is estimated that yearly signatures are most likely due to EAL rather than to the primary standards, so this procedure mostly removes these signatures from TT.

*The smoothed frequencies are interpolated and integrated with a 5-day step since MJD 48984 (28 Dec 1992), at which epoch continuity is ensured with TT(BIPM99). This forms TT(BIPM2003) which is available at ftp://62.161.69.5/pub/tai/scale/.

[TT(BIPM99)-TT(BIPM2003)] remains in the range [-40ns,+25ns] until August 1997. Then the difference gets larger and reaches -170 ns in February 1999. This may be partly due to the influence of the new primary standards introduced in 1999 that were not available for the computation of TT(BIPM99) but affect TT(BIPM2003) already during the end of 1998. Figure 1a shows the difference between TAI and TT(BIPM2003) over 1993-2003. Two main periods may be distinguished, when the frequency of TAI is notably too low: In the first period, 1993-1998, this results from the decision in 1995 to correct the PFS frequencies for the Blackbody frequency shift, automatically shifting the TAI frequency by about -2×10^{-14} , a step which took about 3 years to recover by continuously steering its frequency by 1×10^{-15} every two months. In the second period, about since end 1999, this is due to other causes: when Cs fountains started to contribute significantly, it was observed that their estimation of TAI frequency was somewhat lower than the estimation given by other PFSs. Although this was recognized quite early, the present steering policy has so far failed to bring the TAI frequency close to that of the PFSs probably because a systematic frequency drift in EAL, of unknown origin, adds its effect to counter the frequency steering corrections. The net result is a nearly systematic frequency difference between TAI and TT(BIPM2003) which integrates to some 4 microseconds over 10 years.

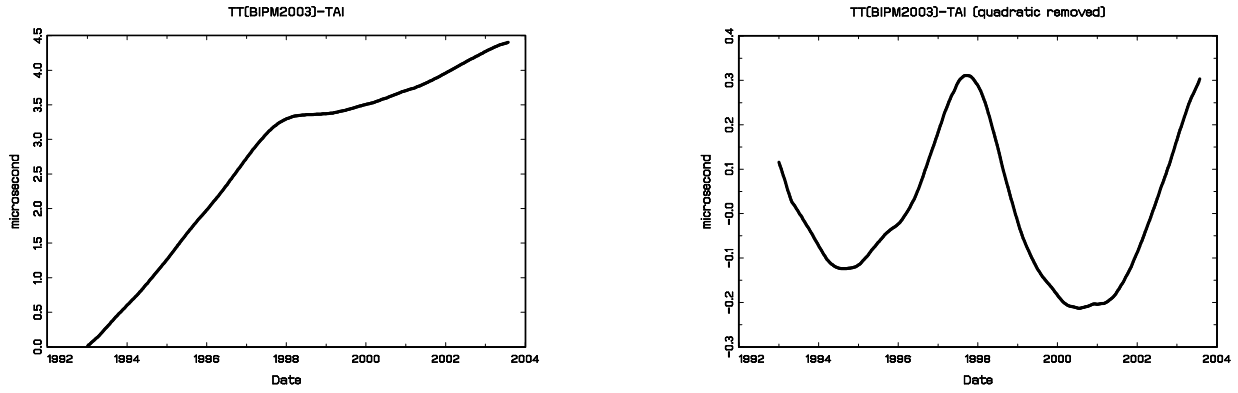

Figure 1: a: Difference between TT(BIPM2003) and TAI (with an offset removed) b: Difference in pulsar timing of using TT(BIPM2003) or TAI as a reference

The most demanding application of a time scale on the long term is the analysis of long series of measurements of the time of arrival of radio pulses from millisecond pulsars [Petit and Tavella

1996]. In such an analysis, several physical parameters of the pulsar are obtained by adjusting a model to the data, assuming that long-term systematic effects from both the reference time scale and the series of measurements do not contaminate this estimation. It is useful to try to estimate in what respect time scales like TAI or TT(BIPM) may differ for this purpose. Because the pulsar rotation period and its derivative are always obtained by adjustment, all comparisons between different time scales must be done after removing the best-fit quadratic between them. Such an adjustment over a period of 10 years yields quasi-periodic differences between the two scales, with apparent period of a few years and amplitude of several hundred ns (Figure 1b). This compares to a timing noise that may be as low as a few hundred ns in the best cases, so this effect is not negligible in principle. However, the timing noise and some other long term effects are generally larger than this for most pulsars. Nevertheless it is always advised to use a post-processed time scale like the new TT(BIPM2003) for pulsar analysis, rather than a real-time scale such as TAI, GPS time or a local atomic time scale realized by a single time laboratory

Another important application of TT(BIPM2003) is to serve as a frequency reference to compare Cs fountain data. Half a dozen Cs fountains from four different laboratories have contributed to the estimation of EAL frequency over the past years. However they operate intermittently and it is generally not possible to directly compare them because their operation is not simultaneous. Then the most convenient way to intercompare them is to use a common reference which is as accurate and stable as possible. TT(BIPM2003) may serve this purpose and the results of such comparisons will be presented in a subsequent paper [Petit 2003].

4. CONCLUSIONS

We compute a post-processed time scale, TT(BIPM2003), basing its stability on EAL and its accuracy on all available PFS measurements. Presently the three sources of uncertainty (time scale instabilities, uncertainties in PFS frequency and in frequency transfer techniques) each contribute at a level which is close to, or slightly below, 1×10^{-15} in fractional frequency so that the uncertainty in the frequency of TT(BIPM2003) is close to 1×10^{-15}. This time scale is considered the best realization of Terrestrial Time and is therefore most suited as a reference for the analysis of pulsar data. It also allows a better comparison of the different PFS measurements that are presently sparse and rarely simultaneous.

It is expected that the accuracy of PFS will progress rapidly in the coming years. Progresses in time scale formation and in time transfer techniques should accompany the progresses in primary frequency standard technology to bring the accuracy of TT(BIPM) and the uncertainty on the TAI frequency well below 1×10^{-15} in the near future.

5. REFERENCES

Azoubib J., Granveaud M., Guinot B., *Metrologia* 13, 87, 1977.

Guinot B., *Astron. Astrophys.*, 192, pp. 370–373, 1988.

Petit G., *Proc.* 31^{st} *PTTI*, pp. 297–304, 1999.

Petit G., *Proc.* 35*th PTTI*, 2003, to be published.

Petit G., Tavella P., *Astron. Astrophys.*, 308, pp. 290–298, 1996.

COMPARISON BETWEEN THE FINITE VLBI MODEL AND THE CONSENSUS MODEL

M. SEKIDO[1], T. FUKUSHIMA[2]
1 : Communications Research Laboratory
893-1 Hirai Kashima Ibaraki, 314-0012 Japan
e-mail: sekido@crl.go.jp
2 : National Astronomical Observatory
2-21-1 Osawa Mitaka Tokyo,181-8588 Japan
e-mail: Toshio.Fukushima@nao.ac.jp

ABSTRACT. For application of VLBI technique to spacecraft navigation, we have developed an analytical formula of VLBI delay model for finite distance radio source with based on linearized parameterized post Newtonian metric. This formula corresponds to the standard VLBI model ('consensus model'), which is widely used in VLBI community all over the world. This finite VLBI model has an accuracy better than 5 pico seconds for a radio source at distance beyond 10^9 m away from the observer on earth based baseline. The deviation of finite VLBI model from the consensus model comes from the curvature of the wavefront. We compared these two models and derived an analytical expression for the difference.

1. INTRODUCTION

Spacecraft navigation is another application field of Very Long Baseline Interferometry (VLBI) other than astronomy and geodesy. VLBI has great sensitivity in direction perpendicular to the line of sight. It is complementary characteristic to the range and range rate (R&RR) measurement, which is widely used for spacecraft navigation in deep space. Thus jointly using VLBI and R&RR together will make increase the accuracy of orbit determination of the spacecraft. An accurate delay model is required in VLBI data processing and analysis, especially for precise astrometry and geodesy. The 'consensus model' [Eubanks, 1991] is widely used as standard VLBI model in world wide VLBI community. That is based on plane wave approximation, however, this standard VLBI model does not have enough accuracy, when radio source is closer than 30 light years from observer (e.g. planets, asteroids, and spacecraft in the solar system). Because curvature of the wave front cannot be ignored in those observations, an alternative VLBI delay model is required for finite distance radio sources.

Sovers & Jacobs (1996) discussed on curvature effect of finite distance radio source. Fukushima (1994) introduced an useful expression of VLBI delay model for finite distance radio source. However, an analytical formula of relativistic VLBI delay model corresponding to the 'Consensus model' was not obviously expressed on their papers. The Jet Propulsion Laboratory (JPL/NASA) have been using VLBI technique for spacecraft navigation [e.g. Border et al., 1982] sometimes. Moyer (2000) has developed formulation of radiometric observation data for spacecraft navigation with based on light time equation (light-time approach). Solving light time

equation by numerical procedure is straightforward, however it need iteration of computation to solve light time equation in the analysis software. We took a VLBI-like approach rather than the light-time approach, because we intended to find a analytical formula for replacement with consensus model so that it can easily be implemented in current apriori computation software (CALC[1]). We derived an analytical formula of VLBI delay model for finite distance radio source (hear after referred as 'finite VLBI model') [Sekido and Fukushima, 2003] based of linearized Parameterized Post Newtonian (PPN) metric, and by following the approaches of Hellings (1986), Shahid-Saless and Hellings (1991), and Fukushima (1994). The form is

$$\tau_2 - \tau_1 = (1+\beta_{02})^{-1} \left\{ \Delta t_g - \frac{\vec{\mathbf{K}}\cdot\vec{\mathbf{b}}}{c}\left[1-(1+\gamma)U - \frac{V_e^2 + 2\vec{\mathbf{V}}_e\cdot\vec{\mathbf{w}}_2}{2c^2}\right] - \frac{\vec{\mathbf{V}}_e\cdot\vec{\mathbf{b}}}{c^2}\left(1+\beta_{02} - \frac{\vec{\mathbf{K}}\cdot(\vec{\mathbf{V}}_e + 2\vec{\mathbf{w}}_2)}{2c}\right)\right\}, \quad (1)$$

where, $\beta_{02} = \hat{\vec{\mathbf{R}}}_{02}\cdot\vec{\mathbf{V}}_2/c$. Target accuracy of this formula is order of pico seconds with ground based baseline for the radio source in the solar system. An expression of the difference between the finite VLBI model and the consensus model is mainly discussed in this paper.

2. PREPARATION OF COMPARISON

Definitions of Parameters and Notation

Variables of large capital indicate quantity in the rest frame of solar system barycenter (hereafter referred as FCB) and small ones denote those of geocentric reference frame (hereafter referred as FCG). Then Barycentric Coordinate Time (TCB) is represented by T and Geocentric Coordinate Time (TCG) is represented by t. Suffix 0,1,2 represent radio source and two VLBI observation stations, respectively. Position vector of i^{th} station in the FCB is expressed by $\vec{\mathbf{X}}_i$. Radio signal is supposed to be emitted at T_0 from the radio source and to arrive at i^{th} observation station at T_i. Relative position vector and its magnitude are denoted as follows:

$$\vec{\mathbf{R}}_{ij} = \vec{X}_i - \vec{X}_j, \quad R_{ij} = |\vec{\mathbf{R}}_{ij}|$$

Definition of other parameters are summarized in Table 1. Pseudo source vector $\vec{\mathbf{K}}$, baseline vector $\vec{\mathbf{B}}$, and those composed from position vectors of different time epoch are defined in FCB as:

$$\begin{aligned} \vec{\mathbf{K}} &= \frac{\vec{\mathbf{R}}_{01}(T_1) + \vec{\mathbf{R}}_{02}(T_1)}{R_{01}(T_1) + R_{02}(T_1)}, \quad \vec{\mathbf{K}}^* = \frac{\vec{\mathbf{R}}_{01}(T_1) + \vec{\mathbf{R}}_{02}(T_2)}{R_{01}(T_1) + R_{02}(T_2)}, \\ \vec{\mathbf{B}} &= \vec{\mathbf{R}}_{02}(T_1) - \vec{\mathbf{R}}_{01}(T_1), \quad \vec{\mathbf{B}}^* = \vec{\mathbf{R}}_{02}(T_2) - \vec{\mathbf{R}}_{01}(T_1), \end{aligned} \quad (2)$$

[1] http://gemini.gsfc.nasa.gov/solve/solve.shtml

Table 1: Notation of parameters

$\vec{\mathbf{V}}_e$	Velocity of the earth motion around the sun in FCB
$\vec{\mathbf{w}}_2$	Velocity of the station 2 due to spin of the earth in FCG.
$\vec{\mathbf{K}}_s$	Source unit vector from the solar system barycenter defined in FCB.
$\vec{\mathbf{b}}$	$= \vec{\mathbf{x}}_2(t_1) - \vec{\mathbf{x}}_1(t_1)$. Baseline vector in FCG.
c	Speed of light
γ	A parameter of linearized PPN metric. $\gamma = 1$ in Einstein's general relativity.
U	$= \sum_p \frac{GM_p}{\lvert\vec{\mathbf{X}}-\vec{\mathbf{X}}_p\rvert c^2}$. Normalized gravitational potential produced by pth body at $\vec{\mathbf{X}}$.
Δt_g	Gravitational delay difference in VLBI observation.

where $\vec{\mathbf{R}}_{0i}(T_j) = \vec{\mathbf{X}}_0(T_0) - \vec{\mathbf{X}}_i(T_j)$. T_0 is obtained with respect to T_1 by solution of light-time equation

$$\begin{aligned} c(T_1 - T_0) &= |\vec{\mathbf{X}}_1(T_1) - \vec{\mathbf{X}}_0(T_0)| \\ &\quad +(1+\gamma)\sum_J \frac{GM_J}{c^2} \ln \left| \frac{R_{0\mathrm{J}} + R_{1\mathrm{J}} s + R_{01}}{R_{0\mathrm{J}} + R_{1\mathrm{J}} - R_{01}} \right|. \end{aligned} \tag{3}$$

Definition of source vector for finite distance radio source

In comparison between the two cases, where distance to the radio source is infinite and finite, there is a freedom of choice on source vector for finite distance radio source. Question is which vector in 'finite' case is regarded as correspond to source unity vector in 'infinite' case. Source vector in consensus model ($\vec{\mathbf{K}}_s$) is defined by a unit vector from barycenter of solar system to radio source in FCB. Sovers & Jacobs(1996) used a geocentric vector to radio source to express the difference between delays of plane wave and curved wavefront. Here we suppose unit vector from station 1 to radio source as correspond to source vector in 'infinite' case.

$$\vec{\mathbf{K}}'_s \stackrel{\mathrm{def}}{=} \frac{\vec{\mathbf{R}}_{01}}{R_{01}} \tag{4}$$

The reason of our choice is because delay of VLBI observation is measured at epoch time of signal's arrival to station 1, i.e. station 1 is the reference station. In addition more important reason is that delay characteristic of finite distance radio source departed from that of plane wave is expressed obviously with our definition. That will be seen in latter section.

Figure 1 illustrate a configuration of VLBI observation of curved wavefront. For simplicity, we eliminate any motion of the earth in discussion only in this section. For instance, baseline vector $\vec{\mathbf{B}}$ used here has to be properly denoted $\vec{\mathbf{B}}^*$ (equation (2)) in real condition.

As seen from Figure 1, geometrical difference of distance between R_{02} and R_{01} is given as

$$\begin{aligned} R_{01} - R_{02} = &\quad \vec{\mathbf{K}}'_s \cdot \vec{\mathbf{B}} - R_{02}(1 - \cos\theta) \\ = &\quad \vec{\mathbf{K}}'_s \cdot \vec{\mathbf{B}} - R_{02}\left(1 - \sqrt{1 - \frac{|\vec{\mathbf{K}}'_s \times \vec{\mathbf{B}}|^2}{R_{02}^2}}\right) \\ = &\quad \vec{\mathbf{K}}'_s \cdot \vec{\mathbf{B}} - R_{02}\Delta C \end{aligned} \tag{5}$$

The second term of the equation represents the effect of curved wavefront. The factor of this term ΔC can be expressed my Maclaurin expansion as

$$\begin{aligned} \Delta C = &\quad \frac{|\vec{\mathbf{K}}'_s \times \vec{\mathbf{B}}|^2}{2R_{02}^2} + \frac{|\vec{\mathbf{K}}'_s \times \vec{\mathbf{B}}|^4}{8R_{02}^4} - \cdots \\ = &\quad \sum_{i=1}^{\infty} \frac{|\vec{\mathbf{K}}'_s \times \vec{\mathbf{B}}|^{2i}}{2iR_{02}^{(2i)}}. \end{aligned} \tag{6}$$

Difference between the Finite VLBI model and the Consensus model

Time difference measured by VLBI observation in TCB time scale is

$$c(T_2 - T_1) = R_{02}(T_2) - R_{01}(T_1) + c\Delta t_g \tag{7}$$

An approximation $\vec{\mathbf{B}}^* = \vec{\mathbf{B}} + \vec{\mathbf{V}}_2(T_2 - T_1)$ has enough accuracy (better than 6 micro meter on ground based baseline). By using this relation, differential range $R_{02}(T_2) - R_{01}(T_1)$ is expressed with pseudo source vector $\vec{\mathbf{K}}$ defined by equation (2) as:

$$\begin{aligned} R_{02}(T_2) - R_{01}(T_1) &= -\vec{\mathbf{K}}^* \cdot \vec{\mathbf{B}}^* \\ &= -\frac{1}{1+\beta_{02}} \vec{\mathbf{K}} \cdot \vec{\mathbf{B}} \end{aligned} \tag{8}$$

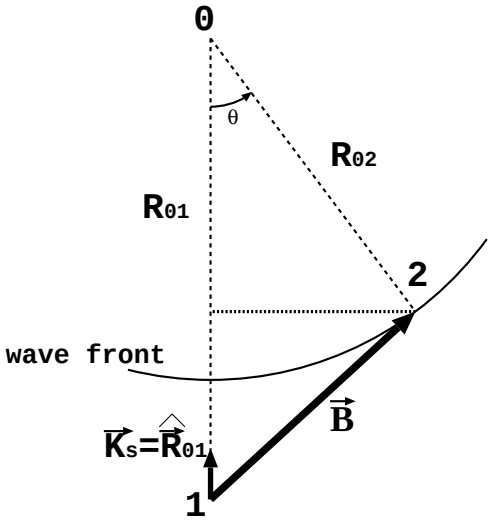

Figure 1: For comparison between the finite VLBI model and the consensus model, $\vec{\mathbf{K}}'_s \stackrel{\text{def}}{=} \widehat{\vec{\mathbf{R}}}_{01}$ is used as definition of source vector corresponding to that in 'infinite' case. Here we are eliminating motion of station 1 and 2 for simplicity. For example, the baseline vector $\vec{\mathbf{B}}$ in this figure must be written as $\vec{\mathbf{B}}^* = \vec{\mathbf{X}}_2(T_2) - \vec{\mathbf{X}}_1(T_1)$ in real condition.

This equation was used to derive the finite distance VLBI model (equation (1)) in other paper [Sekido & Fukushima , 2003]. The same differential range can be expressed with unit source vector $\vec{\mathbf{K}}'_s$ instead of pseudo source vector $\vec{\mathbf{K}}$ as follows:

$$\begin{aligned} R_{02}(T_2) - R_{01}(T_1) &= -\vec{\mathbf{K}}'_s \cdot \vec{\mathbf{B}}^* + R_{02}\Delta C \\ &= -\frac{1}{1 + \frac{\vec{\mathbf{K}}'_s \cdot \vec{\mathbf{V}}_2}{c}} \left(-\vec{\mathbf{K}}'_s \cdot \vec{\mathbf{B}} + R_{02}\Delta C \right) \end{aligned} \tag{9}$$

A relation between $\vec{\mathbf{B}}$ and $\vec{\mathbf{b}}$ is given (e.g. equation (16) of Sekido & Fukushima (2003)) as:

$$\vec{\mathbf{B}} = X_2(T_1) - X_1(T_1) = (1 - \gamma U)\vec{\mathbf{b}} - \frac{\vec{\mathbf{V}}_e \cdot \vec{\mathbf{b}}}{c^2} \left(\frac{\vec{\mathbf{V}}_e}{2} + \vec{\mathbf{w}}_2 \right). \tag{10}$$

And a relation of time interval in TCB $(T_2 - T_1)$ and interval of events in TCG is given as (e.g. equation (17) of Sekido & Fukushima (2003)):

$$T_2 - T_1 = \left(1 + U + \frac{V_e^2}{2c^2} + \frac{\vec{\mathbf{V}}_e \cdot \vec{\mathbf{w}}_2}{c^2} \right) (t_2 - t_1) + \frac{\vec{\mathbf{V}}_e \cdot \vec{\mathbf{b}}}{c^2}. \tag{11}$$

Substituting equations (9), (10), and (11) into equation (7) becomes

$$\begin{aligned} c \left(1 + U + \frac{V_e^2}{2c^2} + \frac{\vec{\mathbf{V}}_e \cdot \vec{\mathbf{w}}_2}{c^2} \right) (t_2 - t_1) = \\ \left(1 + \frac{\vec{\mathbf{K}}'_s \cdot \vec{\mathbf{V}}_2}{c} \right)^{-1} \left[\Delta t_g - (1 - \gamma U)\vec{\mathbf{K}}'_s \cdot \vec{\mathbf{b}} - \frac{\vec{\mathbf{V}}_e \cdot \vec{\mathbf{b}}}{c^2} \left(1 + \frac{\vec{\mathbf{V}}_e \cdot \vec{\mathbf{K}}'_s}{2c} \right) + R_{02}\Delta C \right], \end{aligned} \tag{12}$$

where difference $\vec{\mathbf{V}}_2/c$ and $(\vec{\mathbf{V}}_e + \vec{\mathbf{w}}_2)/c$ was eliminated, since it was order of $(V_e/c)^{-3}$.

Time scale of TT (τ) is related with that of TCG (t) by $dt = d\tau(1 - L_G)$, where $L_G = 6.969290134 \times 10^{-10}$ [McCarthy and Petit, 2003]. Consequently, the form of finite VLBI delay in TT scale expressed with unit source vector $\vec{\mathbf{K}}'_s$ is given by

$$c(\tau_2 - \tau_1) = \left(1 + \frac{\vec{\mathbf{K}}'_s \cdot \vec{\mathbf{V}}_2}{c}\right)^{-1} \left\{\Delta t_g - \vec{\mathbf{K}}'_s \cdot \vec{\mathbf{b}}[1 - (1+\gamma)U - \frac{V_e^2 + 2\vec{\mathbf{V}}_e \cdot \vec{\mathbf{w}}_2}{2c^2}] - \frac{\vec{\mathbf{V}}_e \cdot \vec{\mathbf{b}}}{c}\left(1 + \frac{\vec{\mathbf{V}}_e \cdot \vec{\mathbf{K}}'_s}{2c}\right) + R_{02}\Delta C'\right\}, \quad (13)$$

where spatial coordinate on the geoid ξ was taken so that speed of light c was kept constant as $d\xi = (1 - L_G)dx$, and baseline vector was re-defined by $\vec{\mathbf{b}} = \vec{\xi}_2(\tau_1) - \vec{\xi}_1(\tau_1)$. And $\Delta C' = (1 - U - L_G - \frac{V_e^2 + 2\vec{\mathbf{V}}_e \cdot \vec{\mathbf{w}}_2}{2c^2})\Delta C$ was used.

The consensus model [Eubanks, 1991; McCarthy and Petit, 2003] is given by

$$c(\tau_2 - \tau_1) = \left[1 + \frac{\vec{\mathbf{K}}_s \cdot (\vec{\mathbf{V}}_e + \vec{\mathbf{w}}_2)}{c}\right]^{-1} \left\{c\Delta t_g - \vec{\mathbf{K}}_s \cdot \vec{\mathbf{b}}\left[1 - (1+\gamma)U - \frac{V_e^2 + 2\vec{\mathbf{V}}_e \cdot \vec{\mathbf{w}}_2}{2c^2}\right] - \frac{\vec{\mathbf{V}}_e \cdot \vec{\mathbf{b}}}{c^2}\left(1 + \frac{\vec{\mathbf{K}}_s \cdot \vec{\mathbf{V}}_e}{2c}\right)\right\} \quad (14)$$

Putting the numerator and denominator of right hand side of equation (14) respectively A and B, delay of the consensus model (τ_∞) is $\tau_\infty = A/B$. Regarding $\vec{\mathbf{K}}'_s$ as identical with $\vec{\mathbf{K}}_s$, delay of finite distance VLBI model (τ_F) is written as $\tau_F = \frac{A + R_{02}\Delta C'}{B}$. where difference between $\vec{\mathbf{V}}_2$ and $\vec{\mathbf{V}}_e + \vec{\mathbf{w}}_2$ of the denominators were eliminated, since its factor is $(V_e/c)^{-3}$. Consequently the difference of the two model is given as

$$\tau_F - \tau_\infty = \frac{(1 - U - L_G - \frac{V_e^2 + 2\vec{\mathbf{V}}_e \cdot \vec{\mathbf{w}}_2}{2c^2})}{1 + \frac{\vec{\mathbf{K}}'_s \cdot \vec{\mathbf{V}}_2}{c}} \cdot \frac{R_{02}}{c}\left(1 - \sqrt{1 - \frac{|\vec{\mathbf{K}}'_s \times \vec{\mathbf{B}}^*|^2}{R_{02}^2}}\right) \quad (15)$$

$$= \frac{(1 - U - L_G - \frac{V_e^2 + 2\vec{\mathbf{V}}_e \cdot \vec{\mathbf{w}}_2}{2c^2})}{1 + \frac{\vec{\mathbf{K}}'_s \cdot \vec{\mathbf{V}}_2}{c}} \cdot \frac{R_{02}}{c}\sum_{i=1}^{\infty} \frac{|\vec{\mathbf{K}}'_s \times \vec{\mathbf{B}}^*|^{2i}}{2i R_{02}^{(2i)}}. \quad (16)$$

This difference corresponds to the geometrical delay of curved wavefront multiplied by factor of relativistic time contraction (numerator) and effect of motion of station 2 (denominator). The magnitude of this term is quite large with order of $B^2/2R_{02}$. It reaches up to 50 km in case that the distance to the radio source is 10^9 m and baseline length is 10^7 m, for instance.

A series of VLBI observation campaign were organized in the first half of 2003 for supporting earth swing-by of spacecraft NOZOMI[2]. Several Japanese domestic VLBI stations and Algonquin observatory in Canada joined the campaign. The baseline lengths between Algonquin and Japanese stations were about 9000 km, and NOZOMI approached to the earth in distance 10^9 m or less at the moment of swing-by. Therefore this finite VLBI model was essential for detecting interferometer fringes on the continental baseline in these observations.

[2]Spacecraft NOZOMI was launched for Mars exploration by Institute of Space and Astronautical Sciences of Japan.

References

[1] Border J. S., et al. (1982) Determining Spacecraft Angular Position with Delta VLBI: The Voyager Demonstration. *AIAA/AAS Astrodynamics Conference* Aug. 9-11, AIAA-82-1471.

[2] Eubanks, T. M. (1991) A Consensus Model for Relativistic Effects in Geodetic VLBI. *Proc. of the USNO workshop on Relativistic Models for Use in Space Geodesy*: 60-82

[3] Fukushima, T. (1994) Lunar VLBI observation model. *Astron. Astrophys.*291: 320-323

[4] Hellings, R. W. (1986) RELATIVISTIC EFFECTS IN ASTRONOMICAL TIMING MEASUREMENTS. *Astron. J.*, 91: 650-659

[5] McCarthy, D. D. and Petit, G. (2003), IERS Conventions 2003. *IERS Technical Note* No. 32.

[6] Moyer, T. D. (2000) Formulation for Observed and Computed Values of Deep Space Network Data Types for Navigation. *JPL Monograph* 2 (JPL Publication 00-7).

[7] Seidelmann, P. K. and Fukushima, T. (1992) Why new time scale?. *Astron. Astrophys.*265: 833-838

[8] Shahid-Saless, B. & Hellings, R. W. (1991) A Picosecond Accuracy Relativistic VLBI Model via Fermi Normal Coordinates. *Geophys. Res. Lett.* 18: 1139-1142

[9] Sovers, O. J. & Jacobs C. S. (1996) Observation Model and Parameter Partials for the JPL VLBI Parameter Estimation Software "MODEST"-1996". *JPL Publication* 83-39, Rev. 6: 6–8

LIGHT DEFLECTION AND TIME TRANSFER TO THE POST-POST-MINKOWSKIAN ORDER USING SYNGE'S WORLD FUNCTION

C. LE PONCIN-LAFITTE
SYRTE, CNRS/UMR 8630 Observatoire de Paris
61 avenue de l'Observatoire, F-75014 PARIS, FRANCE
e-mail: leponcin@danof.obspm.fr

P. TEYSSANDIER
SYRTE, CNRS/UMR 8630 Observatoire de Paris
61 avenue de l'Observatoire, F-75014 PARIS, FRANCE
e-mail: pierre.teyssandier@obspm.fr

ABSTRACT. Astrometric missions like GAIA and SIM will require microarcsecond accuracy in the measurement of the direction of light rays. At this level of precision, it is necessary to develop a relativistic modelling of the light deflection up to the order G^2, G being Newton's gravitationnal constant. We emphasize that this modelling may be achieved without integrating the differential equations of null geodesics, by improving the method of the world function developed by Synge. As an example, we give a detailed calculation of the light deflection in a static, spherically symmetric space-time considered in the post-post-Minkowskian approximation. The world function also makes it very easy to determine the time transfer function.

1. INTRODUCTION

With advances in technology, great improvements in astrometric accuracy will certainly be made in the near future. Two major space astrometric missions are already planned to measure the positions of celestial objects with typical uncertainties in the range 1-10 μas (microarcsecond). The Global Astrometric Interferometer for Astrophysics (GAIA, Perryman *et al.* 2001) mission, to be launched not later than 2012, will be capable to measure the positions of 25 million stars with a global uncertainty better than 10 μas and a few million with an uncertainty better than 4 μas. The Space Interferometric Mission (SIM, Danner and Unwin 1999) will be capable of at least 4 μas accuracy for 3000 quasars and fundamental stars.

For these missions, and for those which will follow them, all relativistic effects contributing to the deflection of light must be determined at a level of 1 μas, or significantly better. It was shown that this level of accuracy can be achieved by the GAIA mission if one retains only the perturbative terms of the background metric which are of the first order with respect to the Newtonian gravitational constant G (the so-called post-Minkowskian approximation). However, it must be emphasized that this approximation is sufficient only because the light rays received by GAIA will be propagating sufficiently far from the Sun. If we want to build a relativistic model for any light ray propagating through the Solar System, it will be necessary to take into

account terms of order G^2 in the metric. The aim of the present paper is to furnish a general method allowing the calculation of the deflection of light within the post-post-Minkowskian approximation of any metric.

Since the pioneering works (see, e.g., Will 1988 and Refs. therein), a lot of papers investigated the deflection of light and/or the time delay effects in the linearized, weak-field limit of general relativity (Klioner 1991, Klioner and Kopeikin 1992, Kopeikin 1997, Kopeikin and Schäfer 1999, Ciufolini and Ricci 2002). In (Kopeikin and Schäfer 1999) especially, one finds an exhaustive determination of light rays in the field of an arbitrary large number of moving point masses in terms of retarded Liénard-Wichert potentials.

In contrast with the generality of the results obtained at the first order, the investigations undertaken at the second order in G have been confined to static spherically symmetric fields (see Epstein and Shapiro 1980, Fischbach and Freeman 1980 for the deflection angles, Klioner and Kopeikin 1992, Richter and Matzner 1982 and 1983, Brumberg 1987, for the time delay and light bending).

In the above-mentioned studies, the deflection of light and the time delay are calculated by integrating the differential equations of null geodesics. This procedure is workable as long as one contents oneself with analyzing the effects in the first-order post-Minkowskian approximation or considering the case of a static spherically symmetric field. However, analytical or numerical integrations of the geodesic equations require very cumbersome calculations when the effects in G^2 are taken into account. So we explore an alternative method, based on the two-point world function, as developed by Synge (Synge 1964). This method presents the decisive advantage to avoid the solution of the null geodesic equations. Moreover, the knowledge of the world function allows an explicit determination of the travel time of a photon. We summarize here the results that we have obtained for a general metric within the second post-Minkowskian approximation and we apply them to a static, spherically-symmetric ds^2 containing three post-Minkowskian parameters. Thus we recover with simple quadratures formulae obtained in John 1975 with heavy calculations.

In the following, we suppose that space-time is covered by a global quasi-Cartesian coordinate system $x^\mu = (x^0, x^i) = (ct, \mathbf{x})$, c being the speed of light in a vacuum. The signature of the metric is $(+---)$.

2. THE WORLD FUNCTION

Consider two points x_A and x_B in a given space-time endowed with a metric $g_{\mu\nu}$ and assume that x_A and x_B are connected by a unique geodesic path Γ. Throughout this paper, λ denotes the unique affine parameter along Γ which fulfills the boundary conditions $\lambda_A = 0$ and $\lambda_B = 1$. The so-called world-function of space-time (Synge 1964) is the two-point function $\Omega(x_A, x_B)$ defined by

$$\Omega(x_A, x_B) = \frac{1}{2}\int_0^1 g_{\mu\nu}(x^\alpha(\lambda))\frac{dx^\mu}{d\lambda}\frac{dx^\nu}{d\lambda}d\lambda\,, \tag{1}$$

the integral being taken along Γ. It is easily seen that $\Omega(x_A, x_B) = \varepsilon[s_{AB}]^2/2$, where s_{AB} is the geodesic distance between x_A and x_B and $\varepsilon = 1, 0, -1$ for timelike, null and spacelike geodesics, respectively. It results from Eq. (1) that the world-function $\Omega(x_A, x_B)$ is unchanged if we perform any admissible coordinate transformation.

The utility of the world-function for our purpose comes from the following properties (Synge 1964) :

i) The world function satisfies the Hamilton-Jacobi equations

$$\frac{1}{2}\,g^{\alpha\beta}(x_A)\frac{\partial\Omega}{\partial x_A^\alpha}(x_A, x_B)\frac{\partial\Omega}{\partial x_A^\beta}(x_A, x_B) = \Omega(x_A, x_B)\,, \tag{2}$$

$$\frac{1}{2}\, g^{\alpha\beta}(x_B)\frac{\partial\Omega}{\partial x_B^\alpha}(x_A,x_B)\frac{\partial\Omega}{\partial x_B^\beta}(x_A,x_B)=\Omega(x_A,x_B)\,. \tag{3}$$

ii) The vectors $(dx^\alpha/d\lambda)_A$ and $(dx^\alpha/d\lambda)_B$ tangent to the geodesic Γ respectively at x_A and x_B are given by

$$\left(g_{\alpha\beta}\frac{dx^\beta}{d\lambda}\right)_A=-\frac{\partial\Omega}{\partial x_A^\alpha}\,,\quad \left(g_{\alpha\beta}\frac{dx^\beta}{d\lambda}\right)_B=\frac{\partial\Omega}{\partial x_B^\alpha}\,. \tag{4}$$

As a consequence, if $\Omega(x_A,x_B)$ is explicitly known, the determination of these vectors does not require the integration of the differential equations of the geodesic.

iii) Points x_A and x_B may be linked by a light ray if and only if the condition

$$\Omega(x_A,x_B)=0 \tag{5}$$

is fulfilled. Thus, $\Omega(x_A,x)=0$ is the equation of the light cone $\mathcal{C}(x_A)$ at x_A. This fundamental property shows that the knowledge of $\Omega(x_A,x_B)$ yields (at least in principle) the knowledge of the travel time t_B-t_A of a photon connecting two points x_A and x_B. It must be pointed out, however, that solving the equation $\Omega(ct_A,\boldsymbol{x}_A,ct_B,\boldsymbol{x}_B)=0$ for t_B yields two distinct solutions t_B^+ and t_B^- since the timelike curve $x^i=x_B^i$ cuts the light cone $\mathcal{C}(x_A)$ at two points x_B^+ and x_B^-, x_B^+ being in the future of x_B^-. In the present paper, we shall always regard x_A as the point of emission of the photon and x_B as the point of reception, and we shall write t_B for t_B^+. With this convention, t_B-t_A may be considered either as a function of t_A, $\boldsymbol{x}_A$, $\boldsymbol{x}_B$, or as a function of t_B, $\boldsymbol{x}_A$, $\boldsymbol{x}_B$. So we put

$$t_B^+-t_A=\mathcal{T}_e(t_A,\boldsymbol{x}_A,\boldsymbol{x}_B)=\mathcal{T}_r(t_B,\boldsymbol{x}_A,\boldsymbol{x}_B)\,, \tag{6}$$

and we call $\mathcal{T}_e(t_A,\boldsymbol{x}_A,\boldsymbol{x}_B)$ the emission time transfer function and $\mathcal{T}_r(t_B,\boldsymbol{x}_A,\boldsymbol{x}_B)$ the reception time transfer function.

Consider now a stationary space-time. In this case, we use exclusively coordinates (x^μ) such that the metric does not depend on x^0. Then, the world-function is a function of $x_B^0-x_A^0$, $\boldsymbol{x}_A$ and $\boldsymbol{x}_B$, and (6) reduces to a relation of the form

$$t_B^+-t_A=\mathcal{T}(\boldsymbol{x}_A,\boldsymbol{x}_B)\,. \tag{7}$$

The knowledge of $\mathcal{T}$ enables to determine the direction of light rays since a comparaison between Eq. (5) and Eq. (7) immediately shows that the vectors $(l^\mu)_A$ and $(l^\mu)_B$ defined by their covariant components

$$(l_0)_A=1,\quad (l_i)_A=c\frac{\partial}{\partial x_A^i}\mathcal{T}(\boldsymbol{x}_A,\boldsymbol{x}_B)\,, \tag{8}$$

$$(l_0)_B=1,\quad (l_i)_B=-c\frac{\partial}{\partial x_B^i}\mathcal{T}(\boldsymbol{x}_A,\boldsymbol{x}_B)\,, \tag{9}$$

are tangent to the ray at x_A and x_B, respectively. It must be pointed out that these tangent vectors correspond to an affine parameter such that $l_0=1$ along the ray (note that such a parameter does not coincide with λ). Generally, extracting the time transfer formula Eq. (7) from Eq. (5), next using Eqs. (8)-(9) will be more straightforward than deriving the vectors tangent at x_A and x_B from Eq. (4), next imposing the constraint (5).

In the present work, we assume that the gravitational potentials may be expanded as

$$g_{\mu\nu}=\eta_{\mu\nu}+Gh_{\mu\nu}^{(1)}+G^2h_{\mu\nu}^{(2)}+O(G^3)\,. \tag{10}$$

As a consequence, the world function admits an expansion as follows

$$\Omega(x_A,x_B)=\Omega^{(0)}(x_A,x_B)+G\Omega^{(1)}(x_A,x_B)+G^2\Omega^{(2)}(x_A,x_B)+O(G^3)\,, \tag{11}$$

where $\Omega^{(0)}$ is the Minkowskian world function

$$\Omega^{(0)}(x_A, x_B) = \frac{1}{2}\eta_{\mu\nu}(x_B^\mu - x_A^\mu)(x_B^\nu - x_A^\nu) \tag{12}$$

and $\Omega^{(1)}$ is given by (Synge 1964, Linet and Teyssandier 2002)

$$\Omega^{(1)}(x_A, x_B) = \frac{1}{2}(x_B^\mu - x_A^\mu)(x_B^\nu - x_A^\nu)\int_0^1 h^{(1)}_{\mu\nu}(x_{(0)}(\lambda))d\lambda\,. \tag{13}$$

Using a method inspired by Buchdahl 1990, we show elsewhere (Le Poncin-Lafitte *et al.* 2004) that $\Omega^{(2)}(x_A, x_B)$ may be written in the form

$$\begin{aligned}\Omega^{(2)}(x_A, x_B) &= \frac{1}{2}(x_B^\mu - x_A^\mu)(x_B^\nu - x_A^\nu)\\ &\times\int_0^1 \Big[\, h^{(2)}_{\mu\nu}(x_{(0)}(\lambda)) - \eta^{\rho\sigma}\, h^{(1)}_{\mu\rho}(x_{(0)}(\lambda))\, h^{(1)}_{\nu\sigma}(x_{(0)}(\lambda))\\ &\qquad -\eta^{\rho\sigma}\,\frac{\partial\Omega^{(1)}}{\partial x^\rho}(x_A, x_{(0)}(\lambda))\, h^{(1)}_{\mu\nu,\sigma}(x_{(0)}(\lambda))\Big]\, d\lambda\\ &\qquad +\frac{1}{2}\eta^{\mu\nu}\,\frac{\partial\Omega^{(1)}}{\partial x_B^\mu}(x_A, x_B)\,\frac{\partial\Omega^{(1)}}{\partial x_B^\nu}(x_A, x_B)\,,\end{aligned} \tag{14}$$

where the line integrals are taken along the unperturbed geodesic connecting x_A and x_B defined by the parametric equations

$$x^\alpha_{(0)}(\lambda) = (x_B^\alpha - x_A^\alpha)\lambda + x_A^\alpha\,, \quad 0 \le \lambda \le 1\,. \tag{15}$$

3. APPLICATION TO A STATIC, SPHERICALLY SYMMETRIC BODY

In order to apply the general results obtained above, let us determine the world function and the time transfer function in the second post-Minkowskian approximation when points x_A and x_B are both outside a static, spherically symmetric body of mass M. We suppose that the metric components may be written as

$$\begin{aligned} h^{(1)}_{00} &= -\frac{2M}{c^2 r}\,, \quad h^{(1)}_{0i} = 0\,, \quad h^{(1)}_{ij} = -\frac{2\gamma M}{c^2 r}\delta_{ij}\,,\\ h^{(2)}_{00} &= \frac{2\beta M^2}{c^4 r^2}\,, \quad h^{(2)}_{0i} = 0\,, \quad h^{(2)}_{ij} = -\frac{3\delta M^2}{2c^4 r^2}\delta_{ij}\,,\end{aligned} \tag{16}$$

where β and γ are the usual post-Newtonian parameters and δ is a post-post-Newtonian parameter (in general relativity, $\beta = \gamma = \delta = 1$). Furthermore, we suppose that x_A and x_B are such that the connecting geodesic path is entirely in the exterior space. We use the notations

$$r = |\boldsymbol{x}|\,, \quad r_A = |\boldsymbol{x}_A|\,, \quad r_B = |\boldsymbol{x}_B|, \quad R_{AB} = |\boldsymbol{x}_B - \boldsymbol{x}_A|\,.$$

It is easily seen that $G\Omega^{(1)}(x_A, x_B)$ is the term due to the mass in the multipole expansion of the world function given by Eq. (56) in Linet and Teyssandier 2002 (see also John 1975) :

$$\Omega^{(1)}(x_A^0, \boldsymbol{x}_A, x_B^0, \boldsymbol{x}_B) = -\frac{M}{c^2}\left[(x_B^0 - x_A^0)^2 + \gamma R_{AB}^2\right] F(\boldsymbol{x}_A, \boldsymbol{x}_B)\,, \tag{18}$$

where

$$F(\boldsymbol{x}_A,\boldsymbol{x}_B)=\int_0^1\frac{d\lambda}{|\boldsymbol{x}_{(0)}(\lambda)|}=\frac{1}{R_{AB}}\ln\left(\frac{r_A+r_B+R_{AB}}{r_A+r_B-R_{AB}}\right)\,. \tag{19}$$

For the integrals of second order involving $h^{(2)}_{\mu\nu}$ and terms quadratic in $h^{(1)}_{\mu\nu}$, we find

$$\begin{aligned}&\frac{1}{2}(x^\mu_B-x^\mu_A)(x^\nu_B-x^\nu_A)\int_0^1\left[\,h^{(2)}_{\mu\nu}(x_{(0)}(\lambda))-\eta^{\rho\sigma}\,h^{(1)}_{\mu\rho}(x_{(0)}(\lambda))\,h^{(1)}_{\nu\sigma}(x_{(0)}(\lambda))\right]d\lambda\\&\quad=\frac{M^2}{c^4}\left[(\beta-2)(x^0_B-x^0_A)^2+\left(2\gamma^2-\frac{3\delta}{4}\right)R^2_{AB}\right]E(\boldsymbol{x}_A,\boldsymbol{x}_B)\,,\end{aligned} \tag{20}$$

where $E(\boldsymbol{x}_A,\boldsymbol{x}_B)$ is given by

$$E(\boldsymbol{x}_A,\boldsymbol{x}_B)=\int_0^1\frac{d\lambda}{|\boldsymbol{x}_{(0)}(\lambda)|^2}=\frac{\arccos(\boldsymbol{n}_A\cdot\boldsymbol{n}_B)}{r_Ar_B\sqrt{1-(\boldsymbol{n}_A\cdot\boldsymbol{n}_B)^2}}\,, \tag{21}$$

$\boldsymbol{n}_A$ and $\boldsymbol{n}_B$ being defined as

$$\boldsymbol{n}_A=\boldsymbol{x}_A/r_A\,,\qquad\boldsymbol{n}_B=\boldsymbol{x}_B/r_B\,. \tag{22}$$

For the integral involving the gradient of $\Omega^{(1)}$, we obtain

$$\begin{aligned}&-\frac{1}{2}(x^\mu_B-x^\mu_A)(x^\nu_B-x^\nu_A)\int_0^1\eta^{\rho\sigma}\,\frac{\partial\Omega^{(1)}}{\partial x^\rho}(x_A,x_{(0)}(\lambda))\,h^{(1)}_{\mu\nu,\sigma}(x_{(0)}(\lambda))d\lambda\\&\quad=\frac{M^2}{c^4}\left[(x^0_B-x^0_A)^2+\gamma R^2_{AB}\right]\left[\left(1+\frac{r_A}{r_B}\right)\frac{1}{R^2_{AB}}\frac{(x^0_B-x^0_A)^2+\gamma R^2_{AB}}{r_Ar_B+(\boldsymbol{x}_A\cdot\boldsymbol{x}_B)}\right.\\&\qquad\left.-2\gamma E(\boldsymbol{x}_A,\boldsymbol{x}_B)-\frac{(x^0_B-x^0_A)^2-\gamma R^2_{AB}}{R^2_{AB}}\frac{F(\boldsymbol{x}_A,\boldsymbol{x}_B)}{r_B}\right]\,.\end{aligned} \tag{23}$$

Substituting Eqs. (20) and (23) into Eq. (14), and then carrying out the calculation of the square of the gradient of $\Omega^{(1)}(x_A,x)$, we obtain an expression for the world function as follows

$$\begin{aligned}&\Omega(x_A,x_B)=\frac{1}{2}(x^0_B-x^0_A)^2-\frac{1}{2}R^2_{AB}\\&-\frac{GM}{c^2}\left[(x^0_B-x^0_A)^2+\gamma R^2_{AB}\right]F(\boldsymbol{x}_A,\boldsymbol{x}_B)\\&+\frac{G^2M^2}{c^4}\left\{\frac{(x^0_B-x^0_A)^4}{R^2_{AB}}\left[\frac{1}{r_Ar_B+(\boldsymbol{x}_A\cdot\boldsymbol{x}_B)}-\frac{1}{2}F^2(\boldsymbol{x}_A,\boldsymbol{x}_B)\right]\right.\\&+(x^0_B-x^0_A)^2\left[\frac{2\gamma}{r_Ar_B+(\boldsymbol{x}_A\cdot\boldsymbol{x}_B)}-(2-\beta+2\gamma)E(\boldsymbol{x}_A,\boldsymbol{x}_B)\right.\\&\qquad\left.+(2+\gamma)F^2(\boldsymbol{x}_A,\boldsymbol{x}_B)\right]\\&\left.+R^2_{AB}\left[\frac{\gamma^2}{r_Ar_B+(\boldsymbol{x}_A\cdot\boldsymbol{x}_B)}-\frac{3\delta}{4}E(\boldsymbol{x}_A,\boldsymbol{x}_B)-\frac{\gamma^2}{2}F^2(\boldsymbol{x}_A,\boldsymbol{x}_B)\right]\right\}+O(G^3)\,.\end{aligned} \tag{24}$$

Now substituting for $\Omega(x_A,x_B)$ from Eq. (24) into Eq. (5) and then solving this equation thus obtained for $x^0_B-x^0_A$, we find for the time transfer function in the second post-Minkowskian approximation

$$\begin{aligned}\mathcal{T}(\boldsymbol{x}_A,\boldsymbol{x}_B)\;&=\;\frac{R_{AB}}{c}+\frac{(\gamma+1)GM}{c^3}\ln\left(\frac{r_A+r_B+R_{AB}}{r_A+r_B-R_{AB}}\right)\\&\quad+\frac{G^2M^2R_{AB}}{c^5}\left[\kappa E(\boldsymbol{x}_A,\boldsymbol{x}_B)-\frac{(1+\gamma)^2}{r_A\,r_B+(\boldsymbol{x}_A\cdot\boldsymbol{x}_B)}\right]\,,\end{aligned} \tag{25}$$

where

$$\kappa = 2 - \beta + 2\gamma + \frac{3\delta}{4}\,. \tag{26}$$

For $\gamma = \beta = \delta = 1$, we recover the expression of time transfer found by Brumberg (1987) within general relativity. Now, substituting for $\mathcal{T}$ from Eq. (25) into Eqs. (8)-(9) and then putting $\mathbf{N}_{AB} = (\boldsymbol{x}_B - \boldsymbol{x}_A)/R_{AB}$ yield for the covariant components of the vectors tangent at $\boldsymbol{x}_A$ and $\boldsymbol{x}_B$

$$\mathbf{l}_A = (l_i)_A = -\mathbf{N}_{AB} + G\mathbf{l}_{(1)}(\boldsymbol{x}_A, \boldsymbol{x}_B) + G^2\mathbf{l}_{(2)}(\boldsymbol{x}_A, \boldsymbol{x}_B) + O(G^3)\,, \tag{27}$$

$$\mathbf{l}_B = (l_i)_B = -\mathbf{N}_{AB} - G\mathbf{l}_{(1)}(\boldsymbol{x}_B, \boldsymbol{x}_A) - G^2\mathbf{l}_{(2)}(\boldsymbol{x}_B, \boldsymbol{x}_A) + O(G^3)\,, \tag{28}$$

where contributions $\mathbf{l}_{(1)}$ are given in Linet and Teyssandier (2002)

$$\mathbf{l}_{(1)}(\boldsymbol{x}_A, \boldsymbol{x}_B) = -(\gamma+1)\frac{M}{c^2}\frac{(r_A + r_B)\mathbf{N}_{AB} + R_{AB}\boldsymbol{n}_A}{r_A r_B(1 + \boldsymbol{n}_A.\boldsymbol{n}_B)}\,. \tag{29}$$

For the post-post-Minkowskian effect we find

$$\begin{aligned}
\mathbf{l}_{(2)}(\boldsymbol{x}_A, \boldsymbol{x}_B) \;=\; & \frac{M^2}{c^4 r_A r_B}\left[\frac{(1+\gamma)^2}{1 + \boldsymbol{n}_A.\boldsymbol{n}_B} - \kappa r_A r_B E(\boldsymbol{x}_A, \boldsymbol{x}_B)\right]\mathbf{N}_{AB} \qquad (30)\\
& + \frac{M^2}{c^4 r_A r_B}\frac{R_{AB}}{r_A}\left[\frac{(1+\gamma)^2}{[1 + \boldsymbol{n}_A.\boldsymbol{n}_B]^2} - \kappa\frac{r_A r_B E(\boldsymbol{x}_A, \boldsymbol{x}_B) - \boldsymbol{n}_A.\boldsymbol{n}_B}{1 - (\boldsymbol{n}_A.\boldsymbol{n}_B)^2}\right]\boldsymbol{n}_A\\
& + \frac{M^2}{c^4 r_A r_B}\frac{R_{AB}}{r_A}\left[\frac{(1+\gamma)^2}{[1 + \boldsymbol{n}_A.\boldsymbol{n}_B]^2} - \kappa\frac{1 - (\boldsymbol{n}_A.\boldsymbol{n}_B) r_A r_B E(\boldsymbol{x}_A, \boldsymbol{x}_B)}{1 - (\boldsymbol{n}_A.\boldsymbol{n}_B)^2}\right]\boldsymbol{n}_B\,. \qquad (31)
\end{aligned}$$

4. REFERENCES

Buchdahl, H. A. 1990, *Int. J. Theor. Phys.* **29**, 209.
Brumberg, V. A. 1987, *Kinematics Phys. Celest. Bodies* **3**, 6.
Ciufolini, I. and Ricci, F. 2002, *Class. Quant. Grav.* **19**, 3863.
Danner, R. and Unwin, S. 1999, Space Interferometry Mission, JPL 400-811, 3/99, 70.
Epstein, R. and Shapiro, I. I. 1980, *Phys. Rev.* D **22**, 2947.
Fischbach, E. and Freeman, B. S. 1980, *Phys. Rev.* D **22**, 2950.
John, R. W. 1975, *Exp. Techn. Phys.* **23**, 127.
Klioner, S. A. 1991, *Sov. Astron.* **35**, 523.
Klioner, S. A. and Kopeikin, S. M. 1992, *Astron. J.* **104**, 897.
Kopeikin, S. M. 1997, *J. Math. Phys.* **38**, 2587.
Kopeikin, S. M. and Schäfer, G. 1999, *Phys. Rev.* D **60**, 124002.
Kopeikin, S. M. and Mashhoon B. 2002, *Phys. Rev.* D **65**, 064025.
Linet, B. and Teyssandier, P. 2002, *Phys. Rev.* D **66**, 024045.
Le Poncin-Lafitte, C., Linet, B. and Teyssandier, P., in preparation.
Perryman, M. A. C., *et al.* 2001, *Astron. Astrophys.* **369**, 339.
Richter, G. W. and Matzner, R. A. 1982 *Phys. Rev.* D **26**, 2549.
Richter, G. W. and Matzner, R. A. 1983 *Phys. Rev.* D **28**, 3007.
Synge, J. L. 1964, Relativity: The General Theory (North-Holland, Amsterdam, 1964).
Will, C. M. 1988, *Am. J. Phys.* **56**, 413.

THE BCRS, GCRS AND THE CLASSICAL ASTRONOMICAL REFERENCE SYSTEM

M. SOFFEL
Lohrmann Observatory,
Dresden Technical University,
01062 Dresden, Germany

ABSTRACT. The roles of the BCRS and the GCRS are reviewed. Problems related with the traditional astronomical equinox based reference system in the framework of relativity are discussed.

1. THE BCRS AND THE GCRS

According to IAU2000-Resolution B1.3 (Soffel et al., 2003) the Barycentric Celestial Reference System (BCRS) with coordinates $(t, \mathbf{x})$ is defined by a metric tensor of the form

$$\begin{aligned} g_{00} &= -1 + \frac{2w}{c^2} - \frac{2w^2}{c^4} + \mathcal{O}(c^{-5}) \\ g_{0i} &= -\frac{4}{c^3} w^i + \mathcal{O}(c^{-5}) \\ g_{ij} &= \delta_{ij} \left(1 + \frac{2}{c^2} w \right) + \mathcal{O}(c^{-4}) \,. \end{aligned} \tag{1}$$

Here, the gravito-electric potential w generalizes the usual Newtonian gravitational potential U and the gravito-magnetic potential w^i describes gravitational effects resulting from moving gravitational sources. The order symbols in equation 1 indicate that the validity of the metric tensor is restricted to the first post-Newtonian approximation of Einstein's theory of gravity. By the choice of the metric tensor the orientation of spatial BCRS coordinates is fixed only up to some constant, i.e., time independent rotation. One might think of this orientation to be determined by the ICRS/ICRF. For special purposes, however, the spatial axes might differ from these basic ones by a constant rotation matrix and the orientation, e.g., given by some 'ecliptic of some fixed epoch'.

IAU2000-Resolution B1.3 also specifies the Geocentric Celestial Reference System (GCRS) with coordinates $(T, \mathbf{X})$ by a corresponding geocentric metric tensor, where external bodies contribute only tidal terms that grow with increasing coordinate distance from the geocenter. One can show that because of the acceleration of the geocenter the GCRS is only a local system that cannot be extended to infinity.

Both systems, the BCRS and the GCRS might be considered as quasi-inertial with respect to rotational motion. However, if relativity is taken into account the BCRS and the GCRS are actually quite different systems that are related by some complicated 4-dimensional space-time

transformation (some generalized Lorentz-transformation; e.g., Soffel et al., 2003). Both systems have their own specific roles. The BCRS serves as basis for solar-system ephemerides, for the definition of the ecliptic, for interplanetary spacecraft navigation. It is the fundamental system where concepts such as proper motion or radial velocity of stars can be defined and where the relation with remote objects (quasars etc.), hence to the ICRS, is given directly. On the other hand the GCRS is used for the description of physical processes and time scales in the vicinity of the Earth, the dynamics of the Earth itself, for the introduction of potential coefficients for the Earth's gravity field, for satellite theory etc. Concepts such as rotation axis, CIP, CIO or equator are basically defined in the GCRS whose spatial coordinates differ from those of the ITRS by a time dependent rotation matrix only. To stress again: the barycenter and the geocenter carry their own celestial (quasi-inertial) system.

2. PROBLEMS WITH THE CLASSICAL ASTRONOMICAL EQUINOX BASED SYSTEM IN THE FRAMEWORK OF RELATIVITY

The orientation of some BCRS[E_0] (assuming the standard BCRS to be oriented according to the ICRS) according to some (ccordinate) fixed ecliptic of some epoch presents no problem. One might then construct a corresponding GCRS[E_0] as kinematically non-rotating and thus oriented according to the BCRS[E_0]. Some equator, 'GCRS-ecliptic' (e.g., as $X-Y$-plane) and equinox can then be defined as coordinate quantities in the GCRS. If such a construction, however, in virtue of the complicated 4-dimensional space-time transformation between the BCRS and the GCRS, would yield some useful generalization of the corresponding classical quantities is unclear.

The problem becomes much more serious if some dynamical equinox based system is considered. Even in the Newtonian framework different historical concepts for some moving mean ecliptic exist: some *inertial mean ecliptic* that usually is associated with the name of LeVerrier and some *rotating mean ecliptic*, associated with Newcomb. Note, that the corresponding mean equinoxes differ in right ascension by about 90 mas. For references the reader is referred to (Standish 1981, Kinoshita and Aoki 1983). It is obvious that some dynamical mean ecliptic might be defined as some $t = TCB$ dependent BCRS spatial coordinate plane.

In principle one might invent many ways of mapping such a plane into the GCRS. Let us consider the $(t, \mathbf{x}) \longleftrightarrow (T, \mathbf{X})$ transformation (the relation between the BCRS and the GCRS) in the form

$$\begin{aligned} T &= t - \frac{1}{c^2}\left(A(t) + \mathbf{v}_E \cdot \mathbf{r}_E\right) + \ldots \\ \mathbf{X} &= \mathbf{r}_E \left(1 + \frac{1}{c^2} w_{\rm ext}(\mathbf{x}_E)\right) + \frac{1}{2c^2}\mathbf{v}_E(\mathbf{v}_E \cdot \mathbf{r}_E) + \ldots \end{aligned} \tag{2}$$

Here, $\mathbf{r}_E = \mathbf{x} - \mathbf{x}_E$, $\mathbf{x}_E$ and $\mathbf{v}_E$ are the BCRS coordinate position and velocity of the geocenter and $w_{\rm ext}$ is the gravitational potential of all solar system bodies apart from the Earth. Such a transformation maps 4 space-time coordinates of an event. In that manner one might map the various events $(t, \mathbf{x}_{\rm eclip}(t))$ related with some dynamical BCRS ecliptic into the GCRS. However, a $t =$const. BCRS coordinate plane (mean ecliptic) will NOT be mapped into some $T =$const. GCRS plane and this naive mapping idea does not lead to something useful.

Another idea is due to George Kaplan (Kaplan 2003). One might consider only the orientation of some BCRS (mean) ecliptic as given by some angular momentum vector, defining the corresponding ecliptic pole. Normalize this vector with $\epsilon \to 0 : \mathbf{n}_\epsilon(t)$. Add the position vector of the geocenter to obtain $\mathbf{e}_\epsilon(t)$ and then transform the event $(t, \mathbf{e}_\epsilon(t))$ into the GCRS. Because of the small quantity ϵ only terms linear in $\mathbf{r}_E$ in the transformation are needed and

the transformed spatial vector reads

$$\mathbf{E}_\epsilon = \left(1 + \frac{w_{\rm ext}(\mathbf{x}_E)}{c^2}\right)\mathbf{n}_\epsilon + \frac{1}{2c^2}\mathbf{v}_E(\mathbf{v}_E \cdot \mathbf{n}_\epsilon) + \ldots \qquad (3)$$

Since the ecliptic is usually defined with respect to the Earth-Moon barycenter the second term will not be zero in principle. Actually the whole idea of transforming a direction from the BCRS to the GCRS and to face aberration terms is questionable. Note that the GCRS was NOT constructed by transforming some BCRS-pole.

Another idea would be to transform the BCRS solar-system ephemerides into the GCRS and to define some GCRS-ecliptic there. Still another idea would be to take the spherical angles of some BCRS ecliptic pole at time $t = TCB$ as spherical angles of some ecliptic pole in the GCRS at time $T = TCG$ at the geocenter (i.e., to take the same angles both in the BCRS and in the GCRS).

Possibly for the purpose of historical continuity one might think of such coordinate games. It is obvious, however, that in the spirit of relativity the new paradigm with quantities such as the CIP or the CIO being defined in the GCRS is preferred. Actually the real problem is this: if one is concerned about relativity one needs some overall consistent post-Newtonian scheme to describe Earth's rotation. Only then a definition of some GCRS-ecliptic becomes meaningful and a precession matrix can be defined to post-Newtonian order. However, such a consistent post-Newtonian scheme for the description of Earth's rotation does presently not exist. Clearly these problems have to be investigated in more detail.

3. REFERENCES

Kaplan, G., private communication, 2003
Kinoshita, H., Aoki, S., Celest.Mech., **31**, 329, 1983
Soffel, M., et al., Astron.J., **126**, 2687, 2003
Standish, M., Astron.Astrophys., **101**, L17, 1981

A GALACTIC POSITIONING SYSTEM

B. COLL[(1)], A. TARANTOLA[(2)]

(1) SYRTE-UMR 8630/CNRS - Observatoire de Paris
61, avenue de l'Observatoire - 75005 Paris, France
e-mail: bartolome.coll@obspm.fr

(2) Institut de Physique du Globe de Paris
4, place Jussieu - 75005 Paris, France
e-mail: albert.tarantola@ipgp.jussieu.fr

ABSTRACT. Relativistic Positioning Systems are the best realizations of coordinate systems conceived up to now. We propose to use the signals of millisecond pulsars as a relativistic positioning system valid in and beyond our Solar System. The analogue of a GPS receiver is here a radio telescope, so that such a positioning system is heavy to use, but its interest is strong. Its study constitutes a simplified version of the relativistic positioning system recently proposed as primary reference system for the Earth [1]. A simple qualitative analysis of this last system and its relation to the usual, conventional reference frames may be made, allowing to better understand this new class of coordinate systems.

1. POSITIONING SYSTEMS

A coordinate system is a mathematical object. A detailed protocol for its physical construction in the space-time is called a *location system.* A coordinate system may always be defined by its coordinate (hyper-)surfaces. Consequently, the physical objects needed to define a location system are *nothing but* those physical fields able to describe parameterized (hyper-)surfaces.

The most interesting class of location systems are the *positioning systems*, which allow every event to know immediately its own coordinates. Four sources in arbitrary motion in space-time, broadcasting parameterized light signals, constitute the ingredients for such positioning systems, these signals drawing cones centered on the world line of the sources, i.e., parameterized families of (hyper-)surfaces. The coordinates of a space-time event are then, by definition, the values of the parameters (t^1, t^2, t^3, t^4) of the four signals, as recorded by a receiver at the event.

2. THE GALACTIC POSITIONING SYSTEM

We propose to use millisecond pulsar pulses as the light signals for a positioning system valid for the Solar System and its neighbours. The pulses being sequenced, they need only to be parameterized, that is, enumerated with respect to an origin.

Because of the anomalies in shape and arrival time within the average pulse period [2], it is possible to broadcast a 'signature' of signals allowing any user to identify the origin and,

consequently, to find its proper coordinates.

A Galactic frame has already proposed. Its definition, as well as a first mathematical description, may be found in http://coll.cc . With present-day technology, this locates any space-time event with an accuracy of the order of 4 ns, i.e., of the order of one meter. This is not an extremely precise coordinate system, but it is extremely stable and has a great domain of validity.

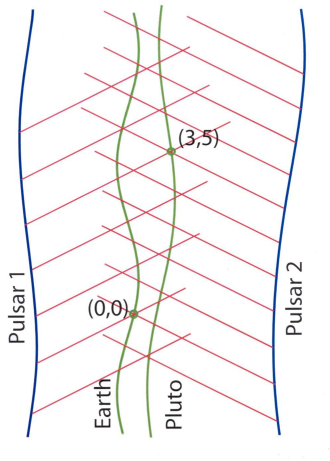

Figure 1: The anomalies in shape and arrival time of pulsar's pulses allow to identify, parameterize and broadcast the pulse chosen as origin. Then, any observer (event) in the Solar System may know its own coordinates.

A first point of interest in the analysis of the Galactic positioning system based on pulsars, is its relatively simple mathematical structure, as compared with its Earth analogue based on a constellation of satellites.

This advantage not only allows *i)* to make easy many calculations, but also *ii)* to give the first explicit example of Minkowskian relativistic positioning systems, *iii)* to interpret it as the instantaneous asymptotic limit of the relativistic GNSS and *iv)* to take it as the order zero in the gravitational field of more realistic models.

The possibility for the Earth to share a common immediate and relativistic coordinate system with other planets and satellites would improve the precision to which we know their position and trajectories. Should we, one day, be able to equip space-crafts with receivers of pulsar signals (in fact, miniature radio telescopes), they could continuously send their space-time position to us. This would help, for instance, in better understanding the vicinity of our Solar System and, in particular, Pioneer 10/11, Galileo and Ulysses acceleration anomalies [3].

We are grateful to François Biraud for helping in the selection of the four pulsars.

3. REFERENCES

1. B. Coll, JSR-2001, JSR-2002; also http://www.coll.cc.
2. D.R. Lorimer, Binary and Millisecond Pulsars at the New Millennium, in http://www.livingreviews.org/lrr-2001-5.
3. J.D. Anderson, M. Martin Nieto and S.G. Turyshev, A Mission to Test the Pioneer Anomaly, Int. J. Mod. Phys., D11 (2002) 1545-1552.

BASIS FOR A NATIVE RELATIVISTIC SOFTWARE INTEGRATING THE MOTION OF SATELLITES

S. PIREAUX, J-P. BARRIOT, G. BALMINO
UMR5562/GRGS, Observatoire Midi-Pyrénées
14 avenue Edouard Belin, 31400 Toulouse, France
e-mail: Sophie.Pireaux@cnes.fr

ABSTRACT. We introduce here a relativistically consistent software called RMI (Relativistic Motion Integrator). We compare it with the GINS software as an example of the classical approach consisting in the Newtonian formalism plus relativistic corrections.

1. THE CLASSICAL APPROACH: GINS

GINS [1] is a software routinely used to evaluate gravity potential models (GRIM4, GRIM5, EIGENS 1-2) from the determination of orbit perturbations, or for precise orbit determinations around the Earth (CHAMP, GRACE, JASON...) and around other solar system bodies, e.g. Mars (MGS...). It is based upon the usual formalism used in space geodesy, i.e. it relies upon the classical Newtonian description of motion, to which relativistic corrections are added. The number and type of corrections needed depend upon the precision in the measurements (clock precision and stability). The relativistic corrections on the forces already taken into account in GINS are: the Schwarzschild effect, function of the position and speed of the satellite; the Lens-Thirring effect, due to the rotation of the attracting body; the geodetic precession, function of the chosen coordinate system and due to the non inertial motion of the gravitational source in the solar system. Corrections are also applied on the measurements: a time tag correction, which stems from the transformation between the Universal Time Coordinate and the International Atomic Time, or the time referred to in the ephemeris; a relativistic time delay correction, due to the curvature of space-time. And finally, a correction on the clock frequency, owing to the presence of a gravitational field, is considered, leading to a relativistic Doppler effect. In relativistic theories, these post-Newtonian measurements corrections are a natural consequence of the distinction between proper time and coordinate time.

The classical "Newton + relativistic corrections" method briefly described here faces three major problems. First of all, it ignores that in General Relativity time and space are intimately related. Secondly, a (complete) review of all the corrections is needed in case of a change in conventions (adopted underlying metric), or if precision is gained in measurements. Thirdly, with such a method, one correction can sometimes be counted twice (for example, the reference frequency provided by the GPS satellites is already corrected for the main relativistic effect), if not forgotten. For those reasons, a new approach was suggested.

2. THE RELATIVISTIC APPROACH: RMI

In the relativistic approach implemented in RMI [2], the geodesic equations of motion are

directly numerically integrated for a chosen metric, with respect to proper time (for a massive particle). RMI is a prototype software taking only gravitational forces into account. It consists mainly of an integrator, plus separate modules containing metric definitions, the coordinate (space-time) transformations, or routines accessing the ephemeris.

To validate the different relativistic contributions in RMI orbits, the GINS software is used to produce template orbits. In a first step, comparison of RMI orbits with GINS orbits calculated for the Earth gravitational monopole plus a Schwarzschild correction shall validate the main relativistic effect in the RMI software, if the corresponding Schwarzschild metric is chosen. Then, harmonic terms (according to one of the geopotential models used in GINS) can further be added to the monopole term in the Schwarzschild metric used in RMI to test the harmonic contributions of the geopotentiel. In order to test the Lens-Thirring effect, the corresponding correction is selected from the GINS interface to produce the template orbits, while the Kerr metric is chosen from the RMI interface. With all Solar System masses set to zero except for the Earth and Sun masses, the GCRS (Geocentric Coordinate Reference System) metric provided by IAU (International Astronomical Union) 2000 resolutions [6,7] should include the additional geodetic precession effect when used to calculate RMI orbits. The latter RMI orbits can then be compared to orbits produced by GINS with the corresponding relativistic correction selected. Finally, the complete GCRS metric shall introduce additional contributions from other Solar System bodies in RMI orbits. These latter effects are simply modeled by Newtonian monopole terms in the GINS software, plus a coupling between the Moon and the Earth's flattening. We must notice that the GCRS metric already takes into acount an additional relativistic effect, the Thomas precession, which is not modeled in the RMI sofware.

Once the RMI software is coherently calibrated for all the relativistic effects considered in the GINS software, RMI will go beyond GINS capabilities. Not only will RMI coherently incorporate the latest IAU resolutions [6,7] regarding metric standards, prescription for time transformations [3,4], and latest IAU 2000/IERS 2003 standards on Earth rotation [5,6], but thanks to its separate modules, it will allow to easily update for metric, geopotential model prescriptions. However, the fondamental advantage of RMI over GINS resides in the fact that it coherently incorporates all the relativistic effects at the required metric order chosen.

3. REFERENCES

[1] GRGS, 2001, Descriptif modèle de forces: logiciel GINS, Note technique du Groupe de Recherche en Géodesie Spatiale (GRGS).

[2] X. Moisson, 2000, Intégration du mouvement des planètes dans le cadre de la relativité générale (thèse), Observatoire de Paris.

[3] A. W. Irwin, T. Fukushima, 1999, A numerical time ephemeris of the Earth, *Astron. Astrophys.*, **338**, 642–652.

[4] SOFA homepage. The SOFA libraries. IAU Division 1: Fundamental Astronomy. ICRS Working Group Task 5: Computation Tools. Standards of Fundamental Astronomy Review Board (2003). http://www.iau-sofa.rl.ac.uk/product.html.

[5] D. D. McCarthy, G. Petit, *IERS conventions (2003)*, IERS technical note 200? (2003). http://maia.usno.navy.mil/conv2000.html.

[6] IAU 2000 resolutions. IAU Information Bulletin, 88 (2001). Erratum on resolution B1.3. Information Bulletin, 89 (2001).

[7] M. Soffel et al., 2003, The IAU 2000 resolutions for astrometry, celestial mechanics and metrology in the relativistic framework: explanatory supplement. astro-ph/0303376v1.

Section VI)

HIGHLIGHTS OF THE 25th IAU GENERAL ASSEMBLY ON REFERENCE SYSTEMS AND FUNDAMENTAL ASTRONOMY

LA 25è ASSEMBLÉE GÉNÉRALE DE L'UAI SUR LES SYSTÈMES DE RÉFÉRENCE ET L'ASTRONOMIE FONDAMENTALE

HIGHLIGHTS OF THE SCIENTIFIC MEETINGS OF DIVISION I "FUNDAMENTAL ASTRONOMY"

N. CAPITAINE
SYRTE/UMR8630-CNRS
Observatoire de Paris, 61 avenue de l'Observatoire, 75014, Paris, France
e-mail: capitain@syrte.obspm.fr

ABSTRACT. This paper summarizes the Division I meetings that have been held during the XXVth General Assembly of the Astronomical Union in Sydney (16-24 July 2003).

1. INTRODUCTION

Division meetings have been organized for the first time during the XXVth General Assembly, according to the recent evolution in the scientific organisation of the IAU. The SOC of the Division I meetings was composed of the Division Board, enlarged with Vice-Presidents of Division Commissions, Presidents of the current Division Working Groups and with the upcoming Division I President, T. Fukushima, who was elected in March 2003. The first meeting (on 17 July) included three sessions devoted to scientific discussions and one session devoted to reports of the Division Working Groups. The second meeting (on 21 July) included one session devoted to the future organization of the Division. At the opening of the first meeting, the memory of P. Bretagnon and Ch. de Veght, who had outstanding contributions to the topics to be discussed and passed away last year, was recalled.

The report of Division I meetings at the General Assembly is being published in IAU Transactions Vol XXVB (2003, O. Engvold ed.) and that of Division I activity during the past triennium including the Working Groups have been published in the Reports in Astronomy (IAU Transactions Vol XXVA, 2003, H. Rickmann ed.). The main points of the presentations and discussion during the Division I meeting are summarized in the following sections.

2. SUMMARY OF THE SCIENTIFIC SESSIONS

Besides organisation issues regarding the Division 1 Working Groups, the two major points that have been discussed in the scientific sessions were the "Implementation of the IAU Resolutions" and the "Precession and Astronomical Standards".

2.1. Implementation of the IAU Resolutions

The session on the implementation of the IAU Resolutions has included a) two presentations on the present status of this implementation, b) a specific consideration of the implementation of the resolutions for the Almanacs (chaired by J. Vondrák) with five presentations and one large discussion, and c) a special discussion on experiences and problems (chaired by P. Wallace) introduced by two presentations.

a) N. Capitaine recalled that the implementation of the IAU 2000 resolutions required the adoption of (i) the IAU 2000 model (Resolution B1.6) to replace the IAU 1976/1980 precession-nutation for the motion of the Celestial Intermediate Pole (CIP) in the Geocentric Celestial Reference System (GCRS), (ii) a conventional model (Resolution B1.7) for high frequency motions of the CIP in the International Terrestrial Reference System (ITRS) and (iii) the conventional relationship for defining UT1 (Resolution B1.8) as proportional to the Earth Rotation Angle (ERA) between the Celestial and Terrestrial Ephemeris Origins (CEO and TEO). Expressions with an accuracy of a few microarcseconds have been provided in a number of scientific papers published in 2002 and 2003 for all the models necessary to implement the IAU 2000 system, using equivalently either the CEO-based or the equinox-based transformations.

D.D McCarthy presented the International Earth rotation and Reference system Service (IERS) implementation of the IAU resolutions in its products. The IERS Conventions now provides an outline of the procedures to be used along with software consistent with those procedures. IERS Bulletins A and B have made the data required to implement the resolutions available since January, 2003. To assist users in the transition period between the previous system and that recommended by the 24th General Assembly, the IERS also continues to provide data consistent with the previous system. It also plans to make available a file of frequently asked questions to assist users in the transition between systems.

b) J. Bangert introduced the special issue of implementing the new resolutions in the almanacs. These publications provide practical astronomical data in an accessible form to satisfy the needs of a wide variety of user applications such as navigation, pointing a telescope, planning an observing session, or scientific research. Implementing the IAU 2000 resolutions in the almanacs must be considered in the context of specific criteria (i.e. a proposed change is implemented only when it (1) will result in more accurate information in the almanac, (2) is based on sound scientific underpinnings, and (3) will result in data or information relevant to the users of the almanac). Moreover, a considerable lag has to be expected between the time a resolution is adopted and the time that it is implemented in the almanacs due to the time needed to develop, implement, and test new production software, and to the normal publication schedule.

Special presentations from various Almanac offices specified how they would implement the IAU resolutions on reference systems and Earth rotation adopted in 1997 and 2000.

G. Kaplan presented the changes in the Astronomical Almanac, prepared jointly by the US and UK nautical almanac offices and based to the greatest extent possible on IAU-endorsed and other internationally recognized standards. Both the reference data and algorithms used must be changed, and some new tabulations added. Some of the required modifications have already been made and others will be introduced into the editions now in preparation.

W. Thuillot reported on this implementation in the French ephemerides, which are prepared by the Intitut de Mécanique Céleste et de calcul des Ephémérides (IMCCE), at Paris Observatory, under the auspices of Bureau des longitudes. The use of new models for precession and nutation will be done at first and the changes in the systems of coordinates will only be introduced in parallel with the usual systems.

T. Fukushima reported on the two kinds of national almanacs in Japan; the more precise and comprehensive one for the nautical use, the Japanese Ephemeris (JE) by the Maritime Safety Agency (MSA), and the more compact for the civil use, the Ephemeris Year Book (EYB) by the National Astronomical Observatory of Japan (NAOJ). The MSA will make no revision of the JE until all the required procedures for the changes are clear. As for EYB, a major revision from the edition of Year 2003 was already made including (1) the change of base planetary/lunar ephemeris from DE200 to DE405, (2) the change of nutation theory from IAU 1980 to Shirai and Fukushima (2001), and (3) the change of geodetic datum from Tokyo datum to the new Tokyo datum, being almost the same as the latest ITRF.

I. Kumkova gave the report prepared by M.L. Sveshnikov, N.I. Glebova, M.V. Lukashova, A.A. Malkov on the Russian astronomical yearbooks (RAS) prepared at the Institute of Applied astronomy in St.-Petersburg. The report recalled that the structure and contents of the IAA RAS are changed regularity to satisfy IAU resolutions and requirements of users. The current plan of implementing the IAU 2000 resolutions includes the replacement of planetary ephemerides, precession-nutation model, stellar catalogue and transfer to the new CEO concept. It will be carried out during 2003-2006.

The presentations and discussion in this session showed that procedures, models and software are available to users for the implementation of the IAU 2000 resolutions and that the implementation has already been done in IERS products and will be done in almanacs in a near future. They have also made it clear that (1) official recommendations are required in order that the almanacs implement the new IAU resolutions based on a common an approved terminology, (2) an important educational effort is needed to inform a wider astronomical community about the new system recommended in IAU 2000 Resolutions.

c) In this context, G. Kaplan presented an alternative to the usual quantities used for positioning the CEO. This scheme may have pedagogical and pratical advantages for the vast majority of astronomers who are unfamiliar with the history of this topic as it consists in a simple vector differential equation for the position of a non-rotating origin on its reference sphere. This directly yields the ICRS right ascension and declination of the CEO, or the ITRF longitude and latitude of the TEO, as a function of time and also yields a simple vector expression for apparent sidereal time.

C. Ma recalled that initial set of FAQs on the recent IAU resolutions has been prepared for linking from relevant web sites and discussed the content, future refinement and expansion, and distribution.

2.2 Precession and Astronomical Standards

The session on Precession and Astronomical Standards has included a) four presentations on improved precession models followed by a discussion (chaired by G. Kaplan) and b) one presentation on astronomical standards followed by a discussion (chaired by V. Dehant).

a) T. Fukushima presented his recent precession solution which uses modified Williams' formulation (1994) for precession and nutation and is based on (i) the planetary precession of Harada and Fukushima (2003) derived from DE405 JPL ephemerides, (ii) the nutation theory of Shirai and Fukushima (2001) and (iii) a fit of the luni-solar precession to VLBI observation of celestial pole offsets (1979-2000). As by-products, he obtained the new determinations of (1) the mean pole offset at J2000.0, (2) the speed of general precession in longitude at J2000.0, (3) the mean obliquity of ecliptic at J2000.0, and (4) the dynamical flattening of the Earth.

N. Capitaine presented the expressions for precession quantities compliant with IAU 2000 that have been obtained by N. Capitaine, P. Wallace and J. Chapront (2003). This includes (1) the currently used precession quantities, in agreement with the MHB corrections to the precession rates, that appear in the IERS Conventions 2000 and (2) the new P03 precession expressions that are dynamically consistent. The P03 precession of the ecliptic is based on most recent theories for the Earth and the Moon and the most precise numerical ephemerides. The P03 solution for the precession of the equator is dynamically consistent and compliant with IAU 2000. This also reported on the most suitable precession quantities to be considered in order to be based on the minimum number of variables and to be the best adapted to the most recent models and observations.

W. Thuillot presented a recent work on precession expressions and consideration about the EOP and a conventional ecliptic that was done by P. Bretagnon, A. Fienga and J.L. Simon

(2003). The new precession quantities consistent with the IAU 2000A model have been derived from the analytical solution of the rotation of the rigid Earth SMART97 which provided together precession and nutation and was based on the new value of the precession rate of the equator in longitude. This work includes the derivatives of the expressions with respect to the precession constant and the obliquity. It also reports on the possible use of Euler angles in IERS publications for a global modelling of the Earth rotation and proposes the definition of a conventional ecliptic plane close to the mean ecliptic J2000 and with a non-rotating origin.

J. Hilton discussed the future directions in precession and nutation. One concern is that the IAU 2000A precession-nutation theory is computationally expensive, requiring over one thousand evaluations of sine and cosine functions to evaluate IAU 2000A just once and IAU 2000B has a reduced precision that was designed to cover only a limited time span around the epoch J2000.0, whereas applications such as the Multiyear Interactive Computer Almanac (MICA), are being developed that require long coverage periods and the ability to reach the accuracy of modern day observations. He concluded that to address this deficiency future precession and nutation theories will need to do one or more of the following: (a) make a serious effort to optimize the code; (b) reduce its precision to match the accuracy with which the Earth orientation can accurately be determined; (c) no longer separate terms that are so close together in frequency space that their individual contributions cannot be determined at the level of accuracy of the observations; (d) move from representation as an analytic theory to a numerically integrated representation.

Presentations and discussion in this session showed that a physically consistent precession should have to be considered in the near future based on an improved precession of the ecliptic and that an IAU Working Group is needed to recommend a new precession model resulting from comparisons of the recent available models.

b) M. Standish discussed the sources and uses of astronomical constants and especially the use of ephemerides based upon the independent variable, "Teph" (which has been used over the past three decades for the ephemerides created at JPL, CfA, and IPA) and compared it with the use of ephemerides based upon the recent IAU-defined "TCB". He showed that Teph and TCB are are both relativistic coordinate times that are mathematically equivalent. Proper use of a Teph-based ephemeris should give results identical to those obtained using a TCB-based ephemeris. He discussed special situations such as navigating a spacecraft in orbit around a remote planet while timing the dynamics on an earth-based clock.

The discussion about astronomical standards has made it clear that a strong coordination is required between the various sources of standards (IAU, IERS or IAG values) in order to improve consistency between the standards for astronomical or geophysical uses. An effort should be done in that sense by the representatives of these bodies in various Committees.

3. SUMMARY OF THE SESSION ON DIVISION I ORGANISATION

The last session of Division I meetings has been devoted to a large discussion on the future of Division I commissions and working groups within the future revised by-laws of the IAU. According to the discussions that have been held during the scientific sessions and during the session devoted to the reports of the Division I Working Groups, Division I Board proposed to continue the Working Groups that have very specific tasks and to establish two new Working Groups: one on "Precession and ecliptic" (Chair: J. Hilton, USA) and the other on "Nomenclature for Fundamental Atronomy" (Chair: N. Capitaine, France). This proposal was presented by the upcoming President, Toshio Fukushima, at the end of the Joint Discussion 16 "The International Celestial Reference System: Maintenance and future realizations" (on 22 July) during which the future of the Working Group ICRS, considering a possible distribution of its tasks to some Division I Commissions, has been discussed.

A BRIEF REPORT ON IAU JOINT DISCUSSION 16, "THE INTERNATIONAL CELESTIAL REFERENCE SYSTEM, MAINTENANCE AND FUTURE REALIZATIONS"

D.D. MCCARTHY
U. S. Naval Observatory
Washington, DC 20392 USA
e-mail: dmc@maia.usno.navy.mil

ABSTRACT. The IAU Joint Discussion 16 (JD16) was held in conjunction with the XXVth General Assembly in July, 2003. Papers related to the maintenance of the International Celestial Reference System were presented in the one-day session, and these were followed by discussion that pointed out the need for standard nomenclature. This issue was addressed by the formation of a Division 1 Working Group on the subject. JD16 also pointed out the requirement for a dynamical expression for precession which was addressed by the creation of a Division 1 Working Group on Precession and the Ecliptic. It also showed that although plans are being implemented to provide reference frames for the future, there is a need for improved coordination of astrometric observations. Finally it should be noted that the discussion pointed out the concern for the future organization of IAU Division 1.

1. INTRODUCTION

The international Astronomical Union (IAU) Joint Discussion 16 (JD16) was held in connection with the XXVth General Assembly of the IAU in Sydney, Australia in July 2003. The title of the meeting was "The International Celestial Reference System, Maintenance and Future Realizations." The International Celestial Reference System (ICRS) has recently been redefined with the adoption of an International Celestial Reference Frame (ICRF) and revised concepts and models to access the system. The ICRF is a radio reference frame and the current realization in optical wavelengths is the HIPPARCOS Catalogue. Maintenance and improvement of the ICRF requires continuing, coordinated observations. Extension and densification of the system to other wavelengths remains as a work to be accomplished. It is also necessary at this time to anticipate the maintenance and extension of the ICRF to meet future needs. The models currently used in the definition of the system also require maintenance to ensure that they are able to meet improving observational accuracy in all wavelengths. The potential significant improvement of reference frames from the results of future space astrometry missions requires planning for the long-term realization of the ICRS. These topics were addressed by a series of invited and contributed presentations

2. PRESENTATIONS

Session 1 of JD 16 was entitled "The International Celestial Reference Frame." It was introduced with a paper by A. Fey and J. Souchay entitled "Status of the International Celestial Reference Frame." C. Ma presented a paper, "Potential refinement of the ICRF" outlining plans to improve the frame. This was followed by a review of recent work done in the Geoscience Australian IVS analysis center by O. Titov. A. M. Gontier and M. Feissel provided a presentation "Contribution of stable radio sources to ICRF improvements" showing the importance of source position stability to the astrometric observations. M. Hosokowa completed the session with a paper that he prepared in conjunction with his colleagues entitled "Astrometric microlensing and degradation of reference frames" that pointed out the limitations on accuracy imposed by microlensing.

Session 2, "Extension of the International Celestial Reference Frame" contained presentations dealing with providing realizations of the reference system in other wavelengths. C. Jacobs in a paper that he prepared with his colleagues entitled "Extending the ICRF to higher radio frequencies: 24 and 43 GHz" pointed out the advantages to moving to higher frequencies. S. Urban followed with a presentation "Densification of the ICRF/HCRF in visible wavelengths" showing plans to improve the reference frame of most concern to the astronomical community. Extension to the infrared was discussed in the paper by N. Zacharias *et al.* entitled "Extending the ICRF into the infrared: 2MASS-UCAC astrometry." C. Pinigin *et al.* presented a paper,"About progress of the link optical-radio systems," and P. Charlot finished the session with a paper, "Source structure" describing recent work in characterizing source structure.

Session 3 dealt with models needed to analyze the astrometric observations that are used to produce the ICRF. V. Dehant in a paper "Geophysical nutation model" described the geophysical background of the recently adopted IAU 2000 precession-nutation model. P. Wallace provided practical implementation procedures in his paper, "Practical consequences of improved precession-nutation model." The philosophy and status of the International Earth Rotation and Reference System Service (IERS) Conventions was described in a presentation by D. McCarthy and G. Petit. T. Fukushima showed a new determination of precession formulas and M. Soffel *et al.* discussed the relativistic concerns with the ICRS in their paper entitled "ICRS, ITRS and the IAU resolutions concerning relativity." J. Vondrak described a reference frame provided largely by historical observations in visual wavelengths made to determine the Earth's orientation in his paper "Earth orientation catalogue - An improved reference frame." I. Platais closed the session with his paper "Astrometry with large un-astrometric telescopes" that outlined work that could be done to improve the ICRF that made use of instrumentation not usually used to make astrometric observation.

The final session was devoted to Space-Based Astrometry and Dynamical Reference Frames. It was introduced with a review of the status of space-based astrometric missions by R. Gaume. F. Mignard followed with a review of recent work on GAIA in his paper "Future space-based celestial reference frame," and the radioastron project was described in a presentation by W. Zharov and colleagues. F. Mignard presented a paper by J. Kovalevsky entitled "Misleading proper motions of galactic objects at the mas level." The relationship of modern dynamical ephemerides to the ICRS was covered by M. Standish in his paper "Relating the dynamical frame and the ephemerides to the ICRF."

3. POSTERS

The work of JD16 was enhanced by a large number of poster contributions. These are listed below.

Wang Wen-Jun, "Celestial three-pole rotations of the Earth."
Hu Hui, "Optical positions of 55 radio stars."
W. Dick, "The ICRS and the IERS information system."
V. Martin, "Ground-based astrometry: optical-radio connection."
P.C. Rocha Poppe, "Relativistic reference systems transformations."
E. Khrutskaya, "Pul-3 catalog of 58483 stars on the Tycho-2 system."
I. Kumkova, "ICRS-ITRS connection consistent with IAU(2000) resolutions."
E. Pitjeva, "The planetary ephemerides EPM and their orientation to ICRF."
M. Stavinschi, "Report of the WG: Future development of ground-based astrometry."
B. Bucciarelli,"Astrometric measurements of radio-stars optical counterparts."
M. Stavinschi, "Reference frames and ground-based astrometry."
S. Lambert, "Coupling between the Earth's rotation rate and nutation."
G. Bourda, "Temporal gravity field and modelisation of Earth rotation."
G. Damljanovic, "ICRF densification via Hipparcos-2MASS cross identification."
F. Mitsumi, "On the construction of radio reference frame using VERA."
A. Fey, "Extending the ICRF to higher frequencies: imaging results."
P. Fedorov, "The star positions and proper motions of stars around ERS."
T. Yano, "Japanese astrometry satellite mission - JASMINE project."
M. Zacharias, "The USNO extragalactic reference frame link program.
A. Kahrin, "An-all wave classification and principle astrometry problem."
D. Boboltz, "Testing the Hipparcos/ICRF link using radio-stars."
J. Souchay, "Numerical approach to the free rotation of celestial bodies."
G. Kaplan, "Another look at non-rotating origins."
O. Roopesh, "IDV sources as ICRF sources: viability and benefits."
O. Roopesh, "USNO/ATNF astrometry and imaging of southern ICRF sources."
F. Bustos, "CDD-based astrometric measurements of photographic plates."
M. Crosta, "Relativistic satellite attitude in the realization of space-borne astrometric catalogues."

3. DISCUSSION

An open discussion prepared and led by P. K. Seidelmann followed the scheduled presentations. Notes from that discussion were taken by N. Zacharias and they form the basis of the following. To initiate the discussion, a list of reference system issues was presented to the participants. These are listed below along with relevant comments by participants.

Items for Discussion

a. Precession-nutation Model
   New precession theory?
   What angles - Newcomb or Williams?
   What nutation model?
   An abbreviated nutation theory with less accuracy?
   Include geodesic precession and nutation?
   Is it a BCRS or GCRS model?

b. Future of Equinox
Introduce Earth Rotation Angle?
Revise definition of ERA?
Dual system by IERS?
Dual system in almanacs?
Transition period specified?
For how long? 2004? Indefinitely?

c. Definition of equinox
Inertial or rotating

d. Introduce Conventional ecliptic
How defined, through x axis of ICRF? by node angle and obliquity?
For what purpose?
With what accuracy?

F. Mignard emphasized that the ecliptic moves and will change with time. D. McCarthy pointed out that this is a subject for the Working Group on precession and that a precise definition of the ecliptic is needed for planetary precession.

e. Terminology issues
CIO and TIO or CEO and TEO?
Stellar angle or Earth Rotation Angle?
right ascensions from equinox only?
right ascensions from CIO?
other terms?

C.Hohenkerk remarked that some concepts seem odd, and that the user is not concerned "which" RA,Dec is used, as long as there is some RA, Dec.

f. Unification of Lists of Constants
IAU Best Estimates
IAU 1976 Astronomical Constants
IERS Best Estimates
IUGG List of Constants
JPL DE 405 Constants
Astronomical Almanac Constants Used
Are all these necessary?
A joint IAU/IUGG committee?

g. Redefinition of UTC
UTC tied to UT1?
Use of "mean solar time"?
Leap seconds or not?

h. Implementation Issues
Who are the users?
What do users need?

What is really used by the IERS?
What is necessary for almanacs offices?
Standardized software?
Documentation required?
Dual availability for how long?
What to do now?

i. Roles of Organizations
WG on Reference systems of IAU Div I
IERS
IAU Comm 5
Others involved?

j. Possible Procedure
IAU /IUGG? WG on Reference Systems with subgroups established now
Dec 2004 WG proposals circulated
Mid 2005 Colloquium for discussion of proposals and draft resolutions
2006 Clarifying resolutions

k. Education Plan
Clear and convincing presentation of reference systems and justifications
Dissemination of information with proposals in Dec 2004
Distribution of 2005 Colloquium Proceedings
Wide distribution of any proposed resolutions well before IAU GA in 2006

In the general discussion following the presentation of the items for discussion K. Johnston said that some issues might not be solved earlier than 2006. P. Wallace argued that we need to get away from the "one-or-the-other" concept and that algorithms are now available for both paradigms so the user can choose. C. Jacobs noted that users need more education so that they can decide how complex they need to go for a given goal in accuracy. P. Wallace replied that there is a misconception that the "new paradigm is more complex," and that this was not true. The non-rotating origin procedure is simpler in concept; like spherical trigonometry and vectors: they are both there to choose. A participant said that this is difficult at the moment, that there is a need for education, and that currently we don't even know what to call things. K. Johnston suggested that there is no need for the general astronomers to make a change because current procedures are sufficient for their requirements. It is only the IERS and space astrometry applications that are concerned about sub-milliarcsecond accuracies and need to use the new more accurate system. It was pointed out that this was true, but people needed to realize that the basic values were coming from new definitions and methods.

At that point there was a break in the discussion, and T. Fukushima, President of Division I, presented some details regarding the future structure of Division I in the context of this discussion. He said that the ICRS WG has been dissolved because it was too large, with too many sub-tasks. As follow-up for two of the sub-tasks, two new Working Groups were being established. These are (1) precession and the ecliptic chaired by J. Hilton and (2) nomenclature in fundamental astronomy chaired by N. Capitaine.

The new IAU structure puts more emphasize on the Divisions and the Commissions are now dynamic, with a finite life time. It is possible to terminate commissions and to create new commissions upon request by the Division and approval by the IAU Executive Committee. Working groups can be established by approval of the Division, without Executive Committee contact. The approval process is fast, and can be done by e-mail, with no need to wait for a General Assembly.

Fukushima initiated a special committee for the re-organization of Division I. Members are T. Fukushima (chair), F. Mignard, I. Platais, G. Petit, and K. Seidelmann. For the 2003-2006 period (*i.e.* before the special committee issues their recommendations), the proposal for ICRS related issues is that Celestial Reference Frame issues will be directed to Commission 8 and that IERS related issues will be directed to Commission 19. A general discussion followed about the roles of Commissions 8 and 19.

A. Fey asked about the current members of the ICRS WG and whether their expertise would be lost until a re-organization was accomplished. Following some discussion T. Fukushima responded that the "WG ICRS" will continue to exist for next six months. During that time a re-arrangement can be organized by e-mail.

4. CONCLUSION

The Joint Discussion pointed out the need for standard nomenclature. This issue was addressed by the formation of a Division 1 Working Group on nomenclature. It also pointed out the requirement for a dynamical expression for precession which was addressed by the creation of a Division 1 Working Group on Precession and the Ecliptic. JD 16 also showed that although plans are being implemented to provide reference frames for the future, there is a need for improved coordination of astrometric observations. Finally it should be noted that the discussion pointed out the concern for the future organization of IAU Division 1. The pproceedings will be published and distributed by the U.S. Naval Observatory.

THOUGHTS ABOUT THE IMPLEMENTATION OF THE IAU 2000 RESOLUTIONS

P.K. SEIDELMANN
University of Virginia
Box 3818 University Station, Charlottesville VA 22903-0818, USA

1. INTRODUCTION

The International Celestial Reference System (ICRS) has been introduced as recommended by the International Astronomical Union (IAU). This is a fixed reference system that is epoch independent. It is implemented by a reference frame, the International Celestial Reference Frame (ICRF), which is based on non-moving distant radio sources. The optical implementation is based on those Hipparcos Catalog stars, which do not have known problems, and densified by optical catalogs on the Hipparcos reference frame.

Since most observations are made from the surface of the Earth, which has many motions, it is still necessary to use a moving, time dependent reference frame. A set of resolutions was adopted by the IAU in 2000, which introduces changes for the moving reference system. This is based on Earth kinematics rather than the solar system dynamics. There is a new precession-nutation model, IAU 2000A, with sub-milliarcsecond accuracies. Based on the new precession-nutation model, the Celestial Intermediate Pole (CIP) has been introduced to replace the Celestial Ephemeris Pole. A new fiducial point, the Celestial Ephemeris Origin (CEO) based on the non-rotating origin has been introduced, as a possible replacement for the equinox. It has the characteristic of having no motion along the instantaneous equator, all its motion is perpendicular to the instantaneous equator. Since observations now permit the determination of sub-daily periodic motions in the Earth's pole, arbitrarily all periodic motions with periods less than two days are considered polar motion.

Some additional changes are the introduction of geodesic precession and nutation in the precession-nutation model, the detection of free core nutation, although that is only represented in observational data and not included in the precession-nutation model.

These resolutions left some unanswered issues. Implementation and terminology issues remain to be considered.

2. INTERNATIONAL CELESTIAL REFERENCE SYSTEM (ICRS)

The ICRS is a fixed reference system that is epochless. It is based on extragalactic radio sources that are so distant that they have no apparent motions. It is specified so that its orientation is close to the FK5 system, within the errors of the FK5. The two reference systems Barycentric Celestial Reference System (BCRS) and Geocentric Celestial Reference System (GCRS) are defined based on gravitational potentials at the two origins. Their coordinate systems are defined to have the same orientations. They define the ICRS. The system includes a system of constants, solar system ephemerides, a precession-nutation model, and standard procedures.

a. The International Celestial Reference Frame (ICRF) is based on selected, well observed, well defined extragalactic radio sources. Unfortunately, they are optically faint. This frame can be determined and maintained to an accuracy of about 0.2 milliarcseconds (mas).

b. The ICRF is realized optically by the Hipparcos Catalog, which is the result of the Hipparcos mission. About 120,000 stars down to 11th magnitude without problems are the basis for the Hipparcos Reference Catalog. This catalog is accurate to about 1 mas at its epoch of 1991.25.

c. The ICRF is densified by the Tycho 2 Catalog, which is likewise limited to 11th magnitude, but it includes 2,000,000 stars with an accuracy of about 20 mas at epoch. Further densification is achieved by the USNO CCD Astrographic Catalog (UCAC) reaching about 16th magnitude with about 70,000,000 stars at accuracies ranging from 20 to 70 mas. The USNO B2.0 catalog contains billions of stars down to 21st magnitude with accuracies around 200 mas.

While the ICRF is epochless as a frame, the optical stars in the implementations have proper motions, so epochs must be specified and positions have to be corrected to specific dates by means of the proper motions.

3. MOVING REFERENCE FRAMES - PROPOSED CHANGES

With the fixed reference frame, ICRF, there is still the need for a moving reference frame, because the Earth from which most observations are made, is still in motion. However, there is not the need to base the moving reference system on the dynamics of the Earth orbit and the motions of the solar system. The ICRS is independent of the Earth dynamics which were the bases for the previous reference systems, like the FK5.

The proposed changes for the new moving reference frames are the following:

a. The new frames will be based on the kinematic motions of the Earth rather than the dynamics of the solar system.

b. A new precession- nutation model, IAU 2000A, that does not separate the two, but rather is a single model to be evaluated.

c. A new pole is introduced as an intermediate between the celestial and terrestrial reference frames. The new pole is determined from the IAU 2000A precession-nutation model and is called the Celestial Intermediate Pole (CIP).

d. A new fiducial point is introduced based on the non-rotating origin. This origin has no motion along the instantaneous equator, all its motion is perpendicular to the instantaneous equator. Thus, its motion along the equator is very slow and takes the form a saw tooth motion over time. The fiducial point is called the Celestial Intermediate Origin (CIO), or the Celestial Ephemeris Origin (CEO). This would replace the equinox.

e. A Terrestrial Intermediate Origin (TIO), or Terrestrial Ephemeris Origin (TEO), is based on the International Terrestrial Reference System (ITRS) of the IUGG. This origin represents the positions on the Earth.

f. The angle between the CIO and TIO is called the Earth Rotation Angle (ERA), or the stellar angle. This can be calculated from a formula or integrated based on the motions involved. This is in place of sidereal time.

g. The International Terrestrial Reference Frame (ITRF) is based on a catalog of positions on the surface of the Earth, similar to the use of a catalog of sources in the sky to define the ICRF.

h. An Intermediate Reference System (IRS) is based on the CIP and the CIO.

i. With the ability to observe the kinematics of the Earth with the Global Positioning System (GPS) on a continuous basis, it is possible to observe sub-daily periodic motions of the kinematics of the Earth. In order to separate nutation from polar motion, an arbitrary division has been introduced. Thus, all periodic motions with periods less than two days are considered polar motion.

j. Free core nutation, which cannot be accurately predicted, is not included in the precession-nutation model and must be added for accurate computations.

k. Geodesic precession and nutation, which are relativistic effects that arise in the transformation between the Geocentric Celestial Reference System (GCRS) and the Barycentric Celestial Reference System (BCRS), are included in the precession-nutation model, IAU 2000A. Thus, if the transformation is to be between a moving and a fixed geocentric reference frame, the geodesic precession and nutation terms must be removed from the precession-nutation model.

While the new moving reference frame has been proposed, the classical system can be improved to provide the same accuracies at least to 1 mas. Since there is a lot of software based on that system and many people are more familiar with it, it can be expected to continue in use. The classical system would use the equinox as the fiducial point, an improved precession theory, an improved separate nutation theory, the CIP pole as above, sidereal time with a new defining expression, and mean and true positions as usual.

4. IMPLEMENTATION ISSUES

The introduction of the ICRS and ICRF as the fixed reference system has been accomplished very smoothly and everyone should be using those. However, there are a number of outstanding issues concerning the implementation of the new moving reference frame system. Specifically:

a. The precession theory has not been properly updated. Thus, the equinox based system, using separate precession and nutation theories, does not have an accurate precession theory available. The new precession-nutation model, IAU 2000A, does not separate the two and only improves the precession constant value. An IAU Working Group has been appointed to solve this problem.

b. What angles should be used in the precession theory, Newcomb's or William's formulations? Should geodesic precession and nutation be included in the model? Is the precession-nutation model barycentric or geocentric? Is an abbreviated nutation theory, with less accuracy, needed by the users?

c. There are two definitions of the equinox; one is based on a uniformly moving ecliptic plane and one is based on the instantaneous position of the intersection of the equatorial and ecliptic planes. The uniformly moving plane definition has been traditionally used in the past. The difference in these definitions is about 0.1 arcsecond.

d. It appears likely that both the equinox and CEO based systems will be used in the future. For best accuracy the CEO system may be necessary, and there is some uncertainty

whether the IERS will provide the necessary data for the two systems as recommended by IAU resolutions. However, it appears certain that many organizations will not make the change to the CEO in the immediate future. Should the dual system be supported by the IERS and the almanac offices and for how long?

e. The concept of a conventional ecliptic has been suggested. How would this be defined? How would it be used and what accuracy would be required for it?

f. There is a lack of agreement so far concerning the nomenclature to be used with the new system. There are choices such as Celestial Ephemeris Origin (CEO) or Celestial Intermediate Origin (CIO), Terrestrial Ephemeris Origin (TEO) or Terrestrial Intermediate Origin (TIO), Earth Rotation Angle or stellar angle, which have not been resolved. There is also the question of the definition of right ascension and the use of that term. Should right ascensions only be measured from the equinox, or should they be measured from other fiducial points and they be specified by types, such as CEO right ascensions, equinox right ascensions, etc?. There is another IAU Working Group established to resolve these issues.

g. There is not a single accepted list of constants to be recommended. There are "best estimates" of constants available from the IAU, IERS, and IAG. The JPL Ephemerides include a list constants used for the ephemerides. The Astronomical Almanac, and other national almanacs, includes lists of constants and their sources, which are the bases for the data in those publications. The 1976 IAU System of Astronomical Constants is the latest official IAU list of constants, but in many cases these are out of date. Thus, it is recommended that everyone providing precise data should cite the constants that have been used. Should there be a joint IAU/IAG committee on constants?

5. REDEFINITION OF UTC

There is an International Telecommunications Union (ITU) study and discussion concerning the continuation of leap seconds. Does UTC need to be within some limit of UT1? Are the official time systems of countries specified in terms of mean solar time? Does that require the continued specification of UTC in terms of UT1 to some accuracy level? Many assume that UTC differs from UT1 by less than one second. Is the inconvenience of leap seconds sufficient to justify discontinuing them? What are the cost and problems of the reprogramming necessary if leap seconds are discontinued? There is an IAU Working Group established to respond to a possible inquiry from the ITU.

6. USER ISSUES

As changes are introduced into the reference systems, questions must be asked: Who are the users? Do users want to understand what is going on? What do users require and what do they really want? What is really used by the IERS for their purposes and is that what should be provided as a service? What is necessary for almanac offices and what should they be providing for their users? Do the users want standardized software, do they want to understand what is in that software, and do they care if it changes? What documentation is required and how much explanation is necessary? Should there be equinox and CEO based systems made available concurrently and, if so, how long should the dual systems be available? What should be done now, based on the current situation?

7. ROLES OF ORGANIZATIONS

What are the roles of the different organizations concerning reference systems? There currently exists a Working Group of IAU Division I on Reference systems, the International Earth Rotation Service (IERS), IUGG, IAG, IAU Commissions 4,5,8,19, and 31. All these groups feel they have some role in reference systems. Are there others who feel they are involved? How is this organizational confusion to be satisfactorily resolved?

8. IAU WORKING GROUPS

In 2003 two new Working groups were established with the specified chairmen: Precession - James Hilton and Nomenclature and Education - Nicole Capitaine. There is also the continuing working group, Definition of UTC - Dennis McCarthy.

9. IMPLEMENTATION POSSIBILITIES

I would suggest the following possible steps to reach a successful implementation:

a. A new Precession Theory needs to be adopted which can be incorporated into the IAU 2000A precession-nutation model, clarifying the two parts of the model. This precession theory would then establish an accurate equinox based reference frame, consistent in accuracy with the CEO based system.

b. Agreement needs to be reached concerning terminology and definitions among the experts.

c. For best accuracy the IERS and other high precision users should use the CIO, TIO, and Earth Rotation Angle (ERA) based system.

d. For many applications, users may continue to use the equinox based system, reaching good accuracy with the new precession theory, IAU 2000A nutation theory, and sidereal time from ERA definition.

e. The IERS and Almanac Offices should continue to provide data for both systems for the foreseeable future. Evaluations should be made after some period of time to determine what is really being used.

f. There clearly is a need for an education program that reaches the astronomical community and the other scientists that use these reference systems.

g. Appropriate resolutions should be presented to the IAU and IAG to formalize the establishment and ensure the continuity of the required reference systems.

10. EDUCATION PLAN

There is a need to educate astronomers, geodesists, space scientists, and others concerning this whole field of activities. Again, the IAU Working Group for the nomenclature is supposed to address this problem. This education program needs to include the following:

a. Clarifying the issues among the experts before trying to educate the whole community.

b. Clear and convincing presentation of reference systems and justifications for their structure in a way that reaches the general astronomy community. A good review article might help.

c. Presentations at astronomical meetings might draw attention to the current situation.

d. Web sites that provide explanations, answers, documentation, standardized software, and the needed data to support the systems.

e. Wide distribution of any proposed resolutions, including explanations, well before IAU General Assembly in 2006.

11. CONCLUSIONS

a. The ICRS has been introduced as fixed epoch independent reference system. It is implemented by the ICRF and optical catalogs, which are all available on one reference frame.

b. The non-rotating origin based system has been introduced and has advantages for submilliarcsecond type accuracies. It will be the basis for Earth Orientation parameters.

c. Many users will continue to use the equinox based system and will need the data to support that system.

d. There are a number of outstanding issues concerning the implementation and nomenclature for the moving reference frame for the future.

e. The dual systems, equinox and CEO, will probably be used for the foreseeable future. This will probably be a subject of discussion and disagreement for some time.

f. There is a need for agreement concerning some standardization of values for constants among the international organizations.

g. The continuing improvements in the accuracies of observations and theories will continue to drive the requirements for improvements in reference systems and their components in the future.

12. REFERENCES

Guinot, B., 1979, *Time and the Earth's Rotation, IAU Symp. 82*, D. D. McCarthy & J. D. H. Pilkington (eds.), D.Reidel Publ. Co, Dordrecht, 7.

IAU 2001, In Proceedings of the twenty-fourth General Assembly, H. Rickman (ed.), Astronomical Society of the Pacific, San Francisco.

IERS 2004, IERS Conventions, International Earth Rotation Service, in press.

Seidelmann, P.K., Kovalevsky, J., 2002, Application of the new concepts and definitions (ICRS, CIP and CEO) in fundamental astronomy, *Astron. Astrophys.*, **392**, 341-351.

Seidelmann, P.K., (ed.) 1991, Explanatory Supplement to the Astronomical Almanac, University Science Books, Mill Valley, CA.

POSTFACE

JOURNÉES 2004 SYSTÈMES DE RÉFÉRENCE SPATIO-TEMPORELS

"Fundamental Astronomy: New concepts and models for high accuracy observations"

Scientific Organizing Committee
N. Capitaine, France (Chair); A. Brzeziński, Poland; P. Defraigne, Belgium; T. Fukushima, Japan; D.D. McCarthy, USA; M. Soffel, Germany; J. Vondrák, Czech R.; Ya. Yatskiv, Ukraine

Local Organizing Committee
J. Souchay (Chair), P. Baudoin, O. Becker, C. Bizouard, G. Bourda, A-M. Gontier, J-B. N'Guyen

Conference location : Observatoire de Paris, France

Scientific objectives
The Journées 2004 "Systèmes de référence spatio-temporels", with the sub-title "Fundamental Astronomy: New concepts and models for high accuracy observations", will be held from 20 to 22 September 2004 at Paris Observatory. These Journées will be the sixteenth conference in this series whose main purpose is to provide a forum for researchers in the fields of Earth rotation, reference frames, astrometry and time. The problems to be discussed in 2004 are related to the International Celestial Reference System (ICRS), including new concepts in fundamental astronomy, the associated nomenclature and the astronomical models for Earth rotation (precession, nutation, atmospheric and oceanic effects, etc.) at the highest level of accuracy consistent with the current and future precision and temporal resolution of the observations of Earth rotation.

The programme of the Journes 2004 will consist in five sessions including discussion on the work of the new IAU Working Groups of Division I: "Precession and the ecliptic" (Session 2) and "Nomenclature in Fundamental Astronomy" (Session 3), as well as the Working Groups on "Relativity in Celestial Mechanics, Astrometry and Metrology" (Session 4) and "The future of UTC" (Session 5). Discussion on the tasks that were previously part of the ICRS Working Group will also take place (Session 1). A kickoff meeting for the Project "Descartes - Nutation" (Chair: V. Dehant) the purpose of which is to support cooperative studies devoted to 'the understanding of the next decimal of precession/nutation, from the theoretical point of view as well as from the observational point of view' will be included in Session 2. Posters summarizing the proposals selected by the Advisory Board of the Descartes - Nutation project will be encouraged. 2004 being the 150 anniversary of Poincar's birth, there will be a special emphasis on Poincare's work on Earth rotation in Session 2.

Scientific programme

Session 1 : Recent and future developments in the realization of the ICRS

Session 2 : Models for Earth rotation: from Poincar to IAU 2000

Session 3 : Nomenclature in fundamental astronomy

Session 4 : Solar System Dynamics

Session 5 : Relativity in the problems of astronomical reference systems and Earth rotation: status and prospects

Session 6 : Future of UTC: Consequences in astronomy

Contact : Nicole Capitaine, Observatoire de Paris 61, avenue de l'Observatoire, 75014, Paris, France Phone : 33 1 40 51 22 31; Fax : 33 1 40 51 22 91; e-mail : capitaine@syrte.obspm.fr,

or see : http://syrte.obspm.fr/journees2004/